

ADVANCES IN
Agronomy

VOLUME 126





VOLUME ONE HUNDRED AND TWENTY SIX

ADVANCES IN
AGRONOMY

ADVANCES IN AGRONOMY

Advisory Board

PAUL M. BERTSCH
University of Kentucky

KATE M. SCOW
University of California, Davis

RONALD L. PHILLIPS
University of Minnesota

LARRY P. WILDING
Texas A&M University

Emeritus Advisory Board Members

JOHN S. BOYER
University of Delaware

EUGENE J. KAMPRATH
North Carolina State University

MARTIN ALEXANDER
Cornell University

Prepared in cooperation with the

**American Society of Agronomy, Crop Science Society of America, and Soil
Science Society of America Book and Multimedia Publishing Committee**

DAVID D. BALTENSPERGER, CHAIR

LISA K. AL-AMOODI

WARREN A. DICK


HARI B. KRISHNAN

SALLY D. LOGSDON

CRAIG A. ROBERTS

MARY C. SAVIN

APRIL L. ULERY



VOLUME ONE HUNDRED AND TWENTY SIX

ADVANCES IN AGRONOMY

Edited by

DONALD L. SPARKS

Department of Plant and Soil Sciences

University of Delaware

Newark, Delaware, USA



ELSEVIER

AMSTERDAM • BOSTON • HEIDELBERG • LONDON
NEW YORK • OXFORD • PARIS • SAN DIEGO
SAN FRANCISCO • SINGAPORE • SYDNEY • TOKYO

Academic Press is an imprint of Elsevier



Academic Press is an imprint of Elsevier
525 B Street, Suite 1800, San Diego, CA 92101-4495, USA
225 Wyman Street, Waltham, MA 02451, USA
32 Jamestown Road, London, NW1 7BY, UK
The Boulevard, Langford Lane, Kidlington, Oxford, OX5 1GB, UK
Radarweg 29, PO Box 211, 1000 AE Amsterdam, The Netherlands

First edition 2014

© 2014 Elsevier Inc. All rights reserved.

No part of this publication may be reproduced, stored in a retrieval system or transmitted in any form or by any means electronic, mechanical, photocopying, recording or otherwise without the prior written permission of the publisher

Permissions may be sought directly from Elsevier's Science & Technology Rights Department in Oxford, UK: phone: (+44) (0) 1865 843830; fax: (+44) (0) 1865 853333; email: permissions@elsevier.com. Alternatively you can submit your request online by visiting the Elsevier web site at <http://elsevier.com/locate/permissions>, and selecting *Obtaining permission to use Elsevier material*

Notice

No responsibility is assumed by the publisher for any injury and/or damage to persons or property as a matter of products liability, negligence or otherwise, or from any use or operation of any methods, products, instructions or ideas contained in the material herein. Because of rapid advances in the medical sciences, in particular, independent verification of diagnoses and drug dosages should be made

ISBN: 978-0-12-800132-5

ISSN: 0065-2113

For information on all Academic Press publications
visit our website at store.elsevier.com

Printed and bound in USA

14 15 16 17 10 9 8 7 6 5 4 3 2 1

		Working together to grow libraries in developing countries
www.elsevier.com • www.bookaid.org		

CONTENTS

Contributors

vii

Preface

ix

1. Soil Chemical Insights Provided through Vibrational Spectroscopy	1
Sanjai J. Parikh, Keith W. Goyne, Andrew J. Margenot, Fungai N.D. Mukome and Francisco J. Calderón	
1. Introduction	2
2. FTIR Sampling Techniques	8
3. Raman Sampling Techniques	15
4. Soil Mineral Analysis	20
5. SOM Spectral Components	36
6. Bacteria and Biomolecules	44
7. Soil Amendments	49
8. Molecular-scale Analysis at the Solid–Liquid Interface	54
9. Real World Complexity: Soil Analysis for Mineral and Organic Components	85
10. FTIR Spectroscopy for SOM Analysis	91
11. Summary	111
Acknowledgments	112
References	112
2. Water-Saving Innovations in Chinese Agriculture	149
Qiang Chai, Yantai Gan, Neil C. Turner, Ren-Zhi Zhang, Chao Yang, Yining Niu and Kadambot H.M. Siddique	
1. Introduction	151
2. Framework of Water-Saving Agriculture	155
3. Water-Resource Management	162
4. Water-Saving Cropping Practices	169
5. Water-Saving Engineering Systems	184
6. Challenges and Opportunities in Water-Saving Agriculture	192
7. Conclusions	193
Acknowledgments	195
References	195

3. The Physiology of Potassium in Crop Production	203
Derrick M. Oosterhuis, Dimitra A. Loka, Eduardo M. Kawakami and William T. Pettigrew	
1. Introduction	204
2. Physiology of Potassium Nutrition	204
3. Stress Mitigation	218
4. Summary	223
References	223
4. Disease and Frost Damage of Woody Plants Caused by <i>Pseudomonas syringae</i>: Seeing the Forest for the Trees	235
Jay Ram Lamichhane, Leonardo Varvaro, Luciana Parisi, Jean-Marc Audergon and Cindy E. Morris	
1. Introduction	236
2. Economic Importance	240
3. Types of Diseases of Woody Plants Caused by <i>P. syringae</i> and Their Importance	241
4. Epidemiology	249
5. The Diversity of <i>P. syringae</i> Causing Disease to Woody Plant Species	257
6. Control of Diseases of Woody Plants Caused by <i>P. syringae</i>	263
7. The Case of Frost Damage due to Ice Nucleation-Active <i>P. syringae</i>	272
8. Conclusions and Perspectives	274
Acknowledgments	275
References	276
<i>Index</i>	297

CONTRIBUTORS

Jean-Marc Audergon

INRA, GAFL, Montfavet cedex, France

Francisco J. Calderón

USDA-ARS, Central Great Plains Research Station, Akron, CO, USA

Qiang Chai

Gansu Provincial Key Laboratory for Aridland Crop Sciences, Gansu Agricultural University, Lanzhou, Gansu, P.R. China; College of Agronomy, Gansu Agricultural University, Lanzhou, Gansu, P.R. China

Yantai Gan

Semi-arid Prairie Agricultural Research Centre, Agriculture and Agri-Food Canada, Swift Current, SK, Canada

Keith W. Goyne

Department of Soil, Environmental and Atmospheric Sciences, University of Missouri, Columbia, MO, USA

Eduardo M. Kawakami

University of Arkansas, Department of Crop, Soil and Environmental Sciences, Fayetteville, AR, USA

Jay Ram Lamichhane

Department of Science and Technology for Agriculture, Forestry, Nature and Energy (DAFNE), Tuscia University, Viterbo, Italy; INRA, Pathologie Végétale, Montfavet cedex, France

Dimitra A. Loka

University of Arkansas, Department of Crop, Soil and Environmental Sciences, Fayetteville, AR, USA

Andrew J. Margenot

Department of Land, Air and Water Resources, University of California Davis, Davis, CA, USA

Cindy E. Morris

INRA, Pathologie Végétale, Montfavet cedex, France

Fungai N.D. Mukome

Department of Land, Air and Water Resources, University of California Davis, Davis, CA, USA

Yining Niu

Gansu Provincial Key Laboratory for Aridland Crop Sciences, Gansu Agricultural University, Lanzhou, Gansu, P.R. China; College of Agronomy, Gansu Agricultural University, Lanzhou, Gansu, P.R. China

Derrick M. Oosterhuis

University of Arkansas, Department of Crop, Soil and Environmental Sciences, Fayetteville, AR, USA

Sanjai J. Parikh

Department of Land, Air and Water Resources, University of California Davis, Davis, CA, USA

Luciana Parisi

INRA, Pathologie Végétale, Montfavet cedex, France

William T. Pettigrew

ARS-USDA, Stoneville, MS, USA

Kadambot H.M. Siddique

The UWA Institute of Agriculture, The University of Western Australia, Crawley, WA, Australia

Neil C. Turner

The UWA Institute of Agriculture, The University of Western Australia, Crawley, WA, Australia

Leonardo Varvaro

Department of Science and Technology for Agriculture, Forestry, Nature and Energy (DAFNE), Tuscia University, Viterbo, Italy

Chao Yang

Semi-arid Prairie Agricultural Research Centre, Agriculture and Agri-Food Canada, Swift Current, SK, Canada

Ren-Zhi Zhang

Gansu Provincial Key Laboratory for Aridland Crop Sciences, Gansu Agricultural University, Lanzhou, Gansu, P.R. China; College of Resources and Environments, Gansu Agricultural University, Lanzhou, Gansu, P.R. China

PREFACE

Volume 126 contains four excellent reviews that will be of broad interest to crop and soil scientists. Chapter One is a comprehensive review of vibrational spectroscopic techniques to investigate natural materials and reaction processes of interest to soil and environmental scientists. Techniques that are discussed in detail, including theoretical, experimental, and application aspects, include Fourier transform infrared and Raman spectroscopy. Chapter Two is a timely review on water-saving innovations that are being employed in Chinese agriculture. Key water-saving technologies and applications are discussed. Chapter Three covers the physiology of potassium in crop production and its role in stress relief. Topics that are discussed include agronomic aspects of potassium requirements and diagnosis of soil and plant potassium status. Chapter Four provides important details on disease and frost damage of woody plants caused by *Pseudomonas syringae*. This is a disease that has been increasing on woody plants, which has significant implications for the forestry industry. The review discusses features of the pathogen, disease epidemiology, pathogen diversity, and methods of disease control.

I am grateful to the authors for their enlightening reviews.

Donald L. Sparks

This page intentionally left blank



Soil Chemical Insights Provided through Vibrational Spectroscopy

Sanjai J. Parikh^{*,1}, Keith W. Goyne[†], Andrew J. Margenot^{*}, Fungai N.D. Mukome^{*} and Francisco J. Calderón[‡]

^{*}Department of Land, Air and Water Resources, University of California Davis, Davis, CA, USA

[†]Department of Soil, Environmental and Atmospheric Sciences, University of Missouri, Columbia, MO, USA

[‡]USDA-ARS, Central Great Plains Research Station, Akron, CO, USA

¹Corresponding author: e-mail address: sjparikh@ucdavis.edu

Contents

1. Introduction	2
1.1 FTIR Spectroscopy	3
1.2 Raman Spectroscopy	5
2. FTIR Sampling Techniques	8
2.1 Transmission	8
2.2 Diffuse Reflectance Infrared Fourier Transform Spectroscopy	9
2.3 Attenuated Total Reflectance Fourier Transform Infrared Spectroscopy	10
2.4 IR Microspectroscopy	12
2.5 SR-FTIR Spectromicroscopy	13
3. Raman Sampling Techniques	15
3.1 Dispersive Raman Spectroscopy	15
3.2 Fourier Transformed Raman Spectroscopy (FT-Raman)	17
3.3 Raman Microspectroscopy	18
3.4 Surface-Enhanced Raman Scattering Spectroscopy	18
4. Soil Mineral Analysis	20
4.1 Phyllosilicates	21
4.2 Allophane and Imogolite	26
4.3 Metal Oxides, Hydroxides, and Oxyhydroxides	28
4.4 Mineral Weathering and Pedogenesis	34
5. SOM Spectral Components	36
6. Bacteria and Biomolecules	44
7. Soil Amendments	49
7.1 Biochar	49
7.2 Compost	53
7.3 Biosolids	53
8. Molecular-scale Analysis at the Solid–Liquid Interface	54
8.1 Organic Molecule Interactions with Mineral Surfaces	55
8.1.1 <i>Low Molecular Weight Organic Acids</i>	59
8.1.2 <i>Herbicides and Pharmaceuticals</i>	64

8.2	Inorganic Molecule Interactions with Mineral Surfaces	72
8.3	Bacteria and Biomolecule Adhesion	78
9.	Real World Complexity: Soil Analysis for Mineral and Organic Components	85
9.1	Soil Heterogeneity and Mineral Analysis	85
9.2	Differentiating Mineral and Organic Spectral Absorbance	87
10.	FTIR Spectroscopy for SOM Analysis	91
10.1	SOM Analysis in Whole Soils	91
10.2	SOM Analysis via Fractions and Extracts	92
10.2.1	<i>Chemical Extracts and Fractionation</i>	93
10.2.2	<i>HS: A Common SOM Extract for FTIR Analyses</i>	93
10.2.3	<i>SOM Analysis Following Physical Fractionation</i>	98
10.3	SOM Analysis via Subtraction Spectra	104
10.4	Spectral Analysis through Addition of Organic Compounds	107
10.5	Quantitative Analysis of Soil Carbon and Nitrogen	109
11.	Summary	111
	Acknowledgments	112
	References	112

Abstract

Vibrational spectroscopy techniques provide a powerful approach to the study of environmental materials and processes. These multifunctional analytical tools can be used to probe molecular vibrations of solid, liquid, and gaseous samples for characterizing materials, elucidating reaction mechanisms, and examining kinetic processes. Although Fourier transform infrared (FTIR) spectroscopy is the most prominent type of vibrational spectroscopy used in the field of soil science, applications of Raman spectroscopy to study environmental samples continue to increase. The ability of FTIR and Raman spectroscopies to provide complementary information for organic and inorganic materials makes them ideal approaches for soil science research. In addition, the ability to conduct in situ, real time, vibrational spectroscopy experiments to probe biogeochemical processes at mineral interfaces offers unique and versatile methodologies for revealing a myriad of soil chemical phenomena. This review provides a comprehensive overview of vibrational spectroscopy techniques and highlights many of the applications of their use in soil chemistry research.



1. INTRODUCTION

Fourier transform infrared (FTIR) and Raman spectroscopies provide scientists with powerful analytical tools for studying the organic and inorganic components of soils and sediments. In addition to their utility for investigating sample mineralogy and organic matter (OM) composition, these techniques provide molecular-scale information on metal and organic sorption processes at the solid–liquid interface. As such, both mechanistic and kinetic studies of important biogeochemical processes can be

conducted. It is the versatility and accessibility of these vibrational spectroscopy techniques that make them a critical tool for soil scientists. In this review FTIR and Raman spectroscopy approaches are introduced and a comprehensive discussion of their applications for soil chemistry research is provided.

The primary objective of this review is to provide a synopsis of vibrational spectroscopy applications with utility for soil chemistry research. In doing so, FTIR and Raman spectroscopy will be presented, their sampling techniques introduced, and relevant studies discussed. Due to the large number of FTIR studies in the field of soil science and related disciplines far exceeding those for Raman, this review is heavily weighted towards FTIR. Additionally, emphasis will be placed on applications of vibrational spectroscopy for studying soil minerals, soil organic matter (SOM), bacteria and biopolymers, and various soil amendments (i.e. biochar, compost, biosolids). Particular attention is given to the analysis of OM in whole soils, fractions, and extracts. Molecular-scale analysis at the mineral-liquid interface and approaches for analyzing soil samples will also be discussed.

Vibrational spectroscopy approaches for studying soil, and the chemical processes occurring within, are some of the most versatile and user-friendly tools for scientists. Today, computer hardware and software capabilities continue to grow and the vast literature of vibrational spectroscopy studies is correspondingly expanding. As highlighted in this review, there is a wealth of information that can be garnered from these analysis techniques and the future of vibrational spectroscopy holds great promise for scientists working in the fields of soil and environmental sciences.

1.1 FTIR Spectroscopy

The development of the FTIR spectrometer relied on the prior invention of the Michelson interferometer by Albert Abraham Michelson in 1880 (Livingston, 1973). With the Michelson interferometer it became possible to accurately measure wavelengths of light. Although Jean Baptiste Joseph Fourier had previously developed the Fourier transform (FT), the calculations to convert the acquired interferograms to spectra remained cumbersome—even following the advent of computers. It was not until the development of the Cooley–Tukey Algorithm in 1965 (Cooley and Tukey, 1965) that computers could rapidly perform FT and modern FTIR spectroscopy became possible. The FTIR spectrometers that soon developed have remained relatively unchanged in recent decades, though advances in computer science have enabled new

methods for data collection, processing, and analysis. Today the methods of data acquisition are becoming increasingly sophisticated and the applications for FTIR continue to grow. Specific collection techniques, such as transmission, diffuse reflectance infrared Fourier transform spectroscopy (DRIFTS), and attenuated total reflectance (ATR) will be discussed later in this review.

Infrared microspectroscopy (IRMS) is a FTIR spectroscopy technique that is developing rapidly and providing exciting new experimental capabilities for soil scientists. The first documentation of combining infrared (IR) spectroscopy with microscopy are several studies from 1949 where the technique was applied to analyze tissue sections and amino acids (Barer et al., 1949; Blout and Mellors, 1949; Gore, 1949). This promising new technique offered imaging and chemical information of samples at a new level of resolution. However, as the two instruments were not integrated and computer technology was still in its infancy, the combination suffered from low signal to noise ratios and slow data processing (Katon, 1996; Shearer and Peters, 1987). Those interested in the early difficulties of these techniques are referred to Messerschmidt and Chase (1989) for details on the theory and causes of design failures in the early instruments. After about two decades, advances in computerization and IR spectroscopy instrumentation (i.e. interferometer, Fourier transformation, detectors) greatly increased the use and applicability of this analytical technique (Carr, 2001; Heymann et al., 2011; Hirschfeld and Chase, 1986; Liang et al., 2008). Despite the extensive use of IRMS in biomedical and material science through the 1980s and 1990s, similar analyses in soils were challenged by appropriate sample preparation (i.e. $\sim 10\ \mu\text{m}$ thin sections). In addition, due to the heterogeneous nature of soil, the spatial resolution of the microscopes used in the instruments was insufficient to characterize most soil samples. For discussion and details on the component setup of IR microscopes the reader is directed to several excellent articles (Katon, 1996; Lang, 2006; Stuart, 2000; Wilkinson et al., 2002). Improvements in microprocessor and computational technologies, and direct coupling of the microscope with IR spectrophotometer improved spatial resolution (typically $75\text{--}100\ \mu\text{m}$) and enabled a new scale of differentiation (Holman, 2010). IRMS can be used with the IR spectrometer in transmission, reflectance, grazed incidence, and ATR modes (Brandes et al., 2004).

FTIR spectroscopy uses polychromatic radiation to measure the excitation of molecular bonds whose relative absorbances provide an index of the abundance of various functional groups (Griffiths and de Haseth, 1986). Molecules with dipole moments are considered to be IR detectable. Dipole

moments can be permanent (e.g. H₂O) or induced through molecular vibration (e.g. CO₂). Absorption of IR light occurs when photon transfer to the molecule excites it to a higher energy state. These “excited states” result in vibrations of molecular bonds, rotations, and translations. The IR spectra contain peaks representing the absorption of IR light by specific molecular bonds as specific frequencies (i.e. wavenumbers) due to stretching (symmetric and asymmetric), bending (or scissoring), rocking, and wagging vibrations. An excellent introduction to FTIR theory and instrumentation is provided by [Smith \(2011\)](#). While not all molecules lend themselves to FTIR analysis, the majority of inorganic and organic compounds in the environment are IR active. In soils and environmental sciences much of the FTIR literature focuses on the mid-infrared (MIR) region of light (approximately 4000 to 400 cm⁻¹).

1.2 Raman Spectroscopy

Raman spectroscopy was first observed experimentally by Raman and Kirishnan in 1928 as a technique using secondary radiation concurrent with the discovery of IR spectroscopy ([Raman and Krishnan, 1928](#)). Due to a greater difficulty in perfecting the technique, Raman spectroscopy initially lagged behind and suffered from less experimental and instrumental development. Significantly hampered by fluorescence, it was not until the early light source used by Raman and Kirishnan (sunlight) was replaced that the technique gained popularity. Initially several different modifications of mercury lamps [including water cooled ([Kerschbaum, 1914](#)), mercury burner ([Hibben, 1939](#)), and cooled mercury burner ([Rank and Douglas, 1948](#); [Spedding and Stamm, 1942](#))] were used but these were affected by sample photodecomposition.

The introduction of lasers by Porto and colleagues ([Leite and Porto, 1966](#); [Porto et al., 1966](#)) paved the way for modern day instruments. The use of a near-infrared (NIR) excitation laser source (Nd:YAG at 1064 nm) in FT-Raman analysis in the late 1980s, coupled with advances in other parts of the instrumentation [detectors ([Epperson et al., 1988](#); [Pemberton et al., 1990](#)) and scattering suppression filters ([Otto and Pully, 2012](#))], overcame the aforementioned major limitation of Raman spectroscopy—fluorescence ([Hirschfeld and Chase, 1986](#)). For a more detailed account of the history of Raman spectroscopy, readers are directed to [Ferraro \(1967\)](#). Novel techniques such as surface-enhanced Raman spectroscopy (SERS) and confocal Raman microspectroscopy have elevated the importance of Raman spectroscopy in the field of soil chemistry ([Corrado et al., 2008](#); [Dickensheets et al., 2000](#);

Francioso et al., 2001; Leyton et al., 2008; Sanchez-Cortes et al., 2006; Szabó et al., 2011; Vogel et al., 1999; Xie and Li, 2003; Yang and Chase, 1998).

In contrast to IR spectroscopy, in which vibrational spectra are measured by the absorption of incident photons, Raman spectroscopy utilizes the scattering of incident photons to observe the transitions between the quantized rotational and vibrational energy states of the molecules. When a monochromatic light source interacts with matter, photons can traverse, absorb, or scatter. Photon scattering can be elastic (Rayleigh) or inelastic (Raman).

In Rayleigh scattering, the frequency of the emitted photons does not change relative to the incident light frequency. This type of scattering arises from approximately 10^{-4} of incident photons and is thus more intense (Smith and Dent, 2005) relative to the inelastic scattering of 10^{-8} of incident photons in Raman scattering (Petry et al., 2003). Inelastic scattering can result from (1) excitation of molecules in the ground state (ν_0) to a higher energy vibrational state (Stokes) and (2) return of molecules in an excited vibrational state to the ground state (anti-Stokes) (Popp and Kiefer, 2006). The different transition schemes are illustrated in Figure 1.1. Due to the small population of molecules in the excited vibrational state at room temperature (calculated from the Boltzmann distribution),

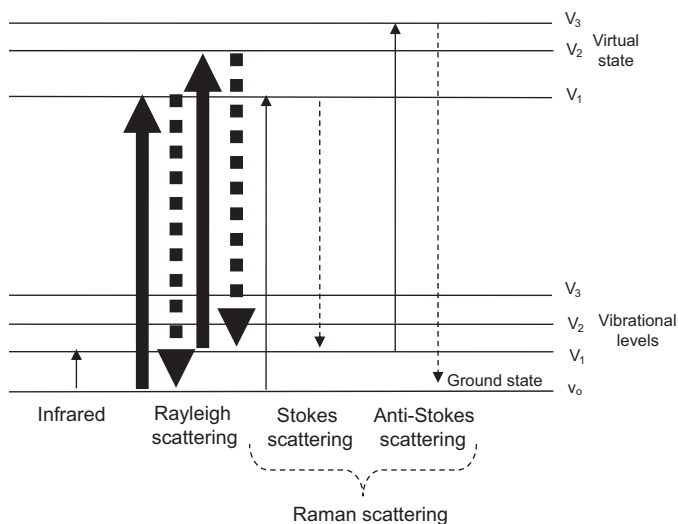


Figure 1.1 Energy level transitions of infrared and Raman spectroscopy. Larger arrows for Rayleigh scattering signify greater abundance. Adapted with permission from Smith and Dent (2005).

anti-Stokes bands are not usually considered important in Raman spectra. The energy of emitted photons is relative to the incident light and hence, although plotted like IR spectra, Raman spectra display the wavenumbers shift in the energy of the incident radiation. For a more comprehensive explanation of the principle, theory and instrumentation of Raman spectroscopy the reader is directed to several resources (Colthup et al., 1990; Ferraro, 2003; Lewis and Edwards, 2001; Long, 1977, 2002; Lyon et al., 1998; Pelletier, 1999; Popp and Kiefer, 2006; Smith, 2005).

The change in polarizability of a molecular bond measured by Raman spectroscopy is more intense in pi bonds of symmetric molecules (e.g. olefinic and aromatic C=C) compared to sigma bonds of atoms of different electronegativity (e.g. O-H, C-N and C-O) (Sharma, 2004). As the latter type of bonds (asymmetric) are more intensely IR active, Raman spectroscopy provides complementary information on symmetric bonds. Additionally, the weakness of Raman bands of asymmetric bonds, particularly O-H, limits spectral interference of water, one of the major limitations of FTIR analysis (Li-Chan et al., 2010). Figure 1.2 shows positions of Raman bands for generalized inorganic and organic samples. As Raman and FTIR are both vibrational spectroscopies, combining these complementary approaches can provide thorough molecular bond characterization of samples. A comparison of Raman and IR spectroscopy pertaining to soil chemistry is summarized in Table 1.1.

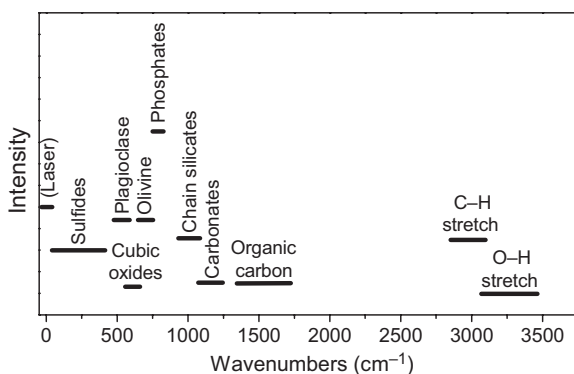


Figure 1.2 Diagram showing general positions of Raman shifts of certain types of minerals and organic matter. Overlapping of bands is minimal, allowing detection of components of complex heterogeneous matrices like soil. Adapted with permission from Fries and Steele (2011).

Table 1.1 Comparison of Raman and Infrared Spectroscopic Analysis for Soil Chemical Analysis

	Raman Spectroscopy	Infrared Spectroscopy
Spectral interference from water	No	Yes
Spectral interference from glass containers	No	Yes
Sample preparation	No	Yes (minimal)
Overlapping of spectral bands	Yes (minimal)	Yes
Intensity of band is quantitative	Yes	Yes (limited)
Sensitive to composition, bonding, chemical environment, phase, and crystalline structure	Yes	No
In situ analysis	Yes	No



2. FTIR SAMPLING TECHNIQUES

There are a variety of sampling approaches that are conducive for analysis of environmental samples. The most common methods of collecting FTIR spectra are transmission, DRIFTS, and ATR. The basic sampling principles for these spectroscopic approaches are illustrated in [Figure 1.3](#). In recent years, FTIR–microspectroscopy (IRMS) is being used more commonly in soil science research. The greatest advances with IRMS have been made by utilizing the energy beam from synchrotron (SR) source to enhance spatial resolution of FTIR.

2.1 Transmission

The simplest method for collecting FTIR data is via transmission ([Figure 1.3\(A\)](#)). This is a relatively inexpensive sampling technique, which has been used extensively since the invention of the FTIR. In transmission, the sample is placed directly in the path of the IR beam and the transmitted light is recorded by the detector. Liquid samples are dried onto IR windows (e.g. ZnSe, Ge, CdTe), and solid samples are ground and mixed with KBr and pressed into pellets or wafers. Transmission is often considered a bulk IR measurement because all components of the sample (e.g. exterior, interior) encounter the beam. Samples must be sufficiently thin ($\sim 1\text{--}20\ \mu\text{m}$ for solid samples, or 0.5–1 mm for KBr pellets) and sufficient light must reach the detector. Soil and mineral samples can be analyzed following careful sample preparation, which can be labor intensive and involves grinding, mixing with KBr, and pressing of pellets or wafers. Since sample desiccation

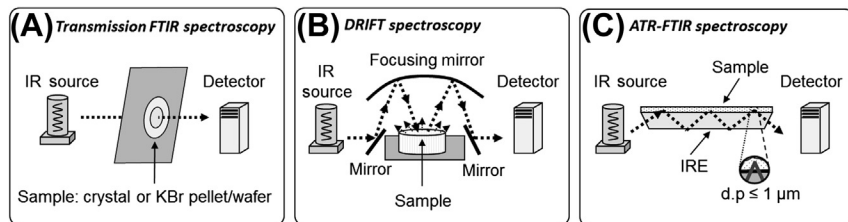


Figure 1.3 Representative illustration of common FTIR sampling approaches including: (A) transmission, (B) diffuse reflectance infrared Fourier transform spectroscopy (DRIFTS), and (C) attenuated total reflectance (ATR)-FTIR. (FTIR, Fourier transform infrared.) Adapted with permission from *Parikh and Chorover (2005)*.

is required for transmission analysis, artifacts such as the dehydration of surface complexes may result.

2.2 Diffuse Reflectance Infrared Fourier Transform Spectroscopy

In DRIFTS, IR radiation penetrates the sample to a depth, which is dependent on the reflective and absorptive characteristics of the sample (e.g. [Figure 1.3\(B\)](#)). This partially absorbed light is then diffusely re-emitted from the sample and collected on a mirror that focuses energy coming from the sample onto the detector. The resulting spectrum is comparable to that produced in transmission mode, but is more dependent on spectral properties of the sample interface ([Griffiths and de Haseth, 1986](#)).

DRIFTS is well suited for soil analysis because the spectra can be obtained directly from the samples with minimal sample preparation. Typically only drying and grinding are required, although, dilution with KBr is sometimes beneficial. Grinding is best done finely and uniformly across the sample set in order to avoid artifacts that could affect the baseline and peak widths (20 mesh should suffice). Coarser soils trap light more effectively than finer soils, resulting in higher overall absorbance and a shifted baseline ([Reeves et al., 2012](#)). Also, mineral bands can be affected by particle size due to variations in specular distortion between small and large silica fragments ([Nguyen et al., 1991](#)). Fine grinding can additionally improve spectral quality by homogenizing soil samples. MIR radiation does not penetrate soil samples very well, so the volume of soil scanned by diffuse reflectance instruments is limited to a few cubic millimeters.

Similar to transmission analysis of pressed pellets, DRIFTS can be used to analyze soil or sediment samples diluted with KBr (typically 2–10% sample by mass). This approach is particularly useful when only small sample

volumes are available or if the sample is strongly IR absorbing. However, quantitative calibrations with soil samples can only be achieved using spectra from “as is” neat samples not diluted with KBr (Janik et al., 1998; Reeves et al., 2001).

2.3 Attenuated Total Reflectance Fourier Transform Infrared Spectroscopy

ATR-FTIR spectroscopy is a tool that can be used for nondestructive in situ studies of soil minerals, humic substances (HS), bacteria, and other samples. As illustrated in Figure 1.3(C), ATR-FTIR spectra provide information on functional groups near the surface ($\sim 1 \mu\text{m}$) of an internal reflection element (IRE) (Nivens et al., 1993a, 1993b). One distinct advantage to ATR-FTIR as compared to other sampling techniques is the relative ease of collecting quality data in the presence of water. Water absorbs strongly in the MIR range (particularly at 1640 cm^{-1} and 3300 cm^{-1}) common to vibrational frequencies of many functionalities (Suci et al., 1998). ATR-FTIR avoids water interference by sending IR light through a highly refractive index prism (IRE). The refracted IR light travels beyond the IRE surface in evanescent waves, probing the solid-liquid interface without penetrating into the bulk solution (Suci et al., 1998). Due to the ability to conduct experiments in the presence of water, ATR-FTIR techniques can be used to examine sorption of aqueous species at crystal and mineral-coated crystal interfaces (Arai and Sparks, 2001; Borer et al., 2009; Goyne et al., 2005; Jiang et al., 2010; Parikh et al., 2011; Peak et al., 1999). ATR-FTIR is a particularly powerful approach for studying sorption because it can provide information on the speciation of bound molecules and differentiate between inner- and outer-sphere complexes. Since FTIR can be used to probe distinct vibrations arising from biomolecules and inorganic solids, ATR-FTIR is additionally useful for investigating processes at the bacteria-mineral and biomolecule-mineral interfaces (Benning et al., 2004; Deo et al., 2001; Omoike et al., 2004; Parikh and Chorover, 2006, 2008).

ATR-FTIR is limited in that only a few crystal materials can be used effectively. Some of the most common IRE's used include ZnSe, Ge, and KRS-5. When choosing an IRE, consideration must be given to the refractive index (RI) of both crystal and sample, wavenumbers range of interest, solubility of the IRE, and acidity of the experiment. Information on various ATR crystals can be easily found from FTIR spectrometer manufacturers and the literature (e.g. Lefèvre, 2004; Smith, 2011). In recent years, the development of single bounce ATR has led to the commonplace use of diamond as

an IRE. Diamond has the advantage of being very durable and resistant to most solution chemistries. Regardless of the crystal used, the IRE must have a high RI such that IR light passing through the crystal is refracted within the crystal. The light traveling from the optically dense medium (IRE) into the rare medium (bacteria/liquid medium) will totally reflect at the interface if the angle of incidence is greater than the critical angle (Chittur, 1998b). The critical angle is calculated using the following equation:

$$\theta_{\text{critical}} = \sin^{-1} \frac{\text{RI of rare medium}}{\text{RI of dense medium}} \quad (1.1)$$

where θ is the incident angle (Chittur, 1998a). A high RI of the IRE and increasing θ will result in a decreased depth of penetration (Schmitt and Flemming, 1998). The IR beam is able to penetrate into the rare medium allowing a sample spectrum to be acquired from the thin layer attached to the crystal surface (Schmitt and Flemming, 1998).

The RI of the IRE (n_1) and sample (n_2) governs the depth of beam penetration. The depth of penetration (d_p) is calculated using the following equation (Mirabella, 1985):

$$d_p = \frac{\lambda}{2\pi \left[\left(\sin^2 \theta \right) - \left(\frac{n_1}{n_2} \right)^2 \right]^{\frac{1}{2}}} \quad (1.2)$$

where λ is the wavelength (cm) and θ is the angle of incidence. The intensity of reflected light traveling through the IRE will be reduced through interactions with IR absorbing material in the rare medium (Chittur, 1998a). IR light is absorbed by the sample on the IRE surface and the IR detector records the amount of light absorbed from the original IR source, thus producing IR absorption bands and an IR spectrum (Nivens et al., 1993a, 1993b).

As shown in Eqn (1.2), the depth of penetration is dependent on θ . Variable angle ATR (VATR)-FTIR permits depth profiling of samples at the IRE-liquid interface by varying θ of the IR beam into the sample to alter the d_p . This technique provides information on the spatial arrangement of samples at the IRE interface on small length scales. The effective angle of incidence (θ_{eff}) is determined using the following equation (Pereira and Yarwood, 1994):

$$\theta_{\text{eff}} = \theta_{\text{fix}} - \sin^{-1} \left[\frac{\sin(\theta_{\text{fix}} - \theta_{\text{var}})}{n_1} \right] \quad (1.3)$$

where θ_{fix} is angle of the crystal face (commonly 45°), and θ_{var} is the scale angle set on the VATR accessory. As an example of how d_p varies as a function of θ_{eff} the depth of penetration for bacteria on a ZnSe IRE is shown in Figure 1.4. For more information on ATR-FTIR, a number of review papers are suggested (Hind et al., 2001; Madejová, 2003; Strojek and Mielczar, 1974).

2.4 IR Microspectroscopy

IRMS is another approach for nondestructive in situ studies of soil components, but with the additional advantage of high spatial resolution. IRMS analysis can be performed in several measurement modes: transmission, diffuse reflection, reflection-absorption, grazing incidence reflection, and attenuated total reflection (Garidel and Boese, 2007). Sample preparation of soil samples is perhaps the most important factor for effectively applying this technique. For example, for IRMS analysis in transmission mode, thin sections of $<10\ \mu\text{m}$ thickness are required to avoid total light adsorption (Gregoriou and Rodman, 2002). This can be achieved by embedding the soil (typically air- or freeze-dried) in an epoxy resin and then microtoming with a diamond or glass knife. In some instances, samples may be better

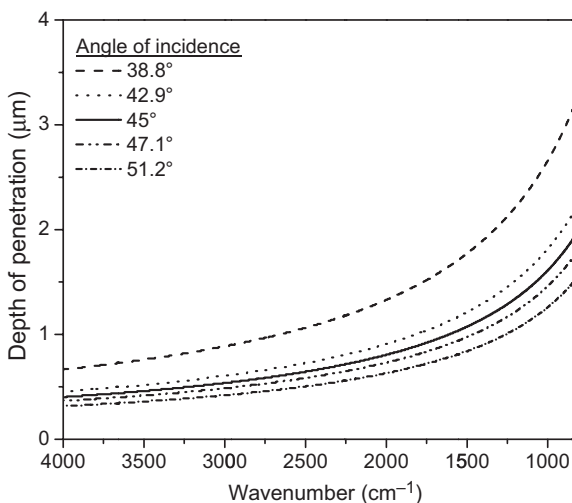


Figure 1.4 Calculated plot of the effect of altering the angle of incidence into an ATR internal reflection element (IRE) on the depth of penetration into the sample. In this case the refractive index (RI) for the IRE was $n_1=2.4$ (e.g. ZnSe or diamond) and the RI for the sample was $n_2=1.38$ (e.g. organic biopolymer or bacteria). (ATR, attenuated total reflectance.)

suiting to drying in liquid nitrogen and cryomicrotoming at subzero temperatures. Cryomicrotoming has been successfully used to analyze OM stability in intact soil microaggregates (Lehmann et al., 2007; Wan et al., 2007). After slicing, the mode of analysis determines the surface to mount the thin sections. For example, transmission electron microscopy grids are used in transmission mode or gold reflective microscope slides for reflection modes.

To obtain high quality spectra, the selected resin must not have adsorption bands that overlap with the sample and the sample surface must be even (Brandes et al., 2004). Polishing or thin sectioning can be used to avoid spectral “fringing”. Fringing occurs from interference between light that has been transmitted directly through the sample and light that has been internally reflected (Griffiths and de Haseth, 2006). The resultant sinusoidal patterns of this phenomenon are not easily subtracted from the spectra, making interpretation difficult (Holman et al., 2009).

Most resins are carbon based, presenting a unique sample preparation challenge for analysis of carbonaceous soil material. This has been overcome through use of noncarbon embeddings such as sulfur (Hugo and Cady, 2004; Lehmann et al., 2005; Solomon et al., 2005). For reflection mode, smooth sample surfaces are required to avoid collection inefficiency arising from excessive scattering of the reflected light. This mode is not favored for analysis of soils because it has a high signal to noise ratio suited to homogeneous samples. For more information regarding sample preparation in other modes, the reader is directed elsewhere (Brandes et al., 2004).

The capability of simultaneously obtaining biochemical information and high-resolution images of soil features using IRMS is currently unmatched. However, the applicability of IRMS to soil science research is limited by several factors including water adsorption and spatial resolution. Intense absorption in the MIR region associated with water is a major challenge for real time and in situ IR analyses. Spatial resolution is typically limited to 3–10 μm due to the diffraction limit of the IR source (Garidel and Boese, 2007). Details on the relationship between the diffraction limit and the wavelength of the IR source are explained in the reference.

2.5 SR-FTIR Spectromicroscopy

The motivation for combining SR radiation with an IR spectrophotometer arises from a desire to improve the signal to noise ratio and to overcome the diffraction limit of conventional IRMS (smallest practical spot size is approximately 20 μm) mainly due to the low brightness of the thermal IR source and use of an aperture (Carr, 2001). SR radiation is electromagnetic

radiation emitted when electrons, moving at velocities close to the speed of light, are forced to move in a high energy electron storage ring and produce a light source that has an intrinsic brilliance 100–1000 times that of light source used in IRMS (Lombi et al., 2011; Martin and McKinney, 2001; Solomon et al., 2012). At present, there are more than 50 light source facilities worldwide dedicated to the production of this radiation for research purposes. The electromagnetic radiation is nonthermal and highly polarized resulting in a reduced S/N ratio and improved spectral and spatial resolution. Another benefit of this technique is that despite the high intensity of the radiation, it does not degrade or change the chemical composition of the sample and elevates the sample temperature by only 0.5 K (Wilkinson et al., 2002). Figure 1.5 presents a schematic layout of the IR spectromicroscope highlighting its key components.

The hybrid technique affords high resolution (down to a few microns in the MIR region) that is no longer limited by the aperture size, but by

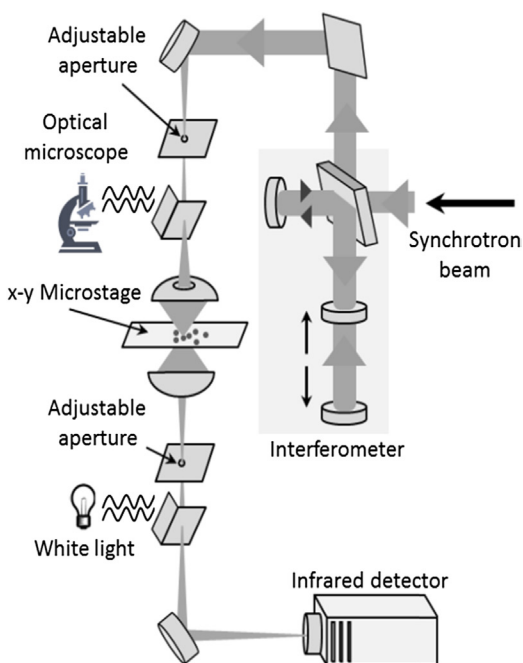


Figure 1.5 Schematic layout of key components of the synchrotron microspectroscope. The microstage (where sample is mounted) is computer controlled, enabling precision mapping. (For color version of this figure, the reader is referred to the online version of this book.) Adapted with permission from Wilkinson et al. (2002).

the optical system's numerical aperture and the wavelength of light, as explained by Carr (2001). The attainable spot size is 0.7 times the diameter of the wavelength of the IR beam, which is a spot size of 2–20 μm in the MIR region (Holman, 2010; Levenson et al., 2008). Until recently, intense absorption in the mid IR region associated with water was a major obstacle to real time and in situ analyses via SR-FTIR but has since been overcome using open channel microfluidics (Holman et al., 2010, 2009).

Several good reviews on the application of SR-FTIR with a focus on soils have been written (Holman, 2010; Holman and Martin, 2006; Lawrence and Hitchcock, 2011; Lombi et al., 2011; Raab and Vogel, 2004). In particular, the excellent review by Holman (2010) was a key resource in compiling this chapter. However, in a recent review comparing advanced in situ spectroscopic techniques and their applications in environmental biogeochemistry research, it is evident that there is opportunity for more studies in this field using this technique (Lombi et al., 2011). Numerous closely related applications of SR-FTIR can be found in literature: surface and environmental science (Hirschmugl, 2002; Sham and Rivers, 2002); biology and biomedicine (Dumas and Miller, 2003; Dumas et al., 2007); fossils (Foriel et al., 2004); fate and organic contaminants transport of pollutants in plants (Dokken et al., 2005a,b), and location and characterization of contaminants in sediments (Ghosh et al., 2000; Song et al., 2001).



3. RAMAN SAMPLING TECHNIQUES

3.1 Dispersive Raman Spectroscopy

Dispersive Raman spectroscopy, commonly referred to as Raman spectroscopy, utilizes visible laser radiation, as the source of incident light (Figure 1.6(A)). As the intensity of the Raman scatter is proportional to $1/\lambda^4$, shorter excitation laser wavelengths result in greater Raman signal (Lyon et al., 1998; Schrader et al., 1991). This technique requires only a few grams of sample with minimal to no sample preparation. Most liquid and solid samples can be analyzed without removal of atmospheric gases and water vapor as required for FTIR analysis. Solid samples can be finely ground to ensure homogeneity of the sample while liquid samples can be analyzed glass tubes or cuvettes. Particle size, although typically not considered to matter, may induce changes in the Raman spectra. In a recent study of several samples (i.e. silicon, quartz graphite, and charcoal, basalt and silicified volcanic sediments) comparing crushed and bulk samples, Foucher et al. (2013) showed differences in the spectra of the silicon and silicified

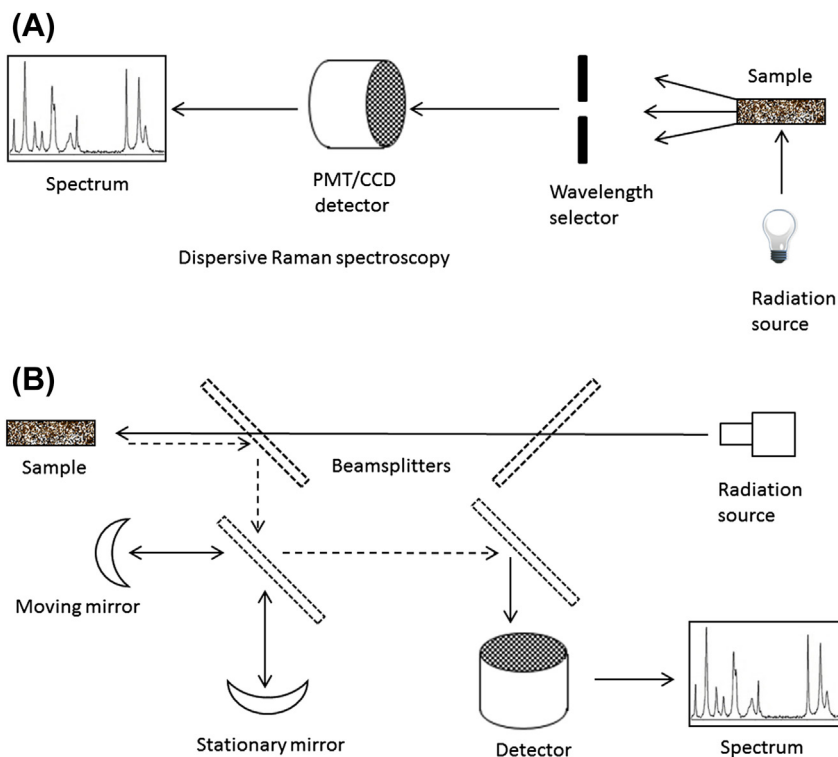


Figure 1.6 Schematic of instrument setup showing difference between (A) Dispersive and (B) Fourier transform Raman spectroscopy. (PMT, Photomultiplier tube; CCD, charged coupled detector.) (For color version of this figure, the reader is referred to the online version of this book.) Adapted with permission from *Das and Agrawal (2011)*.

volcanic sediments, and fewer differences in the others. The authors suggested that crushing results in an increase in the background signal level and peak width, and a slight shift in peak position, due to localized heating from the Raman laser. Interferences from the media and container glass are minimal and only become important for samples that produce a weak Raman signal. This enables analysis of samples to be performed within packaging, reducing the risk of sample contamination and loss. For analyses in polymer containers, greater consideration of potential interference from the container is required.

Despite the ease of sample preparation, this technique is hindered by several effects arising from the analysis process (*Bowie et al., 2000*). Firstly, the intensity of the incident light may result in heating of the sample leading to structural modifications, thermal degradation, and background thermal

radiation (Yang et al., 1994). For whole soil analysis, this technique can be severely limited by fluorescence depending on the sample and the wavelength utilized due to saturation of the silicon charged coupled detector typically used in this type of instrument. This limitation has been partially overcome through the use of software and by varying the wavelength of the incident light, as fluorescence is excitation wavelength-dependent. Oxidative pretreatment of soils with chemicals such as hydrogen peroxide (for removal of unsaturated aliphatic and aromatic compounds) has also been used to minimize sample fluorescence, enabling Raman analysis of soil mineral phases (Edwards et al., 2012). Fluorescence interferences when attempting Dispersive Raman were principally responsible for the development of FT-Raman. Early attempts to perform Dispersive Raman analysis on 50% of all “real samples” (including soils and clays) suffered from severe fluorescence interference and lack of resolution (Ewald et al., 1983; Hirschfeld and Chase, 1986).

3.2 Fourier Transformed Raman Spectroscopy (FT-Raman)

Improvements in Raman instrumentation, particularly incorporation of Fourier spectroscopy (detector signal enhancement), use of NIR excitation lasers of either yttrium vanadate (Nd:YVO₄) and neodymium-doped yttrium aluminum garnet (Nd:YAG) emitting light at a wavelength of 1064 nm (approximately 9400 cm⁻¹), and use of optical filters with very low transmission at the Rayleigh line wavelength have reduced interference by reflecting the interfering light (Hirschfeld and Chase, 1986; Schrader et al., 2000; Zimba et al., 1987). FT-Raman, as Dispersive Raman, requires small amounts of sample and minimal sample preparation. For solid samples, finely ground neat samples can be analyzed. In analysis of inorganic salts, Raman spectral intensity has been shown to increase as sample particle size decreases (Pellow-Jarman et al., 1996). The use of FT-Raman with post spectral processing has been advantageous for overcoming additional shortfalls (e.g. background thermal radiation) associated with Dispersive Raman spectroscopy (Yang et al., 1994) and resulted in improved spectral quality for a number of previously problematic samples, such as HS (Yang and Wang, 1997).

Due to the high wavelength used in FT-Raman, intensity of the Raman signal is very weak [Intensity = 1/(wavelength)⁴] but fluorescence is negligible. Interferometers convert the Raman signal into a single interferogram and the sensitive NIR detectors [e.g. germanium (Ge) and indium gallium arsenide (InGaAs)] used in conjunction, greatly enhance the signal–noise ratio of the resultant signal. FT-Raman has wide applications and several

good reviews detailing the application of this technique to a diverse range of fields are available (Brody et al., 1999a,b; Lewis and Edwards, 2001), including FT-Raman use in soil chemistry (Bertsch and Hunter, 1998; Hayes and Malcolm, 2001; Kizewski et al., 2011). This technique has been adapted to obtain quality data from the soil components: humic and fulvic acids (Yang and Wang, 1997) and clay minerals (Aminzadeh, 1997; Coleyshaw et al., 1994; Frost et al., 2010b; Frost and Palmer, 2011; Frost et al., 1997). However, few studies on more complex samples such as whole soils have been performed (Francioso et al., 1996). The technique has long been touted as an effective astrobiological tool in the exploration of Mars (Bishop and Murad, 2004; Ellery et al., 2004; Popp and Schmitt, 2004). For example, FT-Raman was recently included in the instrumentation of the ExoMars rover. FT-Raman has proven to be a versatile analytical tool, which is opening new scientific frontiers, including inclusion of this instrument on the MARS Rover.

3.3 Raman Microspectroscopy

First introduced in 1990, Raman microspectroscopy combines the robustness of Dispersive Raman spectroscopy with the resolution of optical microscopy to analyze single living cells and chromosomes (Puppels et al., 1990). Since then, the technique has been widely used in many disciplines to study bacteria (Huang et al., 2004; Xie and Li, 2003), fish (Ikoma et al., 2003), ceramics (Durand et al., 2012), and soils (Lanfranco et al., 2003). While, no sample preparation is required. However, due to the small spot size utilized in this technique, homogeneity of the sample and analysis of more than one position is paramount to acquiring a representative spectrum. Raman microspectroscopy offers several advantages over Dispersive and FT-Raman, including smaller minimum quantities of analyte, depth profiling via confocal microscopy, and improved spatial resolution with mapping and correlated imaging.

3.4 Surface-Enhanced Raman Scattering Spectroscopy

SERS was inadvertently first observed in 1974 by Fleischmann et al. (1974) and later explained by Jeanmaire and Van Duyne (1977) and Albrecht and Creighton (1977). This technique essentially incorporates a solution of the analyte into an electrochemical cell (Figure 1.7). When incident radiation is shone on the surface metal, of which the nature and roughness of the surface are critical, surface plasmons are generated from oscillation of the electron density (arising from conduction electrons held in the metal lattice) laterally (at a few microns/nanometers) to the metal surface. For scattering to be observed, the oscillation of the plasmons must be perpendicular to

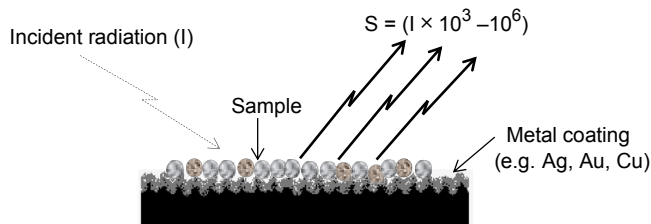


Figure 1.7 Schematic illustration of signal enhancing achieved in surface enhanced Raman scattering (S = enhanced signal). (For color version of this figure, the reader is referred to the online version of this book.)

the metal surface hence the requirement of a rough surface with peaks and valleys (smooth surfaces are inactive). These plasmons generate an enhanced electromagnetic field experienced by the analyte resulting in a scattered Raman signal that is greatly enhanced (Smith, 2005—Modern Raman Spectroscopy).

SERS greatly improves the sensitivity of Dispersive Raman spectroscopy by overcoming the challenge of a low-intensity sample signal. The greatest signal enhancement has been observed using metals such as silver, copper, and gold as coatings and aggregated colloidal suspensions, metal films, and beads as roughened substrates (Huang et al., 1999; Moskovits, 1985; Otto et al., 1992). The Raman signal is increased by up to 10^3 – 10^6 times when compared to the unenhanced signal and two explanations have been used to describe the enhancement (Moskovits, 1985). The first, and likely more important, involves direct electromagnetic interaction of the analyte with the roughened metal surface resulting in scattering from oscillations of surface metal plasmons perpendicular to the metal surface (Campion and Kambhampati, 1998; Das and Agrawal, 2011; Smith, 2005). The second theory involves chemical enhancement from charge transfer from the metal surface to the analyte due to analyte/metal surface binding (Moskovits, 1985; Otto et al., 1992).

Due to its sensitivity and ability to quench fluorescence, SERS has found a number of applications in soil chemistry research. Examples of these applications include: characterization of carbon in soil (Corrado et al., 2008; Francioso et al., 2000, 2001; Francioso et al., 1996); investigation of humic binding mechanisms (Corrado et al., 2008; Francioso et al., 2001; Francioso et al., 1996; Leyton et al., 2008; Liang et al., 1999; Sánchez-Cortés et al., 1998; Sanchez-Cortes et al., 2006; Vogel et al., 1999; Yang and Wang, 1997; Yang and Chase, 1998). In a series of studies, Francioso et al. successfully used

SERS to study different molecular weight humic and fulvic acids extracted from Irish peat using silver as the metal coating. Advances in SERS instrumentation and improvements of the technique have enabled in situ monitoring of soil carbon sequestration (Stokes et al., 2003; Wullschlegler et al., 2003) and application to the qualitative investigation of metal contaminants (e.g. Zn) in soil (Szabó et al., 2011). Several reviews and texts discussing the technique and its application have been written in recent years (Campion and Kambhampati, 1998; Corrado et al., 2008; Etchegoin and Le Ru, 2010; Huang et al., 2010; Katrin et al., 2002; Lombardi and Birke, 2009; Moskovits, 2005; Otto et al., 1992; Stiles et al., 2008).



4. SOIL MINERAL ANALYSIS

Vibrational spectroscopy has many utilities associated with soil mineral studies due to the ability of FTIR and Raman spectroscopies to elucidate local structures and composition changes within samples. Application of these spectroscopic techniques ranges from basic confirmation of mono-mineral samples to pedogenic studies of mineral formation. Additionally, vibrational spectroscopy can be applied solely or in conjunction with other instruments, most notably X-ray diffraction (XRD), for soil mineral confirmation and investigations. Although the utility of vibrational spectroscopy for mineral studies is hampered by similar energies produced from specific bond types (e.g. Si–O and Al–O) commonly found in similar environments within many minerals, FTIR and Raman spectroscopy are well suited for identifying and characterizing amorphous minerals and minerals with hydroxyl, carbonate, and sulfate groups (Amonette, 2002). A variety of FTIR techniques can be employed for mineral analyses, depending on available equipment and study objectives, including transmission with KBr pressed pellets, DRIFTS, and ATR techniques (Madejová, 2003). The wide range of applicable techniques and information obtained makes vibrational spectrometers very useful tools for investigating minerals. There are a number of excellent reviews and resources regarding application of vibrational spectroscopy to minerals including Farmer (1974b), McMillan and Hofmeister (1988), Russell and Fraser (1994), Johnston and Aochi (1996), Madejová and Komadel (2001), and Madejová (2003).

Micro-Raman and FT-Raman are the two Raman techniques most applied to soil mineral analysis. Removal of highly fluorescent OM is a necessary sample pretreatment step (e.g. combustion, chemical oxidation,

and solvent extraction) to ensure applicability of these techniques. Separation of the mineralogical and water-soluble organic fractions in soil samples enabled differentiation between ten different English soils using both fractions (Edwards et al., 2012). The authors utilized differing amounts of hydrogen peroxide (10, 25, and 50%) to remove incremental amounts of the nonparticulate organic matter from the soils. Analysis of the organic and inorganic sections of the Raman spectra of these samples showed differences in the OM (e.g. fulvic and humic fractions and long-aliphatic carbon chains) as well as mineralogy (e.g. calcite, hematite, and gypsum). Similarly, solvent extraction enabled applicability of Raman spectroscopy to perform speciation studies in the solid phases of natural and anthropogenic compounds present in river and estuarine sediments with appreciable clay and OM contents (Villanueva et al., 2008).

4.1 Phyllosilicates

Phyllosilicates, or layer silicates, are the most common minerals in soils. They are composed of one or two sheets of Si in tetrahedral coordination with O, with varying isomorphically substituted Al tetrahedra, fused to cations in octahedral coordination with O or OH. IR spectroscopy has been used to study clay minerals for a great number of years (Farmer, 1958). The utility of this technique is that it can be employed to distinguish between types of clay minerals (1:1 vs. 2:1 layer silicates) and further distinguish minerals within each structural grouping (e.g. kaolinite vs dickite). Structural details (di- vs trioctahedral nature) and compositional information (octahedral layer cations) of samples can be obtained as well.

Differentiation and characterization of layer silicates using FTIR is primarily based on vibrations associated with constituent units of the minerals (the hydroxyl functional group, the silicate anion, and cations residing in the octahedral layer and interlayer) as described by Farmer (1974c). The stretching vibrations of structural hydroxyl groups (OH) are found between 3750 and 3400 cm^{-1} and the bending bands are located between 950 and 600 cm^{-1} . Silicon bonded to oxygen (Si–O) stretching vibrations appear in the 1200–700 cm^{-1} region, and are also observed from 700 to 400 cm^{-1} along with octahedral cation vibrations. Vibrations from interlayer cations are found outside the MIR range between 150 and 70 cm^{-1} (Farmer, 1974c). Major portions of the IR spectrum used to fingerprint clay minerals are illustrated in Figure 1.8 from Madejová (2003). Notable differences in the 1:1 and 2:1 layer silicate spectra (Figure 1.8(A)a–c and d–g, respectively) are observed in OH stretching and Si–O stretching regions.

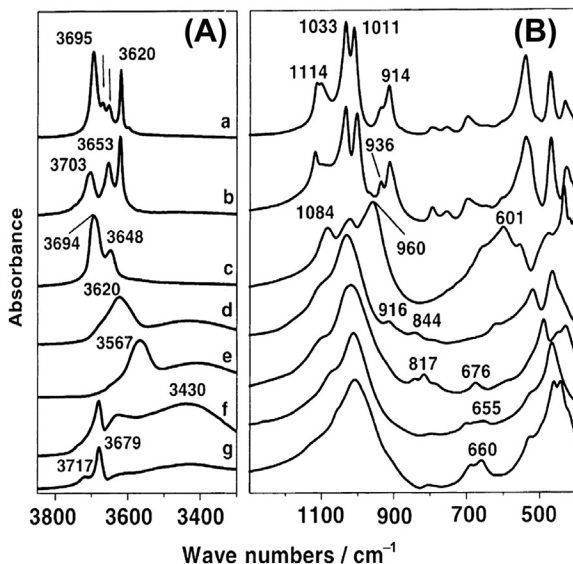


Figure 1.8 Transmission infrared spectra of pressed KBr discs containing samples of the 1:1 layer silicates (a) kaolinite, (b) dickite, (c) chrysotile, and the 2:1 layer silicates (d) SAz-1 montmorillonite, (e) nontronite, (f) hectorite, and (g) saponite for (A) the O-H stretching region and (B) the Si-O stretching and OH bending region. From *Madejová (2003)*, reprinted with permission.

The 1:1 layer silicates exhibit two or more OH stretching vibrations from 3700 to 3620 cm⁻¹ (kaolinite—4, dickite—3, chrysotile—2); whereas, the 2:1 minerals contain only a single OH stretching band. The number and location of the OH stretching bands in the 1:1 layer silicates can further identify the minerals. The absorption band at 3630–3620 cm⁻¹ in kaolinite, dickite, and nacrite (1:1 layer silicates; spectra not shown) is attributed to internal OH groups between the tetrahedral and octahedral sheets. The band at 3700 cm⁻¹ for these three minerals is associated with internal surface OH groups located on the octahedral layer surface that are involved in hydrogen bonding to oxygen atoms of the underlying tetrahedral layer surface (*Madejová, 2003*; *Russell and Fraser, 1994*). The remaining OH stretching bands in kaolinite and dickite are also associated with internal surface OH groups (*Farmer, 2000*), and the assignment of OH bands in chrysotile is unresolved (*Madejová, 2003*). Presence of the single OH stretching vibration in 2:1 layer silicates is attributed to OH coordinated with octahedral cations. The single broad band is attributed to isomorphous substitution within the mineral that disrupts crystalline order and increases structural imperfections (*Russell and Fraser, 1994*), and exact location of

this band in the spectrum is dependent upon the cation(s) to which OH is bonded (Farmer, 1974(C)). For example, the Al_2OH vibration at 3620 cm^{-1} in montmorillonite (Figure 1.8(A)d) is common for smectites with high Al content in the octahedral layer, whereas the band at 3567 cm^{-1} in Figure 1.8(A)e is indicative of Fe_2OH associated with Fe octahedra in nontronites (Madejová, 2003). In the trioctahedral minerals hectorite and saponite (Figure 1.8(A)f–g), OH stretching of Mg (Mg_3OH) in the octahedral layer appears at 3680 cm^{-1} . Čičel and Komadel (1997) describe the use of deconvoluting OH stretching frequencies in IR spectra to quantify the composition of octahedral cations. In micas and smectites, the method provides a fair degree of accuracy (2.5–10% relative error) for determining cation structural formula coefficients when compared to data derived from chemical analyses.

The Si–O stretching and OH bending region (Figure 1.8(B)) can also be quite informative for differentiating between the layer silicates. The 1:1 minerals shown in Figure 1.8(B)a–c and nacrite (spectrum not shown) exhibit three strong Si–O frequencies between 1120 and 950 cm^{-1} (Madejová, 2003; Russell and Fraser, 1994). In contrast, Si–O stretching in the 2:1 layer silicates (Figure 1.8(B)d–g) is noted by a single broad peak residing at 1030 – 1010 cm^{-1} . The di- or trioctahedral nature of a mineral apparently influences where the Si–O stretching band appears within a spectrum, as bands for the trioctahedral minerals which appear are higher wavenumbers (1030 – 1020 cm^{-1}) than the dioctahedral minerals ($\sim 1010\text{ cm}^{-1}$) (Madejová, 2003).

Vibrations from OH bending, referred to as librational frequencies of OH by Farmer (1974b), can also be evaluated for identifying structure of the octahedral layer. The OH bending vibrations in di- and trioctahedral 1:1 layer silicates are noted at 950 – 800 cm^{-1} and 700 – 600 cm^{-1} , respectively (Madejová, 2003). The OH bending portion of the spectrum has particular utility for elucidating the composition of dioctahedral 2:1 layer silicates due to frequency changes with octahedral cation composition (Farmer, 1974b). The following list of vibrational OH frequencies from Farmer (1974c) notes these changes quite well: Al_2OH , 950 – 915 cm^{-1} in all dioctahedral 2:1 species; FeAlOH , $\sim 890\text{ cm}^{-1}$ in montmorillonites; MgAlOH , $\sim 840\text{ cm}^{-1}$ in montmorillonites; and Fe_2OH , $\sim 818\text{ cm}^{-1}$ in nontronites. Several of these bands (Al_2OH , AlMgOH , and Fe_2OH) are readily observed in Figure 1.8(B)d–e. Presence of Al_2OH (916 cm^{-1}) and AlMgOH (844 cm^{-1}) vibrations in the SAz-1 montmorillonite spectrum is indicative of isomorphous substitution within the octahedral layer of this mineral (Madejová, 2003).

Greater details about the detailed structure of clay minerals or “nanoscale architecture” (Johnston, 2010) can also be investigated using vibrational spectroscopy. For example, low-temperature (<30 K) FTIR has been employed for detailed studies of OH stretching vibrations of kaolin group minerals (Balan et al., 2010; Bish and Johnston, 1993; Johnston et al., 2008; Prost et al., 1989). Reductions in temperature enhance resolution of OH stretching vibrations in IR spectra by shifting high frequency bands to higher frequencies (i.e. greater wavenumbers) and low frequency bands to lower frequencies (Prost et al., 1989). Prost et al. (1989) applied this approach to study crystalline kaolinite, dickite, and nacrite, and compared spectra of these minerals to poorly crystalline kaolinites. Their work demonstrated that the relative amounts of dickite-like and nacrite-like structures within poorly crystalline kaolinite increases as crystallinity of the sample decreases.

Johnston et al. (2008) expanded upon the low-temperature work of Prost et al. (1989) by conducting a more detailed study of OH stretching vibrations as a function of temperature. In kaolin group minerals, octahedral layer OH groups and the O of silicon tetrahedra found on opposing sides of the interlayer interact through hydrogen bonding (O(H)⋯O). Using FTIR data collected at 15 and 300 K, Johnston et al. (2008) demonstrated a linear correlation between OH stretching vibrations of kaolin group polytypes (kaolinite, dickite, and nacrite) and the corresponding distances of O(H)⋯O interlayer pairings. Interestingly, the correlation indicates that a 0.001 nm change in distance results in a 4 cm^{-1} shift in band position (Johnston, 2010), and more importantly the relationship provides clear identification of the three polytypes or the degree of disorder within a kaolin group mineral sample. Using this relationship, Johnston et al. (2008) identified structural disorders (dickite- or nacrite-like features) in 9 out of the 10 kaolinite samples analyzed, even in samples considered to be well ordered. Similar to the findings of Prost et al. (1989), the presence of dickite- and nacrite-like features increased with increasing disorder in the crystal structure. Low-temperature FTIR was unable to distinguish whether features represented discrete particles of dickite or nacrite or stacking mistakes in sample, but selected area electron diffraction patterns for Capim kaolinite indicate that the features were due to interstratified stacking mistakes. Thus, the use of low-temperature FTIR appears to be sufficiently sensitive for assessing structural disorders in kaolin group minerals (Johnston et al., 2008). The reader is referred to Johnston (2010) for additional examples regarding the application of FTIR and low-temperature FTIR for the detailed study of clay minerals.

There are numerous other applications of vibrational spectroscopy for the study of clay minerals, and the following studies illustrate the breadth and depth of information that can be gained with FTIR spectroscopy. Johnston et al. (1992) and Schuttlefield et al. (2007) used FTIR to study water interactions and uptake, respectively, onto clay minerals. Komadel et al. (1996) monitored HCl and temperature-induced structural changes in reduced-charge montmorillonites via FTIR analyses. Octahedral sheet evolution with progressive kaolinization was studied by Cuadros and Dudek (2006) using mixed kaolinite–smectite samples and transmission FTIR spectroscopy. Petit and colleagues (Petit et al., 1998, 2006) have developed FTIR-based methodology to quantitatively measure the layer charge properties of clay minerals through evaluation of NH_4^+ deformation vibrations. In addition to these more common bulk FTIR analysis approaches, a number of studies have utilized the spatial resolution provided by FTIR microspectroscopy to investigate in situ changes in clay minerals (Beauvais and Bertaux, 2002; Johnston et al., 1990; Rintoul and Fredericks, 1995). For example, Beauvais and Bertaux (2002) characterized in situ differentiation of kaolinite in lateritic weathering profiles from sample thin sections (30 μm thick). Changes observed in the four O–H stretching bands (between 3550 and 3750 cm^{-1}) were used as a proxy to differentiate among different kaolin species. More recently, Katti and Katti (2006) employed FTIR microscopy and micro-ATR spectroscopy to understand the influence of clay swelling on the misorientation and physical breakdown of montmorillonite platelets. Drying-induced acidity on smectite and kaolinite surfaces was studied using ATR-FTIR by Clarke et al. (2011).

Although less common than FTIR, Raman spectroscopy can also provide important information for the study of phyllosilicates. Abrupt shifts in the three Raman $\nu(\text{OH})$ bands of dickite, combined with XRD analysis, provided evidence for the first documented occurrence of a pressure-induced phase transformation in a 1:1 phyllosilicate (Johnston et al., 2002b). The reversible structural phase transitions occurred between 2.0 and 2.5 GPa as evidenced by shifts in the layers and significant changes in the stacking sequence and interlayer hydrogen bonding structure. In another study, kaolinite-like layered phyllosilicates, bismutoferrite $\text{BiFe}_3^{2+}(\text{Si}_2\text{O}_8)(\text{OH})$, and chapmanite $\text{SbFe}_3^{2+}(\text{Si}_2\text{O}_8)(\text{OH})$ were characterized through Raman and IR spectroscopy. The spectra were related to the molecular structure of the minerals with characteristic Raman bands attributed to the Si–O–Si stretching and bending vibrations and the (Si–O terminal) stretching vibration (Frost et al., 2010a; Rinaudo et al., 2004). Raman microspectroscopy

has also utilized to show water sorption in both the lattice and interlayers of vermiculite and muscovite (Haley et al., 1982).

4.2 Allophane and Imogolite

Allophane and imogolite are hydrated aluminosilicate minerals that exhibit short-range order crystallinity. Most commonly these minerals are found in Andisols or Spodosols (Dahlgren, 1994); however, allophane and imogolite can be precipitated from solution in any soil with sufficiently high concentrations of Si^{4+} and Al^{3+} in soil solution (Harsh et al., 2002). These minerals can be indicative of important pedogenic processes (Chadwick and Chorover, 2001) and they can strongly influence soil chemical processes (Harsh et al., 2002). Thus, identification and quantification of these minerals may be particularly useful for soil chemical and pedogenic studies.

IR spectroscopy is one technique that has application for identifying and quantifying allophane and imogolite in soils (Dahlgren, 1994; Farmer et al., 1977). The spectra of allophane and imogolite contain OH stretching vibrations ($3800\text{--}2800\text{ cm}^{-1}$), H–O–H deformation vibrations from absorbed water ($1700\text{--}1550\text{ cm}^{-1}$), Si–O stretching and OH vibrations ($1200\text{--}800\text{ cm}^{-1}$), and a band at 348 cm^{-1} that may be applicable for quantitative or semiquantitative determination of allophane and imogolite (Harsh et al., 2002). A primary difference between allophane and imogolite IR spectra can be found at $1050\text{--}900\text{ cm}^{-1}$. Imogolite and protoimogolite contain two absorption maxima at ~ 940 and $\sim 1000\text{ cm}^{-1}$; the former is attributed to an unshared hydroxyl in the orthosilicate group and the latter to Si–O vibrations (Harsh et al., 2002; Russell and Fraser, 1994). In contrast, allophane shows only a single Si–O band in this region that varies in location with changes in the Si/Al ratio (Figure 1.9) (Harsh et al., 2002); band position ($1020\text{--}975\text{ cm}^{-1}$) decreases in wavenumbers as Si/Al decreases. Differences in this spectral region of allophane and imogolite are attributed to changes in Si–O polymerization; silicon tetrahedra in imogolite are not polymerized and polymerization increases in allophane with increasing Si/Al ratio (Harsh et al., 2002).

Utilizing the absorbance band at 348 cm^{-1} , quantification of allophane and imogolite content in soils was first proposed by Farmer et al. (1977) and the method is detailed by Dahlgren (1994). There are several challenges associated with using IR spectroscopy to quantify these minerals (Dahlgren, 1994). Obtaining appropriate reference materials for use in developing a standard curve may be challenging, as IR absorption at 348 cm^{-1} varies among allophane samples used as standards (Farmer et al., 1977). Allophane

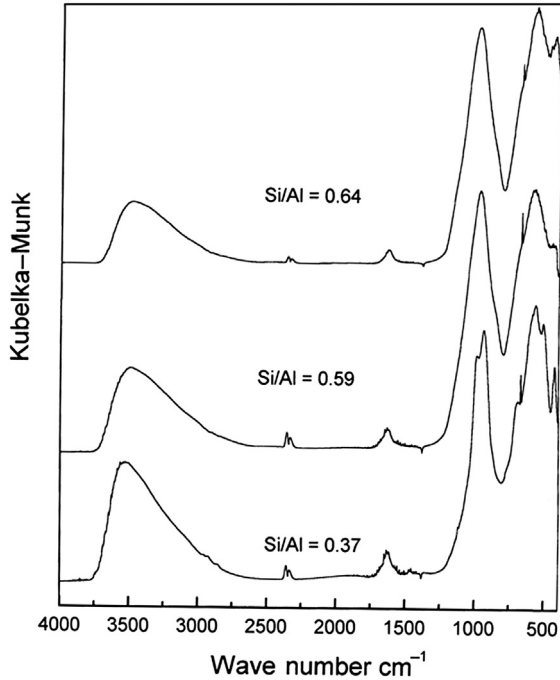


Figure 1.9 Diffuse reflectance Fourier transform infrared (DRIFTS) spectra of allophanes with decreasing Si/Al molar ratio. From Harsh et al. (2002), reprinted with permission.

and imogolite are not the only minerals to express a vibration band at 348 cm^{-1} ; many common layer silicates and metal oxides absorb IR radiation at this wavelength as well (Farmer et al., 1977). Concern about the latter issue has led some to discourage the use of IR spectroscopy for quantifying allophane and imogolite (Joussein et al., 2005), although acquisition of difference spectra for samples before and after varying treatments may mitigate this concern.

Dahlgren (1994) outlines three methods for using IR spectroscopy to quantify allophane/imogolite content in samples (allophane/imogolite is used here to indicate that the methods cannot separate quantities of one mineral or the other when both minerals are present in a sample). Although the methods outlined in Dahlgren (1994) specifically employ transmission analysis of pressed pellets, DRIFTS and ATR-FTIR analysis of powder samples may also be appropriate after additional method development. The first technique involves simple analysis of samples mixed with KBr diluent and heated to $150\text{ }^{\circ}\text{C}$ overnight, followed by mineral quantification based on absorption at 348 cm^{-1} . This approach suffers most greatly from

interferences at 348 cm^{-1} , as it does not adequately account for interference from other minerals absorbing in this portion of the spectrum. The other two recommended techniques mitigate this concern by employing the development of a difference spectrum. Samples are analyzed to obtain spectra prior to and after selective dissolution of allophane/imogolite using acid oxalate or dehydroxylation of allophane/imogolite at $350\text{ }^{\circ}\text{C}$. Spectra collection is followed by computer-aided subtraction of one spectrum from the other to develop a difference spectrum that can be used to quantify allophane/imogolite content at 348 cm^{-1} . Calculation of a difference spectrum should effectively remove contributions at the target wavelength to improve quantification of allophane/imogolite content in the sample, thereby minimizing concerns expressed by [Joussein et al. \(2005\)](#).

4.3 Metal Oxides, Hydroxides, and Oxyhydroxides

IR spectroscopy can be employed to identify and study the structures of metal oxides, hydroxides, and oxyhydroxides, collectively referred to as metal oxides hereafter ([Farmer, 1974a](#); [Lewis and Farmer, 1986](#); [Russell and Fraser, 1994](#); [Russell et al., 1974](#)). The greatest focus of metal oxide FTIR investigations has been on iron oxide structures and properties. Aluminum and manganese (Mn) oxides can be observed with IR spectroscopy as well, although Mn oxides have been received the least attention. A distinct advantage of IR spectroscopy over XRD for studying metal oxides is the ability to characterize poorly crystalline and crystalline metal oxide phases. The FTIR spectra of hematite ($\alpha\text{-Fe}_2\text{O}_3$), goethite ($\alpha\text{-FeOOH}$), gibbsite ($\gamma\text{-Al(OH)}_3$), and diaspore [$\alpha\text{-AlO(OH)}$] are shown in [Figure 1.10](#). Although similarities exist, the ATR-FTIR and DRIFTS spectra can be quite different in band ratios and peak width, due primarily to the differences in the interaction of the sample with the IR beam and the depth of beam penetration into the sample. This figure is an illustrative reminder that MIR spectra are greatly influenced by the sample collection method and caution should be used in making band assignments from the literature when sampling methods differ.

Gibbsite, a crystalline Al(OH)_3 polymorph, is the most commonly occurring crystalline aluminum oxide in soils and bauxite deposits ([Allen and Hajek, 1989](#)). The gibbsite structure consists of Al in sixfold coordination with OH that generates dioctahedral sheets stacked upon one another. There are six distinct structural OH groups in gibbsite: three OH groups are oriented perpendicular to the sheet and three OH are oriented parallel to the sheet (pointed toward empty octahedral sites) ([Huang et al., 2002](#)). The OH groups oriented parallel to the sheet form intralayer hydrogen bonds

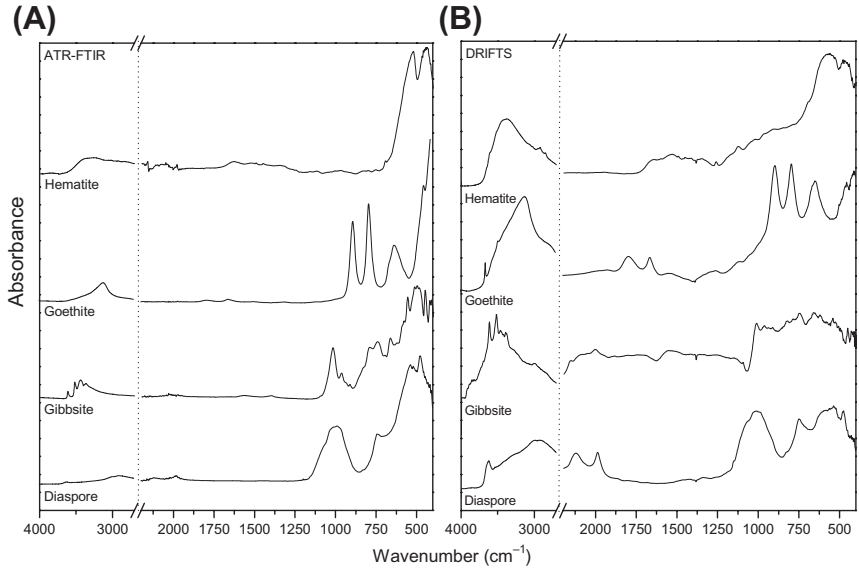


Figure 1.10 Mid-infrared spectra of some common soil minerals collected by (A) ATR-FTIR spectroscopy and (B) DRIFTS. All spectra were collected using a Thermo Nicolet 6700 spectrometer. ATR samples were collected using a single bounce diamond IRE (GladiATR, PIKE Technologies) with no ATR correction performed. Samples for DRIFTS (EasiDiff, PIKE Technologies) were diluted with KBr (10% mineral). (ATR, attenuated total reflectance; FTIR, Fourier transform infrared; IRE, internal reflection element; DRIFTS, diffuse reflectance Fourier transform infrared spectroscopy.)

within a gibbsite sheet, whereas OH oriented perpendicular to the sheet for interlayer hydrogen bonds between gibbsite sheets (Wang and Johnston, 2000). Subsequently, the FTIR spectrum of gibbsite (Figure 1.10) is characterized by OH stretching bands (Russell and Fraser, 1994).

The number of OH stretching bands readily observed in a spectrum of $\text{Al}(\text{OH})_3$ polymorphs as well as band frequency is highly dependent upon the crystallinity of the specimen studied (Elderfield and Hem, 1973). In general, Elderfield and Hem (1973) observed that band resolution increased with crystallinity and the two highest frequency OH stretching bands moved to higher frequencies (as much as 30 cm^{-1}). At ambient temperature, IR spectra of well crystallized gibbsite (Figure 1.10) typically exhibit five OH stretching vibrations at 3620, 3527, 3464, and a doublet at 3391/3373 cm^{-1} ; Al–O and Al–OH vibrations generally appear in aluminum oxides between 1100 and 400 cm^{-1} (Lu et al., 2012). However, Wang and Johnston (2000) employed low temperature (12K) to identify a sixth OH band at 3519 cm^{-1} (Figure 1.11(A)). The sixth band was also observed in Raman spectra

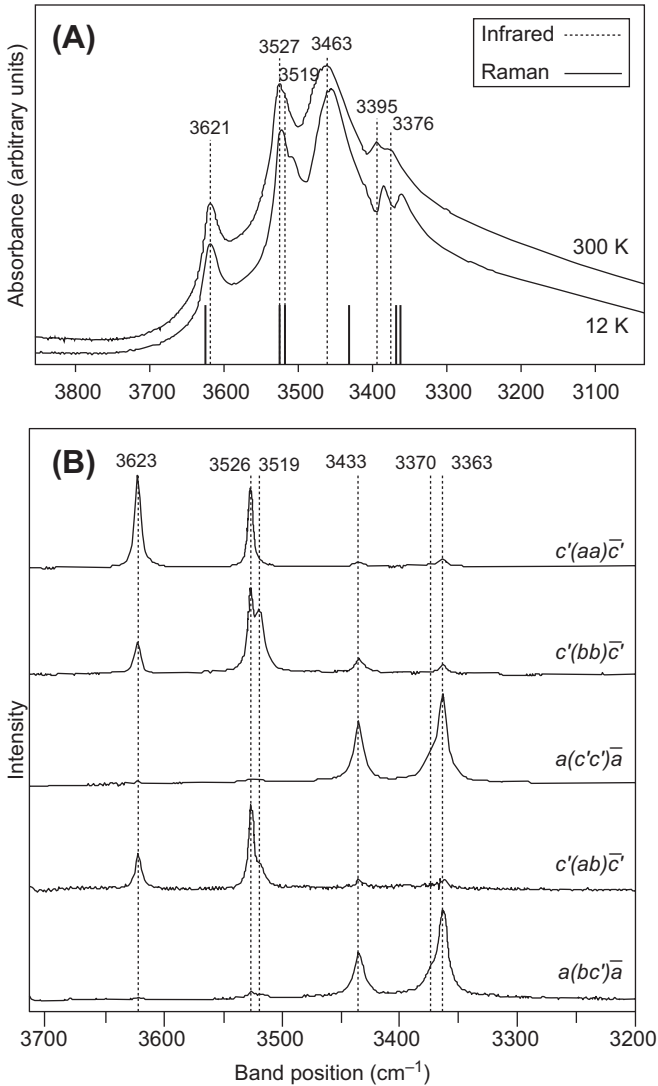


Figure 1.11 (A) FTIR spectra of gibbsite at 12 and 300 K; short vertical lines indicate OH positions in Raman spectrum. (B) Polarized single-crystal Raman spectra of gibbsite at varying Raman scattering geometries (Wang and Johnston, 2000). (FTIR, Fourier transform infrared.) Reprinted with permission.

obtained using polarized single-crystal Raman spectroscopy through the collection of data at different crystal orientations and manipulation of polarization analyzer settings (Figure 1.11(B)). Furthermore, the authors applied the Lippincott and Schroeder (LS-1D) model to predict the location of

the OH stretching vibrations based on interatomic O...O distances, thus permitting assignment of individual OH groups in the crystal structure to specific intra- and interlayer OH bands. Intra- and interlayer OH bands were assigned to the three highest and three lowest frequency OH bands, respectively (Wang and Johnston, 2000).

Balan et al. (2006) modeled IR and Raman spectra of gibbsite using ab initio quantum mechanical calculations and collected ambient temperature FTIR spectra of powdered, synthetic gibbsite. Theoretical vibrational spectra of gibbsite in the OH stretching region matched quite well with the experimental spectra collected by Balan et al. (2006) and Wang and Johnston (2000). Proposed OH stretching assignments to bands were similar between the two studies. However, the ability of theoretical IR spectra to match experimental spectra was highly dependent upon the particle shape modeled (e.g. sphere vs plate). At lower frequencies (1200–200 cm^{-1}), theoretical IR spectra did not match experimental spectra due to particle shape challenges and band overlap. The same challenges were reported by Balan et al. (2008) in a similar approach for studying bayerite ($\beta\text{-Al}(\text{OH})_3$). Ferreira et al. (2011) employed molecular modeling and vibrational spectroscopy to determine if spinel-like or nonspinel structures are present in $\gamma\text{-Al}_2\text{O}_3$. Theoretical IR spectra for spinel-like structures agreed most closely with experimental data and the spinel-like structure was predicted to be thermodynamically more stable (19 kJ mol^{-1} per formula unit greater than nonspinel structure from 0 to 1000 K). The work of Balan et al. (2008, 2006) and Ferreira et al. (2011) demonstrate the potential utility of coupling ab initio calculations with experimentally collected vibrational spectra to further understand the nanoscale architecture of minerals, but also indicate that molecular modeling is currently unable to replace experimental spectra.

As noted earlier, Fe oxides have been extensively studied using vibrational spectroscopy due to their widespread occurrence and diversity, high reactivity, and importance as soil coloring agents. Goethite ($\alpha\text{-FeOOH}$) and hematite ($\alpha\text{-Fe}_2\text{O}_3$) are two of the more common iron oxides found in soils (Allen and Hajek, 1989), but six other Fe oxides (ferrihydrite, green rust, lepidocrocite, maghemite, magnetite, and schwertmannite) are also present (Bigham et al., 2002). Fe oxides are solely or primarily composed of Fe in sixfold coordination with O and OH, although Fe tetrahedra are found in magnetite and maghemite (Schwertmann and Cornell, 2000). MIR spectra of the more commonly found iron oxides can be found in Russell and Fraser (1994), Schwertmann and Cornell (2000),

and [Glotch and Rossman \(2009\)](#). Here, the ATR and DRIFT spectra of goethite and hematite are shown in [Figure 1.10](#). The hematite spectra display prominent peaks at 525 and 443 cm^{-1} in the ATR-FTIR spectrum (578 and 480 cm^{-1} in the DRIFTS spectrum) corresponding to the Fe-O vibrations of hematite ([Schwertmann and Cornell, 1991](#); [Schwertmann and Taylor, 1989](#)).

For goethite, [Blanch et al. \(2008\)](#) assigned the band at 670 cm^{-1} to in-plane OH bending, 633 cm^{-1} to the Fe-O stretch, 497 cm^{-1} to the asymmetric stretch of Fe-O, 450 cm^{-1} was assigned to the Fe(III)-OH stretch, the Fe-OH asymmetric stretch appears at 409 cm^{-1} , and two Fe-O symmetric stretches arise at 361 and 268 cm^{-1} . Easily observed in [Figure 1.10](#) are the peaks associated with OH stretching (3153 cm^{-1}), in-plane OH deformation (839 cm^{-1}), and out-of-plane OH deformation (794 cm^{-1}) ([Russell and Fraser, 1994](#)). It is important to note, however, that these bands broaden and shift to higher frequencies as Al content in the sample increases $>5.85\text{ mol. \%}$. These shifts are attributed to structural strains within the mineral when additional Al atoms are found in the first cation coordination sphere surrounding a substituted Al atom, perhaps resulting in partial ordering of the Al sites and formation of Al-rich clusters ([Blanch et al., 2008](#)). Comparison of vibrations in goethite to the isostructural diaspore ($\alpha\text{-AlOOH}$) provides further comparison for these shifts in frequency (goethite \rightarrow diaspore): $268 \rightarrow 350\text{ cm}^{-1}$; $290 \rightarrow 372\text{ cm}^{-1}$; $361 \rightarrow 518\text{ cm}^{-1}$; $410 \rightarrow 578\text{ cm}^{-1}$; $450 \rightarrow 690\text{ cm}^{-1}$ ([Blanch et al., 2008](#)). Similar work investigating the effect of Al substitution on hydroxyl behavior during the dehydroxylation of goethite was conducted by [Ruan et al. \(2002a\)](#). [Cambier \(1986b\)](#) illustrated the influence of crystallinity on the FTIR spectrum of goethite: spectral bands broaden with decreasing crystallinity. This change was attributed to the weakening of H-bonds within the crystal due to changes in Fe-O bonds associated with the tilting of octahedra rows within the goethite structure ([Cambier, 1986b](#)). In [Cambier \(1986a\)](#), the influence of particle size on goethite spectra was evaluated. [See [Wang et al. \(1998\)](#) for a detailed description of particle size, shape, and internal structure effects on the FTIR spectrum of hematite.] The work of [Blanch et al. \(2008\)](#) and [Cambier \(1986a,b\)](#) illustrate the need to consider the influence of substituted cations, crystallinity, and particle shape when evaluating and interpreting the spectra of specimens.

As with clay minerals, the abundance of studies on Fe oxides using vibrational spectroscopy makes it difficult to mention or discuss any in great detail. However, the following studies indicate the utility of FTIR for studying Fe oxides. [Tejedor-Tejedor and Anderson \(1990\)](#) used ATR-FTIR with

a cylindrical internal reflection (CIR) cell to study changes in the structure of water at the solid–water interface of goethite as a function of pH, ionic strength, and electrolyte anions. Ruan et al. (2001) and Boily et al. (2006) used FTIR to study dehydroxylation of goethite during phase transition to hematite, and Ruan et al. (2002b) applied FTIR microscopy to further study this phenomenon. Similar to Balan et al. (2008, 2006) and Ferreira et al. (2011), Blanchard et al. (2008) employed molecular modeling and FTIR spectroscopy to interpret and assign vibrational bands observed in the spectrum of hematite. Chernyshova et al. (2007) used FTIR and Raman spectroscopy to identify maghemite-like defects in the structure of hematite nanoparticles (7–120 nm) and the role both particle size and growth kinetics have on the formation of structural defects. From the vibrational spectroscopic results, a new general model was developed to describe solid-state transformations of hematite nanoparticles as a function of particle size (Chernyshova et al., 2007).

Mn oxides have not been studied using vibrational spectroscopy to the same extent as Fe and Al oxides, but valuable resources exist for identifying and characterizing Mn oxides. Potter and Rossman (1979) and Julien et al. (2004) captured FTIR and Raman scattering spectra for a large number of Mn oxides. More recently, Zhao et al. (2012a) reported FTIR spectra for six birnessite samples with different mean Mn oxidation states. With respect to other IR applications for Mn oxides, Parikh and Chorover (2005) used four different FTIR techniques to study biogenic Mn oxide formation on *Pseudomonas putida* GB-1. In situ monitoring revealed the development of MnO_x upon addition of MnSO_4 and changes in the spectra of extracellular biomolecules. Interestingly, the spectra of biogenic MnO_x was not identical to the spectra of synthetic Mn oxides due to the incorporation of biomolecules within the solid phase.

Thibau et al. (1978) first reported the Raman spectra of FeO, Fe_3O_4 , $\alpha\text{-Fe}_2\text{O}_3$, $\alpha\text{-FeOOH}$, and $\gamma\text{-FeOOH}$. In other work, Hart et al. were able to completely assign the Raman spectra of hematite and magnetite (Hart et al., 1976). Despite these studies, Raman analysis of iron oxidation products has been hampered by their poor light scattering ability (Thibau et al., 1978), uncertainty over the number of peaks in the spectra (Dünnwald and Otto, 1989), and potential thermal degradation by Raman radiation (Bersani et al., 1999). SERS overcomes these limitations and has been utilized to investigate the structures of hematite ($\alpha\text{-Fe}_2\text{O}_3$), magnetite (Fe_3O_4), wustite (FeO), maghemite ($\gamma\text{-Fe}_2\text{O}_3$), goethite ($\alpha\text{-FeOOH}$), lepidocrocite ($\gamma\text{-FeOOH}$), and $\delta\text{-FeOOH}$ (de Faria et al., 1997).

4.4 Mineral Weathering and Pedogenesis

Vibrational spectroscopy can be a very useful tool for investigating weathering reactions and pedogenesis, and it can be used independently or in conjunction with XRD, electron microscopy, and other molecular spectroscopy analyses to elucidate changes in a system. FTIR and Raman spectroscopies can be employed to identify changes to mineral surfaces and the development of new mineral phases during weathering reactions in the laboratory, and these changes can be evaluated *ex situ* or *in situ*. These approaches are powerful tools for studying mineral transformations and identifying mineral phases within soil samples. Tomić et al. (2010) utilized transmission FTIR and Raman microspectroscopy (with corroboration from XRD analysis) to differentiate between soluble minerals present throughout a morphologically similar vertisol sequence. In this study, the presence of dolomite, aragonite, and calcite in lower soil horizons compared to gypsum was used to explain the surface layer transition of the soils from calcic- to calcimagnesian-vertisols.

Through an ATR-FTIR approach, Cervini-Silva et al. (2005) analyzed powder samples to evaluate the development of new mineral phases following rhabdophane ($\text{CePO}_4 \cdot \text{H}_2\text{O}$) reaction with solutions containing organic acids and chelating agents. FTIR analysis permitted identification of CeO_2 (s) precipitate formation, which explained the lack of Ce^{3+} (aq) in some reaction vessels. Similarly, DRIFTS permitted Goyne et al. (2010) to identify the formation of Ca- and rare earth elements (REE)-oxalate precipitates following reaction of apatite with oxalate at differing aqueous phase concentrations. Goyne et al. (2006) also used DRIFTS analyses to document the formation of Cu precipitates following chalcopyrite (CuFeS_2) reaction with organic ligands under anoxic conditions. The formation of precipitates was in agreement with chemical speciation model results predicting oversaturation of covellite (CuS), and these results were used to explain nonstoichiometric chalcopyrite dissolution and the low Cu concentration in solution.

In a study of mica weathering to hydroxyl interlayered vermiculite (Maes et al., 1999), FTIR spectra in conjunction with XRD patterns were used to document biotite transformation after K^+ extraction and oxidation. The DRIFTS data collected by Choi et al. (2005) during a study of clay mineral weathering in caustic aqueous systems revealed the development of nitrate sodalite and nitrate cancrinite secondary precipitates. In addition to demonstrating differences in formation of these nitrate-containing precipitates as a function of the clay mineral reacted, Cs^+ (aq) and Sr^{2+} (aq) concentration

in the reaction vessel, and time, FTIR data were more useful at identifying mineral precipitation at earlier reaction times than XRD (Choi et al., 2005). Although none of these studies were entirely spectroscopy-centered, they illustrate the utility of FTIR for rapid acquisition of additional data that can aid in explaining mineral weathering. FTIR spectroscopy can be extended to the study of soil mineral composition and transformation during pedogenesis (Caillaud et al., 2004; Chorover et al., 2004). When used in this context, FTIR can be particularly useful for identifying the formation of amorphous minerals.

In situ measurements of mineral weathering or change can also be completed using FTIR. Morris and Wogelius (Morris and Wogelius, 2008) developed a multiple internal reflection flow through cell for capturing FTIR spectra, and applied this to study forsteritic glass dissolution in the presence of phthalic acid. This approach permitted in situ observations of phthalate attachment and subsequent changes on the mineral surface that would otherwise not have been observed. Using an ATR flow through circle cell, Parikh and Chorover (2005) monitored biogenic Mn oxide formation on bacteria biofilms through time. Usher et al. (2005) used ATR-FTIR for in situ monitoring of mineral oxidation upon exposure to oxidizing gases, thereby illustrating that in situ analyses need not be restricted to aqueous studies.

The weathering of limestone (i.e. monuments) due to salt formation was investigated by Kramar et al. (2010) using micro-Raman spectroscopy in conjunction with XRD. Gypsum was identified within the sample by its main Raman band at 1008 cm^{-1} and some twin minor doublet bands, at $414, 494\text{ cm}^{-1}$, and $623, 671\text{ cm}^{-1}$, assigned to ν_2 symmetric and ν_4 antisymmetric bending of the SO_4 tetrahedra. The XRD analysis also corroborated the presence of gypsum in the weather limestone. Furthermore, micro-Raman enabled the observation of minor differences in the weathering processes arising from specific weathering conditions. Raman peaks signifying the presence of magnesium sulfate hydrates (i.e. hexa- and pentahydrates) and niter were observed only in the efflorescence of structures weathered indoors. The assignment of the magnesium sulfate hydrates was based on the extensive Raman study of this series of hydrates by Wang et al. (2006).

The effectiveness of micro-Raman in the investigation of weathering products is also evident in a study of soils present at an abandoned zinc and lead mine by Goienaga et al. (2011). By analyzing samples from the top 2 cm of soil, they were able to identify the presence of 16 primary (including dolomite, calcite, fluorite, graphite, and rutile) and 23 secondary minerals (zinc, cadmium, and lead minerals) resulting from several processes

including: dissolution–precipitation processes; weathering of superficial mineral phases; percolation of dissolved ions; and precipitation. The impact of the deterioration of guardrails, brake linings, and tires in conjunction with exhaust fumes on heavy metals in urban soils has been investigated using Raman spectroscopy and X-ray fluorescence. Zinc (as hydrozincite and zinc nitrate) and barium (as witherite) were determined to be the main contaminants of the soils (Carrero et al., 2012).



5. SOM SPECTRAL COMPONENTS

FTIR spectroscopy is a well-suited analytical tool for studying organic molecules in soil samples. The presence of dipole moments in organic functional groups allows FTIR to be used for sample identification, quantification, and purity analysis for a myriad of organic compounds. In fact, there is a long history of analyzing pharmaceuticals, pesticides, and other organic compounds using this approach. However, due to the observed fluorescence of organic molecules, Raman spectroscopy is typically not the preferred approach for vibrational spectroscopy analysis of organics.

Although considerably more complex than anthropogenic organic compounds, the chemical composition of SOM makes it a suitable substrate for FTIR analysis. Organic molecule bonds, in SOM commonly C–O, C=O, C–C, C–H, O–H, N–H, N=C, and S–H, absorb in the MIR region, with overtones extending to the NIR region (12,000–4000 cm^{-1}), in particular for O–H and N–H. These molecular bonds collectively constitute SOM and influence its interactions with other soil components (e.g. minerals, bacteria, water). The abundance of oxygen (O), nitrogen (N), and sulfur (S) provide SOM with its high chemical reactivity (e.g. cation and anion-exchange capacity, acidity, binding metals and anthropogenic organic compounds). Of these, O is most abundant and exists primarily in carboxyl form, arguably the single most important functional group given its basis for the majority of SOM properties (Hay and Myneni, 2007). Additional O-containing functional groups can be divided broadly into acidic (i.e. enol, phenol) and neutral (i.e. alcohol, ether, ketone, aldehyde, ester) categories. Important N groups are amines and amides. Aromatics, acids, and sugars are also functionally significant moieties (Sparks, 2002). Common assignments for IR absorbing moieties present within SOM are provided in Table 1.2. A recent review of vis-NIR spectroscopy calibration for predicting soil carbon content provides an excellent summary of fundamental SOM absorbances (Stenberg et al., 2010).

Table 1.2 FTIR Vibrational Assignments for Soil Organic Matter Absorbances

Wavenumbers (cm ⁻¹)	Assignment	Sample Type	FTIR Method
3700–3200	O–H and N–H stretch	Humic acids and humin of soil ^a	Transmission ^a
3690–3619	Free O–H, N–H stretch	Humic acids ^{b,c} and fulvic acids of soil ^c	Transmission ^{b,c}
3450–3300	Hydrogen bonded O–H, N–H stretch; greater N–H contribution at lower range	Humic acids of soil ^{d,b,e} and pyrophos- phate extracts of soil ^f	Transmission ^{d,f} , ATR ^e
3110–3000	Aromatic C–H stretch	Humic acids and humin of soil ^{a,f,g} , pyridine extracts of coals ^h	Transmission ^{a,f,h} , ATR ^g
3000–2800	Aliphatic C–H stretch	Humic acids of soil ^{b,f}	Transmission ^{b,f}
2925	Aliphatic C–H antisymmetric stretch	Humic acids of charcoals ⁱ	Transmission ⁱ
2855–2850	Aliphatic C–H symmetric stretch	Humic acids of soil ^a and charcoal ⁱ	Transmission ^{a,i}
2730	CH ₃ deformation	Petroleum-contaminated soil ^l	DRIFTS ^j
2600–2500	H-bonded OH of carboxylic acids	Humic acids of soil ^f	Transmission ^f
1765–1700	Carbonyl C=O stretch ^x	Humic acids of soil ^{a,d,k} and water- extractable OM of soil ^l	Transmission ^{a,d,k,l}
1720	Carboxylic acid C=O stretch	Humic acids of soil ^b , peat ^m	Transmission ^b , ATR ^m
1710	Free organic acid carboxylic C=O	Peat ^m	ATR ^m
1700	Carboxylic acid, ketone, aldehyde C=O stretch	Humic acids of soil ^a	Transmission ^a
1660–1630	Amide C=O stretch (amide I)	Humic acids of soil ^{d,e}	Transmission ^{d,e}
1650	Quinone ketone C=O stretch	Humic acids of soil ^a	Transmission ^a

Continued

Table 1.2 FTIR Vibrational Assignments for Soil Organic Matter Absorbances—cont'd

Wavenumbers (cm ⁻¹)	Assignment	Sample Type	FTIR Method
1650–1600	Aromatic C=C stretch and/or carboxylate C–O asymmetric stretch and/or conjugated ketone C=O stretch	Humic fractions of soil ^{b,o} , peat ^m , soil organic horizons ^p	Transmission ^{b,o,p} , ATR ^{m,n}
1590–1500	Amide N–H bend and C=N stretch (amide II)	Humic acids of soil ^{a,d,k}	Transmission ^{a,d,k}
1570	Aromatic C–H deformation	Humic acids of charcoals ⁱ	Transmission ⁱ
1550–1500	Aromatic C=C stretch	Humic acids of soil ^{a,b}	Transmission ^{a,b}
1470–1370	Aliphatic C–H bend	Humic acids of soil ^{d,k} , peat ^m	Transmission ^{a,k} , ATR ^m
1410–1380	Phenolic C–O stretch, OH deformation	Humic acids of soil ^k , peat ^m	Transmission ^k , ATR ^m
1400–1380	Carboxylate C–O symmetric stretch	Humic acids of soil ^{q,r}	Transmission ^q , DRIFTS ^r
1330–1315	Ester C–O	Humic acids of soils ^a	Transmission ^a
1300	C–H overtone	Soil ^s	DRIFTS ^s
1280–1200	Carboxylic acid C–O stretch, OH deformation, ester, phenol C–O asymmetric stretch	Humic acids of soil ^{d,e}	Transmission ^{d,e}
1190–1127	Alcohol, ether, phenol C–O–C stretch, poly OH stretch	Humic acids of soil ^o and charcoals ⁱ	Transmission ^{i,o}
1170–1120	Aliphatic O–H, C–OH stretch	Humic acids of soil ^b	Transmission ^b
1160–1000	Ester, phenol C–O–C, C–OH stretch, attributed to polysaccharides or polysaccharide-like compounds	Humic acids of soil ^k , soil organic horizons ^p , and compost ^t	Transmission ^{k,p} , ATR ^t

975–700	Aromatic C–H out-of-plane bend; increasing wavenumbers with increasing degree of substitution	Soil ^u , soil organic horizons ^u , humic acids of soil ^{a,b} , charcoal ⁱ	Transmission ^{a,b,i} , DRIFTS ^u , ATR ^u
720	CH ₂ wag	Coal ^v	Transmission ^v
670	OH bending	Biochar ^w	ATR ^w

FTIR: Fourier transform infrared, ATR: attenuated total reflectance (FTIR) spectroscopy, DRIFTS: diffuse reflectance infrared Fourier transform spectroscopy.

^aTatzber et al. (2007).

^bSenesi et al. (2003).

^cScherrer et al. (2010).

^dFernández-Getino et al. (2010).

^eVergnoux et al. (2011).

^fPiccolo et al. (1992).

^gAranda et al. (2011).

^hSobkowiak and Painter (1992).

ⁱAscough et al. (2011).

^jForrester et al. (2013).

^kOlk et al. (2000).

^lHe et al. (2011b).

^mArtz et al. (2008).

ⁿSolomon et al. (2007a).

^oSánchez-Monedero et al. (2002).

^pHaberhauer (1998).

^qEllerbrock et al. (1999).

^rDing et al. (2002).

^sCozzolino and Morón (2006).

^tTandy et al. (2010).

^uCécillon et al. (2012).

^vIbarra et al. (1996).

^wMukome et al. (2013).

^xFor a detailed discussion of carboxyl assignments, see (Hay and Myneni, 2007).

Due to the fact that SOM is a complex and heterogeneous mixture of these functional groups, FTIR spectroscopy requires specialized methodologies and data interpretation, in contrast to pure compounds or simple mixtures of known composition. This, however, is not so much a shortcoming of FTIR spectroscopy as a reflection of the inherent chemical diversity of SOM. Indeed, FTIR spectroscopy is well suited to provide molecular insight to this defining aspect of SOM precisely. The major limitation of FTIR for SOM analysis arises from mineral interference, with the implication that sample selection and/or preparation or spectral treatment are key strategies for overcoming this. A detailed description of SOM analysis in whole soils and SOM fractions and extracts is provided later in this review.

Identification of absorbance bands in FTIR spectra can be challenging in heterogeneous samples like SOM. Sample identity (e.g. bulk soil, SOM extract, compost) can be used a priori to narrow possible assignments or make specific claims to the greater structural environment of the bonds assigned. Even for spectra of SOM-rich or extract samples without interfering or overlapping mineral and inorganic absorbances, heterogeneity among SOM fractions [e.g. particulate organic matter (POM), light fraction (LF)] can make assignments difficult (Calderón et al., 2011b; Stenberg et al., 2010). The heterogeneous nature of SOM limits assignments to only be tentatively made, based on the presence of MIR peaks assigned to specific functional groups whose MIR absorbances are well established in the literature. Additionally, the presence of multiple molecular bonds that absorb MIR light within the same frequency range further limit assignments for SOM. For instance, a common assignment for 1650 cm^{-1} band in samples known to contain nitrogenous OM is amide C=O (amide I), and in the context of SOM this may be broadly assigned as an absorbance of peptides or proteins (Calderón et al., 2011b). Knowing the sample type can help discriminate among possible assignments and justify specific molecular environments. For example, in the case of overlaps between C=N (amide II) and aromatic C=C at 1530 cm^{-1} , or polysaccharide type (e.g. lignin, cellulose, pectin) for $\nu(\text{C-O})$ absorbance ($1160\text{--}1020\text{ cm}^{-1}$).

In cases where identifying SOM composition and/or quantifying functionalities is not necessary, absorbance assignment may be irrelevant. The high sensitivity of FTIR to organic functionalities allows fingerprinting of SOM samples, much in the same way mass spectrometry methods (e.g. py-GC-MS, py-MBMS) can be used to fingerprint soils or OM samples by chemical composition. For instance, FTIR fingerprints of SOM grassland

and forest soils over a 700-m elevation range in France allowed discrimination by canonical variate analysis of sites by vegetation cover, presumably as a result of vegetation influence on SOM composition (Ertlen et al., 2010). Absorbances were collected on bulk soils, which varied significantly in SOM content (4.5–50% soil C); spectra were then corrected for particle size. The potential for overlap of mineral and organic absorbances was not taken into account, but differences in absorption were assumed to be due to SOM (reflecting differing vegetation) given similar mineralogy. Second and third derivatives of absorbances incrementally increased the ability of FTIR to improve discrimination among soil type by SOM.

Arocena et al. (1995) were the first to use IRMS technique to investigate the nature of the organic and mineral components in SOM. The study compared in situ OM spectra with extracted humic acids, showing the effects of the extraction process (appearance of potentially degraded ester band at approximately 1720 cm^{-1} and loss of amide II band at 1520 cm^{-1}). In another application of IR microscopy, DRIFTS mapping was utilized to map the distribution (mm-scale) of OM composition on soil microaggregate surfaces. The authors showed that OM composition was affected by preferential flow-path surfaces arising from earthworm and root activity (Leue et al., 2010a).

SR-FTIR spectroscopy has also shown capabilities of fingerprinting complex materials such as soil organic carbon (SOC). In one study, thin films of humic acids extracted from the silt and clay fractions of natural forests, plantations, and cultivated fields were shown to exhibit qualitative and quantitative differences in aromatic-C, aliphatic-C, phenolic-C, carboxylic-C, and polysaccharide-C (Solomon et al., 2005). Similar humic acid extracts were used to investigate the speciation, composition, and the long-term impact of anthropogenic activities on SOC from soils originating from tropical and subtropical agroecosystems (Solomon et al., 2007a). The use of SR-FTIR spectroscopy with other SR-based techniques, particularly near-edge X-ray absorption fine structure (NEXAFS) spectroscopy, has provided complementary data for microscale analysis of soil components. After overcoming the methodological constraints of sample preparation by embedding their samples in sulfur, Lehmann et al. (2005) determined differences in black and nonblack C from samples analyzed using the two techniques.

The two techniques were also used in the analysis of thin sections of free stable microaggregates. By mapping the spatial distribution of organic carbon in the microaggregates of three soils, Lehmann et al. (2007) showed

the correlation of aliphatic C and the ratio of aliphatic C/aromatic C to kaolinite O–H, in addition to greater microbial-derived OM on the mineral surface, as evidence supporting models of C stabilization in microaggregates. Adsorption of organics on mineral surfaces rather than occlusion of organic debris by adhering clay particles was proposed as the initial dominant process responsible for aggregate formation. Mapping of images using this technique generates considerable data. Overlapping bands, swamping from major bands such as O–H stretching and Si–O–Si stretching, and spectral fringing are a few of the challenges to spectral interpretation that arise (Lawrence and Hitchcock, 2011; Lehmann and Solomon, 2010).

In an early article highlighting the potential application of FT-Raman and SERS to HS, Yang and Chase (1998) highlighted the limitations of Dispersive Raman to the study of HS, namely fluorescence coupled with the dark color of the organic molecules. Utilizing FT-Raman, Yang et al. elucidated the building blocks of HS (through acid hydrolysis to remove labile constituents) to be low, structurally disordered carbon networks with two peaks at $\sim 1600\text{ cm}^{-1}$ and $\sim 1300\text{ cm}^{-1}$ (Yang and Wang, 1997; Yang et al., 1994). Assignment of Raman bands in a complex matrix such as soils is challenging but some of the characteristic peaks are presented in Table 1.3. Due to the variability of samples, this table should be observed only as a guideline for possible assignments. More comprehensive band assignments are available in the literature (Chalmers and Griffiths, 2002; Ferraro, 2003; Smith, 2005). Peaks associated with humic acids are less complex (usually consisting of two broad bands), but show some variation depending on origin (Yang and Wang, 1997).

Due to the significant signal enhancement and quenched fluorescence, more studies have utilized SERS to investigate SOM. Several studies have applied SERS to the characterization of humic acids in soil (Corrado et al., 2008; Francioso et al., 2000, 2001, 1996; Liang et al., 1996; Vogel et al., 1999), including the effect of pH on humic acid structure at different pH values. In a series of studies, Francioso et al. were the first to successfully utilize SERS to ascertain structural and conformational characteristics of humic acids extracted from peat (Francioso et al., 1996). In later work the same authors applied SERS, DRIFTS, and NMR spectroscopy to study humic and fulvic acids extracted from peat, leonardite, and lignite. The peat humic acids had a greater content of oxygenated (COOH, C–OH in carbohydrates and phenols) and aliphatic groups while the humic acids from the leonardite and lignite had a lower content of sugar-like components and polyethers (Francioso et al., 2001).

Table 1.3 Raman Peak Assignments Relevant to Soil Organic Constituents

Raman Shift (cm ⁻¹)	Assignment	Raman Method
3240	Water, symmetric N–H stretch of 2° amines	Dispersive ^a
3059	C=C–H aromatic stretch	SERS ^b
2950–75	CH ₃ symmetric stretch	Dispersive ^d , FT-Raman ^d , SERS ^{b,c,d}
2935	C–H stretch	SERS ^{b,c}
2840–2890	CH ₂ asymmetric stretch	Dispersive ^d , FT-Raman ^d , SERS ^{b,c,d}
2135	Triple C–C, NH ₃ vibrational mode	Dispersive ^a
1735	C=O ester stretch	Dispersive ^d , FT-Raman ^d , SERS ^{b,d}
1635–1680	Amide I: C=O, C–N, N–H	FT-Raman ^e , SERS ^b ,
1580–1600	Aromatic C=C stretch	Dispersive ^a , FT-Raman ^{d,e} , SERS ^f
1550–1575	Amide II: N–H, C–N	Dispersive ^{a,d} , FT-Raman ^d , SERS ^{b,d}
1530	Graphite C=C (G band)	Dispersive ^{b,g}
1440–1460	C–H bending vibration	Dispersive ^{a,d,g} , FT-Raman ^d , SERS ^{b,d}
1380	COOH symmetric stretch	Dispersive ^{a,d} , FT-Raman ^d , SERS ^{d,f}
1300–1340	Diamond C=C (D band)	Dispersive ^{b,g} , FT-Raman ^e
1270	CH ₂ deformation	Dispersive ^d , FT-Raman ^d , SERS ^{b,d}
1145–1160	C–C breathing vibration, C–O asymmetric stretch	FT-Raman ^h
1085	C–O stretch, C–N stretch	Dispersive ^d , FT-Raman ^d , SERS ^{b,d} ,
1061	C–N and C–C stretch	SERS ^b
1030–1130	C–C stretch, C–O stretch, C–O–H deformation	SERS ^b
950–990	Aromatic C–H out-of-plane deformation	Dispersive ^{a,d} , FT-Raman ^d , SERS ^d
897	C–O–C stretch	SERS ^b

SERS: surface enhanced Raman scattering spectroscopy, FT-Raman: Fourier transform Raman spectroscopy.

^aDollish et al., (1974).

^bMaquelin et al. (2002).

^cVogel et al. (1999).

^dYang and Chase (1998).

^eYang and Wang (1997).

^fRoldan et al. (2011).

^gEdwards et al. (2012).

^hSchenzel et al. (2001).

Humic binding mechanisms have also generated several SERS studies (Corrado et al., 2008; Leyton et al., 2008; Liang et al., 1999; Roldán et al., 2011; Sánchez-Cortés et al., 1998; Sanchez-Cortes et al., 2006; Vogel et al., 1999; Yang and Chase, 1998). In a recent study, Roldán et al. (2011) utilized SERS and surface-enhanced fluorescence to investigate the interaction of humic acids extracted from a soil amended for over 30 years with cattle manure, cow slurries, crop residues, and a control sample with the herbicide paraquat (1,1'-dimethyl-4,4'-bipyridinium). Binding mechanisms were attributed to the structure of the HS. The polyphenolic aromatic-rich HS, originating from crop residues, interacted through π - π stacking with similar groups of the pesticide. For the cattle manure and cow slurry HS, the interactions were mostly ionic and occurred through the larger amounts of carboxylate groups. Advances in SERS instrumentation and improvements of the technique have enabled in situ monitoring of soil carbon sequestration (Stokes et al., 2003; Wullschleger et al., 2003). By modifying the SERS surface from "passive" silver to an "active/electro" surface using copper, detection of humic acids at 1000 ppm was possible, although not reproducible. Signal reproducibility was improved by using a hybrid electro-SERS surface (electrochemically enhanced adsorption with an alumina-based copper). In another study, SERS was similarly enhanced through the use of a chelating agent (4-(2-pyridylazo) resorcinol) to detect Zn (II) in contaminated industrial soils (Szabó et al., 2011).



6. BACTERIA AND BIOMOLECULES

In soil environments, bacteria and biopolymers are ubiquitous and play a critical role in aggregate stability, nutrient cycling, and bioremediation. All of these processes involve interactions between biopolymers and mineral surfaces, which are dependent on the nature and quantity of reactive biomolecular functional groups. FTIR spectroscopy has emerged as a fundamental tool for evaluating biomolecule and bacterial composition and its utility has been realized for a diversity of disciplines including microbiology, medicine, engineering, and environmental science. In soil science, the development of FTIR as a tool to examine biological samples has been critical for increasing our mechanistic understanding of cell/biomolecule adhesion on mineral surfaces.

FTIR spectroscopy was first suggested as a tool for bacterial identification over 100 years ago (Coblentz, 1911), and over the years has been used extensively to study microorganisms and biomolecules (Brandenburg

and Seydel, 1996; Fringeli and Günthard, 1981; Jiang et al., 2004; Legal et al., 1991; Levine et al., 1953; Naumann et al., 1996; Nivens et al., 1993a, 1993b; Omoike and Chorover, 2004; Riddle et al., 1956; Schmitt and Flemming, 1998; Wang et al., 2010). Common FTIR band assignments corresponding to lipids, nucleic acids, proteins, and polysaccharides of bacteria and biomolecules are presented in Table 1.4. Naumann et al. (1988, 1991) established FTIR spectroscopy as a method to rapidly identify microorganisms through analysis of specific “fingerprint” spectra. Their method utilizes spectral derivatives and correspondence maps to differentiate and identify bacteria. This approach is commonly used for identification of bacteria from pure cultures and extracts (e.g. Schmitt and Flemming, 1998; Yu and Iru-dayaraj, 2005). Microbial identification via FTIR has also been successful from simple mineral matrices, such as detection of *Bacillus subtilis* spores within bentonite (Brandes Ammann and Brandl, 2011) and *Escherichia coli*

Table 1.4 Pertinent Infrared Assignments for Bacteria and Biopolymer Samples

Wavenumbers (cm ⁻¹)	IR Band Assignment
2956	$\nu_{as}(\text{CH}_3)^a$
2920	$\nu_{as}(\text{CH}_2)^a$
2870	$\nu_s(\text{CH}_3)^a$
2850	$\nu_s(\text{CH}_2)^a$
1720–1729	$\nu_{as}(\text{COOH})^b$
1652–1637	Amide I: C=O, C–N, N–H ^{b,c,d}
1550–1540	Amide II: N–H, C–N ^{a-c}
1460–1454	$\delta(\text{CH}_2)^{b,c}$
1400–1390	$\nu_s(\text{COO}^-)^{b,c}$
1220–1260	$\nu_{as}(\text{PO}_2^-)$ of phosphodiester (hydrated) ^{b,e,f}
1170	$\nu(\text{C–O})^d$
1114–1118	$\nu(\text{C–O–P}, \text{P–O–P})$, aromatic ring vibrations ^{b,d}
1084–1088	$\nu_s(\text{PO}_2^-)$ of phosphodiester, ⁱ ring vibrations, ^b $\nu(\text{C–C})^g$
1045, 1052, 1058	$\nu(\text{C–O–C}, \text{C–C})$ from polysaccharides ^{b,g}
962–968	$\nu(\text{PO}_2^-)^{h,i}$
650–450	$\nu(\text{CH}_2)^j$

ν_{as} : asymmetric stretching vibration, ν_s : symmetric stretching vibration, δ : bending vibration.

^aSchmitt and Flemming (1998).

^bBrandenburg and Seydel (1996).

^cSockalingum et al. (1997).

^dNivens et al. (1993a, 1993b).

^eBrandenburg et al. (1997).

^fNaumann et al. (1991).

^gFringeli and Günthard (1981).

^hBarja et al. (1999).

ⁱQuiles et al. (1999).

^jDeo et al. (2001).

metabolic products on carbonate minerals (Bullen et al., 2008). For details on the use of FTIR to identify and classify microorganisms, readers are referred to Mariey et al. (2001), who give a thorough review of articles from the 1990s which utilize FTIR spectroscopy for characterization of microorganisms, and papers by Maquelin et al. (2003, 2002) who employ FTIR and Raman spectroscopies to identify medically relevant microorganisms.

Due to the presence of SOM, characterization of bacteria within soil samples is not feasible. The organic nature of bacteria results in similarities of peak locations between SOM and microbial samples. For this reason many IR band assignments are common among these samples. However, stark contrasts in typical spectra can be observed and reflect significant differences in the chemical composition, with bacteria having much lower C:N and C:P than SOM (Horwath, 2007). This difference results in prominent amide I (1650 cm^{-1}), amide II (1550 cm^{-1}), and PO_4^{3-} (1240 cm^{-1}) peaks in FTIR spectra of bacteria. As an illustrative example, spectra for various bacterial species collected using multibounce ATR-FTIR on a ZnSe IRE are shown in Figure 1.12(A). CH_2 and CH_3 bonds of aliphatic chains are also prevalent on bacteria and the corresponding symmetric and asymmetric vibrations can be easily observed as a quartet of IR peaks at approximately 2560,

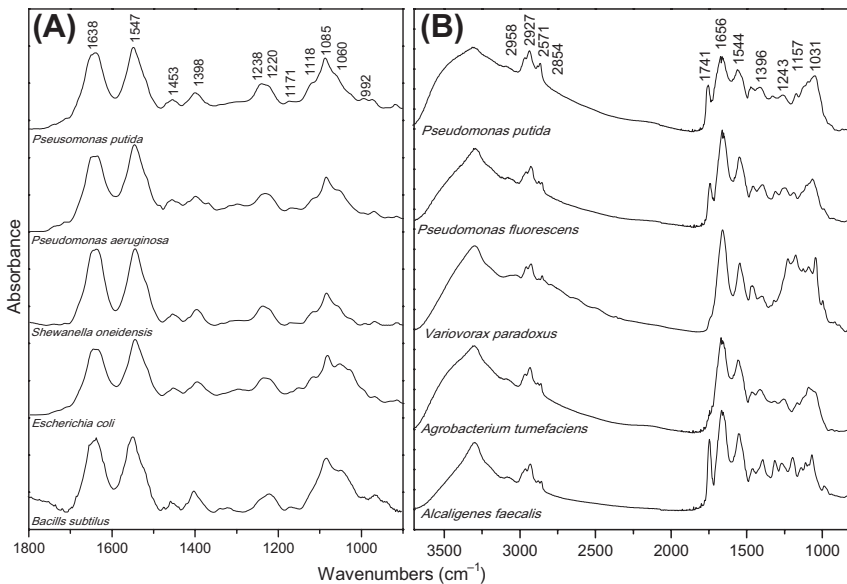


Figure 1.12 FTIR spectra of various bacteria collected by (A) ATR-FTIR on ZnSe and (B) transmission on ZnSe (Thermo Nicolet 6700 spectrometer). (ATR, attenuated total reflectance; FTIR, Fourier transform infrared.)

2930, 2570, and 2855 cm^{-1} . Examples of these peaks are shown in transmission FTIR spectra of various bacteria species in [Figure 1.12\(B\)](#). Although, characterization of in situ soil bacteria is not possible, knowledge regarding the IR spectra of bacteria is very important for understanding processes of bacterial adhesion to mineral surfaces.

A number of studies have used FTIR to characterize and study interactions of specific bacterial components including extracellular polymeric substances (EPS) ([Badireddy et al., 2008](#); [Beech et al., 1999](#); [Eboigbodin and Biggs, 2008](#); [Omoike and Chorover, 2004, 2006](#); [Omoike et al., 2004](#); [Wingender et al., 2001](#)), lipopolysaccharides (LPS) ([Brandenburg, 1993](#); [Brandenburg et al., 2001, 1997](#); [Brandenburg and Seydel, 1990](#); [Kamnev et al., 1999](#); [Parikh and Chorover, 2007, 2008](#)), phospholipids ([Brandenburg et al., 1999](#); [Brandenburg and Seydel, 1986](#); [Cagnasso et al., 2010](#); [Hübner and Blume, 1998](#)), and DNA ([Brewer et al., 2002](#); [Falk et al., 1963](#); [Mao et al., 1994](#); [Pershina et al., 2009](#); [Tsuboi, 1961](#); [Zhou and Li, 2004](#)). In addition, ATR-FTIR has emerged as a powerful tool for studying biofilm formation, composition, and structure ([Beech et al., 2000](#); [Cheung et al., 2000](#); [Schmitt and Flemming, 1999](#); [Spath et al., 1998](#)).

Although less extensively studied, the nondestructive nature and minimal sample handling of Raman techniques, coupled with the invisibility of water have lent themselves well to application of analysis of bacteria and biomolecules. Raman techniques afford a fast and relatively simple way to identify bacteria compared to the tedious and lengthy conventional and instrumental methods as discussed by [Ivnitski et al. \(1999\)](#). As in soil analysis, the development of FT-Raman overcame fluorescence, which hindered Raman analysis of cells due to naturally strongly fluorescent constituents such as enzymes and coenzymes ([Schrader et al., 2000](#)). In one of the first studies applying FT-Raman to bacterial identification, [Naumann et al. \(1995\)](#) obtained reproducible spectra of *Enterobacteriaceae*, *Staphylococcus*, *Bacillus*, and *Pseudomonas* bacterial strains that had no fluorescence interference even for highly colored bacteria. The Raman spectra gave complementary information (C–H bond stretching of the bacterial membrane phospholipids, amino acids, and RNA/DNA) to the FTIR data (amide I/II bands of proteins and oligo/polysaccharides of cell walls). Confocal Raman microspectroscopy has also been used successfully to rapidly identify microorganisms in blood samples ([Maquelin et al., 2003](#)), and similar techniques could likely be applied for environmental analysis. A comparison between Raman and FTIR spectroscopy of bacteria samples from that study is provided in [Figure 1.13](#).

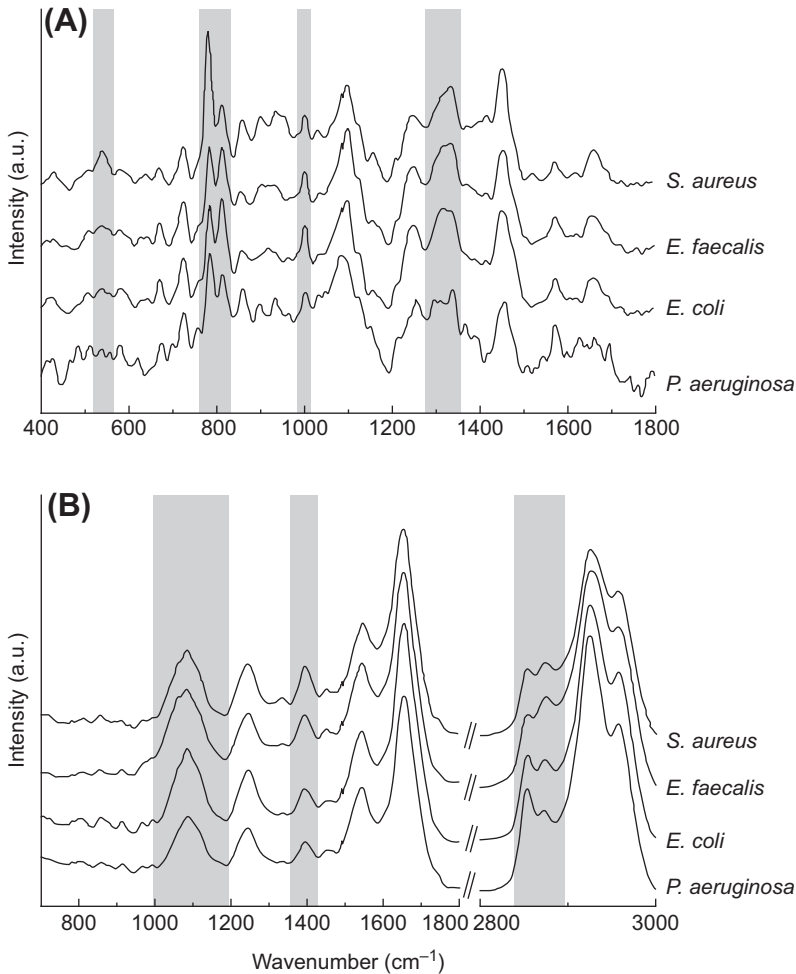


Figure 1.13 Representative Raman (A) and FTIR (B) spectra of four microorganisms (*Staphylococcus aureus*, *Enterococcus faecalis*, *Escherichia coli*, *Pseudomonas aeruginosa*). These spectra demonstrate the complementary and unique information provided by these techniques. Gray boxes have been placed over the spectra to indicate areas of differences. (FTIR, Fourier transform infrared.) Reprinted with permission [Maquelin et al. \(2003\)](#).

The high resolution and size scale necessary for these samples have meant ready application for micro-Raman and SERS. The first study to apply SERS to bacterial cell wall research examined impregnated and coated *E. coli* bacteria with silver colloids and observed sharp and intense SERS spectra ([Efrima and Bronk, 1998](#)). The resulting spectra were relatively

selective, preferentially showing bands associated with molecules and functional groups in the immediate proximity of the metal surface. Many studies have since used this technique to characterize bacteria with rapid analytical times and reproducible data (Kahraman et al., 2007; Naja et al., 2007). Improvements in the SERS substrate (through use of nanoparticles) has increased homogeneity of the substrate resulting in improved reproducibility of the Raman spectra and afforded greater sensitivity to the technique. Liu et al. were able to use this approach to detect fine-scale changes in the bacterial cell wall of single bacterium (*S. aureus*) during the bacterium's different growth stages and bacterial response to antibiotic treatment during early period of antibiotic exposure (Liu et al., 2009). Similarly, by coating volcanic clinopyroxene rocks with silver colloidal nanoparticles, SERS was utilized as a simple, sensitive technique to detect the presence of biomolecules (adenine, guanine, nucleobases, and micro-RNA) on the rocks (Muniz-Miranda et al., 2010). According to the authors, Martian rocks and sediments, believed to be analogous to pyroxene rocks, could be similarly investigated for evidence of life (extinct or extant) particularly using the sharp SERS adenosine band at 735 cm^{-1} . For additional information on Raman spectroscopy in microbiology, readers are referred to an informative review article by Petry et al. (2003).



7. SOIL AMENDMENTS

Characterization of materials using FTIR and Raman spectroscopies is an established method for scientists and is a common quality control practice in various industries. FTIR spectroscopy can serve as a rapid and informative method for analysis of a variety of soil amendments, including biochar, compost, and biosolids. This information can be utilized for quality control, predicting reactivity, and recalcitrance, or to provide insight into interfacial interactions between the amendment and soil constituents.

7.1 Biochar

Biochar is a byproduct of biomass pyrolysis (or gasification) to produce biofuels, as well as an intentional primary product from the partial pyrolysis of biomass. The produced biochar is highly aromatic and has increased C stability relative to the original feedstock materials (Lehmann and Joseph, 2009). Biochar differs from charcoal in that its primary use is not as a source of fuel, and is commonly applied to agricultural fields as a soil amendment.

The use of biochar, or black carbon, as a soil amendment has received increased attention since the discovery of the Terra Preta de Indio soils (approximately 7000 year old anthropogenic influenced soils) in the Amazon. It is proposed that these soils have received historical applications of charcoal, which provide a number of beneficial properties to the soil today (Glaser and Woods, 2004; Sombroek, 1966). Studies on the Terra Preta de Indio soils have shown that they have greater cation exchange capacity (Liang et al., 2006), fertility, and nutrient retention (Glaser, 2007; Lehmann and Joseph, 2009; Smith, 1980; Sohi et al., 2010), and stable stored carbon (Glaser et al., 2002; Sombroek et al., 2003) compared to nearby pedogenically similar soils. Presently much research is focused on attempting to replicate the conditions in these soils using biochar (Busscher et al., 2010; Case et al., 2012; Joseph et al., 2010; Kookana et al., 2011; Laird et al., 2010; Major et al., 2009; Mulvaney et al., 2004; Novak et al., 2009; Singh et al., 2010; Steinbeiss et al., 2009; Verhejien et al., 2010; Zimmerman et al., 2011).

Today, many growers are considering the use of biochar soil amendments for agronomic benefits and climate change mitigation strategies. The diversity of biochar source materials, pyrolysis methods, soils, and agricultural systems lends complexity to determining the appropriate circumstances for biochar amendments; however, it is becoming increasingly clear that the best use for a given biochar is dependent on its physical and chemical properties (Brewer et al., 2009). A number of recent publications have used FTIR and Raman spectroscopies to evaluate the chemical properties of biochar.

In an attempt to determine the difference between charcoal found within the Terra Preta de Indio soils and modern day manufactured biochars, Jorio et al. (2012) utilized Dispersive Raman to examine the carbon nanostructure within these materials. Their results reveal that the charcoal in these soils had an in-plane crystallite size distribution (L_a) of 3–8 nm range while that of several analyzed biochars was between 8 and 12 nm. The crystallite size distribution was approximated from intensity of the D and G bands as according to Cançado et al. (2007). Knowledge of the differences in the carbonaceous material increases the potential for improving biochar production methods to produce carbon of similar nanostructure to that of the Amazonian soils (Jorio, 2012).

FTIR spectroscopy has long been used to examine the chemical characteristics of charcoal materials (O'Reilly and Mosher, 1983; Starsinic et al., 1983; Wolf and Yuh, 1984) and the increased prevalence of biochar has resulted in the routine use of FTIR in biochar analysis (e.g. Brewer et al.,

2009; Fuertes et al., 2010; Keiluweit et al., 2010; Lehmann et al., 2005; Mukome et al., 2013). FTIR spectra of biochar provide information regarding the relative contribution of chemical functional groups (Table 1.5) and give a qualitative indication of the aromaticity of samples.

As a tool for characterization, FTIR spectroscopy can be used to elucidate the impact of pyrolysis temperature on the chemical composition of biochar. Increasing pyrolysis temperature and duration resulted in straw feedstock biochars with decreased peak intensities for C–O, O–H, and aliphatic C–H, concomitant with increased aromatic bands (Peng et al., 2011). A similar result was observed when ponderosa pine shavings and grass clippings were pyrolyzed from 100 to 700 °C and analyzed via FTIR (Keiluweit et al., 2010). The results demonstrate dehydration (decreased O–H), followed by increased lignin- and cellulose-derived products (C=C,

Table 1.5 Functional Group Assignments Corresponding to Biochar Samples as Determined by ATR-FTIR Analysis

Wavenumbers (cm ⁻¹)	Assignment
2924	$\nu(\text{C-H})$ vibrations in CH ₃ and CH ₂ ^{a-f}
2850	$\nu(\text{C-H})$ vibrations in CH ₃ and CH ₂ ^{a-f}
1695	$\nu(\text{C=O})$ vibration aromatic carbonyl/carboxyl C=O stretching ^{a-f}
1640	$\nu(\text{C=C})$ vibration, C=C aromatic ring ^{a-f}
1587	C=C vibration ^{a-f}
1505–1515	Skeletal C=C vibration (lignin) ^{a-f}
1460	$\delta(\text{C-H})$ vibrations in CH ₃ and CH ₂ ^{a-f}
1423	C=C vibration ^{a-f}
1380	$\nu(\text{C-O})$ vibration aromatic and $\delta(\text{C-H})$ vibrations in CH ₃ and CH ₂ _v ^{a-f}
1240–1260	$\nu(\text{C-O})$ vibration phenolic ^{a-f}
1154	Aromatic C–O stretching ^{a,b,e}
1080–1040	Si–O, C–O stretch of polysaccharides ^a
1029	Aliphatic ether C–O and alcohol C–O stretching ^{a,b,d,e}
870	1 adjacent H deformation ^{a,b,d,e}
804	2 adjacent H deformations ^{a,b,d,e}
750	4 adjacent H deformations ^{a,b,d,e}
667	$\gamma(\text{OH})$ bend ^{a,e}

^aHsu and Lo (1999).

^bSharma et al. (2004).

^cKeiluweit et al. (2010).

^dÖzçimen and Ersoy-Meriçboyu (2010).

^eWu et al. (2009).

^fBrewer et al. (2009).

C=O, C–O, C–H), and finally condensation into aromatic ring structures (decrease in number of FTIR bands) for biochars produced at 700 °C. Since FTIR spectroscopy probes chemical bonds with dipole moments, nonpolar materials are not strong IR absorbers; therefore, the FTIR spectra of highly aromatic chars do not have large peaks.

It should be noted that FTIR is not limited to characterization of discrete biochar samples, but can also be used to study and characterize charcoal within soil. For example, the Terra Preta de Indio soils were evaluated using SR ATR-FTIR in order to compare the content of phenolics, aliphatics, aromatics, carboxyls, and polysaccharides in these and adjacent soils having no charcoal added (Solomon et al., 2007b). Analysis of carbon functional groups present in the analyzed samples revealed that the Terra Preta de Indio soils have elevated levels of recalcitrant carbon (aliphatic and aromatic) attributed to historical additions of charcoal and the increased carbon sequestration within these soils.

Although determination of aromaticity and structural disorder of charcoals can be probed with FTIR, Raman spectroscopy provides distinct advantages for determining the structural order of carbonaceous materials. For example, the structural order of carbon nanostructures is routinely evaluated using this approach (Ajayan, 1999; Dresselhaus et al., 2005; Ferrari et al., 2006). Similarly, the amorphous nature of biochars can be determined via Dispersive Raman analysis. Through analysis of the Raman shift at 1500 cm^{-1} (sp^2 carbon), 1150 cm^{-1} (sp^3 -hybridized carbon), and 1530 cm^{-1} (sp^2 -hybridized carbon) the amorphous nature of biochar can be evaluated (Schmidt et al., 2002). Similar to the pyrolysis temperature effects evaluated with FTIR, Raman spectroscopy has demonstrated that the amorphous carbon components of biochar decrease with increased duration of steam gasification (Wu et al., 2009). During feedstock conversion to biochar, Raman bands associated with the disordered carbon decrease relative to aromatic and recalcitrant carbon. Another study using Dispersive Raman spectroscopy as a biochar characterization tool showed changes that occur in the ratio of sp^2 (G band) to sp^3 C (D band) in the material as a function of pyrolysis temperature (Chia et al., 2012). In addition, Dispersive Raman revealed how the sp^2 to sp^3 ratio changes with biochar feedstock (Jawhari et al., 1995; Mukome et al., 2013). The G or graphite-band arises from vibrations of sp^2 C found in graphitic materials and C=C bonds, while the D-band (diamond band) is linked to the breathing modes of disordered graphite rings (Ferrari and Robertson, 2000; Sadezky et al., 2005). On occasion these two broad peaks have been

further deconvoluted into seven peaks and further structural characterization information determined (Kim et al., 2011; Li et al., 2006). A helpful summary of Raman band assignments for charcoal samples is also presented by Wu et al. (2009).

7.2 Compost

Analysis of compost via vibrational spectroscopy results in spectra similar to those observed for SOM and humic fractions. One notable difference between analyses of these samples is that the humification of compost raw materials can be observed as a function of composting time to study the composting process (Chen, 2003; Inbar et al., 1991; Ouattmane et al., 2000; Smidt and Schwanninger, 2005; Wershaw et al., 1996), and characterize compost materials (Carballo et al., 2008b; Niemeyer et al., 1992). The evolution of FTIR spectra of green-waste samples to compost has shown an increase in etherified and peptidic compounds (bands at 1384, 1034, and 1544 cm^{-1}) with a relative decrease of more labile aliphatic carbon pools (2925 and 1235 cm^{-1}) (Amir et al., 2010). This interpretation of the spectral results are consistent with corresponding analysis of total C, H, N, and O content during the composting process. Other studies examining the composting processes highlight the increase of aromatic content and reduction in oxygen containing functional moieties (e.g. carboxylic, carbonylic groups) with increased humification (Fuentes et al., 2007). An excellent discussion of changes in FTIR spectra through observation of indicator bands for product control during waste material processing can be found in Smidt and Schwanninger (2005). Through a process of calibration with database of compost samples, FTIR has also been shown to hold promise as a rapid and cost-effective tool for estimating total C, total N, lignin, and cellulose content of composts (Tandy et al., 2010).

7.3 Biosolids

Due to the comparable composition of biosolids with compost and SOM, FTIR spectra are similar and band assignments are analogous. Biosolid IR spectra have numerous bands attributed to typical organic functional groups such as OH, CH₂, CH₃, C=O, COOH. Composted biosolids tend to be highly aliphatic and similar to fulvic acids extracted from soil and aquatic samples (Pérez-Sanz et al., 2006; Tapia et al., 2010). The addition of iron salts in wastewater treatments plants to coagulate OM can lead to the production of Fe-rich biosolid materials. Combined analysis of Fe content in biosolid extracted humic fractions and carboxyl content of FTIR spectra showed a

positive relationship, suggesting the formation of carboxyl-Fe complexes. Iron chelation by water-soluble HS has shown to increase Fe uptake by plants (Cesco et al., 2002), thus biosolids may serve as a source of Fe fertilizer (Pérez-Sanz et al., 2006).



8. MOLECULAR-SCALE ANALYSIS AT THE SOLID-LIQUID INTERFACE

Vibrational spectroscopy has proven to be an extremely valuable tool for elucidating binding mechanisms for a variety of compounds on environmental surfaces. These versatile techniques have successfully been employed to probe the soil-liquid interface for studies examining the sorption of inorganic ions, natural OM, anthropogenic organic compounds, biomolecules, and bacteria to clay minerals and metal oxides. In this case ATR-FTIR spectroscopy is the tool of choice for elucidating binding mechanisms at interfaces. In each of these cases it is the ability to use coatings to increase sensitivity and permit evaluation of sorption processes that makes ATR-FTIR analytically powerful. Although advanced X-ray techniques are providing new capabilities and additional insights for studies of mineral interfaces, the relative ease, low cost, and analytical power of FTIR spectroscopy approaches makes it an invaluable tool for researchers.

When it comes to FTIR for analysis at the solid-liquid interface, the use of ATR-FTIR is essential. Although DRIFTS has also been used to examine sorption reactions, this approach can introduce artifacts, which make data interpretation difficult and may yield incorrect results. The use of crystal IRE solves this problem and permits examination in the presence of water. The reason this works is that the IR light traveling through the IRE does not penetrate directly through the aqueous medium, but instead an evanescent wave propagates at each reflection point to provide information regarding the IR absorbance by molecules present at the IRE surface. Through the use of a reference water spectrum, water bands can be effectively subtracted to produce spectra revealing the interactions of species, which may be dissolved or bound to the substratum. For soil science research, one of the most important developments of ATR-FTIR was creating coatings on the IRE with relevant mineral phases to examine sorption to these surfaces. The use of IRE coatings was first developed by Hug et al. (Hug, 1997; Hug and Sulzberger, 1994) and has been widely adapted as a standard approach for evaluating sorption to mineral surfaces. These studies even allow discrimination between inner- and outer-sphere sorption mechanisms.

8.1 Organic Molecule Interactions with Mineral Surfaces

Organic molecules reacting with mineral surfaces may undergo a variety of processes such as surface complexation, oxidation/reduction, transformation, and polymerization. Therefore, evaluating the interactions of organic compounds with mineral surfaces is critical for understanding mineral dissolution, SOM stabilization, alteration of a solid's physicochemical properties, organic pollutant fate and transport in soil and sediment, and the formation of biomolecules on early Earth (Duckworth and Martin, 2001; Gu et al., 1995; Hazen and Sverjensky, 2010; Parikh et al., 2011; Wu et al., 2011; Yoon et al., 2004a). Vibrational spectroscopy provides a means to capture a spatially integrated response of the local bonding environment by measuring energies associated with the motion of bonded atoms, which can then be utilized to determine molecular structure (Amonette, 2002; Sposito, 2004). Therefore, vibrational spectroscopy provides a relatively convenient means to measure changes in the molecular structure of an adsorbed species (adsorbate) relative to an aqueous species (adsorptive) or changes in the adsorbent before and after complexation reactions.

Vibrational spectroscopy studies may employ direct observation of adsorbate interactions with an adsorbent or use alternative strategies. Johnston et al. (1993) and Sposito (2004) discuss two alternative strategies and refer to them as the use of adsorbate surrogates and reporter groups. In the case of adsorbate surrogates, a particular chemical species is used as an in situ probe to identify adsorbate–adsorbent interactions that can then be applied to understand adsorption mechanisms for similar compounds (Sposito, 2004). For example, Axe and Persson (2001) and Yoon et al. (2004b) used oxalate as an adsorbate surrogate to understand the interaction of dicarboxylates with metal oxide surfaces. This is in contrast to the use of reporter units, typically hydroxyl groups when working with mineral adsorbents, on the adsorbent surface. When employing reporter units one investigates changes in mineral spectra before and after reaction with an adsorbate to indicate adsorbate bonding characteristics (Sposito, 2004). Johnston and Stone (1990) used the reporter unit approach to study hydrazine sorption to kaolinite. Upon intercalation of hydrazine, the intensity of OH stretching and deformation bands in Raman and FTIR spectra was substantially reduced, and the reductions in intensity were attributed to hydrogen bonding between hydrazine and OH groups of kaolinite present in the interlayer.

A variety of FTIR techniques have been used to investigate organic compound–mineral interactions (e.g. transmission, FTIR, DRIFTS, ATR-FTIR, SR-FTIR). Although the interference from water in a spectrum is typically

diminished in transmission FTIR and DRIFTS analyses due to dehydration of the sample, these methods may provide inaccurate representation of interactions on a hydrated mineral surface. Kang and Xing (2007) and Kang et al. (2008) noted that the carboxylic acid function groups of organic acids tend to form outer-sphere complexes with metal centers on minerals when the spectra of pastes were collected using in situ ATR-FTIR. However, inner-sphere complexes were more predominant in the DRIFTS spectra of freeze-dried samples as noted by shifts in the asymmetric COO^- stretch to higher frequencies. The inducement of inner-sphere coordination on a mineral surface is due not only to dehydration but also to significant decreases in pH upon drying. This can be discerned from the observation of Kang and Xing (2007) that inner-sphere complexation was favored at lower pH, and the work of Dowding et al. (2005) and Clarke et al. (2011) illustrating drastic pH decreases (hydrogen ion activity increased 1000-fold) with increased drying. Although the spectra of powders or pressed pellets is applicable for understanding interactions under extremely dry conditions, it may provide false information regarding the types of surface complexes formed under well hydrated conditions. This may be particularly problematic when attempting to apply mechanistic understanding of bonding observed in transmission FTIR or DRIFTS to explain macroscopic data collected under hydrated conditions (i.e. batch test tube sorption experiments). Therefore, it is more appropriate to study organic interactions with minerals under hydrated conditions using saturated pastes obtained from batch experiments or in situ bonding of organics to mineral-coated crystals when practical.

The assignment of molecular vibrations to spectral features observed at particular frequencies can be quite challenging in complex spectra due to: (1) the wide range of frequencies where some vibrations may appear in a spectrum; (2) the overlap of frequencies associated with two or more vibrations; (3) spectral interferences (e.g. water, CO_2); (4) slight differences in band position within spectra collected using differing FTIR techniques; and (5) insufficient or lack of information on band assignments for a particular compound. One means to aid in the assignment of bands within a spectrum is through the study of spectral changes as a function of pH. Examples of this approach can be found in studies of the fluoroquinolone antibiotics ofloxacin (Goyne et al., 2005) (Figure 1.14) and ciprofloxacin (Gu and Karthikeyan, 2005b; Trivedi and Vasudevan, 2007). Through the collection of aqueous ofloxacin spectra (Figure 1.14), Goyne et al. (2005) were able to observe loss of the $\text{C}=\text{O}$ stretch of the COOH (1710 cm^{-1}) and increased intensity of the COO^- asymmetric (1585 cm^{-1}) and symmetric (1340 cm^{-1}) stretches as pH increased. Decreased intensity of vibration at 1400 cm^{-1} with increased acidity was attributed to protonation of N_4 in

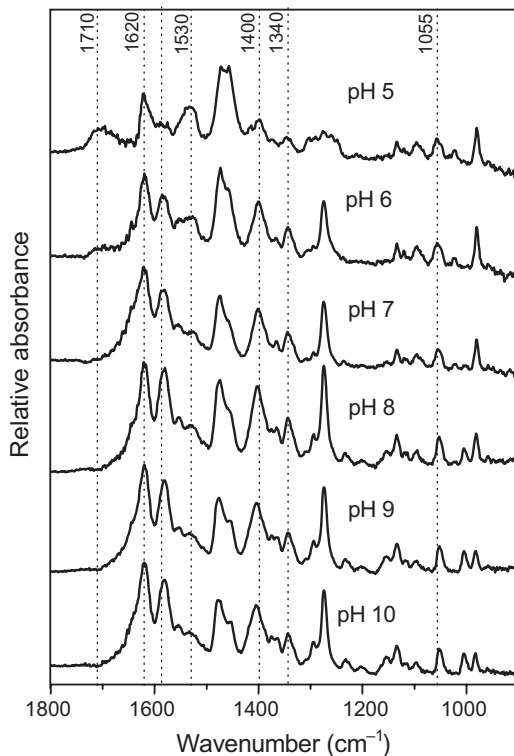


Figure 1.14 ATR-FTIR difference spectra of ofloxacin in 0.02M CaCl₂ background electrolyte solution from pH 5 to 10. Adapted with permission from [Goynet al. \(2005\)](#).

the piperazinyl ring. [Trivedi and Vasudevan \(2007\)](#) used a similar approach; however, they also investigated aqueous spectra of Fe³⁺-ciprofloxacin complexes as a function of pH, which was useful for interpreting the spectra of ciprofloxacin bound to goethite. In addition, prediction of FTIR and Raman spectra using molecular modeling can help to further elucidate observed vibrational bands ([Kubicki and Mueller, 2010](#)).

Indications of inner- and outer-sphere complex formation on mineral surfaces and the types of surface complex structures formed can also be acquired from MIR spectra. Formation of inner-sphere complexes between adsorbates with a carboxylic acid group and mineral surfaces is often indicated by substantial shifts (25–150 cm⁻¹) in the frequency of asymmetric and symmetric COO⁻ stretching relative to a spectrum of the aqueous adsorptive (e.g. [Chorover and Amistadi, 2001](#); [Duckworth and Martin, 2001](#); [Gu et al., 1995](#); [Gu and Karthikeyan, 2005b](#); [Kang and Xing, 2007](#)). With respect to the types of structural complexes formed, there are three common coordination modes developed between

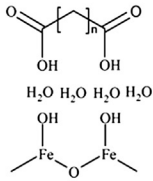
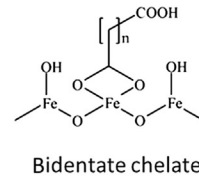
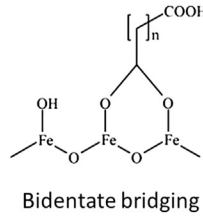
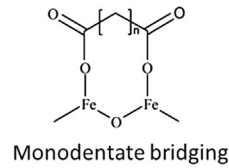
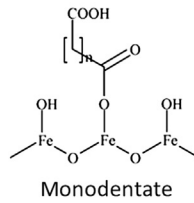
(A) Outer-sphere complex**(B)** Inner-sphere complexes

Figure 1.15 Various adsorption complexes between dicarboxylic acids and an iron oxide surface. Adapted with permission from Kang et al. (2008).

Table 1.6 General Range of Carboxyl Band Separations ($\Delta\nu$), between Unbound Carboxyl Groups ($\Delta\nu_{\text{ionic}}$) and Metal-Carboxyl Complexes ($\Delta\nu_{\text{com}}$), and Corresponding Binding Coordination (Dobson and McQuillan, 1999; Hug and Bahnemann, 2006; Kang et al., 2008)

Coordination	COO ⁻ Band Separation ($\Delta\nu$)	$\Delta\nu_{\text{com}}:\Delta\nu_{\text{ionic}}$	Carboxyl Shift
Monodentate	350–500 cm ⁻¹	$\Delta\nu_{\text{com}} > \Delta\nu_{\text{ionic}}$	$\nu_s(\text{COO}^-)$ lower
Binuclear bidentate	150–180 cm ⁻¹	$\Delta\nu_{\text{com}} < \Delta\nu_{\text{ionic}}$	$\nu_s(\text{COO}^-)$ higher or lower $\nu_{\text{as}}(\text{COO}^-)$ higher or lower
Mononuclear bidentate	60–100 cm ⁻¹	$\Delta\nu_{\text{com}} \ll \Delta\nu_{\text{ionic}}$	$\nu_s(\text{COO}^-)$ higher $\nu_{\text{as}}(\text{COO}^-)$ lower

a carboxylate group and a cation at the mineral surface: (1) monodentate binding; (2) chelating bidentate; and (3) bridging bidentate (Figure 1.15). The formation of these coordination modes can be distinguished through determination of the separation distance (cm⁻¹) between the asymmetric and symmetric COO⁻ stretching vibrations ($\Delta\nu = \nu_{\text{as}}\text{COO}^- - \nu_s\text{COO}^-$) (Alcock et al., 1976; Deacon and Phillips, 1980). As shown in Table 1.6, the range of $\Delta\nu$ for chelating bidentate, bridging bidentate, and unidentate bridging are 60–100 cm⁻¹, 150–180 cm⁻¹, and 350–500 cm⁻¹, respectively

(Dobson and McQuillan, 1999; Kang et al., 2008). It should be noted that these are only typical ranges of $\Delta\nu$ for coordination assignments and analyses can be made on an individual basis by comparing the $\Delta\nu$ of unbound carboxyl groups ($\Delta\nu_{\text{ionic}}$) with those representing metal-carboxyl complexes ($\Delta\nu_{\text{com}}$) such $\Delta\nu_{\text{com}} > \Delta\nu_{\text{ionic}}$ for monodentate binding, $\Delta\nu_{\text{com}} < \Delta\nu_{\text{ionic}}$ for bridging bidentate, and $\Delta\nu_{\text{com}} \ll \Delta\nu_{\text{ionic}}$ for chelating bidentate (Hug and Bahnemann, 2006). The differences in $\Delta\nu$ for the various coordination modes arise due to changes in C–O bond lengths and O–C–O angles upon bonding to a cation that subsequently alter the frequency at which a vibration is observed (Nara et al., 1996).

8.1.1 Low Molecular Weight Organic Acids

There has been a considerable amount of research published examining the interaction of low molecular weight organic molecules at the solid–liquid interface using vibrational spectroscopy. The pioneering work by Tejedor-Tejedor et al. (Tejedor-Tejedor and Anderson, 1990; Tejedor-Tejedor et al., 1992) demonstrated how in situ analysis of organic molecules could be carried out using ATR-FTIR in order to elucidate sorption mechanisms to mineral surfaces. In these companion papers, phthlate (PHTH), *p*-hydroxybenzoate (PHB), and 2,4-dihydroxybenzoate (2,4DHB) were reacted with goethite suspensions and analyzed using a cylindrical ZnSe ATR-FTIR IRE. Through comparison of IR spectra before and after reaction with goethite the authors determined that PHTH and PHB both bound to goethite through bidentate–binuclear surface complexes via both oxygens of a carboxyl group to a single iron atom. For 2,4DHB, a bidentate–mononuclear surface complex through one carboxyl oxygen and one phenolic oxygen was formed on goethite. Since the publication of these papers, the use of ATR-FTIR to elucidate sorption mechanisms of small organic molecules has become commonplace.

Due to interference from a heterogeneous background matrix (SOM and various minerals), it is highly challenging to determine binding mechanisms of small organic molecules in soil samples. For this reason, research in this area has been conducted using pure mineral phases such as Fe oxides (e.g. hematite, goethite), Al oxides (e.g. gibbsite, corundum), Ti-oxides (e.g. rutile, anatase), and phyllosilicates (e.g. smectite, montmorillonite) to examine low molecular weight organic molecule (e.g. amino acids, carboxylic acids) sorption mechanisms. Table 1.7 provides a list of selected studies, which have used FTIR spectroscopy to study these processes. Readers are also directed to Lefèvre et al. (2012) for a recent review of carboxylic acid reactions with mineral surfaces.

Table 1.7 Compiled List of Studies Investigating the Sorption of Amino Acids, Carboxylic Acids, and Other Low Molecular Weight Organic Molecules to Mineral Surfaces

References	Sorbate	Mineral	Analysis Method
Axe and Persson (2001)	Oxalate	Boehmite	ATR-FTIR
Axe et al. (2006)	Oxalate, malonate	Goethite	ATR-FTIR
Barja et al. (2001)	Phosphonate	Goethite	ATR-FTIR
Bargar et al. (1999)	Pb(II)-ethylenediaminetetraacetic acid (EDTA)	Goethite	ATR-FTIR, DRIFTS, EXAFS
Benetoli et al. (2007)	Alanine, methionine, glutamine, cysteine, aspartic acid, lysine, histidine	Bentonite, kaolinite	Transmission FTIR, XRD, Mössbauer
Boily et al. (2000)	Benzenecarboxylate	Goethite	ATR-FTIR
Borer et al. (2009)	Desferrioxamine b	Lepidocrocite	ATR-FTIR
Borda et al. (2003)	Oxalate	Goethite	ATR-FTIR
Bowen et al. (1988)	Dimethyl monophosphate	Montmorillonite	Transmission FTIR
Brigatti et al. (1999)	Cysteine	Montmorillonite, beidellite	Transmission FTIR, XRD, DTC
Cagnasso et al. (2010)	L- α -phosphatidylcholine, phosphatidyl-ethanolamine, phosphatidic acid	Goethite, hematite	ATR-FTIR
Dobson and McQuillan (1999)	Formate, acetate, oxalate, succinate, fumarate, malonate	Titanium oxide, aluminum oxide, zirconium oxide, tantalum oxide	ATR-FTIR
Duckworth and Martin (2001)	Oxalate, malonate, glutarate, succinate, adipate	Hematite	ATR-FTIR
Fitts et al. (1999)	Cu(II)-glutamate	γ -Alumina	ATR-FTIR, EXAFS
Kang and Xing (2007)	Succinic acid, glutaric acid, adipic acid, azelaic acid	Kaolinite, montmorillonite	ATR-FTIR, DRIFTS
Kang et al. (2008)	Succinic acid, glutaric acid, adipic acid, azelaic acid	Goethite	ATR-FTIR, DRIFTS

Gu et al. (1995) Gulley-stahl et al. (2010)	Phthalate, catechol, natural organic matter Catechol	Hematite Manganese oxides, iron oxide, titanium oxides chromium oxide (amorphous nanoparticles)	ATR-FTIR, NMR ATR-FTIR
Ha et al. (2008) Hug and Sulzberger (1994) Hug and Bahnemann (2006)	Lactate Oxalate, acetate Oxalate, malonate, succinate	Hematite Anatase Rutile, anatase, lepidocrocite	ATR-FTIR, QCC ATR-FTIR, SVD ATR-FTIR
Hwang and Lenhart (2008) Johnson et al. (2004) Kubicki et al. (1999)	Maleate acid, fumarate, succinate Maleate Acetate, oxalate, citrate, benzoate, salicy- late, phthalate	Hematite Corundum Quartz, albite, illite, kaolinite, montmorillonite	ATR-FTIR ATR-FTIR ATR-FTIR, MOC
Lackovic et al. (2003) Lefèvre et al. (2012) Mendive et al. (2006) Norén et al. (2008)	Citrate 5-Sulfosalicylic acid Oxalate Sarcosine, 5-carboxy-2-methyl- 1H-imidazole-4-carboxylate (H ₂ MIDA ⁻), ethylenediamine- N,N-diacetic acid (H ₂ EDDA)	Goethite, kaolinite, illite Gibbsite Anatase, rutile Goethite	ATR-FTIR ATR-FTIR ATR-FTIR ATR-FTIR
Norén and Persson (2007)	Acetate, benzoate, cyclohexanecarboxylate	Goethite	ATR-FTIR
Parikh et al. (2011) Parikh and Chorover (2006)	Glutamate, aspartate Phenylphosphonic acid adenosine 5'-monophosphate, 2'-deoxyadenyl- (3'->5')-2'-DNA	Rutile Hematite	ATR-FTIR, QCC ATR-FTIR

Continued

Table 1.7 Compiled List of Studies Investigating the Sorption of Amino Acids, Carboxylic Acids, and Other Low Molecular Weight Organic Molecules to Mineral Surfaces—cont'd

References	Sorbate	Mineral	Analysis Method
Person et al. (1998)	Acetate	γ -Alumina	ATR-FTIR
Person and Axe (2005)	Oxalate, malonate	Goethite	ATR-FTIR
Roddick-Lanzilotta et al. (1998)	Lysine	Anatase, titanium oxide (amorphous)	ATR-FTIR
Roddick-Lanzilotta and McQuillan (1999)	Lysine peptide, polylysine	Titanium oxide (amorphous)	ATR-FTIR
Roddick-Lanzilotta and McQuillan (2000)	Glutamate, aspartate	Anatase	ATR-FTIR
Rosenqvist et al. (2003)	O-phthalate, maleate, fumarate, malonate, oxalate	Gibbsite (nano)	ATR-FTIR
Rotzinger et al. (2004)	Formate, acetate	Rutile	ATR-FTIR
Specht and Frimmel (2001)	Oxalate, malonate, succinate	Kaolinite	ATR-FTIR
Tejedor-Tejedor et al. (1992, 1990)	Phthalate, <i>p</i> -hydroxybenzoate, 2,4-dihydroxybenzoate	Goethite	ATR-FTIR
Weisz et al. (2001)	Oxalate, salicylate		ATR-FTIR
Weisz et al. (2002)	Oxalate, salicylate, nicotinate, pyridine-3,4 dicarboxylic acid, pyridine-2,6 dicarboxylic acid, 2,2-bipyridine-4,4 dicarboxylic acid	Titanium oxide	ATR-FTIR
Yoon et al. (2004a)	Oxalate	Boehmite	ATR-FTIR

EXAFS: extended X-ray absorption fine structure spectroscopy, XRD: X-ray diffraction, DTC: differential thermal calorimetry, QCC: quantum chemical calculations, SVD: singular value decomposition, NMR: nuclear magnetic resonance spectroscopy, MOC: molecular orbital calculations, FTIR: Fourier transform infrared, ATR: attenuated total reflectance.

The combined use of vibrational spectroscopy with chemical modeling techniques provides increased assurance in data interpretation of binding mechanisms and surface coordination complexes. Kubicki and Muller (2010) present an excellent review of computational spectroscopy for environmental chemistry studies and details on methods and applications are found within. This synergistic approach is now commonly used to study the interaction for both small organic (e.g. Adamescu et al., 2010; Ha et al., 2008; Kubicki et al., 1999; Parikh et al., 2011) and inorganic (e.g. Baltrusaitis et al., 2007; Bargar et al., 2005; Paul et al., 2005) molecules with mineral surfaces. For example, quantum chemical calculations were used in conjunction with experimental collection of ATR-FTIR spectra to reveal that lactate binds to hematite nanoparticles through both outer-sphere and inner-sphere coordination (Ha et al., 2008). The chemical modeling improved data interpretation to reveal that inner-sphere coordinated lactate formed primarily monodentate, mononuclear complexes with the hydroxyl functional group facing away from hematite surface.

Kubicki et al. (1999) studied the sorption of a number carboxylic acids (i.e. acetic, oxalic, benzoic, salicylic, phthalic) to common soil minerals (i.e. quartz, albite, illite, kaolinite, montmorillonite) using batch experiments, ATR-FTIR spectroscopy, and molecular orbital calculations. The results reveal that inner-sphere coordination of the carboxylic acids does not occur through Si^{4+} on mineral surfaces. In fact, substantial chemisorption of carboxylic acids to clay minerals was only observed for illite, which was believed to contain trace Fe-hydroxide coatings. The modeling component in this study provides verification of ATR-FTIR spectroscopic interpretations and refines surface complexation structures, such as the monodentate or bidentate bridging of oxalic acid on albite, illite, and kaolinite.

In order to determine the influence of solution chemistry (pH, amino acid concentration) on surface structures of glutamic acid at the rutile ($\alpha\text{-TiO}_2$)-water interface, ATR-FTIR experiments were conducted on rutile thin films and quantum chemical calculations were carried out (Parikh et al., 2011). Correlation of experimental and calculated FTIR peak locations indicated the three potential surface configurations of glutamate on rutile. The proposed surface complexations are (1) bridging bidentate through inner-sphere coordination of both carboxyl groups; (2) chelating-monodentate via inner-sphere coordination of the γ -carboxyl; and (3) bridging bidentate with inner-sphere coordination of the α -carboxyl and outer-sphere coordination of the γ -carboxyl. It is only with the inclusion

of sophisticated modeling techniques along with spectroscopic approaches that elucidation of these specific surface complexes is possible. In these studies the synergistic nature of combining computational modeling with experimental spectroscopy can be exploited to yield high benefits.

8.1.2 *Herbicides and Pharmaceuticals*

Vibrational spectroscopy has been used considerably to evaluate the interactions of agrochemicals and contaminants with layer silicates and metal oxides. Elucidating mechanisms of adsorption between such compounds and minerals is valuable for determining chemical fate and transport in the environment, particularly in subsoil horizons where organic carbon content is generally minimal. [Tables 1.8 and 1.9](#) present a compiled list of studies, which probe the sorption of organic herbicides and antibacterial compounds to mineral surfaces using vibrational spectroscopy.

Several studies have illustrated the sorption of neutral organic herbicides to neutral siloxane surface sites in the interlayer of layer silicates, and the dependence of neutral herbicide sorption on the presence of less hydrated interlayer cations (Cs^+ and K^+) and low charge density ([Boyd et al., 2011](#); [Li et al., 2003](#); [Sheng et al., 2002](#)). We refer the reader to the review article by [Boyd et al. \(2011\)](#) that thoroughly synthesizes these studies and the application of vibrational spectroscopy for studying neutral organic compound interactions with clay minerals; however, we note below a few interesting applications of FTIR found in several of these studies.

[Sheng et al. \(2002\)](#) collected FTIR spectra of the herbicide 4,6-dinitro-*o*-cresol (DNOC) adsorbed to potassium saturated Wyoming smectites to evaluate orientation of DNOC on the clay surface. The FTIR spectra of oriented clay films collected at 0° and 45° of beam incidence show two in-plane bands associated with asymmetric N–O vibrations at 1550 to 1510 cm^{-1} , symmetric N–O stretching vibrations of NO_2 (1356 and 1334 cm^{-1}), and an out-of-plane NO_2 rocking vibration at $\sim 745\text{ cm}^{-1}$. Intensity of in-plane vibrations in 0° spectra was greater than the 45° spectra and the opposite trend was observed for the out-of-plane band. Because intensity of the absorption bands varied with increasing angle of beam incidence, the authors were able to apply linear dichroism to determine that the spectra indicated parallel orientation of DNOC to the clay mineral surfaces ([Sheng et al., 2002](#)). In a more robust study of DNOC and 4,6-dinitro-2-sec-butylphenol adsorption to clay minerals with differing exchangeable cations, [Johnston et al. \(2002a\)](#) used linear dichroism FTIR to reveal that positions of the N–O bands varied little on three K-saturated clays.

Table 1.8 Compiled List of Studies Investigating the Sorption of Antimicrobial Organic Compounds to Mineral Surfaces

References	Sorbate	Mineral	Analysis Method
Aristilde et al. (2010)	Oxytetracycline	Na-montmorillonite	Transmission FTIR, XRD, NMR, MCMS
Chabot et al. (2009)	p-Arsanilic acid	Hematite, maghemite, goethite	ATR-FTIR
Chang et al. (2012)	Tetracycline	Illite	ATR-FTIR, XRD
Chang et al. (2009a, 2009b)	Tetracycline	Palygorskite	ATR-FTIR, XRD
Chen et al. (2010)	Clindamycin, linomycin	Birnessite	Transmission FTIR
Depalma et al. (2008)	p-Arsanilic acid	Hematite, maghemite, goethite	ATR-FTIR
Goyne et al. (2005)	Ofloxacin	Alumina, silica	ATR-FTIR
Gu and Karthikeyan (2005b)	Ciprofloxacin	Hydrous Al-oxide, hydrous Fe-oxide	ATR-FTIR
Gu and Karthikeyan (2005a)	Tetracycline	Hydrous Al-oxide, hydrous Fe-oxide	ATR-FTIR
Kulshrestha et al. (2004)	Oxytetracycline	Montmorillonite	Transmission FTIR, XRD
Li et al. (2010)	Tetracycline	Na-montmorillonite, Ca-montmorillonite, mica-montmorillonite, hectorite	ATR-FTIR, XRD
Li et al. (2011)	Ciprofloxacin	Kaolinite	ATR-FTIR
Nowara et al. (1997)	Enrofloxacin, ciprofloxacin, levofloxacin	Illite, montmorillonite, vermiculite, kaolinite	Transmission FTIR, XRD, Microcalorimetry,
Paul et al. (2012)	Ofloxacin	Anatase	ATR-FTIR
Pei et al. (2010)	Ciprofloxacin	Montmorillonite, kaolinite	ATR-FTIR
Pusino et al. (2000)	Triasulfuron	Montmorillonite	Transmission FTIR
Peterson et al. (2009)	Cephapirin	Quartz, feldspar	Raman microscopy, transmission FTIR

Continued

Table 1.8 Compiled List of Studies Investigating the Sorption of Antimicrobial Organic Compounds to Mineral Surfaces—cont'd

References	Sorbate	Mineral	Analysis Method
Rakshit et al. (2013a)	Oxytetracycline	Magnetite	ATR-FTIR
Rakshit et al. (2013b)	Ciprofloxacin	Magnetite	ATR-FTIR
Trivedi and Vasudevan (2007)	Ciprofloxacin	Goethite	ATR-FTIR
Wang et al. (2010)	Ciprofloxacin	Montmorillonite	Transmission FTIR, XRD
Wu et al. (2010)	Ciprofloxacin	Montmorillonite	Transmission FTIR
Wu et al. (2013a)	Nalidixic acid	Montmorillonite, kaolinite	Transmission FTIR, XRD
Wu et al. (2013b)	Ciprofloxacin	Kaolinite, montmorillonite	Transmission FTIR, XRD
Yan et al. (2012)	Enrofloxacin	Montmorillonite	ATR-FTIR, 2D-COS
Zhao et al. (2012)	Tetracycline	Montmorillonite	FTIR-PAS, XRD

XRD: X-ray diffraction, NMR: nuclear magnetic resonance spectroscopy, MCMS: Monte Carlo molecular simulations, 2D COS: two dimensional correlation spectroscopy, FTIR-PAS: FTIR photoacoustic spectroscopy, ATR: attenuated total reflectance, FTIR: Fourier transform infrared

Table 1.9 Compiled List of Studies Investigating the Sorption of Organic Pesticide Compounds to Mineral Surfaces

References	Sorbate	Mineral	Analysis Method
Adamescu et al. (2010)	Dimethylarsinic acid	Hematite, goethite	ATR-FTIR, QCC
Barja et al. (1999)	Methylphosphonic acid (glyphosate surrogate)	Goethite	ATR-FTIR
Barja and Afonso (2005)	Glyphosate, aminomethylphosphonic acid	Goethite	ATR-FTIR
Celis et al. (1999)	2,4-Dichlorophenoxyacetic acid (2,4-D)	Montmorillonite, ferrihydrite	Transmission FTIR
Chen, et al. (2009)	1-naphthyl methylcarbamate (carbaryl)	Montmorillonite, kaolinite, goethite	Transmission FTIR
Davies and Jabeen (2002)	Isoproturon, N,N-dimethylurea (model compound), 4-isopropylaniline (model compound)	Bentonite, montmorillonite, kaolinite	Transmission FTIR, TGA, XRD
Davies and Jabeen (2003)	Atrazine, 2-chloropyrimidine, 3-chloropyridine	Bentonite, montmorillonite, kaolinite	Transmission FTIR, TGA, XRD
Goyne et al. (2004)	2,4-Dichlorophenoxyacetic acid (2,4-D)	Alumina, silica	ATR-FTIR
Johnston et al. (2002)	4,6-Dinitro- <i>o</i> -cresol, 4,6-dinitro-2-sec-butylphenol	Montmorillonite	Transmission FTIR
Laird et al. (1994)	Atrazine	Soil clay fraction	FTIR-PAS, XRD
Li et al. (2009)	2,4-Dichlorophenoxyacetic acid (2,4-D), acetochlor	Bentonite	Transmission FTIR
de Oliveira et al. (2005)	1-naphthyl methylcarbamate (carbaryl)	Montmorillonite	Transmission FTIR
Pusino et al. (2003)	Quinmerac 7-chloro-3-methylquinoline- 8-carboxylic acid, quinclorac 3,7- dichloroquinoline-8-carboxylic acid	Montmorillonite	Transmission FTIR

Continued

Table 1.9 Compiled List of Studies Investigating the Sorption of Organic Pesticide Compounds to Mineral Surfaces—cont'd

References	Sorbate	Mineral	Analysis Method
Sheals et al. (2002)	Glyphosate	Goethite	ATR-FTIR, XPS
Sheng et al. (2002)	4,6-Dinitro- <i>o</i> -cresol, dichlobenil	Montmorillonite	ATR-FTIR
Shimizu et al. (2010)	Monomethylarsenate, dimethylarsenate	Alumina (amorphous)	ATR-FTIR, EXAFS
Tofan-Lazar and Al-Abadleh (2012a)	Dimethylarsenate	Hematite	ATR-FTIR
Tofan-Lazar and Al-Abadleh (2012b)	Dimethylarsenate (w/phosphate)	Hematite	ATR-FTIR
Undabeytia et al. (2000)	Norflurazon	Montmorillonite, sepiollite	
Wu et al. (2011)	Isoxaflutole	Hydrous Fe-oxide, hydrous Al-oxide	ATR-FTIR, DRIFTS

QCC: quantum chemical calculations, TGA: thermogravimetric analysis, XPS: X-ray photoelectron spectroscopy, XRD: X-ray diffraction, ATR: attenuated total reflectance, FTIR, Fourier transform infrared, FTIR-PAS: FTIR photoacoustic spectroscopy, EXAFS: extended X-ray absorption fine structure spectroscopy, DRIFTS: diffuse reflectance infrared Fourier transform spectroscopy.

However, differences in position of the N–O bands were observed between mono- and divalent exchangeable cations with differing ionic radius and hydration enthalpy. In particular, the symmetric N–O stretching vibration at $\sim 1350\text{ cm}^{-1}$ shifted to lower energy as hydration energy decreased (Johnston et al., 2002a). These changes suggest that the NO_2 group coordinates with metal cations in the clay interlayer, thus suggesting that the dinitrophenol herbicides adsorb to clay minerals through van der Waals interactions with neutral siloxane groups on the mineral surface and coordination with exchangeable cations (Johnston et al., 2002a). FTIR analyses also proved useful for determining mechanisms of carbaryl (1-naphthyl-N-methyl-carbamate) sorption to clay minerals and the importance of interlayer cation–carbonyl interactions for bonding strength (de Oliveira et al., 2005).

Others have used FTIR to investigate the interaction of anionic herbicides and herbicide degradation products with metal oxides to determine the types of complexes and structures formed upon adsorption. Celis et al. (1999) and Goyne et al. (2004) investigated mechanisms of 2,4-dichlorophenoxyacetic acid (2,4-D) sorption to metal oxide surfaces using transmission FTIR and ATR–FTIR, respectively. Both interpreted the acquired spectra as indication that 2,4-D sorbed to variable charge mineral surfaces via electrostatic interaction between the carboxylate group and $\equiv\text{Metal-OH}_2^+$ surface functional groups on Al and Fe oxides. Wu et al. (2011) employed ATR–FTIR and DRIFTS spectroscopy to study the interactions of isoxaflutole degradates to hydrous aluminum and iron oxides. The ATR–FTIR spectra of the diketone nitrile (DKN) and benzoic acid (BA) degradates of isoxaflutole adsorbed to the hydrous metal oxides provided no evidence of inner-sphere complex formation between the ketone carbonyl group of DKN or the carboxylate group of BA with mineral surfaces. In contrast, DRIFTS spectra of the BA–mineral complex suggested the formation of an inner-sphere complex upon freeze-drying based on a shift in the asymmetric COO^- stretch to a lower wavenumbers relative to the aqueous spectrum (Wu et al., 2011).

Adsorption of glyphosate [(N-phosphonomethyl)glycine], glyphosate degradates, and adsorbate surrogates of glyphosate to iron oxides have received considerable study using FTIR. Barja and dos Santos Afonso (1998) conducted ATR–FTIR studies as a function of pH and pD to identify particular bands in the glyphosate spectra and to evaluate changes in the glyphosate spectrum upon complexation with aqueous Fe(III). Three vibrations of the phosphonic group resided between 1320 and 979 cm^{-1} at pH 6–9, and four phosphonic group vibrations were observed in the range

of pH 2–4; carboxylic acid and amino vibrations were assigned to bands between 1736 and 1403 cm^{-1} . Coordination of the phosphonate group with aqueous Fe was indicated by a broad and unresolved band from 1200 to 950 cm^{-1} where stretching vibrations of the PO_2^- and PO_3^- are observed in the free ligand, and the absence of $\text{P}=\text{O}$ and $\text{P}-\text{OH}$ at 1400–1200 cm^{-1} and 917 cm^{-1} , respectively (Barja and dos Santos Afonso, 1998). Barja et al. (1999) employed methylphosphonic acid (MPA) as an adsorbate surrogate for glyphosate in adsorption studies with goethite. In situ CIR-FTIR spectra at low pH suggested that protonated MPA was bound through a monodentate complex between the phosphonate group and the goethite surface; whereas, a bridging bidentate complex was the proposed structure for MPA bonding at high pH. Sheals et al. (2002) and Barja and dos Santos Afonso (2005) studied glyphosate adsorption to goethite using ATR-FTIR and independently concluded that glyphosate sorbed to goethite as inner-sphere complexes similar to those proposed for MPA with no contribution from the carboxylic acid and amino groups.

Although herbicides have been an environmental concern for many decades, the widespread detection of pharmaceuticals and personal care products in the environment (e.g. Kolpin et al., 2002) has stimulated interest in the interactions of these contaminants with soil. Reactions of antibiotics at the solid–water interface have received particular attention and vibrational spectroscopy has improved understanding of antibiotic sorption processes to minerals. Reaction of minerals and antibiotics from the fluoroquinolone and tetracycline classes have been studied quite extensively using FTIR spectroscopy (e.g. Goyne et al., 2005; Gu and Karthikeyan, 2005a, b; Kulshrestha et al., 2004; Li et al., 2011). Lincosamide and β -lactam interactions with minerals have been studied as well but to a lesser extent (Chen et al., 2010; Peterson et al., 2009).

Fluoroquinolones form strong complexes with Fe and Al oxides via ligand exchange reactions, and ATR-FTIR studies have indicated the potential for two differing complexes to form with metal centers of the mineral. Spectra of ofloxacin sorbed to Al oxide in Goyne et al. (2005) were interpreted as indication of mononuclear bidentate complexation of Al with the ketone and carboxylate functional groups, and this assertion was supported by molecular modeling. Gu and Karthikeyan (2005b) also interpreted spectra of ciprofloxacin adsorbed to hydrous iron oxide as indication of ketone and carboxylate participation in the complex, although they proposed mononuclear monodentate complex formation between one of the oxygen in the carboxylate group and a metal center on hydrous aluminum

oxide. In contrast, [Trivedi and Vasudevan \(2007\)](#) observed spectroscopic evidence that ciprofloxacin complexes with iron atoms in goethite through a bidentate complex with both oxygen atoms in the carboxylate group. Molecular modeling by [Aristilde and Sposito \(2008\)](#) suggests that both types of bidentate complexes are possible. FTIR studies of fluoroquinolone interaction with 1:1 and 2:1 layer silicates have helped reveal differences in sorption between the layer silicates (e.g. intercalation vs external sorption), the influence of exchange cations on adsorption, participation of the carboxylate, ketone, and protonated N in the piperazinyl group in adsorption as a function of pH, and the influence of coadsorbing cations ([Li et al., 2011](#); [Nowara et al., 1997](#); [Pei et al., 2010](#); [Wang et al., 2011](#); [Wu et al., 2010](#); [Yan et al., 2012](#)). Similar types of FTIR studies focused on tetracycline class antibiotic adsorption have proved useful in evaluating the mechanisms and the types of complexes formed between tetracyclines and minerals ([Chang et al., 2009a, 2009b](#); [Gu and Karthikeyan, 2005a](#); [Kulshrestha et al., 2004](#); [Li et al., 2010](#); [Zhao et al., 2012b](#)).

Organoarsenicals have been used historically as herbicides, insecticides, fungicides, and antibacterial compounds and their reaction with mineral surfaces have also been widely studied using vibrational spectroscopy (e.g. [Cowen et al., 2008](#); [Depalma et al., 2008](#); [Shimizu et al., 2010](#)). Although most instances of arsenic contamination can be attributed to weathering geologic sources, the industrial production of organoarsenicals, particularly for use in agriculture, is also of concern. Until recently *p*-arsanilic acid (and roxarsone) was commonly used as an additive to poultry feed and therefore an understanding of their interactions with soil minerals is important. ATR-FTIR spectroscopy was instrumental in determining that *p*-arsanilic acid formed inner-sphere complexes with iron (oxyhydr)oxide minerals ([Chabot et al., 2009](#)). And although this binding mechanism suggests limited transport of *p*-arsanilic acid in iron rich soils, this study also showed that aqueous phosphate can desorb *p*-arsanilic acid and thus has potential to enhance its transport, particularly important for poultry manure amended soils. Similar studies were also conducted using both ATR-FTIR spectroscopy and quantum chemical calculations to elucidate dimethylarsinic acid inner- and outer-sphere binding mechanisms to goethite ([Adamescu et al., 2010](#)). More recently, Tofan-Lazar and Al-Abadleh ([Tofan-Lazar and Al-Abadleh, 2012a,b](#)) have used ATR-FTIR to study the reaction kinetics of dimethylarsinic acid and phosphate (absence/presence of surface arsenic) sorption to hematite and goethite.

8.2 Inorganic Molecule Interactions with Mineral Surfaces

FTIR is a well-developed tool for probing the solid–solution interface to examine the processes of inorganic ion sorption. In particular, ATR–FTIR has proven to be a useful tool for determining the sorption mechanism (i.e. inner-sphere vs outer-sphere) of oxyanions to mineral surfaces, typically in cases where binding occurs and there is no change in the IR spectrum following reaction with the solid surface where outer-sphere sorption is taking place. However, the presence of new peaks or shifts in the wavenumbers of existing peaks is commonly attributed to inner-sphere coordination. Due to the fact that only molecules with a dipole moment (permanent or induced) are IR active, FTIR studies are best suited for oxyanions, which have relatively large dipole moments.

Of all the applications of vibrational spectroscopy in the area of soil chemistry, the use of FTIR to study inorganic ion sorption to mineral surfaces is the most complete and advances in recent years have somewhat slowed. As a result, prior review papers cover this area quite well. For example, [Suarez et al. \(1999\)](#) provide an excellent review of oxyanion (i.e. phosphate, borate, selenate, selenite) sorption mechanisms and present data showing inner-sphere coordination for arsenate and arsenite to amorphous Fe and Al oxides from ATR–FTIR and DRIFTS analysis. In addition, this review places an emphasis on pH and mineral surface charge [i.e. point of zero charge (pzc)] for oxyanion sorption coordination, in part through inclusion of electrophoretic mobility (EM) and titration data. In a slightly more recent review, [Lefèvre \(2004\)](#) provides a thorough and insightful article on ATR–FTIR theory and its application to studying inorganic ion sorption to metal oxides and hydroxides. In that review the adsorption of sulfate, carbonate, phosphate, nitrate, perchlorate, borate, selenite/selenate, and arsenate to metal oxides and hydroxides is addressed. Included in both of the aforementioned review papers are excellent tables summarizing FTIR band assignments for a number of dissolved and mineral-coordinated anions. In addition, a review of surface interactions of inorganic arsenic on mineral surfaces using a variety of spectroscopic techniques, including FTIR and Raman, is provided by [Wang and Mulligan \(2008\)](#). Due to the existence of these quality reviews, the study of inorganic ions on mineral surfaces will not be discussed in great detail here. [Table 1.10](#) provides references for studies which probe inorganic ion sorption to soil minerals through vibrational spectroscopy.

Due largely to the common occurrence of elevated phosphate levels in agricultural soils, and concerns associated to its transport to surface waters

Table 1.10 Compiled List of Studies Investigating the Sorption of Inorganic Ions to Mineral Surfaces

References	Sorbate	Mineral	Analysis Method
Arai and Sparks (2001)	Phosphate	Ferrihydrite	ATR-FTIR
Arai et al. (2004)	Arsenate (w/carbonate)	Hematite	ATR-FTIR, XAS
Baltrusaitis et al. (2007)	Nitrate	Corundum, γ -alumina	Transmission FTIR, QCC
Bargar et al. (2005)	Carbonate	Hematite	ATR-FTIR, DFT
Beattie et al. (2008)	Sulfate, Cu ^{II}	Goethite	ATR-FTIR
Connor and McQuillan (1999)	Phosphate	Titanium oxide	ATR-FTIR, Raman, CCM
Elzinga and Sparks (2007)	Phosphate	Hematite	ATR-FTIR
Elzinga and Kretzschmar (2013)	Phosphate (w/Cd ^{II})	Hematite	ATR-FTIR
Goldberg and Johnston (2001)	Arsenite, arsenate	Fe-oxide (amorphous), Al-oxide (amorphous)	ATR-FTIR
Gong (2001)	Phosphate	Titanium oxide	ATR-FTIR
Guan et al. (2005)	Sodium pyrophosphate, sodium tripolyphosphate	Aluminum hydroxide (amorphous)	ATR-FTIR
Hug (1997)	Sulfate	Hematite	ATR-FTIR
Hug and Sulzberger (1994)	Sulfate	Anatase	ATR-FTIR, SVD
Johnston and Chrysochoou (2012)	Chromate	Ferrihydrite	ATR-FTIR, QCC
Luengo et al. (2006)	Phosphate	Goethite	ATR-FTIR
Luxton et al. (2008)	Silicate	Goethite	ATR-FTIR
McAuley and Cabaniss (2007)	Arsenate, sulfate, selenate	Goethite	ATR-FTIR
Michelmore et al. (2000)	Phosphate	Titanium oxide, silica	ATR-FTIR, Electrophoresis

Continued

Table 1.10 Compiled List of Studies Investigating the Sorption of Inorganic Ions to Mineral Surfaces—cont'd

References	Sorbate	Mineral	Analysis Method
Myneni et al. (1998)	Arsenate	Ettringite	ATR-FTIR
Ostergren et al. (2000)	Carbonate	Goethite	ATR-FTIR, EXAFS
Parfitt and Smart (1977)	Sulfate	Goethite	Transmission FTIR
	Sulfate	Goethite, akaganeite, lepidocrocite, hematite, amorphous Fe-hydroxide	Transmission FTIR
Parikh et al. (2008)	Arsenite, arsenate	Hydrous manganese oxide	ATR-FTIR
Parikh et al. (2010)	Arsenite, arsenate, phosphate	Hydrous manganese oxide, goethite	ATR-FTIR
Paul et al. (2005)	Sulfate	Hematite	ATR-FTIR, MO/DFT
Peak et al. (1999)	Sulfate	Goethite	ATR-FTIR
Pena et al. (2006)	Arsenite, arsenate	Titanium oxide	ATR-FTIR, EXAFS
Persson et al. (1996)	Phosphate	Goethite	DRIFTS
Roddick-Lanzilotta et al. (2002)	Arsenate	Hydrous Fe-oxide	ATR-FTIR
Suarez et al. (1999)	Arsenite, arsenate	Fe-oxide (amorphous), al-oxide (amorphous)	ATR-FTIR, DRIFTS
Su and Suarez (1995)	Boron	Fe-oxide, allophane, kaolinite	ATR-FTIR
Su and Suarez (1997a)	Boron	Allophane	DRIFTS
Su and Suarez (1997b)	Carbonate	Gibbsite, goethite, hydrous al-oxide, hydrous Fe-oxide	ATR-FTIR
Su and Suarez (2000)	Selenite, selenate	Goethite, Fe-oxide (amorphous)	ATR-FTIR, DRIFTS, Electrophoresis

Sun and Doner (1996)	Arsenite, arsenate	Goethite	ATR-FTIR, transmission FTIR
Sun and Doner (1998)	Arsenite	Goethite, birnessite	ATR-FTIR, XANES
Szlachta et al. (2012)	Arsenite, selenite	Fe-Mn hydrous oxide	DRIFTS, XPS
Tejedor-Tejedor and Anderson (1986)	Nitrate, perchlorate	Goethite	ATR-FTIR
Tejedor-Tejedor and Anderson (1990)	Phosphate	Goethite	ATR-FTIR
Tofan-Lazar and Al-Abadleh (2012b)	Phosphate (w/dimethylarsenate)	Hematite	ATR-FTIR
	Carbonate	Goethite	ATR-FTIR
Voegelin and Hug (2003)	Arsenite	Ferrihydrite	ATR-FTIR
Wijnja and Schulthess (1999)	Carbonate, nitrate	γ -Alumina	ATR-FTIR
Wijnja and Schulthess (2001)	Carbonate	Goethite	ATR-FTIR, DRIFTS, H ⁺ Coadsorption

XAS: X-ray absorption spectroscopy, QCC: quantum chemical calculations, DFT: density function theory, CCM: constant capacitance modeling, SVD: singular value decomposition, EXAFS: extended X-ray absorption fine structure spectroscopy, MO/DFT: molecular orbital/density function theory, XANES: X-ray absorption near-edge structure, XPS: X-ray photoelectron spectroscopy, ATR: attenuated total reflectance, FTIR, Fourier transform infrared, EXAFS: extended X-ray absorption fine structure spectroscopy, DRIFTS: diffuse reflectance infrared Fourier transform spectroscopy.

and subsequent impact on eutrophication, its interactions with soil minerals continue to be studied. Over the last 25 years FTIR spectroscopy has provided critical insight into the interactions of phosphate with various soil minerals. Some of the more impactful studies on phosphate sorption to iron oxides are found in [Tejedor-Tejedor and Anderson \(1990\)](#), [Persson et al. \(1996\)](#), and [Arai and Sparks \(2001\)](#), providing fundamental knowledge regarding the formation of inner-sphere phosphate complexes. Building on these studies, [Elzinga and Sparks \(2007\)](#) utilized the molecular-scale power of ATR-FTIR to examine the surface coordination of phosphate to hematite as a function of pH/pD (3.5–7.0). In this study, the authors compare spectra collected at various pH/pD values and suggest that multiple monoprotonated phosphate inner-sphere surface complexes (i.e. monodentate binuclear, monodentate mononuclear) are observed at the hematite–water interface. More recently, the impact of metal cations (i.e. Cd^{II}) on phosphate sorption to goethite has been investigated using ATR-FTIR ([Elzinga and Kretzschmar, 2013](#)). In this study, phosphate sorption to goethite was enhanced in the presence of Cd^{II}, increasing with increased pH values. ATR-FTIR spectra indicated that Cd^{II} results in a distortion of the orthophosphate tetrahedron at low pH values, thus impacting phosphate protonation. This research demonstrates the importance of considering divalent metals, such as Cd^{II}, on the fate of phosphate in soil environments.

[Lanfranco et al. \(2003\)](#) successfully utilized Raman microspectroscopy to determine the presence of mixed-metal hydroxylapatites (Ca and Cd substituted) in manually doped soil at concentrations as low as 0.1% despite fluorescence interference. They were also able to determine the relative composition of the mixed-metal hydroxylapatites due to variance in Raman active bands as a function of the Cd content. This type of analysis illustrates the potential of Raman spectroscopy in the investigation of utilizing phosphates for remediation of metal contaminated soils. Several other studies have focused on using Raman spectroscopy to investigate phosphorus in soils ([Bogrekeci, 2006](#); [Zheng et al., 2012](#)). [Zheng et al. \(2012\)](#) recently used the technique to determine soil phosphorus concentrations and obtained a good correlation between the Raman signal and concentration (validation $R^2 = 0.937$). Application of Raman spectroscopy for this determination is significant as it enables simple and rapid determination of this soil nutrient comparable to other techniques such as UV-vis and NIR without interference from soil moisture, a major limitation of these techniques.

The coupling of FTIR with advanced modeling techniques for validation, and enhancement, of spectral interpretation also aids elucidation of

inorganic ion interactions at mineral surfaces. For example, [Paul et al. \(2005\)](#) utilized ATR-FTIR and molecular orbit/density functional theory (MO/DFT) to study sulfate sorption to hematite in aqueous and with subsequent dehydration. The results of this study reveal that sulfate binds at the mineral-water interface through a bidentate bridging or monodentate coordination, but following dehydration sulfate changes species to form a bidentate bridging or monodentate bisulfate complex. This study is an excellent example of the ability of vibrational spectroscopy to provide information regarding both sorption mechanisms and surface speciation information. These authors ([Kubicki et al., 2007](#)) also present an excellent theoretical (MO/DFT) study to model FTIR and extended X-ray absorption fine structure spectra of carbonate, phosphate, sulfate, arsenate, and arsenite on various Fe- and Al oxides. In another study, [Bargar et al. \(2005\)](#) used a similar approach to examine the speciation of adsorbed carbonate on hematite. Correlation between vibrational frequency calculations and experimental data suggested carbonate exists as both a monodentate binuclear inner-sphere complex and also fully or partially solvated species (i.e. outer-sphere) bound to the surface via hydrogen bonding. In a more recent study, chromate sorption to ferrihydrite was probed using this combined experimental and theoretical approach ([Johnston and Chrysochoou, 2012](#)). The authors conclude that at pH greater than pH 6.5 monodentate complexes are prevalent, whereas bidentate surface species are observed at pH < 6. The continuing advances in computer processing capabilities and affordability are making the use of molecular calculations accessible and providing significant advances to vibrational spectroscopy analysis on mineral surfaces.

Vibrational spectroscopy can also provide additional methodologies and insights for studying reaction kinetics of inorganic ions on mineral surfaces. The use of ATR-FTIR to monitor reaction kinetics has shown very good agreement with traditional batch approaches; for example, for phosphate sorption to goethite ([Luengo et al., 2006, 2007](#)). However, it was not until recent years that very rapid reactions could be studied using FTIR. Software and computing advances now permit rapid collection of data for vibrational spectroscopy and thus permit kinetic study or rapid sorption or transformation (e.g. redox) reactions. Reactions that occur on timescales of just minutes are difficult to observe in situ with most conventional techniques; however, the development of rapid-scan instrumentation and software opens up the possibilities for kinetic FTIR studies. The first application of a rapid-scan ATR-FTIR approach to study oxyanion sorption and transformation focused on the oxidative transformation of arsenite to arsenate on a hydrous

Mn oxide (HMO) mineral surface (Parikh et al., 2008). In that study, a temporal resolution of 2.55 s per scan was presented (24 scans, 8 cm^{-1} resolution) and revealed 50% of the oxidation reaction occurred within the first 1 min of reaction. It was additionally shown that following oxidation of arsenite, arsenate rapidly bound to the HMO surface leading to surface passivation. A follow-up study examined the impact of competing ions (i.e. phosphate), minerals (i.e. $\alpha\text{-FeOOH}$), and bacteria (i.e. *Pseudomonas fluorescens*, *Alcaligenes faecalis*) on the rate and extent of arsenite oxidation via the same hydrous Mn oxide (Parikh et al., 2010) via batch and rapid-scan ATR-FTIR analysis. The data reveal that although the initial rates of oxidation are not greatly impacted, competing ions, biomolecules, and surfaces have a large impact on the extent of reaction via blocking of reactive surface sites and sorption of reaction products. These studies not only demonstrate the rapid nature of Mn oxide catalyzed oxidation of arsenite, but also highlight the importance of considering the heterogeneous nature of natural systems when studying environmental processes. In other studies examining inorganic redox transformations, SR-FTIR provided spatial and temporal resolution to reveal that microbial reduction of toxic Cr (VI) to less toxic Cr (III) from a heavy metal polluted site is stimulated via biodegradation of toluene (Holman et al., 1999). Holman et al. (2002) also used SR-FTIR to show that biodegradation rates of polycyclic aromatic hydrocarbons are enhanced by the presence of humic acids, suggesting that additional labile carbon sources can enhance bioremediation of contaminated soils.

8.3 Bacteria and Biomolecule Adhesion

The development of FTIR as a tool to examine bacteria and biomolecule samples has been critical for increasing our mechanistic understanding of bacteria and biomolecule adhesion on mineral surfaces. This application is particularly well suited to ATR-FTIR spectroscopy investigations as non-destructive in situ studies of bacteria, microbial biofilms, and biomolecules can be conducted in the presence of water biofilms (Nichols et al., 1985; Nivens et al., 1993a, 1993b; Schmitt and Flemming, 1998; Schmitt et al., 1995). In addition, overlapping IR bands arising from biological samples and the mineral substratum are reduced due to the differing “fingerprint” regions for organic and inorganic samples. Table 1.11 provides citations for a number of studies, which have utilized FTIR spectroscopy to study bacteria and biomolecule interactions with mineral surfaces.

The exterior surfaces of bacterial cells are complex, comprised of surface proteins, nucleic acids, EPS, LPS (Gram-negative bacteria), teichoic

Table 1.11 Compiled List of Studies Investigating the Sorption of Bacteria and Biomolecules on Mineral Surfaces

References	Sorbate	Mineral	Analysis Method
Borer et al. (2009)	Aerobactin (<i>E. coli</i>)	Lepidocrocite	ATR-FTIR
Brandes Ammann and Brandl (2011)	<i>Bacillus</i> sp. spores	Bentonite	Transmission FTIR, reflection FTIR
Bullen et al. (2008)	Microbial metabolites	Calcite	ATR-FTIR
Cao et al. (2011)	EPS (<i>Bacillus subtilis</i>)	Montmorillonite, kaolinite, goethite	ATR-FTIR
Deo et al. (2001)	<i>Paenibacillus polymyxa</i> <i>Shewanella putrefaciens</i>	Hematite, corundum, Quartz	Transmission FTIR
Gao and Chorover (2011)	<i>Cryptosporidium parvum</i> oocysts	Hematite	ATR-FTIR
Gao et al. (2009)	<i>Cryptosporidium parvum</i> oocysts	Hematite	ATR-FTIR
McWhirter et al. (2003)	<i>P. aeruginosa</i> , pyoverdine (<i>P. aeruginosa</i>)	Titanium oxide, iron oxide	ATR-FTIR
McWhirter et al. (2002)	<i>P. aeruginosa</i>	Titanium oxide	ATR-FTIR
Ojeda et al. (2008)	<i>P. putida</i>	Hematite	ATR-FTIR
Omoike and Chorover (2004)	EPS (<i>B. subtilis</i>)	Goethite	ATR-FTIR
Omoike and Chorover (2006)	EPS (<i>B. subtilis</i>)	Goethite	DRIFTS, transmission FTIR
Omoike et al. (2004)	EPS (<i>B. subtilis</i> , <i>P.aeruginosa</i>)	Goethite	ATR-FTIR, QCC
Parikh and Chorover (2006)	<i>S. oneidensis</i> , <i>P. aeruginosa</i> , <i>B. subtilis</i>	Hematite	ATR-FTIR
Parikh and Chorover (2008)	LPS (<i>P. aeruginosa</i>)	Corundum, hematite	ATR-FTIR
Rong et al. (2010)	<i>P. putida</i>	Kaolinite, montmorillonite	Transmission FTIR, SEM, ITC
Rong et al. (2010)	<i>P. putida</i>	Goethite	Transmission FTIR, SEM, ITC
Upritchard et al. (2011)	<i>E. coli</i> , enterobactin (<i>E. coli</i>)	Titanium oxide, boehmite	ATR-FTIR
Upritchard et al. (2007)	<i>P. aeruginosa</i> , pyoverdine (<i>P. aeruginosa</i>)	Titanium oxide, iron oxide, boehmite	ATR-FTIR
Vasiliadou et al. (2011)	<i>P. putida</i>	Kaolinite	ATR-FTIR, ¹ H-NMR

QCC: quantum chemical calculations, SEM: scanning electron microscopy, ITC: isothermal titration calorimetry, NMR: nuclear magnetic resonance spectroscopy, ATR: attenuated total reflectance, FTIR, Fourier transform infrared, EXAFS: extended X-ray absorption fine structure spectroscopy, DRIFTS: diffuse reflectance infrared Fourier transform spectroscopy.

acids (Gram-positive bacteria), and other surface biosynthetic molecules that likely are involved in the adhesion process (Wingender et al., 1999). Through ATR-FTIR studies, it has been noted that a certain degree of universality of surface functional groups between bacteria (i.e. Gram-negative, Gram-positive) exists. FTIR spectra reveal that hydroxyl, carboxyl, phosphoryl, and amide groups are common among bacterial cell walls and that the negative charge of bacteria arises from the deprotonation of carboxylates and phosphates (Jiang et al., 2004). The charge of biomolecular functional groups on bacteria surfaces, and of the substratum, is certainly important for the adhesion process.

It is well established that bacteria and many environmental particles exhibit a net negative charge at environmental pH values (Rijnaarts et al., 1995). For example, silica is negatively charged at $\text{pH} > 2.0$ to 3.0 (Sposito, 1989). However, in weathering environments, many siliceous surfaces become coated with a veneer of hydrous Al- and Fe- oxides, which can confer net positive charge even at circumneutral pH (Sposito, 1989). It is therefore significant that ATR-FTIR spectroscopy can be used to examine biomolecule-mineral interactions with surfaces of varying chemical composition and charge. Depending on the sample being studied, untreated IREs (e.g. ZnSe, diamond) can be used to collect spectrum of aqueous phase samples and Ge (GeO_2), due to similarity between the surface chemistry silica, is often used as a surrogate for studying interactions with siliceous minerals. ZnSe is a hydrophobic crystalline material (Reiter et al., 2002; Song et al., 1992) with a point of zero net proton charge (PZNPC) that is < 4 (Tickanen et al., 1997). Ge, on the other hand, has a hydroxylated surface, similar to silica, and is relatively hydrophilic (Snabe and Petersen, 2002). A corresponding PZNPC for Ge was not found in the literature, however it is also presumed to be < 4 when considering that the isoelectric point (IEP) of silica ranges from 2.0 to 2.5 (Gun'ko et al., 1998; Sparks, 1995) and that doping of SiO_2 up to 20% GeO_2 (by mass) had only minimal effects on the IEP (Gun'ko et al., 1998). ATR-FTIR experiments probing biomolecule interactions with other charged surfaces can be conducted using a variety of static and flow-through approaches in the presence of soil minerals. While some studies have examined interactions using mineral suspensions (e.g. Jiang et al., 2010; Parikh and Chorover, 2006; Rong et al., 2010; Vasiliadou et al., 2011), a number of studies have utilized mineral coatings (e.g. Fe-, Al-, Ti-oxides) on IREs in order to modify the surface chemistry of the substratum and examine sorption to a range of environmentally relevant surfaces (e.g. Elzinga et al., 2012; McWhirter et al., 2002; Ojeda et al., 2008; Parikh

and Chorover, 2006). With these approaches the interactions of bacteria and various biomolecules can be monitored in situ with ATR-FTIR to provide insight into their binding mechanisms with various surfaces.

FTIR studies have revealed that bacterial adhesion to clay minerals and other negatively charged surfaces are primarily mediated by interactions with proteins, such as extracellular enzymes, and hydrogen bonding. For example, under flow conditions using a cylindrical ZnSe IRE, *P. putida* (GB-1) biofilm growth corresponds to increased spectral absorbance in the amide I and II regions. Additionally, bacterial adhesion was inhibited when biogenic Mn-oxides were present on the cell exterior due to blocking of positively charged proteinaceous moieties and electrostatic repulsion between the ZnSe IRE and the negatively charged coated bacteria (Parikh and Chorover, 2005). As these experiments were performed with live bacteria it is not possible to conclusively distinguish between membrane-bound proteins and those in the EPS. Combined batch sorption and FTIR studies have demonstrated the preferential adsorption of proteinaceous constituents to montmorillonite and kaolinite, which are primarily negatively charged at environmental pH values (Cao et al., 2011). In this study numerous shifts in peaks associated with the vibrations of water molecules (e.g. 1634 to 1647 cm^{-1}), Si-O (e.g. 1124 to 992 cm^{-1}), and Al-OH (e.g. 906 to 913 cm^{-1}) indicate that the EPS sorption was mediated through hydrogen bonding. Similar nonelectrostatic forces are also involved in live bacterial interactions with these mineral surfaces. Following reaction of *P. putida* with kaolinite and montmorillonite shifts in the IR absorption bands of water molecules (e.g. 3450 to 3442 cm^{-1} and 1637 to 1647 cm^{-1} for kaolinite) are likewise attributed to hydrogen bonding—with much greater sorption observed to kaolinite (Rong et al., 2008). Hydrogen bonding has also been observed in the binding of the O-antigen from bacterial LPS (*E. coli*, *Citrobacter freundii*, *Stenotrophomonas maltophilia*) to TiO_2 , SiO_2 , and Al_2O_3 films on a ZnSe IRE (Jucker et al., 1997).

The ubiquity of negatively charged functional groups in EPS and on the surface of bacteria leads to favorable binding with positively charged mineral surfaces, such as Fe-, Al-, and Ti-oxides. The ability to coat IRE with these minerals makes FTIR a powerful approach for elucidating biomolecule and bacteria binding mechanisms. The collective data reveal that bacterial adhesion to metal oxide surfaces, which are typically positively charged at environmental pH values, is facilitated by carboxylate (Gao and Chorover, 2009; Gao et al., 2009; Ojeda et al., 2008), phosphate (Cao et al., 2011; Elzinga et al., 2012; Omoike et al., 2004; Parikh and Chorover, 2006), and catecholate (McWhirter et al., 2003; Upritchard et al., 2007, 2011)

groups associated with the EPS or cell surfaces. Of course, environmental factors such as pH and bacterial growth conditions have a large effect on these interactions.

Carboxyl groups are present within polysaccharides, amino acids, siderophores, and many other components of EPS, all of which can contribute to conditioning film formation and cell adhesion. Carboxyl groups can form both inner-sphere and outer-sphere complexes with metal oxides surfaces, with the inner-sphere complexes favored at acidic pH (Boily et al., 2000; Gao et al., 2009; Ha et al., 2008; Hwang and Lenhart, 2008). Substantial progress has been made in understanding bacterial adhesion processes through the use of model compounds. For example, elucidation of carboxylate binding mechanisms has been facilitated through FTIR experiments examining amino acids (Norén et al., 2008; Parikh et al., 2011; Roddick-Lanzilotta et al., 1998; Roddick-Lanzilotta and McQuillan, 2000) and model carboxylic acids (Boily et al., 2000; Deacon and Phillips, 1980; Ha et al., 2008; Norén and Persson, 2007). In fact, studies by Alcock and coauthors (1976) and later refined by others (Chu et al., 2004; Deacon and Phillips, 1980; Dobson and McQuillan, 1999), demonstrate that carboxyl binding mechanisms can be inferred through the separation differences ($\Delta\nu$) between the asymmetric carboxylate [$\nu_{as}(\text{COO}^-)$] and the symmetric carboxylate [$\nu_s(\text{COO}^-)$] stretching vibrations [i.e. $\Delta\nu = \nu_{as}(\text{COO}^-) - \nu_s(\text{COO}^-)$] as summarized in Table 1.6.

Following the spectral interpretations for model carboxylate compounds, there is evidence for carboxyl involvement during adhesion of *P. putida* to hematite ($\alpha\text{-Fe}_2\text{O}_3$) under flow conditions, possibly forming bidentate bridging complexes to the mineral surface [$\nu_s(\text{COO}^-)$ shift from 1400 to 1415 cm^{-1} ; $\Delta\nu \approx 150 \text{ cm}^{-1}$], with additional binding interactions through polysaccharides and phosphoryl groups (Ojeda et al., 2008). However, in this case the location of the $\nu_{as}(\text{COO}^-)$ is masked by the amide II band at 1550 cm^{-1} and some uncertainty in $\Delta\nu$ remains. In addition, the determination of surface coordination using this approach was developed for simple organic acids and interpretation of chemically heterogeneous systems such as this may require additional verification through chemical modeling studies. Therefore, although the shift of the $\nu_s(\text{COO}^-)$ is still indicative of inner-sphere coordination (Dobson and McQuillan, 1999; Duckworth and Martin, 2001; Ha et al., 2008), it is possible that other surface complexes exist.

Recent FTIR studies by Gao et al. (Gao and Chorover, 2011; Gao et al., 2009) highlight the importance of carboxyl groups in mediating the adhesion of *Cryptosporidium parvum* oocysts to a hematite ($\alpha\text{-Fe}_2\text{O}_3$) surface, also by extending $\Delta\nu$ interpretation to more complex systems. In these experiments shifts of peaks corresponding to carboxyl groups splitting of

the $\nu_s(\text{COO}^-)$ were used to determine that in NaCl solutions oocysts bind to hematite primarily in monodentate complexes at low pH and in bidentate complexes with increased pH. However, it is noted that at pH values above the PZNPC for hematite, FTIR spectra closely resemble spectra corresponding to unbound oocysts and that outer-sphere coordination is observed. In this study, IR spectra were deconvoluted, permitting determination of $\nu_{as}(\text{COO}^-)$ peak location for calculation of $\Delta\nu$ to empirically determine the oocyst surface coordination.

Siderophores, which are released from bacteria and found within EPS, provide additional functional groups of negative charge, which may mediate cell adhesion processes to metal oxides. Siderophores are a class of low molecular weight Fe^{3+} chelating compounds released by almost all bacteria, including *Pseudomonas* sp. and *E. coli*, in order to increase iron bioavailability (Crowley et al., 1991). The siderophore pyoverdine is produced by *Pseudomonas aeruginosa* and has carboxyl, hydroxyl, hydroxamate, and catecholate functional groups that can bind to Fe^{3+} (McWhirter et al., 2003; Upritchard et al., 2007). Enterobactin, the siderophore produced by *E. coli*, has both salicylate and catecholate binding sites (Upritchard et al., 2011). FTIR studies investigating these biomolecules suggest that pyoverdine and enterobactin play an important role in mediating cell adhesion to metal oxides surfaces (McWhirter et al., 2003; Upritchard et al., 2007, 2011), primarily through inner-sphere binding of catecholate groups to metal centers (e.g. Fe, Ti). These binding mechanisms were determined through analysis of IR spectra of bacteria, siderophores, and model catecholate compounds. For bacterial cells grown in minimal growth media and reacted with TiO_2 coated IREs, a peak at 1286 cm^{-1} for *P. aeruginosa* is consistent with pyoverdine and a peak around 1260 cm^{-1} for *E. coli* is consistent with enterobactin. Other FTIR studies with model siderophores (i.e. desferroxamine B, aerobactin) with lepidocrocite ($\gamma\text{-FeOOH}$) demonstrate possible inner-sphere sorption mechanisms through hydroxamate and outer-sphere coordination via carboxyl groups (Borer et al., 2009). The potential role of siderophores in mediating bacterial adhesion will be maximized in conditions of Fe scarcity, where siderophore production is the greatest (Crowley et al., 1991).

Due to the fact that most of the negative charge on bacterial cell walls are attributed to carboxyl and phosphoryl groups, the role of bacterial phosphate groups should also be considered. Due to the strong polarity of the P–O bond, FTIR spectroscopy is an ideal tool for examining phosphate binding to metal oxides. Phosphate groups originating from phospholipids, DNA, LPS, and other extracellular biomolecules provide potential binding sites to initiate bacterial adhesion to metal oxide surfaces. The binding of

phosphate with Fe oxide surfaces is well documented in numerous ATR-FTIR spectroscopic studies (Barja et al., 2001, 1999; Cagnasso et al., 2010; Tejedor-Tejedor and Anderson, 1990). Omoike et al. (2004) used a combined ATR-FTIR spectroscopy and modeling approach to demonstrate the occurrence of P–O–Fe bonds (1037 cm^{-1}) for extracted EPS reacted with goethite ($\alpha\text{-FeOOH}$) (Figure 1.16). The complementary modeling calculated frequencies for phosphodiester clusters on $\alpha\text{-FeOOH}$ of 1045 cm^{-1} for a monodentate cluster [$\nu_s(\text{FeO-PO})$] and 1027 cm^{-1} for a bidentate cluster [$\nu_s(\text{FeO-P-Ofe})$]. Due to the good correlation between experimental and calculated frequencies the authors suggest that phosphodiester bonds in DNA are involved in the binding of EPS to the mineral surface. Similarly,

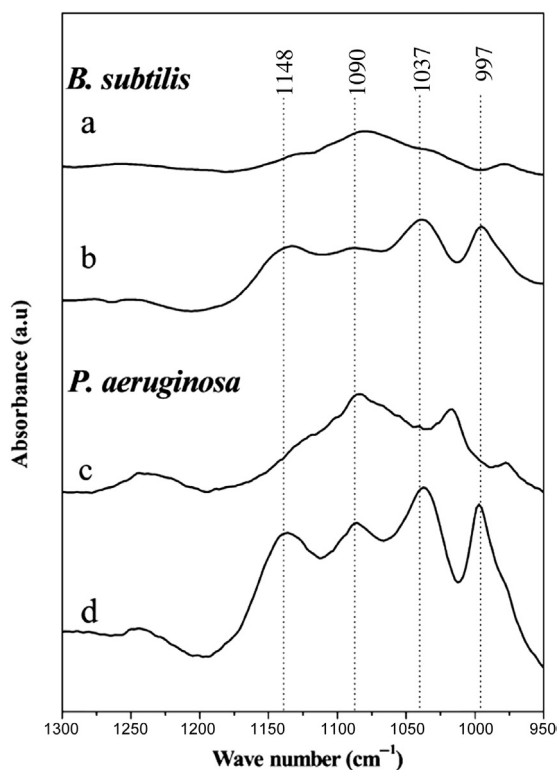


Figure 1.16 ATR-FTIR spectra ($1300\text{--}950\text{ cm}^{-1}$) of solution phase EPS and adsorbed EPS after 60 min reaction time: (a) *B. subtilis* EPS (free), (b) *B. subtilis* EPS after contact with goethite, (c) *P. aeruginosa* EPS (free), and (d) *P. aeruginosa* EPS after contact with goethite (17.9 mg L^{-1} EPS suspension, pH 6.0, and 10 mM NaCl). (ATR, attenuated total reflectance; FTIR, Fourier transform infrared; EPS, exopolysaccharide.) Reprinted with permission from Omoike et al. (2004).

another ATR-FTIR study revealed that phosphatidic acid (phospholipid) reaction with both Fe oxides and hematite ($\alpha\text{-Fe}_2\text{O}_3$) produce Fe-O-P IR bands at 992 ($\alpha\text{-Fe}_2\text{O}_3$) and 997 cm^{-1} ($\alpha\text{-FeOOH}$) which are attributed to inner-sphere coordination of phosphate groups (Cagnasso et al., 2010).

The importance of bimolecular-P interactions with Fe oxides was also demonstrated with ATR-FTIR for live bacteria to $\alpha\text{-Fe}_2\text{O}_3$ (Elzinga et al., 2012; Parikh and Chorover, 2006). When *Shewanella oneidensis*, *P. aeruginosa*, and *B. subtilis* cells were deposited in a ZnSe IRE coated with $\alpha\text{-Fe}_2\text{O}_3$, FTIR peaks emerged at approximately 1020 and 1040 cm^{-1} and were attributed to inner-sphere coordination to the mineral surface (Parikh and Chorover, 2006). Elzinga et al. (2012) demonstrate the impact of pH and contact time for *Shewanella putrefaciens* adhesion to $\alpha\text{-Fe}_2\text{O}_3$. The results of this study show that the initial binding of bacterial cells is mediated by bacterial phosphate groups; however, as bacterial contact times increase to 24 h, FTIR peaks corresponding to proteins and carboxyl groups become more apparent. Additionally, changes in pH impact the protonation of bacterial functional groups and thus impact their coordination to the hematite surface. Although corresponding studies with model compounds (i.e. phenylphosphonic acid, adenosine 5—monophosphate, 2'-deoxyadenyl(3'→5')-2'-deoxyadenosin, DNA) provide additional credence for an important role of bacterial phosphate groups (Parikh and Chorover, 2006), the precise source of phosphate in the EPS mixtures remains unclear.



9. REAL WORLD COMPLEXITY: SOIL ANALYSIS FOR MINERAL AND ORGANIC COMPONENTS

9.1 Soil Heterogeneity and Mineral Analysis

There has long been a desire to use FTIR spectroscopy to identify and quantify specific minerals in mineral/OM assemblages (Russell and Fraser, 1994). The potential utility and challenges for determining allophane/iron-oxide content in soils using FTIR have previously been noted; however, there are other significant challenges for analysis of soil minerals that must be considered as well. Russell and Fraser (1994) identify six factors that must be considered for quantitative determination of minerals using FTIR: (1) particle size of a sample should be $<2\ \mu\text{m}$ to minimize scattering and maximize sample absorption of radiation; (2) diligence must be expressed when weighing and transferring samples during sample preparation; (3) samples should be uniformly dispersed and thoroughly mixed when diluents are

employed (e.g. KBr) for sample preparation; (4) interference of bands from nontargeted minerals or OM should be minimized by choosing bands associated with the target mineral that are adequately isolated in the spectrum; (5) availability of specific mineral standards and the matching of standards to minerals in a sample (e.g. similar crystallinity, elemental composition), the latter is particularly challenging when little is known about the specimen being studied; and (6) the technique employed must generate highly reproducible results. [Reeves et al. \(2005\)](#) expand upon some of these issues and note that differences in methods of FTIR spectra collection (e.g. transmission vs. DRIFTS) may present challenges for utilizing mineral libraries to develop quantitative measures of minerals using FTIR.

Many studies investigating the utility of FTIR for mineral quantification have investigated artificially mixed mineral matrices to calibrate and validate a particular approach ([Bertaux et al., 1998](#); [Madejová et al., 2002](#); [Matteson and Herron, 1993](#)). Others have calibrated their approach using mineral assemblages and validated the approach using clays or rocks of known mineral composition as determined by XRD ([Breen et al., 2008](#); [Kaufhold et al., 2012](#)). There have also been some who have applied models to quantify mineral content in soils ([Bruckman and Wriessnig, 2013](#)). Although mineral quantification with FTIR can be quite challenging, depending on the intended application the level of difficulty in quantification of soil mineral composition using FTIR may not present a significant issue. However, to achieve more widespread application, it is necessary to validate an MIR method using soils, which contain a complex assemblage of minerals and OM. An alternative approach to using MIR spectroscopy is visible/near-infrared (VNIR) spectroscopy, which has been demonstrated by [Viscarra Rossel et al. \(2009, 2006\)](#) to show some promise.

The presence of exploration rovers on Mars has increased interest in the use of vibration spectroscopy for identifying and quantifying specific minerals in mineral assemblages ([Bishop et al., 2008, 2004](#); [Villar and Edwards, 2006](#)). For example, [Bishop et al. \(2004\)](#) demonstrated the use of VNIR and MIR spectroscopy for identifying hydrated sulfates in samples from acidic environments on Earth that may have application for identifying minerals in sulfate-rich rocks and soils on Mars. [Villar and Edwards \(2006\)](#) discuss and demonstrate the potential for the use of Raman spectroscopy for identifying minerals, such as carbonates, on Mars. [Bishop et al. \(2004\)](#) discuss phyllosilicate diversity in rock outcrops on Mars determined from VNIR data captured by the Mars Reconnaissance Orbiter/Compact Reconnaissance Imaging Spectrophotometer. Although soils of Mars are presumed to

lack extensive OM quantities (Summons et al., 2011), which would further convolute the vibrational spectra, it seems possible or even probable that significant advancements for accurately identifying and quantifying minerals in Earth's soil using vibrational spectroscopy may be associated with extraterrestrial exploration efforts.

9.2 Differentiating Mineral and Organic Spectral Absorbance

Soils contain organic C in a great variety of chemical forms. The soil C molecular structure is important, because it is one of the potential determinants of SOM recalcitrance, which has significant implications for soil and environmental quality. Soils contain a rich organic chemical diversity, from labile fatty acids, carbohydrates, and proteins, to more processed and condensed molecules, and highly insoluble, nonhydrolyzable forms of older C. Soil C molecular structure is an active area of research with many extraction methods and instrumentation technologies being evaluated. These approaches include combustion analyses, NMR spectroscopy, incubation and curve fitting, and pyrolysis molecular beam mass spectrometry (py-MBMS), among others. These methods are all contributing to our understanding of soil C quality, but MIR spectroscopy is a particularly valuable tool for soil scientists. This is especially true when different methodologies are used side-by-side, affording a more comprehensive picture of the chemical makeup of soil samples.

One of the challenges for soil scientists studying soil C chemistry via MIR data is identifying the spectral bands that can be fully or partially ascribed to organics, as opposed to the regions that are more affected by mineral absorption. Soils are predominantly mineral in nature, and even Histosols can have a substantial mineral content, which can hinder spectral interpretation (Reeves, 2012). Soil MIR spectra generally contain several regions that can be highly influenced by minerals. The presence of kaolinite, smectite, or illite clays will result in a peak near 3620 cm^{-1} due to hydroxyl stretching in aluminosilicate (Nguyen et al., 1991) (Figure 1.17). The region between 1790 and 2000 cm^{-1} often has three characteristic peaks due to silicates. It is not surprising then that absorbance within this region can correlate negatively with total soil C and N (Calderón et al., 2011a). Carbonates absorb in the region between 2995 and 2860 cm^{-1} and can cause a peak with a shoulder near 2520 cm^{-1} . The carbonate absorbance between 2995 and 2860 cm^{-1} will interfere with aliphatic CH bands, so it is beneficial to decalcify soil samples before scanning in order to rid the sample of carbonate interference (Reeves, 2012). Perhaps one of the most obvious mineral features in neat soil spectra is the “w”-shaped silicate inversion band

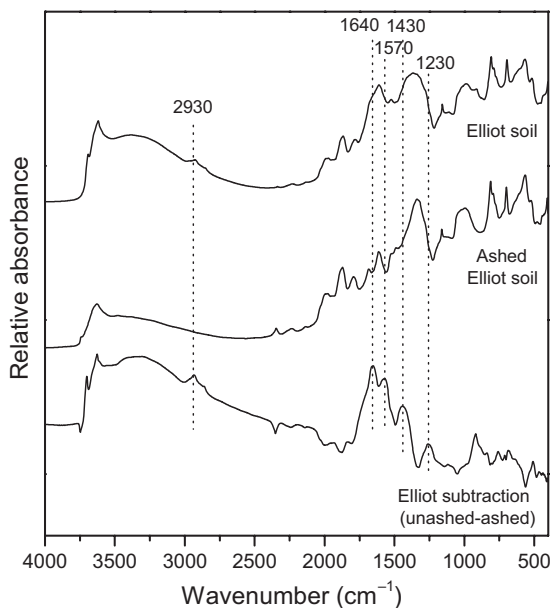


Figure 1.17 DRIFTS spectra of Elliott soil, ashed Elliott soil (550 °C for 3 h), and subtraction of the unashed-ashed spectra. Soil obtained from the International Humic Substances Society. (DRIFTS, diffuse reflectance Fourier transform infrared spectroscopy.)

that occurs between 1280 and 1070 cm^{-1} due to specular reflection (Figure 1.17). This inverted band may interfere with absorbance from carbonyls and other important functional groups. The inverted band is not present in KBr diluted samples (typically 5–10% soil or mineral), forming a broad peak instead, but the advantages of scanning a KBr–soil mixture need to be weighed against the convenience of scanning neat soils.

Studies on NMR spectroscopy of soils have used pretreatment with hydrofluoric acid (HF) in order to reduce the influence of minerals on the soil spectra, and that way enhance the resolution of organic signals (Rumpel et al., 2006). However, SOM molecular structure can be studied by DRIFTS on undiluted soils as long as mineral interferences and specular reflection are taken in account (Demyan et al., 2012) and there are no artifacts of HF treatment (e.g. Rumpel et al., 2006). Furthermore, the ability to detect mineral features (e.g. clays, sands, and carbonates) may be a benefit rather than a disadvantage, because soil texture and clay protection are important pieces of the puzzle in the study of SOC dynamics. Pretreated or whole soil spectra both hold important, albeit different kinds of information. It is all a matter of properly resolving the soil spectral traits that are relevant for a given research question.

Previous work has relied on ashing (e.g. 550 °C, 3 h) of the soil sample followed by the subtraction of the ashed soil spectrum from the intact soil spectrum. The ashing removes the organic C from the sample, so the subtraction helps to accentuate some of the organic bands in the spectrum (Calderón et al., 2011a,c; Sarkhot et al., 2007b). Figure 1.17 shows the ash subtracted spectrum, the intact soil spectrum, and the subtraction for a soil sample. The subtracted spectrum highlights several organic bands including the 2930–2830 cm⁻¹ bands for aliphatic C–H (Haberhauer and Gerzabek, 1999). The peak at 1640 cm⁻¹ is possibly C=O from amides, aromatic C=C, or carboxylates. The subtracted features at 1570 cm⁻¹ (amide II band), 1430 cm⁻¹ (C–O vibrations or C–H deformation), and 1230 cm⁻¹ (aromatic ring C–H) also comprise organic absorbances.

Recently, it has been noted that these ashing subtractions need to be interpreted with caution because the heating of minerals can affect their spectral properties, and the removal of organics can cause artifacts due to altered specular reflection in the sample (Reeves, 2012). However, the aliphatic CH regions (3000–2800 cm⁻¹) and the region between 1750 and 1600 cm⁻¹ are relatively free of those artifacts and can be accurately subtracted. This is significant because the range between 1750 and 1600 cm⁻¹ is considered part of the fingerprint region that contains information about many important functional groups like amides, carboxylates, and aromatics that can be determinants of SOM quality. Subtractions outside these regions will need more judicious interpretation and involve assumptions that may or may not be met. While the accuracy of ashing subtraction spectra for analytical purposes may be limited, these spectra may still be useful when fingerprinting of soils is the chief objective, as in forensic studies (Cox et al., 2000). Additional discussion on removal of organic C from soil is provided in section 10.3.

For future studies, other modes of oxidation, such as hypochlorite treatment, should be investigated as alternatives to ashing–subtraction so that the effects of the heating of clays can be avoided. Another interesting approach will be to simply use wet chemistry extraction procedures to isolate different soil C pools and that way avoid the presence of mineral bands altogether. For example, HS can be obtained from soils and the characteristics of the humic and fulvic acids can be studied in detail via DRIFTS. Also, as previously mentioned, soils can be extracted with hot water and the dried extracts scanned directly to study the extracted carbon fraction, which is thought to contain labile organics (Demyan et al., 2012). Already a common FTIR–extract approach is DRIFTS of organics extracted sequentially by water and sodium pyrophosphate (He et al., 2012, 2011b; Kaiser and

Ellerbrock, 2005; Kaiser et al., 2007). Other possible fruitful approaches could include the analysis of nonhydrolyzable soil C, which has been shown to be old and recalcitrant (Follett et al., 2007). For the study of low mean residence time (MRT) SOM, density fractionation allows for the isolation of the LF (see below), a mostly organic material that consists of recently added plant residues (Calderón et al., 2011c).

Several studies have used ratios of specific spectral bands in environmental samples and soils to study the chemical composition of SOM (Artz et al., 2006; Calderón et al., 2006; Ellerbrock et al., 2005). Ellerbrock et al. (2005) related the wettability of soils to hydrophilic to hydrophobic band ratios. Artz et al. (2006) calculated the ratio of carboxylate to polysaccharide peak intensities and related it to the decomposability of organic soils. The band ratio approach can thus be used to minimize inorganic interferences and in effect normalize the data to resolve baseline issues. For example, Demyan et al. (2012) used the ratio of 1620–2930 cm^{-1} band areas as an index of SOM stability. This ratio is thought to measure the proportion of conjugated groups (aromatics, carboxylic acids, quinones) to aliphatic methyl groups, thus giving an index for SOM condensation. Assis et al. (2012) used the band ratio approach to determine hydrophobicity and condensation in SOM, which are related to the resistance to decomposition of SOM. The ratio 2929 to 1035 cm^{-1} represents apolar methyl groups to polar (C–O, –OH) groups. Similarly Matějková and Šimon (2012) used 3000–2800 cm^{-1} as an indicator of hydrophobic component, and 1740–1600 cm^{-1} to indicate hydrophilic components. Ding et al. (2002) calculated the ratios of labile (O-containing) to recalcitrant functional groups in humic acids. Oxygen containing groups are preferentially utilized by soil microbes, so absorbances such as 1727, 1650, 1160, 1127, 1050 cm^{-1} were considered labile, while absorbances at 2950, 2924, 2850, 1530, 1509, 1457, 1420, 779 cm^{-1} were considered resistant. Recently, Veum et al. (2014) used approaches similar to Demyan et al. (2012) and Ding et al. (2002) to study relationships between DRIFTS derived indices of decomposition stage (i.e. potentially reduced biological reactivity) and other measures of SOM lability. The authors noted all five decomposition indices (three relating aromatic to aliphatic moieties and two relating recalcitrant to O-containing functional groups) were negatively related to soil microbial dehydrogenase activity ($r = -0.63$ to -0.76 ; $p < 0.05$), potassium permanganate oxidizable-C ($r = -0.83$ to -0.95 ; $p < 0.001$), and water-extractable OC ($r = -0.66$ to -0.82 ; $p < 0.05$). Although the argument for using the lack of O-containing functional groups as an indicator/estimate of more resistant groups requires further testing (e.g. fatty acids rich in C–H

are relatively easily degraded by soil microbes), the work of [Veum et al. \(2014\)](#) demonstrates a linkage between DRIFTS measures of decomposition stage and microbial function.



10. FTIR SPECTROSCOPY FOR SOM ANALYSIS

Most soils are predominantly composed of minerals, from purely mineral soils to the outlier of 25% soil OC of Histosols ([Woodwell, 1984](#)). In general, surface horizons tend to contain more SOM (1–5% soil OC) and OC content in some subsoil horizons may be nearly undetectable. This relatively low OC content in soils presents a challenge for the spectroscopic study of OM, and the challenge is currently addressed by three broad experimental approaches. These FTIR spectroscopy approaches include: (1) whole soils, with low absorbance values for OM bands nonetheless quantified; (2) soil fractions enriched in OM, or SOM extracts with minor mineral components; and (3) calculation of subtraction or difference spectra, in which a spectrum of SOM is obtained indirectly by subtraction of an SOM removal treatment (e.g. combustion, oxidation).

10.1 SOM Analysis in Whole Soils

Some chemical insights of SOM can be gained from scans of whole soils. Meaningful quantification or even detection of SOM can be difficult due to the low intensity of organic absorbances relative to the dominance of mineral absorbances, in particular silicates [$\nu(\text{Si}-\text{O})$ 1070–950 cm^{-1}]. Considerable overlap of SOM and mineral absorbances can occur, in particular 1400–400 cm^{-1} , making unambiguous assignments for mineral and organic moieties challenging ([Calderón et al., 2011b](#)). Advantages of using soil samples include minimal or no sample preparation, quantitative assessments of SOM, and additional data on the soil matrix (e.g. moisture content, soil mineralogy). For instance, whole soil samples have been employed in indices of hydrophobicity–hydrophilicity contributed to by OM ([Ellerbrock and Gerke, 2004](#); [Ellerbrock et al., 2005](#); [Matejkova and Simon, 2012](#); [Simon, 2007](#); [Šimon et al., 2009](#); [Simonetti et al., 2012](#)). Areas of the aliphatic $\nu(\text{C}-\text{H})$ band at 3000–2800 cm^{-1} as the hydrophobic region and a hydrophilic region of $\nu(\text{C}=\text{O})$ at 1740–1600 cm^{-1} of whole soil spectra provided hydrophobic/hydrophilic ratios. Intensity of absorbance of these functionally defined regions was also employed to obtain indexes of hydrophobicity. These regions correspond to SOM components related to wettability ([Ellerbrock et al., 2005](#)). Previous work has established hydrophobic

components of FTIR absorbances (Capriel et al., 1995) and these as a function of management (Capriel, 1997).

Employing the same ratio of absorbances to track soil wettability and sorption properties, more recent studies have extended to different spatial scales and dimensions of SOM, from the three-dimensional microaspect of soil aggregates to landscapes. SOM hydrophobicity was evaluated with the aliphatic:carbonyl band ratios previously described over a chronosequence in the Swiss Alps (Egli et al., 2010). The same band ratio has been used for in situ FTIR mapping of soil physical structures, including pores, cracks, and earthworm tunnels, revealing significant heterogeneity in hydrophobicity and general SOM composition at the millimeter scale (Ellerbrock et al., 2009). It should be noted that in situ FTIR often requires untangling primary reflection, primary absorption, and diffuse reflection (i.e. Kubelk–Munk transformation) as a result of surface topology effects. A recent review addresses the physics of DRIFTS spectroscopy and the use of data transformation like Kubelk–Munk, to account for potentially interfering reflectance behaviors (Torrent and Barrón, 2008).

Performing FTIR of SOM with bulk soil on the same soil type is a strategy to control for mineral absorbances in order to highlight differences in SOM-based spectral features. This increases the sensitivity of organic bands with possible or partial mineral contributions, and is well suited for block treatment experiments (Demyan et al., 2012; Giacometti et al., 2013).

10.2 SOM Analysis via Fractions and Extracts

The dominance of FTIR spectra by mineral absorptions in whole soil samples typically prevents detailed investigation of SOM. As a result, researchers commonly use extractions of representative or C-enriched fractions in order to obtain detailed FTIR data on the organic component of soil (Simonetti et al., 2012). SOM fractions can be highly enriched in OM or are dominantly OM, allowing for better detection. This can be particularly useful for evaluating the effects of land-use, climate, and vegetation on SOM. The use of SOM fractions or extracts complements the theoretical approach to SOM as the sum of a number of pools of organic carbon, often overlapping at functional and structural levels. Moreover, these enriched OM fractions enable, greater FTIR detection of organic bands. FTIR of organic fractions can be used to track changes in SOM composition over time and in response to land management. Molecular resolution of SOM enhances the utility of these fractions beyond mass balance values and also allows controlling for potentially confounding effects of composition variation within a fraction.

Chemical and physical fractionation of samples enriched in or composed of SOM allows comparative changes in chemical composition to be assessed from the increased resolution of organics compared to whole soils. Chemical and physical fractionation can be coupled to increase the specificity of FTIR data, as was done by Simonetti et al. by extracting humic acids from macroaggregates, microraggregates, and the silt + clay fraction (Simonetti et al., 2012). FTIR analysis of SOM using chemical and physical fractionations are discussed below.

10.2.1 Chemical Extracts and Fractionation

In the literature, a number of chemical extracts of SOM have been analyzed by FTIR. Commonly studied fractions are dissolved organic matter (DOM) or water-extractable organic matter (WEOM) (He et al., 2011a, 2012; Kaiser and Ellerbrock, 2005; Kaiser et al., 2007; Peltre et al., 2011), and HS, which will be discussed shortly. Kaiser and He also report the use of pyrophosphate-extractable organic matter (PEOM) as an SOM fraction of intermediate stability suitable for FTIR characterization, using the ground freeze-dried extract to avoid water interference (He et al., 2011b; Kaiser and Ellerbrock, 2005). ^{14}C dating and greater carbonyl absorbance of $\nu(\text{C}=\text{O})$ at 1710 and 1690 cm^{-1} in spectra of PEOM relative to WEOM suggests the former as an older, more stabilized fraction (Kaiser and Ellerbrock, 2005). FTIR characteristics of PEOM characterized were sensitive to soil type and crop rotation, unless fertilized by manure, which consistently increased carbonyl content of amide and carboxylate $\nu(\text{C}=\text{O})$ at 1740 – 1700 and 1640 – 1600 cm^{-1} , respectively. The lower $\nu(\text{C}=\text{O})$ absorbance of WEOM suggests PEOM as a more appropriate pool for evaluating organic amendments on SOM (Kaiser et al., 2007, 2008). Organic absorbances of WEOM extracts from potato cropping systems reflected irrigation treatment types through aliphatic $\nu(\text{C}-\text{H})$ at 3020 – 2800 cm^{-1} and aromatic $\nu(\text{C}=\text{C})$ at 1640 – 1600 cm^{-1} , in contrast to PEOM (He et al., 2011b). The high sensitivity of WEOM to labile organics make FTIR spectra of this fraction a means to track changes in aliphatic and proteinaceous material during municipal waste composting (He et al., 2011a).

10.2.2 HS: A Common SOM Extract for FTIR Analyses

The most common method of SOM fractionation for FTIR employs an OM pool referred to as HS. HS have been traditionally understood as a pool of stabilized, recalcitrant SOM (Kleber and Johnson, 2010; Schnitzer and Monreal, 2011). HS are an alkaline-soluble fraction of SOM, and FTIR is

performed on further fractions based on solubility in acid and base (Kerek et al., 2003; Mao et al., 2008; Senesi et al., 2007; Simonetti et al., 2012; Watanabe et al., 2007). These operationally defined components of HS include humic acids (HA), fulvic acids (FA) and humin, with similar postulated structures but differing and characteristic molecular weight, elemental composition, and functional group content (Khan, 1975). One of the early applications of FTIR in soil was the analysis of HS (e.g. Filip et al., 1974; Kodama and Schnitzer, 1971), and the FTIR characterization of HS composition from not only soils but also sediments and aquatic environments is well established. For this reason, discussion will focus on more recent advances in FTIR of HS and its applications in various contexts. For a review of FTIR analysis of HS readers are referred to Stevenson and Goh (1971).

FTIR spectroscopy of HS is particularly insightful when used in tandem with complementary molecular-level characterizations. FTIR provides information on functional groups, often coupled with ^{13}C NMR spectroscopy to corroborate observed distribution of carbon environments, or vice versa. The uniqueness of FTIR in these complementary approaches lies in its ability to provide molecular context to carbon environments measured by NMR. Additionally, noncarbon components of SOM and HA, such as sulfur and phosphate, can be simultaneously characterized with FTIR (Tatzber et al., 2008).

Along with NMR spectroscopy, elemental analysis is commonly coupled with FTIR for molecular-level analyses of HS (Tatzber et al., 2008). In the latter case, FTIR is used as a standard and non-destructive component of a spectroscopic toolkit to fully characterize HS, including UV–vis spectroscopy, fluorescence spectroscopy, electron spin resonance spectroscopy and NMR spectroscopy (Matilainen et al., 2011). Mass spectrometry methods are also common (e.g. Baglieri et al., 2012), and photochemical characterization has been suggested as an additional spectroscopic measurement (Uyguner-Demirel and Bekbolet, 2011).

FTIR spectra of HS have been frequently employed as a marker pool to monitor changes in the more recalcitrant portion of SOM. Though the utility of alkaline extracts as an SOM pool of functional significance is contested (Kleber and Johnson, 2010; Schmidt et al., 2011), these pools may find limited use as a standardized extract for monitoring SOM. Multiple FTIR studies on SOM employ HS, and direct comparisons of DRIFT and transmission (Baes and Bloom, 1989), and DRIFT and photoacoustic (PAS) FTIR (Du et al., 2013a) reveal that comparable spectra of HS are obtained across the varied sampling approaches.

FTIR has helped further understanding of HS chemistry, corroborating and revealing characteristics of HS fractions like functional group differences between HA and FA, and the variation of these as a function of environment. For instance, C–H bending vibrations at 1460 cm^{-1} suggest alkyl enrichment of FA relative to HA (Zhang et al., 2009), though aliphatic content of HS as measured by C–H stretching at $3000\text{--}2800\text{ cm}^{-1}$ can vary significantly as function of age and/or soil depth (Mafra et al., 2007; Marinari et al., 2010; Tatzber et al., 2007).

HS are particularly rich in functional groups detectable by FTIR such as carboxylic, carbonyl, and hydroxyl moieties that can interact with agrochemicals and heavy metals through complexation, ion exchange, and reduction (Sparks, 2002). FTIR has been used to understand sorption of Hg^{2+} to HA and FA, occurring through C=O (1628 cm^{-1}) and O–H (3446 cm^{-1}) groups (Zhang et al., 2009), quantify functional group differences between HA and FA to predict suitability for iron ore aggregation (Han et al., 2011), and reveal HA sorption and oxidative-mediation of Sb(III) to Sb(IV) of soils along highways (Ceriotti and Amarasiwardena, 2009). Binding mechanisms with HS have been elucidated for cations like Cu^{2+} (Alvarez-Puebla et al., 2004; Piccolo and Stevenson, 1982), Pb^{2+} , Ca^{2+} (Piccolo and Stevenson, 1982), and Al^{3+} (Elkins and Nelson, 2002), and agrochemicals, including atrazine (Martin-Neto et al., 1994; Sposito, 1996), hydroxyatrazine (Martin-Neto et al., 2001), glyphosphate (Piccolo and Celano, 1994), paraquat and chlordimeform (Maqueda et al., 1993), and metribuzin (Landgraf et al., 1998).

The carboxyl groups that lend HS much of its characteristic properties, including pH-dependent structure and high chemical reactivity (e.g. metal complexation, pH buffering), can be studied by FTIR in great detail. Hay and Myneni found evidence of highly similar structures for HA of different origins using the carboxylate $\nu_a(\text{C–O})$ band as a sensitive indicator of structural environment (Hay and Myneni, 2007). ATR-FTIR of five HS obtained from the International Humic Substances Society revealed a common carboxylate $\nu_s(\text{C–O})$ peak at 1578 cm^{-1} with similar narrow peak width, suggesting a high degree of structural similarity in carboxylate moieties of HS independent of source (e.g. soil, river). Comparison of the peak position of the carboxylate band of the five HS with a suite of carboxylate-containing model compounds suggested the presence of carboxyl structures similar to those of low molecular weight aliphatic acids of gluconate, D-lactate, methoxyacetate, acetoxyacetate, and malonate, and aromatic acids of salicylate and furancarboxylate. The strong pH-dependence

of the carboxylate band in FTIR spectra highlights increasing deprotonation of carboxylic acids with increasing pH (Gondar et al., 2005; Martin-Neto et al., 1994).

FTIR spectroscopy of HS can be used to evaluate agricultural management effects on SOM. Such studies commonly employ a handful of select absorbance bands and/or band ratios, and typically address the impact of the two main ways in which management can alter SOM quantity and quality: tillage and amendments. HA composition changes have been tracked by FTIR in agroecosystems as a function of amendments, including manure (Watanabe et al., 2007), organic waste (Brunetti et al., 2012), and fertilizers (Ferrari et al., 2011; Simonetti et al., 2012; Watanabe et al., 2007), cover crops (Ding et al., 2006) tillage, irrigation, and crop rotations (Ding et al., 2002; He et al., 2011b), or some combination thereof (Senesi et al., 2007; Verchot et al., 2011). However, some may question the use of FTIR data on HS to draw conclusions about the larger SOM pool. Though HS extracts are generally free of mineral absorbances, their recalcitrance as a stabilized OM pool can make them ineffective windows into SOM changes, even with extreme treatments or over many seasons. For instance, only at high manure addition rates ($160 \text{ Mg ha}^{-1} \text{ yr}^{-1}$) were the effects of continuous manure application reflected in HA composition (Watanabe et al., 2007). Spectra of HA across manure treatments were highly similar, and the absorbance intensity of the amide I band best discriminated among manure treatments, suggesting differences in peptidic or proteinaceous forms in soil organic N pools. Also unique to the HA spectra of high manure treatment was increased absorbance at the aliphatic C–H band $3000\text{--}2900 \text{ cm}^{-1}$ and carbohydrate C–O band $1150\text{--}1040 \text{ cm}^{-1}$. Similarly, effects of high manure application have been observed in intermediately labile SOM fractions like PEOM as increased absorption of carbonyl C=O at 1710 cm^{-1} (Kaiser and Ellerbrock, 2005). Across a variety of land-use in the Philippines, including primary forest, restored forest, and plantations, there were no appreciable differences of HA and FA as characterized by FTIR, though differences were also not found by elemental analysis (Navarrete et al., 2010).

FTIR of HS has been used to evaluate differential tillage regimes on humification and SOM quality. In contrast to SOM as a nutrient reservoir, tillage may provide a more suitable context for FTIR of HS because soil disturbance is known to affect SOM dynamics and decomposition, including humification processes (Tatzber et al., 2008). This approach is often used to evaluate tillage practices, including no-till (Ding et al., 2002; González Pérez et al., 2004; Tatzber et al., 2007). Similarly, the effects of fallow and

amendment treatments have been tracked through changes in ^{14}C -labeled HA functionalities over a 36-year experiment with FTIR and NMR. With manure vs straw treatment, and crop diversification and land cover (rotation vs. monoculture vs. fallow), general aromatic and carbonyl content decreased, with specific decreases in benzene and methyl absorbances, whereas amide bands and sulfone and/or ester absorbance increased (Ohno et al., 2009; Tatzber et al., 2009). HA functionalities sensitive to tillage and amendments include aromatic $\nu(\text{C-H})$ at 3050 cm^{-1} , carbonyl $\nu(\text{C=O})$ at 1700 cm^{-1} , amide $\nu(\text{C=O})$ at 1650 cm^{-1} (amide I) amide $\nu(\text{C-N})$ at 1420 cm^{-1} (amide III), sulfone $\nu(\text{S=O})$ at 1315 cm^{-1} with possible ester contributions, aromatic out-of-plane $b(\text{C-H})$ at $873\text{--}728\text{ cm}^{-1}$, and $\text{sp}^3\text{-CH}_2$ and mono-/di-substituted benzene rings at 766 cm^{-1} . FTIR of HS is also sensitive to climate, vegetation cover, and geologic features, allowing discrimination of HA by soil suborder level and humus type (Fernández-Getino et al., 2010).

FTIR for HS characterization extends beyond agricultural contexts and finds use in related areas like archeology, air and water quality, and compost production. FTIR has been used to study the mechanisms of HA formation in archeological samples (Ascough et al., 2011), analyze HA-like fractions from dust macromolecules (Zhao and Peng, 2011), and evaluate water fouling and treatment (Howe et al., 2002; Kanokkantapong et al., 2006). The use of FTIR for analyzing composition and quality of composts, industrial organic wastes, and sewage sludge, and their effects on SOM quality as soil amendments or disposed wastes, is well established (Martínez et al., 2012; Smidt and Meissl, 2007) and has been used to monitor humification during composting (Jouraiphy et al., 2008; Smidt and Schwanninger, 2005) as well as discerning compost quality as a function of feedstock and method (Carballo et al., 2008a; Fialho et al., 2010).

One HS-specific FTIR approach to monitor changes in recalcitrant or long MRT SOM involves two HA subfractions differentiated by cation-binding affinity: calcium-bound humic acid (CaHA) and noncalcium-bound, mobile humic acid (MHA) (Olk et al., 2000; Ve et al., 2004; Whitbread, 1994). MHA is younger and N-rich relative to CaHA, which is consequently less involved in nutrient cycling. Peptide enrichment of the MHA accounts for its greater ability to provision N (Mao et al., 2008). Notably, FTIR can only partly distinguish the increased peptide content of MHA relative to CaHA due to masking of peptide absorbances [amide $\nu(\text{C=O})$, $\nu(\text{C=N})$] by aromatic signals [C-O-CH_3 1224 cm^{-1} , $\nu(\text{COO}^-)$], illustrating a potential drawback in FTIR of heterogeneous organic samples. Yet

unlike NMR, FTIR was able to detect differences in phosphate [$\nu(\text{P-O})$ 1075–1028 cm^{-1}], with partial overlap of alcohol $\nu(\text{O-H})$ and ether $\nu(\text{C-O})$ among HA subfractions and soils, reflecting known differences in soil P content. Phosphate P–O bonds at 1100–1000 cm^{-1} have been shown to be detectable in FTIR spectra of HS and correlate with phosphorus content of humic fractions (He et al., 2006). The MHA-CaHA FTIR method has also been used to assess N storage in soils for nutrient management in various crop systems, including lowland rice, legumes, and turfgrass (Kerek et al., 2003; Olk et al., 1999, 2000; Slepetiene et al., 2010).

10.2.3 SOM Analysis Following Physical Fractionation

Physical fractionation of soils according to settling properties and aggregate size affords a way of obtaining different types of SOM that vary in their chemistry, decomposability, and age (Assis et al., 2012; Calderón et al., 2011c). Physical fractionation of SOM is commonly performed to understand C cycling and SOM partitioning. These fractions, including soil aggregates, are particularly favorable for FTIR study because they provide distinct information on their own. FTIR characterization, which can be performed with little or no additional sample preparation to molecularly resolve these fractions. FTIR analysis of physical fractions can thus improve understanding of organomineral interactions that exert controls on SOM stabilization and turnover (Kögel-Knabner et al., 2008; Six et al., 2004; Wiseman and Püttmann, 2006). Physical aggregate fractions can serve as C-enriched soil samples with increased organic IR absorbance for improved SOM characterization. SOM composition among individual aggregate fractions and bulk soil allows detailed evaluation of the effect of different tillage and cropping regimes on soil chemistry and nutrient cycling (Calderón et al., 2011a; Davinic et al., 2012b; Tõnon et al., 2010; Verchot et al., 2011). The use of FTIR for characterizing soil physical fractions is not limited to providing mean SOM composition on ground samples; surface and other spatial characterization is possible (Leue et al., 2010b).

While there are different fractionation schemes being used today, the fractions may consist of a LF that floats in a high-density solution, POM that is rich in organics but usually contains some sand, and finally the finer materials that separate by settling such as the clay-sized and silt-sized fractions (Haile-Mariam et al., 2008). Different fractionation procedures are also able to separate occluded soil C fractions or free fractions that occur inside and outside of soil aggregates (Assis et al., 2012). Aggregate classes in effect contain different forms of SOM that vary in their role in soil C

accrual. Intraaggregate microaggregates, for example, are thought to contain protected/recalcitrant C important for C sequestration. Macroaggregates, in turn, are responsive to tillage and contain some labile C (Oades, 1984). Sarkhot et al. (2007b) studied aggregate size fractions from a forested Spodosol and showed that polysaccharide bands in 250- to 150- μm aggregates could be indicative of aggregate binding agents secreted by microorganisms. One interesting aspect of physical fractionations is that clays and sands become enriched in different SOM chemical fractions and depleted in others, which needs to be taken into account during spectral interpretation (Fultz, 2012).

One advantage of soil physical fractions for FTIR is minimization of particle size effects on IR reflectance. Heterogeneous particle size of samples, like bulk soils, can produce inaccurate absorbances as a result of different reflectance patterns, in particular for DRIFTS. For instance, the homogeneity of textures within soil sets is thought to be partly responsible for the success of FTIR-calibrated models for soil C and N prediction (Cozzolino and Morón, 2006). Increased particle size homogeneity improves the consistency of diffuse reflectance (Dahm and Dahm, 2001). Absorbance is inversely proportional to particle size, such that soil samples containing a range of clay- to sand-sized particles may produce biases in FTIR data like disproportionately greater absorbance of sand-associated OM. The accuracy of FTIR quantification of soil C and N often varies by texture class within a given soil, and depending on the particular soil a texture fraction can have significantly different predictive accuracy (Cozzolino and Morón, 2006). For instance, soil C often strongly correlates with clay and silt C. In some cases correlations between C or N fractions and texture fractions are poor despite a theoretical expectation otherwise. For instance, stronger correlations can be found between soil C and fine sand C relative to coarse sand C (Cozzolino and Morón, 2006). In addition to confounding effects on reflectance, particle size heterogeneity can also encompass SOM variation that leads to absorbance bias by certain functional groups. Given the diversity of organic functional groups, components of SOM can differ in their absorbance of IR and thus be differentially sensitive to FTIR quantification. For instance, POM encompasses a range of humification products, generally increasing in humification with decreasing POM size. Large POM is thought to represent lightly processed litter ($>1000\ \mu\text{m}$) whereas small POM contains humified SOM ($<53\ \mu\text{m}$). The accuracy of FTIR measurements of soil C and N are lower for clay fractions compared to fractions of larger SOM size, mostly notable POM and sand-associated OM. This is thought to reflect the different sensitivity of FTIR to broad differences

in SOM quality, like nonhumified vs humified OM (Yang et al., 2012). Likewise, FTIR calibration models of SOM content have found improved predictions with decreasing particle size, which are thought to be the result of coarser particles ($>20\ \mu\text{m}$) having more heterogeneous SOM distribution (Barthès et al., 2008).

The use of FTIR spectroscopy in conjunction with size fractionations has yielded good insights regarding the chemistry of different forms of C in soil. For example, spectral data shows that the LF and POM are possibly made up of partially decomposed plant residues of relatively short MRT. Calderón et al. (2011c) showed that spectral differences between the size fractions are maintained across soils from different locations from the Corn Belt. For example, the LF absorbs markedly at 3400 and $1750\text{--}1350\ \text{cm}^{-1}$ (Figure 1.18). The POM also has relatively high absorbance at $1360\ \text{cm}^{-1}$. Long-term incubation shows that the LF loses absorbance at $3400\ \text{cm}^{-1}$, and $2920\text{--}2860\ \text{cm}^{-1}$, suggesting the decomposition of labile

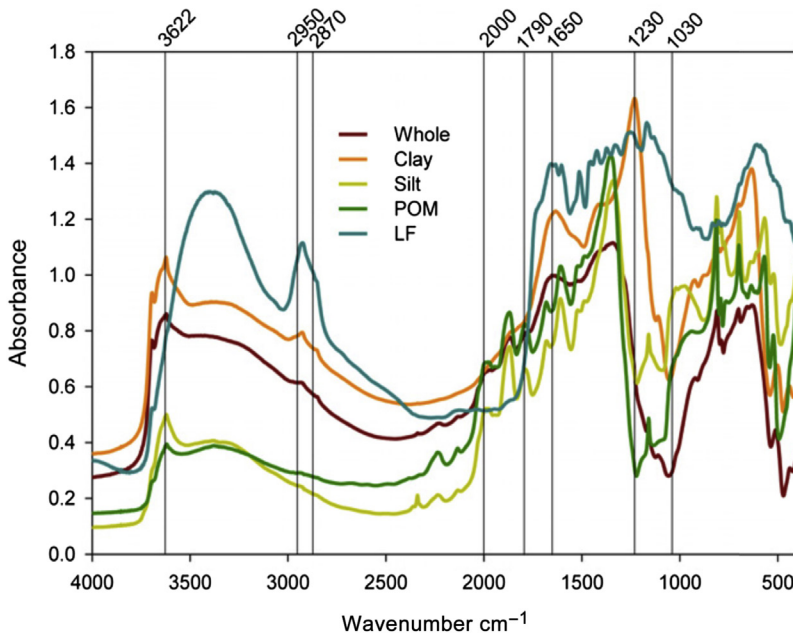


Figure 1.18 DRIFTS spectra of size and density fractions of SOM isolated in a clay loam ($20\ \text{g C kg}^{-1}$ soil) under long-term continuous maize cropping. Shown are spectra for whole soil, clay fraction, silt fraction, particulate organic matter (POM), and light fraction (LF). (DRIFTS, diffuse reflectance Fourier transform infrared spectroscopy; SOM, soil organic matter.) (For color version of this figure, the reader is referred to the online version of this book.) Reprinted with permission from Calderón et al. (2011).

residue C. In contrast, incubation increased the band at 1630 cm^{-1} indicating that this band represents more processed forms of plant-derived C. The study by [Assis et al. \(2012\)](#) shows that the LF from an oxisol can be separated into occluded and free fractions, and that the occluded material has a higher degree of condensation according to DRIFTS band ratios. This study also found that the free and occluded LF were affected differently by cultivation, showing that size fractionations can be a sensitive way to monitor the effects of agricultural management.

In physical aggregate fractions, the finer silt and clay fractions typically contain older, more processed C. The OC signal in these fine fractions is characterized by aromatic bands suggesting humification ([Calderón et al., 2011c](#)). The clay fraction contains more than half of the total soil C in many agricultural soils, so it is not surprising that high SOM soils have greater absorbance than low SOM soils at 1230 cm^{-1} , a band for aromatics and characteristic of clay minerals too. Future research should try to elucidate if absorbance at 1230 cm^{-1} is primarily due to organic or mineral absorbance in neat samples, because it is possible that the relationship of soil C with this band is a result of a correlation by proxy of C with clay mineral abundance. Clay fraction DRIFTS spectra do change during laboratory incubation ([Calderón et al., 2011c](#)), suggesting that soil C cycling dynamics can be very complex, with fractions that are thought to be old, but are not necessarily recalcitrant.

A classic example of the utility of FTIR for analysis of soil physical fractions involves examining SOM composition among soil aggregates as a function of management. For example, aggregate fractions (macro, $>212\text{ }\mu\text{m}$; meso, $212\text{--}53\text{ }\mu\text{m}$; microaggregates $53\text{--}20\text{ }\mu\text{m}$) of two mineralogically and texturally distinct soils (Ferralsol and Arenosol) were analyzed for organic absorbances ([Verchot et al., 2011](#)). Certain aggregate classes displayed a distinct FTIR signature with characteristic peaks independent of soil or management (e.g. tillage, crop type and rotation), whereas the SOM absorbances of other aggregate classes varied by site. Across soils and treatments, microaggregate spectra exhibited polysaccharide (C–O, 1018 cm^{-1}) enrichment and depletion of ketone and carboxyl ($\nu(\text{C}=\text{O})$ 1778 cm^{-1}) and aromatic (C=C, 1635 cm^{-1}) moieties relative to mesoaggregate OM, for which opposite FTIR trends were observed. In contrast, macroaggregate OM composition varied by soil type. Comparison of macroaggregate with bulk soil spectra indicated that macroaggregates were poor in all but aliphatic C–H deformation (1370 cm^{-1}) and polysaccharide C–O in the clay-rich Ferralsol ($420\text{ g clay kg}^{-1}$ soil), but poor in aliphatic C–H stretching (2930 cm^{-1})

and phenolic O–H (3435 cm^{-1}) in the Arenosol ($180\text{ g clay kg}^{-1}$ soil). Similar aggregate characterization by additional FTIR studies suggest shared OM composition of aggregate classes within a range of edaphic factors, pointing to common mechanisms of organomineral stabilization and turnover by physical size. It is notable that despite the large range in soil C contents of these soils ($5\text{--}24\text{ g C kg}^{-1}$ soil), bulk soil FTIR did not detect substantial differences among tillage (minimal vs. conventional) and crop rotation (continuous maize vs maize-legume vs maize-fallow), in contrast to aggregate FTIR. This illustrates the high suitability of C-enriched fractions and extracts for capturing SOM response to treatment effects, rather than bulk soil samples, with FTIR. These soil fractions can also provide the necessary resolution of SOM into various pools to track SOM cycling and responses to managements.

In another study using FTIR to examine physical fractions, [Demyan et al. \(2012\)](#) fractionated SOM from a Haplic Chernozem using a procedure that involved flotation, centrifugation, and heavy liquid density separation. They baseline-corrected band areas centered at 2930 , 1620 , 1530 , and 1159 cm^{-1} in bulk soil and identified them as organic with minimal mineral interference. The lighter density SOM fractions correlated with bulk soil absorbance at 2930 cm^{-1} , while peak areas centered at 1620 cm^{-1} correlated with the denser SOM fractions, indicating that the SOM fractionation by density also resulted in a separation according to C stability.

Partial Least Squares (PLS) calibrations using FTIR for different POM size fractions at a field scale has also been developed ([Bornemann et al., 2010](#)). The PLS loadings, which show the spectral bands responsible for the calibration results, were used to identify the spectral bands that were useful to resolve the different POM fractions. Absorbance between 1000 and 1080 cm^{-1} was used as an indicator of cellulose in the POM classes. Hydroxyl and carbonyl groups (1320 and 1660 cm^{-1} , respectively) increased with decreasing POM size. Lignin, aliphatic C–H, aromatic, and cellulose bands allowed calibration for the different POM fractions. Besides the calibration analysis, this study gave insights about SOM spatial variability, and the role of the different fractions in SOM accumulation.

A recent study by [Davinic et al. \(2012a\)](#) incorporated two data-rich technologies to shed light into the relationship between SOM chemistry and microbiology. Nucleic acid pyrosequencing and DRIFTS were used to investigate soil bacterial communities and how they are associated with different soil C chemical attributes in macroaggregates, microaggregates,

silt, and clay fractions. Pyrosequencing showed that different microenvironments, such as macroaggregates and microaggregates, have distinct bacterial communities and ecological niches. DRIFTS was used to highlight spectral features that distinguished the different fractions, which included organic and mineral bands. With this approach, [Davinic et al. \(2012a\)](#) showed not only that each aggregate size fraction has a particular microbial composition, but that within each aggregate type different microbial taxa correlate with particular organic or mineral DRIFTS bands. Such combinations of DRIFTS with other soil microbiology analyses techniques will help us further our understanding of soil microbial ecology.

Physical fractions of acidic (pH 4.4) and alkaline (pH 7.8) forest soils at Rothamsted Research site revealed fraction-specific pH effects on SOM distribution and quality ([Tonon et al., 2010](#)). Less-processed 'light' fractions (free LF, intraaggregate LF) representing recent plant residue inputs accounted for a greater portion of total soil C in the acidic soil compared to the alkaline soil, with greater thermolabile SOM composition in the latter like lignin (guaiacyl lignin of softwoods at 1518 cm^{-1}). In contrast, no soil pH effect was observed for the quantitative distribution and quality of clay and silt-associated OM, 'heavy' fractions representing processed and stabilized SOM. A lack of these same thermolabile compounds and a dominance of absorbances consistent with NMR identification of aliphatics (e.g. C–H deformation $1460\text{--}1440\text{ cm}^{-1}$) characterized the clay and silt SOM. In the acidic soil, increased absorbance of carboxylic acid $\nu(\text{C}=\text{O})$ at 1724 cm^{-1} of LFs suggested greater protonation. The dominance of $\nu(\text{O}-\text{H})$ at 3620 cm^{-1} from montmorillonite and kaolinite clays and low aliphatic absorbance area at $\nu_{a,s}(\text{C}-\text{H})$ at $2950\text{--}2800\text{ cm}^{-1}$ was proposed to reflect mineral–organic interactions: hydrophobic association of aliphatic chains with clays lead to shielding of the latter. Another possible organomineral association detectable by FTIR was carboxylic acid $\nu(\text{C}=\text{O})$ at 1724 cm^{-1} and carboxylate $\nu(\text{C}=\text{O})$ at 1660 cm^{-1} . Present in LFs with limited or no stabilization by minerals, the carboxylic acid band was nonexistent in heavy fractions and the carboxylate band appeared to have shifted downfield to $1630\text{--}1620\text{ cm}^{-1}$, suggesting carboxylate complexation with mineral surfaces. However, this assignment was not certain given the possible overlap of phyllosilicate interlayer water ($b(\text{O}-\text{H})$ $1660\text{--}1630\text{ cm}^{-1}$). This suggests that one benefit of samples containing mineral components, in spite of possible interference with organic absorbances, is providing insight to interactions of organic and mineral constituents of soils.

10.3 SOM Analysis via Subtraction Spectra

A promising but less utilized approach to FTIR study of SOM is to remove mineral absorbances by subtraction of a mineral background. This may be thought of as a spectral correction, akin to correcting for water vapor or CO₂ contamination in extracts and the sample chamber (Kaiser et al., 2007, 2008), accounting for an interfering background (Ellerbrock and Gerke, 2004), or accentuating organic absorbances rather than providing a definite SOM spectrum (Sarkhot et al., 2007a). For instance, subtraction from bulk soil of the mineral component provides a difference or subtraction spectrum of SOM. Spectra of C enriched extracts or fractions, like humic acids and soil aggregates, can also be improved with respect to organic absorbances by subtracting a mineral background. The background or subtracted spectrum is most appropriately obtained by treating the sample to remove SOM (e.g. ashing, oxidation), though in model systems a pure mineral standard can be used. Subtraction of the treated sample spectrum from that of the bulk soil spectrum yields a subtraction spectrum representing the SOM removed during preparation of the background sample. In this regard, the subtraction method offers the possibility of calculating spectra of soil components isolated by fractionation, extractive or destructive.

Important considerations in the subtraction approach for FTIR of SOM include the type of SOM removal and possible treatment artifacts. It is necessary to know how the amount and kind of SOM was removed from the original sample for the subtraction background. Accordingly, using fractionations that isolate fractions of known function, vs largely operational fractions, makes subtraction spectra more useful for SOM characterization by FTIR. Certain fractionations may be better suited for subtraction approaches due to the effects of fractionation method (e.g. chemical oxidation by-products) on subtraction spectra quality. Artifacts of treatment in background samples can compromise the utility of subtraction spectra, though it has been argued that this depends on the overlap of affected regions and regions of interest (Reeves, 2012). For instance, soil ashing for SOM removal can alter mineral absorbances via phyllosilicate dehydration and collapse. One of the early uses of ashed subtraction spectra of total SOM was for obtaining sensitive fingerprints of soils for forensic purposes (Cox et al., 2000). Here the objective was not exact identification or quantitative analysis of SOM composition, but discrimination among soils using the putatively greater site-specificity of SOM composition as characterized by FTIR. The approach takes advantage of the high site-specificity of SOM and FTIR sensitivity to organic compounds to provide soil forensics with

a more sensitive means of fingerprinting soils. Thus, artifacts of treatment in subtraction spectra were not an unacceptable concern. This method has found continued use in soil forensics (Dawson and Hillier, 2010; Lorna et al., 2008).

An early application of the ashing subtraction method was for removing mineral absorbances from DRIFTS spectra of DOM fractions (Chefetz et al., 1998). It has been since used largely to calculate subtraction spectra of the total SOM pool, as well as to remove trace mineral absorbances in soil C extracts. There is great variation in the temperature and duration of ashing, ranging from 400 to 650 °C and 2–8 h (Calderón et al., 2011a,b; Cheshire et al., 2000; Kaiser et al., 2008; McCarty et al., 2010; Reeves et al., 2005, 2001; Sarkhot et al., 2007a,b; Simon, 2007) across a diversity of soil textures and mineralogies, suggesting the need to investigate upper limits of ashing conditions by soil type to avoid artifacts of subtraction that may result from mineral alteration. Theoretically, knowledge of a soil's mineral composition could inform ashing maximum temperatures. Alternatively, these conditions can be empirically established for a given soil by monitoring FTIR mineral bands sensitive to thermal alteration over a range of ashing conditions. For instance, Kaiser et al. (2007) evaluated ashing temperatures from 400 to 900 °C using changes in the intensity and position of the dominant silicate band of Si-O-Si stretching at 1100–1000 cm^{-1} as an indicator of mineral alteration unacceptable for calculating subtraction spectra. Ashing above 400 °C produced intensity changes and peak shifts in the silicate band (Kaiser et al., 2007, 2008). To ensure full SOM removal at this lower temperature, soils were ashed for 8 h. However, other soils may contain minerals that degrade at temperatures lower than 400 °C. As a precautionary measure, in the absence of information on the thermosensitivity of a soil, ashing for subtraction spectra should be performed at a default maximum of 400 °C.

Alternative methods exist for SOM removal with minimal collateral damage to minerals and consequentially insignificant, spectroscopically minimal, or well-defined artifacts in subtraction spectra. Methods for SOM removal have been developed for obtaining pure mineral samples for mineralogical analysis (Soukup et al., 2008) and particle size analysis (Gray et al., 2010; Leifeld and Kögel-Knabner, 2001; Vdović et al., 2010), including hydrogen peroxide, sodium hypochlorite, disodium peroxodisulfate, sodium dithionite, and sodium pyrophosphate, with varying C removal and sensitivity to mineralogy (Mikutta et al., 2005). Given their emphasis on maintaining mineral integrity, in particular with XRD, these methods are highly suitable for obtaining artifact-free mineral samples for subtraction spectra

of SOM. Less mineralogically sensitive reagents include hydrofluoric acid, hydrochloric acid, and potassium permanganate (Favilli et al., 2008; von Lützow et al., 2007).

Hydrogen peroxide has been suggested as an alternative to ashing for FTIR analysis of SOM (Reeves, 2012), though its efficacy depends on clay mineral type and content (Eusterhues et al., 2003) and it can dissolve mineral oxides (Mikutta et al., 2005), hence the use of hydrogen peroxide for field identification of Mn oxides. A comparative study of common oxidants for SOM removal developed a modified version of hypochlorite oxidation (Anderson, 1961) that maximizes OC loss while minimizing mineralogical changes, including relatively sensitive pedogenic oxides (Siregar et al., 2005). This has been corroborated by evaluation of SOM removal from the clay fraction by various oxidative and extractive methods (Cheshire et al., 2000; Favilli et al., 2008) (Figure 1.19). Different ranges of C loss by a single method within and among studies [e.g. hydrogen peroxide, (Leifeld and Kögel-Knabner, 2001; Plante et al., 2004; von Lützow et al., 2007)] suggest

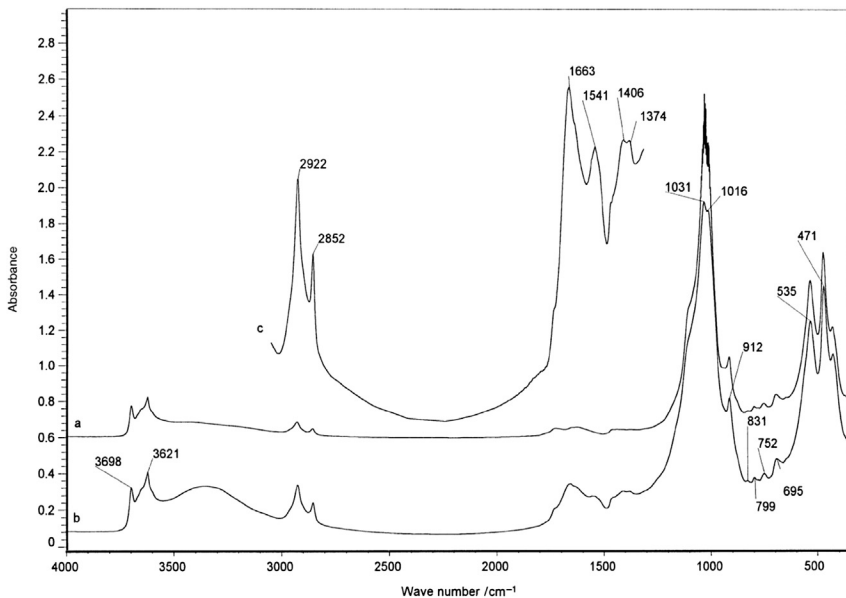


Figure 1.19 Subtraction spectra of SOM in the clay fraction of a pasture Spodosol surface horizon (56 g C kg^{-1} soil). Transmission FTIR spectrum of SOM (C) was calculated by subtraction of sodium hypochlorite-oxidized clay fraction spectrum (A), from the spectrum of the sodium pyrophosphate and sodium hydroxide extracted of this fraction (B). (SOM, soil organic matter; FTIR, Fourier transform infrared.) Reprinted with permission from Cheshire et al. (2000).

the influence of mineralogy, and SOM quality and quantity. Reagents may selectively remove distinct SOM pools of varying chemical thermostability and physical occlusion (Eusterhues et al., 2003; von Lützow et al., 2007), and combinations of oxidants and/or hydrolytic agents can obtain high SOM removal rates (Favilli et al., 2008). Alternative SOM removal methods include low-temperature ashing (LTA), in which radio frequency excites molecular oxygen at $<100\text{ }^{\circ}\text{C}$ to remove strongly absorbed OM from clay minerals (D'Acqui et al., 1999; Sullivan and Koppi, 1987), and potentially negative pressure treatments. FTIR and XRD comparative analysis of LTA and hydrogen peroxide treatments of bitumen and model clays found comparable loss of aliphatic C–H absorbance, but peroxide dissolution of siderite, confirmed by CEC measurements (Adegoroye et al., 2009).

Clearly, there is an abundance of soil C removal techniques for providing mineral backgrounds for SOM subtraction spectra. It should be noted that incomplete SOM removal is only a disadvantage when net SOM characterization is sought. These oxidative and hydrolytic treatments double as wet chemical methods for fractionating SOM by degree of physical protection, chemical stability, and MRT (von Lützow et al., 2007). They can be especially powerful when coupled to analytical techniques such as ^{14}C dating (e.g. Eusterhues et al., 2003, 2005). With the subtractive approach, FTIR can be used to characterize SOM to improve understanding of these fractions beyond MRT and C/N content. This approach extends beyond destructive fractionation and includes extractive fractionations, which offer the opportunity to cross-check subtractive data by direct FTIR analysis of the extract (in some cases purification is needed, via dialysis for removal of salts). For instance, comparison of SOM subtraction spectra of sodium hydroxide (i.e. HS), sodium pyrophosphate, and sodium hypochlorite treatments of soil clay fractions reveals significant differences in OM reflecting differences in the selectivity and reactivity of reagents (Cheshire et al., 2000).

10.4 Spectral Analysis through Addition of Organic Compounds

One way to validate IR band identification is to add a substance of known spectral properties to soil and then observe changes in absorbance patterns of the soil mixture. The differences can be visualized by subtracting the mixture spectrum from the pure soil spectrum, in which case the subtracted spectrum should show the spectral characteristic of the added substance. Figure 1.20 shows the spectra of soil, humic acid, soil plus humic acid mix, and the subtraction spectrum. The OH/NH region centered at 3400 cm^{-1}

does not show a prominent feature in the subtracted spectrum because absorbance in this band is not particularly different in soils and humic acids. The same can be said about the aliphatic C–H bands between 2930 and 2870 cm^{-1} . However, the regions where the humic acid and soil spectra are different are accentuated. For example, absorbance at 2540 cm^{-1} , which forms a slight rise in the humic acid spectrum but is negligible in pure soil, is shown as a prominent feature of the subtracted spectrum. This band is perhaps underutilized in soil analyses. It is due to overtones of the –COH stretch, and has been identified as important in the development of soil C calibrations (Janik et al., 2007). The humic acid also absorbs strongly at the 1750 cm^{-1} aromatic C=C band, which is characteristic of lignins and humic acids in general. Absorbance at 1750 cm^{-1} is greater in shallow soils than in deeper soils, so it could be used as a marker for SOM accretion in C sequestration scenarios (Calderón et al., 2011a). Absorbance at 1550, 1470, and 1230 cm^{-1} form smaller peaks in the subtraction spectrum due in part to the aromatic absorbance in the humic acid. It is interesting to note that the band at 1230 cm^{-1} falls within the silicate inversion band in neat soils, showing that spectral changes due to organics in this region can be amenable to subtraction and interpretation despite the inversion caused by reflection from sand particles.

Note that the 3630 cm^{-1} clay, 1890 cm^{-1} silica, 1370 cm^{-1} phenolic/carboxylate, 800 cm^{-1} silica, and 695 cm^{-1} silica bands were more intense on the soil spectrum and formed negative peaks in the subtracted spectrum (Figure 1.20). This suggests little interaction of the added humic acid with the soil in these regions and underscores the mineral character of these bands.

The argument could be made that the amendment-subtraction approach could be vulnerable to artifacts such as coating or matrix effects. It is possible that an added standard could coat the clay particles due to electrostatic attraction and shield the soil components from adequate exposure to the IR beam. This is especially true in the MIR range due to the higher energy and lower penetration of the IR energy. Also, it should be kept in mind that some of the older C in soil may be in close association with clays and not easily detected by DRIFTS. In contrast, the added substance should have a relatively good presentation to the IR beam due to its recent incorporation. Nevertheless, this approach can be seen mimicking a soil amendment such as compost addition to soil in the field. Future studies should explore which spectral bands will respond quantitatively according to Beer–Lambert law, and which spectral bands are more prone to artifacts derived from soil amendment interaction.

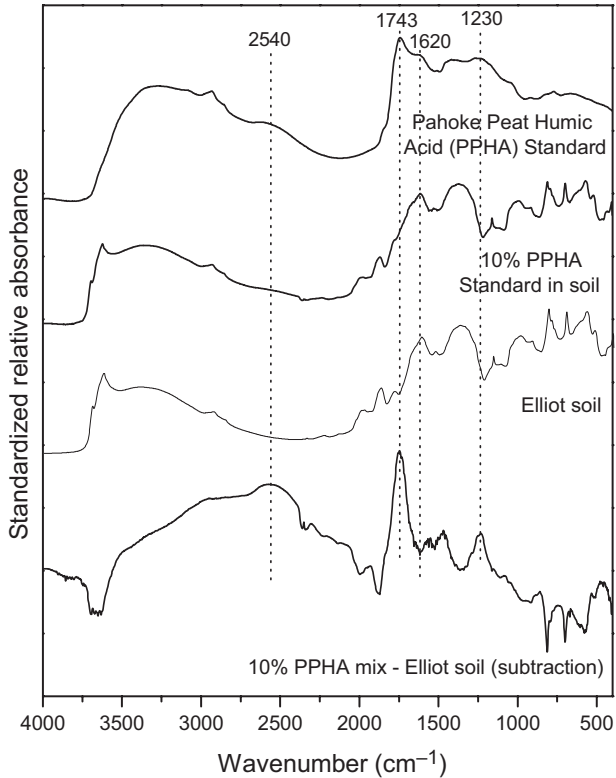


Figure 1.20 DRIFTS spectra of Elliott soil, Pahokee Peat Humic Acid Standard, soil-standard mixture (10% standard in soil by wt), and subtraction of the mix and pure soil spectra. The spectral data was standardized in order for the spectra to have the same mean and standard deviation. Soil and humic acid standards were obtained from the International Humic Substances Society. (DRIFTS, diffuse reflectance Fourier transform infrared spectroscopy; PPHA, Pahokee Peat Humic Acid.)

10.5 Quantitative Analysis of Soil Carbon and Nitrogen

Diffuse reflectance NIR spectroscopy has been used for decades to develop predictive calibrations for the analysis of grains, forages, and other agricultural materials (Roberts et al., 2004). IR calibrations are valuable because they can be used instead of expensive, complex, and time consuming chemical analyses. NIR and MIR spectroscopies have been used successfully to calibrate for soil parameters like soil C, N, as well as mineral features (Reeves, 2010). Given a sample set of adequate size and acceptable distribution of the C data, both NIR and MIR (i.e. DRIFTS) can produce calibrations for total soil C, although MIR often outperforms NIR (McCarty et al., 2010;

Mimmo et al., 2002; Reeves et al., 2005). One exception is when the soil samples are field moist, in which case DRIFTS calibrations fail due to its higher sensitivity to moisture (Reeves, 2010). Because of this, DRIFTS may be amenable for laboratory-based calibrations, but NIR has more potential for field on-site calibrations.

As with all calibrations of any kind, it is important to include a sample set that brackets the samples to be predicted in terms of C content and soil type (Reeves et al., 2012). Prediction accuracy benefits from having samples in the calibration set that are geographically proximate and compositionally similar to the samples to be predicted.

Soil C measurement was the original motive for developing calibrations with FTIR data. Indeed, MIR and NIR can be used to measure soil total C and N accurately (McCarty et al., 2002; Mimmo et al., 2002; Reeves et al., 2005, 2001). However, the last decade has seen a proliferation of calibration work for soil properties other than total C and N. DRIFTS has been used to predict alkyl, carbonyl, and aromatic C in soil and litter samples quantified via NMR (Ludwig et al., 2008). Recent work shows that we can potentially calibrate for other parameters in soil such as metals, carbonates (inorganic C), enzymes, potential nitrification, and pH (Du et al., 2013b; McCarty et al., 2002; Mimmo et al., 2002; Reeves et al., 2001; Siebielec et al., 2004). Because DRIFTS contains information related to organic and inorganic components that relate to texture and particle size distribution, calibrations can also be developed for soil physical attributes including moisture retention, bulk density, or hydraulic conductivity (Janik et al., 2007; Minasny et al., 2008; Tranter et al., 2008). For example, PLS regression coefficients show that absorbance at the 3630 cm^{-1} clay band, and at the 1640 cm^{-1} amide I or phenyl C–C band are important for calibrations for soil water retention (Tranter et al., 2008).

Sometimes predictions can be based on surrogate calibrations, meaning that an alternative to the analyte of interest is detected and a calibration is built inadvertently by correlation. For example, calibrations for pH could be based on the fact that the DRIFTS is measuring other soil qualities related to pH, such as carbonates, which have defined prominent features in the MIR (Reeves, 2010). Reeves et al. (2006) hypothesized that calibrations for $\delta^{13}\text{C}$ are possible due to a surrogate relationship of isotope ratios and soil C pool chemistry. It is important to note that surrogate calibrations can fall apart when the relationship between the analyte and the surrogate soil property changes, such as when the calibration is used to predict a soil sample with widely different parent material or geographic origin from the samples in the calibration set (Reeves, 2010).



11. SUMMARY

Vibrational spectroscopy can be a versatile and highly informative analytical tool for soil scientists. Although FTIR and Raman spectroscopies have great utility for characterization of pure samples, it is the continued development of computer science, sampling modules, and methodologies that continue to make vibrational spectroscopy a powerful approach for studying complex matrices such as soils. In particular, FTIR provides a relatively low cost approach for probing molecular composition and interactions on soil particles and at the mineral–liquid interface. The ability of FTIR to provide information on the chemical arrangement and composition of inorganic and organic moieties makes it somewhat unique and ideal analysis approach for soil scientists. Simultaneously providing information on soil minerals and OM composition or organic contaminant binding mechanisms is a benefit not provided by many other instrumental methods.

The existence of diverse methodologies that complement vibrational spectroscopy studies further enhance their potential impact. Studies of soil minerals benefit greatly by coupling FTIR and Raman spectroscopy with XRD to provide confirmation of mineral structures. Similarly, NMR spectroscopy is an excellent method to pair with FTIR for studies of SOM. Advanced synchrotron techniques, such as NEXAFS, also can be used in conjunction with FTIR to elucidate metal binding mechanisms on mineral surfaces. Additionally, the continued development of molecular modeling approaches is greatly improving spectral interpretations and providing detailed molecular-level information for molecular interactions on mineral and organic surfaces. These approaches highlight synergistic analytical methodologies which are becoming increasingly important tools for soil scientists.

Continued advances in the instrumentation and methodologies for vibrational spectroscopy hold great promise for soil science research. For example, advances in microfluidic sampling cells for SR-FTIR are making analysis in the presence of water possible. This will provide exciting capabilities for examining processes at the mineral–water interface with high spatial resolution. Confocal Raman microspectroscopy is another methodology with great potential to develop into a powerful tool for soil scientists. Using this approach sample depth profiling of soil aggregates or films on minerals could be probed with high spatial resolution.

Vibrational spectroscopy has provided a wealth of important data on soil chemical processes since it was first developed in the mid-1900s. Each

ensuing decade has witnessed significant advances in analytical capabilities, affording soil scientists with ever increasing tools to study soil minerals, OM, and their interactions. This review has highlighted some of the more recent applications and discoveries of vibrational spectroscopy, demonstrating a diverse set of approaches for studying important soil chemical processes. Future research efforts will benefit greatly from the continuing evolution of vibrational spectroscopy. It is anticipated that advances will provide new methodologies and provide exciting opportunities for studies of a variety of biogeochemical processes in soil.

ACKNOWLEDGMENTS

S.J. Parikh and K.W. Goynne acknowledge support from the United States Department of Agriculture (USDA) National Institute of Food and Agriculture (NIFA) for Hatch Formula Funding (provided to their respective institutions) and multistate regional project W-2082. A.J. Margenot acknowledges support from USDA NIFA Organic Agriculture Research and Education Initiative Award 2009-01415.

Disclaimer and EEO/Non-Discrimination statement

Mention of trade names or commercial products in this publication is solely for the purpose of providing specific information and does not imply recommendation or endorsement by the U.S. Department of Agriculture. USDA is an equal opportunity provider and employer.

REFERENCES

- Adamescu, A., Mitchell, W., Hamilton, I.P., Al-Abadleh, H.A., 2010. Insights into the surface complexation of dimethylarsinic acid on iron (Oxyhydr)oxides from ATR-FTIR studies and quantum chemical calculations. *Environ. Sci. Technol.* 44, 7802–7807.
- Adegoroye, A., Uhlik, P., Omotoso, O., Xu, Z., Masliyah, J., 2009. A comprehensive analysis of organic matter removal from clay-sized minerals extracted from oil sands using low temperature ashing and hydrogen peroxide. *Energy & Fuels* 23, 3716–3720.
- Ajayan, P.M., 1999. Nanotubes from carbon. *Chem. Rev.* 99, 1787–1799.
- Albrecht, M.G., Creighton, J.A., 1977. Anomalously intense Raman spectra of pyridine at a silver electrode. *J. Am. Chem. Soc.* 99, 5215–5217.
- Alcock, N.W., Tracy, V.M., Waddington, T.C., 1976. Acetates and acetato-complexes. 2. spectroscopic studies. *J. Chem. Dalt. Trans.* 2243–2246.
- Allen, B.L., Hajek, B.F., 1989. Mineral occurrence in soil environments. In: Dixon, J.B., Weed, S.B. (Eds.), *Minerals in Soil Environments*. Vol. SSSA Book Ser. 1. SSSA, Madison, WI.
- Alvarez-Puebla, R.A., Valenzuela-Calahorra, C., Garrido, J.J., 2004. Cu(II) retention on a humic substance. *J. Colloid Interface Sci.* 270, 47–55.
- Aminzadeh, A., 1997. Fluorescence bands in the FT-Raman spectra of some calcium minerals. *Spectrochim. Acta Part A Mol. Biomol. Spectrosc.* 53, 693–697.
- Amir, S., Jouraiphy, A., Meddich, A., El Gharous, M., Winterton, P., Hafidi, M., 2010. Structural study of humic acids during composting of activated sludge-green waste: elemental analysis, FTIR and C-13 NMR. *J. Hazard. Mater.* 177, 524–529.
- Amonette, J.E., 2002. Methods for determination of mineralogy and environmental availability. Vol. SSSA Book Ser. 7. In: Dixon, J.B., Schulze, D.G. (Eds.), *Soil Mineralogy with Environmental Applications*. SSSA, Madison, WI.

- Anderson, J.U., 1961. An improved pretreatment for mineralogical analysis of samples containing organic matter. *Clays Clay Miner.* 10, 380–388.
- Arai, Y., Sparks, D.L., 2001. ATR-FTIR spectroscopic investigation on phosphate adsorption mechanisms at the ferrihydrite-water interface. *J. Colloid Interface Sci.* 241, 317–326.
- Arai, Y., Sparks, D.L., Davis, J.A., 2004. Effects of dissolved carbonate on arsenate adsorption and surface speciation at the hematite-water interface. *Environ. Sci. Technol.* 38, 817–824.
- Aranda, V., Ayora-Cañada, M.J., Domínguez-Vidal, A., Martín-García, J.M., Calero, J., Delgado, R., et al., 2011. Effect of soil type and management (organic vs. conventional) on soil organic matter quality in olive groves in a semi-arid environment in Sierra Mágina Natural Park (S Spain). *Geoderma* 164, 54–63.
- Aristilde, L., Sposito, G., 2008. Molecular modeling of metal complexation by a fluoroquinolone antibiotic. *Environ. Toxicol. Chem.* 27, 2304–2310.
- Aristilde, L., Marichal, C., Miéché-Brendlé, J., Lanson, B., Charlet, L., 2010. Interactions of Oxytetracycline with a Smectite Clay: A Spectroscopic Study with Molecular Simulations. *Environ. Sci. Technol.* 44, 7839–7845.
- Arocena, J.M., Pawluk, S., Dudas, M.J., Gajdostik, A., 1995. In situ investigation of soil organic matter aggregates using infrared microscopy. *Can. J. Soil. Sci.* 75, 327–332.
- Artz, R.R.E., Chapman, S.J., Campbell, C.D., 2006. Substrate utilisation profiles of microbial communities in peat are depth dependent and correlate with whole soil FTIR profiles. *Soil Biol. Biochem.* 38, 2958–2962.
- Artz, R.R.E., Chapman, S.J., Jean Robertson, A.H., Potts, J.M., Laggoun-Défarge, F., Gogo, S., et al., 2008. FTIR spectroscopy can be used as a screening tool for organic matter quality in regenerating cutover peatlands. *Soil Biology and Biochemistry* 40, 515–527.
- Ascough, P.L., Bird, M.I., Francis, S.M., Lebl, T., 2011. Alkali extraction of archaeological and geological charcoal: evidence for diagenetic degradation and formation of humic acids. *J. Archaeol. Sci.* 38, 69–78.
- Assis, C.P., Jucksch, I., Mendonca, E.S., Neves, J.C.L., Silva, L.H.M., Wendling, B., 2012. Distribution and quality of the organic matter in light and heavy fractions of a red Latosol under different uses and management practices. *Commun. Soil Sci. Plant Anal.* 43, 835–846.
- Axe, K., Persson, P., 2001. Time-dependent surface speciation of oxalate at the water-boehmite (γ -AlOOH) interface: implications for dissolution. *Geochim. Cosmochim. Acta* 65, 4481–4492.
- Axe, K., Vejgard, M., Persson, P., 2006. An ATR-FTIR spectroscopic study of the competitive adsorption between oxalate and malonate at the water-goethite interface. *J. Colloid Interface Sci.* 294, 31–37.
- Badireddy, A.R., Korpel, B.R., Chellam, S., Gassman, P.L., Engelhard, M.H., Lea, A.S., Rosso, K.M., 2008. Spectroscopic characterization of extracellular polymeric substances from *Escherichia coli* and *Serratia marcescens*: suppression using sub-inhibitory concentrations of Bismuth Thiols. *Biomacromolecules* 9, 3079–3089.
- Baes, A.U., Bloom, P.R., 1989. Diffuse reflectance and transmission Fourier transform infrared (DRIFT) spectroscopy of humic and fulvic acids. *Soil Sci. Soc. Am. J.* 53, 695–700.
- Baglieri, A., Gennari, M., Ioppolo, A., Leinweber, P., Nègre, M., 2012. Comparison between the humic acids characteristics of two andisols of different age by: FT-IR and $^1\text{H-NMR}$ spectroscopy and py-FIMS. *Geochem. Int.* 50, 148–158.
- Balan, E., Blanchard, M., Hochepied, J.-F., Lazzeri, M., 2008. Surface modes in the infrared spectrum of hydrous minerals: the OH stretching modes of bayerite. *Phys. Chem. Minerals* 35, 279–285.
- Balan, E., Delattre, S., Guillaumet, M., Salje, E.K.H., 2010. Low-temperature infrared spectroscopic study of OH-stretching modes in kaolinite and dickite. *Am. Mineral.* 95, 1257–1266.

- Balan, E., Lazzeri, M., Morin, G., Mauri, F., 2006. First-principles study of the OH-stretching modes of gibbsite. *Am. Mineral.* 91, 115–119.
- Baltrusaitis, J., Schuttlefield, J., Jensen, J.H., Grassian, V.H., 2007. FTIR spectroscopy combined with quantum chemical calculations to investigate adsorbed nitrate on aluminium oxide surfaces in the presence and absence of co-adsorbed water. *Phys. Chem. Chem. Phys.* 9, 4970–4980.
- Barer, R., Cole, A.R.H., Thompson, H.W., 1949. Infra-red spectroscopy with the reflecting microscope in physics, chemistry and biology. *Nature* 163, 198–201.
- Bargar, J.R., Kubicki, J.D., Reitmeyer, R., Davis, J.A., 2005. ATR-FTIR spectroscopic characterization of coexisting carbonate surface complexes on hematite. *Geochim. Cosmochim. Acta* 69, 1527–1542.
- Bargar, J.R., Persson, P., Brown Jr., G.E., 1999. Outer-sphere adsorption of Pb(II)EDTA on goethite. *Geochim. Cosmochim. Acta* 63, 2957–2969.
- Barja, B.C., Afonso, M.D., 2005. Aminomethylphosphonic acid and glyphosate adsorption onto goethite: a comparative study. *Environ. Sci. Technol.* 39, 585–592.
- Barja, B.C., dos Santos Afonso, M., 1998. An ATR-FTIR study of glyphosate and its Fe(III) complex in aqueous solution. *Environ. Sci. Technol.* 32, 3331–3335.
- Barja, B.C., Herszage, J., Alfonso, M.D., 2001. Iron(III)-phosphonate complexes. *Polyhedron* 20, 1821–1830.
- Barja, B.C., Tejedor-Tejedor, M.I., Anderson, M.A., 1999. Complexation of Methylphosphonic acid with the surface of goethite particles in aqueous solution. *Langmuir* 15, 2316–2321.
- Barthès, B.G., Brunet, D., Hien, E., Enjalric, F., Conche, S., Freschet, G.T., d'Annunzio, R., Toucet-Louri, J., 2008. Determining the distributions of soil carbon and nitrogen in particle size fractions using near-infrared reflectance spectrum of bulk soil samples. *Soil Biol. Biochem.* 40, 1533–1537.
- Beattie, D.A., Chapelet, J.K., Gräfe, M., Skinner, W.M., Smith, E., 2008. In Situ ATR FTIR Studies of SO₄ Adsorption on Goethite in the Presence of Copper Ions. *Environ. Sci. Technol.* 42, 9191–9196.
- Beauvais, A., Bertaux, J., 2002. In situ characterization and differentiation of kaolinites in lateritic weathering profiles using infrared microspectroscopy. *Clays Clay Miner.* 50, 314–330.
- Beech, I., Hanjagsit, L., Kalaji, M., Neal, A.L., Zinkevich, V., 1999. Chemical and structural characterization of exopolymers produced by *Pseudomonas* sp NCIMB 2021 in continuous culture. *Microbiology UK* 145, 1491–1497.
- Beech, I.B., Gubner, R., Zinkevich, V., Hanjagsit, L., Avci, R., 2000. Characterisation of conditioning layers formed by exopolymeric substances of *Pseudomonas* NCIMB 2021 on surfaces of AISI 316 stainless steel. *Biofouling* 16, 93–104.
- Benetoli, L.O.B., de Souza, C.M.D., da Silva, K.L., Souza, I.G.D., de Santana, H., Paesano, A., et al., 2007. Amino acid interaction with and adsorption on clays: FT-IR and Mossbauer Spectroscopy and X-ray diffractometry investigations. *Origins of Life and Evolution of Biospheres* 37, 479–493.
- Benning, L.G., Phoenix, V.R., Yee, N., Tobin, M.J., 2004. Molecular characterization of cyanobacterial silicification using synchrotron infrared micro-spectroscopy. *Geochim. Cosmochim. Acta* 68, 729–741.
- Bersani, D., Lottici, P.P., Montenero, A., 1999. Micro-Raman investigation of iron oxide films and powders produced by sol-gel syntheses. *J. Raman Spectrosc.* 30, 355–360.
- Bertaux, J., Frohlich, F., Ildefonse, P., 1998. Multicomponent analysis of FTIR spectra: quantification of amorphous and crystallized mineral phases in synthetic and natural sediments. *J. Sediment. Res.* 68, 440–447.
- Bertsch, P.M., Hunter, D.B., 1998. Elucidating fundamental mechanisms in soil and environmental chemistry: the role of advanced analytical, spectroscopic, and microscopic methods. *Future Prospects Soil Chem. SSSA Special Publ.* 103–122.

- Bigham, J.M., Fitzpatrick, R.W., Schulze, D.G., 2002. Iron oxides. Vol. SSSA Book Ser. 7. In: Dixon, J.B., Schulze, D.G. (Eds.), *Soil Mineralogy with Environmental Applications*. SSSA, Madison, WI.
- Bish, D.L., Johnston, C.T., 1993. Rietveld refinement and Fourier-transform infrared spectroscopic study of the dickite structure at low-temperature. *Clays Clay Miner.* 41, 297–304.
- Bishop, J.L., Dobrea, E.Z.N., McKeown, N.K., Parente, M., Ehlmann, B.L., Michalski, J.R., Milliken, R.E., Poulet, F., Swayze, G.A., Mustard, J.F., Murchie, S.L., Bibring, J.-P., 2008. Phyllosilicate diversity and past aqueous activity revealed at Mawrth Vallis, Mars. *Science* 321, 830–833.
- Bishop, J.L., Dyar, M.D., Lane, M.D., Banfield, J.F., 2004. Spectral identification of hydrated sulfates on Mars and comparison with acidic environments on Earth. *Int. J. Astrobiol.* 3, 275–285.
- Bishop, J.L., Murad, E., 2004. Characterization of minerals and biogeochemical markers on Mars: a Raman and IR spectroscopic study of montmorillonite. *J. Raman Spectrosc.* 35, 480–486.
- Blanch, A.J., Quinton, J.S., Lenehan, C.E., Pring, A., 2008. The crystal chemistry of Al-bearing goethites: an infrared spectroscopic study. *Mineral. Mag.* 72, 1043–1056.
- Blanchard, M., Lazzeri, M., Mauri, F., Balan, E., 2008. First-principles calculation of the infrared spectrum of hematite. *Am. Mineral.* 93, 1019–1027.
- Blout, E.R., Mellors, R.C., 1949. Infrared spectra of tissues. *Science* 110, 137–138.
- Bogrekcı, I., Lee, W.S., 2006. The effect of particle size on sensing phosphorus by Raman spectroscopy. In: ASABE Annual Meeting.
- Boily, J.-F., Nilsson, N., Persson, P., Sjöberg, S., 2000. Benzenecarboxylate surface complexation at the goethite (α -FeOOH)/water interface: I. A mechanistic description of pyromellitate surface complexes from the combined evidence of infrared spectroscopy, potentiometry, adsorption data, and surface complexation modeling. *Langmuir* 16, 5719–5729.
- Boily, J.-F., Szanyi, J., Felmy, A.R., 2006. A combined FTIR and TPD study on the bulk and surface dehydroxylation and decarbonation of synthetic goethite. *Geochim. Cosmochim. Acta* 70, 3613–3624.
- Borda, M.J., Strongin, D.R., Schoonen, M.A., 2003. A novel vertical attenuated total reflectance photochemical flow-through reaction cell for Fourier transform infrared spectroscopy. *Spectrochimica Acta Part a-Molecular and Biomolecular Spectroscopy* 59, 1103–1106.
- Borer, P., Hug, S.J., Sulzberger, B., Kraemer, S.M., Kretzschmar, R., 2009. ATR-FTIR spectroscopic study of the adsorption of desferrioxamine B and aerobactin to the surface of lepidocrocite (γ -FeOOH). *Geochim. Cosmochim. Acta* 73, 4661–4672.
- Bornemann, L., Welp, G., Amelung, W., 2010. Particulate organic matter at the field scale: rapid acquisition using mid-infrared spectroscopy. *Soil Sci. Soc. Am. J.* 74, 1147–1156.
- Bowen, J.M., Powers, C.R., Ratcliffe, A.E., Rockley, M.G., Hounslow, A.W., 1988. Fourier transform infrared and Raman spectra of dimethyl methylphosphonate adsorbed on montmorillonite. *Environ. Sci. Technol.* 22, 1178–1181.
- Bowie, B.T., Chase, D.B., Griffiths, P.R., 2000. Factors affecting the performance of benchtop Raman spectrometers. Part II: effect of sample. *Appl. Spectrosc.* 54, 200A–207A.
- Boyd, S.A., Johnston, C.T., Laird, D.A., Teppen, B.J., Li, H., 2011. Comprehensive study of organic contaminant adsorption by clays: methodologies, mechanisms, and environmental implications. In: *Biophysico-chemical Processes of Anthropogenic Organic Compounds in Environmental Systems*. John Wiley & Sons, Inc., pp. 51–71.
- Brandenburg, K., 1993. Fourier-transform infrared-spectroscopy characterization of the lamellar and nonlamellar structures of free lipid-A and Re lipopolysaccharides from *Salmonella minnesota* and *Escherichia coli*. *Biophys. J.* 64, 1215–1231.

- Brandenburg, K., Funari, S.S., Koch, M.H.J., Seydel, U., 1999. Investigation into the acyl chain packing of endotoxins and phospholipids under near physiological conditions by Waxes and FTIR spectroscopy. *J. Struct. Biol.* 128, 175–186.
- Brandenburg, K., Jurgens, G., Muller, M., Fukuoka, S., Koch, M.H.J., 2001. Biophysical characterization of lipopolysaccharide and lipid A Inactivation by lactoferrin. *Biol. Chem.* 382, 1215–1225.
- Brandenburg, K., Kusumoto, S., Seydel, U., 1997. Conformational studies of synthetic lipid A analogues and partial structures by infrared spectroscopy. *Biochim. Biophys. Acta Biomembranes* 1329, 183–201.
- Brandenburg, K., Seydel, U., 1986. Orientation measurements on ordered multibilayers of phospholipids and sphingolipids from synthetic and natural origin by ATR Fourier-transform infrared-spectroscopy. *Z. Naturforsch. C-A J. Biosci.* 41, 453–467.
- Brandenburg, K., Seydel, U., 1990. Investigation into the fluidity of lipopolysaccharide and free lipid-A membrane systems by fourier-transform infrared- spectroscopy and differential scanning calorimetry. *Eur. J. Biochem.* 191, 229–236.
- Brandenburg, K., Seydel, U., 1996. Fourier transform infrared spectroscopy of cell surface polysaccharides. In: Mantsch, H.H., Chapman, D. (Eds.), *Infrared Spectroscopy of Biomolecules*. John Wiley and Sons, Inc., New York, pp. 203–237.
- Brandenburg, K., Seydel, U., Schromm, A.B., Loppnow, H., Koch, M.H.J., Rietschel, E.T., 1996. Conformation of lipid A, the Endotoxic Center of Bacterial Lipopolysaccharide. *J. Endotoxin Res.* 3, 173–178.
- Brandes Ammann, A., Brandl, H., 2011. Detection and differentiation of bacterial spores in a mineral matrix by Fourier transform infrared spectroscopy (FTIR) and chemometrical data treatment. *BMC Biophys.* 4, 14.
- Brandes, J.A., Lee, C., Wakeham, S., Peterson, M., Jacobsen, C., Wirick, S., Cody, G., 2004. Examining marine particulate organic matter at sub-micron scales using scanning transmission X-ray microscopy and carbon X-ray absorption near edge structure spectroscopy. *Mar. Chem.* 92, 107–121.
- Breen, C., Clegg, F., Herron, M.M., Hild, G.P., Hillier, S., Hughes, T.L., Jones, T.G.J., Matteson, A., Yarwood, J., 2008. Bulk mineralogical characterisation of oilfield reservoir rocks and sandstones using diffuse reflectance infrared Fourier transform spectroscopy and partial least squares analysis. *J. Petroleum Sci. Eng.* 60, 1–17.
- Brewer, C.E., Schmidt-Rohr, K., Satrio, J.A., Brown, R.C., 2009. Characterization of biochar from fast pyrolysis and gasification systems. *Environ. Prog. Sustain. Energy* 28, 386–396.
- Brewer, S.H., Anthireya, S.J., Lappi, S.E., Drapcho, D.L., Franzen, S., 2002. Detection of DNA Hybridization on gold surfaces by polarization modulation infrared reflection absorption spectroscopy. *Langmuir* 18, 4460–4464.
- Brigatti, M.F., Lugli, C., Montorsi, S., Poppi, L., 1999. Effects of exchange cations and layer-charge location on cysteine retention by smectites. *Clays Clay Miner.* 47, 664–671.
- Brody, R.H., Carter, E.A., Edwards, H.G.M., Pollard, A.M., 1999a. FT-Raman spectroscopy, applications. In: Editor-in-Chief: John, C.L. (Ed.), *Encyclopedia of Spectroscopy and Spectrometry* second ed. Academic Press, Oxford, pp. 732–740.
- Brody, R.H., Carter, E.A., Edwards, H.G.M., Pollard, A.M., 1999b. FT-Raman spectroscopy, applications. In: Editor-in-Chief: John, C.L. (Ed.), *Encyclopedia of Spectroscopy and Spectrometry*, Elsevier, Oxford, pp. 649–657.
- Bruckman, V.J., Wriessnig, K., 2013. Improved soil carbonate determination by FT-IR and X-ray analysis. *Environ. Chem. Lett.* 11, 65–70.
- Brunetti, G., Farrag, K., Plaza, C., Senesi, N., 2012. Advanced techniques for characterization of organic matter from anaerobically digested grapemarc distillery effluents and amended soils. *Environ. Monit. Assess.* 184, 2079–2089.

- Bullen, H.A., Oehrle, S.A., Bennett, A.F., Taylor, N.M., Barton, H.A., 2008. Use of attenuated total reflectance Fourier transform infrared spectroscopy to identify microbial metabolic products on carbonate mineral surfaces. *Appl. Environ. Microbiol.* 74, 4553–4559.
- Busscher, W.J., Novak, J.M., Evans, D.E., Watts, D.W., Niandou, M.A.S., Ahmedna, M., 2010. Influence of Pecan Biochar on physical properties of a Norfolk Loamy sand. *Soil Sci.* 175, 10–14.
- Cagnasso, M., Boero, V., Franchini, M.A., Chorover, J., 2010. ATR-FTIR studies of phospholipid vesicle interactions with alpha-FeOOH and alpha-Fe₂O₃ surfaces. *Colloids Surf. B Biointerfaces* 76, 456–467.
- Caillaud, J., Proust, D., Righi, D., Martin, F., 2004. Fe-rich clays in a weathering profile developed from serpentinite. *Clays Clay Miner.* 52, 779–791.
- Calderón, F.J., McCarty, G.W., Reeves, J.B., 2006. Pyrolysis-MS and FT-IR analysis of fresh and decomposed dairy manure. *J. Anal. Appl. Pyrolysis* 76, 14–23.
- Calderón, F.J., Mikha, M.M., Vigil, M.F., Nielsen, D.C., Benjamin, J.G., Reeves III, J.B., 2011a. Diffuse-reflectance mid-infrared spectral properties of soils under alternative crop rotations in a semi-arid climate. *Commun. Soil Sci. Plant Anal.* 42, 2143–2159.
- Calderón, F.J., Reeves, J.B., Collins, H.P., Paul, E.A., 2011b. Chemical differences in soil organic matter fractions determined by diffuse-reflectance mid-infrared spectroscopy (All rights reserved. No part of this periodical may be reproduced or transmitted in any form or by any means, electronic or mechanical, including photocopying, recording, or any information storage and retrieval system, without permission in writing from the publisher. Permission for printing and for reprinting the material contained herein has been obtained by the publisher) *Soil Sci. Soc. Am. J.* 75, 568–579.
- Calderón, F.J., Reeves III, J.B., Collins, H.P., Paul, E.A., 2011c. Chemical differences in soil organic matter fractions determined by diffuse-reflectance mid-infrared spectroscopy. *Soil Sci. Soc. Am. J.* 75, 568–579.
- Cambier, P., 1986a. Infrared study of goethites of varying crystallinity and particle size; I, interpretation of OH and lattice vibration frequencies. *Clay Miner.* 21, 191–200.
- Cambier, P., 1986b. Infrared study of goethites of varying crystallinity and particle size; II, crystallographic and morphological changes in series of synthetic goethites. *Clay Miner.* 21, 201–210.
- Campion, A., Kambhampati, P., 1998. Surface-enhanced Raman scattering. *Chem. Soc. Rev.* 27, 241–250.
- Cançado, L.G., Jorio, A., Pimenta, M.A., 2007. Measuring the absolute Raman cross section of nanographites as a function of laser energy and crystallite size. *Phys. Rev. B* 76, 064304.
- Cao, Y.Y., Wei, X., Cai, P., Huang, Q.Y., Rong, X.M., Liang, W., 2011. Preferential adsorption of extracellular polymeric substances from bacteria on clay minerals and iron oxide. *Colloids Surf. B Biointerfaces* 83, 122–127.
- Capriel, P., 1997. Hydrophobicity of organic matter in arable soils: influence of management. *Eur. J. Soil Sci.* 48, 457–462.
- Capriel, P., Beck, T., Borchert, H., Gronholz, J., Zachmann, G., 1995. Hydrophobicity of the organic matter in arable soils. *Soil Biol. Biochem.* 27, 1453–1458.
- Carballo, T., Gil, M., Gómez, X., González-Andrés, F., Morán, A., 2008a. Characterization of different compost extracts using Fourier-transform infrared spectroscopy (FTIR) and thermal analysis. *Biodegradation* 19, 815–830.
- Carballo, T., Gil, M.V., Gomez, X., Gonzalez-Andres, F., Moran, A., 2008b. Characterization of different compost extracts using Fourier-transform infrared spectroscopy (FTIR) and thermal analysis. *Biodegradation* 19, 815–830.
- Carr, G.L., 2001. Resolution limits for infrared microspectroscopy explored with synchrotron radiation. *Rev. Sci. Instrum.* 72, 1613–1619.

- Carrero, J.A., Goienaga, N., Olivares, M., Martínez-Arkarazo, I., Arana, G., Madariaga, J.M., 2012. Raman spectroscopy assisted with XRF and chemical simulation to assess the synergic impacts of guardrails and traffic pollutants on urban soils. *J. Raman Spectrosc.* 43, 1498–1503.
- Case, S.D.C., McNamara, N.P., Reay, D.S., Whitaker, J., 2012. The effect of biochar addition on N₂O and CO₂ emissions from a sandy loam soil—the role of soil aeration. *Soil Biol. Biochem.* 51, 125–134.
- Cécillon, L., Certini, G., Lange, H., Forte, C., Strand, L.T., 2012. Spectral fingerprinting of soil organic matter composition. *Organic Geochemistry* 46, 127–136.
- Celis, R., Hermosin, M.C., Cox, L., Cornejo, J., 1999. Sorption of 2,4-dichlorophenoxyacetic acid by model particles simulating naturally occurring soil colloids. *Environ. Sci. Technol.* 33, 1200–1206.
- Cerriotti, G., Amarasiwardena, D., 2009. A study of antimony complexed to soil-derived humic acids and inorganic antimony species along a Massachusetts highway. *Microchem. J.* 91, 85–93.
- Cervini-Silva, J., Fowle, D.A., Banfield, J., 2005. Biogenic dissolution of a soil cerium-phosphate mineral. *Am. J. Sci.* 305, 711–726.
- Cesco, S., Nikolic, M., Römheld, V., Varanini, Z., Pinton, R., 2002. Uptake of ⁵⁹Fe from soluble ⁵⁹Fe-humate complexes by cucumber and barley plants. *Plant Soil* 241, 121–128.
- Chabot, M., Hoang, T., Al-Abadleh, H.A., 2009. ATR-FTIR studies on the nature of surface complexes and desorption efficiency of p-arsanilic acid on iron (oxyhydr)oxides. *Environ. Sci. Technol.* 43, 3142–3147.
- Chadwick, O.A., Chorover, J., 2001. The chemistry of pedogenic thresholds. *Geoderma* 100, 321–353.
- Chalmers, J.M., Griffiths, P.R., 2002. *Handbook of Vibrational Spectroscopy*. J. Wiley.
- Chang, P.-H., Li, Z., Jiang, W.-T., Jean, J.-S., 2009a. Adsorption and intercalation of tetracycline by swelling clay minerals. *Appl. Clay Sci.* 46, 27–36.
- Chang, P.-H., Li, Z., Yu, T.-L., Munkhbayer, S., Kuo, T.-H., Hung, Y.-C., et al., 2009b. Sorptive removal of tetracycline from water by palygorskite. *J. Hazard. Mater.* 165, 148–155.
- Chang, P.-H., Li, Z., Jean, J.-S., Jiang, W.-T., Wang, C.-J., Lin, K.-H., 2012. Adsorption of tetracycline on 2:1 layered non-swelling clay mineral illite. *Applied Clay Science* 67–68, 158–163.
- Chefetz, B., Hader, Y., Chen, Y., 1998. Dissolved organic carbon fractions formed during composting of municipal solid waste: properties and significance. *Acta Hydrochim. Hydrobiol.* 26, 172–179.
- Chen, H., He, X., Rong, X., Chen, W., Cai, P., Liang, W., et al., 2009. Adsorption and biodegradation of carbaryl on montmorillonite, kaolinite and goethite. *Applied Clay Science* 46, 102–108.
- Chen, W.-R., Ding, Y., Johnston, C.T., Teppen, B.J., Boyd, S.A., Li, H., 2010. Reaction of lincosamide antibiotics with manganese oxide in aqueous solution. *Environ. Sci. Technol.* 44, 4486–4492.
- Chen, Y.N., 2003. Nuclear magnetic resonance, infra-red and pyrolysis: application of spectroscopic methodologies to maturity determination of composts. *Compost Sci. Util.* 11, 152–168.
- Chernyshova, I.V., Hochella Jr., M.F., Madden, A.S., 2007. Size-dependent structural transformations of hematite nanoparticles. 1. Phase transition. *Phys. Chem. Chem. Phys.* 9, 1736–1750.
- Cheshire, M.V., Dumat, C., Fraser, A.R., Hillier, S., Staunton, S., 2000. The interaction between soil organic matter and soil clay minerals by selective removal and controlled addition of organic matter. *Eur. J. Soil Sci.* 51, 497–509.
- Cheung, H.Y., Sun, S.Q., Sreedhar, B., Ching, W.M., Tanner, P.A., 2000. Alterations in extracellular substances during the biofilm development of *Pseudomonas aeruginosa* on aluminium plates. *J. Appl. Microbiol.* 89, 100–106.

- Chia, C.H., Gong, B., Joseph, S.D., Marjo, C.E., Munroe, P., Rich, A.M., 2012. Imaging of mineral-enriched biochar by FTIR, Raman and SEM-EDX. *Vib. Spectrosc.* 62, 248–257.
- Chittur, K.K., 1998a. FTIR/ATR for protein adsorption to biomaterial surfaces. *Biomaterials* 19, 357–369.
- Chittur, K.K., 1998b. Surface techniques to examine the biomaterial-host interface: an introduction to the papers. *Biomaterials* 19, 301–305.
- Choi, S., Crosson, G., Mueller, K.T., Seraphin, S., Chorover, J., 2005. Clay mineral weathering and contaminant dynamics in a caustic aqueous system - II. Mineral transformation and microscale partitioning. *Geochim. Cosmochim. Acta* 69, 4437–4451.
- Chorover, J., Amistadi, M.K., 2001. Reaction of forest floor organic matter at goethite, birnessite and smectite surfaces. *Geochim. Cosmochim. Acta* 65, 95–109.
- Chorover, J., Amistadi, M.K., Chadwick, O.A., 2004. Surface charge evolution of mineral-organic complexes during pedogenesis in Hawaiian basalt. *Geochim. Cosmochim. Acta* 68, 4859–4876.
- Chu, H.A., Hillier, W., Debus, R.J., 2004. Evidence that the C-terminus of the D1 polypeptide of photosystem II is ligated to the manganese ion that undergoes oxidation during the S-1 to S-2 transition: an isotope-edited FTIR study. *Biochemistry* 43, 3152–3166.
- Čičel, B., Komadel, P., 1997. Structural formulae of layer silicates. In: Amonette, J.E., Zelazny, L.W. (Eds.), *Quantitative Methods in Soil Mineralogy*. SSSA, Madison, WI, pp. 114–136.
- Clarke, C.E., Aguilar-Carrillo, J., Roychoudhury, A.N., 2011. Quantification of drying induced acidity at the mineral-water interface using ATR-FTIR spectroscopy. *Geochim. Cosmochim. Acta* 75, 4846–4856.
- Coblentz, W.W., 1911. Radiometric investigation of water of crystallisation, light filters and standard absorption bands. *Bull. Bur. Stand.* 7, 619–668.
- Coleyshaw, E.E., Griffith, W.P., Bowell, R.J., 1994. Fourier-transform Raman spectroscopy of minerals. *Spectrochim. Acta Part A Mol. Spectrosc.* 50, 1909–1918.
- Colthup, N.B., Daly, L.H., Wiberley, S.E., 1990. *Introduction to Infrared and Raman Spectroscopy*. Academic Press.
- Connor, P.A., McQuillan, A.J., 1999. Phosphate adsorption onto TiO₂ from aqueous solutions: An in situ internal reflection infrared spectroscopic study. *Langmuir* 15, 2916–2921.
- Cooley, J.W., Tukey, J.W., 1965. An algorithm for machine calculation of complex Fourier series. *Math. Comput.* 19, 297.
- Corrado, G., Sanchez-Cortes, S., Francioso, O., Garcia-Ramos, J.V., 2008. Surface-enhanced Raman and fluorescence joint analysis of soil humic acids. *Anal. Chim. Acta* 616, 69–77.
- Cowen, S., Duggal, M., Hoang, T., Al-Abadleh, H.A., 2008. Vibrational spectroscopic characterization of some environmentally important organoarsenicals—a guide for understanding the nature of their surface complexes. *Can. J. Chem. Rev. Can. Chim.* 86, 942–950.
- Cox, R.J., Peterson, H.L., Young, J., Cusik, C., Espinoza, E.O., 2000. The forensic analysis of soil organic by FTIR. *Forensic Sci. Int.* 108, 107–116.
- Cozzolino, D., Morón, A., 2006. Potential of near-infrared reflectance spectroscopy and chemometrics to predict soil organic carbon fractions. *Soil Tillage Res.* 85, 78–85.
- Crowley, D.E., Wang, Y.C., Reid, C.P.P., Szaniszló, P.J., 1991. Mechanisms of iron acquisition from siderophores by microorganisms and plants. *Plant Soil* 130, 179–198.
- Cuadros, J., Dudek, T., 2006. FTIR investigation of the evolution of the octahedral sheet of kaolinite-smectite with progressive kaolinization. *Clays Clay Miner.* 54, 1–11.
- D'Acqui, L.P., Churchman, G.J., Janik, L.J., Ristori, G.G., Weissmann, D.A., 1999. Effect of organic matter removal by low-temperature ashing on dispersion of undisturbed aggregates from a tropical crusting soil. *Geoderma* 93, 311–324.
- Dahlgren, R.A., 1994. Quantification of allophane and imogolite. In: Amonette, J.E., Zelazny, L.W. (Eds.), *Quantitative Methods in Soil Mineralogy*. SSSA, Madison, WI, pp. 430–451.

- Dahm, D.J., Dahm, K.D., 2001. The Physics of Near Infrared Scattering. American Association of Cereal Chemists, St. Paul, Minnesota.
- Das, R.S., Agrawal, Y.K., 2011. Raman spectroscopy: recent advancements, techniques and applications. *Vib. Spectrosc.* 57, 163–176.
- Davies, J.E.D., Jabeen, N., 2002. The adsorption of herbicides and pesticides on clay minerals and soils. Part 1. Isoproturon. *Journal of Inclusion Phenomena and Macrocyclic Chemistry* 43, 329–336.
- Davies, J.E.D., Jabeen, N., 2003. The adsorption of herbicides and pesticides on clay minerals and soils. Part 2. Atrazine. *Journal of Inclusion Phenomena and Macrocyclic Chemistry* 46, 57–64.
- Davinic, M., Fultz, L.M., Acosta-Martinez, V., Calderón, F.J., Cox, S.B., Dowd, S.E., Allen, V.G., Zak, J.C., Moore-Kucera, J., 2012a. Pyrosequencing and mid-infrared spectroscopy reveal distinct aggregate stratification of soil bacterial communities and organic matter composition. *Soil Biol. Biochem.* 46, 63–72.
- Davinic, M., Fultz, L.M., Acosta-Martinez, V., Calderón, F.J., Cox, S.B., Dowd, S.E., Allen, V.G., Zak, J.C., Moore-Kucera, J., 2012b. Pyrosequencing and mid-infrared spectroscopy reveal distinct aggregate stratification of soil bacterial communities and organic matter composition. *Soil Biol. Biochem.* 46, 63–72.
- Dawson, L.A., Hillier, S., 2010. Measurement of soil characteristics for forensic applications. *Surf. Interface Anal.* 42, 363–377.
- de Faria, D.L.A., Venâncio Silva, S., de Oliveira, M.T., 1997. Raman microspectroscopy of some iron oxides and oxyhydroxides. *J. Raman Spectrosc.* 28, 873–878.
- de Oliveira, M.F., Johnston, C.T., Premachandra, G.S., Teppen, B.J., Li, H., Laird, D.A., Zhu, D.Q., Boyd, S.A., 2005. Spectroscopic study of carbaryl sorption on smectite from aqueous suspension. *Environ. Sci. Technol.* 39, 9123–9129.
- Deacon, G.B., Phillips, R.J., 1980. Relationships between the carbon–oxygen stretching frequencies of carboxylato complexes and the type of carboxylate coordination. *Coord. Chem. Rev.* 33, 227–250.
- Demyan, M.S., Rasche, F., Schulz, E., Breulmann, M., Mueller, T., Cadisch, G., 2012. Use of specific peaks obtained by diffuse reflectance Fourier transform mid-infrared spectroscopy to study the composition of organic matter in a Haplic Chernozem. *Eur. J. Soil Sci.* 63, 189–199.
- Deo, N., Natarajan, K.A., Somasundaran, P., 2001. Mechanisms of adhesion of *Paenibacillus polymyxa* onto hematite, corundum and quartz. *Int. J. Mineral Process.* 62, 27–39.
- Depalma, S., Cowen, S., Hoang, T., Al-Abadleh, H.A., 2008. Adsorption thermodynamics of p-arsanilic acid on iron (oxyhydr)oxides: In-situ ATR-FTIR studies. *Environ. Sci. Technol.* 42, 1922–1927.
- Dickensheets, D.L., Wynn-Williams, D.D., Edwards, H.G.M., Schoen, C., Crowder, C., Newton, E.M., 2000. A novel miniature confocal microscope/Raman spectrometer system for biomolecular analysis on future Mars missions after Antarctic trials. *J. Raman Spectrosc.* 31, 633–635.
- Ding, G., Liu, X., Herbert, S., Novak, J., Amarasiwardena, D., Xing, B., 2006. Effect of cover crop management on soil organic matter. *Geoderma* 130, 229–239.
- Ding, G., Novak, J.M., Amarasiwardena, D., Hunt, P.G., Xing, B., 2002. Soil organic matter characteristics as affected by tillage management. *Soil Sci. Soc. Am. J.* 66, 421–429.
- Dobson, K.D., McQuillan, A.J., 1999. In situ infrared spectroscopic analysis of the adsorption of aliphatic carboxylic acids to TiO₂, ZrO₂, Al₂O₃, and Ta₂O₅ from aqueous solutions. *Spectrochim. Acta Part A Mol. Biomol. Spectrosc.* 55, 1395–1405.
- Dokken, K.M., Davis, L.C., Erickson, L.E., Castro-Diaz, S., Marinkovic, N.S., 2005a. Synchrotron Fourier transform infrared microspectroscopy: a new tool to monitor the fate of organic contaminants in plants. *Microchem. J.* 81, 86–91.
- Dokken, K.M., Davis, L.C., Marinkovic, N.S., 2005b. Using SR-IMS to study the fate and transport of organic contaminants in plants. *Spectroscopy* 20, 14–18.

- Dollish, F.R., Fateley, W.G., Bentley, F.F., 1974. Characteristic Raman frequencies of organic compounds. Wiley.
- Dowding, C.E., Borda, M.J., Fey, M.V., Sparks, D.L., 2005. A new method for gaining insight into the chemistry of drying mineral surfaces using ATR-FTIR. *J. Colloid Interface Sci.* 292, 148–151.
- Dresselhaus, M.S., Dresselhaus, G., Saito, R., Jorio, A., 2005. Raman spectroscopy of carbon nanotubes. *Phys. Rep. Rev. Sect. Phys. Lett.* 409, 47–99.
- Du, C., He, Z., Zhou, J., 2013a. Characterization of soil humic substances using mid-infrared photoacoustic spectroscopy. In: Xu, J., Wu, J., He, Y. (Eds.), *Functions of Natural Organic Matter in Changing Environment*. Springer, Netherlands, pp. 43–47.
- Du, C., Ma, Z., Zhou, J., Goyne, K.W., 2013b. Application of mid-infrared photoacoustic spectroscopy in monitoring carbonate content in soils. *Sens. Actuators B Chem.* 188, 1167–1175.
- Duckworth, O.W., Martin, S.T., 2001. Surface complexation and dissolution of hematite by C-1-C-6 dicarboxylic acids at pH = 5.0. *Geochim. Cosmochim. Acta* 65, 4289–4301.
- Dumas, P., Miller, L., 2003. Biological and biomedical applications of synchrotron infrared microspectroscopy. *J. Biol. Phys.* 29, 201–218.
- Dumas, P., Sockalingum, G.D., Sulé-Suso, J., 2007. Adding synchrotron radiation to infrared microspectroscopy: what's new in biomedical applications? *Trends Biotechnol.* 25, 40–44.
- Dünnwald, J., Otto, A., 1989. An investigation of phase transitions in rust layers using Raman spectroscopy. *Corros. Sci.* 29, 1167–1176.
- Durand, J.-C., Jacquot, B., Salehi, H., Margerit, J., Cuisinier, F.G., 2012. Confocal Raman microscopy and SEM/EDS investigations of the interface between the zirconia core and veneering ceramic: the influence of a liner and regeneration firing. *J. Mater. Sci. Mater. Med.* 23, 1343–1353.
- Eboigbodin, K.E., Biggs, C.A., 2008. Characterization of the extracellular polymeric substances produced by *Escherichia coli* using infrared spectroscopic, proteomic, and aggregation studies. *Biomacromolecules* 9, 686–695.
- Edwards, H., Munshi, T., Scowen, I., Surtees, A., Swindles, G.T., 2012. Development of oxidative sample preparation for the analysis of forensic soil samples with near-IR Raman spectroscopy. *J. Raman Spectrosc.* 43, 323–325.
- Efrima, S., Bronk, B.V., 1998. Silver colloids impregnating or coating bacteria. *J. Phys. Chem. B* 102, 5947–5950.
- Egli, M., Mavris, C., Mirabella, A., Giaccai, D., 2010. Soil organic matter formation along a chronosequence in the Morteratsch proglacial area (Upper Engadine, Switzerland). *CATENA* 82, 61–69.
- Elderfield, H., Hem, J.D., 1973. The development of crystalline structure in aluminum hydroxide polymorphs. *Mineral. Mag.* 39, 89–96.
- Elkins, K.M., Nelson, D.J., 2002. Spectroscopic approaches to the study of the interaction of aluminum with humic substances. *Coord. Chem. Rev.* 228, 205–225.
- Ellerbrock, R., Höhn, A., Gerke, H., 1999. Characterization of soil organic matter from a sandy soil in relation to management practice using FT-IR spectroscopy. *Plant and Soil* 213, 55–61.
- Ellerbrock, R.H., Gerke, H.H., 2004. Characterizing organic matter of soil aggregate coatings and biopores by Fourier transform infrared spectroscopy. *Eur. J. Soil Sci.* 55, 219–228.
- Ellerbrock, R.H., Gerke, H.H., Bachmann, J., Goebel, M.-O., 2005. Composition of organic matter fractions for explaining wettability of three forest soils. *Soil Sci. Soc. Am. J.* 69, 57–66.
- Ellerbrock, R.H., Gerke, H.H., Boehm, C., 2009. In situ DRIFT characterization of organic matter composition on soil structural surfaces. *Soil Sci. Soc. Am. J.* 73, 531–540.
- Ellery, A., Wynn-Williams, D., Parnell, J., Edwards, H.G.M., Dickensheets, D., 2004. The role of Raman spectroscopy as an astrobiological tool in the exploration of Mars. *J. Raman Spectrosc.* 35, 441–457.

- Elzinga, E.J., Huang, J.-H., Chorover, J., Kretzschmar, R., 2012. ATR-FTIR spectroscopy study of the influence of pH and contact time on the adhesion of *Shewanella putrefaciens* bacterial cells to the surface of hematite. *Environ. Sci. Technol.* 46, 12848–12855.
- Elzinga, E.J., Kretzschmar, R., 2013. In situ ATR-FTIR spectroscopic analysis of the co-adsorption of orthophosphate and Cd(II) onto hematite. *Geochim. Cosmochim. Acta* 117, 53–64.
- Elzinga, E.J., Sparks, D.L., 2007. Phosphate adsorption onto hematite: an in situ ATR-FTIR investigation of the effects of pH and loading level on the mode of phosphate surface complexation. *J. Colloid Interface Sci.* 308, 53–70.
- Epperson, P.M., Sweedler, J.V., Bilhorn, R.B., Sims, G.R., Denton, M.B., 1988. Applications of charge transfer devices in spectroscopy. *Anal. Chem.* 60, 327A–335A.
- Ertlen, D., Schwartz, D., Trautmann, M., Webster, R., Brunet, D., 2010. Discriminating between organic matter in soil from grass and forest by near-infrared spectroscopy. *Eur. J. Soil Sci.* 61, 207–216.
- Etchegoin, P.G., Le Ru, E.C., 2010. Basic electromagnetic theory of SERS. In: *Surface Enhanced Raman Spectroscopy*. Wiley-VCH Verlag GmbH & Co. KGaA, pp. 1–37.
- Eusterhues, K., Rumpel, C., Kleber, M., Kögel-Knabner, I., 2003. Stabilisation of soil organic matter by interactions with minerals as revealed by mineral dissolution and oxidative degradation. *Org. Geochem.* 34, 1591–1600.
- Eusterhues, K., Rumpel, C., Kögel-Knabner, I., 2005. Stabilization of soil organic matter isolated via oxidative degradation. *Org. Geochem.* 36, 1567–1575.
- Ewald, M., Belin, C., Berger, P., Weber, J.H., 1983. Corrected fluorescence spectra of fulvic acids isolated from soil and water. *Environ. Sci. Technol.* 17, 501–504.
- Falk, M., Hartman, K.A., Lord, R.C., 1963. Hydration of deoxyribonucleic acid. 3. A spectroscopic study of effect of hydration on structure of deoxyribonucleic acid. *J. Am. Chem. Soc.* 85, 391–394.
- Farmer, V.C., 1958. The infra-red spectra of talc, saponite, and hectorite. *Mineral. Mag.* 31, 829–845.
- Farmer, V.C., 1974a. The anhydrous oxide minerals. Vol. Mineral. Soc. Monograph 4. In: Farmer, V.C. (Ed.), *The Infrared Spectra of Minerals*. Mineral. Soc., London, UK, pp. 183–204.
- Farmer, V.C., 1974b. *The Infrared Spectra of Minerals*. Mineralogical Society, London.
- Farmer, V.C., 1974c. The layer silicates. Vol. Mineral. Soc. Monograph 4. In: Farmer, V.C. (Ed.), *The Infrared Spectra of Minerals*. Mineral. Soc., London, UK, pp. 331–363.
- Farmer, V.C., 2000. Transverse and longitudinal crystal modes associated with OH stretching vibrations in single crystals of kaolinite and dickite. *Spectrochim. Acta Part A* 56, 927–930.
- Farmer, V.C., Fraser, A.R., Russell, J.D., Yoshinaga, N., 1977. Recognition of imogolite structures in allophanic clays by infrared spectroscopy. *Clay Miner.* 12, 55–57.
- Favilli, F., Egli, M., Cherubini, P., Sartori, G., Haeblerli, W., Delbos, E., 2008. Comparison of different methods of obtaining a resilient organic matter fraction in Alpine soils. *Geoderma* 145, 355–369.
- Fernández-Getino, A.P., Hernández, Z., Piedra Buena, A., Almendros, G., 2010. Assessment of the effects of environmental factors on humification processes by derivative infrared spectroscopy and discriminant analysis. *Geoderma* 158, 225–232.
- Ferrari, A.C., Meyer, J.C., Scardaci, V., Casiraghi, C., Lazzeri, M., Mauri, F., Piscanec, S., Jiang, D., Novoselov, K.S., Roth, S., Geim, A.K., 2006. Raman spectrum of graphene and graphene layers. *Phys. Rev. Lett.* 97.
- Ferrari, A.C., Robertson, J., 2000. Interpretation of Raman spectra of disordered and amorphous carbon. *Phys. Rev. B* 61, 14095–14107.
- Ferrari, E., Francioso, O., Nardi, S., Saladini, M., Ferro, N.D., Morari, F., 2011. DRIFT and HR MAS NMR characterization of humic substances from a soil treated with different organic and mineral fertilizers. *J. Mol. Struct.* 998, 216–224.

- Ferraro, J.R., 1967. Advances in Raman instrumentation and sampling techniques. In: Szymanski, H. (Ed.), *Raman Spectroscopy*. Springer, US, pp. 44–81.
- Ferraro, J.R., 2003. *Introductory Raman Spectroscopy*, second ed. Academic Press, Amsterdam.
- Ferreira, A.R., Martins, M.J.F., Konstantinova, E., Capaz, R.B., Souza, W.F., Chiaro, S.S.X., Leitão, A.A., 2011. Direct comparison between two structural models by DFT calculations. *J. Solid State Chem.* 184, 1105–1111.
- Fialho, L.L., Lopes da Silva, W.T., Milori, D.M.B.P., Simões, M.L., Martin-Neto, L., 2010. Characterization of organic matter from composting of different residues by physico-chemical and spectroscopic methods. *Bioresour. Technol.* 101, 1927–1934.
- Filip, Z., Haider, K., Beutelspacher, H., Martin, J.P., 1974. Comparisons of IR-spectra from melanins of microscopic soil fungi, humic acids and model phenol polymers. *Geoderma* 11, 37–52.
- Fitts, J.P., Persson, P., Brown, G.E., Parks, G.A., 1999. Structure and bonding of Cu(II)-glutamate complexes at the gamma-Al₂O₃-water interface. *J. Colloid Interface Sci.* 220, 133–147.
- Fleischmann, M., Hendra, P.J., McQuillan, A.J., 1974. Raman spectra of pyridine adsorbed at a silver electrode. *Chem. Phys. Lett.* 26, 163–166.
- Follett, R.F., Paul, E.A., Pruessner, E.G., 2007. Soil carbon dynamics during a long-term incubation study involving C-13 and C-14 measurements. *Soil Sci.* 172, 189–208.
- Foriel, J., Philippot, P., Susini, J., Dumas, P., Somogyi, A., Salomé, M., Khodja, H., Ménez, B., Fouquet, Y., Moreira, D., López-García, P., 2004. High-resolution imaging of sulfur oxidation states, trace elements, and organic molecules distribution in individual microfossils and contemporary microbial filaments. *Geochim. Cosmochim. Acta* 68, 1561–1569.
- Forrester, S.T., Janik, L.J., McLaughlin, M.J., Soriano-Disla, J.M., Stewart, R., Dearman, B., 2013. Total Petroleum Hydrocarbon Concentration Prediction in Soils Using Diffuse Reflectance Infrared Spectroscopy. *Soil Sci. Soc. Am. J.* 77, 450–460.
- Foucher, F., Lopez-Reyes, G., Bost, N., Rull-Perez, F., Rüßmann, P., Westall, F., 2013. Effect of grain size distribution on Raman analyses and the consequences for in situ planetary missions. *J. Raman Spectrosc.* 44, 916–925.
- Francioso, O., Ciavatta, C., Sánchez-Cortés, S., Tugnoli, V., Sitti, L., Gessa, C., 2000. Spectroscopic characterization of soil organic matter in long-term amendment trials. *Soil Sci.* 165, 495–504.
- Francioso, O., Sánchez-Cortés, S., Tugnoli, V., Marzadori, C., Ciavatta, C., 2001. Spectroscopic study (DRIFT, SERS and ¹H NMR) of peat, leonardite and lignite humic substances. *J. Mol. Struct.* 565–566, 481–485.
- Francioso, O.S.-C., S., Tugnoli, V., Ciavatta, C., Sitti, L., Gessa, C., 1996. Infrared, Raman, and nuclear magnetic resonance (¹H, ¹³C, and ³¹P) spectroscopy in the study of fractions of peat humic acids. *Appl. Spectrosc.* 50, 1165–1174.
- Fries, M., Steele, A., 2011. Raman Spectroscopy and Confocal Raman Imaging in Mineralogy and Petrography. In: Dieing, T., Hollricher, O., Toporski, J. (Eds.), *Confocal Raman Microscopy*, vol. 158. Springer Berlin Heidelberg, pp. 111–135.
- Fringeli, U.P., Günthard, H.H., 1981. Infrared membrane spectroscopy. In: Grell, E. (Ed.), *Membrane Spectroscopy*. Springer-Verlag, Berlin, pp. 270–332.
- Frost, R.L., Bahfenne, S., Čejka, J., Sejkora, J., Plášil, J., Palmer, S.J., 2010a. Raman and infrared study of phyllosilicates containing heavy metals (Sb, Bi): bismutoferrite and chapmanite. *J. Raman Spectrosc.* 41, 814–819.
- Frost, R.L., Bahfenne, S., Čejka, J., Sejkora, J., Plášil, J., Palmer, S.J., 2010b. Raman spectroscopic study of the hydrogen-arsenate mineral pharmacolite Ca(AsO₃OH)·2H₂O—implications for aquifer and sediment remediation. *J. Raman Spectrosc.* 41, 1348–1352.
- Frost, R.L., Palmer, S.J., 2011. Raman spectroscopic study of the minerals diadochite and destinezite Fe³⁺₂(PO₄,SO₄)₂(OH)·6H₂O: implications for soil science. *J. Raman Spectrosc.* 42, 1589–1595.

- Frost, R.L., Thu Ha, T., Kristof, J., 1997. FT-Raman spectroscopy of the lattice region of kaolinite and its intercalates. *Vib. Spectrosc.* 13, 175–186.
- Fuentes, M., Baigorri, R., Gonzalez-Gaitano, G., Garcia-Mina, J.M., 2007. The complementary use of H-1 NMR, C-13 NMR, FTIR and size exclusion chromatography to investigate the principal structural changes associated with composting of organic materials with diverse origin. *Org. Geochem.* 38, 2012–2023.
- Fuertes, A.B., Arbestain, M.C., Sevilla, M., Macia-Agullo, J.A., Fiol, S., Lopez, R., Smernik, R.J., Aitkenhead, W.P., Arce, F., Macias, F., 2010. Chemical and structural properties of carbonaceous products obtained by pyrolysis and hydrothermal carbonisation of corn stover. *Aust. J. Soil. Res.* 48, 618–626.
- Fultz, L.M., 2012. Dynamics of Soil Aggregation, Organic Carbon Pools, and Greenhouse Gases in Integrated Crop-Livestock Agroecosystems in the Texas High Plains. Tech University, Texas.
- Gao, X., Chorover, J., 2009. In-situ monitoring of cryptosporidium parvum oocyst surface adhesion using ATR-FTIR spectroscopy. *Colloids Surf. B Biointerfaces* 71, 169–176.
- Gao, X., Chorover, J., 2011. Amphiphile disruption of pathogen attachment at the hematite (α -Fe₂O₃)-Water interface. *Langmuir* 27, 5936–5943.
- Gao, X., Metge, D.W., Ray, C., Harvey, R.W., Chorover, J., 2009. Surface complexation of carboxylate adheres cryptosporidium parvum oocysts to the hematite-water interface. *Environ. Sci. Technol.* 43, 7423–7429.
- Garidel, P., Boese, M., 2007. Non-invasive Fourier transform infrared microspectroscopy and imaging techniques. In: Méndez-Vilas, A., Diaz, J. (Eds.), *Basic Principles and Application, in Modern Research and Educational Topics in Microscopy*.
- Ghosh, U., Gillette, J.S., Luthy, R.G., Zare, R.N., 2000. Microscale location, characterization, and association of polycyclic aromatic hydrocarbons on harbor sediment particles. *Environ. Sci. Technol.* 34, 1729–1736.
- Giacometti, C., Demyan, M.S., Cavani, L., Marzadori, C., Ciavatta, C., Kandeler, E., 2013. Chemical and microbiological soil quality indicators and their potential to differentiate fertilization regimes in temperate agroecosystems. *Appl. Soil Ecol.* 64, 32–48.
- Glaser, B., 2007. Prehistorically modified soils of central Amazonia: a model for sustainable agriculture in the twenty-first century. *Philos. Trans. Roy. Soc. B: Biol. Sci.* 362, 187–196.
- Glaser, B., Lehmann, J., Zech, W., 2002. Ameliorating physical and chemical properties of highly weathered soils in the tropics with charcoal—a review. *Biol. Fertil. Soils* 35, 219–230.
- Glaser, B., Woods, W.I., 2004. *Amazon Dark Earths: Explorations in Space and Time*. Springer, Berlin.
- Glotch, T.D., Rossman, G.R., 2009. Mid-infrared reflectance spectra and optical constants of six iron oxide/oxyhydroxide phases. *Icarus* 204, 663–671.
- Goienaga, N., Arrieta, N., Carrero, J.A., Olivares, M., Sarmiento, A., Martínez-Arkarazo, I., Fernández, L.A., Madariaga, J.M., 2011. Micro-Raman spectroscopic identification of natural mineral phases and their weathering products inside an abandoned zinc/lead mine. *Spectrochim. Acta Part A Mol. Biomol. Spectrosc.* 80, 66–74.
- Goldberg, S., Johnston, C.T., 2001. Mechanisms of arsenic adsorption on amorphous oxides evaluated using macroscopic measurements, vibrational spectroscopy, and surface complexation modeling. *J. Colloid Interface Sci.* 234, 204–216.
- Gondar, D., Lopez, R., Fiol, S., Antelo, J.M., Arce, F., 2005. Characterization and acid-base properties of fulvic and humic acids isolated from two horizons of an ombrotrophic peat bog. *Geoderma* 126, 367–374.
- Gong, W., 2001. A real time in situ ATR-FTIR spectroscopic study of linear phosphate adsorption on titania surfaces. *Int. J. Miner. Process* 63, 147–165.
- González Pérez, M., Martín-Neto, L., Saab, S.C., Novotny, E.H., Milori, D.M.B.P., Bagnato, V.S., Colnago, L.A., Melo, W.J., Knicker, H., 2004. Characterization of humic acids from a Brazilian Oxisol under different tillage systems by EPR, ¹³C NMR, FTIR and fluorescence spectroscopy. *Geoderma* 118, 181–190.

- Gore, R.C., 1949. Infrared spectrometry of small samples with the reflecting microscope. *Science* 110, 710–711.
- Goyne, K.W., Brantley, S.L., Chorover, J., 2006. Effects of organic acids and dissolved oxygen on apatite and chalcopyrite dissolution: Implications for using elements as organomarkers and oxymarkers. *Chem. Geol.* 234, 28–45.
- Goyne, K.W., Brantley, S.L., Chorover, J., 2010. Rare earth element release from phosphate minerals in the presence of organic acids. *Chem. Geol.* 278, 1–14.
- Goyne, K.W., Chorover, J., Kubicki, J.D., Zimmerman, A.R., Brantley, S.L., 2005. Sorption of the antibiotic ofloxacin to mesoporous and nonporous alumina and silica. *J. Colloid Interface Sci.* 283, 160–170.
- Goyne, K.W., Chorover, J., Zimmerman, A.R., Komarneni, S., Brantley, S.L., 2004. Influence of mesoporosity on the sorption of 2,4-dichlorophenoxyacetic acid onto alumina and silica. *J. Colloid Interface Sci.* 272, 10–20.
- Gray, A.B., Pasternack, G.B., Watson, E.B., 2010. Hydrogen peroxide treatment effects on the particle size distribution of alluvial and marsh sediments. *The Holocene* 20, 293–301.
- Gregoriou, V.G., Rodman, S.E., 2002. Quantitative depth profile analysis of micrometer-thick multilayered thin coatings using step-scan FT-IR photoacoustic spectroscopy. *Anal. Chem.* 74, 2361–2369.
- Griffiths, P.R., de Haseth, J.A., 1986. *Fourier Transform Infrared Spectrometry*. John Wiley and Sons, NY.
- Griffiths, P.R., de Haseth, J.A., 2006. Sampling the interferogram. In: *Fourier Transform Infrared Spectrometry*. John Wiley & Sons, Inc, pp. 57–74.
- Gu, B.H., Schmitt, J., Chen, Z., Liang, L.Y., McCarthy, J.F., 1995. Adsorption and desorption of different organic-matter fractions on iron-oxide. *Geochim. Cosmochim. Acta* 59, 219–229.
- Gu, C., Karthikeyan, K.G., 2005a. Interaction of tetracycline with aluminum and iron hydrous oxides. *Environ. Sci. Technol.* 39, 2660–2667.
- Gu, C., Karthikeyan, K.G., 2005b. Sorption of the antimicrobial ciprofloxacin to aluminum and iron hydrous oxides. *Environ. Sci. Technol.* 39, 9166–9173.
- Guan, X.H., Liu, Q., Chen, G.H., Shang, C., 2005. Surface complexation of condensed phosphate to aluminum hydroxide: An ATR-FTIR spectroscopic investigation. *J. Colloid Interface Sci.* 289, 319–327.
- Gun'ko, V.M., Zarko, V.I., Turov, V.V., Leboda, R., Chibowski, E., Gun'ko, V.V., 1998. Aqueous suspensions of highly disperse silica and germania/silica. *J. Colloid Interface Sci.* 205, 106–120.
- Gulley-Stahl, H., Hogan, P.A., Schmidt, W.L., Wall, S.J., Buhrlage, A., Bullen, H.A., 2010. Surface Complexation of Catechol to Metal Oxides: An ATR-FTIR, Adsorption, and Dissolution Study. *Environ. Sci. Technol.* 44, 4116–4121.
- Ha, J., Hyun Yoon, T., Wang, Y., Musgrave, C.B., Brown, J.G.E., 2008. Adsorption of organic matter at mineral/water interfaces: 7. ATR-FTIR and quantum chemical study of lactate interactions with hematite nanoparticles. *Langmuir* 24, 6683–6692.
- Haberhauer, 1998. Comparison of the composition of forest soil litter derived from three different sites at various decompositional stages using FTIR spectroscopy. *Geoderma* 83, 331–342.
- Haberhauer, G., Gerzabek, M.H., 1999. Drift and transmission FT-IR spectroscopy of forest soils: an approach to determine decomposition processes of forest litter. *Vib. Spectrosc.* 19, 413–417.
- Haile-Mariam, S., Collins, H.P., Wright, S., Paul, E.A., 2008. Fractionation and long-term laboratory incubation to measure soil organic matter dynamics. *Soil Sci. Soc. Am. J.* 72, 370–378.
- Haley, L.V., Wylie, I.W., Koningstein, J.A., 1982. An investigation of the lattice and interlayer water vibrational spectral regions of muscovite and vermiculite using Raman microscopy. *A Raman microscopic study of layer silicates. J. Raman Spectrosc.* 13, 203–205.

- Han, G., Jiang, T., Li, G., Huang, Y., Zhang, Y., 2011. Investigation on modified humic substances based Binders for iron ore agglomeration. *J. Eng. Mater. Technol.* 134, 010901.
- Harsh, J., Chorover, J., Nizeyimana, E., 2002. Allophane and imogolite. In: Dixon, J.B., Schulze, D.G. (Eds.), *Soil Mineralogy with Environmental Applications*. SSSA, Madison, WI, pp. 291–322. Vol. SSSA Book Ser. 7.
- Hart, T.R., Adams, S.B., Tempkin, H., 1976. Flammarion Sciences, Paris.
- Hay, M.B., Myneni, S.C.B., 2007. Structural environments of carboxyl groups in natural organic molecules from terrestrial systems. Part 1: Infrared spectroscopy. *Geochim. Cosmochim. Acta* 71, 3518–3532.
- Hayes, M.H.B., Malcolm, R.L., 2001. Considerations of compositions and of aspects of the structures of humic substances. *Humic Subst. Chem. Contam. Access Publ.* 3–39.
- Hazen, R.M., Sverjensky, D.A., 2010. Mineral surfaces, geochemical complexities, and the origins of life. *Cold Spring Harb. Perspect. Biol.* 2.
- He, X., Xi, B., Wei, Z., Guo, X., Li, M., An, D., Liu, H., 2011a. Spectroscopic characterization of water extractable organic matter during composting of municipal solid waste. *Chemosphere* 82, 541–548.
- He, Z., Honeycutt, C.W., Zhang, H., 2011b. Elemental and Fourier transform-infrared spectroscopic analysis of water- and pyrophosphate-extracted soil organic matter. *Soil Sci.* 176, 183–189. <http://dx.doi.org/10.1097/SS.0b013e318212865c>.
- He, Z., Honeycutt, C.W., Olanya, O.M., Larkin, R.P., Halloran, J.M., Frantz, J.M., 2012. Comparison of soil phosphorus status and organic matter composition in potato fields with different crop rotation systems. In: He, Z., Larkin, R., Honeycutt, W. (Eds.), *Sustainable Potato Production: Global Case Studies*. Springer, Netherlands, pp. 61–79.
- He, Z., Ohno, T., Cade-Menun, B.J., Erich, M.S., Honeycutt, C.W., 2006. Spectral and chemical characterization of phosphates associated with humic substances trade or manufacturers' names mentioned in the paper are for information only and do not constitute endorsement, recommendation, or exclusion by the USDA-ARS. *Soil Sci. Soc. Am. J.* 70, 1741–1751.
- Heymann, K., Lehmann, J., Solomon, D., Schmidt, M.W.I., Regier, T., 2011. C 1s K-edge near edge X-ray absorption fine structure (NEXAFS) spectroscopy for characterizing functional group chemistry of black carbon. *Org. Geochem.* 42, 1055–1064.
- Hibben, J.H., 1939. *The Raman Effect and Its Chemical Applications*. Reinhold Publishing Corp., New York, NY.
- Hind, A.R., Bhargava, S.K., McKinnon, A., 2001. At the solid/liquid interface: FTIR/ATR – the tool of choice. *Adv. Colloid Interface Sci.* 93, 91–114.
- Hirschfeld, T., Chase, B., 1986. FT-Raman spectroscopy: development and justification. *Appl. Spectrosc.* 40, 133–137.
- Hirschmugl, C.J., 2002. *Frontiers in infrared spectroscopy at surfaces and interfaces*. *Surf. Sci.* 500, 577–604.
- Holman, H.-Y.N., 2010. Chapter 4–Synchrotron infrared spectromicroscopy for studying chemistry of microbial activity in geologic materials. In: Balwant, S., Markus, G. (Eds.), *Developments in Soil Science*, vol. 34. Elsevier, pp. 103–130.
- Holman, H.-Y.N., Bechtel, H.A., Hao, Z., Martin, M.C., 2010. Synchrotron IR spectromicroscopy: chemistry of living cells. *Anal. Chem.* 82, 8757–8765.
- Holman, H.-Y.N., Miles, R., Hao, Z., Wozel, E., Anderson, L.M., Yang, H., 2009. Real-time chemical imaging of bacterial activity in biofilms using open-channel microfluidics and synchrotron FTIR spectromicroscopy. *Anal. Chem.* 81, 8564–8570.
- Holman, H.-Y.N., Nieman, K., Sorensen, D.L., Miller, C.D., Martin, M.C., Borch, T., McKinney, W.R., Sims, R.C., 2002. Catalysis of PAH biodegradation by humic acid shown in synchrotron infrared studies. *Environ. Sci. Technol.* 36, 1276–1280.
- Holman, H.N., Perry, D.L., Martin, M.C., Lamble, G.M., McKinney, W.R., Hunter-Cevera, J.C., 1999. Real-time characterization of biogeochemical reduction of Cr(VI) on Basalt surfaces by SR-FTIR imaging. *Geomicrobiol. J.* 16, 307–324.

- Holman, H.Y.N., Martin, M.C., 2006. Synchrotron radiation infrared spectromicroscopy: a noninvasive chemical probe for monitoring biogeochemical processes. In: Donald, L.S. (Ed.), *Advances in Agronomy*, vol. 90. Academic Press, pp. 79–127.
- Horwath, W.R., 2007. Carbon cycling and formation of soil organic matter. In: Paul, E.A. (Ed.), *Soil Microbiology, Ecology, and Biochemistry*. Academic Press, San Diego, CA.
- Howe, K.J., Ishida, K.P., Clark, M.M., 2002. Use of ATR/FTIR spectrometry to study fouling of microfiltration membranes by natural waters. *Desalination* 147, 251–255.
- Hsu, J.-H., Lo, S.-L., 1999. Chemical and spectroscopic analysis of organic matter transformations during composting of pig manure. *Environ. Pollut.* 104, 189–196.
- Huang, P.M., Wang, M.K., Kämpf, N., Schultze, D.G., 2002. Aluminum hydroxides. Vol. SSSA Book Ser. 7. In: Dixon, J.B., Schulz, L.A. (Eds.), *Soil Mineralogy with Environmental Applications*. SSSA, Madison, WI, pp. 261–289.
- Huang, Q.J., Li, X.Q., Yao, J.L., Ren, B., Cai, W.B., Gao, J.S., Mao, B.W., Tian, Z.Q., 1999. Extending surface Raman spectroscopic studies to transition metals for practical applications: III. Effects of surface roughening procedure on surface-enhanced Raman spectroscopy from nickel and platinum electrodes. *Surf. Sci.* 427–428, 162–166.
- Huang, W.E., Griffiths, R.I., Thompson, I.P., Bailey, M.J., Whiteley, A.S., 2004. Raman microscopic analysis of single microbial cells. *Anal. Chem.* 76, 4452–4458.
- Huang, W.E., Li, M., Jarvis, R.M., Goodacre, R., Banwart, S.A., 2010. Chapter 5-Shining light on the microbial World: the application of Raman microspectroscopy. In: Allen, I.L., Sima, S., Geoffrey, M.G. (Eds.), *Advances in Applied Microbiology*, vol. 70. Academic Press, pp. 153–186.
- Hübner, W., Blume, A., 1998. Interactions at the lipid–water interface. *Chem. Phys. Lipids* 96, 99–123.
- Hug, S.J., 1997. In situ Fourier transform infrared measurements of sulfate adsorption on hematite in aqueous solutions. *J. Colloid Interface Sci.* 188, 415–422.
- Hug, S.J., Bahnemann, D., 2006. Infrared spectra of oxalate, malonate and succinate adsorbed on the aqueous surface of rutile, anatase and lepidocrocite measured with in situ ATR-FTIR. *J. Electron Spectrosc. Relat. Phenom.* 150, 208–219.
- Hug, S.J., Sulzberger, B., 1994. In-situ fourier-transform infrared spectroscopic evidence for the formation of several different surface complexes of oxalate on TiO₂ in the aqueous-phase. *Langmuir* 10, 3587–3597.
- Hugo, R.C., Cady, S.L., 2004. Preparation of geological and biological TEM specimens by embedding in sulfur. *Microsc. Today* 12, 28–30.
- Hwang, Y.S., Lenhart, J.J., 2008. Adsorption of C4-dicarboxylic acids at the hematite/water interface. *Langmuir* 24, 13934–13943.
- Ikoma, T., Kobayashi, H., Tanaka, J., Walsh, D., Mann, S., 2003. Physical properties of type I collagen extracted from fish scales of *Pagrus major* and *Oreochromis niloticus*. *Int. J. Biol. Macromol.* 32, 199–204.
- Ibarra, J., Muñoz, E., Moliner, R., 1996. FTIR study of the evolution of coal structure during the coalification process. *Organic Geochemistry* 24, 725–735.
- Inbar, Y., Chen, Y., Hadar, Y., 1991. Carbon-13 CPMAS NMR and FTIR Spectroscopic analysis of organic-matter transformations during composting of solid-wastes from wineries. *Soil Sci.* 152, 272–282.
- Ivnitski, D., Abdel-Hamid, I., Atanasov, P., Wilkins, E., 1999. Biosensors for detection of pathogenic bacteria. *Biosens. Bioelectron.* 14, 599–624.
- Janik, L.J., Merry, R.H., Skjemstad, J.O., 1998. Can mid infrared diffuse reflectance analysis replace soil extractions? *Australian Journal of Experimental Agriculture* 38, 681–696.
- Janik, L.J., Skjemstad, J.O., Shepherd, K.D., Spouncer, L.R., 2007. The prediction of soil carbon fractions using mid-infrared-partial least square analysis. *Aust. J. Soil Res.* 45, 73–81.
- Jawhari, T., Roid, A., Casado, J., 1995. Raman spectroscopic characterization of some commercially available carbon black materials. *Carbon* 33, 1561–1565.

- Jeanmaire, D.L., Van Duyne, R.P., 1977. Surface raman spectroelectrochemistry: Part I. Heterocyclic, aromatic, and aliphatic amines adsorbed on the anodized silver electrode. *J. Electroanal. Chem. Interfacial Electrochem.* 84, 1–20.
- Jiang, W., Saxena, A., Song, B., Ward, B.B., Beveridge, T.J., Myneni, S.C.B., 2004. Elucidation of functional groups on gram-positive and gram-negative bacterial surfaces using infrared spectroscopy. *Langmuir* 20, 11433–11442.
- Jiang, W., Yang, K., Vachet, R.W., Xing, B.S., 2010. Interaction between oxide nanoparticles and biomolecules of the bacterial cell envelope as examined by infrared spectroscopy. *Langmuir* 26, 18071–18077.
- Johnson, S.B., Yoon, T.H., Kocar, B.D., Brown, G.E., 2004. Adsorption of Organic Matter at Mineral/Water Interfaces. 2. Outer-Sphere Adsorption of Maleate and Implications for Dissolution Processes. *Langmuir* 20, 4996–5006.
- Johnston, C.P., Chrysochoou, M., 2012. Investigation of chromate coordination on ferrihydrite by in situ ATR-FTIR spectroscopy and theoretical frequency calculations. *Environ. Sci. Technol.* 46, 5851–5858.
- Johnston, C.T., 2010. Probing the nanoscale architecture of clay minerals. *Clay Miner.* 45, 245–279.
- Johnston, C.T., Agnew, S.F., Bish, D.L., 1990. Polarized single-crystal Fourier-transform infrared microscopy of Ouray dickite and Keokuk kaolinite. *Clays Clay Miner.* 38, 573–588.
- Johnston, C.T., Aochi, Y.O., 1996. Fourier transform infrared and Raman spectroscopy. Vol. SSSA Book Ser. 5. In: *Methods of Soil Analysis. Part 3. Chemical Methods.* SSSA, Madison, WI, pp. 269–321.
- Johnston, C.T., Kogel, J.E., Bish, D.L., Kogure, T., Murray, H.H., 2008. Low-temperature FTIR study of kaolin-group minerals. *Clays Clay Miner.* 56, 470–485.
- Johnston, C.T., Sheng, G., Teppen, B.J., Boyd, S.A., De Oliveira, M.F., 2002a. Spectroscopic study of dinitrophenol herbicide sorption on smectite. *Environ. Sci. Technol.* 36, 5067–5074.
- Johnston, C.T., Sposito, G., Earl, W.L., 1993. Characterization of environmental particles by Fourier transform infrared and nuclear magnetic resonance spectroscopy. In: Buffle, J., van Leeuwen, H.P. (Eds.), *Environmental Particles*, vol. 2. Lewis Publishers., Boca Raton, FL.
- Johnston, C.T., Sposito, G., Erickson, C., 1992. Vibrational probe studies of water interactions with montmorillonite. *Clays Clay Miner.* 40, 722–730.
- Johnston, C.T., Stone, D.A., 1990. Influence of hydrazine on the vibrational-modes of kaolinite. *Clays Clay Miner.* 38, 121–128.
- Johnston, C.T., Wang, S.-L., Bish, D.L., Dera, P., Agnew, S.F., Kenney, J.W., 2002b. Novel pressure-induced phase transformations in hydrous layered materials. *Geophys. Res. Lett.* 29, 17-1–17-4.
- Jorio, A., 2012. Raman spectroscopy in graphene-based systems: prototypes for nanoscience and nanometrology. *ISRN Nanotechnol.* 16.
- Jorio, A., Ribeiro-Soares, J., Cançado, L.G., Falcão, N.P.S., Dos Santos, H.F., Baptista, D.L., Martins Ferreira, E.H., Archanjó, B.S., Achete, C.A., 2012. Microscopy and spectroscopy analysis of carbon nanostructures in highly fertile Amazonian anthrosoils. *Soil Tillage Res.* 122, 61–66.
- Joseph, S.D., Camps-Arbestain, M., Lin, Y., Munroe, P., Chia, C.H., Hook, J., van Zwieten, L., Kimber, S., Cowie, A., Singh, B.P., Lehmann, J., Foidl, N., Smernik, R.J., Amonette, J.E., 2010. An investigation into the reactions of biochar in soil. *Aust. J. Soil Res.* 48, 501–515.
- Jouraiaphy, A., Amir, S., Winterton, P., El Gharous, M., Revel, J.C., Hafidi, M., 2008. Structural study of the fulvic fraction during composting of activated sludge-plant matter: elemental analysis, FTIR and ¹³C NMR. *Bioresour. Technol.* 99, 1066–1072.
- Joussein, E., Petit, S., Churchman, J., Theng, B., Righi, D., Delvaux, B., 2005. Halloysite clay minerals—a review. *Clay Miner.* 40, 383–426.

- Jucker, B.A., Harms, H., Hug, S.J., Zehnder, A.J.B., 1997. Adsorption of bacterial surface polysaccharides on mineral oxides is mediated by hydrogen bonds. *Colloids Surf. B Biointerfaces* 9, 331–343.
- Julien, C.M., Massot, M., Poinsignon, C., 2004. Lattice vibrations of manganese oxides—Part 1. Periodic structures. *Spectrochim. Acta Part A Mol. Biomol. Spectrosc.* 60, 689–700.
- Kahraman, M., Yazici, M.M., Sahin, F., Bayrak, O.F., Culha, M., 2007. Reproducible surface-enhanced Raman scattering spectra of bacteria on aggregated silver nanoparticles. *Appl. Spectrosc.* 61, 479–485.
- Kaiser, M., Ellerbrock, R.H., 2005. Functional characterization of soil organic matter fractions different in solubility originating from a long-term field experiment. *Geoderma* 127, 196–206.
- Kaiser, M., Ellerbrock, R.H., Gerke, H.H., 2007. Long-term effects of crop rotation and fertilization on soil organic matter composition. *Eur. J. Soil Sci.* 58, 1460–1470.
- Kaiser, M., Ellerbrock, R.H., Gerke, H.H., 2008. Cation exchange capacity and composition of soluble soil organic matter fractions (All rights reserved. No part of this periodical may be reproduced or transmitted in any form or by any means, electronic or mechanical, including photocopying, recording, or any information storage and retrieval system, without permission in writing from the publisher. Permission for printing and for reprinting the material contained herein has been obtained by the publisher) *Soil Sci. Soc. Am. J.* 72, 1278–1285.
- Kamnev, A.A., Antonyuk, L.P., Matora, L.Y., Serebrennikova, O.B., Sumaroka, M.V., Colina, M., Renou-Gonnord, M.F., Ignatov, V.V., 1999. Spectroscopic characterization of cell membranes and their constituents of the plant-associated soil bacterium *Azospirillum brasilense*. *J. Mol. Struct.* 481, 387–393.
- Kang, S., Xing, B., 2007. Adsorption of dicarboxylic acids by clay minerals as examined by in situ ATR-FTIR and ex situ DRIFT. *Langmuir* 23, 7024–7031.
- Kang, S.H., Amarasiriwardena, D., Xing, B.S., 2008. Effect of dehydration on dicarboxylic acid coordination at goethite/water interface. *Colloids Surf. A Physicochem. Eng. Aspects* 318, 275–284.
- Kanokkantapong, V., Marhaba, T.F., Panyapinyophol, B., Pavasant, P., 2006. FTIR evaluation of functional groups involved in the formation of haloacetic acids during the chlorination of raw water. *J. Hazard. Mater.* 136, 188–196.
- Katon, J.E., 1996. Infrared microspectroscopy. A review of fundamentals and applications. *Micron* 27, 303–314.
- Katrin, K., Harald, K., Irving, I., Ramachandra, R.D., Michael, S.F., 2002. Surface-enhanced Raman scattering and biophysics. *J. Phys. Condens. Matter* 14, R597.
- Katti, K.S., Katti, D.R., 2006. Relationship of swelling and swelling pressure on silica-water interactions in montmorillonite. *Langmuir* 22, 532–537.
- Kaufhold, S., Hein, M., Dohrmann, R., Ufer, K., 2012. Quantification of the mineralogical composition of clays using FTIR spectroscopy. *Vib. Spectrosc.* 59, 29–39.
- Keiluweit, M., Nico, P.S., Johnson, M.G., Kleber, M., 2010. Dynamic molecular structure of plant biomass-derived black carbon (Biochar). *Environ. Sci. Technol.* 44, 1247–1253.
- Kerek, M., Drijber, R.A., Gaussoin, R.E., 2003. Labile soil organic matter as a potential nitrogen source in golf greens. *Soil Biol. Biochem.* 35, 1643–1649.
- Kerschbaum, F.P., 1914. *Instrumentenk* 34, 43.
- Khan, S.U., 1975. *Soil Organic Matter*. Elsevier Science.
- Kim, P., Johnson, A., Edmunds, C.W., Radosevich, M., Vogt, F., Rials, T.G., Labbé, N., 2011. Surface functionality and carbon structures in lignocellulosic-derived biochars produced by fast pyrolysis. *Energy & Fuels* 25, 4693–4703.
- Kizewski, F., Liu, Y.-T., Morris, A., Hesterberg, D., 2011. Spectroscopic Approaches for phosphorus speciation in soils and other environmental systems (All rights reserved. No part of this periodical may be reproduced or transmitted in any form or by any means,

- electronic or mechanical, including photocopying, recording, or any information storage and retrieval system, without permission in writing from the publisher) *J. Environ. Qual.* 40, 751–766.
- Kleber, M., Johnson, M.G., 2010. Advances in understanding the molecular structure of soil organic matter: implications for interactions in the environment. In: Donald, L.S. (Ed.), *Advances in Agronomy*, vol. 106. Academic Press, pp. 77–142.
- Kodama, H., Schnitzer, M., 1971. Evidence for interlamellar adsorption of organic matter by clay in a podzol soil. *Can. J. Soil. Sci.* 51, 509–512.
- Kögel-Knabner, I., Guggenberger, G., Kleber, M., Kandeler, E., Kalbitz, K., Scheu, S., Eusterhues, K., Leinweber, P., 2008. Organo-mineral associations in temperate soils: Integrating biology, mineralogy, and organic matter chemistry. *J. Plant Nutr. Soil. Sci.* 171, 61–82.
- Kolpin, D.W., Furlong, E.T., Meyer, M.T., Thurman, E.M., Zaugg, S.D., Barber, L.B., Buxton, H.T., 2002. Pharmaceuticals, hormones, and other organic wastewater contaminants in US streams, 1999–2000: a national reconnaissance. *Environ. Sci. Technol.* 36, 1202–1211.
- Komadel, P., Bujdak, J., Madejová, J., Sucha, V., Elsass, F., 1996. Effect of non-swelling layers on the dissolution of reduced-charge montmorillonite in hydrochloric acid. *Clay Miner.* 31, 333–345.
- Kookana, R.S., Sarmah, A.K., Van Zwieten, L., Krull, E., Singh, B., 2011. Chapter three—biochar application to soil: agronomic and environmental benefits and unintended consequences. In: Donald, L.S. (Ed.), *Advances in Agronomy*, vol. 112. Academic Press, pp. 103–143.
- Kramar, S., Urosevic, M., Pristacz, H., Mirtiĉ, B., 2010. Assessment of limestone deterioration due to salt formation by micro-Raman spectroscopy: application to architectural heritage. *J. Raman Spectrosc.* 41, 1441–1448.
- Kubicki, J.D., Kwon, K.D., Paul, K.W., Sparks, D.L., 2007. Surface complex structures modelled with quantum chemical calculations: carbonate, phosphate, sulphate, arsenate and arsenite. *Eur. J. Soil Sci.* 58, 932–944.
- Kubicki, J.D., Mueller, K.T., 2010. Computational spectroscopy in environmental chemistry. In: Grunenberg, J. (Ed.), *Computational Spectroscopy: Methods, Experiments and Applications*. Wiley-VCH Verlag GmbH & Co. KGaA, Weinheim, Germany, pp. 323–351.
- Kubicki, J.D., Schroeter, L.M., Itoh, M.J., Nguyen, B.N., Apitz, S.E., 1999. Attenuated total reflectance fourier-transform infrared spectroscopy of carboxylic acids adsorbed onto mineral surfaces. *Geochim. Cosmochim. Acta* 63, 2709–2725.
- Kulshrestha, P., Giese, R.F., Aga, D.S., 2004. Investigating the molecular interactions of oxy-tetracycline in clay and organic matter: Insights on factors affecting its mobility in soil. *Environ. Sci. Technol.* 38, 4097–4105.
- Lackovic, K., Johnson, B.B., Angove, M.J., Wells, J.D., 2003. Modeling the adsorption of citric acid onto Mulloorina illite and related clay minerals. *J. Colloid Interface Sci.* 267, 49–59.
- Laird, D.A., Fleming, P., Davis, D.D., Horton, R., Wang, B., Karlen, D.L., 2010. Impact of biochar amendments on the quality of a typical Midwestern agricultural soil. *Geoderma* 158, 443–449.
- Laird, D.A., Yen, P.Y., Koskinen, W.C., Steinheimer, T.R., Dowdy, R.H., 1994. Sorption of atrazine on soil clay components. *Environ. Sci. Technol.* 28, 1054–1061.
- Landgraf, M.D., da Silva, S.C., Rezende, M. O. de O., 1998. Mechanism of metribuzin herbicide sorption by humic acid samples from peat and vermicompost. *Anal. Chim. Acta* 368, 155–164.
- Lanfranco, A.M., Schofield, P.F., Murphy, P.J., Hodson, M.E., Mosselmans, J.F.W., Valsami-Jones, E., 2003. Characterization and identification of mixed-metal phosphates in soils: the application of Raman spectroscopy. *Mineral. Mag.* 67, 1299–1316.
- Lang, P.L., 2006. Microspectroscopy. In: *Encyclopedia of Analytical Chemistry*. John Wiley & Sons, Ltd.

- Lawrence, J.R., Hitchcock, A.P., 2011. Synchrotron-based X-ray and FTIR absorption spectromicroscopies of organic contaminants in the environment. In: *Biophysico-chemical Processes of Anthropogenic Organic Compounds in Environmental Systems*. John Wiley & Sons, Inc., pp. 341–368.
- Lefèvre, G., 2004. In situ Fourier-transform infrared spectroscopy studies of inorganic ions adsorption on metal oxides and hydroxides. *Adv. Colloid Interface Sci.* 107, 109–123.
- Lefèvre, G., Preočanin, T., Lützenkirchen, J., 2012. Attenuated total reflection - infrared spectroscopy applied to the study of mineral - aqueous electrolyte solution interfaces: a general overview and a case study. In: Grunenberg, J. (Ed.), *Computational Spectroscopy: Methods, Experiments and Applications*. Wiley-VCH Verlag GmbH & Co. KGaA, Weinheim, Germany.
- Legal, J.M., Manfait, M., Theophanides, T., 1991. Applications of FTIR spectroscopy in structural studies of cells and bacteria. *J. Mol. Struct.* 242, 397–407.
- Lehmann, J., Joseph, S. (Eds.), 2009. *Biochar for Environmental Management: Science and Technology*. Earthscan Ltd, London, UK.
- Lehmann, J., Kinyangi, J., Solomon, D., 2007. Organic matter stabilization in soil microaggregates: implications from spatial heterogeneity of organic carbon contents and carbon forms. *Biogeochemistry* 85, 45–57.
- Lehmann, J., Liang, B.Q., Solomon, D., Lerotic, M., Luizao, F., Kinyangi, J., Schafer, T., Wirrick, S., Jacobsen, C., 2005. Near-edge X-ray absorption fine structure (NEXAFS) spectroscopy for mapping nano-scale distribution of organic carbon forms in soil: application to black carbon particles. *Glob. Biogeochem. Cycles* 19.
- Lehmann, J., Solomon, D., 2010. Chapter 10—Organic carbon chemistry in soils observed by synchrotron-based spectroscopy. In: Balwant, S., Markus, G. (Eds.), *Developments in Soil Science*, vol. 34. Elsevier, pp. 289–312.
- Leifeld, J., Kögel-Knabner, I., 2001. Organic carbon and nitrogen in fine soil fractions after treatment with hydrogen peroxide. *Soil Biol. Biochem.* 33, 2155–2158.
- Leite, R.C.C., Porto, S.P.S., 1966. Enhancement of Raman cross section in CdS due to resonant absorption. *Phys. Rev. Lett.* 17, 10–12.
- Leue, M., Ellerbrock, R.H., Gerke, H.H., 2010a. DRIFT mapping of organic matter composition at intact soil aggregate surfaces. *Vadose Zone J.* 9, 317–324.
- Leue, M., Ellerbrock, R.H., Gerke, H.H., 2010b. DRIFT mapping of organic matter composition at intact soil aggregate surfaces (All rights reserved. No part of this periodical may be reproduced or transmitted in any form or by any means, electronic or mechanical, including photocopying, recording, or any information storage and retrieval system, without permission in writing from the publisher) *Vadose Zone J.* 9, 317–324.
- Levenson, E., Lerch, P., Martin, M.C., 2008. Spatial resolution limits for synchrotron-based infrared spectromicroscopy. *Infrared Phys. Technol.* 51, 413–416.
- Levine, S., Stevenson, H.J.R., Chambers, L.A., Kenner, B.A., 1953. Infrared spectrophotometry of enteric bacteria. *J. Bacteriol.* 65, 10–15.
- Lewis, D.G., Farmer, V.C., 1986. Infrared-absorption of surface hydroxyl-groups and lattice-vibrations in lepidocrocite (γ -FeOOH) and boehmite (γ -AlOOH). *Clay Miner.* 21, 93–100.
- Lewis, I.R., Edwards, H.G.M., 2001. *Handbook of Raman Spectroscopy: From the Research Laboratory to the Process Line*. Marcel Dekker.
- Leyton, P., Córdova, I., Lizama-Vergara, P.A., Gómez-Jeria, J.S., Aliaga, A.E., Campos-Vallette, M.M., Clavijo, E., García-Ramos, J.V., Sanchez-Cortes, S., 2008. Humic acids as molecular assemblers in the surface-enhanced Raman scattering detection of polycyclic aromatic hydrocarbons. *Vib. Spectrosc.* 46, 77–81.
- Li-Chan, E., Chalmers, J.M., Griffiths, P., 2010. *Applications of Vibrational Spectroscopy in Food Science*. John Wiley & Sons, Ltd, West Sussex, UK.

- Li, H., Sheng, G.Y., Teppen, B.J., Johnston, C.T., Boyd, S.A., 2003. Sorption and desorption of pesticides by clay minerals and humic acid-clay complexes. *Soil Sci. Soc. Am. J.* 67, 122–131.
- Li, X., Hayashi, J.-i., Li, C.-Z., 2006. FT-Raman spectroscopic study of the evolution of char structure during the pyrolysis of a Victorian brown coal. *Fuel* 85, 1700–1707.
- Li, J., Li, Y., Lu, J., 2009. Adsorption of herbicides 2,4-D and acetochlor on inorganic-organic bentonites. *Applied Clay Science* 46, 314–318.
- Li, Z., Hong, H., Liao, L., Ackley, C.J., Schulz, L.A., MacDonald, R.A., Mihelich, A.L., Emard, S.M., 2011. A mechanistic study of ciprofloxacin removal by kaolinite. *Colloids Surf. B Biointerfaces* 88, 339–344.
- Li, Z., Kolb, V.M., Jiang, W.-T., Hong, H., 2010. FTIR and XRD investigations of tetracycline intercalation in smectites. *Clays Clay Miner.* 58, 462–474.
- Liang, B., Lehmann, J., Solomon, D., Kinyangi, J., Grossman, J., O'Neill, B., Skjemstad, J.O., Thies, J., Luizao, F.J., Petersen, J., Neves, E.G., 2006. Black carbon increases cation exchange capacity in soils. *Soil Sci. Soc. Am. J.* 70, 1719–1730.
- Liang, B., Lehmann, J., Solomon, D., Sohi, S., Thies, J.E., Skjemstad, J.O., Luizão, F.J., Engelhard, M.H., Neves, E.G., Wirrick, S., 2008. Stability of biomass-derived black carbon in soils. *Geochim. Cosmochim. Acta* 72, 6069–6078.
- Liang, E.J., Yang, Y., Kiefer, W., 1999. Surface-enhanced raman spectra of fulvic and humic acids adsorbed on copper electrodes. *Spectrosc. Lett.* 32, 689–701.
- Liang, E.J., Yang, Y.H., Kiefer, W., 1996. Surface-enhanced Raman spectra of fulvic and humic acids on silver nitrate-modified Fe–C–Cr–Ni surface. *J. Environ. Sci. Health. Part A Environ. Sci. Eng. Toxicol.* 31, 2477–2486.
- Liu, T.-T., Lin, Y.-H., Hung, C.-S., Liu, T.-J., Chen, Y., Huang, Y.-C., Tsai, T.-H., Wang, H.-H., Wang, D.-W., Wang, J.-K., Wang, Y.-L., Lin, C.-H., 2009. A high speed detection platform based on surface-enhanced raman scattering for monitoring antibiotic-induced chemical changes in bacteria cell wall. *PLoS One* 4, e5470.
- Livingston, D., 1973. *The Master of Light: A Biography of Albert A. Michelson*. University of Chicago Press, Chicago, IL.
- Lombardi, J.R., Birke, R.L., 2009. A unified view of surface-enhanced Raman scattering. *Acc. Chem. Res.* 42, 734–742.
- Lombi, E., Hettiarachchi, G.M., Scheckel, K.G., 2011. Advanced in situ spectroscopic techniques and their applications in environmental biogeochemistry: introduction to the special section. *J. Environ. Qual.* 40, 659–666.
- Long, D.A., 1977. *Raman Spectroscopy*. McGraw-Hill.
- Long, D.A., 2002. *The Raman Effect: A Unified Treatment of the Theory of Raman Scattering by Molecules*. Wiley.
- Lorna, D., Colin, C., Stephen, H., Mark, B., 2008. Methods of characterizing and fingerprinting soils for forensic application. In: *Soil Analysis in Forensic Taphonomy*. CRC Press, pp. 271–315.
- Lu, S., Chunfeng, H., Sakka, Y., Qing, H., 2012. Study of phase transformation behaviour of alumina through precipitation method. *J. Phys. Appl. Phys.* 45, 215302 (6 pp.)–215302 (6 pp.).
- Ludwig, B., Nitschke, R., Terhoeven-Urselmans, T., Michel, K., Flessa, H., 2008. Use of mid-infrared spectroscopy in the diffuse-reflectance mode for the prediction of the composition of organic matter in soil and litter. *J. Plant Nutr. Soil Sci. Z. Pflanzenernahrung Bodenkunde* 171, 384–391.
- Luengo, C., Brigante, M., Antelo, J., Avena, M., 2006. Kinetics of phosphate adsorption on goethite: comparing batch adsorption and ATR-IR measurements. *J. Colloid Interface Sci.* 300, 511–518.
- Luengo, C., Brigante, M., Avena, M., 2007. Adsorption kinetics of phosphate and arsenate on goethite. A comparative study. *J. Colloid Interface Sci.* 311, 354–360.
- Luxton, T.P., Eick, M.J., Rimstidt, D.J., 2008. The role of silicate in the adsorption/desorption of arsenite on goethite. *Chem. Geol.* 252, 125–135.

- Lyon, L.A., Keating, C.D., Fox, A.P., Baker, B.E., He, L., Nicewarner, S.R., Mulvaney, S.P., Natan, M.J., 1998. Raman spectroscopy. *Anal. Chem.* 70, 341–362.
- Madejová, J., 2003. FTIR techniques in clay mineral studies. *Vib. Spectrosc.* 31, 1–10.
- Madejová, J., Keckes, J., Paalkova, H., Komadel, P., 2002. Identification of components in smectite/kaolinite mixtures. *Clay Miner.* 37, 377–388.
- Madejová, J., Komadel, P., 2001. Baseline studies of the Clay minerals society source clays: infrared methods. *Clays Clay Miner.* 49, 410–432.
- Maes, E., Vielvoye, L., Stone, W., Delvaux, B., 1999. Fixation of radiocaesium traces in a weathering sequence mica→vermiculite→hydroxy interlayered vermiculite. *Eur. J. Soil Sci.* 50, 107–115.
- Mafrá, A.L., Senesi, N., Brunetti, G., Miklós, A.A.W., Melfi, A.J., 2007. Humic acids from hydromorphic soils of the upper Negro river basin, Amazonas: chemical and spectroscopic characterisation. *Geoderma* 138, 170–176.
- Major, J., Steiner, C., Downie, A., Lehmann, J., 2009. Biochar effects on nutrient leaching. In: Joseph, J.L.A.S. (Ed.), *Biochar for Environmental Management—Science and Technology*. Earthscan, London, pp. 227–249.
- Mao, J., Olk, D.C., Fang, X., He, Z., Schmidt-Rohr, K., 2008. Influence of animal manure application on the chemical structures of soil organic matter as investigated by advanced solid-state NMR and FT-IR spectroscopy. *Geoderma* 146, 353–362.
- Mao, Y., Daniel, L.N., Whittaker, N., Saffiotti, U., 1994. DNA binding to crystalline silica characterized by Fourier-transform infrared spectroscopy. *Environ. Health Perspect.* 102, 165–171.
- Maqueda, C., Morillo, E., Martín, E., Undabeytia, T., 1993. Interaction of pesticides with the soluble fraction of natural and artificial humic substances. *J. Environ. Sci. Health Part B* 28, 655–670.
- Maquelin, K., Kirschner, C., Choo-Smith, L.P., Ngo-Thi, N.A., Van Vreeswijk, T., Stammler, M., Endtz, H.P., Bruining, H.A., Naumann, D., Puppels, G.J., 2003. Prospective study of the performance of vibrational spectroscopies for rapid identification of bacterial and fungal pathogens recovered from blood cultures. *J. Clin. Microbiol.* 41, 324–329.
- Maquelin, K., Kirschner, C., Choo-Smith, L.P., van den Braak, N., Endtz, H.P., Naumann, D., Puppels, G.J., 2002. Identification of medically relevant microorganisms by vibrational spectroscopy. *J. Microbiol. Methods* 51, 255–271.
- Marley, L., Signolle, J.P., Amiel, C., Travert, J., 2001. Discrimination, classification, identification of microorganisms using FTIR spectroscopy and chemometrics. *Vib. Spectrosc.* 26, 151–159.
- Marinari, S., Dell'Abate, M.T., Brunetti, G., Dazzi, C., 2010. Differences of stabilized organic carbon fractions and microbiological activity along Mediterranean Vertisols and Alfisols profiles. *Geoderma* 156, 379–388.
- Martin-Neto, L., Tragheta, D.G., Vaz, C.M.P., Crestana, S., Sposito, G., 2001. On the interaction mechanisms of atrazine and hydroxyatrazine with humic substances. *J. Environ. Qual.* 30, 520–525.
- Martin-Neto, L., Vieira, E.M., Sposito, G., 1994. Mechanism of atrazine sorption by humic acid: a spectroscopic study. *Environ. Sci. Technol.* 28, 1867–1873.
- Martin, M.C., McKinney, W.R., 2001. The first synchrotron infrared beamlines at the advanced light source: spectromicroscopy and fast timing. *Ferroelectrics* 249, 1–10.
- Martínez, E.J., Fierro, J., Sánchez, M.E., Gómez, X., 2012. Anaerobic co-digestion of FOG and sewage sludge: study of the process by Fourier transform infrared spectroscopy. *Int. Biodeterior. Biodegrad.* 75, 1–6.
- Matejkova, S., Simon, T., 2012. Application of FTIR spectroscopy for evaluation of hydrophobic/hydrophilic organic components in arable soil. *Plant Soil Environ.* 58, 192–195.
- Matilainen, A., Gjessing, E.T., Lahtinen, T., Hed, L., Bhatnagar, A., Sillanpää, M., 2011. An overview of the methods used in the characterisation of natural organic matter (NOM) in relation to drinking water treatment. *Chemosphere* 83, 1431–1442.

- Matteson, A., Herron, M.M., 1993. Quantitative mineral analysis by Fourier transform infrared spectroscopy. Soc. Core Anal. Conf. Pap. 9308, 1–15.
- McAuley, B., Cabaniss, S.E., 2007. Quantitative detection of aqueous arsenic and other oxoanions using attenuated total reflectance infrared spectroscopy utilizing iron oxide coated internal reflection elements to enhance the limits of detection. *Analytica Chimica Acta* 581, 309–317.
- McCarty, G.W., Reeves Iii, J.B., Gurel, S., Katkat, A.V., 2010. Evaluation of methods for measuring soil organic carbon in West African soils. *Afr. J. Agric. Res.* 5, 2169–2177.
- McCarty, G.W., Reeves, J.B., Reeves, V.B., Follett, R.F., Kimble, J.M., 2002. Mid-infrared and near-infrared diffuse reflectance spectroscopy for soil carbon measurement. *Soil Sci. Soc. Am. J.* 66, 640–646.
- McMillan, P.F., Hofmeister, A.M., 1988. Infrared and Raman spectroscopy. In: Hawthorne, F.C. (Ed.), *Review in Mineralogy: Spectroscopic methods in mineralogy and geology*, vol. 18, pp. 99–159 (Miner. Soc. Am.).
- McWhirter, M.J., Bremer, P.J., Lamont, I.L., McQuillan, A.J., 2003. Siderophore-mediated covalent bonding to metal (oxide) surfaces during biofilm initiation by *Pseudomonas aeruginosa* bacteria. *Langmuir* 19, 3575–3577.
- McWhirter, M.J., McQuillan, A.J., Bremer, P.J., 2002. Influence of ionic strength and pH on the first 60 min of *Pseudomonas aeruginosa* attachment to ZnSe and to TiO₂ monitored by ATR-IR spectroscopy. *Colloids Surf. B Biointerfaces* 26, 365–372.
- Mendive, C.B., Bredow, T., Blesa, M.A., Bahnemann, D.W., 2006. ATR-FTIR measurements and quantum chemical calculations concerning the adsorption and photoreaction of oxalic acid on TiO₂. *Physical Chemistry Chemical Physics* 8, 3232–3247.
- Messerschmidt, R.G., Chase, D.B., 1989. FT-Raman microscopy: discussion and preliminary results. *Appl. Spectrosc.* 43, 11–15.
- Michelmore, A., Gong, W.Q., Jenkins, P., Ralston, J., 2000. The interaction of linear polyphosphates with titanium dioxide surfaces. *Physical Chemistry Chemical Physics* 2, 2985–2992.
- Mikutta, R., Kleber, M., Kaiser, K., Jahn, R., 2005. Review. *Soil Sci. Soc. Am. J.* 69, 120–135.
- Mimmo, T., Reeves, J.B., McCarty, G.W., Galletti, G., 2002. Determination of biological measures by mid-infrared diffuse reflectance spectroscopy in soils within a landscape. *Soil Sci.* 167, 281–287.
- Minasny, B., McBratney, A.B., Tranter, G., Murphy, B.W., 2008. Using soil knowledge for the evaluation of mid-infrared diffuse reflectance spectroscopy for predicting soil physical and mechanical properties. *Eur. J. Soil Sci.* 59, 960–971.
- Mirabella, F.M.J., 1985. Internal reflection spectroscopy. *Appl. Spectrosc. Rev.* 21, 45–78.
- Morris, P.M., Wogelius, R.A., 2008. Phthalic acid complexation and the dissolution of forsteritic glass studied via in situ FTIR and X-ray scattering. *Geochim. Cosmochim. Acta* 72, 1970–1985.
- Moskovits, M., 1985. Surface-enhanced spectroscopy. *Rev. Mod. Phys.* 57, 783–826.
- Moskovits, M., 2005. Surface-enhanced Raman spectroscopy: a brief retrospective. *J. Raman Spectrosc.* 36, 485–496.
- Mukome, F.N.D., Zhang, X., Sillva, L.C.R., Six, J., Parikh, S.J., 2013. Use of chemical and physical characteristics to investigate trends in biochar feedstocks. *J. Agric. Food Chem.* 61, 2196–2204.
- Mulvaney, R.L., Yaremych, S.A., Khan, S.A., Swiader, J.M., Horgan, B.P., 2004. Use of diffusion to determine soil cation-exchange capacity by ammonium saturation. *Commun. Soil Sci. Plant Anal.* 35, 51–67.
- Muniz-Miranda, M., Gellini, C., Salvi, P.R., Pagliai, M., 2010. Surface-enhanced Raman micro-spectroscopy of DNA/RNA bases adsorbed on pyroxene rocks as a test of in situ search for life traces on Mars. *J. Raman Spectrosc.* 41, 12–15.

- Myneni, S.C.B., Traina, S.J., Waychunas, G.A., Logan, T.J., 1998. Vibrational spectroscopy of functional group chemistry and arsenate coordination in ettringite. *Geochim. Cosmochim. Acta* 62, 3499–3514.
- Naja, G., Bouvrette, P., Hrapovic, S., Luong, J.H.T., 2007. Raman-based detection of bacteria using silver nanoparticles conjugated with antibodies. *Analyst* 132, 679–686.
- Nara, M., Torii, H., Tasumi, M., 1996. Correlation between the vibrational frequencies of the carboxylate group and the types of its coordination to a metal ion: an ab initio molecular orbital study. *J. Phys. Chem.* 100, 19812–19817.
- Naumann, D., Fijala, V., Labischinski, H., Giesbrecht, P., 1988. The rapid differentiation and identification of pathogenic bacteria using Fourier transform infrared spectroscopic and multivariate statistical analysis. *J. Mol. Struct.* 174, 165–170.
- Naumann, D., Helm, D., Labischinski, H., 1991. Microbiological characterizations by FT-IR spectroscopy. *Nature* 351, 81–82.
- Naumann, D., Keller, S., Helm, D., Schultz, C., Schrader, B., 1995. FT-IR spectroscopy and FT-Raman spectroscopy are powerful analytical tools for the non-invasive characterization of intact microbial cells. *J. Mol. Struct.* 347, 399–405.
- Naumann, D., Schultz, C.P., Helm, D., 1996. What can infrared spectroscopy tell us about the structure and composition of intact bacterial cells? In: Mantch, H.H., Chapman, D. (Eds.), *Infrared Spectroscopy of Biomolecules*. John Wiley and Sons, New York, pp. 279–310.
- Navarrete, I.A., Tsutsuki, K., Navarrete, R.A., 2010. Humus composition and the structural characteristics of humic substances in soils under different land uses in Leyte, Philippines. *Soil Sci. Plant Nutr.* 56, 289–296.
- Nguyen, T.T., Janik, L.J., Raupach, M., 1991. Diff use reflectance infrared fourier transform (DRIFT) spectroscopy in soil studies. *Aust. J. Soil Res.* 29, 49–67.
- Nichols, P.D., Henson, J.M., Guckert, J.B., Nivens, D.E., White, D.C., 1985. Fourier transform-infrared spectroscopic methods for microbial ecology – analysis of bacteria, bacteria-polymer mixtures and biofilms. *J. Microbiol. Methods* 4, 79–94.
- Niemeyer, J., Chen, Y., Bollag, J.M., 1992. Characterization of humic acids, composts, and peat by diffuse reflectance Fourier-transform infrared-spectroscopy. *Soil Sci. Soc. Am. J.* 56, 135–140.
- Nivens, D.E., Schmitt, J., Sniatecki, J., Anderson, T.R., Chambers, J.Q., White, D.C., 1993a. Multichannel ATR/FT-IR spectrometer for on-line examination of microbial biofilms. *Appl. Spectrosc.* 47, 668–671.
- Nivens, D.E., Chambers, J.Q., Anderson, T.R., Tunlid, A., Smit, J., White, D.C., 1993. Monitoring Microbial Adhesion and Biofilm Formation by Attenuated Total Reflection Fourier-Transform Infrared Spectroscopy. *J. Microbiol. Methods* 17, 199–213.
- Norén, K., Loring, J.S., Persson, P., 2008. Adsorption of alpha amino acids at the water/goethite interface. *J. Colloid Interface Sci.* 319, 416–428.
- Norén, K., Persson, P., 2007. Adsorption of monocarboxylates at the water/goethite interface: the importance of hydrogen bonding. *Geochim. Cosmochim. Acta* 71, 5717–5730.
- Novak, J.M., Busscher, W.J., Laird, D.L., Ahmedna, M., Watts, D.W., Niandou, M.A.S., 2009. Impact of biochar amendment on fertility of a Southeastern Coastal Plain soil. *Soil Sci.* 174, 105–112.
- Nowara, A., Burhenne, J., Spiteller, M., 1997. Binding of fluoroquinolone carboxylic acid derivatives to clay minerals. *J. Agric. Food Chem.* 45, 1459–1463.
- O'Reilly, J.M., Mosher, R.A., 1983. Functional groups in carbon black by FTIR spectroscopy. *Carbon* 21, 47–51.
- Oades, J.M., 1984. Soil organic matter and structural stability: mechanisms and implications for management. *Plant Soil* 76, 319–337.
- Ohno, T., He, Z., Tazisong, I.A., Senwo, Z.N., 2009. Influence of tillage, cropping, and nitrogen source on the chemical characteristics of humic acid, fulvic acid, and water-soluble soil organic matter fractions of a long-term cropping system study. *Soil Sci.* 174, 652–660. <http://dx.doi.org/10.1097/SS.0b013e3181c30808>.

- Ojeda, J.J., Romero-Gonzalez, M.E., Pouran, H.M., Banwart, S.A., 2008. In situ monitoring of the biofilm formation of *Pseudomonas putida* on hematite using flow-cell ATR-FTIR spectroscopy to investigate the formation of inner-sphere bonds between the bacteria and the mineral. *Mineral. Mag.* 72, 101–106.
- Olk, D.C., Brunetti, G., Senesi, N., 1999. Organic matter in double-cropped lowland rice soils: chemical and spectroscopic properties. *Soil Sci.* 164, 633–649.
- Olk, D.C., Brunetti, G., Senesi, N., 2000. Decrease in humification of organic matter with intensified lowland rice cropping a wet chemical and spectroscopic investigation. *Soil Sci. Soc. Am. J.* 64, 1337–1347.
- Omoike, A., Chorover, J., 2004. Spectroscopic study of extracellular polymeric substances from *Bacillus subtilis*: aqueous chemistry and adsorption effects. *Biomacromolecules* 5, 1219–1230.
- Omoike, A., Chorover, J., 2006. Adsorption to goethite of extracellular polymeric substances from *Bacillus subtilis*. *Geochim. Cosmochim. Acta* 70, 827–838.
- Omoike, A., Chorover, J., Kwon, K.D., Kubicki, J.D., 2004. Adhesion of bacterial exopolymers to α -FeOOH: inner-sphere complexation of phosphodiester groups. *Langmuir* 20, 11108–11114.
- Ostergren, J.D., Trainor, T.P., Bargar, J.R., Brown, G.E., Parks, G.A., 2000. Inorganic ligand effects on Pb(II) sorption to goethite (α -FeOOH) – I. Carbonate. *J. Colloid Interface Sci.* 225, 466–482.
- Otto, A., Mrozek, I., Grabhorn, H., Akemann, W., 1992. Surface-enhanced Raman scattering. *J. Phys. Condens. Matter* 4, 1143.
- Otto, C., Pully, V.V., 2012. Hyperspectral Raman microscopy of the living cell. In: Ghomi, M. (Ed.), *Applications of Raman Spectroscopy to Biology*, Vol. 5. Ios Press Inc., pp. 148–173.
- Quatmane, A., Provenzano, M.R., Hafidi, M., Senesi, N., 2000. Compost maturity assessment using calorimetry, spectroscopy and chemical analysis. *Compost Sci. Util.* 8, 124.
- Özçimen, D., Ersoy-Meriçboyu, A., 2010. Characterization of biochar and bio-oil samples obtained from carbonization of various biomass materials. *Renewable Energy* 35, 1319–1324.
- Parfitt, R.L., Smart, R.S.C., 1977. Infrared spectra from binuclear bridging complexes of sulphate adsorbed on goethite ($[\text{small } \alpha]\text{-FeOOH}$). *Journal of the Chemical Society, Faraday Transactions 1: Physical Chemistry in Condensed Phases* 73, 796–802.
- Parfitt, R.L., Smart, R.S.C., 1978. Mechanism of sulfate adsorption on iron-oxides. *Soil Science Society of America Journal* 42, 48–50.
- Parikh, S.J., Chorover, J., 2005. FTIR spectroscopic study of biogenic Mn-oxide formation by *Pseudomonas putida* GB-1. *Geomicrobiol. J.* 22, 207–218.
- Parikh, S.J., Chorover, J., 2006. ATR-FTIR spectroscopy reveals bond formation during bacterial adhesion to iron oxide. *Langmuir* 22, 8492–8500.
- Parikh, S.J., Chorover, J., 2007. Infrared spectroscopy studies of cation effects on lipopolysaccharides in aqueous solution. *Colloids Surf. B Biointerfaces* 55, 241–250.
- Parikh, S.J., Chorover, J., 2008. ATR-FTIR study of lipopolysaccharides at mineral surfaces. *Colloids Surf. B Biointerfaces* 62, 188–198.
- Parikh, S.J., Kubicki, J.D., Jonsson, C.M., Jonsson, C.L., Hazen, R.M., Sverjensky, D.A., Sparks, D.L., 2011. Evaluating glutamate and aspartate binding mechanisms to rutile (α -TiO₂) via ATR-FTIR spectroscopy and quantum chemical calculations. *Langmuir* 27, 1778–1787.
- Parikh, S.J., Lafferty, B.J., Meade, T.G., Sparks, D.L., 2010. Evaluating environmental influences on As(III) oxidation kinetics by a poorly crystalline Mn-oxide. *Environ. Sci. Technol.* 44, 3772–3778.
- Parikh, S.J., Lafferty, B.J., Sparks, D.L., 2008. An ATR-FTIR spectroscopic approach for measuring rapid kinetics at the mineral/water interface. *J. Colloid Interface Sci.* 320, 177–185.

- Paul, K.W., Borda, M.J., Kubicki, J.D., Sparks, D.L., 2005. Effect of dehydration on sulfate coordination and speciation at the Fe-(Hydr)oxide-water interface: a molecular orbital/density functional theory and Fourier transform infrared spectroscopic investigation. *Langmuir* 21, 11071–11078.
- Paul, T., Machesky, M.L., Strathmann, T.J., 2012. Surface Complexation of the Zwitterionic Fluoroquinolone Antibiotic Ofloxacin to Nano-Anatase TiO₂ Photocatalyst Surfaces. *Environ. Sci. Technol.* 46, 11896–11904.
- Peak, D., Ford, R.G., Sparks, D.L., 1999. An in situ ATR-FTIR investigation of sulfate bonding mechanisms on goethite. *J. Colloid Interface Sci.* 218, 289–299.
- Pei, Z., Shan, X.-Q., Kong, J., Wen, B., Owens, G., 2010. Coadsorption of ciprofloxacin and Cu(II) on montmorillonite and kaolinite as affected by solution pH. *Environ. Sci. Technol.* 44, 915–920.
- Pelletier, M.J., 1999. *Analytical Applications of Raman Spectroscopy*. Wiley.
- Pellow-Jarman, M.V., Hendra, P.J., Lehnert, R.J., 1996. The dependence of Raman signal intensity on particle size for crystal powders. *Vib. Spectrosc.* 12, 257–261.
- Peltre, C., Thuriès, L., Barthès, B., Brunet, D., Morvan, T., Nicolardot, B., Parnaudeau, V., Houot, S., 2011. Near infrared reflectance spectroscopy: a tool to characterize the composition of different types of exogenous organic matter and their behaviour in soil. *Soil Biol. Biochem.* 43, 197–205.
- Pemberton, J.E., Sobocinski, R.L., Sims, G.R., 1990. The effect of charge traps on Raman spectroscopy using a Thomson-CSF charge coupled device detector. *Appl. Spectrosc.* 44, 328–330.
- Pena, M., Meng, X.G., Korfiatis, G.P., Jing, C.Y., 2006. Adsorption mechanism of arsenic on nanocrystalline titanium dioxide. *Environ. Sci. Technol.* 40, 1257–1262.
- Peng, X., Ye, L.L., Wang, C.H., Zhou, H., Sun, B., 2011. Temperature- and duration-dependent rice straw-derived biochar: characteristics and its effects on soil properties of an Ultisol in southern China. *Soil Tillage Res.* 112, 159–166.
- Pereira, M.R., Yarwood, J., 1994. Depth-profiling of polymer laminates using Fourier-transform infrared (ATR) spectroscopy—the barrier film technique. *J. Polym. Sci. Part B Polym. Phys.* 32, 1881–1887.
- Pérez-Sanz, A., Lucena, J.J., Graham, M.C., 2006. Characterization of Fe-humic complexes in an Fe-enriched biosolid by-product of water treatment. *Chemosphere* 65, 2045–2053.
- Pershina, A., Sazonov, A., Ogorodova, L., 2009. Investigation of the interaction between DNA and cobalt ferrite nanoparticles by FTIR spectroscopy. *Russ. J. Bioorg. Chem.* 35, 607–613.
- Persson, P., Axe, K., 2005. Adsorption of oxalate and malonate at the water-goethite interface: molecular surface speciation from IR spectroscopy. *Geochim. Cosmochim. Acta* 69, 541–552.
- Persson, P., Karlsson, M., Ohman, L.O., 1998. Coordination of acetate to Al(III) in aqueous solution and at the water-aluminum hydroxide interface: A potentiometric and attenuated total reflectance FTIR study. *Geochim. Cosmochim. Acta* 62, 3657–3668.
- Persson, P., Nilsson, N., Sjöberg, S., 1996. Structure and bonding of orthophosphate ions at the iron oxide aqueous interface. *J. Colloid Interface Sci.* 177, 263–275.
- Peterson, J.W., O'Meara, T.A., Seymour, M.D., Wang, W., Gu, B., 2009. Sorption mechanisms of cephapirin, a veterinary antibiotic, onto quartz and feldspar minerals as detected by Raman spectroscopy. *Environ. Pollut.* 157, 1849–1856.
- Petit, S., Righi, D., Madejová, J., Decarreau, A., 1998. Layer charge estimation of smectites using infrared spectroscopy. *Clay Miner.* 33, 579–591.
- Petit, S., Righi, D., Madejová, J., 2006. Infrared spectroscopy of NH₄⁽⁺⁾-bearing and saturated clay minerals: a review of the study of layer charge. *Appl. Clay Sci.* 34, 22–30.
- Petry, R., Schmitt, M., Popp, J., 2003. Raman spectroscopy—a prospective tool in the life sciences. *ChemPhysChem* 4, 14–30.

- Piccolo, A., Celano, G., 1994. Hydrogen-bonding interactions between the herbicide glyphosate and water-soluble humic substances. *Environ. Toxicol. Chem.* 13, 1737–1741.
- Piccolo, A., Stevenson, F.J., 1982. Infrared spectra of Cu^{2+} Pb^{2+} and Ca^{2+} complexes of soil humic substances. *Geoderma* 27, 195–208.
- Piccolo, A., Zaccaro, P., Genevini, P.G., 1992. Chemical characterization of humic substances extracted from organic-waste-amended soils. *Bioresource Technology* 40, 275–282.
- Plante, A.F., Chenu, C., Balabane, M., Mariotti, A., Righi, D., 2004. Peroxide oxidation of clay-associated organic matter in a cultivation chronosequence. *Eur. J. Soil Sci.* 55, 471–478.
- Popp, J., Kiefer, W., 2006. Raman scattering, fundamentals. In: *Encyclopedia of Analytical Chemistry*. John Wiley & Sons, Ltd.
- Popp, J., Schmitt, M., 2004. Raman spectroscopy breaking terrestrial barriers! *J. Raman Spectrosc.* 35, 429–432.
- Porto, S.P.S., Tell, B., Damen, T.C., 1966. Near-forward Raman scattering in zinc oxide. *Phys. Rev. Lett.* 16, 450–452.
- Potter, R.M., Rossman, G.R., 1979. Tetravalent manganese oxides—identification, hydration, and structural relationships by infrared-spectroscopy. *Am. Mineral.* 64, 1199–1218.
- Prost, R., Dameme, A., Huard, E., Driard, J., Leydecker, J.P., 1989. Infrared study of structural oh in kaolinite, dickite, nacrite, and poorly crystalline kaolinite at 5-K to 600-K. *Clays Clay Miner.* 37, 464–468.
- Puppels, G.J., de Mul, F.F.M., Otto, C., Greve, J., Robert-Nicoud, M., Arndt-Jovin, D.J., Jovin, T.M., 1990. Studying single living cells and chromosomes by confocal Raman microspectroscopy. *Nat. Commun.* 347, 301–303.
- Pusino, A., Braschi, I., Gessa, C., 2000. Adsorption and degradation of triasulfuron on homoionic montmorillonites. *Clays Clay Miner.* 48, 19–25.
- Pusino, A., Gelsomino, A., Fiori, M.G., Gessa, C., 2003. Adsorption of Two Quinolinecarboxylic Acid Herbicides on Homoionic Montmorillonites. *Clays Clay Miner.* 51, 143–149.
- Quiles, F., Burneau, A., Keiding, K., 1999. In situ ATR-FTIR. Characterization of organic macromolecules aggregated with metallic colloids. In: Berthelin, J., Huang, P.M., Bollag, J.-M., Andreuz, F. (Eds.), *Effect of Mineral-Organic Microorganism Interactions on Soil and Freshwater Environments*. Klumer Academic / Plenum Publishers, New York, pp. 133–142.
- Raab, T.K., Vogel, J.P., 2004. Ecological and agricultural applications of synchrotron IR microscopy. *Infrared Phys. Technol.* 45, 393–402.
- Rakshit, S., Elzinga, E.J., Datta, R., Sarkar, D., 2013a. In Situ Attenuated Total Reflectance Fourier-Transform Infrared Study of Oxytetracycline Sorption on Magnetite. *J. Environ. Qual.* 42, 822–827.
- Rakshit, S., Sarkar, D., Elzinga, E.J., Punamiya, P., Datta, R., 2013b. Mechanisms of ciprofloxacin removal by nano-sized magnetite. *J. Hazard. Mater.* 246–247, 221–226.
- Raman, C.V., Krishnan, K.S., 1928. A new type of secondary radiation. *Nat. Commun.* 121, 501–502.
- Rank, D.H., Douglas, A.E., 1948. Light scattering in optical glass. *J. Opt. Soc. Am.* 38, 966–970.
- Reeves, J.B., Francis, B.A., Hamilton, S.K., 2005. Specular reflection and diffuse reflectance spectroscopy of soils. *Appl. Spectrosc.* 59, 39–46.
- Reeves III, J.B., 2010. Near- versus mid-infrared diffuse reflectance spectroscopy for soil analysis emphasizing carbon and laboratory versus on-site analysis: where are we and what needs to be done? *Geoderma* 158, 3–14.
- Reeves III, J.B., 2012. Mid-infrared spectral interpretation of soils: is it practical or accurate? *Geoderma* 189, 508–513.
- Reeves III, J.B., McCarty, G.W., Calderón, F.J., Hively, H.D., 2012. *Advances in Spectroscopic Methods for Quantifying Soil Carbon*, first ed. (Coordinated Agricultural Research through GRACEnet to Address our Changing Climate).

- Reeves III, J.B., Follett, R.F., McCarty, G.W., Kimble, J.M., 2006. Can near or mid-infrared diffuse reflectance spectroscopy be used to determine soil carbon pools? *Commun. Soil. Sci. Plant Anal.* 37, 2307–2325.
- Reeves, J.B., McCarty, G.W., Reeves, V.B., 2001. Mid-infrared diffuse reflectance spectroscopy for the quantitative analysis of agricultural soils. *J. Agric. Food Chem.* 49, 766–772.
- Reiter, G., Siam, M., Falkenhagen, D., Gollneritsch, W., Baurecht, D., Fringeli, U.P., 2002. Interaction of a bacterial endotoxin with different surfaces investigated by in situ Fourier transform infrared attenuated total reflection spectroscopy. *Langmuir* 18, 5761–5771.
- Riddle, J.W., Kabler, P.W., Kenner, B.A., Bordner, R.H., Rockwood, S.W., Stevenson, H.J.R., 1956. Bacterial identification by infrared spectrophotometry. *J. Bacteriol.* 72, 593–603.
- Rijnaarts, H.H.M., Norde, W., Bouwer, E.J., Lyklema, J., Zehnder, A.J.B., 1995. Reversibility and mechanism of bacterial adhesion. *Colloids Surf. B Biointerfaces* 4, 5–22.
- Rinaudo, C., Roz, M., Boero, V., Franchini-Angela, M., 2004. FT-Raman spectroscopy on several di- and trioctahedral T—O—T phyllosilicates. *Neues Jahrb. Mineral. Monatsh.* 537–554.
- Rintoul, L., Fredericks, P.M., 1995. Infrared microspectroscopy of Bauxitic Pisoliths. *Appl. Spectrosc.* 49, 1608–1616.
- Roberts, C.A., Workman, J., Reeves III, J.B., 2004. Near-infrared Spectroscopy in Agriculture. American Societies of Agronomy, Crop and Soil Science, Madison, WI.
- Roddick-Lanzilotta, A.D., Connor, P.A., McQuillan, A.J., 1998. An in situ infrared spectroscopic study of the adsorption of lysine to TiO_2 from an aqueous solution. *Langmuir* 14, 6479–6484.
- Roddick-Lanzilotta, A.D., Mcquillan, A.J., 1999. An in Situ Infrared Spectroscopic Investigation of Lysine Peptide and Polylysine Adsorption to TiO_2 From Aqueous Solutions. *J. Colloid Interface Sci* 217, 194–202.
- Roddick-Lanzilotta, A.D., McQuillan, A.J., 2000. An in situ infrared spectroscopic study of glutamic acid and of aspartic acid adsorbed on TiO_2 : Implications for the biocompatibility of titanium. *J. Colloid Interface Sci.* 227, 48–54.
- Roddick-Lanzilotta, A.J., McQuillan, A.J., Craw, D., 2002. Infrared spectroscopic characterisation of arsenate (V) ion adsorption from mine waters, Macraes mine, New Zealand. *Applied Geochemistry* 17, 445–454.
- Roldán, M.L., Corrado, G., Francioso, O., Sanchez-Cortes, S., 2011. Interaction of soil humic acids with herbicide paraquat analyzed by surface-enhanced Raman scattering and fluorescence spectroscopy on silver plasmonic nanoparticles. *Anal. Chim. Acta* 699, 87–95.
- Rong, X., Chen, W., Huang, Q., Cai, P., Liang, W., 2010. *Pseudomonas putida* adhesion to goethite: studied by equilibrium adsorption, SEM, FTIR and ITC. *Colloids Surf. B Biointerfaces* 80, 79–85.
- Rong, X., Huang, Q., He, X., Chen, H., Cai, P., Liang, W., 2008. Interaction of *Pseudomonas putida* with kaolinite and montmorillonite: a combination study by equilibrium adsorption, ITC, SEM and FTIR. *Colloids Surf. B Biointerfaces* 64, 49–55.
- Rosenqvist, J., Axe, K., Sjöberg, S., Persson, P., 2003. Adsorption of Dicarboxylates on Nano-Sized Gibbsite Particles: Effects of Ligand Structure on Bonding Mechanisms. *Colloid Surf. A-Physicochem. Eng. Asp.* 220, 91–104.
- Rotzinger, F.P., Kesselman-Truttman, J.M., Hug, S.J., Shklover, V., Gratzel, M., 2004. Structure and vibrational spectrum of formate and acetate adsorbed from aqueous solution onto the TiO_2 rutile (110) surface. *Journal of Physical Chemistry B* 108, 5004–5017.
- Ruan, H.D., Frost, R.L., Klopogge, J.T., 2001. The behavior of hydroxyl units of synthetic goethite and its dehydroxylated product hematite. *Spectrochim. Acta Part A Mol. Biomol. Spectrosc.* 57, 2575–2586.
- Ruan, H.D., Frost, R.L., Klopogge, J.T., Duong, L., 2002a. Infrared spectroscopy of goethite dehydroxylation. II. Effect of aluminium substitution on the behaviour of hydroxyl units. *Spectrochim. Acta Part A Mol. Biomol. Spectrosc.* 58, 479–491.

- Ruan, H.D., Frost, R.L., Klopogge, J.T., Duong, L., 2002b. Infrared spectroscopy of goethite dehydroxylation: III. FT-IR microscopy of in situ study of the thermal transformation of goethite to hematite. *Spectrochim. Acta Part A Mol. Biomol. Spectrosc.* 58, 967–981.
- Rumpel, C., Rabia, N., Derenne, S., Quenea, K., Eusterhues, K., Koegel-Knabner, I., Mariotti, A., 2006. Alteration of soil organic matter following treatment with hydrofluoric acid (HF). *Org. Geochem.* 37, 1437–1451.
- Russell, J.D., Fraser, A.R., 1994. Infrared methods. In: Wilson, M.J. (Ed.), *Clay Mineralogy: Spectroscopic and Chemical Determinative Methods*. Chapman & Hall, London, UK, pp. 11–67.
- Russell, J.D., Parfitt, R.L., Fraser, A.R., Farmer, V.C., 1974. Surface structures of gibbsite goethite and phosphated goethite. *Nature* 248, 220–221.
- Sadezky, A., Muckenhuber, H., Grothe, H., Niessner, R., Pöschl, U., 2005. Raman microspectroscopy of soot and related carbonaceous materials: spectral analysis and structural information. *Carbon* 43, 1731–1742.
- Sánchez-Cortés, S., Francioso, O., Ciavatta, C., García-Ramos, J.V., Gessa, C., 1998. pH-dependent adsorption of fractionated peat humic substances on different silver colloids studied by surface-enhanced Raman spectroscopy. *J. Colloid Interface Sci.* 198, 308–318.
- Sanchez-Cortes, S.C.G., Trubetskaya, O.E., Trubetskoj, O.A., Hermosin, B., Saiz-Jimenez, C., 2006. Surface-enhanced Raman spectroscopy of chernozem humic acid and their fractions obtained by coupled size exclusion chromatography-polyacrylamide gel electrophoresis (SEC-PAGE). *Appl. Spectrosc.* 60, 48–53.
- Sánchez- Monedero, M.A., Roig, A., Cegarra, J., Bernal, M.P., Paredes, C., 2002. Effects of HCl-HF purification treatment on chemical composition and structure of humic acids. *European Journal of Soil Science* 53, 375–381.
- Sarkhot, D.V., Comerford, N.B., Jokela, E.J., Reeves, J.B., Harris, W.G., 2007a. Aggregation and aggregate carbon in a forested southeastern coastal plain spodosol (All rights reserved. No part of this periodical may be reproduced or transmitted in any form or by any means, electronic or mechanical, including photocopying, recording, or any information storage and retrieval system, without permission in writing from the publisher. Permission for printing and for reprinting the material contained herein has been obtained by the publisher) *Soil Sci. Soc. Am. J.* 71, 1779–1787.
- Sarkhot, D.V., Comerford, N.B., Jokela, E.J., Reeves III, J.B., Harris, W.G., 2007b. Aggregation and aggregate carbon in a forested southeastern coastal plain spodosol. *Soil Sci. Soc. Am. J.* 71, 1779–1787.
- Schenzel, K., Fischer, S., 2001. NIR FT Raman Spectroscopy—a Rapid Analytical Tool for Detecting the Transformation of Cellulose Polymorphs. *Cellulose* 8, 49–57.
- Scherrer, S., Diniz, I., Morais, H., 2010. Climate and host plant characteristics effects on lepidopteran caterpillar abundance on *Miconia ferruginata* DC. and *Miconia pohliana* Cogn (Melastomataceae). *Brazilian Journal of Biology* 70, 103–109.
- Schmidt, M.W.I., Skjemstad, J.O., Jager, C., 2002. Carbon isotope geochemistry and nano-morphology of soil black carbon: black chernozemic soils in central Europe originate from ancient biomass burning. *Glob. Biogeochem. Cycles* 16.
- Schmidt, M.W.I., Torn, M.S., Abiven, S., Dittmar, T., Guggenberger, G., Janssens, I.A., Kleber, M., Kogel-Knabner, I., Lehmann, J., Manning, D.A.C., Nannipieri, P., Rasse, D.P., Weiner, S., Trumbore, S.E., 2011. Persistence of soil organic matter as an ecosystem property. *Nature* 478, 49–56.
- Schmitt, J., Flemming, H.C., 1998. FTIR-spectroscopy in microbial and material analysis. *Int. Biodeterior. Biodegrad.* 41, 1–11.
- Schmitt, J., Flemming, H.C., 1999. Water binding in biofilms. *Water Sci. Technol.* 39, 77–82.
- Schmitt, J., Nivens, D., White, D.C., Flemming, H.C., 1995. Changes of biofilm properties in response to sorbed substances—an FTIR-ATR study. *Water Sci. Technol.* 32, 149–155.

- Schnitzer, M., Monreal, C.M., 2011. Chapter three—Quo Vadis soil organic matter research? A biological link to the chemistry of humification. In: Donald, L.S. (Ed.), *Advances in Agronomy*, vol. 113. Academic Press, pp. 143–217.
- Schrader, B., Hoffmann, A., Keller, S., 1991. Near-infrared Fourier transform Raman spectroscopy: facing absorption and background. *Spectrochim. Acta Part A Mol. Spectrosc.* 47, 1135–1148.
- Schrader, B., Schulz, H., Andreev, G.N., Klump, H.H., Sawatzki, J., 2000. Non-destructive NIR-FT-Raman spectroscopy of plant and animal tissues, of food and works of art. *Talanta* 53, 35–45.
- Schuttlefield, J.D., Cox, D., Grassian, V.H., 2007. An investigation of water uptake on clays minerals using ATR-FTIR spectroscopy coupled with quartz crystal microbalance measurements. *J. Geophys. Res. Atmos.* 112.
- Schwertmann, U., Cornell, R.M., 1991. *Iron Oxides in the Laboratory: Preparation and Characterization*, second ed. Wiley-VCH, Weinheim.
- Schwertmann, U., Cornell, R.M., 2000. *Iron Oxides in the Laboratory*. Wiley-VCH, Weinheim, Germany.
- Schwertmann, U., Taylor, R.M., 1989. Iron oxides. In: Klute, A. (Ed.), *Methods of Soil Analysis, Part 1—Physical and Mineralogical Methods*, vol. 5. SSSA, Madison, WI, pp. 379–438.
- Senesi, N., D'Orazio, V., Ricca, G., 2003. Humic acids in the first generation of EURO-SOILS. *Geoderma* 116, 325–344.
- Senesi, N., Plaza, C., Brunetti, G., Polo, A., 2007. A comparative survey of recent results on humic-like fractions in organic amendments and effects on native soil humic substances. *Soil Biol. Biochem.* 39, 1244–1262.
- Sham, T.K., Rivers, M.L., 2002. A brief overview of synchrotron radiation. *Rev. Mineral. Geochem.* 49, 117–147.
- Sharma, B.K., 2004. *Instrumental Methods of Chemical Analysis*. Goel Publishing House, Meerut, India.
- Sharma, R.K., Wooten, J.B., Baliga, V.L., Lin, X., Geoffrey Chan, W., Hajaligol, M.R., 2004. Characterization of chars from pyrolysis of lignin. *Fuel* 83, 1469–1482.
- Sheals, J., Sjöberg, S., Persson, P., 2002. Adsorption of glyphosate on goethite: molecular characterization of surface complexes. *Environ. Sci. Technol.* 36, 3090–3095.
- Shearer, J.C., Peters, D.C., 1987. Fourier transform infrared microspectrophotometry as a failure analysis tool. In: Roush, P.B. (Ed.), *The design, sample handling, and applications of infrared microscopes*. ASTM Committee E-13 on Molecular Spectroscopy Federation of Analytical Chemistry Spectroscopy Societies.
- Sheng, G.Y., Johnston, C.T., Teppen, B.J., Boyd, S.A., 2002. Adsorption of dinitrophenol herbicides from water by montmorillonites. *Clays Clay Miner.* 50, 25–34.
- Shimizu, M., Ginder-Vogel, M., Parikh, S.J., Sparks, D.L., 2010. Molecular scale assessment of methylarsenic sorption on aluminum oxide. *Environ. Sci. Technol.* 44, 612–617.
- Siebielc, G., McCarthy, G.W., Stuczynski, T.I., Reeves, J.B., 2004. Near- and mid-infrared diffuse reflectance spectroscopy for measuring soil metal content. *J. Environ. Qual.* 33, 2056–2069.
- Simon, 2007. Quantitative and qualitative characterization of soil organic matter in the long-term fallow experiment with different fertilization and tillage. *Archives Agronomy Soil Sci.* 53, 241–251.
- Šimon, T., Javůrek, M., Mikanová, O., Vach, M., 2009. The influence of tillage systems on soil organic matter and soil hydrophobicity. *Soil Tillage Res.* 105, 44–48.
- Simonetti, G., Francioso, O., Nardi, S., Berti, A., Brugnoli, E., Francesco Morari, E.L., 2012. Characterization of humic carbon in soil aggregates in a long-term experiment with manure and mineral fertilization. *Soil Sci. Soc. Am. J.* 76, 880–890.

- Singh, B., Singh, B.P., Cowie, A., 2010. Characterisation and evaluation of biochars for their application as a soil amendment. *Aust. J. Soil Res.* 48, 516–525.
- Siregar, A., Kleber, M., Mikutta, R., Jahn, R., 2005. Sodium hypochlorite oxidation reduces soil organic matter concentrations without affecting inorganic soil constituents. *Eur. J. Soil Sci.* 56, 481–490.
- Six, J., Bossuyt, H., Degryze, S., Deneff, K., 2004. A history of research on the link between (micro)aggregates, soil biota, and soil organic matter dynamics. *Soil Tillage Res.* 79, 7–31.
- Slepetiene, A., Liaudanskiene, I., Slepetys, J., Velykis, A., 2010. The influence of reduced tillage, winter crops and ecologically managed long-term mono- and multi-component swards on soil humic substances. *Chem. Ecol.* 26, 97–109.
- Smith, E., Dent, G., 2005. "Modern Raman spectroscopy: A practical approach," Hoboken, NJ, J. Wiley.
- Smidt, E., Meissl, K., 2007. The applicability of Fourier transform infrared (FT-IR) spectroscopy in waste management. *Waste Manag.* 27, 268–276.
- Smidt, E., Schwanninger, M., 2005. Characterization of waste materials using FTIR spectroscopy: process monitoring and quality assessment. *Spectrosc. Lett.* 38, 247–270.
- Smith, B., 2011. *Fundamentals of Fourier Transform Infrared Spectroscopy*. CRC Press, Boca Raton.
- Smith, E., 2005. *Modern Raman Spectroscopy: A Practical Approach*. J. Wiley, Hoboken, NJ.
- Smith, N.J.H., 1980. Anthrosols and human carrying capacity in Amazonia*. *Ann. Assoc. Am. Geogr.* 70, 553–566.
- Snabe, T., Petersen, S.B., 2002. Application of infrared spectroscopy (attenuated total reflection) for monitoring enzymatic activity on substrate films. *J. Biotechnol.* 95, 145–155.
- Sobkowiak, M., Painter, P., 1992. Determination of the aliphatic and aromatic CH contents of coals by FT-i.r.: studies of coal extracts. *Fuel* 71, 1105–1125.
- Sockalingum, G.D., Bouhedja, W., Pina, P., Allouch, P., Mandray, C., Labia, R., et al., 1997. ATR-FTIR Spectroscopic Investigation of Imipenem-Susceptible and -Resistant *Pseudomonas aeruginosa* Isogenic Strains. *Biochem. Biophys. Res. Commun.* 232, 240–246.
- Sohi, S.P., Krull, E., Lopez-Capel, E., Bol, R., 2010. Chapter 2-A review of biochar and its use and function in soil. In: Donald, L.S. (Ed.), *Advances in Agronomy*, vol. 105. Academic Press, pp. 47–82.
- Solomon, D., Lehmann, J., Kinyangi, J., Liang, B.Q., Schafer, T., 2005. Carbon K-edge NEXAFS and FTIR-ATR spectroscopic investigation of organic carbon speciation in soils. *Soil Sci. Soc. Am. J.* 69, 107–119.
- Solomon, D., Lehmann, J., Kinyangi, J., Amelung, W., Lobe, I., Pell, A., Riha, S., Ngoze, S., Verchot, L.O.U., Mbugua, D., Skjemstad, J.A.N., Schäfer, T., 2007a. Long-term impacts of anthropogenic perturbations on dynamics and speciation of organic carbon in tropical forest and subtropical grassland ecosystems. *Glob. Change Biol.* 13, 511–530.
- Solomon, D., Lehmann, J., Thies, J., Schäfer, T., Liang, B., Kinyangi, J., Neves, E., Petersen, J., Luizão, F., Skjemstad, J., 2007b. Molecular signature and sources of biochemical recalcitrance of organic C in Amazonian Dark Earths. *Geochim. Cosmochim. Acta* 71, 2285–2298.
- Solomon, D., Lehmann, J., Wang, J., Kinyangi, J., Heymann, K., Lu, Y., Wirick, S., Jacobsen, C., 2012. Micro- and nano-environments of C sequestration in soil: a multi-elemental STXM-NEXAFS assessment of black C and organomineral associations. *Sci. Total Environ.* 438, 372–388.
- Sombroek, W., Ruivo, M.L., Fearnside, P.M., Glaser, B., Lehmann, J., 2003. Amazonian Dark Earths as carbon stores and sinks. In: Lehmann, J., Kern, D.C., Glaser, B., Woods, W.I. (Eds.), *Amazonian Dark Earths: Origin, Properties, Management*. Kluwer Academic Publishers, The Netherlands, pp. 125–139.
- Sombroek, W.G., 1966. *Amazon Soils A Reconnaissance of the Soils of the Brazilian Amazon Region*.

- Song, Y.P., Yarwood, J., Tsibouklis, J., Feast, W.J., Cresswell, J., Petty, M.C., 1992. Fourier-transform infrared spectroscopic studies on alternate-layer Langmuir-Blodgett-films with nonlinear optical-properties. *Langmuir* 8, 262–266.
- Song, Z., Chouparova, E., Jones, K.W., Feng, H., Marinkovic, N.S., 2001. FTIR Investigation of Sediments from NY/NJ Harbor, San Diego Bay, and the Venetian Lagoon. NLSL(Activity Report).
- Soukup, D.A., Buck, B.J., Harris, W., 2008. Preparing soils for mineralogical analyses. In: Ulery, A.L., Drees, L.R. (Eds.), *Methods of Soil Analysis, Part 5—Mineralogical Methods*. Soil Science Society of America, Madison, WI.
- Sparks, D.L., 1995. *Environmental Soil Chemistry*. Academic Press, Inc., San Diego, CA.
- Sparks, D.L., 2002. *Environmental Soil Chemistry*. Elsevier Science.
- Spath, R., Flemming, H.C., Wuertz, S., 1998. Sorption properties of biofilms. *Water Sci. Technol.* 37, 207–210.
- Spedding, F.H., Stamm, R.F., 1942. The Raman spectra of the sugars in the solid state and in solution I. The Raman spectra of alpha- and beta-D-glucose. *J. Chem. Phys.* 10, 176–183.
- Specht, C.H., Frimmel, F.H., 2001. An in Situ ATR-FTIR Study on the Adsorption of Dicarboxylic Acids Onto Kaolinite in Aqueous Suspensions. *Physical Chemistry Chemical Physics* 3, 5444–5449.
- Spósito, G., 1989. *The Chemistry of Soils*. Oxford University Press, New York.
- Spósito, G., 2004. *The Surface Chemistry of Natural Particles*. Oxford University Press, New York.
- Spósito, G., Martín-Neto, L., Yang, A., 1996. Atrazine Complexation by Soil Humic Acids. *J. Environ. Qual.* 25, 1203–1209.
- Starsinic, M., Taylor, R.L., Walker Jr., P.L., Painter, P.C., 1983. FTIR studies of Saran chars. *Carbon* 21, 69–74.
- Steinbeiss, S., Gleixner, G., Antonietti, M., 2009. Effect of biochar amendment on soil carbon balance and soil microbial activity. *Soil Biol. Biochem.* 41, 1301–1310.
- Stenberg, B., Viscarra Rossel, R.A., Mouazen, A.M., Wetterlind, J., 2010. Chapter five—visible and near infrared spectroscopy in soil science. In: Donald, L.S. (Ed.), *Advances in Agronomy*, vol. 107. Academic Press, pp. 163–215.
- Stevenson, F.J., Goh, K.M., 1971. Infrared spectra of humic acids and related substances. *Geochim. Cosmochim. Acta* 35, 471–483.
- Stiles, P.L., Dieringer, J.A., Shah, N.C., Van Duyne, R.P., 2008. Surface-enhanced Raman spectroscopy. *Annu. Rev. Anal. Chem.* 1, 601–626.
- Stokes, D.L., Wullschleger, S., Martin, M., Vo-Dinh, T., 2003. *Raman Spectroscopy and Instrumentation for Monitoring Soil Carbon Systems*. Environmental Sciences Division Oak Ridge National Laboratory.
- Strojek, J.W., Mielczar, J.A., 1974. Internal-reflection spectroscopy for investigations of sorption on powders. *Rocz. Chem.* 48, 1747–1751.
- Stuart, B., 2000. Infrared spectroscopy. In: Kirk-Othmer Encyclopedia of Chemical Technology. John Wiley & Sons, Inc.
- Su, C., Suarez, D.L., 1995. Coordination of Adsorbed Boron: A FTIR Spectroscopic Study. *Environ. Sci. Technol.* 29, 302–311.
- Su, C.M., Suarez, D.L., 1997a. Boron sorption and release by allophane. *Soil Science Society of America Journal* 61, 69–77.
- Su, C.M., Suarez, D.L., 1997b. In situ infrared speciation of adsorbed carbonate on aluminum and iron oxide. *Clays Clay Miner.* 45, 814–825.
- Su, C., Suarez, D.L., 2000. Selenate and Selenite Sorption on Iron Oxides An Infrared and Electrophoretic Study *Soil Sci. Soc. Am. J.* 64, 101–111.
- Suarez, D.L., Goldberg, S., Su, C., 1999. Evaluation of oxyanion adsorption mechanisms on oxides using FTIR spectroscopy and electrophoretic mobility. In: *Mineral-Water Interfacial Reactions*, vol. 715, American Chemical Society, pp. 136–178.

- Suci, P.A., Vransky, J.D., Mittelman, M.W., 1998. Investigation of interactions between antimicrobial agents and bacterial biofilms using attenuated total reflection Fourier transform infrared spectroscopy. *Biomaterials* 19, 327–339.
- Sullivan, L.A., Koppi, A.J., 1987. In-situ soil organic matter studies using scanning electron microscopy and low temperature ashing. *Geoderma* 40, 317–332.
- Summons, R.E., Amend, J.P., Bish, D., Buick, R., Cody, G.D., Des Marais, D.J., Dromart, G., Eigenbrode, J.L., Knoll, A.H., Sumner, D.Y., 2011. Preservation of martian organic and environmental records: final report of the Mars biosignature working group. *Astrobiology* 11, 157–181.
- Sun, X.H., Doner, H.E., 1996. An investigation of arsenate and arsenite bonding structures on goethite by FTIR. *Soil Science* 161, 865–872.
- Sun, X.H., Doner, H.E., 1998. Adsorption and oxidation of arsenite on goethite. *Soil Science* 163, 278–287.
- Szabó, L., Leopold, L., Cozar, B., Leopold, N., Herman, K., Chiş, V., 2011. SERS approach for Zn(II) detection in contaminated soil. *Central Eur. J. Chem.* 9, 410–414.
- Szlachta, M., Gerda, V., Chubar, N., 2012. Adsorption of arsenite and selenite using an inorganic ion exchanger based on Fe–Mn hydrous oxide. *J. Colloid Interface Sci.* 365, 213–221.
- Tandy, S., Healey, J.R., Nason, M.A., Williamson, J.C., Jones, D.L., Thain, S.C., 2010. FT-IR as an alternative method for measuring chemical properties during composting. *Bioresour. Technol.* 101, 5431–5436.
- Tapia, Y., Cala, V., Eymar, E., Frutos, I., Gárate, A., Masaguer, A., 2010. Chemical characterization and evaluation of composts as organic amendments for immobilizing cadmium. *Bioresour. Technol.* 101, 5437–5443.
- Tatzber, M., Stemmer, M., Spiegel, H., Katzlberger, C., Haberhauer, G., Gerzabek, M.H., 2008. Impact of different tillage practices on molecular characteristics of humic acids in a long-term field experiment—an application of three different spectroscopic methods. *Sci. Total Environ.* 406, 256–268.
- Tatzber, M., Stemmer, M., Spiegel, H., Katzlberger, C., Haberhauer, G., Mentler, A., Gerzabek, M.H., 2007. FTIR-spectroscopic characterization of humic acids and humin fractions obtained by advanced NaOH, Na₄P₂O₇, and Na₂CO₃ extraction procedures. *J. Plant Nutr. Soil. Sci.* 170, 522–529.
- Tatzber, M., Stemmer, M., Spiegel, H., Katzlberger, C., Zehetner, F., Haberhauer, G., Garcia-Garcia, E., Gerzabek, M.H., 2009. Spectroscopic behaviour of ¹⁴C-labeled humic acids in a long-term field experiment with three cropping systems. *Soil Res.* 47, 459–469.
- Tejedor-Tejedor, M.I., Anderson, M.A., 1986. *In situ* attenuated total reflection Fourier-transform infrared studies of the goethite (α-FeOOH)-aqueous solution interface. *Langmuir* 2, 203–210.
- Tejedor-Tejedor, M.I., Anderson, M.A., 1990. Protonation of phosphate on the surface of goethite as studied by CIR-FTIR and electrophoretic mobility. *Langmuir* 6, 602–611.
- Tejedor-Tejedor, M.I., Yost, E.C., Anderson, M.A., 1992. Characterization of benzoic and phenolic complexes at the goethite aqueous-solution interface using cylindrical internal-reflection fourier-transform infrared-spectroscopy. 2. Bonding structures. *Langmuir* 8, 525–533.
- Tejedor-Tejedor, M.I., Yost, E.C., Anderson, M.A., 1990. Characterization of benzoic and phenolic complexes at the goethite aqueous-solution interface using cylindrical internal-reflection Fourier-transform infrared-spectroscopy. 1. Methodol. *Langmuir* 6, 979–987.
- Thibau, R.J., Brown, C.W., Heidersbach, R.H., 1978. Raman spectra of possible corrosion products of iron. *Appl. Spectrosc.* 32, 532–535.
- Tickanen, L.D., Tejedor-Tejedor, M.I., Anderson, M.A., 1997. Quantitative characterization of aqueous suspensions using variable-angle ATR-FTIR spectroscopy: determination of optical constants and absorption coefficient spectra. *Langmuir* 13, 4829–4836.

- Tofan-Lazar, J., Al-Abadleh, H.A., 2012a. ATR-FTIR studies on the adsorption/desorption kinetics of dimethylarsinic acid on iron-(oxyhydr)oxides. *J. Phys. Chem. A* 116, 1596–1604.
- Tofan-Lazar, J., Al-Abadleh, H.A., 2012b. Kinetic ATR-FTIR studies on phosphate adsorption on iron (oxyhydr)oxides in the absence and presence of surface arsenic: molecular-level insights into the ligand exchange mechanism. *J. Phys. Chem. A* 116, 10143–10149.
- Tomić, Z., Makreski, P., Gajić, B., 2010. Identification and spectra-structure determination of soil minerals: Raman study supported by IR spectroscopy and X-ray powder diffraction. *J. Raman Spectrosc.* 41, 582–586.
- Tonon, G., Sohi, S., Francioso, O., Ferrari, E., Montecchio, D., Giocchini, P., Ciavatta, C., Panzacchi, P., Powlson, D., 2010. Effect of soil pH on the chemical composition of organic matter in physically separated soil fractions in two broadleaf woodland sites at Rothamsted, UK. *Eur. J. Soil Sci.* 61, 970–979.
- Torrent, J., Barrón, V., 2008. Diffuse reflectance spectroscopy. In: Ulery, A.L., Drees, L.R. (Eds.), *Methods of Soil Analysis, Part 5-Mineralogical Methods*. Soil Science Society of America, Madison, WI.
- Tranter, G., Minasny, B., McBratney, A.B., Viscarra Rossel, R.A., Murphy, B.W., 2008. Comparing spectral soil inference systems and mid-infrared spectroscopic predictions of soil moisture retention. *Soil. Sci. Soc. Am. J.* 72, 1394–1400.
- Trivedi, P., Vasudevan, D., 2007. Spectroscopic investigation of ciprofloxacin speciation at the goethite-water interface. *Environ. Sci. Technol.* 41, 3153–3158.
- Tsuboi, M., 1961. Infrared spectra and secondary structure of deoxyribonucleic acid. *Prog. Theor. Phys. Suppl.* 17, 99–107.
- Undabeytia, T., Nir, S., Rubin, B., 2000. Organo-clay formulations of the hydrophobic herbicide norflurazon yield reduced leaching. *Journal of Agricultural and Food Chemistry* 48, 4767–4773.
- Upritchard, H.G., Yang, J., Bremer, P.J., Lamont, I.L., McQuillan, A.J., 2007. Adsorption to metal oxides of the *Pseudomonas aeruginosa* siderophore pyoverdine and implications for bacterial biofilm formation on metals. *Langmuir* 23, 7189–7195.
- Upritchard, H.G., Yang, J., Bremer, P.J., Lamont, I.L., McQuillan, A.J., 2011. Adsorption of enterobactin to metal oxides and the role of siderophores in bacterial adhesion to metals. *Langmuir* 27, 10587–10596.
- Usher, C.R., Paul, K.W., Narayansamy, J., Kubicki, J.D., Sparks, D.L., Schoonen, M.A.A., Strongin, D.R., 2005. Mechanistic aspects of pyrite oxidation in an oxidizing gaseous environment: an in situ HATR-IR isotope study. *Environ. Sci. Technol.* 39, 7576–7584.
- Uyguner-Demirel, C.S., Bekbolet, M., 2011. Significance of analytical parameters for the understanding of natural organic matter in relation to photocatalytic oxidation. *Chemosphere* 84, 1009–1031.
- Vasiliadou, I.A., Papouli, D., Chrysikopoulos, C.V., Panagiotaras, D., Karakosta, E., Fardis, M., Papavassiliou, G., 2011. Attachment of *Pseudomonas putida* onto differently structured kaolinite minerals: a combined ATR-FTIR and H-1 NMR study. *Colloids Surf. B Biointerfaces* 84, 354–359.
- Vdović, N., Obhodaš, J., Pikelj, K., 2010. Revisiting the particle-size distribution of soils: comparison of different methods and sample pre-treatments. *Eur. J. Soil Sci.* 61, 854–864.
- Ve, N.B., Olk, D.C., Cassman, K.G., 2004. Nitrogen mineralization from humic acid fractions in rice soils depends on degree of humification. *Journal Series No. 14403 from the Agricultural Research Division, Univ. of Nebraska. Soil Sci. Soc. Am. J.* 68, 1278–1284.
- Verchot, L.V., Dutaur, L., Shepherd, K.D., Albrecht, A., 2011. Organic matter stabilization in soil aggregates: understanding the biogeochemical mechanisms that determine the fate of carbon inputs in soils. *Geoderma* 161, 182–193.
- Verheijen, F., Jeddery, S., Bastos, A., van der Velde, C.M., Dias, I., 2010. *Biochar Application to Soils*. Institute for Environment and Sustainability, European Communities.

- Vergnoux, A., Guiliano, M., Di Rocco, R., Domeizel, M., Théraulaz, F., Doumenq, P., 2011. Quantitative and mid-infrared changes of humic substances from burned soils. *Environmental Research* 111, 205–214.
- Veum, J., Goyne, K., Kremer, R., Miles, R., Sudduth, K., 2014. Biological indicators of soil quality and soil organic matter characteristics in an agricultural management continuum. *Biogeochemistry* 117, 81–99.
- Villanueva, U., Raposo, J.C., Castro, K., de Diego, A., Arana, G., Madariaga, J.M., 2008. Raman spectroscopy speciation of natural and anthropogenic solid phases in river and estuarine sediments with appreciable amount of clay and organic matter. *J. Raman Spectrosc.* 39, 1195–1203.
- Villalobos, M., Leckie, J.O., 2001. Surface complexation modeling and FTIR study of carbonate adsorption to goethite. *J. Colloid Interface Sci.* 235, 15–32.
- Villar, S.E.J., Edwards, H.G.M., 2006. Raman spectroscopy in astrobiology. *Anal. Bioanal. Chem.* 384, 100–113.
- Viscarra Rossel, R.A., Cattle, S.R., Ortega, A., Fouad, Y., 2009. In situ measurements of soil colour, mineral composition and clay content by vis-NIR spectroscopy. *Geoderma* 150, 253–266.
- Viscarra Rossel, R.A., McGlynn, R.N., McBratney, A.B., 2006. Determining the composition of mineral-organic mixes using UV-vis-NIR diffuse reflectance spectroscopy. *Geoderma* 137, 70–82.
- Voegelin, A., Hug, S.J., 2003. Catalyzed oxidation of arsenic(III) by hydrogen peroxide on the surface of ferrihydrite: An in situ ATR-FTIR study. *Environ. Sci. Technol.* 37, 972–978.
- Vogel, E., Geßner, R., Hayes, M.H.B., Kiefer, W., 1999. Characterisation of humic acid by means of SERS. *J. Mol. Struct.* 482–483, 195–199.
- von Lützow, M., Kögel-Knabner, I., Ekschmitt, K., Flessa, H., Guggenberger, G., Matzner, E., Marschner, B., 2007. SOM fractionation methods: relevance to functional pools and to stabilization mechanisms. *Soil Biol. Biochem.* 39, 2183–2207.
- Wan, J., Tyliszczak, T., Tokunaga, T.K., 2007. Organic carbon distribution, speciation, and elemental correlations within soil microaggregates: applications of STXM and NEXAFS spectroscopy. *Geochim. Cosmochim. Acta* 71, 5439–5449.
- Wang, A., Freeman, J.J., Jolliff, B.L., Chou, I.M., 2006. Sulfates on Mars: a systematic Raman spectroscopic study of hydration states of magnesium sulfates. *Geochim. Cosmochim. Acta* 70, 6118–6135.
- Wang, C.-J., Li, Z., Jiang, W.-T., Jean, J.-S., Liu, C.-C., 2010. Cation exchange interaction between antibiotic ciprofloxacin and montmorillonite. *J. Hazard. Mater.* 183, 309–314.
- Wang, C.J., Li, Z., Jiang, W.T., 2011. Adsorption of ciprofloxacin on 2:1 dioctahedral clay minerals. *Appl. Clay Sci.* 53, 723–728.
- Wang, H., Hollywood, K., Jarvis, R.M., Lloyd, J.R., Goodacre, R., 2010. Phenotypic characterization of *Shewanella oneidensis* MR-1 under aerobic and anaerobic growth conditions by using Fourier transform infrared spectroscopy and high-performance liquid chromatography analyses. *Appl. Environ. Microbiol.* 76, 6266–6276.
- Wang, S., Mulligan, C.N., 2008. Speciation and surface structure of inorganic arsenic in solid phases: a review. *Environ. Int.* 34, 867–879.
- Wang, S.L., Johnston, C.T., 2000. Assignment of the structural OH stretching bands of gibbsite. *Am. Mineral.* 85, 739–744.
- Wang, Y.S., Muramatsu, A., Sugimoto, T., 1998. FTIR analysis of well-defined α - Fe_2O_3 particles. *Colloids Surf. A Physicochem. Eng. Aspects* 134, 281–297.
- Watanabe, A., Kawasaki, S., Kitamura, S., Yoshida, S., 2007. Temporal changes in humic acids in cultivated soils with continuous manure application. *Soil. Sci. Plant Nutr.* 53, 535–544.
- Weisz, A.D., Regazzoni, A.E., Blesa, M.A., 2001. ATR-FTIR study of the stability trends of carboxylate complexes formed on the surface of titanium dioxide particles immersed in water. *Solid State Ionics* 143, 125–130.

- Weisz, A.D., Rodenas, L.G., Morando, P.J., Regazzoni, A.E., Blesa, M.A., 2002. FTIR study of the adsorption of single pollutants and mixtures of pollutants onto titanium dioxide in water: oxalic and salicylic acids. *Catal. Today* 76, 103–112.
- Wershaw, R.L., Leenheer, J.A., Kennedy, K.R., Noyes, T.I., 1996. Use of ^{13}C NMR and FTIR for elucidation of degradation pathways during natural litter decomposition and composting I. Early stage leaf degradation. *Soil Sci.* 161, 667–679.
- Whitbread, A., 1994. Soil organic matter: its fractionation and role in soil structure. In: Lefroy, R., Blair, G., Craswell, E. (Eds.), *Soil Organic Matter Management for Sustainable Agriculture*, vol. 56. ACIAR, Canberra, pp. 124–130 (ACT, Ubon, Thailand).
- Wilkinson, T.J., Perry, D., McKinney, M., Martin, M.Z., 2002. Physics and forensics. In: *Physics World*, Vol. 15, pp. 43–46.
- Wingender, J., Neu, T.R., Flemming, H.C., 1999. What are bacterial extracellular polymeric substances? In: Wingender, J., Neu, T.R., Flemming, H.C. (Eds.), *Microbial Extracellular Polymeric Substances: Characterization, Structure, and Function*. Springer, Berlin, pp. 1–15.
- Wingender, J., Strathmann, M., Rode, A., Leis, A., Flemming, H.-C., 2001. Isolation and biochemical characterization of extracellular polymeric substances from *Pseudomonas aeruginosa*. In: Doyle, R.J. (Ed.), *Microbial Growth in Biofilms, Part A: development and molecular biological aspects*, vol. 336. Academic Press, New York, pp. 303–314.
- Wijnja, H., Schulthess, C.P., 1999. ATR-FTIR and DRIFT spectroscopy of carbonate species at the aged gamma- Al_2O_3 /water interface. *Spectrochimica Acta Part a-Molecular and Biomolecular Spectroscopy* 55, 861–872.
- Wijnja, H., Schulthess, C.P., 2001. Carbonate adsorption mechanism on goethite studied with ATR-FTIR, DRIFT, and proton coadsorption measurements. *Soil Science Society of America Journal* 65, 324–330.
- Wiseman, C.L.S., Püttmann, W., 2006. Interactions between mineral phases in the preservation of soil organic matter. *Geoderma* 134, 109–118.
- Wolf, E.E., Yuh, S.J., 1984. Kinetic and FTIR studies of steam gasification of coal chars catalyzed by alkali salts. *Abstr. Pap. Am. Chem. Soc.* 187, 43. FUEL.
- Woodwell, G.M., 1984. The Role of Terrestrial Vegetation in the Global Carbon Cycle: Measurement by Remote Sensing. Published on behalf of the Scientific Committee on Problems of the Environment (SCOPE) of the International Council of Scientific Unions (ICSU) by Wiley, New York.
- Wu, H., Yip, K., Tian, F., Xie, Z., Li, C.-Z., 2009. Evolution of char structure during the steam gasification of biochars produced from the pyrolysis of various Mallee biomass components. *Ind. Eng. Chem. Res.* 48, 10431–10438.
- Wu, Q., Li, Z., Hong, H., Yin, K., Tie, L., 2010. Adsorption and intercalation of ciprofloxacin on montmorillonite. *Appl. Clay Sci.* 50, 204–211.
- Wu, S.H., Goyne, K.W., Lerch, R.N., Lin, C.-H., 2011. Adsorption of isoxaflutole degradates to aluminum and iron hydrous oxides. *J. Environ. Qual.* 40, 528–537.
- Wu, Q., Li, Z., Hong, H., 2013a. Adsorption of the quinolone antibiotic nalidixic acid onto montmorillonite and kaolinite. *Applied Clay Science* 74, 66–73.
- Wu, Q., Li, Z., Hong, H., Li, R., Jiang, W.-T., 2013b. Desorption of ciprofloxacin from clay mineral surfaces. *Water Res.* 47, 259–268.
- Wullschlegel, S.D., Martin, M.Z., Vo-Dinh, T., Griffin, G.D., Stokes, D.L., Wintenberg, A.L., 2003. *Advanced Instrumentation for In Situ Field Monitoring of Soil Carbon Sequestration*. Oak Ridge National Laboratory.
- Xie, C., Li, Y.-q., 2003. Confocal micro-Raman spectroscopy of single biological cells using optical trapping and shifted excitation difference techniques. *J. Appl. Phys.* 93, 2982–2986.
- Yan, W., Hu, S., Jing, C., 2012. Enrofloxacin sorption on smectite clays: effects of pH, cations, and humic acid. *J. Colloid Interface Sci.* 372, 141–147.

- Yang, X.M., Xie, H.T., Drury, C.F., Reynolds, W.D., Yang, J.Y., Zhang, X.D., 2012. Determination of organic carbon and nitrogen in particulate organic matter and particle size fractions of Brookston clay loam soil using infrared spectroscopy. *Eur. J. Soil Sci.* 63, 177–188.
- Yang, Y.-h., Li, B.-n., Tao, Z.-y., 1994. Characterization of humic substances by laser Raman spectroscopy. *Spectrosc. Lett.* 27, 649–660.
- Yang, Y.-h., Wang, T., 1997. Fourier transform Raman spectroscopic characterization of humic substances. *Vib. Spectrosc.* 14, 105–112.
- Yang, Y., Chase, H.A., 1998. Applications of Raman and surface-enhanced Raman scattering techniques to humic substances. *Spectrosc. Lett.* 31, 821–848.
- Yoon, T.H., Johnson, S.B., Musgrave, C.B., Brown, G.E., 2004a. Adsorption of organic matter at mineral/water interfaces: I. ATR-FTIR spectroscopic and quantum chemical study of oxalate adsorbed at boehmite/water and corundum/water interfaces. *Geochim. Cosmochim. Acta* 68, 4505–4518.
- Yoon, T.H., Johnson, S.B., Brown, G.E., 2004b. Adsorption of Suwannee River fulvic acid on aluminum oxyhydroxide surfaces: An in situ ATR-FTIR study. *Langmuir* 20, 5655–5658.
- Yu, C., Irudayaraj, J., 2005. Spectroscopic characterization of microorganisms by Fourier transform infrared microspectroscopy. *Biopolymers* 77, 368–377.
- Zhang, J., Dai, J., Wang, R., Li, F., Wang, W., 2009. Adsorption and desorption of divalent mercury (Hg^{2+}) on humic acids and fulvic acids extracted from typical soils in China. *Colloids Surf. A Physicochem. Eng. Aspects* 335, 194–201.
- Zhao, J., Peng, P.A., Song, J., Ma, S., Sheng, G., Fu, J., 2011. Characterization of macromolecular organic matter in atmospheric dust from Guangzhou, China. *Atmos. Environ.* 45, 5612–5620.
- Zhao, W., Liu, F., Feng, X., Tan, W., Qiu, G., Chen, X., 2012a. Fourier transform infrared spectroscopy study of acid birnessites before and after Pb^{2+} adsorption. *Clay Miner.* 47, 191–204.
- Zhao, Y., Gu, X., Gao, S., Geng, J., Wang, X., 2012b. Adsorption of tetracycline (TC) onto montmorillonite: cations and humic acid effects. *Geoderma* 183, 12–18.
- Zheng, L., Lee, W.S., Li, M., Katti, A., Yang, C., Li, H., Sun, H., 2012. Analysis of Soil Phosphorus Concentration Based on Raman Spectroscopy. 852718–852718.
- Zhou, Y., Li, Y., 2004. Studies of interaction between poly(allylamine hydrochloride) and double helix DNA by spectral methods. *Biophys. Chem.* 107, 273–281.
- Zimba, C.G., Hallmark, V.M., Swalen, J.D., Rabolt, J.F., 1987. Fourier-transform Raman-spectroscopy of long-chain molecules containing strongly absorbing chromophores. *Appl. Spectrosc.* 41, 721–726.
- Zimmerman, A.R., Gao, B., Ahn, M.-Y., 2011. Positive and negative carbon mineralization priming effects among a variety of biochar-amended soils. *Soil Biol. Biochem.* 43, 1169–1179.



Water-Saving Innovations in Chinese Agriculture

Qiang Chai^{*,‡,1}, Yantai Gan^{†,1}, Neil C. Turner[¶], Ren-Zhi Zhang^{*,‡}, Chao Yang[†], Yining Niu^{*,‡} and Kadambot H.M. Siddique[¶]

*Gansu Provincial Key Laboratory for Aridland Crop Sciences, Gansu Agricultural University, Lanzhou, Gansu, P.R. China

†Semi-arid Prairie Agricultural Research Centre, Agriculture and Agri-Food Canada, Swift Current, SK, Canada

‡College of Agronomy, Gansu Agricultural University, Lanzhou, Gansu, P.R. China

¶The UWA Institute of Agriculture, The University of Western Australia, Crawley, WA, Australia

‡College of Resources and Environments, Gansu Agricultural University, Lanzhou, Gansu, P.R. China

¹Corresponding authors: e-mail address: Gan@agr.gc.ca; chaiq@gsau.edu.cn

Contents

1. Introduction	151
1.1 Water Availability and Food Security	151
1.2 Water Shortage in Northern China	152
1.3 Agriculture in Northwest China	152
1.4 Objectives	155
2. Framework of Water-Saving Agriculture	155
2.1 Definition of Water-Saving Agriculture	155
2.2 Quantification of Crop Water Use	156
2.2.1 <i>Evapotranspiration</i>	156
2.2.2 <i>Crop Water Requirement</i>	157
2.2.3 <i>Soil Water Balance</i>	158
2.2.4 <i>Water-Use Efficiency</i>	159
2.2.5 <i>Water Footprint</i>	160
2.3 Thinking at the System Level	161
2.4 Case Studies	162
3. Water-Resource Management	162
3.1 Basic Rules and Regulations	163
3.2 Water Users' Associations and Villagers' Committees	164
3.3 Water-Use Rights	165
3.4 Water Prices and Water-Use Fees	166
3.5 Education, Training, and Coordination	168
3.6 Off-Farm Employment	169
4. Water-Saving Cropping Practices	169
4.1 Crop Responses to Water Deficits	169
4.2 Interaction of Water Use and Nutrient Availability	171
4.3 No-Till and Subsoiling	172

4.4	Mulching	173
4.4.1	<i>Ridge–Furrow Plastic Mulching</i>	173
4.4.2	<i>Straw Mulching</i>	176
4.4.3	<i>Gravel–Sand Mulching</i>	179
4.5	Regulated Deficit Irrigation	181
4.6	Chemical Regulation	183
5.	Water-Saving Engineering Systems	184
5.1	Land Leveling, Terracing, and Contour Farming	184
5.2	Rainwater Catchments	184
5.3	Improvement of Irrigation Canals	187
5.4	Spray Irrigation, Drip Irrigation, and Subsurface Drip Irrigation	188
5.5	Fertigation	189
5.6	“She-Shi Agriculture - 设施农业”	190
6.	Challenges and Opportunities in Water-Saving Agriculture	192
7.	Conclusions	193
	Acknowledgments	195
	References	195

Abstract

Water scarcity, water pollution, and water-related waste threaten humanity globally, largely due to the limited supply of freshwater on the planet, the unbalanced distribution of water resources, and the excessive consumption of water from the growing population and its economic development. China is facing severe water shortages; the northern part of the country has an average freshwater availability of 760 cubic meter per capita per year, 25% below the internationally accepted threshold for water scarcity. Agriculture in northwest China relies on annual precipitation of 50–500 mm, 70% of which occurs from July to September, and annual evaporation from 1500 to 2600 mm. In the Hexi Corridor regions where annual precipitation is below 150 mm, farming largely depends on irrigation with water from Qilian Mountain snowmelt. However, permanent snow on the mountain has moved upwards at a rate of 0.2–1.0 m annually, and groundwater in the valley has declined at a rate of 0.5–1.8 m year⁻¹. Consequently, some natural oases, along the old Silk Road, have shrunk or disappeared and wells have dried up. At the meantime, some farms use irrigation water at a rate as high as 11,000 m³ ha⁻¹, much greater than crop water requirements for high yield. In recent years, many innovative research projects have dealt with the water issue in arid and semiarid northwestern China. In this chapter, we summarize some key water-saving technologies developed from some of these recently completed research projects, and discuss integrated and innovative approaches for the development of water-saving agricultural systems. Our goal is to encourage the use of innovative water-saving technologies to reduce agricultural water use, increase crop water-use efficiency, and improve agricultural productivity.



1. INTRODUCTION

1.1 Water Availability and Food Security

Water is the most abundant compound on the planet with about 70% of the earth's surface covered by water (Siddique, 2004), but only about 2.5% of the earth's water supply is freshwater (Turner, 2001; Gleick and Palaniappan, 2010). A large proportion of the freshwater is trapped in glaciers, permanent snow or deep groundwater, with only about 0.26% available for human consumption (Sivakumar, 2011). We drink on average 4l of water per day, in one form or another, but the food we consume each day requires 2000l of water to produce. Today roughly 40% of the world grain harvest comes from irrigated land. During the last half of the twentieth century, the world's irrigated area had expanded from close to 100 million ha in 1950 to roughly 700 million ha in 2000. However, the growth in irrigation has come to a near standstill, expanding only 10% between 2000 and 2010.

Overpumping of aquifers has put water-based food production systems under severe pressure. The countries currently overpumping their aquifers include the world's three biggest agricultural producers—China, India, and the United States. The world's second largest economy, China, has water resources of about 2200 cubic meter per capita, one-quarter of the world's average (Liu, 2006), and is one of the 13 countries classified as lacking adequate water resources (Geng et al., 2010). However, China produces 80% of its food on irrigated farmland (Zhang et al., 2006). In the recent two decades, the availability of water resources (surface water and groundwater) in China has declined rapidly, approaching the internationally accepted threshold of water stress of $1700\text{ m}^3\text{ person}^{-1}\text{ year}^{-1}$. Over the next 20 years, the water available for agricultural use in China will exhibit zero or even negative growth (Liu, 2006). Irrigation has played a crucial role in producing sufficient food for China's 1.3 billion people and ensuring its food security. However, water shortage is becoming a bottleneck for the future food security of China. Also, rapid urbanization is causing severe conflict between industrial and agricultural uses of water. As a result, the allocation of freshwater resources to agriculture may need to be reduced in order to ensure the freshwater needs of other sectors of the growing economy. Therefore, the development of water-saving strategies and technologies to decrease water consumption and increase water-use efficiency (WUE) in crop production is a major goal of China's agriculture.

1.2 Water Shortage in Northern China

In northern China, the water shortage is more severe than the rest of the country, with freshwater availability about 760 cubic meter per capita per year, 25% below the internationally accepted thresholds of water scarcity (Shalizi, 2006). Dominated by a continental monsoon climate, annual precipitation varies from 500 mm in the northeast decreasing to as little as 50 mm in the northwest (Figure 2.1(A)). About 70% of annual precipitation is from July to September, often in the form of heavy and sudden storms. Annual potential evaporation ranges from 1500 to 2600 mm (Deng et al., 2006). In the Hexi Corridor of Gansu Province (Figure 2.1(B)), the major source of water for all sectors originates from the accumulation of snow in the Qilian Mountain in winter, with summer snowmelt feeding the rivers and groundwater in the valleys and providing a source of water for drinking and for crop irrigation in so-called oasis agriculture. In the last two decades, the measurable snow level on the Qilian Mountain has moved upwards at a rate of 0.2–1.0 m annually (Che and Li, 2005), whereas the underground water table in the valleys supplied by water from the mountains has persistently fallen and the availability of groundwater has declined substantially. In the Zhangye district of Gansu Province (Figure 2.1(B)), the number of wells constructed for the exploitation of groundwater has increased exponentially, while the depth of the underground water table has declined at a rate of 1.84 m year⁻¹ in recent decades (Figure 2.2(A)). The overexploitation of groundwater has caused some of the oases to shrink, wells to dry up, with little water to flow into reservoirs. Consequently, some natural oases, along the old Silk Road, are gradually disappearing. It is expected that the quantity of water available for economic development will unavoidably decrease in the near future if the deteriorating situation cannot be mitigated.

1.3 Agriculture in Northwest China

In northwest China, the total water resources available for agricultural use averages 530 m³ ha⁻¹, far less than the national average 2800 m³ ha⁻¹. Limited water resources are causing desertification with an estimated 1.6 million ha farmland being challenged by sand dunes (Figure 2.2(B)). Desertification has rapidly expanded in recent years with some farm families losing their land and stopping farming. However, in many towns and villages, gross irrigation amounts used for field crops have been substantially higher than the amounts of water crops require for normal production. Calculated from the outflow of wells and river gates, gross irrigation water used is 7500 m³ ha⁻¹ in the Hexi Corridor of Gansu Province, 10,980 m³ ha⁻¹ in the Huangshui

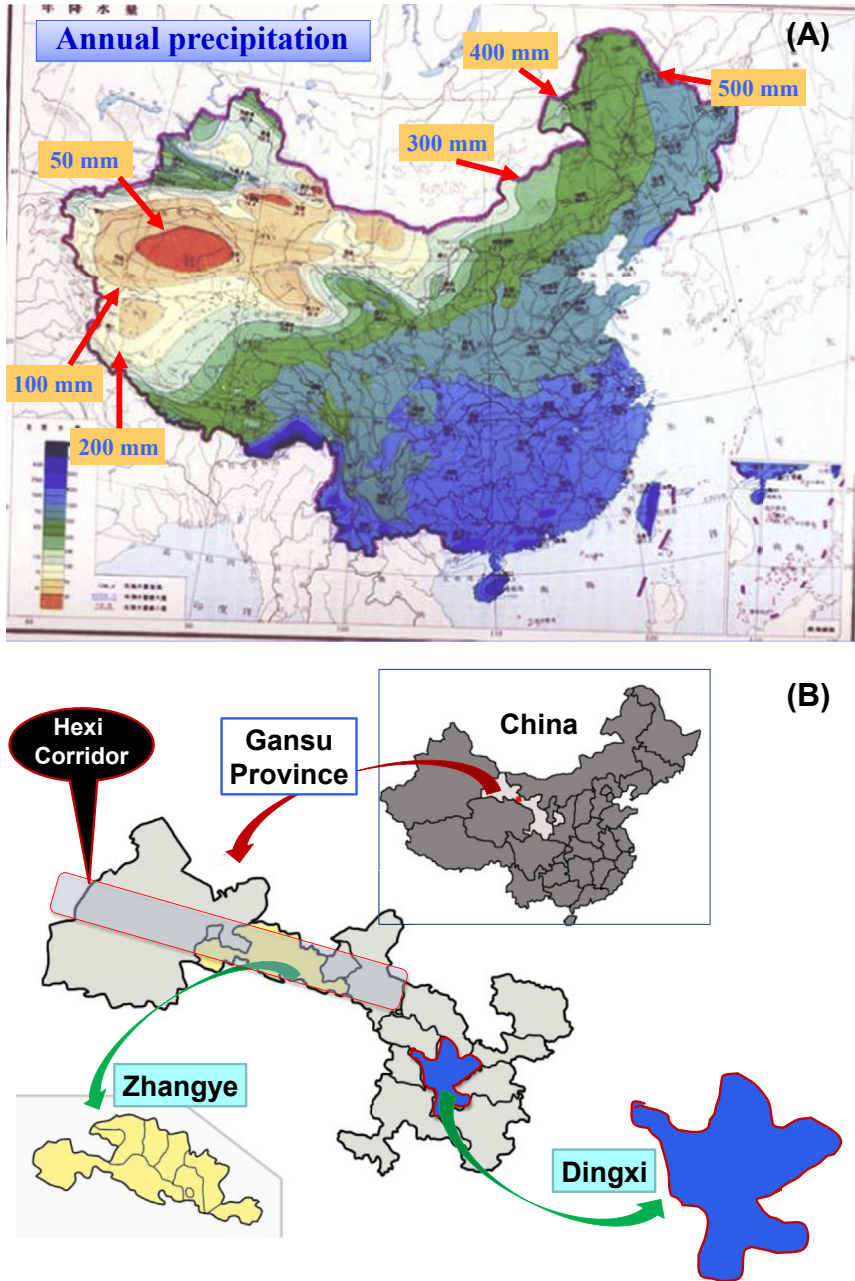


Figure 2.1 (A) Map showing annual precipitation in China highlighting the annual precipitation from 500 mm in the northeast to 50 mm in the northwest, and (B) the location of the Zhangye (representing a typical irrigated area) and Dingxi (representing a typical rainfed area) districts in Gansu Province, China. (For color version of this figure, the reader is referred to the online version of this book.)

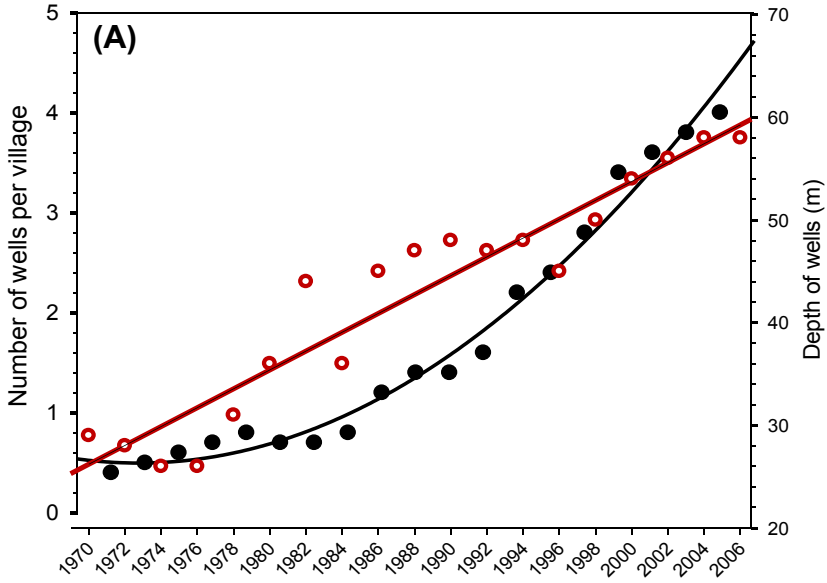


Figure 2.2 Overexploitation of groundwater and overuse of water resources have caused serious water-related problems, as shown by (A) the increasing number of wells and depth of the groundwater table from 1970 to 2006 in Zhangye (*modified from Zhang et al. (2007)*), and (B) moving sand dunes at the edge of an oasis along the old Silk Road. (For color version of this figure, the reader is referred to the online version of this book.)

area of Qinghai Province, $11,300\text{ m}^3\text{ ha}^{-1}$ in the Hetao area of Ningxia Province, and $14,500\text{ m}^3\text{ ha}^{-1}$ in the northern area of Xingjiang Province (Zhang et al., 2005). About half of the irrigation water is lost during transfer from the rivers and wells to the fields. The average WUE of major irrigated grain crops in northwest China is $0.8\text{ kg ha}^{-1}\text{ mm}^{-1}$, much lower than the $1.5\text{--}2.6\text{ kg ha}^{-1}\text{ mm}^{-1}$ for the same crops grown in the Yangling areas of Shaanxi Province where water-saving technologies have been adopted (Zhang et al., 2005). Some field experiments show that in northwest China, $3900\text{ m}^3\text{ ha}^{-1}$ of irrigation water is sufficient to meet the requirements of spring wheat with a grain yield of 7.5 ton ha^{-1} . Thus, there is huge opportunity to develop water-saving agriculture in northwest China.

1.4 Objectives

In this chapter, we summarize some of the key water-saving technologies that have been developed from recently completed research projects in arid and semiarid northwestern China, and discuss integrated and innovative approaches for the development of water-saving agricultural systems for this region. Our overall goal is to use an all-embracing approach with the innovative water-saving technologies to decrease agricultural water use, increase WUE, and maintain or increase crop productivity. We focus our discussion on four aspects: (1) a framework of water-saving agriculture; (2) water-resource management; (3) water-saving practices; and (4) water-saving engineering solutions with an emphasis on crop productivity.



2. FRAMEWORK OF WATER-SAVING AGRICULTURE

2.1 Definition of Water-Saving Agriculture

The definition of water-saving agriculture varies within the scientific literature (Belder et al., 2004; Deng et al., 2006; Li et al., 2008; Luo, 2010; Wang et al., 2002, 2010; Zhou et al., 2011). Some published work from China concentrates on the use of improved farming practices to increase water productivity in irrigated areas and increase precipitation use efficiency (PUE) in dryland areas, while others focus on approaches to raise the water utilization rate and WUE by increasing crop yield and maximizing water use and its efficiency. Other studies have examined the opportunity of utilizing engineering facilities to catch and preserve more rainwater and make it available for agriculture. Those previous studies have provided some essential concepts for agricultural activities to take full advantage of natural rainfall and irrigation resources. However, there is a lack of understanding

of water-saving agriculture at a system level. In this review, we define water-saving agriculture as the “systematic management of natural precipitation and water resources, allocation and application of consumable water to meet the need of agricultural activities, and use of precipitation and irrigation in an effective, efficient and economic manner”. We consider that water-saving agriculture is not a simple saving exercise, but rather a comprehensive management system at regional, local, and farm–field levels.

2.2 Quantification of Crop Water Use

When searching for water-saving strategies and practices for agriculture, one needs to determine the relationship between water availability, water consumption by a crop, and crop responses and performance. The terminology used in water-saving studies includes evapotranspiration (ET), crop water consumption, crop water productivity (CWP), WUE, and water footprint, among others.

2.2.1 Evapotranspiration

It is well known that evaporation and transpiration are the two processes occurring simultaneously in a soil–crop system (Turner et al., 2001). Evaporation from the soil is mainly determined by water availability in the topsoil and the fraction of solar radiation reaching the soil surface (Allen et al., 1998). When a crop is small, soil surface water is predominately lost by soil evaporation as a large proportion of the soil surface is exposed to solar radiation. As the crop canopy gradually closes with crop development, plant transpiration becomes the main process. ET is typically affected by several factors including the weather (radiation, air temperature, humidity, and wind speed), crop factors (crop type, variety, plant growth stage, plant density and ground cover, and crop rooting characteristics), and agronomic practices and environmental conditions (soil type, soil salinity, fertility level, plant diseases, and soil water content).

In water-saving research in northern China, ET is typically estimated using (1) small-scale field plot monitoring experiments (Jiang and Zhang, 2004), (2) large-scale or long-term field experiments (Sun et al., 2010), and (3) remote-sensing technology on a geographic scale (Li et al., 2008).

In the cases of (1) and (2), the crop reference ET is estimated using the Penman–Monteith equation (Allen et al., 1998), as follows:

$$ET_o = \frac{0.408 \Delta (R_n - G) + \gamma \frac{900}{T + 273} U_2 (e_s - e_a)}{\Delta + \gamma (1 + 0.34 U_2)} \quad (2.1)$$

Where ET_o is crop reference ET (mm day^{-1}), R_n is net radiation at the crop surface ($\text{MJ m}^{-2} \text{day}^{-1}$), G is soil heat flux density ($\text{MJ m}^{-2} \text{day}^{-1}$), T is air temperature at 2 m height ($^{\circ}\text{C}$), u_2 is the wind speed at 2 m height (m s^{-1}), e_s is saturation vapor pressure (kPa), e_a is actual vapor pressure (kPa), $e_s - e_a$ is saturation vapor pressure deficit (kPa), Δ is slope vapor pressure curve ($\text{kPa } ^{\circ}\text{C}^{-1}$), and γ is the psychrometric constant ($\text{kPa } ^{\circ}\text{C}^{-1}$).

ET is expressed in millimeters per unit time. For example, an ET of one millimeter per day from a crop is equal to a loss of $10 \text{ m}^3 \text{ ha}^{-1} \text{ day}^{-1}$. The reference ET is estimated for a hypothetical short-grass reference surface and provides a standard with which ET can be compared for different periods of the year, different regions, or different crop species (Allen et al., 1998).

We noted that several authors also use “potential ET” in their water-saving studies, instead of crop reference ET. Nevertheless, ET estimated from small-plot experiments may not be reliable over large geographic areas due to spatial variation in rainfall, soil texture, crop management practices and climatic variation. With today’s modern technology of remote sensing, some researchers have used remote-sensing data to estimate ET in water-saving research (Li et al., 2008; Xiong et al., 2006). Of the models available for estimating ET on a geographic scale, the “Surface Energy Balance Algorithm for Land” (SEBAL) model originated from Wageningen University (Bastiaanssen et al., 2005), is one of the best. Using satellite data as inputs, the SEBAL model can quantify the energy balance to estimate aspects of the hydrological cycle. Land surface characteristics, such as surface albedo, leaf area index, vegetation index, and surface temperature are derived from satellite imagery. Using a time series of satellite and meteorological data, ET can be calculated on a daily, weekly, monthly, or yearly basis (Li et al., 2008). Several Chinese researchers in the field of water-saving agriculture found that daily ET estimation by the SEBAL model is effective and efficient with an estimation error ranging from 4% to 15% (Li et al., 2008; Xiong et al., 2006).

2.2.2 Crop Water Requirement

Research focusing on water-saving agriculture has recently emphasized the use of “crop water requirement”, (CWR) aiming at supplying a precise amount of water to a crop based on crop needs. CWR refers to the amount of water required to compensate for ET losses from a crop field during a specified period of time. CWR can be expressed in millimeters per day, per month, or per season; these can be used for management purposes in estimating irrigation water requirements, irrigation scheduling, and water delivery scheduling (Todorovic, 2005). In crop management

practices, CWR can be used as a guide to determine the balance between the amount of extractable soil water available for the crop and the amount of water needed to be supplied at a particular growth stage. In a wet soil, the water has a high potential energy, is relatively free to move and is easily taken up by plant roots. In a dry soil, however, the water is bound by capillary and absorptive forces to the soil matrix, and is less easily extracted by crop plants. When the potential energy of the soil water decreases to a threshold value (usually, the lower limit of plant extractable soil water), the crop is unable to extract the water from the soil and becomes water stressed. Thus, the CWR of a particular crop at a particular growth stage can be estimated by multiplying the crop coefficient with the crop reference ET, as follows:

$$\text{CWR} = K_s K_c \text{ET}_o \quad (2.2)$$

where CWR is under water stress, K_s describes the effect of water stress on crop transpiration (K_s is <1 under soil water-limiting conditions, with evaporation from soil not a large component of ET), K_c is the crop coefficient which can be estimated using a “crop coefficient curve” developed for different crop species, and ET_o is the crop reference ET calculated using Eqn (2.1) above.

The amount of irrigation water needed by a crop is roughly the difference between CWR and precipitation on a weekly or monthly basis.

$$\text{IW} = \text{CWR} - P_r \quad (2.3)$$

where IW is irrigation water required and P_r is precipitation during the given period (weekly or monthly).

2.2.3 Soil Water Balance

The soil water content in the rooting zone changes with losses and gains of water. Rainfall, irrigation, and capillary rise of groundwater add water to the root zone, whereas soil evaporation, crop transpiration and deep drainage remove water from the root zone. Therefore, in water-saving research, ET can be estimated using the soil water balance equation for the growing season or individual growth periods, as follows:

$$\text{ET} = P_r + I_r + \Delta S + W_g - D - R \quad (2.4)$$

where P_r is precipitation, I_r is irrigation water, ΔS is the change in soil water content over the measured soil depth during the growth period, W_g is water

used by crops through capillary rise from groundwater, D is deep drainage below the root zone, and R is surface runoff (all in millimeters).

Water-saving research in northwestern China's arid and semiarid environments is usually based in regions where the groundwater table is at least 4–5 m below the surface, thus, the capillary rise (W_g) is usually negligible. Also, runoff is usually considered negligible in irrigated areas where the land is typically level (Jin et al., 2007; Mu et al., in press; Xie et al., 2005), but as discussed later, runoff from sloping land in rainfed areas can be substantial during intense rainfall events. During the crop growing season, ΔS is the soil water content of the entire rooting zone measured at harvest minus the soil water content over the same depth at sowing (depending on rainfall, irrigation and ET, the value may be positive or negative). The gravimetric soil moisture content at sowing and at harvest is converted to volumetric units (mm) using the bulk density of the soil measured for each depth. In most arid and semiarid environments, deep drainage (D) is negligible in rainfed systems, but it can be substantial in irrigated systems. Deep drainage is estimated using a recharge coefficient (α) multiplied by the amount of irrigation (I_r) and effective rainfall (P_r), as shown by Sun et al. (2010):

$$D = \alpha (P_r + I_r) \quad (2.5)$$

where α changes with soil texture, soil conditions, crop management, and irrigation method and quantity.

2.2.4 Water-Use Efficiency

WUE is typically calculated using the formula:

$$\text{WUE} = Y/\text{ET} \quad (2.6)$$

where Y can be (1) economic yield in kg ha^{-1} (e.g., grain yield in cereals, seed yield in legumes, tuber yield in potatoes and root crops, and leaf yield in vegetables), (2) biomass yield in kg ha^{-1} , or (3) energy yield (MJ ha^{-1}) (Chai et al., 2014), depending on the nature of the study. In all cases, the denominator ET (mm) is the total actual ET determined using Eqn (2.4) above. Therefore, the unit of WUE is typically in $\text{kg ha}^{-1} \text{mm}^{-1}$.

In some cases, the term PUE (Turner, 2011; Gan et al., 2013) or irrigation water-use efficiency (WUE_i) (Sun et al., 2010) are used to describe the efficiency of precipitation during the growing season or the amount of irrigation applied to the crop, respectively.

For PUE, the denominator in Eqn (2.6) changes to the amount of precipitation (mm) as snow or rain received during the cropping season, whereas WUE_i is usually defined as follows:

$$WUE_i = \frac{(Y_i - Y_d)}{I_r} \quad (2.7)$$

where Y_i is crop yield with irrigation and Y_d is crop yield without irrigation or an equivalent rainfed plot, and I_r is the amount of irrigation water applied (Sun et al., 2010). The unit of WUE_i is in $\text{kg ha}^{-1} \text{mm}^{-1}$.

CWP is an alternative term that has been used for WUE by some researchers, and is defined as follows:

$$CWP = \frac{Y}{10 \text{ ET}} \quad (2.8)$$

where CWP has a unit of kg m^{-3} , Y is the grain yield (kg ha^{-1}) and ET is total ET over the entire growing season (mm) estimated using Eqn (2.4) above. Because one hectare is $10,000 \text{ m}^2$, then 1 mm (0.001 m) of ET from 1 ha of cropped land equates to 10 m^3 . Thus, the ET denominator is multiplied by 10 to obtain the CWP in kg m^{-3} .

2.2.5 Water Footprint

Water footprint is one of the newest indicators used to quantify water use associated with the production of a particular product. By definition, the water footprint of a product is the volume of freshwater appropriated to produce the product, taking into account the volumes of water consumed and polluted in the different steps of the supply chain. Water footprint analysis not only determines water consumption and scarcity, but also reflect the embodied or virtual water in imports and exports (Dong et al., 2013). The concept of the water footprint may also help policy makers make rational policies for water-resources management.

Despite the importance of this new measure for water use, the application of water footprint in water-saving agriculture in China is still in its early stages, and there is limited information available on how to determine the water footprint for agricultural products in northwest China. Cai et al. (2012) used a regional input-output model to calculate the water footprint in Gansu Province and found a reduction in agricultural water use at the regional level is a key measure for lowering the water footprint of agricultural products. Zeng et al. (2012) studied the water footprint within the

Heihe River Basin of northwest China and found that agricultural production was the largest water consumer, accounting for 96% of the water footprint (92% for crop production and 4% for livestock), and the remaining 4% was for industrial and domestic sectors. The assessment of the water footprint of agricultural production considers both the “green” water component (i.e., water conserved in the soil) and the “blue” water component (i.e., surface water and groundwater). An interesting finding from the study of [Zeng et al. \(2012\)](#) was that the percent “green” water component was larger than the “blue” water component in the agriculture production of the Heihe River Basin. These results indicate that strategies and practices for soil water conservation and use of “green” water in soils will be the key to lowering the water footprint for crop production and achieving more sustainable water use in arid and semiarid northwest China.

2.3 Thinking at the System Level

In this chapter, we consider the two major areas of water-saving in China: (1) in irrigated areas mainly focusing on water-resource management, the precise control of the quantity of irrigation water, and the use of improved farming practices and advanced engineering systems to match irrigation water supplies with the requirements of agricultural activities; and (2) in areas beyond the reach of any irrigation network, mainly focusing on the effective use of natural precipitation and the wise use of excessive precipitation by collection of rainwater and its application in various agricultural activities.

At the system level, the main components of water-saving agriculture include, but are not limited to the following:

1. Establishment of relevant laws, regulations, and policies for effective water-resource management taking into account factors affecting the quantity, quality, spatial and temporal distribution and necessary adjustment of water resources available to the target region, villages/towns, and individual households ([Section 3.1](#) below).
2. Establishment of environmentally friendly, efficient water-use farming practices to reduce water consumption, or improving PUE and WUE. The current focus is on reshaping the existing farming structure and improving cropping systems in line with the current distribution pattern of water resources ([Section 4](#)).
3. Development of advanced and practically feasible engineering facilities—including rainwater catchments, irrigation water canals, channels,

ditches, cisterns, and wells—to collect, store, transport, and control rain-water/irrigation, reduce water leakage, and evaporation from storage facilities and during transport (Section 5).

4. Development or adoption of suitable equipment, instrumentation and facilities for the measurement, allocation, quantity control, and distribution of irrigation water (Sections 3.2–3.4).
5. Establishment of research, development and education teams to teach/demonstrate successful water-saving practices to end users (Section 3.5).
6. Engagement of regional and local governments, water-use associations, and individual farmers in water-saving campaigns. This may involve a variety of factors, including relevant social and political factors (Sections 3.1–3.4).

2.4 Case Studies

In this chapter, we periodically use two case studies to highlight/demonstrate how some of the water-saving agricultural approaches have been used effectively and efficiently in Chinese agriculture. One case study is from the Zhangye district (Figure 2.1(B)), a typical oasis area in the Hexi Corridor with all industries heavily reliant on irrigation water from the Qilian Mountain snowmelt. The other case study is from Dingxi (Figure 2.1(B)), a typical rainfed agricultural area of northwestern China without irrigation, located at the western end of the Loess Plateau, one of the most fragile ecoregions in the world. In this region, it is not the amount of rainfall limiting crop production but rather the extreme variability in rainfall, with high rainfall intensities, few rain events, and poor spatial and temporal distribution of rainfall. The greatest untapped potential is to increase percent precipitation captured by the soil that is subsequently used for transpiration relative to percent precipitation lost by evaporation.



3. WATER-RESOURCE MANAGEMENT

In dealing with some of the key issues of water shortage in northwestern China, water-resource management is widely recognized as the top priority on the water-saving agenda. Using Zhangye (representing irrigated areas) and Dingxi (representing rainfed areas) as examples, some of the key measures that the Central Government of China and local authorities have undertaken for effective water-resource management are outlined below.

3.1 Basic Rules and Regulations

Lawmakers and the general public in northwestern China have recognized that strong support from the various levels of government through the establishment, implementation and enforcement of laws, regulations and policies is needed to establish effective water-resource management systems. In irrigated areas, many rules are now in place, guiding both the use of surface water and the exploitation of groundwater. Groundwater use is regulated, monitored and supervised. For example, in Zhangye, a single well and quantity-limited withdrawal system has been in place for a number of years for which a “withdrawal permission license” is required, so that lawmakers can monitor and control groundwater exploitation.

In addition, many engineering techniques have been combined with crop production technologies to legally save irrigation water. Guidelines have been established for water use by small-scale farmers vs large-scale agricultural enterprises; regions with primarily surface water vs those with underground water; production of staple food crops vs cash crops such as fruits and vegetables; field-scale farming vs greenhouse high-value cropping; and production systems with low water use and low income vs those with high income and high water consumption.

In general, these rules have been effective in controlling groundwater exploitation, the protection of groundwater resources and the prevention of land degradation. However, current water-resource management lacks detailed regulations for protecting groundwater quality, an important issue for its long-term sustainable use. No rules are in place for maintaining and protecting the water quality of the rivers and streams used for irrigation. In many villages and towns, groundwater pollution is a serious issue, which damages the eco-environment and affects drinking water quality. The main cause of groundwater pollution appears to be the low ratio of sewage disposal to water use, the lack of water treatment, and sewage recycling (Zhang et al., 2005). It has been suggested that a “law on water pollution” be established to minimize groundwater pollution and protect the groundwater environment. This is one of the most challenging areas to be tackled in water-saving agriculture in irrigated areas. One positive aspect, however, may be that sewage-contaminated groundwater, as opposed to contamination by industrial contaminants, may be considered a rich source of nutrients in agriculture, as human waste has long been used as a fertilizer in China.

3.2 Water Users' Associations and Villagers' Committees

In more recent years, with the development of water-resource management systems, government officials, farmer representatives and key marketers have joined together to form a Water Users' Association. Members can participate in relevant meetings providing advice and suggestions to the management team and, more importantly, engage in key actions of the management. In particular, the association is involved in the establishment of guidelines for allocating water quotas to various sectors/farms, decisions on water prices, and the supervision of trading of water rights among end users. The involvement of key stakeholders and end users in water-resource management has been beneficial in the adoption of water-saving technologies.

Farmers are the largest users of irrigation water. With their active participation in water-resource management, farmers move from being passive to active in water-saving actions. In Zhangye, the farmer members of the Water Users' Association are engaged in optimizing cropping systems to save water. They realize that different crop species require different amounts of water for growth, with cereals (namely wheat and maize) being the highest water-use crops in the area. Reducing the area sown to cereals has been an effective way to save water. At the same time, increasing the proportion of low water-use crops, such as sweet pepper (*Capsicum annuum*) and tomato (*Solanum lycopersicum*), has not only reduced total water use but also increased economic returns per unit of water used.

Another unique, informal and loosely managed organization is the villagers' committee found in some irrigated regions such as Zhangye. Villagers are often considered to be the best source of knowledge, especially when new opportunities arise such as choosing to implement a new policy initiative, introducing a high-value crop species, using new farming equipment or products, or practicing a water-saving measure. The villagers voluntarily form a villagers' committee for a particular area. Often, the active villagers communicate with the county water resources department and other local authorities to obtain new information and knowledge. Through informal meetings or direct visits to ordinary farmers, villagers' committee members intentionally or unintentionally express their concerns about a particular issue. For example, in many villages of the Zhangye district, the groundwater table has declined significantly over the past two decades, but most ordinary farmers have paid little attention to it. In fact, farmers may increase irrigation with high-value crops, drill deeper wells to reach the declining groundwater table, and only reduce water use if water prices increase.

The influence of the villagers' committee has been to motivate farmers to change their behavior and adopt various water-saving measures.

These observations suggest that the villagers' committee can stimulate behavioral change for the entire village community. In rural China, especially in the northwest, villages and towns are a crucial community for socioeconomic development for the region, and thus we consider that villagers' committees will play a crucial role in influencing farmers' actions for water-saving measures and promoting overall economic development.

3.3 Water-Use Rights

Water-use rights have been considered critical for controlling total amounts and efficiency of water used. In northwest China, it is typical that local government considers the total available water resources for the region as a total water right, and then allocates individual rights to subgovernment agencies and different industries. Industries and sectors request water rights based on their estimated total water requirements, and the decision makers allocate water rights to match these requirements. In most cases, however, the total water requirements are more than the amounts allocated due to water shortages. As a result, some industry projects and cropping structures need to be adjusted.

Usually, water rights are hierarchically allocated to villages and towns, and water quotas are then assigned to each individual farmer on the basis of the cultivated land. The water quota is determined on the basis of the cropping systems and the area sown to designated crop species allowed by the local government. Crop species sown without a government agreement or prearrangement may be rejected for a water right. In such cases, farmers are encouraged to trade their water rights between farmers or between farmers and the government, under the supervision of the Water Users' Association. However, trading of a water right is not common in many cases due to concerns about legal, administrative, and fiscal issues associated with such trades (Zhang, 2007a).

The precise measurement of the quantity of water is essential for controlling water allocation and clarifying water rights. In a large, state-funded water-saving project conducted in Zhangye (Zhang et al., 2005), equipment was developed to measure and control water amounts from the regional level near the water resource to field plots. Manually moveable water controllers are typically inserted into branch canals and field ditches delivering water directly to villages and towns. At field sites, portable water measurement

devices are usually used to control the amounts of water applied to each field. For surface water, farmers can meter the volumes of irrigation water according to the size of the section and the speed of water flow, whereas for groundwater, farmers measure the amounts of water by taking into account the conditions of the wells and the amount of electricity used. These types of water-control systems are easy to operate and provide a means of protection of the water rights of farmers.

At the regional level, intelligent decision-making systems are attached to the equipment near water sources and wells so that water flow can be cut automatically according to a predesignated flow system. In addition, computer-assisted systems have improved the precision and efficiency of water flow and allocation. In the irrigated areas of Hexi Corridor, the allocation of water resources and amounts has recently been related to economic outcomes. The production of high water-use crops, such as wheat, maize, and wheat-based intercropping systems (Figure 2.3(A)) has been restricted, whereas highly profitable plant species such as wolfberry or GouQi (*Lycium chinensis*, *Lycium barbarum*) (Figure 2.3(B)) have been given priority in the allocation of water rights. Whether or not this policy will be effective in saving water in the long term requires more research and confirmation.

3.4 Water Prices and Water-Use Fees

In the irrigated areas of northwest China, water prices have been established and a water-use fee is paid by each user. Water prices are designed to cover the cost of collection of fees by water officers, management of supply systems, and fees for service providers. In rainfed agricultural areas, the criteria for collecting a water-use fee is typically based on the balance between water prices paid by water users and the cost of maintaining water-conservation facilities. For the production of field crops, water prices are set per cubic meter. With the help of local authorities or villagers' committee members, farmers determine their total water-use fees based on their cropping systems and the amounts of water to be used.

Governmental officials and water managers generally believe that the current water price in many areas is lower than it should be. It has been suggested that doubling water prices is needed to recover the costs of the provision of water and to encourage water saving. However, despite the apparently low water prices, some farmers still consider that flooding their fields is expensive. The truth is that in most villages and towns, water fees are charged based on the water flow measured at the entrance of the branch water canals instead of the entrance to the fields. Due to

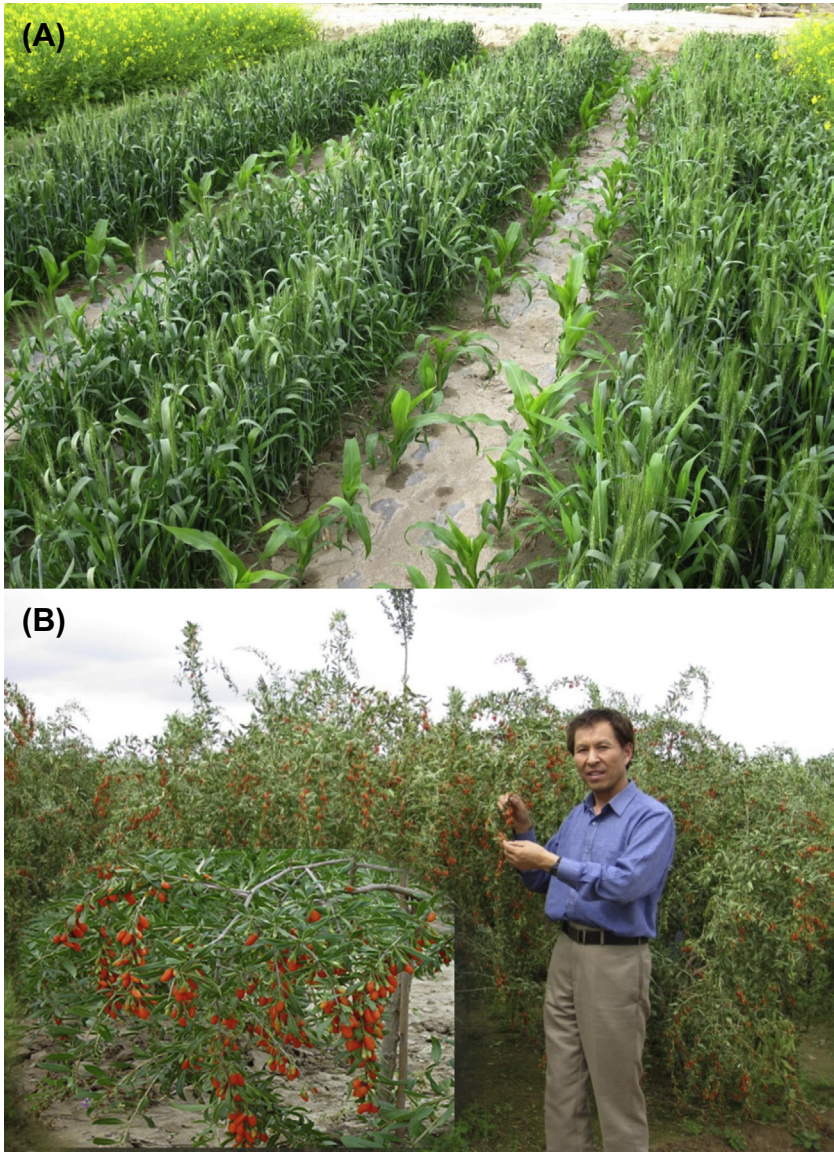


Figure 2.3 (A) A high water-use wheat and maize intercropping system with flood irrigation, and (B) a low water use high-value wolfberry or GouQi (*Lycium chinensis*, *Lycium barbarum*) crop with drip irrigation. (For color version of this figure, the reader is referred to the online version of this book.)

the low quality of the canal infrastructure, water losses are high between these two points. Therefore, the quantity of water a farmer receives on farmland is less than the quantity paid for. As a result, the fee per cubic meter of water measured at the entrance of the branch canal is actually much higher than the book value. Nevertheless, in our view, the regulation of water prices is of great importance for water-saving practices, and this needs to be further improved in the irrigation areas of north-west China.

3.5 Education, Training, and Coordination

In irrigated areas of northwest China, the willingness of farmers to adopt water-saving technologies and the effectiveness of the outcomes are driven by several factors, including the following:

- Economic factors, mainly the cost of adopting new water-saving technologies and potential returns over time. A technology with high water-saving ability, but low production outcomes, is difficult for farmers to accept.
- Natural environmental factors, mainly the availability of water resources, and whether the land, soil, and climatic conditions are suitable for the adoption of new technologies.
- Social environmental factors, mainly in regard to market penetration and saturation, the costs and availability of transportation, information networks, and cultural differences between regions.
- Governmental policies, mainly allocation of water rights, water-use fees, current government allowances and potential government subsidies.
- Farmers' educational backgrounds, their attitudes in choosing irrigation technologies, and their ability to understand, implement, and adopt water-saving practices.

There is a need for coordination among individual farmers, villagers' committees, government officials and business personnel in order to adopt new technologies in a systematic way. The coordination needs to (1) implement government policies on water-saving measures; (2) allocate water rights in various sectors from the origin of the water resource; (3) optimize cropping structures to reduce the proportion of low income, high water use crops and to increase the proportion of efficient water-use crops; (4) improve water prices at the village level and for individual farmers; (5) promote relatively simple, easily adopted programs for monitoring day-to-day water-use activities; and (6) provide suggestions on compensatory policies to water-saving participants on the level of subsidy.

3.6 Off-Farm Employment

With the rapid urbanization and migration of labor from rural to urban areas in northern China, debate exists over whether off-farm employment provides any benefits to water-saving campaigns. In a recent study, [Wachong Castro et al. \(2010\)](#) examined the relationship between off-farm employment and water saving in agriculture using a sample of households located in the Minle County of Zhangye district. The researchers found a significant negative relationship between off-farm employment and water use per unit of farmland, suggesting that increasing off-farm employment can reduce water use in agriculture in large parts of northern China.

There are several possible reasons for the improved water-saving results with increased off-farm employment: (1) participants in off-farm employment generally increase total household income which can help finance production inputs (such as fertilizers and hybrid seeds), purchase more water if the water quota is not reached, and increase agricultural investment in irrigation infrastructure to improve the quality of canals and avoid water leakage; (2) involvement in off-farm employment means that less household labor is available which affects the choice of crops and technology; (3) households with members involved in off-farm employment often experience a reduction in local food consumption which may affect the household's agricultural production decisions or water use; and (4) agricultural production and WUE need to increase to meet the financial burden of family members who move to urban areas for their schooling.



4. WATER-SAVING CROPPING PRACTICES

4.1 Crop Responses to Water Deficits

It is well known that plants can express three types of drought resistance ([Turner et al., 2001](#)): (1) drought escape (such as matching plant phenology to water supply, genetic enhancement for longer flowering duration and increased plasticity of yield components); (2) dehydration postponement (such as maintaining turgor through stomatal closure, increased water uptake, reduced water loss, or osmotic adjustment); and (3) dehydration tolerance (such that plant cells continue metabolism at lower water status, or reconstitute membranes and become functional within hours of rewatering). Under those principles, many water-saving studies conducted in northern China in recent years have focused on determining CWRs and responses to water deficit in major crops (such as wheat, maize, rice, summer

rape, and potato). Well defined for some key physiological processes are the effects of water deficits, regulated deficit irrigation (RDI), dry and wet watering cycles, and supplemental irrigation. In this chapter, we discuss key results from some of those water-saving studies.

The crop physiological processes that are affected by water deficit are plant growth, stomatal closure, reduced transpiration and photosynthesis, and increased dry matter remobilization. Information on these can be used to aid irrigation scheduling to reduce water use, minimize waste of irrigation water, and improve WUE and CWP.

Water deficits affect *plant growth*. Leaf expansion is very sensitive to water supply and a reduction in leaf area through decreased cell expansion is a key mechanism by which a plant responds to water deficit. Reduced cell expansion at the vegetative stage significantly impacts flowering in oilseeds (Liu et al., 2012), tiller initiation in cereals (Fricke, 2002) and tuber yield in potato (Jung et al., 2010). However, transient water shortage imposed at the vegetative to early reproductive stages may trigger reproductive growth and interorgan compensation (French and Turner, 1991; Liang et al., 2000). In cereals, more late emerging tillers or kernels per spikelet will be produced (Ma et al., 2013). The mechanism responsible for the compensatory effect is not well defined in some crop species, but researchers have assumed that this is most likely due to the fact that meristematic tissues are generally positioned within the plant in a relatively protected environment compared with the expanded leaves and stem, and therefore it may take more severe water stress for the meristem to lose its turgor when water shortage occurs (Kwiatkowska, 2008).

Water deficits affect *transpiration* and *photosynthesis* significantly in most crops under field conditions in northern China. A parabolic relationship between photosynthesis and transpiration is shown in wheat (Wang and Liu, 2003). Under drought, plant transpiration can continue to increase even after photosynthesis reaches a maximum. Thus, reducing stomatal conductance and preventing excessive transpiration beyond maximal photosynthesis can be used as a water-saving strategy in wheat production. Osmotic adjustment allows for the maintenance of photosynthesis and growth by stomatal adjustment and photosynthetic adjustment (Turner, 2004). Furthermore, plant transpiration and photosynthesis will respond differently depending on the level of water deficit. Mild and moderate water deficits reduce the rate of photosynthesis due to stomatal closure (Deng et al., 2000), whereas severe water deficits usually affect enzyme activities that are responsible for photosynthetic capacity (Du et al., 1998).

In plants, three sources of carbohydrates exist: (1) those stored in vegetative tissues prior to seed development, which can be *remobilized* to the seeds during grain filling; (2) those stored temporarily in vegetative tissues after the beginning of seed development, which can be remobilized to grains; and (3) those produced during seed development and are readily transferable directly to the grains (Pheloung and Siddique, 1991; Kobata et al., 1992). Studies on main grain crops such as wheat, rice and maize in northern China have shown that mild water stress stimulates stored carbohydrates in vegetative tissues prior to flowering and seed development (Yang et al., 2003) and contribute effectively to the seeds that develop after flowering (Ehdaie et al., 2006). Water stress during grain development usually shortens the duration of grain filling, but the rate of grain filling increases so that final grain weight is not reduced.

4.2 Interaction of Water Use and Nutrient Availability

In the Loess Plateau areas of northwest China, grain production is typically among the hills and gullies, and the main challenge for dryland farming has been and continues to be the lack of sufficient water supply coupled with low soil fertility. Optimizing the relationship between nutrients and water availability has been recognized as a key factor for improving sustainable productivity of the crops in the region.

Several studies conducted on the Loess Plateau have shown that increased soil nutrients increase both crop yield and WUE (Fan et al., 2005; Liu and Ma, 1998). In a 24-year fertilization experiment conducted in Pingliang, Gansu, Fan et al. (2005) showed that mean wheat yield was 4.7 ton ha⁻¹ for plots fertilized annually with manure plus N and P, which was 3.6 times the yield of unfertilized plots. Similarly, mean maize yield for fertilized plots was 2.5 times that of unfertilized plots receiving the same precipitation. They also found that over 24 years, crop yields continuously decreased in plots without fertilizer application. In contrast, soil organic carbon, total N and total P gradually built up in fertilized plots. Shen et al. (2013) showed that fertilizer application improved crop root systems, which in turn improved crop water use and nutrient absorption, and hence increased crop yield and WUE.

Organic carbon in Loess Plateau soils is generally below 5.8 g kg⁻¹ (Xin et al., 2011) because most crop straw is removed from fields for feed or fuel and only a small amount of manure is applied back to the soil. The addition of organic matter to the soil increases the water-holding capacity of the soil (Fan et al., 2005; Liu et al., 2013). In a 7-year field study, Liu et al. (2013) showed that the application of manure coupled with N and P fertilizer significantly improved the soil water-holding capacity over time. The average

soil water content in the 0–10 m soil profile over 5 years was 42.2 mm in plots receiving manure and N and P, which was 23.2 mm higher than that in plots without fertilization. After 7 years, soil water in the upper 2 m of soil in fertilized plots was kept in balance, while significant soil water depletion reached the 1.4 m soil layer in plots without fertilization. Fertilization increased crop root volumes in the soil, and thereby enhanced the water-holding capacity of the soil. As a result, annual grain yields in plots with manure plus N and P were 210% higher than yields in nonfertilized plots and 54% higher than yields in plots with added N and P, but no manure. Increased crop yield with fertilization means to increase carbon input to the soil and lower the carbon footprint of crop products (Gan et al., 2012a, 2012b). These and other studies suggest that in arid and semiarid areas, the improvement of soil fertility through various means such as manure application and fertilization can help build up soil carbon pools, improve water-holding capacity of the soil, and enhance crop productivity in a sustainable manner.

4.3 No-Till and Subsoiling

Conservation tillage, such as no-till or minimum tillage, has been practiced worldwide as a means of conserving soil moisture, maintaining soil structure and improving soil properties (Ding and Zhang, 2002; Siddique et al., 2012). In recent years, this practice has been included in the water-saving campaign to replace traditional plow tillage in northwestern China. Studies have shown that conservation tillage practices can decrease soil disturbance, increase soil water conservation and improve soil aggregate stability (Huang et al., 2012a; Li et al., 2011; Zhang, 2007b). Most of the tillage studies found that no-till combined with stubble retention on the soil surface increased soil water storage in the entire soil profile due to improved water infiltration and reduced runoff (Huang et al., 2012a; Li et al., 2011). Stalk mulch on the soil surface effectively prevents soil water from evaporating and runoff, allowing rainwater to infiltrate into the soil in a timely manner (Li et al., 2011; Xie et al., 2007). The increased water status in topsoil layers with no-till also promoted crop root development (Huang et al., 2012a). Wheat crops grown under no-till had more extensive root growth in the top 0.1 m soil layer compared to a conventionally tilled soils (Huang et al., 2012a).

However, some studies have shown that long-term no-till practices can cause severe soil compaction, reduce soil porosity, and decrease the availability of soil water and nutrients, consequently reducing WUE and crop yield (Huang et al., 2012b). Serious hardpans in the 0.2–0.3 m soil depth often occur with no-till, restricting crop root development in deeper soil. To

overcome this problem, subsoiling—which involves tillage to a soil depth of 0.2–0.3 m—has been introduced (He et al., 2009; Hou et al., 2012b; Li et al., 2007a). Subsoiling has improved soil structure by eliminating soil compaction and overcoming some of the disadvantages caused by no-till (Hou et al., 2012a). The subsoiling effect can last as long as 4 years, so subsoiling is only required once every few years (He et al., 2007; Qin et al., 2008). To utilize the benefits of no-till without soil compaction, one has combined no-till practices with subsoiling in a rotational pattern (named rotational tillage) in recent years. In a 3-year study with no-till alternating with subsoiling, Hou et al. (2012b) demonstrated that rotational tillage decreased soil bulk density, improved soil porosity, improved soil water status and increased the amount of soil water stored during the summer fallow and growing season compared with conventional tillage. The tillage–subsoiling rotation increased wheat yields by 10% and improved WUE by 7% compared to conventional tillage.

4.4 Mulching

A number of mulching systems have been developed during the water-saving campaign in northwest China. Various types of mulches such as thin plastic film, gravel and sand, rock fragments, crop straw, concrete, volcanic ash, paper pellets, and livestock manures have been applied to the soil surface for water conservation in both dryland and irrigated areas (Gan et al., 2008, 2013). Among the mulching practices, plastic film, crop straw, and gravel and sand are the most popular and have shown significant, positive results.

4.4.1 Ridge–Furrow Plastic Mulching

Locally developed seeders are used to form ridges and lay plastic film in one operation (Figure 2.4(A)). At present, the seeds are usually sown manually by making a hole on the plastic film covering the soil surface (Figure 2.4(B)). There are a number of ridge–furrow planting configurations (Gan et al., 2013): a typical configuration is to sow maize on the covered strips (Figure 2.4(C)). Studies have shown that combining plastic mulch with a ridge–furrow planting configuration (RF-system), when managed well as shown in Figure 2.4(D), is an advanced step in increasing water conservation compared to conventional unmulched or flat-plot planting system (CF-system).

There are a number of benefits of the RF-system, including improved soil temperature, decreased soil evaporation, increased crop yield, and improved WUE (Table 2.1). A major benefit is that the RF-system channels rainwater to the furrows, and allows water to penetrate into deeper soil profile, reduces

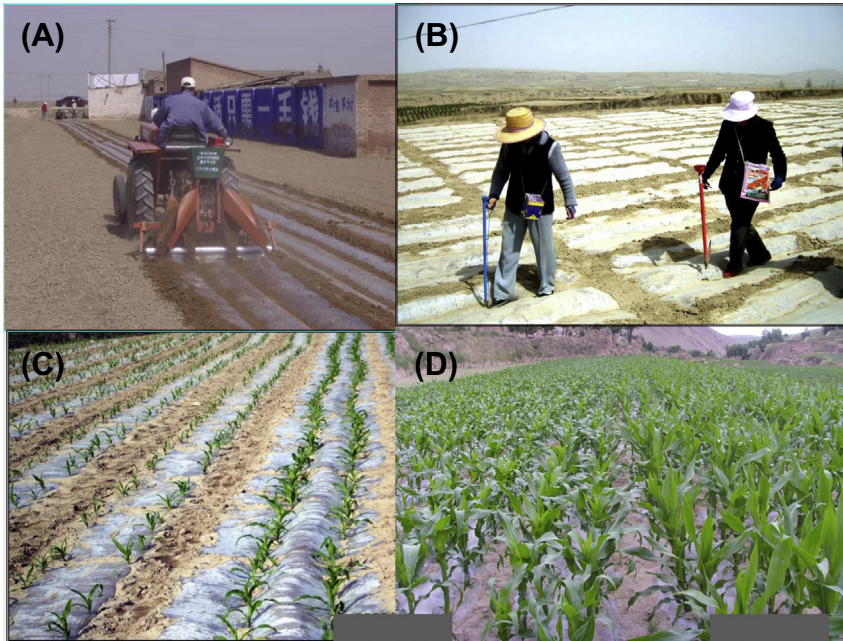


Figure 2.4 The water-saving technology of ridge–furrow plastic mulching: (A) a locally developed seeder used to form ridges and lay film in one operation, (B) seeds being sown manually by making holes in the plastic film, (C) a maize crop growing in the furrows, and (D) a well-managed maize crop. *Photos provided by Professor Feng-Min Li of Lanzhou University.* (For color version of this figure, the reader is referred to the online version of this book.)

soil evaporation and makes water available for crop transpiration (Gan et al., 2013). In a rain-simulation study in the laboratory, Ren et al. (2008) demonstrated that soils with an RF-system had consistently higher soil water contents throughout the experimental period compared with soils in a CF-system. In field studies, Li et al. (2007b) observed that furrows with covered ridges contained 10–50% more soil water than furrows without covered ridges. In C_4 crops such as maize and sorghum, the plastic mulch also heats the soil in spring, thereby speeding up the time to flowering and enabling grain production that is not possible without plastic mulch.

In some dryland areas, rainfall occurs in heavy and intense showers, resulting in runoff and erosion especially if the land is sloping. If the RF-system runs along the contour, the ridges serve as physical barriers that minimize runoff and allow water to penetrate into deeper soil layers. Research has demonstrated that integration of plastic-covered ridges with furrows

Table 2.1 Examples of the Effects of Plastic-Covered Ridge–Furrow Systems (RF-Systems) Compared to Conventional Uncovered or Flat-Plot (CF-System) Systems on Water-Use Efficiency and Crop Yields in Arid and Semiarid Northwest China

Study Site		Study Year	Crop	Advantages of RF-System over CF-System	References
Water-Use Efficiency					
Gaolan	35°54'N, 104°06'E	2001–2002	Potato	Significantly higher ($P < 0.01$)	Wang et al. (2005)
Shaanxi	34°20'N, 108°04'E	2006–2007	Maize	Significantly higher ($P < 0.01$); under simulated rainfall (230 and 340 mm), PUE increased by 73 and 40% in 2006; 77 and 43% in 2007	Ren et al. (2009)
Gaolan	36°13'N, 103°47'E	1998–1999	Maize	Significantly higher ($P < 0.01$); 1.9 times greater in 1998; 1.4 times greater in 1999	Li et al. (2001)
Yuzhong	36°02'N, 104°25'E	2001–2003	Alfalfa	Significantly higher ($P < 0.01$); PUE greater in each growing season	Jia et al. (2006)
Crop Yields					
Shaanxi	35°15'N, 110°18'E	2008–2010	Maize	Increased yield by 13% compared with control with no mulch in furrow	Li et al. (2013)
Yangling	34°20'N, 108°04'E	2006–2007	Maize	Yield increased by 11–75% compared to the nonmulched control when rainfall < 440 mm	Ren et al. (2008)
Linxia	36°13'N, 103°47'E	2002–2003	Alfalfa	Alfalfa dry weight increased 165% compared to uncovered ridge control	Li et al. (2007a,b)
Canghemao	39°6'N, 111°06'E	2010–2011	Prose millet	Millet yield increased by 74–147% compared to control	Qu et al. (2012)

PUE = precipitation use efficiency.

covered with straw is an ideal system for increasing soil water infiltration and preventing runoff (Ren et al., 2008; Wang et al., 2011).

In a comprehensive review on the subject, Gan et al. (2013) concluded that the increased crop yield with RF-systems is primarily attributable to six factors: (1) *increased water availability*—the plastic mulch directly inhibits evaporation of water from the soil surface, promotes water movement from deeper soil layers to the topsoil by vapor transfer, and enhances the topsoil water content during critical stages of crop growth; (2) *improved soil temperatures*—the increased soil temperatures under plastic mulch not only speed up seedling emergence and early growth, but also increase the rate of plant development. The latter effect is crucial for maize production in the cooler regions of northwest China where maize grown without plastic-film mulching has delayed tasselling with poor kernel formation; (3) *enhanced light*—light is reflected from the raised, plastic-surfaced ridges to the plant canopy growing in the furrows, allowing more light to penetrate through the base and side of the canopy. As a result, mulching with plastic film usually increases the leaf area index of plants, and thus enhances net photosynthesis of the crop (Zhang et al., 2011); (4) *increased nutrient availability*—fertilizers are typically applied to the crop through man-made holes in the plastic mulch and are therefore protected by the plastic cover so that the potential loss of N fertilizer through volatilization is minimized. Nutrient uptake and use efficiency are usually higher under plastic-covered RF-systems than under a CF-systems, an effect that is independent of growing-season precipitation (Ren et al., 2009); (5) *improved soil carbon*—crops grown in RF-systems have increased above- and below-ground biomass (Niu et al., 2004), and thus the potential for more organic matter to be returned to the soil, thereby increasing the light and heavy fractions of soil organic carbon, and enhancing soil microbial biomass carbon and biodiversity (Zhou et al., 2011; Lin et al., 2008); and (6) *reduced weed pressure*—RF-systems reduce weed problems since physical cover of the soil surface with plastic film limits weed emergence.

4.4.2 Straw Mulching

In the early days in northwestern China, crop residues were commonly used as animal feed or burned, leading to a severe reduction in soil organic matter content. In recent years, with the initiation of the water-saving agriculture, local governments in areas where crop residues are not considered the main source of fuel or fodder for farm families have encouraged farmers to return crop residues back to the field to enhance soil moisture

conservation (Huang et al., 2006). In maize and wheat production systems, the straw is typically chopped and spread evenly on the soil surface followed by direct seeding. It is also used in seedbed preparation where the straw is placed manually on the soil surface after shallow rotary tillage and sowing. In some areas, straw is used in RF-planting systems as mulch on the furrows while plastic film covers the ridges.

Many studies have confirmed that straw mulch significantly conserves soil moisture. In a tillage study with winter wheat where no-till (NT), no-till with standing stubble (NTSS), no-till with straw mulch on the soil surface (NTS) were compared with conventional tillage (CT) without straw mulch, Huang et al. (2012a) showed that wheat had the highest grain yield in the NTS system (7440 kg ha^{-1}) followed by NTSS (7040 kg ha^{-1}); CT yielded the lowest (6400 kg ha^{-1}) (Table 2.2). Compared to the CT system, NT, NTSS and NTS improved yields by 6–12%, 7–13%, and 16–17%, respectively. Similarly, the three conservation tillage systems improved WUE by 8–10%, 8–10%, and 17–18%, respectively, compared with CT.

The increased yield with straw mulching is largely due to (1) improved soil water storage (Huang et al., 2006; Li et al., 2005), (2) reduced soil bulk density (Hassan et al., 2007; Ishaq et al., 2001), and (3) improved crop root systems. In the study by Huang et al. (2012a), wheat plants grown in the NT, NTSS, and NTS systems significantly improved mean root density at the 0–0.7 m depth by 6–19% at jointing, 14–33% at heading, 13–34% at flowering, and 17–44% at maturity compared to the CT system (Fig. 2.5). The larger rooting systems in the NTSS and NTS systems take up more water and nutrients, ultimately improving crop yields and WUE.

However, reduced soil temperatures with straw mulching are a concern in areas with cool springs during seedling emergence. Also, some crops may be more sensitive to the straw of other crops due to allelopathic effects (Farooq et al., 2011). In a study of a winter-wheat rotation with summer maize, Zhou et al. (2011) found that straw mulching increased the yield of maize but decreased the yield of wheat, which was attributed to reduced soil temperatures and delayed wheat growth in early spring (Dong et al., 2008), while minimizing temperature fluctuations during summer, favoring maize flowering, and grain filling.

In this chapter, we identified some key technical aspects for successful straw mulch systems in semiarid northwestern China, which include: (1) the ground should be covered with crop straw immediately after harvest until sowing the next crop, (2) crops should be sown using an NT drill with minimal soil disturbance to maintain crop residues on the soil surface, (3) weeds

Table 2.2 Effects of Different Tillage Systems (CT, NT, NTSS, NTS) on Winter-Wheat Grain Yield, WUE, Water Use and Soil Water Storage at Various Depths at Sowing in 2006–2007 and 2007–2008, at Huangyang Town (37°30'N, 103°5'E), Northwest China

	2006–2007				2007–2008			
	CT	NT	NTSS	NTS	CT	NT	NTSS	NTS
Grain yield (kg ha ⁻¹)	6533b	7300ab	7366a	7633a	6275a	6644a	6713a	7257a
WUE (kg ha ⁻¹ mm ⁻¹)	11.3b	12.4ab	12.4ab	13.3a	10.3a	11.2a	11.1a	12.1a
Water use (mm)	578.2a	589.3a	594.6a	574.6a	608.2a	595.2c	603.4ab	600.2bc
Soil Water (mm) at Various Depths (m) at Sowing								
0–0.1	10.6a	10.8a	11.6a	11.6a	19.2c	21.5b	21.9ab	22.5a
0.1–0.2	12.6b	14.5a	14.5a	14.8a	19.6d	20.6c	23.6b	24.7a
0.2–0.3	14.2c	15.7b	15.8b	17.2a	18.7b	19.1b	23.5a	23.7a
0.3–0.5	30.2b	33.8a	33.1a	33.6a	41.8a	43.8a	42.3a	44.0a
0.5–0.7	34.5b	41.6a	41.4a	42.1a	43.8a	37.4d	40.9c	43.1b
0.7–0.9	33.2b	36.9ab	37.7a	38.8a	40.3b	37.9d	38.4c	43.8a
0.9–1.2	44.9b	46.2b	47.6b	53.8a	53.1c	51.2d	54.1b	58.1a
1.2–1.5	46.7b	43.0c	46.8b	49.9a	45.8c	51.7b	54.6a	51.8b
Total	226.9c	242.6b	248.7b	261.6a	282.2a	283.1a	299.5a	311.7a

Means within rows in the same year followed by the different letters are significantly different at $P < 0.05$. CT, conventional; NT, no-till; NTSS, no-till with standing stubble; NTS, no-till with straw mulch, WUE, water-use efficiency.

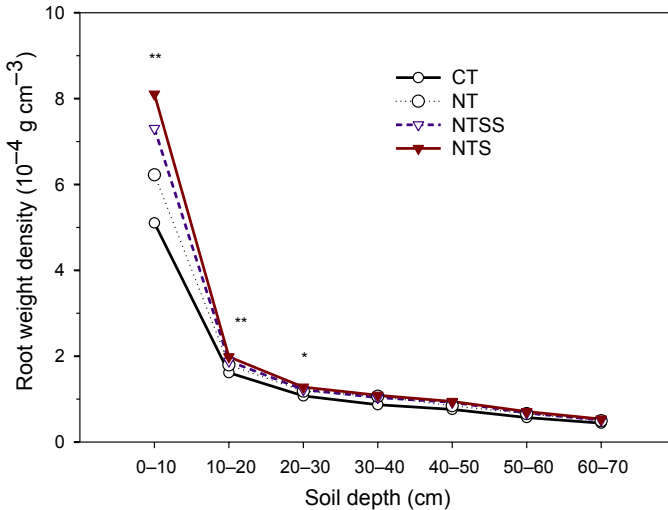


Figure 2.5 Mean root weight densities of winter wheat grown with conventional tillage (CT), no-till (NT), no-till with standing stubble (NTSS), and no-till with straw mulch (NTS) from 2006 to 2008 at Huangyang town (37°30'N, 103°5'E), northwest China. Data from Huang *et al.* (2012a). (For color version of this figure, the reader is referred to the online version of this book.)

should be controlled using herbicides or hand-weeding to ensure no cultivation throughout the cropping year, and (4) crops sensitive to soil temperature at emergence should be sown at a higher seed rate to ensure adequate plant establishment.

4.4.3 Gravel–Sand Mulching

In the transitional zone between arid and semiarid regions of northwest China, gravel, sand, or rock fragments are often applied to the soil surface (Li and Liu, 2003; Gan *et al.*, 2013) and the crop is directly sown through the gravel–sand covered fields with minimal disturbance. Historically, gravel–sand covered fields have been used to produce high-value fruits such as wolfberry or GouQi (*Lycium barbarum* L.) and watermelon (*Citrullus lanatus* T.) (Figure 2.6(A)), but with modern devices available for digging, collecting and transporting, this technique has spread to field crops (Figure 2.6(B)). Gravel–sand mulching is usually conducted in fields where a local source of sand and gravel is readily available. However, construction of such a seedbed is extremely labor intensive, and productivity from a well-constructed gravel–sand mulched field may only last 8–12 years (Gan *et al.*, 2008) as soil nutrients and organic matter under the mulch deplete rapidly over time.

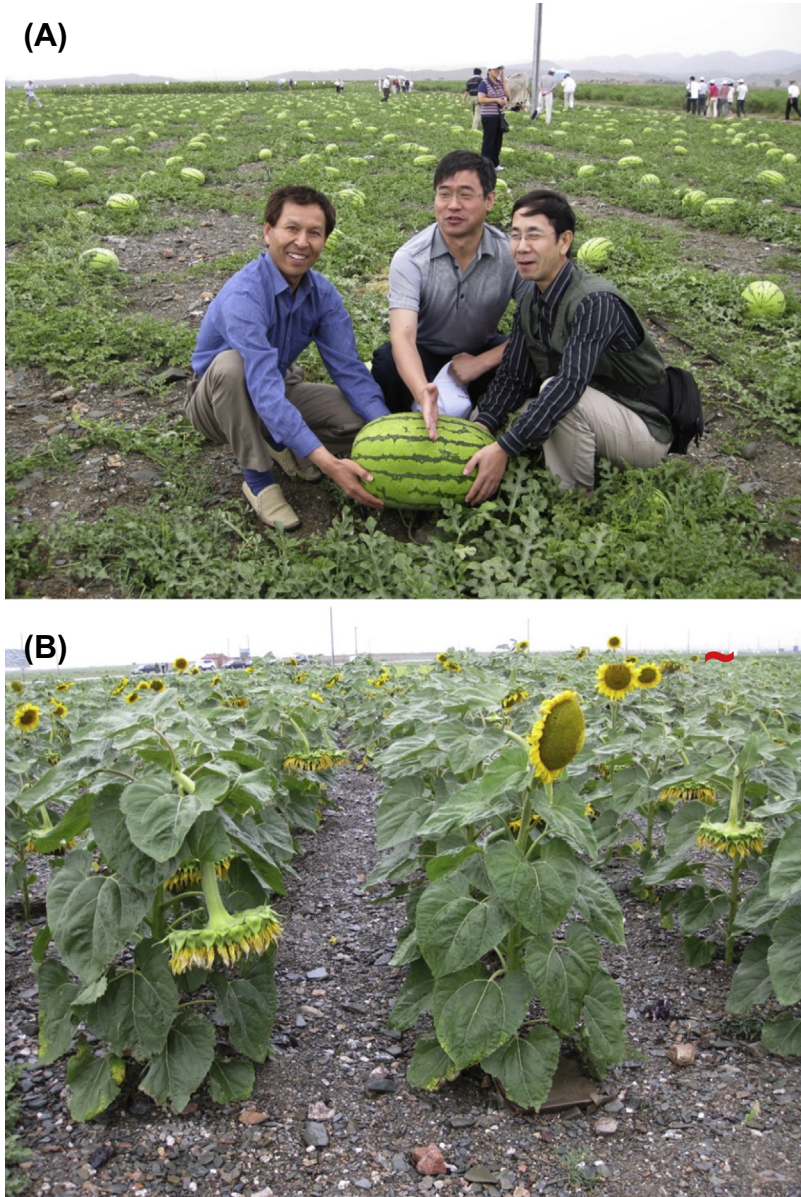


Figure 2.6 Gravel–sand covered fields used for the production of fruits and vegetables, such as (A) watermelon (*Citrullus lanatus* T.), and (B) a sunflower (*Helianthus annuus* L.) crop. (For color version of this figure, the reader is referred to the online version of this book.)

4.5 Regulated Deficit Irrigation

RDI is an irrigation practice in which a crop is watered below full CWRs in order to reduce water use and increase WUE. This practice has been used in many irrigated areas of northwestern China. There are three different methods to apply RDI:

1. RDI at different stages of crop development (RDIC) where full irrigation is applied at critical growth stages with less applied at noncritical growth stages.

RDIC is based on the principle that the response of crop plants to water stress varies at different growth stages, and less irrigation applied to the crop at noncritical stages may not reduce normal plant production. For example, under Mediterranean conditions, the most sensitive growth stages of wheat are at stem elongation and booting, followed by anthesis and grain filling (García Del Moral et al., 2003). High wheat yields have been achieved by exposing wheat plants to mild water deficit at the seedling stage and more severe water deficits at the tillering to stem elongation stage in northwest China (Kang et al., 2002). Studies have also shown that RDIC improved grain yields and WUE in maize (Kang et al., 2000), wheat (Zhang et al., 1998), cotton (Hu et al., 2002), and other crops. In cotton, RDIC is used to stimulate flowering/budding and has been shown to enhance yield and WUE by 57% (Zhang and Cai, 2001; Hu et al., 2002).

2. Partial root zone drying (PRD) where half the root system is irrigated, while the remaining half is exposed to drying soil, as shown in Figure 2.7. The wetting and drying of the root zone is alternated at a frequency allowing the previously well-watered side of the root zone to dry down while the previously dried side is fully irrigated.

PRD is based on two assumptions: (1) the part of the root system in drying soil may respond to drying by sending a root-sourced signal to the shoot where stomata may close to reduce water loss (Dry and Loveys, 1999), and (2) with reduced water availability, a small narrowing of the stomata opening may reduce water loss substantially with little effect on photosynthesis (Dry et al., 2000). When subjected to mild water stress with PRD, plants can accumulate low molecular-weight substances to regulate the osmotic potential (osmotic adjustment) of plants by (1) reducing osmotic stress (Song and Wang, 2002), (2) providing an efficient acclimation to plant-available water (Liu et al., 2005), and (3) allowing plants to experience less oxidative stress or damage induced by water deficits (Hu et al., 2010). As leaf water potential does not decrease with PRD,

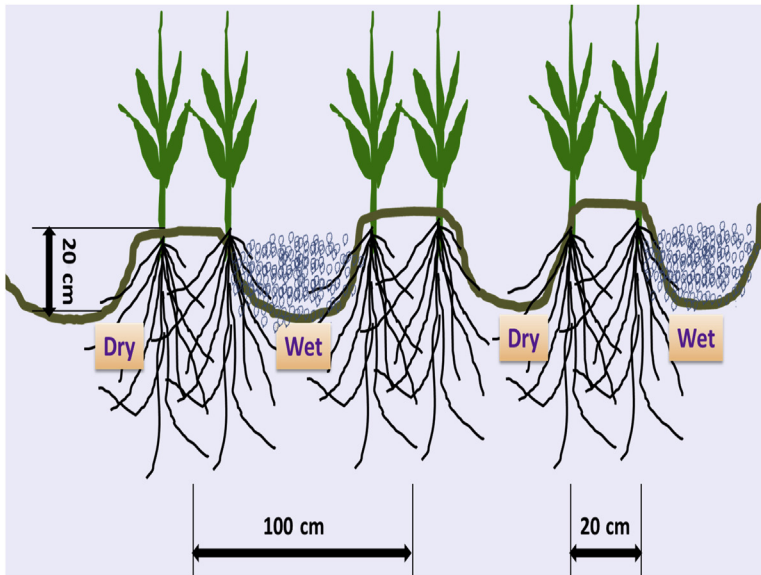


Figure 2.7 A typical partial root zone drying system in which half of the rooting zone is irrigated, and half is unirrigated and allowed to dry. The wet and dry sides of the root zone are alternated so that the previously watered side of the root zone is allowed to dry down while the previously dry side is fully irrigated. (For color version of this figure, the reader is referred to the online version of this book.)

irrigation to part of the root zone does not negatively affect crop growth and development, and instead PRD may stimulate protective processes in the plants.

Many studies in northwestern China have shown the positive effects of PRD. In a pot experiment with maize, for example, [Li et al. \(2010\)](#) found that, compared to the conventional full-watering treatment, PRD for 49 days during jointing and tasselling reduced water consumption by 33%, and increased canopy WUE by 42%. In cotton, alternate-row furrow irrigation reduced water use by 31–33% ([Du et al., 2008](#)) and increased cottonseed yield by 13–24% ([Du et al., 2006](#)). PRD enhanced N recovery in maize by 16% ([Li et al., 2007a](#)), due to the stimulated growth of secondary roots ([Zhang and Tardieu, 1996](#)), increased root surface areas ([Wang et al., 2009](#)), and improved uptake of nutrients and water ([Kang et al., 1998](#)). PRD also induces compensatory water absorption from the wetted zone and reduces plant transpiration ([Du et al., 2006](#)), increases soil mineral N availability ([Liang et al., 2013](#)), and maintains or increases crop yields ([Graterol et al., 1993](#)). These studies clearly demonstrate that RDIC and PRD have the potential to save irrigation water and serve as promising water-saving innovations.

3. Supplemental irrigation where unscheduled irrigation is used to supplement the shortfall of precipitation at strategic times of crop growth.

Supplement irrigation is another water-saving practice used in dryland farming in northwestern China. It is mostly used in areas where rainfall fluctuates greatly within or between seasons and irrigation water is available for supplementation. Good irrigation scheduling requires the availability of water at the correct time and the right amount of water to be applied to match actual field conditions (Bai and Dong, 2001). This requires information on soil moisture conditions and reliable forecasting of weather conditions. Research has shown that, when managed well, supplemental irrigation can maintain and increase yields with limited amounts of irrigation. This system may work best when combined with RDIC or PRD, as it improves the distribution of moisture in the rooting zone and reduces soil evaporation due to the reduced surface area of wet soil exposed by PRD (Xie et al., 2011). However, sophisticated irrigation management scheduling is required to reduce the amount of supplemental water without a substantial reduction in crop yield.

4.6 Chemical Regulation

Under water deficiency, plants use some self-adapting mechanisms such as stomatal closure (Deng et al., 2000) and leaf rolling (Chaves et al., 2009) to reduce transpiration, but these mechanisms often slow plant growth (Kwiatkowska, 2008) and induce abscission (Du et al., 1998). Plant hormones, particularly abscisic acid, have been shown to signal soil drying and reduce transpiration and water loss (Davies and Zhang, 1991; Lu et al., 2003), but have not been widely adopted as they may be rapidly catabolized under field conditions. Recent studies under controlled conditions suggest that drenching the soil with abscisic acid and β -aminobutyric acid can decrease or slow water use and increase WUE (Du et al., 2012, 2013).

In a study using a foliar spray of uniconazole—a plant growth regulator that belongs to a group of triazoles—on wheat plants, Duan et al. (2008) showed that plants receiving uniconazole spray increased the root dry weight that helps absorb soil water and transport it to growing parts, and thus significantly compensated for the harmful effects caused by water deficit. As a result, uniconazole increased WUE by 22–25% under mild water deficit, and alleviated the physiological damage caused by water deficiency. Other studies showed that plants treated with uniconazole reduced water loss by transpiration, delayed permanent wilting (Xu et al., 1995) and improved stress tolerance (Lu et al., 2003). Enhanced antioxidant enzyme systems may be responsible for the

reduction of stress-related oxidative damage to cell membranes (El-Khallal and Nafie, 2003; Du et al., 2012, 2013). More detailed research is needed to evaluate the effectiveness and consistency of uniconazole, abscisic, β -aminobutyric acid, and other phytohormones as potential water-saving chemicals.



5. WATER-SAVING ENGINEERING SYSTEMS

5.1 Land Leveling, Terracing, and Contour Farming

As a result of agricultural water-saving campaigns in northern China, investment in land leveling, terracing, and contour farming has increased significantly in recent years. Land leveling refers to flattening of farmland so that rain or irrigation water is more evenly distributed over the field and runoff is minimized. Land leveling in northern China is commonly done by manual labor coupled with small tractors (Figure 2.8(A)). Land leveling is expensive largely due to the high rates charged for renting equipment such as tractors, but some small-scale farmers often work together with their neighbors. Most importantly, farmers recognize that investing in land leveling can help save money spent on water, can achieve higher crop yields, is an important soil conservation measure and is economically viable in the long term.

In the semiarid Loess Plateau, most farmland slopes at an angle of 10–25°, which makes it highly susceptible to erosion. Cultivating such slopes can result in annual erosion of up to 48 ton ha⁻¹ of fertile topsoil (Wei et al., 2000). Changing such sloping land into contoured terraces (Figure 2.8(B)) can prevent water and soil erosion, ultimately improve soil fertility and facilitate crop production, particularly for high-value crops such as fruit trees. Farming experiences in northwest China have shown that building terraces has enhanced water infiltration, raised the rainfall utilization rate and created high-yielding farmland. Combined with other agricultural techniques, both land leveling and contour terracing play a major role in increasing agricultural productivity and improving WUE on this hard to farm, fragile ecoregion.

5.2 Rainwater Catchments

In areas with annual rainfall between 250 and 400 mm, Chinese farmers typically use various catchment facilities to collect rainwater during the rainy season for drinking, livestock, and supplementary irrigation of crops. Rainwater catchment facilities are normally built along roadside (Figure 2.9(A)), sloping land (Figure 2.9(B)), and uncultivated infertile (Fig. 2.9(C)) and marginal land covered with plastics (Figure 2.9(D)).



Figure 2.8 (A) Land leveling, and (B) contour terraces in northwestern China. *Photos provided by Soil and Water Conservation Department, Ministry of Water Resources, China.* (For color version of this figure, the reader is referred to the online version of this book.)

In addition, on some sloping land, water retention facilities can be built to collect rainwater within the field (Figure 2.10). When heavy and sudden rainfall occurs, the rainwater that has insufficient time to infiltrate the soil and runoff is collected in the field catchment facilities for use later as the crop grows. Farming experience has shown that this practice is beneficial in years with heavy and sudden rainfall events during

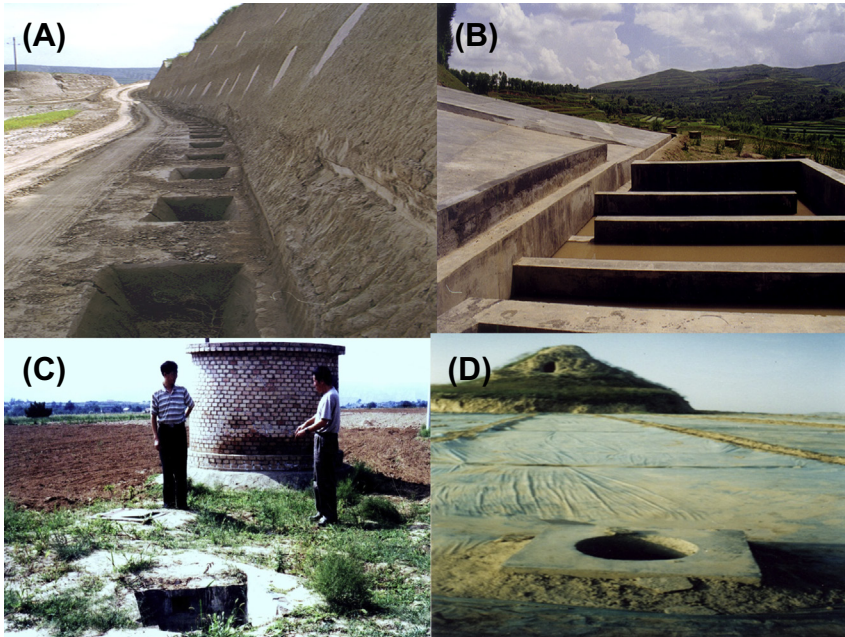


Figure 2.9 Rainwater catchment facilities in northwestern China: (A) at the roadside, (B) on a sloping hillside, (C) on uncultivated areas, and (D) marginal land, in which plastic film is used to cover the soil surface and catch rainwater for supplemental irrigation. (For color version of this figure, the reader is referred to the online version of this book.)



Figure 2.10 A rainwater catchment facility built in the middle of a field to catch runoff from intense summer rainfall events and used for supplemental irrigation later in the crop season. (For color version of this figure, the reader is referred to the online version of this book.)

the cropping season, provided that the infield catchment facility is well maintained and kept free of silt. Due to the limited volume of water that can be stored in the field catchment facility, this water-saving practice is usually used in combination with plastic and straw mulching (Sections 3.4 and 3.5), PRD (Section 3.7) or by adjusting crop growth by changing the sowing date and optimizing soil fertility to maximize the use of the stored rainwater.

Many experiments conducted in Dingxi by Gansu Research Institute for Water Conservation have demonstrated the benefits of rainwater harvesting. Even though the construction of rainwater catchment facilities is costly, it provides a means of meeting the needs of drinking water and water for livestock, and facilitates poverty alleviation and socioeconomic development in the region. By combining rainwater harvesting and supplemental irrigation to high-value crops such as fruit and vegetables, the economic returns are high. Therefore, rainwater catchments not only provide a means of utilizing rainwater for dryland farming, but also serve as a strategic measure for socioeconomic development in semiarid regions.

5.3 Improvement of Irrigation Canals

In the irrigation areas of northwest China, the use of surface irrigation water is traditionally below 50% of that extracted from the rivers and creeks (Zhang et al., 2005) because of losses during transportation. Conventional water transportation is mainly through clay-paved canals, channels, and ditches with substantial losses due to evaporation and leaching. With the development of water-saving agriculture, investments have been made to improve water transportation systems.

Considering environmental conditions, economics and feasibility, the most suitable surface water transportation is via main canals between regions and branch canals between villages/towns that are paved with reinforced concrete (Figure 2.11(A)), and the “U”-shaped channels heading to individual fields paved with either permanent sod or concrete blocks (Figure 2.11(B)). Based on studies in Zhangye, such a surface water transportation system can improve the water utilization rate by up to 75%, reduce irrigation amounts by $5100 \text{ m}^3 \text{ ha}^{-1}$ compared with $>11,000 \text{ m}^3 \text{ ha}^{-1}$ under traditional systems (Zhang et al., 2005). Covering the U-shaped channels increases water productivity even further, but to date this has not been widely adopted.



Figure 2.11 Improved water transportation systems: (A) a reinforced concrete main canal taking water to major distribution points, and (B) a “U”-shaped channel made from concrete blocks taking water to individual fields. (For color version of this figure, the reader is referred to the online version of this book.)

5.4 Spray Irrigation, Drip Irrigation, and Subsurface Drip Irrigation

Flood irrigation has been predominantly used for field crops in north-west China, where water losses from evaporation and leaching are very high. As a result of the water-saving campaign in recent years, the development of spray irrigation, surface irrigation and subsurface drip irrigation technology has been recognized. Spray irrigation is currently being

adopted in some small areas, where main channels are paved with reinforced concrete and other ditches heading to the fields are equipped with plastic pipes. Pipe-based spraying systems improve the water utilization rate by up to 80% and reduce average irrigation amounts by as much as $7500 \text{ m}^3 \text{ ha}^{-1}$ compared with traditional transportation systems (Zhang et al., 2005).

In arid regions, drip and subsurface drip irrigation have been gradually adopted in recent years. This technology allows a small volume of soil to remain moist by frequent applications of low volumes of water. This limits the rooting zone to the moist soil (Du et al., 2010) and reduces water drainage from the rooting zone (Wang et al., 2006). In particular, subsurface drip irrigation substantially minimizes soil evaporation compared to surface drip irrigation and improves irrigation WUE by 95% (Zhang et al., 2005).

In areas such as the Zhangye district, irrigation tubing and drippers are either buried 30–40 mm below the soil surface or placed under the plastic film used to cover the soil surface in RF-systems (Section 3.4). For wealthy farmers, large enterprises, and agriculture specialty companies, underfilm drip irrigation is the most popular technology and is used to produce high-value cash crops such as tomato, sweet chili, hops, and grapes. When combined with plastic mulching, subsurface drip irrigation effectively reduces evaporation and save significant water. Studies at Zhangye have shown that subsurface drip irrigation reduced water use in the production of tomato by 46%, sweet chili by 48%, hops by 36%, and grapes by 62% with yields equivalent to or 4–10% greater than traditional drip irrigation (Zhang et al., 2005).

5.5 Fertigation

Low soil fertility coupled with high evaporation is the major factor limiting agricultural productivity in northwestern China. Fertigation is a crop management practice that allows a timely supply of water through drip irrigation coupled with an accurate rate of fertilizer application, thereby simultaneously improving crop nutrient uptake and WUE. This agricultural technique has been used widely in other semiarid regions of the world (Castellanos et al., 2012), but it is relatively new in China (Liang et al., 2013).

Most studies conducted in northwestern China have responded positively to fertigation, with reduced water consumption (Yu et al., 2010), and increased crop yield and nutrient use efficiency (Liang et al., 2013; Pan et al., 2011; Yu et al., 2010) in many crops. For example, in a study

with cucumber (*Cucumis sativus*), Yu et al. (2010) found that drip fertigation saved irrigation water by 21–27%, reduced fertilizer inputs by 4–49%, and increased yields by 10–18%, compared with conventional drip irrigation. Similar positive responses have been shown in other parts of China in crops such as maize (Liang et al., 2013), banana (*Musa acuminata*) (Pan et al., 2011) and sugarcane (*Saccharum officinarum*) (Chen et al., 2012). In the study on banana, Pan et al. (2011) showed that fertigation increased the concentration of available P by 108%, enhanced microbial biomass and root activity in the soil by 26–68%, and improved root distribution in the 0–0.8 m soil layer by 9% compared with conventional fertilization. Their study suggests that fertigation increased nutrient uptake efficiency as a result of increased root activity, root distribution, and microbial biomass.

This technology is one of the newer water-saving technologies in China, focusing on the integration of advanced production techniques together in one system, including film mulching, drip irrigation, and fertilization with supplemental irrigation. In some studies, automatic fertigation has been developed where soil moisture, soil nutrients, atmospheric temperature, and humidity are monitored and fertigation adjusted by a computer-based decision-making system. In the Zhangye project, two greenhouses were constructed in 2004, each 3100 m²; ornamental lily, produced over the winter months from September to the following May, had a production value up to 1.5 million Chinese Yuan (eq. \$280,000 US in 2013) on a per hectare basis (Zhang et al., 2001). Irrigation required was 1800 m³ water⁻¹ ha⁻¹, about half that of conventional underfilm irrigation. This farming practice allows limited water to be applied to crops on both temporal and spatial scales, and is a “more crop per drop” technology.

5.6 “She-Shi Agriculture - 设施农业”

In northwestern China, there is considerable marginal, desert-type farmland with plentiful sunshine not seen in other parts of the country. One goal for water-saving agriculture in this region is to improve the use of solar energy while supplying irrigation water in balance with plant growth requirements. In recent years, the central and local governments have made large investments into the development of so-called “She-shi agriculture” to take advantage of the rich sunshine to produce high-value crops year-round. The Chinese “She-shi agriculture” refers to the production systems for high-value crops using a mass (group) of greenhouse-like facilities built on the marginal, desertlike land. Typically, each unit of the mass of the facility is built in a south-to-north orientation (Figure 2.12(A)). The northern

wall is constructed with stones, bags of clay (Figure 2.12(B)), or compressed crop straw (Figure 2.12(C)) to act as a heat sink, with the remaining walls covered by durable plastic. The roofing plastic is covered by a layer of straw matting at night in winter to retain the heat, but rolled up in summer when not required. Inside the facility, mulch is used as a ground cover to reduce water loss from soil evaporation, particularly in summer when the plastic roof is rolled back (Figure 2.12(D)). The “She-shi agriculture” differs from traditional greenhouses or glasshouses in terms of the structure, functionality, effectiveness, and durability.

The Chinese “She-shi agriculture” facilities are built on the marginal and desert-type of land with low cost, which helps expand farmers’ production capacities and incomes drastically. The facility allows farmers to produce high-value vegetables in winter months when prices are high, and create secondary jobs for rural communities especially during the off-season. Also, the “She-shi

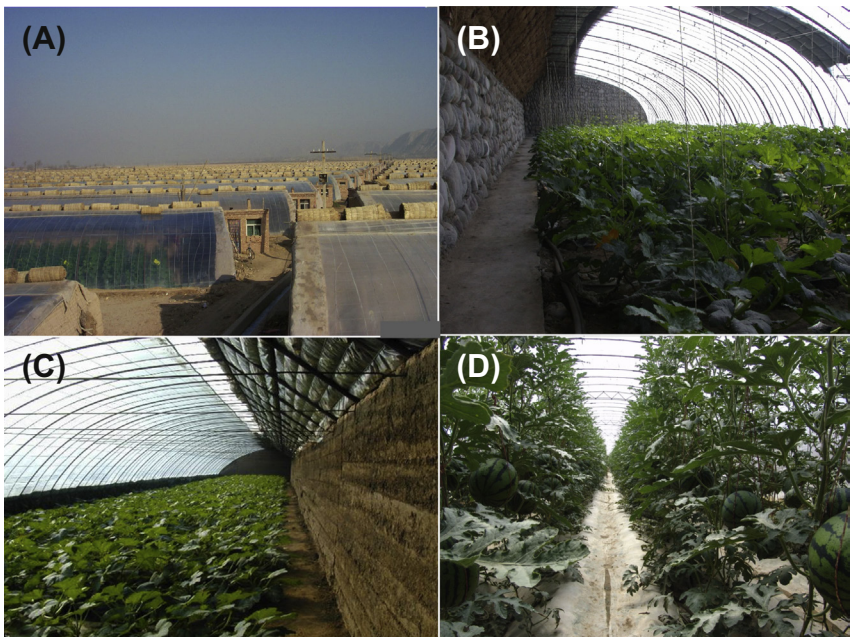


Figure 2.12 Facility agriculture consists of (A) a group of greenhouse-like facilities constructed in an arid region with northern walls in an east–west orientation to capture radiation from the south, (B) the north-side walls constructed with stones or bags of clay, and (C) with compressed straw, and the remaining walls covered by durable plastic, and (D) a watermelon crop being grown with plastic-film mulch. *Photos provided by Li Jie at Gansu Agricultural University, China.* (For color version of this figure, the reader is referred to the online version of this book.)

agriculture” is a form of water-saving technology and can drastically improve WUE in the production of high-value crops. At present, the operation of the “She-shi agriculture” facilities is labor intensive as the straw matting placed over the plastic may have to be rolled up or rolled down manually as needed, and the plastic cover has to be renewed every one or two seasons. Those issues can be addressed with the development of some automatic systems in the near future.



6. CHALLENGES AND OPPORTUNITIES IN WATER-SAVING AGRICULTURE

In arid and semiarid northwestern China, agricultural environments are likely to deteriorate in the short term with serious challenges facing agriculture, largely because:

1. The arid and semiarid regions of China are experiencing global warming with temperatures increasing over the last few decades, and this trend is predicted to continue (Turner, 2011). A consequence of global warming is a shortening of the time to flowering and maturity, with a consequent reduction in crop yield (Turner and Rao, 2013).
2. With the need for increased crop yields, more irrigation will be needed to maintain and increase agricultural production. Groundwater will continue to deepen in irrigation areas (Zhang, 2007a,b), largely due to the overexploitation of groundwater in the past and current farming systems (Zhang et al., 2005). Also, there is a trend of decreasing snowfall and an upward movement of the snowbelt on the Qilian Mountain (Che and Li, 2005). Whether or not this would affect groundwater availability in the Hexi Corridor of northwest China remains to be determined.
3. The challenge of meeting increasing requirements for water resources by urbanization, other industries and economic development is becoming an unprecedented issue in China; competition for water between various industrial sectors and agriculture will increase, forcing a reduced quota for agricultural water use; how to efficiently and effectively allocate and share limited water resources between industries and agriculture will be a central focus of various levels of government and society as a whole.
4. Academically, our understanding is still limited in regard to adaptive pathways and physiological mechanisms of crop responses to water deficits and the environment. We still do not know enough about how different crop species respond to factors like frequency and degree of drought, speed of onset of drought, and patterns of soil water and atmospheric water deficits.

Of equal importance, there are many opportunities for agriculture going forward in northwest China, which can be exploited in the near future as the innovative water-saving technologies summarized in this chapter are broadly adopted and others are developed. For example, about 90% of farmers in the irrigated areas of northwest China still use traditional border and flood irrigation methods, with an annual water demand by a crop as high as $11,000\text{ m}^3\text{ ha}^{-1}$. In contrast, subsurface drip irrigation uses water at a rate of about $3200\text{ m}^3\text{ ha}^{-1}$ or less. This suggests that adoption of subsurface drip irrigation alone could save at least 50% of available water, particularly in fruit and vegetable production.



7. CONCLUSIONS

Global food demands are expected to double by 2050 due to a growing human population and increased needs for feed, fiber, and bio-fuel. To produce sufficient grain to meet demand, crop production must increase by a staggering 140% or more according to Food and Agriculture Organization estimates. A sustainable increase of crop yields in developing countries will play a critical role in reducing the pressure of global grain demand and food security. China, the second largest world economy, has taken drastic steps to increase grain production to feed its 1.3 billion people and satisfy various industrial needs. From 2003 to 2011, the country increased cereal production by about 30%, more than double the world average. In the next two to three decades, 30–50% more grains will be needed to meet the country's projected demands. China is now facing serious water shortages, especially in northwest regions where average freshwater availability is below the internationally defined “water scarcity” level.

This chapter has reviewed more than 150 recent publications on water scarcity and management, and suggests that some of the water-shortage issues in northwestern China can be effectively addressed by adopting innovative technologies to achieve water savings without restraining future agricultural production and endangering China's self-sufficiency for food. A comprehensive water-saving system needs to be established sooner rather than later, which should include the following key actions/components. **First**, drastically increase the investment in developing water-saving technologies; this may need both public and private investments. Public investment should focus on infrastructure improvement of the quality, durability, and efficiency of irrigation channels, canals, ditches,

and water-measuring instrumentation, whereas private investment should focus on constructing contour banks and terraces, land leveling, rainwater catchment and “She-shi” agriculture i.e., 设施农业 in Chinese. **Second**, adopt an improved engineering system, where the focus is on (1) construction of an effective water transport system to optimize water distribution from the water source to farm fields with minimum water leakage, (2) development of efficient water-measuring instrumentation for water-resource control, allocation, and metering of water use, and (3) installation of drip irrigation and subsurface drip irrigation for ordinary farmers at an affordable price. **Third**, build a water-resource management system under the framework of water saving, where decision makers, water-user associations, villagers’ committees and individual farmers are engaged in the establishment of necessary laws, regulations and policies for water-resource management activities/programs, such as water quota allocation, water-use rights, water trading, water pricing and off-farm employment opportunities. **Fourth**, reinforce research and development, where public research institutes and relevant universities take a leading role in the water-saving campaign by (1) providing training courses, establishing “Sites of Excellence” to demonstrate the effectiveness of water-saving measures, encouraging farmers to participate in water-resource management, and engendering a sense of concern, and (2) developing new water-saving technologies in farming. Genetic enhancement of drought-resistant cultivars, implementation of RDI, partial root zone drying, drip irrigation, rainwater catchment for supplemental irrigation and practices for conserving soil moisture are some key research areas that need to be addressed.

Considering that water availability and use has serious socioeconomic and political consequences, we suggest the need to establish a “water-saving society” which would include research institutes and universities, local service organizations, government bodies, market-developers, and farmers and their associations integrated into one system. The system’s focus should be on developing a chain of efficiencies: water transport efficiency (with minimum leakage and evaporation losses during water transportation to the fields), water distribution efficiency (allocating more water to those crops with low water use and high returns such as vegetables and fruits as opposed to cereals), cropping efficiency (increasing crop WUE) and field application efficiency (using subsurface or surface drip irrigation vs furrow and flood irrigation). With integration, the problem of water shortage can be reduced and even mitigated.

ACKNOWLEDGMENTS

The authors are grateful for the financial support of the “863 High-Tech Project Fund of China” and the “111 program B07051 of the Chinese Ministry of Education”. Thanks also go to the support from Agriculture and Agri-Food Canada, The University of Western Australia Institute of Agriculture, and Gansu Agricultural University.

REFERENCES

- Allen, R.G., Pereira, L.S., Raes, D., Smith, M., 1998. Crop Evapotranspiration: Guidelines for Computing Crop Water Requirements. Food and Agriculture Organization of the United Nations, Rome.
- Bai, Q.J., Dong, S.T., 2001. Agricultural high-efficient water usage and sustainable development of water saving agriculture. *J. Shandong Agric. Univ.* 32, 331–335.
- Bastiaansen, W.G.M., Noordman, E.J.M., Pelgrum, H., Davids, G., Thoreson, B.P., Allen, R.G., 2005. SEBAL model with remotely sensed data to improve water-resources management under actual field conditions. *J. Irrig. Drain. Eng.* 131, 85–93.
- Belder, P., Bouman, B.A.M., Cabangon, R., Guoan, L., Quilang, E.J.P., Yuanhua, L., Spiertz, J.H.J., Tuong, T.P., 2004. Effect of water-saving irrigation on rice yield and water use in typical lowland conditions in Asia. *Agric. Water Manage.* 65, 193–210.
- Cai, Z., Shen, L., Liu, J., Zhao, X., 2012. Applying input-output analysis method for calculation of water footprint and virtual water trade in Gansu Province. *Acta Ecol. Sin.* 32, 6481–6488.
- Castellanos, M.T., Tarquis, A.M., Ribas, F., Cabello, M.J., Arce, A., Cartagena, M.C., 2012. Nitrogen fertigation: an integrated agronomic and environmental study. *Agric. Water Manage.* 120, 46–55.
- Chai, Q., Qin, A.Z., Gan, Y., Yu, A., 2014. Higher yield and lower carbon emission by intercropping maize with rape, pea and wheat in arid irrigation areas. *Agron. Sustain. Dev.* 34: 535–543. <http://dx.doi.org/10.1007/s13593-013-0161-x>
- Chaves, M.M., Flexas, J., Pinheiro, C., 2009. Photosynthesis under drought and salt stress: regulation mechanisms from whole plant to cell. *Ann. Bot-London* 103, 551–560.
- Che, T., Li, X., 2005. Spatial distribution and temporal variation of snow water resources in China during 1993–2002. *J. Glaciol. Geocryol.* 27, 64–67.
- Chen, G.F., Tang, Q.Z., Li, Y.R., Huang, Y.Y., Liu, B., Xu, L., Huang, H.R., 2012. Effects of sub-soil drip fertigation on sugarcane in field conditions. *Sugar Technol.* 14, 418–421.
- Davies, W.J., Zhang, J., 1991. Root signals and the regulation of growth and development of plants in drying soil. *Ann. Rev. Plant Biol.* 42, 55–76.
- Deng, X.P., Shan, L., Ma, Y.Q., Inanaga, S., 2000. Diurnal oscillation in the intercellular CO₂ concentration of spring wheat under the semiarid conditions. *Photosynthetica* 38, 187–192.
- Deng, X.P., Shan, L., Zhang, H., Turner, N.C., 2006. Improving agricultural water use efficiency in arid and semiarid areas of China. *Agric. Water Manage.* 80, 23–40.
- Ding, H.W., Zhang, H.S., 2002. Changes of groundwater resources in recent 50 years and their impact on ecological environment in Hexi Corridor. *Nat. Resour. J.* 17, 691–697.
- Dong, H., Geng, Y., Sarkis, J., Fujita, T., Okadera, T., Xue, B., 2013. Regional water footprint evaluation in China: a case of Liaoning. *Sci. Total Environ.* 442, 215–224.
- Dong, H., Li, W., Tang, W., Zhang, D., 2008. Furrow seeding with plastic mulching increases stand establishment and lint yield of cotton in a saline field. *Agron. J.* 100, 1640–1646.
- Dry, P.R., Loveys, B.R., 1999. Grapevine shoot growth and stomatal conductance are reduced when part of the root system is dried. *Vitis* 38, 151–156.
- Dry, P.R., Loveys, B.R., Düring, H., 2000. Partial drying of the rootzone of grape. I. Transient changes in shoot growth and gas exchange. *Vitis* 39, 3–7.

- Du, T., Kang, S., Sun, J., Zhang, X., Zhang, J., 2010. An improved water use efficiency of cereals under temporal and spatial deficit irrigation in north China. *Agric. Water Manage.* 97, 66–74.
- Du, T., Kang, S., Zhang, J., Li, F., 2008. Water use and yield responses of cotton to alternate partial root-zone drip irrigation in the arid area of north-west China. *Irrig. Sci.* 26, 147–159.
- Du, T., Kang, S., Zhang, J., Li, F., Hu, X., 2006. Yield and physiological responses of cotton to partial root-zone irrigation in the oasis field of northwest China. *Agric. Water Manage.* 84, 41–52.
- Du, Y.C., Nose, A., Wasano, K., Uchida, Y., 1998. Responses to water stress of enzyme activities and metabolite levels in relation to sucrose and starch synthesis, the Calvin cycle and the C4 pathway in sugarcane (*Saccharum* sp.) leaves. *Aus. J. Plant Physiol.* 25, 253–260.
- Du, Y.L., Wang, Z.Y., Fan, J.W., Turner, N.C., Wang, T., Li, F.M., 2012. b-Aminobutyric acid increases abscisic acid accumulation and desiccation tolerance and decreases water use but fails to improve grain yield in two spring wheat cultivars under soil drying. *J. Exp. Bot.* 63, 4849–4860.
- Du, Y.L., Wang, Z.Y., Fan, J.W., Turner, N.C., He, J., Wang, T., Li, F.M., 2013. Exogenous abscisic acid reduces water loss and improves antioxidant defense, desiccation tolerance and transpiration efficiency in two spring wheat cultivars subjected to a soil water deficit. *Funct. Plant Biol.* 40, 494–506.
- Duan, L., Guan, C., Li, J., Eneji, A.E., Li, Z., Zhai, Z., 2008. Compensative effects of chemical regulation with uniconazole on physiological damages caused by water deficiency during the grain filling stage of wheat. *J. Agron. Crop Sci.* 194, 9–14.
- Ehdaie, B., Alloush, G.A., Madore, M.A., Waines, J.G., 2006. Genotypic variation for stem reserves and mobilization in wheat: I. postanthesis changes in internode dry matter. *Crop Sci.* 46, 735–746.
- El-Khalla, S.M., Nafie, E.M., 2003. Alleviation of drought damage for two cultivars of wheat seedlings by application of growth regulators brassinolide and uniconazole. *Egypt J. Physiol. Sci.* 24, 297–317.
- Fan, T., Stewart, B.A., Yong, W., Junjie, L., Guangye, Z., 2005. Long-term fertilization effects on grain yield, water-use efficiency and soil fertility in the dryland of Loess Plateau in China. *Agric. Ecosyst. Environ.* 106, 313–329.
- Farooq, M., Jabran, K., Cheema, Z.A., Wahid, A., Siddique, K.M.H., 2011. The role of allelopathy in agricultural pest management. *Pest Manag. Sci.* 67, 493–506.
- French, R.J., Turner, N.C., 1991. Water deficits change dry matter partitioning and seed yield in narrow-leaved lupins (*Lupinus angustifolius* L.). *Aus. J. Agric. Res.* 42, 471–484.
- Fricke, W., 2002. Biophysical limitation of leaf cell elongation in source-reduced barley. *Planta* 215, 327–338.
- Gan, Y., Huang, G.B., Li, L.L., Liu, J.H., Hu, Y.G., 2008. Unique conservation tillage practices in northwest China. *WASWAC*. 3, 429–444.
- Gan, Y., Liang, C., Campbell, C.A., Zentner, R.P., Lemke, R.L., Wang, H., Yang, C., 2012a. Carbon footprint of spring wheat in response to fallow frequency and soil carbon changes over 25 years on the semiarid Canadian prairie. *Eur. J. Agron.* 43, 175–184. doi :10.1016/j.eja.2012.07.004.
- Gan, Y., Liang, C., Huang, G., Malhi, S.S., Brandt, S.A., Katema-Mupondwa, F., 2012b. Carbon footprint of canola and mustard is a function of the rate of N fertilizer. *Int. J. Life Cycle Assess.* 17, 58–68. doi :10.1007/s11367-011-0337-z.
- Gan, Y., Siddique, K.H.M., Turner, N.C., Li, X.G., Niu, J.Y., Yang, C., Liu, L., Chai, Q., 2013. Ridge-furrow mulching systems—an innovative technique for boosting crop productivity in semiarid rain-fed environments. *Adv. Agron.* 118, 429–476.
- García Del Moral, L.F., García Del Moral, M.B., Molina-Cano, J.L., Slafer, G.A., 2003. Yield stability and development in two- and six-rowed winter barleys under Mediterranean conditions. *Field Crop Res.* 81, 109–119.

- Geng, Y., Mitchell, B., Tsuyoshi, F., Nakayama, T., 2010. Perspectives on small watershed management in China: the case of Biliu. *Int. J. Sust. Dev. World* 17, 172–179.
- Gleick, P.H., Palaniappan, M., 2010. Peak water limits to freshwater withdrawal and use. *Proc. Natl. Acad. Sci. U.S.A.* 107, 11155–11162.
- Graterol, Y.E., Eisenhauer, D.E., Elmore, R. W., 1993. Alternate-furrow irrigation for soybean production. *Agric. Water Manage.* 24, 133–145.
- Hassan, F.U., Ahmad, M., Ahmad, N., Abbasi, M.K., 2007. Effects of subsoil compaction on yield and yield attributes of wheat in the sub-humid region of Pakistan. *Soil. Till. Res.* 96, 361–366.
- He, J., Kuhn, N.J., Zhang, X.M., Zhang, X.R., Li, H.W., 2009. Effects of 10 years of conservation tillage on soil properties and productivity in the farming-pastoral ecotone of inner Mongolia, China. *Soil. Use Manage.* 25, 201–209.
- He, X.F., Cao, H., Li, F.M., 2007. Econometric analysis of the determinants of adoption of rainwater harvesting and supplementary irrigation technology (RHSIT) in the semiarid Loess Plateau of China. *Agric. Water Manage.* 89, 243–250.
- Hou, X., Li, R., Han, Q., Wang, W., Jia, Z., 2012a. Effects of different tillage patterns during summer fallow on soil water conservation and crop water use efficiency. *Trans. Chin. Soc. Agric. Eng.* 28, 94–100.
- Hou, X., Li, R., Jia, Z., Han, Q., Wang, W., Yang, B., 2012b. Effects of rotational tillage practices on soil properties, winter wheat yields and water-use efficiency in semi-arid areas of north-west China. *Field Crop Res.* 129, 7–13.
- Hu, C.S., Zhang, X.Y., Cheng, Y.S., Pei, D., 2002. An analysis on dynamics of water table and overdraft in the piedmont of Mt. Taihang. *Syst. Sci. Compr. Stud. Agric.* 18, 89–91.
- Hu, T., Yuan, L., Wang, J., Kang, S., Li, F., 2010. Antioxidation responses of maize roots and leaves to partial root-zone irrigation. *Agric. Water Manage.* 98, 164–171.
- Huang, G.B., Chai, Q., Feng, F.X., Yu, A.Z., 2012a. Effects of different tillage systems on soil properties, root growth, grain yield, water use efficiency of Winter wheat (*Triticum aestivum* L.) in arid northwest China. *J. Integ. Agric.* 11, 1286–1296.
- Huang, G.B., Guo, Q.Y., Zhang, R.Z., Pang, L., Li, G., Chan, K.Y., Yu, A.Z., 2006. Effects of conservation tillage on soil moisture and crop yield in a phased rotation system with spring wheat and field pea in dryland. *Acta Ecol. Sin.* 26, 1176–1185.
- Huang, Y.H., Jiang, D., Zhuang, D.F., Wang, J.H., Yang, H.J., Ren, H.Y., 2012b. Evaluation of relative water use efficiency (RWUE) at a regional scale: a case study of Tuhai-Majia Basin, China. *Water Sci. Technol.* 66, 927–933.
- Ishaq, M., Hassan, A., Saeed, M., Ibrahim, M., Lal, R., 2001. Subsoil compaction effects on crops in Punjab, Pakistan. I. Soil physical properties and crop yield. *Soil. Till. Res.* 59, 57–65.
- Jia, Y., Li, F.M., Wang, X.L., Yang, S.M., 2006. Soil water and alfalfa yields as affected by alternating ridges and furrows in rainfall harvest in a semiarid environment. *Field Crop Res.* 97, 167–175.
- Jiang, T., Zhang, Q., 2004. Climatic changes driving on floods in the Yangtze Delta, China during 1000–2002. *CyberGeo*, 296.
- Jin, H., Hongwen, L., Kuhn, N.J., Xuemin, Z., Wenying, L., 2007. Soil loosening on permanent raised-beds in arid northwest China. *Soil. Till. Res.* 97, 172–183.
- Jung, J., O'Donoghue, E.M., Dijkwel, P.P., Brummell, D.A., 2010. Expression of multiple expansin genes is associated with cell expansion in potato organs. *Plant Sci.* 179, 77–85.
- Kang, S., Liang, Z., Hu, W., Zhang, J., 1998. Water use efficiency of controlled alternate irrigation on root-divided maize plants. *Agric. Water Manage.* 38, 69–76.
- Kang, S., Liang, Z., Pan, Y., Shi, P., Zhang, J., 2000. Alternate furrow irrigation for maize production in an arid area. *Agric. Water Manage.* 45, 267–274.
- Kang, S.Z., Xu, D., Li, W.H., Li, M., 2002. Some thinking on the basic principle and key technology of water-saving in agriculture and ecology in arid and semiarid areas of Northwest China. *Bull. Nat. Nat. Sci. Foundat. China* 5, 274–278.

- Kobata, T., Palta, J.A., Turner, N.C., 1992. Rate of development of postanthesis water deficits and grain filling of spring wheat. *Crop Sci.* 32, 1238–1242.
- Kwiatkowska, D., 2008. Flowering and apical meristem growth dynamics. *J. Exp. Bot.* 59, 187–201.
- Li, F., Liang, J., Kang, S., Zhang, J., 2007a. Benefits of alternate partial root-zone irrigation on growth, water and nitrogen use efficiencies modified by fertilization and soil water status in maize. *Plant Soil* 295, 279–291.
- Li, F., Wei, C., Zhang, F., Zhang, J., Nong, M., Kang, S., 2010. Water-use efficiency and physiological responses of maize under partial root-zone irrigation. *Agric. Water Manage.* 97, 1156–1164.
- Li, H., Zheng, L., Lei, Y., Li, C., Liu, Z., Zhang, S., 2008. Estimation of water consumption and crop water productivity of winter wheat in North China Plain using remote sensing technology. *Agric. Water Manage.* 95, 1271–1278.
- Li, J., Inanaga, S., Li, Z., Eneji, A.E., 2005. Optimizing irrigation scheduling for winter wheat in the North China Plain. *Agric. Water Manage.* 76, 8–23.
- Li, L.L., Huang, G.B., Zhang, R.Z., Bill, B., Guangdi, L., Kwong, Y.C., 2011. Benefits of conservation agriculture on soil and water conservation and its progress in China. *Agric. Sci. China* 10, 850–859.
- Li, R., Hou, X., Jia, Z., Han, Q., Ren, X., Yang, B., 2013. Effects on soil temperature, moisture, maize yield of cultivation with ridge and furrow mulching in the rainfed area of the Loess Plateau, China. *Agric. Water Manage.* 116, 101–109.
- Li, X., Su, D., Yuan, Q., 2007b. Ridge-furrow planting of alfalfa (*Medicago sativa* L.) for improved rainwater harvest in rainfed semiarid areas in Northwest China. *Soil. Till. Res.* 93, 117–125.
- Li, X.Y., Gong, J.D., Gao, Q.Z., Li, F.R., 2001. Incorporation of ridge and furrow method of rainfall harvesting with mulching for crop production under semiarid conditions. *Agr. Water Manage.* 50, 173–183.
- Li, X.Y., Liu, L.Y., 2003. Effect of gravel mulch on aeolian dust accumulation in the semiarid region of northwest China. *Soil. Till. Res.* 70, 73–81.
- Liang, H., Li, F., Nong, M., 2013. Effects of alternate partial root-zone irrigation on yield and water use of sticky maize with fertigation. *Agric. Water Manage.* 116, 242–247.
- Liang, Z., Kang, S., Shi, P., 2000. Effect of alternate furrow irrigation on maize production, root density and water-saving benefit. *Sci. Agric. Sin.* 33, 26–32.
- Lin, X., Scranton, M.I., Chistoserdov, A.Y., Varela, R., Taylor, G.T., 2008. Spatiotemporal dynamics of bacterial populations in the anoxic Cariaco Basin. *Limnol. Oceanogr.* 53, 37–51.
- Liu, C.A., Li, F.R., Zhou, L.M., Zhang, R.H., Yu, J., Lin, S.L., Wang, L.J., Siddique, K.H.M., Li, F.M., 2013. Effect of organic manure and fertilizer on soil water and crop yields in newly-built terraces with loess soils in a semi-arid environment. *Agric. Water Manage.* 117, 123–132.
- Liu, J., Hua, W., Yang, H.L., Zhan, G.M., Li, R.J., Deng, L.B., Wang, X.F., Liu, G.H., Wang, H.Z., 2012. The BnGRF2 gene (GRF2-like gene from *Brassica napus*) enhances seed oil production through regulating cell number and plant photosynthesis. *J. Exp. Bot.* 63, 3727–3740.
- Liu, J., Ma, Y., 1998. Characteristic, protection and utilization of water resources in arid regions in Northwest China. *Agric. Res. Arid Areas* 16, 103–107.
- Liu, X., Ai, Y., Zhang, F., Lu, S., Zeng, X., Fan, M., 2005. Crop production, nitrogen recovery and water use efficiency in rice-wheat rotation as affected by non-flooded mulching cultivation (NFMC). *Nutr. Cycl. Agroecosys.* 71, 289–299.
- Liu, Y.H., 2006. The chinese ministry of science and technology of rural and social development division. In: *The Development Strategies on Water-saving Agriculture in China*. Chinese Agric. Sci. Tech. Press, Beijing.
- Lu, S.Y., Chen, S.M., Chen, S.P., Guo, Z.F., 2003. Effects of ABA, paclobutrazol and uniconazole on the drought resistance of bermudagrass. *Acta Prata. Sin.* 12, 100–104.

- Luo, L.J., 2010. Breeding for water-saving and drought-resistance rice (WDR) in China. *J. Exp. Bot.* 61, 3509–3517.
- Ma, S.C., Li, F.M., Yang, S.J., Li, C.X., Xu, B.C., Zhang, X.C., 2013. Effects of root pruning on non-hydraulic root-sourced signal, drought tolerance and water use efficiency of winter wheat. *J. Integ. Agric.* 12, 989–998.
- Mu, Y.P., Chai, Q., Yu, A.Z., Yang, C.H., Qi, W.H., Feng, F.X., Kong, X.F., 2013. Performance of wheat/maize intercropping is a function of belowground interspecies interactions. *Crop Sci.* 53, 2186–2194. Doi:10.2135/cropsci2012.11.0619.
- Niu, J.Y., Gan, Y.T., Huang, G.B., 2004. Dynamics of root growth in spring wheat mulched with plastic film. *Crop Sci.* 44, 1682–1688.
- Pan, N., Shen, H., Wu, D.M., Deng, L.S., Tu, P.F., Gan, H.H., Liang, Y.C., 2011. Mechanism of improved phosphate uptake efficiency in banana seedlings on acidic soils using fertigation. *Agric. Water Manage.* 98, 632–638.
- Pheloung, P.C., Siddique, K.H.M., 1991. Contribution of stem dry matter to grain yield in wheat cultivars. *Aus. J. Plant Physiol.* 18, 53–64.
- Qin, H.L., Gao, W.S., Ma, Y.C., Ma, L., Yin, C.M., Chen, Z., Chen, C., 2008. Effects of subsoiling on soil moisture under no-tillage for two years. *Agric. Sci. China* 7, 88–95.
- Qu, Y., Su, W., Panpan, Z., Li, C., Jinfeng, G., Xiaoli, G., Pengke, W., Shuhuai, J., Baili, F., 2012. Effects of different water harvesting on soil water, growth and yield of the proso millet (*Panicum miliaceum* L.) in a semiarid region of northwest China. *J. Agr. Sci.* 4, 106–113.
- Ren, X., Chen, X., Jia, Z., 2009. Ridge and furrow method of rainfall concentration for fertilizer use efficiency in farmland under semiarid conditions. *Appl. Eng. Agric.* 25, 905–913.
- Ren, X., Jia, Z., Chen, X., 2008. Rainfall concentration for increasing corn production under semiarid climate. *Agric. Water Manage.* 95, 1293–1302.
- Shalizi, Z., 2006. Addressing China's Growing Water Shortages and Associated Social and Environmental Consequences. World Bank, Washington D. C., USA.
- Shen, J., Li, C., Mi, G., Li, L., Yuan, L., Jiang, R., Zhang, F., 2013. Maximizing root/rhizosphere efficiency to improve crop productivity and nutrient use efficiency in intensive agriculture of China. *J. Exp. Bot.* 64, 1181–1192.
- Siddique, K.H.M., 2004. Water deficits: development. *Encycl. Plant Crop Sci.*, 1284–1287.
- Siddique, K.H.M., Johansen, C., Turner, N.C., Jeuffroy, M.H., Hashem, A., Sakar, D., Gan, Y., Alhgamdi, S.S., 2012. Innovations in agronomy for food legumes. A review. *Agron. Sust. Dev.* 32, 45–64.
- Sivakumar, B., 2011. Water crisis: from conflict to cooperation—an overview. *Hydrol. Sci. J.* 56, 531–552.
- Song, S., Wang, Y., 2002. Molecular response of plant to drought stress. *China Agr. Econ. Rev.* 13, 1037–1044.
- Sun, H., Shen, Y., Yu, Q., Flerchinger, G.N., Zhang, Y., Liu, C., Zhang, X., 2010. Effect of precipitation change on water balance and WUE of the winter wheat-summer maize rotation in the North China Plain. *Agric. Water Manage.* 97, 1139–1145.
- Todorovic, M., 2005. Crop water requirements. *Water Encycl.*, 557–558.
- Turner, N.C., 2001. Optimising water use. In: Geiger, H.H., Struik, P.C. (Eds.), *Crop Science: Progress and Prospects*. CABI Publishing, Wallingford, UK, pp. 119–135.
- Turner, N.C., 2004. Agronomic options for improving rainfall-use efficiency of crops in dryland farming systems. *J. Exp. Bot.* 55, 2413–2425.
- Turner, N.C., 2011. More from less – improvements in precipitation use efficiency in Western Australian wheat production. In: Tow, P., Cooper, I., Partridge, I., Birch, C. (Eds.), *Rainfed Farming Systems*. Springer, Dordrecht, Heidelberg, London, New York, pp. 777–790.
- Turner, N.C., Rao, K.P.C., 2013. Simulation analysis of factors affecting sorghum yield at selected sites in eastern and southern Africa, with emphasis on increasing temperatures. *Agr. Syst.* 121, 53–62.
- Turner, N.C., Wright, G.C., Siddique, K.H.M., 2001. Adaptation of grain legumes (pulses) to water-limited environments. *Adv. Agron.* 71, 193–231.

- Wachong Castro, V., Heerink, N., Shi, X., Qu, W., 2010. Water savings through off-farm employment? *China Agr. Econ. Rev.* 2, 167–184.
- Wang, H., Liu, C., 2003. Experimental study on crop photosynthesis, transpiration and high efficient water use. *China Agr. Econ. Rev.* 14, 1632–1636.
- Wang, H., Liu, F., Andersen, M.N., Jensen, C.R., 2009. Comparative effects of partial root-zone drying and deficit irrigation on nitrogen uptake in potatoes (*Solanum tuberosum* L.). *Irrig. Sci.* 27, 443–448.
- Wang, H.X., Li, Y.Y., Ren, T.Z., Pang, H.C., 2011. Effects of different irrigation modes in winter wheat growth season on the grain yield and water use efficiency of winter wheat–summer maize. *China Agr. Econ. Rev.* 22, 1759–1764.
- Wang, J., Li, D.Q., Gu, L.S., 2002. The response to water stress of the antioxidant system in maize seedling roots with different drought resistance. *Acta Bot. Boreali-Occident. Sin.* 22, 285–290.
- Wang, X.L., Li, F.M., Jia, Y., Shi, W.Q., 2005. Increasing potato yields with additional water and increased soil temperature. *Agric. Water Manage.* 78, 181–194.
- Wang, Y., Cai, H., Zhang, X., Gao, H., Sun, X., 2006. Effects of root-divided alternative irrigation on physiological characteristics and yield of flue-cured tobacco. *Agric. Res. Arid Areas* 24, 93–98.
- Wang, Y.B., Wu, P.T., Zhao, X.N., Li, J.L., Lv, L., Shao, H.B., 2010. The optimization for crop planning and some advances for water-saving crop planning in the semiarid loess plateau of China. *J. Agron. Crop Sci.* 196, 55–65.
- Wei, Y., Guangrong, D., Yujiang, Y., Yingjie, M., 2000. Climate instability in the Yili region, Xinjiang during the last glaciation. *Chin. Sci. Bull.* 45, 1604–1609.
- Xie, R.Z., Li, S.K., Li, X.J., Jin, Y.Z., Wang, K.R., Chu, Z.D., Gao, S.J., 2007. The analysis of conservation tillage in China-conservation tillage and crop production: reviewing the evidence. *Sci. Agric. Sin.* 40, 1914–1924.
- Xie, T., Liu, X., Sun, T., 2011. The effects of groundwater table and flood irrigation strategies on soil water and salt dynamics and reed water use in the Yellow River Delta, China. *Ecol. Model* 222, 241–252.
- Xie, Z.K., Wang, Y.J., Li, F.M., 2005. Effect of plastic mulching on soil water use and spring wheat yield in arid region of northwest China. *Agric. Water Manage.* 75, 71–83.
- Xin, Z., Yu, X., Li, Q., Lu, X.X., 2011. Spatiotemporal variation in rainfall erosivity on the Chinese Loess Plateau during the period 1956–2008. *Reg. Environ. Change* 11, 149–159.
- Xiong, J., Wu, B., Zhou, Y., Li, J., 2006. Estimating evapotranspiration using remote sensing in the Haihe basin. *IGARSS*, 1044–1047.
- Xu, H.Y., Zhou, Q.W., Yang, M.C., 1995. The effect of PP333 on drought resistance in wheat seedlings. *Acta Agron. Sin.* 21, 124–128.
- Yang, H., Zhang, X., Zehnder, A.J.B., 2003. Water scarcity, pricing mechanism and institutional reform in northern China irrigated agriculture. *Agric. Water Manage.* 61, 143–161.
- Yu, L.P., Huang, G.H., Liu, H.J., Wang, X.P., Wang, M.Q., 2010. Effects of sprinkler irrigation amount on winter wheat growth, water consumption, water use efficiency. *China Agr. Econ. Rev.* 21, 2031–2037.
- Zeng, Z., Liu, J., Koenenman, P.H., Zarate, E., Hoekstra, A.Y., 2012. Assessing water footprint at river basin level: a case study for the Heihe River Basin in northwest China. *Hydrol. Earth Syst. Sci.* 16, 2771–2781.
- Zhang, G.H., Shen, J.M., Zhang, C.Y., Liu, S.Y., 2006. Characteristic of variations of surface runoff and groundwater recharge in the middle Heihe River valley, northwestern Gansu, China. *Geol. Bull. China.* 25, 251–255.
- Zhang, J., 2007a. Barriers to water markets in the Heihe River basin in northwest China. *Agric. Water Manage.* 87, 32–40.
- Zhang, J., Sui, X., Li, B., Su, B., Li, J., Zhou, D., 1998. An improved water-use efficiency for winter wheat grown under reduced irrigation. *Field Crop Res.* 59, 91–98.

- Zhang, J., Tardieu, F., 1996. Relative contribution of apices and mature tissues to ABA synthesis in droughted maize root systems. *Plant Cell. Physiol.* 37, 598–605.
- Zhang, M., Duan, L., Tian, X., He, Z., Li, J., Wang, B., Li, Z., 2007. Uniconazole-induced tolerance of soybean to water deficit stress in relation to changes in photosynthesis, hormones and antioxidant system. *J. Plant Physiol.* 164, 709–717.
- Zhang, Q., 2007b. Strategies for developing green super rice. *Proc. Natl. Acad. Sci. U.S.A.* 104, 16402–16409.
- Zhang, T., Huang, G.B., Han, Z.M., 2005. Arid Inland (Zhangye) River Irrigation-Saving Technology Systems Integration and Demonstration in Northwest China. A 863 State Project Report. pp. 48. The People's Republic of China ministry of Science and technology, Beijing.
- Zhang, Y., Shen, Y., Sun, H., Gates, J.B., 2011. Evapotranspiration and its partitioning in an irrigated winter wheat field: a combined isotopic and micrometeorologic approach. *J. Hydrol.* 408, 203–211.
- Zhang, Y., Yuan, Y., Liu, Q., 2001. Proceedings on cultivar improvement and biotechnology in *Lilium*. *J. Beijing For. Univ.* 23, 56–59.
- Zhang, Z., Cai, M., 2001. Effect of underground water on ground stress measurement. *Metal. Mine* 11, 42.
- Zhou, J.B., Wang, C.Y., Zhang, H., Dong, F., Zheng, X.F., Gale, W., Li, S.X., 2011. Effect of water saving management practices and nitrogen fertilizer rate on crop yield and water use efficiency in a winter wheat-summer maize cropping system. *Field Crop Res.* 122, 157–163.

This page intentionally left blank



The Physiology of Potassium in Crop Production

Derrick M. Oosterhuis^{*,1}, Dimitra A. Loka^{*},

Eduardo M. Kawakami^{*} and William T. Pettigrew[†]

^{*}University of Arkansas, Department of Crop, Soil and Environmental Sciences, Fayetteville, AR, USA

[†]ARS-USDA, Stoneville, MS, USA

¹Corresponding author: e-mail address: oosterhu@uark.edu

Contents

1. Introduction	204
2. Physiology of Potassium Nutrition	204
2.1 Enzyme and Organic Compound Synthesis Regulation	205
2.2 Water Relations	206
2.3 Leaf Movements	208
2.4 Meristematic Growth and Plant Growth Regulation	209
2.5 Stomatal Regulation	211
2.6 Photosynthesis	212
2.7 Respiration	214
2.8 Assimilate Transport	214
2.9 Nitrate Transport–Potassium Interactions	215
2.10 Potassium Channels	217
3. Stress Mitigation	218
3.1 Drought Stress	218
3.2 Cold Stress	219
3.3 Salt Stress	220
3.4 Biotic Stress	221
3.5 Potassium and Stress Signaling	222
4. Summary	223
References	223

Abstract

Potassium (K) plays a major role in the basic functions of plant growth and development. In addition, K is also involved in numerous physiological functions related to plant health and tolerance to biotic and abiotic stress. However, deficiencies occur widely resulting in poor growth, lost yield, and reduced fiber quality. This review describes the physiological functions of K and the role in stress relief and also provides some agronomic aspects of K requirements, diagnosis of soil and plant potassium status, and amelioration. The physiological processes described include enzymes and

organic compound synthesis regulation, water relations and stomates, photosynthesis, transport, cell signaling, and plant response to drought stress, cold stress, salt stress, as well as biotic stresses.



1. INTRODUCTION

Potassium (K) is the mineral element, next to nitrogen, required in the largest amount by plants. For optimal growth and productivity, modern crop production requires a large amount of K, particularly during reproductive development. The K requirement for optimal plant growth is 2–5% of the plant dry weight (Marschner, 1995), however, the amount of K utilized by the crop varies depending on the crop species, and the quantity of K⁺ in the soil available to the plants. Additionally, K uptake is influenced by the environmental conditions during the growing season and the management practices used (Mullins et al., 1997). Proper plant nutrition for optimal crop productivity requires that nutrient deficiencies be avoided. However, potassium deficiencies have been reported to occur all around the world for a variety of reasons such as soil types and management practices (Rengel and Damon, 2008), or removal of crop residues for use in the biofuel industry (Romhel and Kirkby, 2010). In addition, even though farmers in the USA and elsewhere are using substantially more commercial fertilizer than 40 years ago the ratio of nitrogen: potassium input has been significantly decreased from 100:63 in 1960 to 100:27 in 2000 (Maene, 2001). This has prompted a renewed focus on K management with some emphasis on understanding K fertilizer requirements and use by the plants. An efficient fertilizer regime requires an accurate knowledge of the nutrient status of the soil, as well as a reliable tissue analysis during the season to fine-tune the fertility status and avoid any unforeseen deficiencies. Fundamental to this is an understanding of the role of the nutrient in plant metabolism and yield formation. This review provides an overview of the physiology of K nutrition in crop growth, and provides an overview of K fertility requirements and deficiency symptoms in field crops.



2. PHYSIOLOGY OF POTASSIUM NUTRITION

Potassium (K) is the most abundant cation in the plant cells, with high mobility within short-distance transport (i.e., between individual cells and between neighbor tissues), as well as within long distance translocation through the xylem and phloem (Marschner, 1995). Since K is not

metabolized into organic compounds in the plant, K is predominately present in the cationic form (Wyn Jones et al., 1979). Potassium can be stored, both in the cell cytoplasm and vacuole, and the distribution among these two locations is the major factor for determining the K function in the plant (Marschner, 1995). These characteristics convey K as a major nutrient responsible for controlling many physiological and biochemical processes in the plant, such as enzyme activation, cell osmotic potential regulation, soluble and insoluble molecular anions neutralization, and cell pH stabilization (Marschner, 1995). This section of this review will summarize the role of K in a few key aspects of plant physiology.

2.1 Enzyme and Organic Compound Synthesis Regulation

In the plant, K is responsible for activation and/or stimulation of a number of enzymes (Suelter, 1970). The activation of enzymes is resulted from a change in the conformation of the inactive enzyme structure caused by a ligation of K to a specific site in the protein (Marschner, 1995). Potassium availability has an influence in the activity of more than 60 enzymes (Wyn Jones and Pollard, 1983) involved in a variety of metabolic process as mainly related to protein and carbohydrates synthesis (Marschner, 1995; Mengel et al., 2001).

The optimum concentration of K for maximum enzyme activation is about 50 mM (Nitsos and Evans, 1969). However cytoplasmic concentration of K is known to be between 100 and 200 mM (Leigh and Wyn Jones, 1984) in order to optimize protein synthesis in the cell (Wyn Jones et al., 1979). For this reason, cytoplasmic K concentration is maintained constant by the pool of K in the vacuole (Leigh and Wyn Jones, 1984; Walker et al., 1996), and changes in the level of cytoplasmic K will be observed only when vacuolar K concentration has been depleted to a minimal vital concentration (Walker et al., 1996). The importance of K in protein synthesis is clear when a decrease in N incorporation into protein is exhibited by K deficient plants (Marschner, 1995; Mengel et al., 2001). Amino acid polymerization is one of the main steps where K has been shown to regulate protein turnover in plants (Conway, 1964). In the review of Mengel et al. (2001), a K effect on ribulose biphosphate carboxylase activity, nitrate reduction process, and ribosome polypeptide syntheses have been described. Furthermore Marschner (1995) reported a central role of K in the translation process, and activity and synthesis of nitrate reductase.

In carbohydrates synthesis, K has been reported to affect a number of enzymes including, glucose starch synthase (Hawker et al., 1974, 1979), glucose pyrophosphorylase (Hawker et al., 1979), β -amylase (Berg et al., 2009),

sucrose synthase (Berg et al., 2009), invertase (Ward, 1960), amylase (Li et al., 1997), phosphofructokinase (Lauchli and Pfluger, 1978), pyruvate kinase (Memon et al., 1985; Matoh et al., 1988). Among all enzymes affected by K availability, pyruvate kinase is probably the most important. Pyruvate kinase has a central role in plant metabolism because it regulates the conversion of phosphoenol pyruvate to pyruvate (Kayne, 1973). Armengaud et al. (2009), studying the effect of K nutrition in *Arabidopsis* roots, observed that despite the fact that a number of enzymes involved in the glycolysis and N assimilation processes were regulated by K, the primary effect of low K availability on metabolic disorders were directly related to inhibition of pyruvate kinase activity. The central role of K on carbohydrates synthesis has been described to be the main reasons for the presence of high concentration of reducing sugars, and low starch content in K deficient plants (Marschner, 1995; Amtmann et al., 2008). In cotton, K fertilization increased leaf protein content (Akhtar et al., 2009), and decreased leaf starch (Bednarz and Oosterhuis, 1999; Akhtar et al., 2009) and sucrose (Zhao et al., 2001). Similarly, Pettigrew (1999) reported that K application decreased leaf glucose, root starch, root glucose, and root fructose content. This effect on carbohydrates was possibly due to an increase in metabolites utilization and translocation (Bednarz and Oosterhuis, 1999). The effect of K on phloem translocation will be discussed in more details later in this review.

2.2 Water Relations

Potassium plays an integral role in plant–water relations (Hsiao and Läuchli, 1986) and is involved in numerous physiological functions within the plant where water is involved including stomatal opening and closing, assimilate translocation, enzyme activation, and leaf heliotropic movements. Water potential, the thermodynamic energy status of water, is well recognized as an indicator of plant–water status (Begg and Turner, 1976). Water potential consists of various components, the main ones being osmotic potential and pressure potential. The magnitude of these two components regulates water potential.

While organic compounds synthesis is regulated by cytoplasmic K concentration, water potential is mainly affected by K concentration in the cell vacuole (Hsiao and Lauchi, 1986). Potassium salts (e.g., KNO_3 , KCl , K-malate) are the common forms of K in the vacuoles, which have a major role in regulating cell osmotic potential in order to maintain adequate turgor pressure for cell functioning (MacRobbie, 1977). The K content in the vacuole has a sole purpose of “biophysical” regulation, and no biochemical functions have been described (Leigh and Wyn Jones, 1984). Potassium is the

most important vacuolar solute that regulates cell osmoregulation process (Mengel and Arneke, 1982; Beringer et al., 1986; Morgan, 1992). However, in contrast with the cytoplasmic pool, the vacuolar K can be replaced by other solutes, i.e., Na (Bednarz and Oosterhuis, 1999), Mg, and amino acids for maintenance of vital water potential values, when K availability is low (Leigh and Wyn Jones, 1984). Vacuolar K content can be variable, ranging from 9 to 174 mM depending on plant species and growing medium (Hsiao and Lauchi, 1986). Leigh and Wyn Jones (1984) reported that the critical minimum concentration of K in the vacuole is about 10–20 mM, and if vacuolar K concentration falls below these values an effect in the cytoplasmic K pool can occur resulting in disruption of vital metabolic processes (i.e., enzyme activation and protein synthesis). In cotton, K fertilization was reported to increase turgor pressure and decrease water and osmotic potential values (Pervez et al., 2004). Pettigrew (1999) observed that application of K to cotton plants resulted in an increase of 17% in turgor pressure, and did not affect water and osmotic potential of leaf tissues.

Another important aspect of K in regulating plant–water relation attributes is the possible role of K in cell osmotic adjustment. Osmotic adjustment is the process of increasing solute concentration in the cell vacuole in order to maintain lower values of water potential during periods of salinity and/or water deficit stress (Hsiao et al., 1976; Morgan, 1984; Taiz and Zeigler, 2010). In water-stressed cotton, although osmotic adjustment is known to occur both in leaf and root tissue, a greater effect was observed in roots compared to leaves (Oosterhuis and Wullshleger, 1987). Potassium ions have been reported to accumulate under water and/or salinity stress in different crops, such as sorghum (*Sorghum bicolor*) (Weimberg et al., 1982), sunflower (*Helianthus annuus*, L.) (Jones et al., 1980), beans (*Vicia faba* L.) (Mengel and Arneke, 1982), and annual clovers (*Trifolium* sp.) (Iannucci et al., 2002). Morgan (1992) observed that 78% of the osmotic adjustment in water-stressed wheat (*Triticum aestivum* L.) plants was attributed to K, and only 22% to organic solutes. In water-stressed chickpeas (*Cicer arietinum*), K importance in regulation of osmotic adjustment processes decreased with plant age (Moinuddin and Imas, 2007). In contrast, K does not appear to play a major role in osmotic adjustment of cotton plants. In an early study of Cutler and Rains (1978), K concentration did not change with water potential of drought stressed cotton; in this case organic solutes (i.e., soluble sugars and malate) were the main regulator of the osmoregulation process. Similarly, Stark (1991) observed that although K accumulated in leaves of salt-stressed cotton plants, K by itself was not a precondition for osmotic

adjustment regulation. Results of no effect of K on osmotic adjustment have also been reported in millet (*Pennisetum glaucum*) (Ashraf et al., 2002), maize (*Zea mays* L.) (Sharp et al., 1990), sorghum (Turner et al., 1978), and panic grass (*Panicum scribnerianum*) (Ford and Wilson, 1981). However, K has been reported to stimulate osmotically active solute, such as malate (Beringer, 1978 cited by Moinuddin and Imas, 2007) and proline (Weimberg et al., 1982), thus it is likely that K can also indirectly affect osmotic adjustment of plants.

2.3 Leaf Movements

Certain plants exhibit reversible leaf movements in response to environmental conditions (Satter and Galston, 1973). Leaf movements (paraheliotropic) in leguminous crops have been well documented (Kawashima, 1969; Oosterhuis et al., 1985; Berg and Heuchlin, 1990), and have also been reported in other crops such as cotton (diaheliotropic) (Miller, 1975). The organ of movement of the leaf is the pulvinus (or the pulvinule of a leaflet) situated at the point where the petiole joins the leaflet lamina (Satter and Galston, 1981). Differential changes in osmotic potential in different parts of the pulvinus have been used to explain the movements (Carlson, 1973; Gorton, 1987). Leaf movements in *Albizzia* and *Samanea* are apparently controlled by differential turgor changes in the pulvinal motor cells (Satter and Galston, 1981) which, in turn, appear to be a consequence of K^+ flux into and out of the pulvinus (Satter and Galston, 1973; Schrempf et al., 1976). Oosterhuis and Walker (1984) reported that the bending and straightening of soybean (*Glycine max*) leaflets under conditions of water stress were due to differential changes in osmotic potential (Ψ_s) and turgor (Ψ_p) in the ventral and dorsal sides of the pulvinule associated with changes in K concentration. The greatest change in Ψ_s and Ψ_p was shown to coincide with the maximum rate of change in leaflet angle with the onset of water stress. They suggested that under conditions of water stress K^+ flux may have the role of regulating movements of the leaflet by inducing changes in turgor in opposing sides of the pulvinule. Ion channels are understood to be the conduits for the movement of K^+ (Koller, 2000), and water channels (aquaporins) serve as the water conduits through the pulvinule cell membranes (Moshelion et al., 2002; Uehlein and Kaldenhoff, 2008).

The importance of K in the regulation of cell osmotic potential and subsequently turgor pressure, results in an indirect effect of K in other physiological processes, such as cell growth, stomata movement, and photosynthesis, which will be discussed in more details throughout this review.

2.4 Meristematic Growth and Plant Growth Regulation

Potassium is essential for cell growth, a vital process for adequate plant functioning and development (Marschner, 1995; Hepler et al., 2001). The most acceptable concept for plant cell elongation is known as the acid growth. This theory involves three different processes: acid-induced cell wall loosening, osmoregulation, cell wall synthesis, and deposition (Rayle and Cleland, 1992). The cell growth is initiated with an acidification of the cell apoplast that triggers cell wall loosening and activation of hydrolyzing enzymes (Hager et al., 1971). This acid stimulus is regulated by the ATPase in the plasmalemma that pumps H^+ from the cytoplasm to the apoplast. The role of K in this process is to stimulate and control the ATPase cycle in the cell (Mengel et al., 2001). Potassium has been reported to stimulate ATPase in chloroplast inner envelope vesicles (Shingles and McCarty, 1994) and to regulate the activity of ATPase by controlling the dephosphorylation of subunit in the ATPase structure (Buch-Pedersen et al., 2006). The importance of osmoregulation in cell growth is to regulate wall stress relaxation in the cell (Taiz and Zeiger, 2010) and the role of K on cell osmoregulation was described above. The major constraint for cell growth is the rigid cell wall, and without wall stress relaxation, the cell growth would only result in thicker cell walls. The stress relaxation is responsible for a mechanical cell expansion, and it is regulated by high turgor pressure that is caused by water intake, due to a decrease in osmotic potential (Taiz and Zeiger, 2010). The last steps for the cell growth process include cell wall synthesis and deposition. Cell walls are composed by cellulose, hemicellulose, lignin, pectin, and protein (Taiz and Zeiger, 2010). As previously mentioned, K is important for carbohydrates and protein synthesis, thus K can indirectly affect cell growth by regulating the production of major components utilized in cell wall metabolism. Furthermore, K can also affect the availability of cell wall constituents by regulating phloem transport, this effect will be discussed later in the review. In addition to being one of the cell wall components, proteins can also be responsible for regulating the acid-induced cell wall loosening process (Taiz and Zeiger, 2010).

Another important role of K in cell growth is the regulation of plant growth regulators (Mengel et al., 2001). Auxin (IAA) activity is the primary controller of the acid growth process (Rayle and Cleland, 1992). However, IAA-induced cell elongation is dependent of protein synthesis (Cocucci and Rosa, 1980), since K regulates cell protein turnover, the occurrence of a combined effect between K and IAA can exist. Claussen et al. (1997), studying the relationship between K channels and IAA, observed that the

IAA-induced cell growth in maize did not occur in the absence of K^+ ions. Furthermore, an effect of IAA on K channel activity has also been reported (Thiel and Weise, 1999). A synergistic effect between gibberellin (GA) and K has also been reported (Marschner, 1995). La Guardia and Benlloch (1980) observed that GA regulates plant remobilization of K and that stem elongation was favored when both GA and K were present. In grape fruits application of GA has been reported to increase the concentration of K in the fruit (Zhenming et al., 2008). In wheat, the presence of K has been reported to be indispensable for the GA induced stem elongation process (Chen et al., 2001). Similar results were observed by Nishizawa et al. (2002), in which they reported that K must be taken up from the soil, in order for wheat stem elongation to occur. Potassium has also been reported to affect the role of cytokinin in plants (Mengel et al., 2001). Green and Muir (1978) observed that the stimulation of cucumber cotyledons growth caused by cytokinin was enhanced by the presence of K. In contrast to K causing an increase in the growth response of cytokinin, K application has been reported to decrease ethylene evolution in cucumber seedlings (Green, 1983). Similarly, drought stressed sunflower grown in adequate levels of K exhibited a decrease in ethylene synthesis in comparison to plants under low K conditions (Benlloch-Gonzalez et al., 2010). Ethylene production appears to be important in the tolerance and regulation of K deficiency stress response in plants (Jung et al., 2009). Green and Muir (1979) studying the relationship among K, cytokinin, and abscisic acid (ABA) on cotyledon expansion, observed that both the cytokinin growth stimulation and ABA growth inhibition was higher with the presence of K. They concluded that the ABA growth inhibition was mediated by an interference in the uptake and accumulation of K in the plant. Furthermore, ABA has been reported to regulate the transport and accumulation of K in roots of higher plants (Roberts and Snowman, 1999); and also to decrease K uptake by inhibiting the K^+/H^+ ion exchange system (Watanabe and Takahashi, 1997). Other compounds, such as jasmonic acid (Ashley et al., 2006) and polyamines (Adams et al., 1990; Sarjala and Kaunisto, 1993) have also been reported to be affected by K availability. In addition, polyamines are also involved in the regulation of K channels (Kusano et al., 2008).

In cotton, the fiber development is probably the most evident process in which K affects cell growth. As previously mentioned, water potential regulation is an important event in cell growth. Dhindsa et al. (1975) reported that K and malate accounted for more than 50% of the fiber osmotic potential during fiber growth. They also observed that the level of K peaked when

fiber growth was the highest and that fiber growth was adversely affected by the absence of K. Similarly, Ruan et al. (2001) reported that high expression of K^+ transporters occurs during cotton fiber development. The K availability is known to have an influence in cotton growth, with effects on plant leaf area index (LAI), number of main stem nodes, plant height, and plant dry matter (Pettigrew and Merdith, 1997). Reddy and Zhao (2005) reported that K fertilization increased plant growth and biomass partitioning to fruits. Growth of cotton roots is also affected by K, Zhang et al. (2009) observed that lack of K decreased root growth, as a result of low IAA and high ethylene activity. Additional K effects on cotton growth have been described in different studies (Bednarz and Oosterhuis, 1999; Pettigrew, 1999, 2003; Zhao et al., 2001).

2.5 Stomatal Regulation

Stomatal functioning is important for providing CO_2 for photosynthesis while keeping water losses to a minimal level, thus the regulation of stomata opening and closing is crucial for efficient plant productivity. The mechanism of stomates movement is known to be regulated by turgor pressure, which is controlled mostly by K ion concentration (Marschner, 1995). The concentration of K on stomates guard cells, depending on plant species, can increase from 100 mM, when closed, to 800 mM, when opened (Taiz and Zeiger, 2010). A detailed explanation of the stomates activity has been described by Taiz and Zeiger (2010). In summary, light radiation into the plant cell activates three important metabolic processes involved in stomates opening: proton pump ATPase, solute uptake, and organic solute synthesis. The H^+ pumping ATPase creates an electrochemical potential that favor the uptake of K and the companion anions Cl^- and/or malate. The increase of these solutes and sucrose in the guard cell vacuole cause a decrease in the osmotic potential. Then, an uptake of water occurs, increasing turgor pressure, which results in stomate opening. In contrast, the closure of stomates is mainly regulated by ABA activity. In this process, the ABA stimulates Ca uptake into the cell, which blocks the K^+ channels and favors the extrusion of anions (Cl^-) into the cell apoplast. The increase in the intercellular Ca inhibits the proton pump ATPase, causing a depolarization in the cell membrane, resulting in extrusion of vacuolar and cytoplasmic K^+ to the cell apoplast. Thus, stomates close due to a decrease in turgor pressure, caused by high osmotic potential due to low intercellular solute concentration.

Recently, an unexpected role of K in plant stomatal regulation was described by [Benlloch-Gonzalez et al. \(2008\)](#). They observed that K deprivation increased stomatal conductivity of water-stressed plants. Report of increased water uptake and decreased water use efficiency under K deficiency also support this evidence ([Fournier et al., 2005](#)). However, since K is important in the stomatal opening process, the lack of K is expected to decrease, not increase, plant stomatal conductivity. An interaction effect between ABA and ethylene has been proposed to explain this behavior ([Benlloch-González et al., 2010](#)). As previously mentioned, ABA regulates stomatal closure and ethylene synthesis increases under K deficiency. Inhibition of stomatal closure caused by ethylene interference with the activity of ABA has been reported ([Tanaka et al., 2005](#)). [Benlloch-Gonzalez et al. \(2010\)](#) could not confirm this effect, but they observed that increased stomatal conductance in K deficient water-stressed plants disappeared with application of an ethylene synthesis inhibitor. They concluded that the high stomatal conductance under deprivation of K, could be a mechanism to increase xylem sap movement, in order to avoid K deficiency in the plant.

2.6 Photosynthesis

Potassium impacts photosynthesis of the crop canopy via two mechanisms: (1) solar radiation interception, and (2) photosynthesis per unit leaf area. Collectively, these two phenomenon regulate the pool of photo assimilates available for plant growth.

One of the more obvious consequences of plant growth under K deficient conditions is a reduction in the plant stature ([Cassman et al., 1989](#); [Ebelhar and Varsa, 2000](#); [Heckman and Kamprath, 1992](#); [Pettigrew and Meredith, 1997](#)). Accompanying this reduction in plant stature is an overall reduction in LAI ([Jordan-Meille and Pellerin, 2004](#); [Kimbrough et al., 1971](#); [Pettigrew and Meredith, 1997](#)) for the crop canopy. Reductions in both the overall number of leaves produced and in the size of individual leaves lead to this reduced overall LAI seen in K deficient conditions. Smaller size of the individual leaves was related to a reduced leaf area expansion as observed with soybean leaves ([Huber, 1985](#)) and maize ([Jordan-Meille and Pellerin, 2004](#)). This lower leaf area expansion under K deficient conditions is most likely related to the role potassium plays in lowering the osmotic potential and thereby raising the turgor pressure to drive cell expansion ([Dhindsa et al., 1975](#); [Mengel and Arneke, 1982](#)).

Not only is the sunlight intercepting leaf surface area diminished when plants are grown under K deficient conditions, but the rate of photosynthesis

per unit of that leaf surface area is also reduced (Bednarz et al., 1998; Huber, 1985; Longstreth and Nobel, 1980; Pier and Berkowitz, 1987; Wolf et al., 1976). Potassium impacts photosynthesis through influences on both stomatal and nonstomatal aspects of photosynthesis. The role that K plays in regulating stomatal aperture is well established and has previously been discussed in detail earlier in this chapter and therefore will not be dwelt within this section. This stomatal aperture regulation controls the flow of CO₂ into and the flow of H₂O vapor out of the intercellular spaces, thus affecting the level of CO₂ available at the reaction site for photosynthesis.

Nonstomatal factors can also be impacted by the potassium level to regulate the photosynthetic rate. Much of the nonstomatal potassium effects are tied into the role that potassium plays in photophosphorylation, rather than the effect that it has on the enzymes involved in carbon assimilation (Huber, 1985). Peoples and Koch (1979), however, reported reduced Rubisco activities caused by potassium deficiencies. Huber (1985) then countered and speculated that this response reported by Peoples and Koch (1979) was more due to reduced enzyme synthesis rather than reduce activity from the individual enzymes. This reduced photophosphorylation seen under K⁺ deficient conditions is related to an inner chloroplast membrane ATPase that maintains a high stromal pH needed for the efficient conversion from light energy to chemical energy by pumping protons out of the stroma into the cytosol while allowing K⁺ flux into the stroma (Berkowitz and Peters, 1993). An adequate potassium supply is critical for maintaining optimal activity of this ATPase (Shingles and McCarty, 1994). In addition, the reduced translocation of carbon assimilates out of the chloroplast (Ashley and Goodson, 1972; Mengel and Haeder, 1977; Mengel and Viro, 1974) could lead to feedback inhibition in the nonstomatal component of the photosynthetic process (Pettigrew, 2008; Cakmak, 2005). There is also evidence that plants not receiving adequate potassium levels can have an increased production of reactive oxygen species (ROS) in the photosynthetic tissue that can lead to photooxidative damage under higher light intensities (Cakmak, 2005). This decreased efficiency in processing excited electrons created by sunlight capture for K⁺ deficient plants is not surprising considering the overall reduced photosynthesis and photoassimilate transport exhibited by those plants.

Although both stomatal and nonstomatal photosynthetic factors can be impacted by the level of available potassium, the timing and extent of any potassium deficiency development can dictate which of these factors plays the predominant role in regulating the photosynthetic production.

For example, [Bednarz et al. \(1998\)](#) reported that during the early onset of a developing potassium deficiency, stomatal conductance was principle component regulating photosynthesis. However, as the potassium deficiency became more pronounced and extreme, nonstomatal or biochemical factors emerge as the overriding factors for the decreased photosynthesis.

The result of this combined potassium deficiency induced reduction in overall LAI, solar radiation interception, and photosynthetic rate per unit leaf area is the generation of a smaller pool of photosynthetic assimilates available for growth. Ultimately, a smaller pool of photosynthetic assimilates will reduce the yield levels that can be attained and compromise the quality of the lint that is produced ([Pettigrew, 2008](#)).

2.7 Respiration

Similarly to photosynthesis, dark respiration has also been reported to be affected by K levels since its function depends on the sum of nonstructural carbohydrates and not on the previous day total assimilation ([Cunningham and Syvertsen, 1977](#)). Under conditions of K deficiency dark respiration rates were initially increased until the deficiency became severe, after which dark respiration was suppressed ([Okamoto, 1969](#)). It was hypothesized that respiration rates were increased due to enhanced mitochondrial activity, and that was supported by [Yeo et al. \(1977\)](#) who in experiments on maize under limited K supply observed significantly higher numbers of mitochondria per cell in roots, stems, and leaves.

2.8 Assimilate Transport

Transpiration may influence translocation of carbon and nitrogen compounds from production sites to sinks. Potassium has been reported to control transpiration rates through its effect on stomatal function ([Blatt, 1988](#)) and consequently the root–shoot transport of mineral salts, nitrate, and amino acids ([Ben-Zioni et al., 1971](#); [Marschner, 1995](#); [Schobert et al., 1998](#)). The membrane potential of the sieve tube/companion cell complex is controlled by K concentrations ([Wright and Fischer, 1981](#)). Since apoplasmic phloem loading of sucrose in source leaves mediated by a proton–sucrose cotransport requires a steep transmembrane pH gradient, high potassium concentrations are needed for efficient phloem loading of sucrose. [Deeken et al. \(2002\)](#) in experiments with *Arabidopsis* reported that loss of the AKT2/3 potassium channel resulted in decreased phloem loading of sucrose. In addition, K influences the rate of phloem loading not only by promoting the efflux of assimilates into the apoplast prior to

phloem loading (Mengel and Haeder, 1977; Doman and Geiger, 1979), but also by regulating activation and function of invertase in the sink organs (Oparka, 1990). Furthermore, K not only is essential for maintenance of osmotic and pH gradients between the phloem and the parenchyma cells within the sieve tubes that are required for phloem loading and transport of assimilates (Marschner, 1995), but also provides the energy needed for the transmembrane phloem re-loading processes (Gajdanowicz et al., 2011). Carbohydrate translocation, therefore, is largely dependent on plant K levels with many researchers reporting that lower than optimum K levels result in accumulation of carbohydrates in several plant species (Haeder et al., 1973; Mengel and Viro, 1974; Geiger and Conti, 1983; Cakmak et al., 1994a,b; Amtmann et al., 2008; Amtmann and Armengaud, 2009), including cotton (Bednarz and Oosterhuis, 1999; Pettigrew, 1999; Zhao et al., 2001). In addition to the increased carbohydrate concentrations in the leaves of K deficient cotton plants, Zhao et al. (2001) noticed that stem sucrose concentrations of K deficient plants were significantly lower compared to the control, suggesting either an inhibition of sucrose entry in the transport pool or a compromise in the phloem-loading mechanism. In support of those observations, Ashley and Goodson (1972) observed that insufficient K severely reduced the translocation ^{14}C -labeled photosynthate. Translocation rates are also dependent on transpiration rates. However, Bednarz et al. (1998) reported that K starvation increased transpiration rates while the opposite was observed by Zhao et al. (2001) and Pervez et al. (2004). More research needs to be focused on the effect of K supply on photosynthate translocation and phloem loading in cotton. Furthermore, studies need to be extended to include nitrogen compound translocation since similar inhibitions and accumulations have been reported for amino acids and other nitrogen compounds to occur under K deficiency in tobacco (*Nicotiana tabacum* L.) (Koch and Mengel, 1974), as well as in rice (*Oryza sativa* L.), soybean, and sunflower (Yamada et al., 2002).

2.9 Nitrate Transport–Potassium Interactions

Nitrogen exists in several ionic and nonionic forms in soil, however, the two monovalent ionic forms, anion NO_3^- and cation NH_4^+ are the forms mostly taken up by plants (Marschner, 1995). Research has revealed that a positive relationship exists between N and K (Cai and Qin, 2006) and increased K rates are required at higher N rates (Mondal, 1982). However, nitrogen form, rate and timing of application have been reported to affect K behavior in the soil as well as its uptake by the plants. NH_4^+ has similar

charges and hydrated diameters with K^+ (Wang and Wu, 2010) and it has been reported that NH_4^+ inhibits the high-affinity transport system which is functional primarily at low external K^+ concentrations (<1 mM) while the low-affinity transport system, which operates primarily at high external K^+ levels remains relatively unaffected (Nieves-Cordones et al., 2007; Szczerba et al., 2009). On the other hand, NO_3^- is a univalent anion that serves as a counterion to K^+ (Lu and Li, 2005, Maathuis, 2009) and it has been shown that NO_3^- uptake is more efficient with K^+ as counterion compared to Ca^{2+} , Mg^{2+} , or Na^+ and similarly K^+ uptake has been reported to increase with nitrate fertilization (Pettersson and Jensen, 1983). K^+ is also involved in the NO_3^- transport in the xylem to the shoot since after retranslocation of K-malate to the roots and subsequent decarboxylation of the organic acids, HCO_3^- is exchanged for NO_3^- (Ben-Zioni et al., 1971; Marschner et al., 1996). Lu and Li (2005) observed that using NH_4^+ -N as the only source of N caused a decrease in K uptake compared to NO_3^- -N, however, NH_4^+ resulted in more K being translocated to the leaves than NO_3^- -N in terms of the quantities of xylem-transported K. K^+ depletion of the nutrient solution has been reported to increase NH_4^+ uptake while it suppressed NO_3^- absorption, translocation, and assimilation and resulting in reduction in leaf nitrate reductase activity (Ali et al., 1991). K^+ deficiency was also reported to result in downregulation of root nitrate transporters (Armengaud et al., 2004), which was quickly reversed after resupply of K^+ . Apart from nitrate reductase, asparaginase, another important enzyme in N metabolism was shown to be controlled by K supply (Sodek et al., 1980) while pyruvate kinase, a central integrator of C and N metabolism was suggested to be the main target of K^+ deficiency (Ammann et al., 2008). Additionally, K^+ deficiency has been observed to result in amino acids, amide, and polyamine accumulation in tissues (Evans and Sorger, 1966) indicating that K^+ plays a pivotal role in the transport of N compounds to the site of protein synthesis and their further stabilization while a number of studies has shown that K^+ application enhances protein and amino acids content in grain crops (Yang et al., 2004). Furthermore Koch and Mengel (1974) reported that adequate supply of K was needed for optimum translocation of amino acids and nitrate as well as incorporation of nitrogen into proteins in tobacco. Reduced K^+ uptake and accumulation has been shown to occur under NH_4^+ toxicity conditions since NH_4^+ significantly suppresses the high-affinity pathway system and especially KUP transporters (Martinez-Cordero et al., 2004).

2.10 Potassium Channels

Potassium is taken up against its concentration gradient through K^+ transporters and channels located in the plasma membrane of root cells (Ashley et al., 2006) while two independent transport mechanisms are employed: (1) a selective, high-affinity pathway that allows active K^+ uptake at low concentrations (<1 mM) and involves plasma membrane proton pumping ATPase complexes, and (2) a passive, low-affinity, channel-mediated pathway that mainly functions at high external concentrations (>1 mM) (Epstein et al., 1963; Britto and Kronzucker, 2008). A highly mobile nutrient, not only within short-distance transport, such as between individual cells and neighboring tissues, but also within long distance transport, such as through xylem and phloem, K is transported throughout the plant with the help of three channel families, Shaker, tandem-pore (TPK), and inwardly rectifying (Kir), and three transporter families, KUP/HAK/KT (K^+/H^+ symporters), HKT (K^+/H^+ or K^+/Na^+ transporters), and CPA (cation/ H^+ antiporters) (Cherel, 2004; Amtmann and Armengaud, 2009; Wang and Wu, 2010). Shaker type channels are involved in K uptake, long distance K transport, and K release, and they mainly occur in the plasma membrane. They have a high selectivity for K and channel gating is activated in response to changes in membrane potential with depolarization of membrane resulting in outward rectifying K channels (K moving out of the cytosol) and hyperpolarization of membrane resulting in inward rectifying K channels (K moving into the cytosol). Additionally, Shaker type channels are the main K conduits during cellular movement exemplified by stomatal function. Furthermore, a main component of low-affinity K uptake pathway in the roots has been identified as an inward rectifying K channel of the Shaker family (AKT1 for *Arabidopsis*) (Hirsch et al., 1998) and is mainly expressed in the plasma membrane of root cortical and epidermal cells (Maathuis and Sanders, 1996). Two pore K (TPK) channels in contrast to Shaker channels are less if any affected by changes in the membrane potential (Gobert et al., 2007). They are involved in K homeostasis and they have been reported to regulate membrane potential; however, they are not characterized in great detail.

KUP/HAK/KT (K^+/H^+ symporters) are capable of both low and high affinity of K^+ (Ahn et al., 2004; Rodríguez-Navarro and Rubio, 2006). Their expression has been shown to increase under K starvation conditions (Armengaud et al., 2004; Gierth et al., 2005). Their roles include high-affinity K^+ uptake at the root:soil boundary, intracellular distribution, turgor driven growth (Rigas et al., 2001; Elumalai et al., 2002), and general K homeostasis (Rodríguez-Navarro and Rubio, 2006).

When external $[K^+]$ becomes increasingly low, K^+ uptake needs to be energized and this occurs through H^+ coupled systems that have been shown to operate in root plasma membranes. The coupling stoichiometry is 1:1 and $K^+ : H^+$ symports can drive 10^6 fold K accumulation (Maathuis and Sanders, 1996). KUP/HAK/KT: K^+ uptake permeases, CHXs:cation- H^+ exchangers are encoding K^+ / H^+ symporters (Britto and Kronzucker, 2008; Zhao et al., 2008) and are found to catalyze K^+ influx to cells at low apoplasmic $[K^+]$ (Zhao et al., 2008). Similarly to KUP/HAK/KT family of transporters, HKT have been reported to be expressed in roots and they are involved in efflux and influx of ions however, they are relatively permeable to K^+ .

K^+ transporter and channel families have been extensively investigated in *Arabidopsis* with less information existing on crops, such as barley (*Hordeum vulgare* L.), wheat, beans, rice, maize, tomato (*Lycopersicon esculentum* L.) (Ashley et al., 2006; Szczerba et al., 2009).



3. STRESS MITIGATION

3.1 Drought Stress

As mentioned above, K levels significantly affect the efficiency of plant photosynthetic machinery with lower than optimum levels resulting in significant decreases in CO_2 fixation due to its involvement in ribulose biphosphate carboxylase/oxygenase activation and stomatal function through turgor regulation. Water deficit stress significantly reduces photosynthetic rates due to stomatal limitations, decreases in leaf stomatal conductance that result in decreased CO_2 fixation rates (Lawlor and Cornic, 2002), as well as due to nonstomatal or metabolic impairment where activities of photosynthetic enzymes, such as ribulose biphosphate carboxylase/oxygenase and ribulose biphosphate are disturbed (Gimenez et al., 1992; Medrano et al., 1997; Tezara et al., 1999). Efficiency and function of adenosine triphosphate synthase has also been reported to be reduced under conditions of water stress (Younis et al., 1979; Tezara et al., 1999) resulting in disturbances of stromal pH values (Berkowitz and Gibbs, 1983) and concomitant reductions in energy production. Most importantly, however, due to the decreased efficiency of the photosynthetic mechanism to utilize the incoming light energy, production of ROS is increased (Lawlor and Cornic, 2002).

Water-stressed chloroplasts have been observed to suffer increased leakage of K resulting in further suppression of photosynthesis (Sen Gupta and Berkowitz, 1987) while high K levels have been associated with maintenance of optimum pH values in the chloroplast's stroma and optimal function of

photosynthetic mechanism (Pier and Berkowitz, 1987). Research with spinach (*Spinacia oleracea* L.) and wheat indicated that water-stressed plants containing higher than optimum quantities of K were able to maintain efficient photosynthetic activity (Berkowitz and Whalen, 1985; Pier and Berkowitz, 1987) due to the alleviating effects of K on chloroplast stromal pH balance and dehydration. Further investigation on wheat also reported that detrimental effects of water stress on photosynthetic activity were minimized when K supply was sufficient (Sen Gupta et al., 1989) and similar results were also obtained from mung beans (*Vigna radiata* L.) and cowpea (*Vigna unguiculata* L.) (Sangakkara et al., 2000) leading researchers to suggest that modification of K plant concentrations can maintain CO₂ assimilation rates by regulating stomatal function and balancing cell water relations (Cakmak and Engels, 1999; Mengel et al., 2001). Research with cotton has indicated the importance of K supply on the photosynthetic functions. However, limited attention has been given to the combination of K and water stress. Bar-Tsur and Rudich (1987) observed that K-deprived cotton plants were able to survive successive water stress, nevertheless with significant growth inhibition.

3.2 Cold Stress

Lower than optimum or freezing temperatures result in photooxidative damage to plant chloroplasts and reduce their CO₂ fixation capacity since their membrane structure is significantly damaged (Marschner, 1995; Thomashow, 1999). Increased ROS production has also been related to cold or freezing temperatures (Prasad et al., 1994; Huner et al., 1998; Foyer et al., 2002; Devi et al., 2012) due to the impaired photosynthetic electron transport chain. In addition, leaf stomatal conductance rates were significantly decreased (Ort, 2002) and similar reductions have also been observed for ribulose biphosphate carboxylase activity, while membrane fluidity was greatly affected (Makino et al., 1994; Allen and Ort, 2001). Beringer and Trolldenier (1978) indicated that a high cell K concentration has the ability to enhance cold tolerance by decreasing the cell's osmotic potential. Further research revealed a positive correlation between K availability and cold stress tolerance, with lower than optimum K concentrations escalating the negative effects of cold stress (Kafkafi, 1990; Yermiyahu and Kafkafi, 1990). In contrast, increased K levels enhanced plant defenses against cold stress by acting as an osmolyte, lowering the freezing point of sap and preventing cell dehydration (Kafkafi, 1990; Kant and Kafkafi, 2002). In addition, significant yield losses and extensive leaf damage due to cold temperatures

were reported to occur under low K fertilization, while the effects were alleviated once K supply was increased in a number of vegetable crops such as potato (*Solanum tuberosum* L.) and tomato (Hakerlerler et al., 1997). In experiments with maize, Farooq et al. (2008) observed that seed treatment with KCl was able to enhance frost tolerance by increasing production of antioxidant enzymes, such as catalase, ascorbate peroxidase, and superoxide dismutase and similar results were reported by Devi et al. (2012) in ginseng (*Panax ginseng* L.).

3.3 Salt Stress

Increased salt levels inhibit plant growth by inducing both osmotic and ionic stresses (Shabala and Cuin, 2007) while also damaging the photosynthetic machinery (Sudhir and Murthy, 2004; Chaves et al., 2009). High Na levels in the soil solution significantly reduce K uptake by the plant, while in the cytoplasm water is driven out of the cell vacuole resulting in decreased cell turgor (Yeo et al., 1991; Zhu et al., 1997). High concentrations of Na cations compete in the soil with K cations substantially reducing their uptake by the plants (Zhu, 2003). As a consequence, higher concentrations of Na in the cytoplasm compete with K for uptake sites at the plasma membrane, including both low-affinity and high-affinity transporters (Shabala et al., 2006) and more Na crosses the plasma membrane resulting in a significant membrane depolarization (Shabala et al., 2005). Under such circumstances passive K uptake is impossible and an increased K leakage from the cell is observed (Shabala and Cuin, 2007). Furthermore, in order for the cell to retain metabolic functions through osmotic adjustment, significant quantities of ATP are used for de novo synthesis of compatible osmolytes synthesis, making active K acquisition even more problematic.

Regarding CO₂ fixation, photosynthetic capacity and quantum yield of oxygen evolution have been reported to significantly decrease under conditions of high Na concentrations (Sudhir and Murthy, 2004; Chaves et al., 2009) resulting in detrimental increases of ROS production and further chlorophyll and membrane damage (Kaya et al., 2001; Cakmak, 2005). Higher K levels as well as increased capacity of plants to accumulate K have been associated with increased salt resistance initially in *Arabidopsis* (Liu and Zhu, 1997; Zhu et al., 1998) and later in wheat (Rascio et al., 2001; Santa-Maria and Epstein, 2001), cucumber (*Cucumis sativus* L.), and pepper (*Piper nigrum* L.) (Kaya et al., 2001) due to potassium's ability to enhance the plants' antioxidative mechanism. In cotton, a relatively salt tolerant crop with a threshold level of 7.7 dS m⁻¹ (Maas, 1986), research has been mainly

focused on the effects of partial replacement of K^+ with Na^+ (Cooper et al., 1967; Joham and Amin, 1964) and their effect on cotton yield. Later research indicated that substituting K supply with appropriate amounts of Na could be beneficial for cotton yield (Chen, 1992; Zhang et al., 2006) while Bednarz and Oosterhuis (1999) observed that a similar treatment could delay K deficiency development.

3.4 Biotic Stress

Disease resistance is genetically controlled but it is mediated through physiological and biochemical processes and is interrelated with the nutritional status of the plant or pathogen. It is generally observed that highly resistant plants are less affected by alterations in nutrition than plants tolerant to disease, and highly susceptible plants may remain susceptible with nutrient conditions that greatly increase the resistance of intermediate or tolerant plants (Huber and Arny, 1985). Potassium plays a significant role in plant protection against biotic stresses since high concentrations of K have been reported to alleviate detrimental effects of disease and pest infestations (Perrenoud, 1990; Prabhu et al., 2007). This has been attributed to the regulation by K of primary metabolic plant functions. In more detail, high levels of K in the plant promote the synthesis of high molecular weight compounds, such as proteins, starch and cellulose while simultaneously suppressing the formation of soluble sugars, organic acids, and amides, compounds indispensable for feeding pathogens and insects (Marschner, 1995; Amtmann et al., 2008). In addition, the accumulation of inhibitory amino acids, phytoalexins, phenols and auxins is dependent on the level of K (Perrenoud, 1990) while K deficiency results in inorganic N accumulation, due to poor translocation, and phenols (with fungicidal properties) break down (Kiraly, 1976). Exuded arginine that inhibits sporangial germination of *Phytophthora infestans* on potato increases as the level of K increases (Alten and Orth, 1941). Additionally, canopy discoloration due to K deficiency has been observed to be more prone to attack by parasites, while cracks and lesions on leaf surfaces that develop under low K supply provide additional access (Krauss, 2001). In tomato, Kirali (1976) observed that higher K supply successfully suppressed disease incidence, and similar results were reported in soybean (Mondal et al., 2001) and wheat (Sweeney et al., 2000). K application on cotton has been reported to decrease root rot (*Phymatotrichum omnivorum*) (Tsai and Bird, 1975), wilt (*Verticillium alboatrum*) (Hafez et al., 1975), as well as wilt and root rot caused by *Fusarium oxysporum* sp. (Prabhu et al., 2007). Ramasami and Shanmugam (1976) reported that K application

decreased seedling blight (*Rhizoctonia solani*) in cotton, however, the opposite results were observed by Blair and Curl (1974). Miller (1969) reported that increased K application rates decreased leaf blight (*Cercospora gossypina*–*Alternaria solani* complex) while KNO_3 significantly reduced the severity of *Alternaria* leaf blight of cotton at the middle canopy level (Bhuiyan et al., 2007). Furthermore, reductions from nematode (*Meloidogyne incognita*, *Rotylenchulus reniformis*) damage due to high K supply were also reported by Oteifa and Elgindi (1976). Cotton cultivars exuding more carbohydrate and K and less Mg and Ca have been reported to have less seedling disease and establish higher plant populations than plants exuding less carbohydrate and K (Tsai and Bird, 1975).

3.5 Potassium and Stress Signaling

Apart from its major role in plant protection from a variety of abiotic and biotic stresses, K has been suggested to be significantly involved in plant stress responses (Ashley et al., 2006; Wang and Wu, 2010). Depolarization of the membrane is observed in response to other fungal elicitors (Rossard et al., 2006) as well as to herbivory (Maffei et al., 2007). Changes in the external K concentration have a great impact on the membrane potential because the conductance of the plasma membrane is larger for K than any other ion. A high external K concentration depolarizes the membrane while a low external concentration hyperpolarizes the membrane (Amtmann et al., 2008). Potassium deficiency not only induced K transporter upregulation (Gierth et al., 2005; Lee et al., 2007), but additionally controlled stress-signaling mechanisms such as ROS synthesis (Schachtman and Shin, 2007) as well as hormone synthesis (Ashley et al., 2006). ROS production, and especially production of hydrogen peroxide (H_2O_2), increased under conditions of limited K supply (Shin and Schachtman, 2004) with H_2O_2 further activating K uptake mechanisms in order to increase K plant status. In addition, genes regulating jasmonic acid and auxin synthesis were upregulated at low plant K concentrations (Armengaud et al., 2004) while ethylene production rates were increased two-fold in K-starved *Arabidopsis* plants compared to control plants (Shin and Schachtman, 2004). In cotton, research indicated that K deficiency resulted in increased abscisic acid concentrations in the roots and the xylem sap while cytokinins (zeatin riboside and isopentenyl adenosine) levels were decreased in the xylem sap and leaves (Wang et al., 2012) indicating that K affects the hormonal balance in cotton.



4. SUMMARY

This review has described the fundamental role K plays in plant growth and crop development. Its involvement in several physiological functions, such as water relations, enzyme activation, stomatal regulation and photosynthesis, assimilate and nitrate transport was summarized and potassium deficiency was described and related to them. In addition, potassium's major role in plant health and tolerance to abiotic and biotic stress as well as stress signaling was underlined. However, research has mainly focused on *Arabidopsis* with little information existing on crop species. Considering potassium's major role in yield development and quality research should focus on expanding its scope in major crop species hence, enable farmers to achieve optimal utilization of K fertilization and additionally provide targets for future genetic improvement efforts.

REFERENCES

- Adams, D.O., Franke, K.E., Christensen, L.P., 1990. Elevated putrescine levels in grapevine leaves that display symptoms of potassium deficiency. *Am. J. Enol. Vitic.* 41, 121–125.
- Ahn, S.J., Shin, R., Schachtman, D.P., 2004. Expression of KT/KUP genes in *Arabidopsis* and the role of root hairs in K⁺ uptake. *Plant Physiol.* 134, 1135–1145.
- Akhtar, M.E., Khan, M.Z., Ahmad, S., Ashraf, M., Sardar, A., 2009. Effect of potassium on micromorphological and chemical composition of three cotton (*Gossypium hirsutum* L.) genotypes. *Afr. J. Biotech.* 8, 3511–3518.
- Ali, A.A., Ikeda, M., Yamada, Y., 1991. Effects of supply of K, Ca, and Mg on the absorption and assimilation of ammonium- and nitrate- N in tomato plants. *Soil. Sci. Plant Nutr.* 37, 283–289.
- Allen, D.J., Ort, D.R., 2001. Impact of chilling temperatures on photosynthesis in warm climate plants. *Trends Plant Sci.* 6, 36–42.
- Alten, F., Orth, H., 1941. Untersuchungen über den aminosäuregehalt und die anfälligkeit der kartoffel gegen die kraut- und kollenfäule (*Phytophthora infestans*). *Phytopathol. Z.* 13, 243–247.
- Amtmann, A., Troufflard, S., Armengaud, P., 2008. The effect of potassium nutrition on pest and disease resistance in plants. *Physiol. Plant* 133, 682–691.
- Amtmann, A., Armengaud, P., 2009. Effects of N, P, K, and S on metabolism: new knowledge gained from multilevel analysis. *Curr. Opin. Plant Biol.* 12, 275–283.
- Armengaud, P., Breitling, R.M., Amtmann, A., 2004. The potassium-dependent transcriptome of *Arabidopsis* reveals a prominent role of jasmonic acid in nutrient signaling. *Plant Phys.* 136, 2556–2576.
- Armengaud, P., Sulpice, R., Miller, A.J., Stitt, M., Amtmann, A., Gibon, Y., 2009. Multilevel analysis of primary metabolism provides new insights into the role of potassium nutrition for glycolysis and nitrogen assimilation in *Arabidopsis* roots. *Plant Phys.* 150, 772–785.
- Ashley, D.A., Goodson, R.D., 1972. Effect on time and plant potassium status on ¹⁴C-labeled photosynthate movement in cotton. *Crop Sci.* 12, 686–690.
- Ashley, M.K., Grant, M., Grabov, A., 2006. Plant responses to potassium deficiencies: a role for potassium transport proteins. *J. Exp. Bot.* 57, 425–436.

- Ashraf, M., Ashfaq, A., Ashraf, M.Y., 2002. Effects of increased supply of potassium on growth and nutrient content in pearl millet under water stress. *Biol. Plant* 45, 141–144.
- Bar-Tsur, A., Rudich, J., 1987. Osmotic adjustment of cotton to moderate potassium chloride stress and subsequent water stress during early stage of development. *Agron. J.* 79, 166–171.
- Bednarz, C.W., Oosterhuis, D.M., Evans, R.D., 1998. Leaf photosynthesis and carbon isotope discrimination of cotton in response to potassium deficiency. *Environ. Exp. Bot.* 39, 131–139.
- Bednarz, C.W., Oosterhuis, D.M., 1999. Physiological changes associated with potassium deficiency in cotton. *J. Plant Nutr.* 22, 303–313.
- Begg, J.E., Turner, N.C., 1976. Crop water deficits. *Adv. Agron.* 28, 161–217.
- Benlloch-González, M., Arquero, O., Fournier, J.M., Barranco, D., Benlloch, M., 2008. K starvation inhibits water-stress-induced stomatal closure. *J. Plant Physiol.* 165, 623–630.
- Benlloch-González, M., Romera, J., Cristescu, S., Harren, F., Fournier, J.M., Benlloch, M., 2010. K starvation inhibits water-stress-induced stomatal closure via ethylene synthesis in sunflower plants. *J. Exp. Bot.* 61, 11–39.
- Ben-Zioni, A., Vaadia, Y., Lips, S.H., 1971. Nitrate uptake by roots as regulated by nitrate reduction products of the shoot. *Physiol. Plant* 24, 288–290.
- Berg, W.K., Cunningham, S.M., Brouder, S.M., Joern, B.C., Johnson, K.D., Volenec, J.J., 2009. Influence of phosphorus and potassium on alfalfa yield, taproot C and N pools, and transcript levels of key genes after defoliation. *Crop Sci.* 49, 974–982.
- Berg, V.S., Heuchelin, S., 1990. Leaf orientation of soybean seedlings: I. effect of water potential and photosynthetic photon flux density on paraheliotropism. *Crop Sci.* 30, 631–638.
- Beringer, H., 1978. Functions of potassium in plant metabolism with particular reference to yield. In: Potassium in soils and crops. Intl. Potash Institute, New Delhi, India, pp. 185–202.
- Beringer, H., Trolldenier, G., September 4–8, 1978. The influence of K nutrition on the response of plants to environmental stress. In: “Potassium Research—Review and Trends” Proceedings of 11th Congress of the International Potash Institute, Bern, Switzerland, pp. 189–222.
- Beringer, H., Koch, K., Lindhauer, M.G., 1986. Sucrose accumulation and osmotic potentials in sugar beet at increasing levels of potassium nutrition. *J. Sci. Food Agric.* 37, 211–218.
- Berkowitz, G.A., Gibbs, M., 1983. Reduced osmotic potential inhibition of photosynthesis. Site-specific effects of osmotically induced stromal acidification. *Plant Phys.* 71, 905–911.
- Berkowitz, G.A., Whallen, C., 1985. Leaf K^+ interaction with water stress inhibition of non-stomatal controlled photosynthesis. *Plant Phys.* 79, 189–193.
- Berkowitz, G.A., Peters, J.S., 1993. Chloroplast inner envelope ATPase acts as a primary H^+ pump. *Plant Physiol.* 102, 261–267.
- Bhuiyan, S.A., Boyd, M.C., Dougall, A.J., Martin, C., Hearnden, M., 2007. Effects of foliar application of potassium nitrate on suppression of *Alternaria* leaf blight of cotton (*Gossypium hirsutum*) in northern Australia. *Aust. Plant Pathol.* 36, 462–465.
- Blair, W.C., Curl, E.A., 1974. Influence of fertilization regimes on the rhizosphere microflora and *Rhizoctonia* disease of cotton seedlings. *Proc. Am. Phytopath. Soc.* 1, 28–29.
- Blatt, M.R., 1988. Potassium-dependent, bipolar of K^+ channels in guard cells. *J. Membr. Biol.* 102, 235–246.
- Britto, D.T., Kronzucker, H.J., 2008. Cellular mechanisms of potassium transport in plants. *Physiol. Plant* 133, 637–650.
- Buch-Pedersen, M.J., Rudashevskaya, E.L., Berner, T.S., Venema, K., Palmgren, M.G., 2006. Potassium as an intrinsic uncoupler of the plasma membrane H -ATPase. *J. Biol. Chem.* 281, 38285–38292.
- Cai, Z.C., Qin, S.W., 2006. Dynamics of crop yields and soil organic carbon in a long-term fertilization experiment in the Huang-Huai-Hai Plain of China. *Geoderma* 136, 708–715.

- Cakmak, I., Hengeler, C., Marschner, H., 1994a. Partitioning of shoot and root dry matter and carbohydrates in bean plants suffering from Phosphorus, potassium, and magnesium deficiency. *J. Exp. Bot.* 45, 1245–1251.
- Cakmak, I., Hengeler, C., Marschner, H., 1994b. Changes in phloem export of sucrose in leaves in response to phosphorus, potassium and magnesium deficiency. *J. Exp. Bot.* 45, 1251–1257.
- Cakmak, I., Engels, C., 1999. Role of mineral nutrients in photosynthesis and yield formation. In: Rengel, Z. (Ed.), *Mineral Nutrition of Crops: Mechanisms and Implications*. The Haworth Press, New York, pp. 141–168.
- Cakmak, I., 2005. The role of potassium in alleviating detrimental effects of abiotic stresses in plants. *J. Plant Nutr. Soil Sci.* 168, 521–530.
- Carlson, J.G., 1973. Morphology. In: Caldwell, B.E. (Ed.), *Soybeans: Improvement, Production and Uses*, pp. 17–95. Am. Soc. Agron., Madison, WI.
- Cassman, K.G., Kerby, T.A., Roberts, B.A., Bryant, D.C., Brouder, S.M., 1989. Differential response to two cotton cultivars to fertilizer and soil potassium. *Agron. J.* 81, 870–876.
- Chaves, M.M., Flexas, J., Pinheiro, C., 2009. Photosynthesis under drought and salt stress: regulation mechanisms from whole plant to cell. *Ann. Bot.* 103, 551–560.
- Chen, G.A., 1992. Na effect on the growth of cotton and K and Na absorption. *Soil* 24, 201–204.
- Chen, L., Nishizawa, T., Higashitani, A., Suge, H., Wakui, Y., Takeda, K., Takahashi, H., 2001. A variety of wheat tolerant to deep-seeding conditions: elongation of the first internode depends on the response to gibberellin and potassium. *Plant Cell Environ.* 24, 469–476.
- Cherel, I., 2004. Regulation of K^+ channel activities in plants: from physiological to molecular aspects. *J. Exp. Bot.* 55, 337–351.
- Claussen, M., Lüthe, H., Blatt, M., Böttger, M., 1997. Auxin-induced growth and its linkage to potassium channels. *Planta* 201, 227–234.
- Cocucci, M.C., Rosa, S.D., 1980. Effects of canavanine on IAA—and fusicoccin—stimulated cell enlargement, proton extrusion and potassium uptake in maize coleoptiles. *Physiol. Plant* 48, 239–242.
- Conway, T.W., 1964. On the role of ammonium or potassium ion in amino acid polymerization. *Proc. Natl. Acad. Sci.* 51, 1216–1220.
- Cooper, R.B., Blaser, R.E., Brown, R.E., 1967. Potassium nutrition effects on net photosynthesis and morphology of Alfalfa. *Soil. Sci. Soc. Am. J.* 31, 231–235.
- Cunningham, G.L., Syvertsen, J.P., 1977. The effect of nonstructural carbohydrate levels on dark CO_2 release in creosotebush. *Photosynthetica* 11, 291–295.
- Cutler, J.M., Rains, D.W., 1978. Effects of water stress and hardening on the internal water relations and osmotic constituents of cotton leaves. *Physiol. Plant* 42, 261–268.
- Deeken, R., Geiger, D., Fromm, J., Kokoreva, O., Ache, P., Langenfeld-Heyser, R., Sauer, N., May, T., Hedrich, R., 2002. Loss of the AKT2/3 potassium channel affects sugar loading into the phloem of *Arabidopsis*. *Planta* 216, 334–344.
- Devi, B.S.R., Kim, J.Y., Selvi, S.K., Lee, S., Yang, D.C., 2012. Influence of potassium nitrate on antioxidant level and secondary metabolite genes under cold stress in *Panax ginseng*. *Rus. J. Plant Physiol.* 59, 318–325.
- Dhindsa, R.S., Beasley, C.A., Ting, I.P., 1975. Osmoregulation in cotton fiber: accumulation of potassium and malate during growth. *Plant Physiol.* 56, 394–398.
- Doman, D.C., Geiger, D.R., 1979. Effect of exogenously supplied foliar potassium on phloem loading in *Beta vulgaris* L. *Plant Physiol.* 64, 528–533.
- Ebelhar, S.A., Varsa, E.C., 2000. Tillage and potassium placement effects on potassium utilization by corn and soybean. *Commun. Soil. Sci. Plant Anal.* 31, 11–14.
- Elumalai, R.P., Nagpal, P., Reed, J.W., 2002. A mutation in *Arabidopsis* KT2/KUP2 potassium transporter gene affects shoot cell expansion. *Plant Cell* 14, 119–131.
- Epstein, E., Rains, D., Elzam, O., 1963. Resolution of dual mechanisms of potassium absorption by barley roots. *Proc. Natl. Acad. Sci.* 49, 684–692.

- Evans, H.J., Sorger, G.J., 1966. Role of mineral elements with emphasis on the univalent cations. *Ann. Rev. Plant Phys.* 17, 47–76.
- Farooq, M., Aziz, T., Chemma, Z.A., Hussian, M., Khaliq, A., 2008. Activation of antioxidant system by KCl improves the chilling tolerance in hybrid maize. *J. Agron. Crop Sci.* 194, 438–448.
- Ford, C.W., Wilson, J.R., 1981. Changes in levels of solutes during osmotic adjustment to water stress in leaves of four tropical pasture species. *Aust. J. Plant Physiol.* 8, 77–91.
- Fournier, J.M., Roldan, A.M., Sanchez, C., Alexandre, G., Benlloch, M., 2005. K starvation increases water uptake in whole sunflower plants. *Plant Sci.* 168, 823–829.
- Foyer, C.H., Vanacker, H., Gomez, L.D., Harbinson, J., 2002. Regulation of photosynthesis and antioxidant metabolism in maize leaves at optimal and chilling temperatures: review. *Plant Physiol. Biochem.* 40, 659–668.
- Gajdanowicz, P., Michard, E., Sandmann, M., Rocha, M., Dreyer, I., 2011. Potassium gradients serve as a mobile energy source in plant vascular tissues. *Proc. Natl. Acad. Sci.* 108, 864–869.
- Geiger, D.R., Conti, T.R., 1983. Relation of increased potassium nutrition to photosynthesis and translocation of carbon. *Plant Physiol.* 71, 141–144.
- Gierth, M., Maser, P., Schroeder, J.I., 2005. The potassium transporter *AtHAK5* functions in K-deprivation induced high affinity K uptake and *AKT1* K channel contribution to K uptake kinetics in *Arabidopsis* roots. *Plant Physiol.* 137, 1105–1114.
- Gimenez, C., Mitchell, V.J., Lawlor, D.W., 1992. Regulation of photosynthetic rate of two sunflower hybrids under water stress. *Plant Physiol.* 98, 516–524.
- Gobert, A., Isayenko, S., Voelker, C., Czempinski, K., Maathuis, F.J.M., 2007. The two-pore channel *TPK1* gene encodes the vacuolar K⁺ conductance and plays a role in K⁺ homeostasis. *Proc. Natl. Acad. Sci.* 104, 10726–10731.
- Gorton, H.L., 1987. Water relations in pulvini from *Samanea saman*. *Plant Physiol.* 83, 945–950.
- Green, J.F., Muir, R.M., 1979. An analysis of the role of potassium in the growth effects of cytokinin, light and abscisic acid on cotyledon expansion. *Physiol. Plant* 46, 19–24.
- Green, J.F., Muir, R.M., 1978. The effect of potassium on cotyledon expansion induced by cytokinins. *Physiol. Plant* 43, 213–218.
- Green, J., 1983. The effect of potassium and calcium on cotyledon expansion and ethylene evolution induced by cytokinins. *Physiol. Plant* 57, 57–61.
- Haeder, H.E., Mengel, K., Forster, H., 1973. The effect of potassium on translocation of photosynthates and yield patterns of potato plants. *J. Sci. Food Agric.* 24, 1479–1487.
- Hafez, A.A.R., Stout, P.R., DeVay, J.E., 1975. Potassium uptake by cotton in relation to Verticillium wilt. *Agron. J.* 67, 359–361.
- Hager, A., Menzel, H., Krauss, A., 1971. Versuche und hypothese zur primarwirkung des auxins beim streckungswachstum. *Planta* 100, 47–75.
- Hakerlerler, H., Oktay, M., Eryuce, N., Yagmur, B., 1997. Effect of potassium sources on the chilling tolerance of some vegetable seedlings grown in hotbeds. In: Johnston, A.E. (Ed.), *Food Security in the WANA Region, the Essential Need for Balanced Fertilization*, pp. 317–327. Basel, Switzerland.
- Hawker, J.S., Marschner, H., Downton, W.J.S., 1974. Effects of sodium and potassium on starch synthesis in leaves. *Funct. Plant Biol.* 1, 491–501.
- Hawker, J.S., Marschner, H., Krauss, A., 1979. Starch synthesis in developing potato tubers. *Physiol. Plant* 46, 25–30.
- Heckman, J.R., Kamprath, E.J., 1992. Potassium accumulation and corn yield related to potassium fertilizer rate and placement. *Soil. Sci.* 56, 141–148.
- Hepler, P.K., Vidali, L., Cheung, A.Y., 2001. Polarized cell growth in higher plants. *Annu. Rev. Cell. Dev. Biol.* 17, 159–187.
- Hirsch, R.E., Lewis, B.D., Spalding, E.P., Sussman, M.R., 1998. A role for the *AKT1* potassium channel in plant nutrition. *Science* 280, 918–921.

- Hsiao, T.C., Läuchli, A., 1986. A role for potassium in plant-water-relations. In: Tinker, B., Läuchli, A. (Eds.), *Advances in Plant Nutrition*, pp. 281–311 (Praeger Scientific, New York).
- Hsiao, T.C., Acevedo, E., Fereres, E., Henderson, D., 1976. Water stress, growth, and osmotic adjustment. *Phil. Trans. R. Soc. Lon. B. Biol. Sci.* 273, 479–500.
- Huber, S.C., 1985. Role of potassium in photosynthesis and respiration. In: Munson, R.D. (Ed.), *Potassium in Agriculture*. ASA, CSSA, SSSA, Madison, WI, pp. 369–391.
- Huber, D.M., Arny, D.C., 1985. Interaction of potassium with plant disease. In: Munson, R.D. (Ed.), *Potassium in Agriculture*. ASA, CSSA, SSSA, Madison, WI, pp. 467–488.
- Huner, N.P.A., Oquist, G., Sarhan, E., 1998. Energy balance and acclimation to light and cold. *Trends Plant Sci.* 3, 224–230.
- Iannucci, A., Russo, M., Arena, L., Di Fonzo, N., Martiniello, P., 2002. Water deficit effects on osmotic adjustment and solute accumulation in leaves of annual clovers. *Eur. J. Agron.* 16, 111–122.
- Joham, H.E., Amin, J.V., 1964. Role of sodium in the potassium nutrition of cotton. *Soil. Sci.* 99, 220–226.
- Jones, M.M., Osmond, C.B., Turner, N.C., 1980. Accumulation of solutes in leaves of sorghum and sunflower in response to water deficits. *Aust. J. Plant Physiol.* 7, 193–205.
- Jordan-Meille, I., Pellerin, S., 2004. Leaf area establishment of a maize (*Zea mays* L.) field crop under potassium deficiency. *Plant Soil.* 265, 75–92.
- Jung, J.Y., Shin, R., Schachtman, D.P., 2009. Ethylene mediates response and tolerance to potassium deprivation in *Arabidopsis*. *Plant Cell* 21, 607–621.
- Kafkafi, U., 1990. The functions of plant K in overcoming environmental stress situations. In: 22nd Colloquium. International Potash Institute, Bern, Switzerland, pp. 81–93.
- Kant, S., Kafkafi, U., 2002. Potassium and abiotic stresses in plants. In: Pasricha, N.S., Bansal, S.K. (Eds.), *Plant Roots: The Hidden Half*. Marcel Dekker Incorporated, New York, pp. 435–449.
- Kawashima, R., 1969. Studies on the leaf orientation-adjusting movement in soybean plants. I. The leaf orientation-adjusting movement and light intensity on leaf surface. *Proc. Crop Sci. Soc. Jpn.* 38, 718–729 (in Japanese with English summary).
- Kaya, C., Kimak, H., Higgs, D., 2001. Enhancement of growth and normal growth parameters by foliar application of potassium and phosphorus in tomato cultivars grown at high (NaCl) salinity. *J. Plant Nutr.* 24, 357–367.
- Kayne, F.J., 1973. In: Boyer, P.D. (Ed.), *The Enzymes*, Vol. 8. Academic Press, New York, pp. 353–382.
- Kimbrough, E.L., Blaser, R.E., Wolf, D.D., 1971. Potassium effects on regrowth of alfalfa (*Medicago sativa* L.). *Agron. J.* 63, 836–839.
- Kirali, Z., 1976. Plant disease resistance as influenced by biochemical effects of nutrients in fertilizers. In: “Fertilizer Use and Plant Health. Proceedings of 12th College of International Potash Institute, pp. 33–46. Izmir, Turkey.
- Koch, K., Mengel, K., 1974. The influence of the level of potassium supply to young tobacco plants (*Nicotiana tabacum* L.) on short-term uptake and utilisation of nitrate nitrogen (¹⁵N). *Sci. Food Agric.* 25, 165–471.
- Koller, D., 2000. Plants in search of sunlight. *Adv. Bot. Res.* 33, 36–131.
- Krauss, A., 2001. Potassium and biotic stress. In: Workshop on Potassium in Argentina’s Agricultural Systems. Intl. Potash Institute, Buenos Aires, Argentina, pp. 281–293.
- Kusano, T., Berberich, T., Tateda, C., Takahashi, Y., 2008. Polyamines: essential factors for growth and survival. *Planta* 228, 367–381.
- La Guardia, M.D., Benlloch, M., 1980. Effects of potassium and gibberellic acid on stem growth of whole sunflower plants. *Physiol. Plant* 49, 443–448.
- Läuchli, A., Pflüger, R., 1978. Potassium transport through plant cell membranes and metabolic role of potassium in plants. In: Potassium Research Review and Trends. Intl. Potash Institute, Bern, Switzerland, pp. 111–164.

- Lawlor, M.M., Cornic, G., 2002. Photosynthetic carbon assimilation and associated metabolism in relation to water deficits in higher plants. *Plant Cell Environ.* 25, 275–294.
- Lee, S.C., Lan, W.Z., Kim, B.G., Li, L., Cheong, Y.H., Pandey, G.K., Buchanan, B.B., Luan, S., 2007. A protein phosphorylation/dephosphorylation network regulates a plant potassium channel. *Proc. Natl. Acad. Sci.* 104, 15959–15964.
- Leigh, R.A., Wyn Jones, R.G., 1984. A hypothesis relating critical potassium concentrations for growth to the distribution and functions of this ion in the plant cell. *New Phytol.* 97, 1–13.
- Li, R., Volenec, J.J., Joern, B.C., Cunningham, S.M., 1997. Potassium and nitrogen effects on carbohydrate and protein metabolism in alfalfa roots. *J. Plant Nutr.* 20, 511–529.
- Liu, J., Zhu, J.K., 1997. Proline accumulation and salt stress-induced gene expression in a salt-hypersensitive mutation of *Arabidopsis*. *Plant Physiol.* 114, 591–596.
- Longstreth, D.J., Nobel, P.S., 1980. Nutrient influences on leaf photosynthesis: effects of nitrogen, phosphorus, and potassium for *Gossypium hirsutum* L. *Plant Physiol.* 65, 541–543.
- Lu, Y.X., Li, C.J., 2005. Transpiration, potassium uptake and flow in tobacco as affected by nitrogen forms and nutrient levels. *Ann. Bot.* 95, 991–998.
- Maas, E.V., 1986. Salt tolerance of plants. *Appl. Agric. Res.* 1, 12–26.
- Maathuis, F.J.M., Sanders, D., 1996. Mechanisms of potassium absorption by higher plant roots. *Physiol. Plant* 96, 158–168.
- Maathuis, F.J.M., 2009. Physiological functions of mineral macronutrients. *Curr. Opin. Plant Biol.* 12, 250–258.
- MacRobbie, E.A.C., 1977. Functions of ion transport in plant cells and tissues. *Int. Rev. Biochem.* 13, 211–247.
- Maene, L.M., 2001. Global Potassium Fertilizer Situation, Current Use and Perspectives. 3–5 December. International Potash Institute, New Delhi, India, pp. 1–10.
- Maffei, M.E., Mithofer, A., Boland, W., 2007. Insects feeding on plants: rapid signals and responses preceding the induction of phytochemical release. *Phytochem* 68, 2946–2959.
- Makino, A., Nakano, H., Mae, T., 1994. Effects of growth temperature on the responses of ribulose-1,5-bisphosphate carboxylase, electron transport components, and sucrose synthesis enzymes to leaf nitrogen in rice and their relationships to photosynthesis. *Plant Physiol.* 105, 1231–1238.
- Marschner, H., 1995. Functions and mineral nutrients. In: *Mineral Nutrition of Higher Plants*. Academic press, London, UK, pp. 213–255.
- Marshner, H., Kirkby, E.A., Cakmak, I., 1996. Effect of mineral nutritional status on shoot-root partitioning of photoassimilates and cycling of mineral nutrients. *J. Exp. Bot.* 47, 1255–1263.
- Martinez-Cordero, M.A., Vicente, M., Francisco, R., 2004. Cloning and functional characterization of the high-affinity K⁺ transporter HAK1 of pepper. *Plant Mol. Biol.* 56, 413–421.
- Matoh, T., Yasuoka, S., Ishikawa, T., Takahashi, E., 1988. Potassium requirement of pyruvate kinase extracted from leaves of halophytes. *Physiol. Plant* 74, 675–678.
- Medrano, H., Parry, M.A., Socias, X., Lawlor, D.W., 1997. Long term water stress inactivates rubisco in subterranean clover. *Ann. Appl. Biol.* 131, 491–501.
- Memon, A.R., Siddiqi, M.Y., Class, A.D.M., 1985. Efficiency of K utilization by barley varieties: activation of pyruvate kinase. *J. Exp. Bot.* 36, 79–90.
- Mengel, K., Viro, M., 1974. Effects on potassium supply on the transport of photosynthates to the fruits of tomatoes (*Lycopersicon esculentum*). *Plant Physiol.* 30, 295–300.
- Mengel, K., Haeder, H.E., 1977. Effect of potassium supply on the rate phloem sap exudation and the composition of phloem sap of *Ricinus communis*. *Plant Physiol.* 59, 282–284.
- Mengel, K., Arneke, W.W., 1982. Effect of potassium on the water potential, the pressure potential, the osmotic potential and cell elongation in leaves of *Phaseolus vulgaris*. *Physiol. Plant* 54, 402–408.
- Mengel, K., Kirkby, E.A., Kosegarten, H., Appel, T., 2001. *Principles of Plant Nutrition*. Kluwer Academic Publishers, Dordrecht, the Netherlands, pp. 481–511.

- Miller, J.W., 1969. The effect of soil moisture and plant nutrition on the *Cercospora-Alternaria* leaf blight complex of cotton in Missouri. *Phytopathology* 59, 767–769.
- Miller, C.S., 1975. Short interval leaf movements of cotton. *Plant Physiol.* 55, 562–566.
- Moinuddin, Imas, P., 2007. Evaluation of potassium compared to other osmolytes in relation to osmotic adjustment and drought tolerance of chickpea under water deficit environments. *J. Plant Nutr.* 30, 517–535.
- Mondal, S.S., 1982. Potassium nutrition at high levels of N fertilization on rice. In: *Potash Review*. Intl. Potash Institute, Bern, Switzerland, pp. 1–4.
- Mondal, S.S., Pramanik, C.K., Das, J., 2001. Effect of nitrogen and potassium on oil yield, nutrient uptake and soil fertility in soybean (*Glycine max*) – sesame (*Sesamum indicum*) intercropping system. *Indian J. Agric. Sci.* 71, 44–46.
- Morgan, J.M., 1984. Osmoregulation and water stress in higher plants. *Ann. Rev. Plant Phys.* 35, 299–319.
- Morgan, J.M., 1992. Osmotic components and properties associated with genotypic differences in osmoregulation in wheat. *Funct. Plant Biol.* 19, 67–76.
- Moshelion, M., Becker, D., Biela, A., Uehlein, N., Hedrich, R., Otto, B., Levi, H., Moran, N., Kaldenhoff, R., 2002. Plasma membrane aquaporins in the motor cells of *Samanea saman*: diurnal and circadian regulation. *Plant Cell* 14, 727–739.
- Mullins, G.L., Burmester, C.H., Reeves, D.W., 1997. Cotton response to in-row subsoiling and potassium fertilizer placement in Alabama. *Soil. Till. Res.* 40, 145–154.
- Nieves-Cordones, M., Martínez-Cordero, M.A., Martínez, V., Rubio, F., 2007. An NH_4^+ -sensitive component dominates high-affinity K^+ uptake in tomato plants. *Plant Sci.* 172, 273–280.
- Nishizawa, T., Chen, L., Higashitani, A., Takahashi, H., Takeda, K., Suge, H., 2002. Responses of the first internodes of hong mang mai wheat to ethylene, gibberellins and potassium. *Plant Prod. Sci.* 5, 93–100.
- Nitsos, R.E., Evans, H.J., 1969. Effects of univalent cations on the activity of particulate starch synthetase. *Plant Physiol.* 44, 1260–1266.
- Okamoto, S., 1969. The respiration in leaf discs from young taro plants under a moderate potassium deficiency. *Soil. Sci. Plant Nutr.* 15, 274–279.
- Oosterhuis, D.M., Walker, S., Eastham, J., 1985. Soybean leaflet movements as an indicator of crop water stress. *Crop Sci.* 25, 1101–1106.
- Oosterhuis, D.M., Walker, S., 1984. Changes in the soybean leaflet pulvinule during inversion with water stress. *Plant Phys. Suppl.* 75, 176.
- Oosterhuis, D.M., Wulschleger, S.D., 1987. Osmotic adjustment in cotton (*Gossypium hirsutum* L.) leaves and roots in response to water stress. *Plant Physiol.* 84, 1154–1157.
- Oparka, K.J., 1990. What is phloem unloading? *Plant Physiol.* 94, 393–396.
- Ort, D.R., 2002. Chilling-induced limitations on photosynthesis in warm climate plants: contrasting mechanisms. *Environ. Control Biol.* 40, 7–18.
- Oteifa, B.A., Elgindi, A.Y., 1976. Potassium nutrition of cotton (*Gossypium barbadense*, L) in relation to nematode infection by *Meloidogyne incognita* and *Rotylenchulus reniformis*. In: “Fertilizer Use and Plant Health”. Proceedings of 12th College of International Potash Institute, pp. 301–306. Izmir, Turkey.
- Peoples, T.R., Koch, D.W., 1979. Role of potassium in carbon dioxide assimilation in *Medicago sativa* L. *Plant Physiol.* 63, 878–881.
- Perrenoud, S., 1990. Potassium and plant health. In: *IPI-Research Topics No. 3*. Intl. Potash Institute, Basel, Switzerland, p. 365.
- Pervez, H., Ashraf, M., Makhdom, M.I., 2004. Influence of potassium nutrition on gas exchange characteristics and water relations in cotton (*Gossypium hirsutum* L.). *Photosynthetica* 42, 251–255.
- Pettersson, S., Jensen, P., 1983. Variations among species and varieties in uptake and utilization of potassium. *Plant Soil.* 72, 231–237.

- Pettigrew, W.T., 2003. Relationship between insufficient potassium and crop maturity in cotton. *Agron. J.* 95, 1323–1329.
- Pettigrew, W.T., 2008. Potassium influences on yield and quality production for maize, wheat, soybean and cotton. *Physiol. Plant* 133, 670–681.
- Pettigrew, W.T., 1999. Potassium deficiency increases specific leaf weights and leaf glucose levels in field-grown cotton. *Agron. J.* 91, 962–968.
- Pettigrew, W.T., Meredith, W.R., 1997. Dry matter production, nutrient uptake, and growth of cotton as affected by potassium fertilization. *J. Plant Nutr.* 20, 531–548.
- Pier, P.A., Berkowitz, G.A., 1987. Modulation of water stress effects on photosynthesis by altered leaf K^+ . *Plant Physiol.* 85, 655–661.
- Prabhu, A.S., Fageria, N.K., Huber, D.M., Rodriguez, F.A., 2007. Potassium and plant disease. In: Datnoff, L.E., Elmer, W.H., Huber, D.M. (Eds.), *Mineral Nutrition and Plant Disease*. The American Phytopathological Soc. Press, Saint Paul, MN, pp. 57–78.
- Prasad, T.K., Anderson, M.D., Martin, B.A., Stewart, C.R., 1994. Evidence of chilling-induced oxidative stress in maize seedlings and a regulatory role for hydrogen peroxide. *Plant Cell* 6, 65–74.
- Ramasami, R., Shanmugam, N., 1976. Effect of nutrients on the incidence of *Rhizoctonia* seedling disease of cotton. *Indian Phytopathol.* 29, 465–466.
- Rascio, A., Russo, M., Mancuzzo, L., Platani, C., Nicastrò, G., Di Fonzo, N., 2001. Enhanced osmotolerance of a wheat mutant selected for potassium accumulation. *Plant Sci.* 160, 441–448.
- Rayle, D.L., Cleland, R.E., 1992. The acid growth theory of auxin-induced cell elongation is alive and well. *Plant Physiol.* 99, 1271–1274.
- Reddy, K.R., Zhao, D., 2005. Interactive effects of elevated CO_2 and potassium deficiency on photosynthesis, growth, and biomass partitioning of cotton. *Field Crops Res.* 94, 201–213.
- Rengel, Z., Damon, P.M., 2008. Crops and genotypes differ in efficiency of uptake and use. *Physiol. Plant* 133, 624–636.
- Rigas, S., Debrosses, G., Haralampidis, K., Vicente-Agullo, F., Feldmann, K.A., Grabov, A., Dolan, L., Hatzopoulos, P., 2001. TRH1 encodes a potassium transporter required for tip growth in *Arabidopsis* root hairs. *Plant Cell* 13, 139–151.
- Roberts, S.K., Snowman, B.N., 1999. The effects of ABA on channel-mediated K^+ transport across higher plant roots. *J. Exp. Bot.* 51, 1585–1594.
- Rodriguez-Navarro, A., Rubio, F., 2006. High-affinity potassium and sodium transport systems in plants. *J. Exp. Bot.* 57, 1149–1160.
- Romheld, V., Kirkby, E.A., 2010. Research in potassium in agriculture: needs and prospects. *Plant Soil.* 335, 155–180.
- Rossard, S., Luini, E., Perault, J.M., Bonmont, J., Roblin, G., 2006. Early changes in membrane permeability, production of oxidative burst and modification of PAL activity induced by ergosterol in cotyledons of *Mimosa pudica*. *J. Exp. Bot.* 57, 1245–1252.
- Ruan, Y.L., Llewellyn, D.J., Furbank, R.T., 2001. The control of single-celled cotton fiber elongation by developmentally reversible gating of plasmodesmata and coordinated expression of sucrose and K transporters and expansin. *Plant Cell* 13, 47–60.
- Sangakkara, U.R., Frehner, M., Nosberger, J., 2000. Effect of soil moisture and potassium fertilizer on shoot water potential, photosynthesis and partitioning of carbon in mungbean and cowpea. *J. Agron. Crop Sci.* 185, 201–207.
- Santa-Maria, G.E., Epstein, E., 2001. Potassium/sodium selectivity in wheat and the amphiploid cross wheat \times *Lophopyrum elongatum*. *Plant Sci.* 160, 523–534.
- Sarjala, T., Kaunisto, S., 1993. Needle polyamine concentrations and potassium nutrition in scots pine. *Tree Phys.* 13, 87–96.
- Satter, R.L., Galston, A.W., 1973. Leaf movements: Rosetta stone of plant behavior. *Bioscience* 23, 407–416.

- Satter, R.L., Galston, A.W., 1981. Mechanisms of control of leaf movements. *Ann. Rev. Plant Phys.* 32, 83–110.
- Schobert, C., Baker, L., Komor, E., Hayashi, H., Chino, M., Lucas, W.J., 1998. Identification of immunologically related proteins in sieve-tube exudate collected from monocotyledonous and dicotyledonous plants. *Planta* 206, 245–252.
- Schrempf, M., Satter, R.L., Galston, A.W., 1976. Potassium-linked chloride fluxes during rhythmic leaf movement of *Albizia Julibrissin*. *Plant Physiol.* 58, 190–192.
- Sen Gupta, A., Berkowitz, G.A., 1987. Osmotic adjustment, symplast volume, and nonstomatically mediated water stress inhibition of photosynthesis in wheat. *Plant Physiol.* 85, 1040–1047.
- Sen Gupta, A., Berkowitz, G.A., Pier, P.A., 1989. Maintenance of photosynthesis at low leaf water potential in wheat. Role of potassium status and irrigation history. *Plant Physiol.* 89, 1358–1365.
- Shabala, L., Cuin, T.A., Newman, I.A., Shabala, S., 2005. Salinity induced ion flux patterns from the excised roots of *Arabidopsis* SOS mutants. *Planta* 222, 1041–1050.
- Shabala, S., Demidichic, V., Shabala, L., Cuin, T.A., Smith, S.J., Miller, A.J., Davies, J.M., Newman, I.A., 2006. Extracellular Ca^{2+} ameliorates NaCl induced loss from *Arabidopsis* root and leaf cells by controlling plasma membrane K permeable channels. *Plant Physiol.* 141, 1653–1665.
- Shabala, S., Cuin, T.A., 2007. Potassium transport and plant salt tolerance. *Physiol. Plant* 133, 651–669.
- Schachtman, D., Shin, R., 2007. Nutrient sensing and signaling: NPKS. *Annu. Rev. Plant Biol.* 58, 47–69.
- Sharp, R.E., Hsiao, T.E., Silk, W.K., 1990. Growth of the maize primary root at low water potentials. II. Role of growth and deposition of hexose and potassium in osmotic adjustment. *Plant Physiol.* 93, 1337–1346.
- Shin, R., Schachtman, D.P., 2004. Hydrogen peroxide mediates plant root cell response to nutrient deprivation. *Proc. Natl. Acad. Sci.* 101, 8827–8832.
- Shingles, R., McCarty, R.E., 1994. Direct measurement of ATP-dependent proton concentration changes and characterization of a K-stimulated ATPase in pea chloroplast inner envelope vesicles. *Plant Physiol.* 106, 731–737.
- Sodek, L., Lea, P.J., Mifflin, D.J., 1980. Distribution and properties of a potassium-dependent asparaginase isolated from developing seeds of *Pisum sativum* and other plants. *Plant Physiol.* 65, 22–26.
- Stark, C., 1991. Osmotic adjustment and growth of Salt-stressed cotton as improved by a bioregulator. *J. Agron. Crop Sci.* 167, 326–334.
- Sudhir, P., Murthy, S.D.S., 2004. Effects of salt stress on basic processes of photosynthesis. *Photosynthetica* 42, 481–486.
- Suelter, C.H., 1970. Enzymes activated by monovalent cations. *Science* 168, 789–795.
- Sweeney, D.W., Granade, G.V., Eversmeyer, M.G., Whitney, D.A., 2000. Phosphorus, potassium, chloride, and fungicide effects on wheat yield and leaf rust severity. *J. Plant Nutr.* 23, 1267–1281.
- Szczerba, M.W., Britto, D.T., Kronzucker, H.J., 2009. K^+ transport in plants: physiology and molecular biology. *J. Plant Physiol.* 166, 447–466.
- Taiz, L., Zeiger, E., 2010. In: *Plant Physiology*. Sinauer Associates Inc., Sunderland, MA.
- Tanaka, Y., Sano, T., Tamaoki, M., Nakajima, N., Kondo, N., Hasezawa, S., 2005. Ethylene inhibits abscisic acid-induced stomatal closure in *Arabidopsis*. *Plant Physiol.* 138, 2337–2343.
- Tezara, W., Mitchell, V.J., Driscoll, S.D., Lawlor, D.W., 1999. Water stress inhibits plant photosynthesis by decreasing coupling factor and ATP. *Nature* 401, 914–917.
- Thiel, G., Weise, R., 1999. Auxin augments conductance of K inward rectifier in maize coleoptile protoplasts. *Planta* 208, 38–45.

- Thomashow, M.F., 1999. Plant cold acclimation: freezing tolerance genes and regulatory mechanisms. *Annu. Rev. Physiol. Plant Mol. Biol.* 50, 571–599.
- Tsai, H.Y., Bird, L.S., 1975. Microbiology of host pathogen interactions for resistance to seedling disease and multiadversity resistance in cotton. In: *Proceedings of the Beltwide Cotton Production Research Conference*, pp. 39–45. Memphis, TN.
- Turner, N.C., Begg, J.E., Tonnet, M.L., 1978. Osmotic adjustment of sorghum and sunflower crops in response to water deficits and its influence on the water potential at which stomata close. *Funct. Plant Biol.* 5, 597–608.
- Uehlein, N., Kaldenhoff, R., 2008. Aquaporins and plant leaf movements. *Ann. Bot.* 101, 1–4.
- Walker, D.J., Leigh, R.A., Miller, A.J., 1996. Potassium homeostasis in vacuolate plant cells. *Proc. Natl. Acad. Sci.* 93, 10510–10514.
- Wang, Y., Wu, W.H., 2010. Plant sensing and signaling in response to K⁺ deficiency. *Mol. Plant* 3, 280–287.
- Wang, Y., Du, M., Eneji, E., Wang, B., Tian, X., 2012. Mechanism of phytohormone involvement in feedback regulation of cotton leaf senescence induced by potassium deficiency. *J. Exp. Bot.* 63, 5887–5901.
- Ward, G.M., 1960. Potassium in plant metabolism. III. Some carbohydrates changes in the wheat seedling associated with varying rates of potassium supply. *Can. J. Plant Sci.* 40, 729–735.
- Watanabe, H., Takahashi, K., 1997. Effects of abscisic acid, fusicoccin, and potassium on growth and morphogenesis of leaves and internodes in dark-grown rice seedlings. *Plant Growth Regul.* 109, 109–114.
- Weimberg, R., Lerner, H.R., Poljakoff-Mayber, A., 1982. A relationship between potassium and proline accumulation in salt-stressed *Sorghum bicolor*. *Physiol. Plant* 55, 5–10.
- Wolf, D.D., Kimbrough, E.L., Blaser, R.E., 1976. Photosynthetic efficiency in alfalfa with increasing potassium nutrition. *Crop Sci.* 16, 292–294.
- Wright, J.P., Fisher, D.B., 1981. Measurement of the sieve tube membrane potential. *Plant Physiol.* 67, 845–848.
- Wyn Jones, R.G., Brady, C.J., Speirs, J., 1979. Ionic and osmotic relations in plant cells. In: Laidman, D.L., Wyn Jones, R.G. (Eds.), *Recent Advances in the Biochemistry of Cereals*. Academic Press, London, UK, pp. 63–103.
- Wyn Jones, R.J., Pollard, A., 1983. Proteins, enzymes and inorganic ions. In: Lauchli, A., Pirson, A. (Eds.), *Encyclopedia of Plant Physiology*. Springer, Berlin, pp. 528–562.
- Yamada, S., Osaki, M., Shimano, T., Yamada, M., Ito, M., Permana, A.T., 2002. Effect of potassium nutrition on current photosynthesized carbon distribution to carbon and nitrogen compounds among rice, soybean, and sunflower. *J. Plant Nutr.* 25, 1957–1973.
- Yang, X.E., Liu, J.X., Li, H., Luo, A.C., 2004. Potassium internal use efficiency, relative to growth vigor, potassium distribution and carbohydrate allocation in rice genotypes. *J. Plant Nutr.* 27, 837–852.
- Yeo, A.R., Kramer, D., Lauchli, A., Gullasch, J., 1977. Ion distribution in salt-stressed mature *Zea mays* roots in relation to ultra-structure and retention of sodium. *J. Exp. Bot.* 28, 17–29.
- Yeo, A.R., Lee, K.S., Izard, P., Boursier, P.J., Flowers, T.J., 1991. Short-term and long-term effects of salinity on leaf growth in rice (*Oryza sativa* L.). *J. Exp. Bot.* 42, 881–889.
- Yermiyahu, U., Kafkafi, U., 1990. Yield increase and stem brittle decrease in response to increasing concentrations of potassium and NO₃⁻/NH₄⁺ in White Carnation CV. Stand. Hassadeh 90, 742–746.
- Younis, H.M., Boyer, J.S., Govindjee, 1979. Conformation and activity of chloroplast factor exposed to low chemical potential of water in cells. *Biochim. Biophys. Acta* 548, 328–340.
- Zhang, Y., Li, Q., Zhou, X., Zhai, C., Li, R., 2006. Effects of partial replacement of potassium by sodium on cotton seedlings development and yield. *J. Plant Nutr.* 29, 1845–1854.
- Zhang, Z., Yang, F., Tian, X., 2009. Coronatine-induced lateral formation in cotton (*Gossypium hirsutum*) seedlings under potassium-sufficient and -deficient conditions in relation to auxin. *J. Plant Nutr. Soil Sci.* 172, 435–444.

- Zhao, D., Oosterhuis, D.M., Bednarz, C.W., 2001. Influence of potassium deficiency on photosynthesis, chlorophyll content, and chloroplast ultrastructure of cotton plants. *Photosynthetica* 39, 103–109.
- Zhao, J., Cheng, N.H., Motes, C.M., Blancaflor, E.B., Moore, M., Gonzales, N., Padmanaban, S., Sze, H., Ward, J.M., Hirschi, K.D., 2008. AtCHX13 is a plasma membrane K⁺ transporter. *Plant Physiol.* 148, 796–807.
- Zhenming, N., Xuefeng, X., Yi, W., Tianzhong, L., Jin, K., Zhenhai, H., 2008. Effects of leaf-applied potassium, gibberellin and source-sink ratio on potassium absorption and distribution in grape fruits. *Sci. Hort.* 115, 164–167.
- Zhu, J., Hasegawa, P.M., Bressan, R.A., 1997. Molecular aspects of osmotic stress in plants. *Crit. Rev. Plant Sci.* 16, 253–277.
- Zhu, J.K., Liu, J., Xiong, L., 1998. Genetic analysis of salt tolerance in *Arabidopsis thaliana*: evidence of a critical role for potassium nutrition. *Plant Cell* 10, 1181–1192.
- Zhu, J.K., 2003. Regulation of ion homeostasis under salt stress. *Curr. Opin. Plant Biol.* 6, 441–445.

This page intentionally left blank



Disease and Frost Damage of Woody Plants Caused by *Pseudomonas syringae*: Seeing the Forest for the Trees

Jay Ram Lamichhane^{*,†}, Leonardo Varvaro^{*}, Luciana Parisi[†], Jean-Marc Audergon[‡] and Cindy E. Morris^{†,1}

^{*}Department of Science and Technology for Agriculture, Forestry, Nature and Energy (DAFNE), Tuscia University, Viterbo, Italy

[†]INRA, Pathologie Végétale, Montfavet cedex, France

[‡]INRA, GAFL, Montfavet cedex, France

¹Corresponding author: e-mail address: Cindy.Morris@avignon.inra.fr

Contents

1. Introduction	236
2. Economic Importance	240
3. Types of Diseases of Woody Plants Caused by <i>P. syringae</i> and Their Importance	241
3.1 Parenchymatic or Localized Diseases	242
3.2 Vascular or Systemic Diseases	242
4. Epidemiology	249
4.1 Sources of Inoculum	249
4.2 Ports of Entry for Infection of Plant Tissues	252
4.3 Means of Dissemination	254
4.4 Variability in Host Genotype Susceptibility	255
5. The Diversity of <i>P. syringae</i> Causing Disease to Woody Plant Species	257
6. Control of Diseases of Woody Plants Caused by <i>P. syringae</i>	263
6.1 Exclusion, Elimination, or Reduction of Pathogen Inoculum	263
6.2 Enhancing Crop Genetic Diversity	268
6.3 Inhibition of <i>P. syringae</i> Virulence Mechanisms	270
7. The Case of Frost Damage due to Ice Nucleation-Active <i>P. syringae</i>	272
8. Conclusions and Perspectives	274
Acknowledgments	275
References	276

Abstract

Pseudomonas syringae is a phytopathogenic bacterium that causes diseases of monocots, herbaceous dicots, and woody dicots, worldwide. On woody plants, reports of disease due to *P. syringae* have markedly increased in the last years and the diseases have been recognized as a major threat to the primary products of agroforestry practices. Detection

in Italy of a new highly aggressive population of *P. syringae* in 2008 on kiwifruit, which caused severe epidemics in the following years throughout the kiwifruit-growing areas of Asia, Europe, Oceania, and South America, rendered the entire kiwifruit industry vulnerable to the disease. Similarly, occurrence of an aggressive population of *P. syringae* on horse chestnut in 2002 in the Netherlands has rapidly established itself as a major threat to horse chestnut throughout Northwest Europe. To better understand the origin of such disease epidemics, a thorough knowledge of the pathogen is needed in *sensu lato*. Here, we report the most important features of the pathogen and its hosts in an attempt to clarify some key aspects. In particular, the diseases and the economic losses they cause, disease epidemiology, pathogen diversity, and the possible means of disease control have been discussed throughout the manuscript. In addition to the ability to cause the disease, the damage caused to woody plants through the ice nucleation activity of this bacterium is discussed.



1. INTRODUCTION

The economic importance of a given plant species is an attribute of the quantity of services and products that it provides for humans. Edible components, firewood, and timber are usually considered to be the most important primary products obtained from plants. In addition, secondary products such as biofuels and plant-based medicines have a nonnegligible value for humans. Perennial plants are composed of the hard fibrous material consisting of secondary xylem tissue known as wood (Hickey and King, 2001; Plomion et al., 2001). Each year, most woody plants form new layers of woody tissue that are deposited on the inner side of the cambium, located immediately under the bark. However, in some monocotyledons, such as palms and dracaenas, the wood is formed in bundles scattered through the interior of the trunk (Chase, 2004). A few herbaceous perennial species such as *Uraria picta*, some other species belonging to the *Polygonaceae* family and herbaceous perennials from alpine and dry environments, that have a thickened and short hard perennial stem known as caudex (Welsh, 1981), develop wood-like stems. However, these species are not truly woody and they only develop hard densely packed stem tissue. Woody perennial plants, because of their long life cycle, ensure a regular income for growers and represent an important economic source for a large number of individuals. In addition to their primary products, the environmental services of trees are particularly significant to human life. Examples are prevention of soil erosion and land degradation (Wilkinson, 1999), carbon sequestration (Nowak and Crane, 2002), reduction of building energy consumption (Akbari, 2002), and of air pollution (Nowak et al., 2006). Among the numerous diseases of woody plants, those caused by *Pseudomonas syringae* have become markedly important in recent years. Since only the beginning of this century, 55 reports of disease outbreaks in 25 countries have been associated with *P. syringae* in 25 different woody hosts (Table 4.1). These

Table 4.1 Disease Outbreaks on Woody Plants Caused by *Pseudomonas syringae* Reported Worldwide Since 2000

Continent	Country	Occurrence Year	Host	Incidence		
				(%)	Pathogen	Reference
Asia-Pacific	China	2006	Pear	NR	Pss	Xu et al. (2008)
		2008	Kiwifruit	NR	Psa	CABI/EPPO (2008)
	Iran	2001–2003	Almond	NR	Pss	Samavatian (2006)
		2003–2004	Chinaberry	NR	Pme	Taghavi and Hasani (2010)
		2005	Apricot, peach	NR	Pss	Karimi-Kurdistani and Harighi (2008)
		2008	Olive	NR	Pss	Ashorpour et al. (2008)
		2007–2008	Jasmine	NR	Psav	Taghavi and Hasani (2012)
		2012	Hazelnut	NR	Ps	Mahdavian and Hasanzadeh (2012)
	Korea	1997–2000	Kiwifruit	NR	Psa	Koh et al. (2012)
	Nepal	2006–2007	Olive	NR	Pssav	Balestra et al. (2009a)
	Syria	2007	Olive	70	Pssav	Alabdalla et al. (2009)
	Turkey	1999–2001	Apricot	80	Pss	Kotan and Sahin (2002)
		2004	Orange, mandarin	100	Pss	Mirik et al. (2005)
		2008	Peach	10	Ps	Ozakatan et al. (2008)
		2009–2010	Kiwifruit	3	Psa	Bastas and Karakaya (2012)
		Australia	2000	Grapevine	NR	Ps
	2001		Olive	NR	Ps	Hall et al. (2003)
	2003		Olive	NR	Pssav	Hall et al. (2004)
	2006–2007		Grapevine	60	Pss	Whitelaw-Weckert et al. (2011)
	2007		Mango	NR	Pss	Golzar and Cother (2008)
2011	Kiwifruit		NR	Psa	EPPO (2011a)	
New Zealand	2010	Kiwifruit	NR	Psa	Everett et al. (2011)	

Continued

Table 4.1 Disease Outbreaks on Woody Plants Caused by *Pseudomonas syringae* Reported Worldwide Since 2000—cont'd

Continent	Country	Occurrence Year	Host	Incidence (%)	Pathogen	Reference	
Europe	Belgium	2007	Horse chestnut	NR	Psaes	Bultreys et al. (2008)	
	Bulgaria	2004–2005	Firethorn	NR	Pss	Bobev et al. (2008)	
		2004–2006	Apricot	85	Ps	Ivanova (2009)	
	Czech Republic	2008–2010	Horse chestnut	NR	Psaes	Mertelik et al. (2013)	
		France	2007	Horse chestnut	NR	Ps	Bardoux and Rousseau (2007)
	2008		Brazilian jasmine	NR	Psav	Eltlbany et al. (2012)	
	2010		Kiwifruit	NR	Psa	Vanneste et al. (2011b)	
	Germany	2006	Hazelnut	NR	Psc	Poschenrieder et al. (2006)	
		2007	Horse chestnut	NR	Psaes	Schmidt et al. (2008)	
	Ireland	2010	Horse chestnut	NR	Psaes	EPPO (2011c)	
	Italy	2003	Onondaga	NR	Psv	Garibaldi et al. (2005)	
		2004	White bird of paradise	40	Psl	Polizzi et al. (2005)	
			Hazelnut	NR	Psc	Cirvilleri et al. (2007)	
		2005	Nectarine	30–35	Pss	Scortichini and Janse (2008)	
		2006	Apricot	30	Pss	Scortichini (2006)	
		2007	Kiwifruit	30	Pv	Balestra et al. (2008)	
		2007–2008	Kiwifruit	10–70	Psa	Balestra et al. (2009b)	
		2013	Sweet olive	NR	Psav	Cinelli et al. (2013a)	
		Lithuania	2007	Cherry and plum	NR	Pss, Psm1, Psm2	Vasinauskienė et al. (2008)
		Norway	2010	Horse chestnut	NR	Psaes	Talgå et al. (2012)
Portugal	2007	Kiwifruit	30	Ps	Balestra et al. (2009c)		
	2010	Kiwifruit	30	Psa	Balestra et al. (2010)		

	Spain	2011	Kiwifruit	80	Psa	Abelleira et al. (2011)
		1999–2000	Kiwifruit	40	Ps	González and Ávila (2005)
	Switzerland	2011	Kiwifruit	NR	Psa	EPPO (2011d)
	The Netherlands	2002–2003	Horse chestnut	NR	Psaes	Dijkshoorn-Dekker (2005)
		2009–2010	Plum	50	Pss, Psm	Wenneker et al. (2012)
	The UK	2000–2001	Wild cherry	50–100	Pss, Psm1, Psm2	Vicente et al. (2004)
		2003	Horse chestnut	70	Psaes	Webber et al. (2008)
		2006	Onondaga	NR	Psv	Stead et al. (2006)
North America	The USA	2002	Sweet cherry	NR	Pss, Psm1	Renick et al. (2008)
South America	Brazil	2006	Coffee	1–2	Pstab	Destéfano et al. (2010)
	Chile	2011	Kiwifruit	NR	Psa	EPPO (2011b)

Note: NR, not reported; Ps, *Pseudomonas syringae*; Pss, *P. syringae* pv. *syringae*; Psav, *P. savastanoi*; Pssav, *P. savastanoi* pv. *savastanoi*; Psm1 and Psm2, *P. syringae* pv. *morsprunorum* race 1 and 2; Psa, *P. syringae* pv. *actinidiae*; Psaes, *P. syringae* pv. *aesculi*; Psc, *P. syringae* pv. *coryli*; Pme, *P. meliae*; Pstab, *P. syringae* pv. *tabaci*; Psv, *P. syringae* pv. *viburni*.

reports are also snapshots of recurring chronic problems, such as olive knot disease in Italy or apricot canker in France, that have been important over the past century. Hence, it can be assumed that this rate portends additional future outbreaks. To mitigate the consequences of such a disease emergence, it is important to understand the underlying causes. In this light, we have reviewed the literature in order to highlight the salient features of *P. syringae* as a pathogen of woody plant species and to underscore what remains unknown about the diseases it causes.



2. ECONOMIC IMPORTANCE

Reliable estimates of economic losses caused by plant pathogens are not only a prerequisite for optimal crop management at the farm level but also for basic decisions on broader issues such as research priorities and pesticide regulations. Although several methods have been proposed to evaluate economic losses caused by plant pathogens (Heaton et al., 1981; James, 1974), only few data are available in the literature. Insufficient information on the biological effects of the pathogens on their host is the major obstacle preventing more accurate crop-loss assessment in monetary terms. Crop-loss assessments have been made for major annual staple and cash crops (Oerke, 2005; Oerke et al., 1994). However, data inadequacies are particularly acute in the case of perennial crops, where intertemporal effects operate. For perennial plants, their health in any given season is likely to influence their health in future seasons (Heaton et al., 1981).

Bacterial cankers of perennial trees caused by *P. syringae* provoke serious economic losses around the world. Cankers are characterized by systemic wilting and dieback of twigs, branches or the entire tree resulting from systemic spread of the pathogen in the vessels. On hazelnut, bacterial canker was reported to be the most important factor limiting the cultivation and further expansion of hazelnut production in Greece (Psallidas, 1993) since its first outbreak (Psallidas and Panagopoulos, 1979). In Italy, *P. syringae* destroyed thousands of hectares of hazelnut, with an annual loss of approximately US\$ 1.5 million (Scortichini, 2002; Scortichini and Tropiano, 1994). Similarly, the recent bacterial canker epidemic of kiwifruit has decimated thousands of hectares around the world. In New Zealand alone, yield losses caused by the disease in 2012 were estimated to be 21% (90,820 ton less than in 2011) with economic losses of US\$ 76 million (<http://www.kvh.org.nz/newsroom>). However, the most dramatic consequences of the disease can be seen for the long term. A risk analysis, performed in 2012, estimated that over the next five years bacterial

canker of kiwifruit might cost between NZ\$ 310 million to 410 million to the New Zealand kiwifruit industry (Vanneste, 2012). It is estimated that over a 15-year period the cost might jump to NZ\$ 885 million (Greer and Saunders, 2012). In the Bay of Plenty area of New Zealand alone, 360 to 470 fulltime jobs might be lost between 2012 and 2016 due to the bacterial canker epidemic on kiwifruit (Greer and Saunders, 2012). Although no estimation has been made for Italy, the situation in that country might be even worse, given the intensity and diffusion of the bacterial canker epidemics (Scortichini et al., 2012; Vanneste, 2012). Due to the extent and serious impact of bacterial canker, it is thought that kiwifruit plantings in Italy will be significantly reduced over the next three to five years (<http://www.kvh.org.nz/newsroom>).

Bacterial canker also affects tree species in the genus *Prunus* (stone fruits and almond) (English et al., 1980; Kennelly et al., 2007; Vicente et al., 2004). In South Africa, annual damage caused by bacterial canker of stone fruit crops is estimated to be over US\$ 10 million (Hattingh et al., 1989). Damage caused by *P. syringae* is not limited to field production but also occurs in nurseries where sudden wilting is a major problem. For example, annual losses in woody plant nurseries in Oregon are estimated at US\$ 8 million (Scheck et al., 1996).

In Germany, bacterial canker causes annual tree mortality rates as high as 30% on plum (Hinrichs-Berger, 2004). In Oregon (the USA), bacterial canker is responsible for 17% annual tree deaths for sweet cherry (Spotts et al., 1990). The incidence of bacterial canker is reported to be 50–100% on wild cherry in the UK (Vicente et al., 2004), 50% on plum in the Netherlands (Wenneker et al., 2012), and 80% on apricot in Turkey (Kotan and Sahin, 2002). In addition to stone fruits, *P. syringae* diseases are economically important also on pome fruits (Mansvelt and Hattingh, 1986). The disease results in economic losses in pear production around the world (English et al., 1980; Fahy and Lloyd, 1983; Manceau et al., 1990; Montesinos and Vilardell, 1991). Another very recent epidemic caused by *P. syringae* is bleeding canker of horse chestnut. The disease is widespread in many European countries (Bultreys et al., 2008; Schmidt et al., 2008; Webber et al., 2008). However, no data are available on the potential losses.



3. TYPES OF DISEASES OF WOODY PLANTS CAUSED BY *P. SYRINGAE* AND THEIR IMPORTANCE

A broad range of crops is susceptible to diseases caused by the group of Gram-negative bacteria referred to as *P. syringae* (Bull et al., 2010). Concerning perennial plants, the literature suggests that a large number

of woody tree species are attacked by this pathogen. An exhaustive list of diseases of perennial plants caused by *P. syringae* is reported in Table 4.2. Deciduous fruit and nut trees (Kennelly et al., 2007; Mansvelt and Hattingh, 1986), ornamental trees and shrubs (Garibaldi et al., 2005; Temsah et al., 2007a,b), deciduous forest tree species (Ark, 1939; Green et al., 2009; Menard et al., 2003), and evergreen fruit trees (Young, 2004) are among the known hosts of *P. syringae*. Overall, phytopathogenic *P. syringae* causes two types of diseases on woody plants (Agris, 2005), those whose symptoms are confined to parenchymatic tissue and those whose symptoms are manifested in vascular tissue.

3.1 Parenchymatic or Localized Diseases

One family of diseases of woody plants caused by *P. syringae* is characterized by the presence of localized symptoms affecting parenchymatic tissues. In this case, the pathogen does not move throughout the host vascular system. Typical symptoms are leaf spots (Destéfano et al., 2010; Goto, 1983a, 1983b; Roberts, 1985a), fruit spots (Bedford et al., 1988; Burr and Hurwitz, 1981), apical necrosis (Cazorla et al., 1998; Golzar and Cother, 2008), blossom and bud blasts (Kennelly et al., 2007; Manceau et al., 1990; Mansvelt and Hattingh, 1986; Young, 1987), bud rot and necroses (Cazorla et al., 1998; Conn et al., 1993), shoot tip dieback (McKee, 1955; Polizzi et al., 2005; Ramos and Kamidi, 1981; Tomihama et al., 2009), and gall or outgrowth on stems, leaves, and trunks (Kamiunten et al., 2000; Ogimi, 1977; Ogimi et al., 1990, 1992; Temsah et al., 2007a,b). The resulting localized infections rarely kill the plants and losses are due mainly to damage to flowers and photosynthetic parts (leaves).

3.2 Vascular or Systemic Diseases

Vascular diseases are characterized by the systemic movement of the disease throughout the plant and in particular the vessels (phloem and xylem). The vascular diseases caused by *P. syringae* are generally devastating. Sudden wilting and dieback (Scortichini, 2002), presence of extended cankers on stems, branches, and main trunks (Jones, 1971; Latorre and Jones, 1979a; Little et al., 1998; Sakamoto, 1999; Young, 1988a), and production of exudates and gummosis (Kennelly et al., 2007; Green et al., 2009; Scortichini et al., 2012) are common symptoms.

To attack stems, branches, and trunks, *P. syringae* infects the woody tissue of the plant. Of all the plant tissues, woody tissue has the highest content of lignin, a complex phenolic polymer common to vascular plants. Plant lignin

Table 4.2 Pathogens from the *Pseudomonas syringae* Complex Reported to be Virulent on Woody Plants

Organism	Phylogroup ^a	Disease	Host(s)	Plant Type	References ^b
<i>P. syringae</i> pv.					
<i>actinidiae</i> ^{f,h}	1	Bacterial canker	Kiwifruit	Tree	Scortichini et al. (2012)
<i>avellanae</i> ^{f,h}	1	Bacterial canker	European hazelnut	Tree	Scortichini (2002)
<i>avii</i> ^{f,h}	1	Bacterial canker	Wild cherry	Tree	Menard et al. (2003)
<i>berberidis</i> ^g	1	Bacterial leaf spot	<i>Berberis</i> spp.	Woody shrub	Roberts (1985b)
<i>lachrymans</i> ^g	1	Bacterial blight	White bird of paradise	Tree	Polizzi et al. (2005)
<i>morsprunorum</i> ^{f,h}	1	Bacterial canker	Stone fruit	Tree	Crosse (1966)
<i>persicae</i> ^{f,h}	1	Bacterial dieback	Peach	Tree	Young (1988a)
<i>theae</i> ^g	1	Bacterial shoot blight	Tea	Tree	Tomihama et al. (2009)
<i>viburni</i> ^s	1	Bacterial blight	<i>Viburnum</i> spp.	Woody shrub	Thornberry and Anderson (1931a)
<i>aceris</i> ^g	2	Bacterial leaf spot	Maple	Tree	Ark (1939)
<i>dysoxylis</i> ^g	2	Bacterial leaf diseases	Kohekohe	Tree	Hutchinson (1949)
<i>papulans</i> ^g	2	Blister spot	Apple	Tree	Bedford et al. (1988)

Continued

Table 4.2 Pathogens from the *Pseudomonas syringae* Complex Reported to be Virulent on Woody Plants—cont'd

Organism	Phylogroup ^a	Disease	Host(s)	Plant Type	References ^b
<i>syringae</i>	2	Blossom blight	Lilac	Tree	Young (1991)
		Apical necrosis ^g	Mango	Tree	Cazorla et al. (1998)
		Influorescence rot	Grapevine	Liana	Whitelaw-Weckert et al. (2011)
		Bacterial canker ^{f,h}	Stone fruit	Tree	Jones (1971), Latorre and Jones (1979a)
		Bacterial canker ^f	Olive	Tree	Hall et al. (2003)
		Blister bark ^{f,h}	Apple	Tree	Mansvelt and Hattingh (1986)
		Blossom blight ^g	Pear	Tree	Moragrega et al. (2003)
		Bacterial blight and canker ^f	Hazelnut	Tree	Scortichini et al. (2002)
		Bacterial blight ^g	Kiwifruit	Tree	Young (1988b)
		Bacterial canker ^{f,h}	Almond	Tree	Little et al. (1998)
		Citrus blast ^g	Orange and mandarin	Tree	Mirik et al. (2005)
		Fruit scab ^g	Nectarine	Tree	Scortichini and Janse (2008)
		Bacterial canker ^f	Amurmaackia	Tree	Sakamoto (1999)
		Bacterial canker ^{f,h}	Blueberry	Woody shrub	Canfield et al. (1986)
		Leaf blight ^g	Cornellian cherry	Tree	Mmbaga and Nnodu (2006)
		Bacterial dieback	Willow	Tree	Ramstedt et al. (1994)
Dieback and canker	Poplar	Tree	Whitebread (1967)		
Sucker and twig dieback	Black alder	Tree	Scortichini (1997)		

<i>P. amygdali</i> ^{c,f,h}	3	Hyperplastic canker	Almond	Tree	Psallidas and Panagopoulos (1975)
<i>P. ficusectae</i> ^g	3	Bacterial leaf spot	Japanese fig	Tree	Goto (1983b)
<i>P. meliae</i> ^f	3	Bacterial gall	Chinaberry	Tree	Ogimi (1977)
<i>P. tremae</i> ^f	3	Bacterial gall	Pigeon wood	Tree	Ogimi et al. (1988a)
<i>P. savastanoi</i> pv.					
<i>savastanoi</i> ^f	3	Olive knot	European olive	Tree	Young (2004)
		Knot	Privet	Woody shrub	Janse (1982)
		Knot	Forsythia	Woody shrub	Janse (1982)
		Knot	Jasmine	Woody shrub	Janse (1982)
<i>nerii</i> ^f	3	Knot	Oleander	Woody shrub	Janse (1982)
<i>fraxini</i> ^f	3	Knot	Ash	Tree	Janse (1982)
<i>retacarpa</i> ^f	3	Knot	Spanish broom	Woody shrub	Garcia de los Rios (1999)
ND ^f		Knot	Buckthorn	Woody shrub	Temsah et al. (2007a,b)
ND ^f		Knot	Myrtle	Woody shrub	Temsah et al. (2007a,b)
ND ^f		Knot	Sweet olive	Woody shrub	Cinelli et al. (2013a)
ND ^f		Knot	Brazilian jasmine	Woody shrub	Eltbany et al. (2012)

Continued

Table 4.2 Pathogens from the *Pseudomonas syringae* Complex Reported to be Virulent on Woody Plants—cont'd

Organism	Phylogroup ^a	Disease	Host(s)	Plant Type	References ^b
<i>P. syringae</i> pv.					
<i>aesculi</i> ^{f,h}	3	Bleeding canker	Horse chestnut	Tree	Green et al. (2010)
<i>castaneae</i> ^{d,f}	3	Bacterial canker	Chestnut	Tree	Takanashi and Shimizu (1989)
<i>cerasicola</i> ^f	3	Bacterial gall	Cherry	Tree	Kamiunten et al. (2000)
<i>ciccaronei</i> ^f	3	Bacterial spot	Carob	Tree	Ercolani and Calderola (1972)
<i>daphniphylli</i> ^f	3	Bacterial gall	Hime-yuzuriha	Tree	Ogimi et al. (1990)
<i>dendropanacis</i> ^f	3	Bacterial gall disease	Kakuremino	Woody shrub	Ogimi et al. (1988b)
<i>eriobotryae</i> ^f	3	Bacterial stem canker	Loquat	Woody shrub	McRae and Hale (1986)
<i>mori</i> ^g	3	Bacterial blight	Mulberry	Tree	Takahashi (1980)
<i>myricae</i> ^f	3	Bacterial knot disease	Yamamomo	Tree	Ogimi and Higuchi (1981)
<i>photiniae</i> ^g	3	Leaf spots and shoot blight	Red-leaf photinia	Woody shrub	Goto (1983a)
<i>rhapiolepidis</i> ^f	3	Bacterial gall	Sharinbai	Tree	Ogimi et al. (1992)
<i>tabaci</i> ^g	3	Bacterial leaf spot	Coffee	Woody shrub	Destéfano et al. (2010)
<i>ulmi</i> ^g	3	Bacterial spot/shoot blight	Elm	Tree	Sutic and Tesic (1958)

<i>garcae</i> ^g	4	Bacterial blight	Coffee	Woody shrub	Ramos and Kamidi (1981)
<i>philadelphia</i> ^g	5	Bacterial blight	Sweet mock-orange	Woody shrub	Roberts (1985a)
<i>ribicola</i> ^g	7	Leaf spot and defoliation	Golden currant	Woody shrub	Bohn and Maloit (1946)
<i>P. viridiflava</i> ^g	7	Blossom blight Tree apoplexy	Kiwifruit Peach	Tree Tree	Young (1988b) Scortichini and Morone (1997)
<i>coryli</i> ^{e,f}	ND	Twig dieback and canker	European hazelnut	Tree	Scortichini et al. (2005)

ND: not determined.

^aPhylogroups according to the study of Parkinson et al. (2011).

^bCited references are articles that provide general overviews of the disease and/or description of the pathogen.

^cThis pathogen is described as a forgotten pathogen in a recent work by Janse (2010).

^dThis pathogen is described as a forgotten pathogen in a recent work by Janse (2010).

^eThis pathogen is identified as *P. s. pv. syringae* belonging to group II as described by O'Brien et al. (2012).

^fThe pathogen attacks also woody tissues.

^gThe pathogen attacks only leaves and succulent parts of plant.

^hThe pathogen is vascular and highly aggressive.

can be broadly divided into three classes, softwood (gymnosperm), hardwood (angiosperm), and grass (graminaceous) lignin (Pearl, 1967). Lignin has a fundamental role in water transport, mechanical support, and biodefense (Robinson, 1990). Within a plant, lignin content varies greatly in different tissues. For example, lignin content is very low in young shoots and high in woody tissues (Novaes et al., 2010). The lignin content of woody perennial plants can vary from 15% to 40% (Sarkanen and Ludwig, 1971) whereas in annual plants it represents only from 4% to 10% of the oven-dry weight (Sullivan, 1955). How *P. syringae* can overcome such a robust barrier and cause a collapse of woody tissues is not known.

Interestingly, *P. syringae*-induced vascular diseases have been reported exclusively on deciduous trees (Green et al., 2009; Hattingh et al., 1989; Kennelly et al., 2007) while only parenchymatic diseases are caused on evergreen woody plants (Ramos and Kamidi, 1981; Young, 2004) (Table 4.2). Many aspects of the annual growth cycle differ significantly between deciduous and evergreen plants. Adaptation to a cold or dry season and to low nutrient levels has led to the differentiation of deciduous and evergreen woody plants (Monk, 1966). The annual phenology of deciduous trees is the process that begins with flower budbreak followed by leaf budbreak and sprouting in the spring and culminates in leaf fall in autumn followed by winter dormancy (Arora et al., 2003). These characteristics differentiate a deciduous tree from evergreens where such phenomena do not occur in synchrony for the whole tree. Accordingly, the risk of *P. syringae* infection might be strikingly higher on deciduous trees given the synchronized abundance of tender tissues and natural openings into the vascular system. Succulent swelling buds and shoots are fragile and highly sensitive to frost damage, thereby predisposing deciduous trees to frost damage induced by *P. syringae* (Gross et al., 1984; Nejad et al., 2004; Ramstedt et al., 1994). On the other hand, complete leaf fall that creates an enormous availability of leaf scars for a long period of time perfectly coincides with climatic conditions that are ideal for the survival and multiplication of *P. syringae* (Agrios, 2005; Scortichini, 2002). The presence of dormant buds, during the winter, represents an ideal overwintering site for *P. syringae* (Crosse, 1956; Roos and Hattingh, 1986; Sundin et al., 1988). On the contrary, evergreen species do not have autumn leaf shedding. However, leaf shed occurs very gradually over the years in evergreen plants (Aerts, 1995). Leaf spots caused by *P. syringae* are also almost exclusively reported on deciduous trees (Hattingh et al., 1989; Kennelly et al., 2007). It is not known why a ubiquitous epiphyte such as *P. syringae* (Hirano and Upper, 1990) causes foliar diseases only on a

very limited number of evergreen hosts, despite whole-year availability of leaf surfaces. In addition to the higher number of infection sites in deciduous trees, several studies have provided evidence of differences in protein content of bark between deciduous trees, including deciduous fruit trees (Kang and Titus, 1987; Kuroda et al., 1990; Lang and Tao, 1990; Mattheis and Ketchie, 1990), and evergreen woody plants (Craker et al., 1969; Hummel et al., 1990). For example, higher levels of polypeptide accumulation in bark tissues were observed in the deciduous peach compared with the evergreen one (Arora et al., 1992). Probably such polypeptides are involved in the process of vascularization of *P. syringae*. But this will need to be established by in-depth future studies. Species with both deciduous and evergreen traits, such as *Viburnum* spp., might provide some new insights in this regard.



4. EPIDEMIOLOGY

As for all plant diseases, biotic, abiotic and/or edaphic factors play an important role in epidemiology. Throughout the cultivation areas, these factors have been reported to weaken plant health and predispose them to pathogen attacks. In particular, soil texture, low soil pH, soil depth, tree nutrition, tree age, nematode parasitism, and environmental factors such as rain can influence *P. syringae* disease development (English et al., 1961, 1980; Scortichini, 2002, 2010; Scortichini et al., 2012; Vigouroux and Bussi, 1994). In addition, cultural practices such as rootstock selection, height of grafting and early fall pruning have been reported to affect *P. syringae* disease susceptibility of apricot and peach (Dunquesne and Gall, 1975; Fratantuono et al., 1998; Lownsbery et al., 1977; Prunier et al., 1999; Vigoroux et al., 1987, 1997). Likewise, the correlation among tree water content, effect of exposure to freezing temperature, and necrosis caused by *P. syringae* has been reported for apricot (Klement et al., 1974; Vigoroux, 1989), cherry (Sobiczewski and Jones, 1992), and peach (Cao et al., 2013; Vigoroux, 1999; Weaver, 1978). There are few generalities that can be made about the impact of abiotic factors and the production practices to which they are linked. On the other hand, biotic factors concerning both the plant and the pathogen have been received in the most intense study and offer the opportunity to identify key factors critical in disease development as illustrated below.

4.1 Sources of Inoculum

Overall, epiphytic populations, latent infection, overwintering sites on the infected hosts, the presence of orchard groundcovers, weeds, and detached

plant parts (pollen and leaf litter) represent the inoculum reservoir of *P. syringae*. All these inoculum sources appear to be important in the epidemiology of diseases caused by *P. syringae*. Epiphytic populations of this pathogen on asymptomatic plants are the immediate source of inoculum for disease. Differences in epiphytic populations of *P. syringae* were observed on leaves of apple trees grown in two different orchards: one with a history of disease, the other where the disease had not been observed previously (Bedford et al., 1988). Larger pathogen population sizes were found in association with greater disease incidence in the orchard with a prior history of the disease. Similarly, epiphytic populations of *P. syringae* as the source of inoculum for disease have been demonstrated on olive (Young, 2004), maple and pear trees (Malvick and Moore, 1988), and stone fruits (Roos and Hattingh, 1986). Monitoring of *P. syringae* epiphytic populations associated with nursery trees in Oregon showed that the population increased rapidly and peaked during the first 2–3 weeks after budbreak (Baca et al., 1987; Moore and Malvick, 1987) increasing markedly the risk of bud infection.

Establishment of *P. syringae* populations inside symptomless tissues could represent a very important source of primary inoculum. For this reason, vegetative propagation of the apparently healthy but latently infected mother plants could be an important source of inoculum. Widespread disease dissemination with propagation material such as dormant cuttings or budwoods, and *in vitro*-propagated shoots can be therefore relevant. On hazelnut, a large-scale dissemination of *P. syringae* is thought to have occurred through distribution of latently infected suckers (Scortichini, 2002). In addition, infected nursery stock of olive has been reported as the main cause of *P. syringae* introduction into new regions (Young, 2004). The isolation of pathogenic *P. syringae* from the vascular tissues of symptomless cherry (Cameron, 1970) and pear trees (Whitesides and Spotts, 1991) clearly explains the latent presence of the pathogen also in deciduous woody hosts. Indeed, infected nursery materials have been reported as the main inoculum reservoir of *P. syringae* in *Prunus* spp. (Dowler and Petersen, 1967; Lyskanowska, 1976; Mansvelt and Hattingh, 1988).

Woody plants provide the unique overwintering sites compared to annual plants. The role of dormant buds in deciduous trees as an overwintering site for *P. syringae* has been demonstrated in South Africa (Roos and Hattingh, 1986a), in the United Kingdom (Crosse, 1956), and in the USA (Sundin et al., 1988). On apple, a consistent population of *P. syringae* has been recovered from the innermost bud tissues and the population was larger than that found in the external tissues (Bedford et al., 1988; Burr and Katz,

1984). Dormant buds in cherry are colonized via infection of leaf scars during autumn at leaf fall. Climatic conditions during leaf shedding typically include cooler temperatures and wind-driven rains during which *P. syringae* is transported from leaf surfaces to leaf scars where systemic colonization occurs (Crosse, 1956). Once *P. syringae* enters through leaf scars, it moves systematically throughout the plant and colonizes dormant buds where the pathogen overwinters. In the following spring, dormant and apparently healthy but infected buds provide the inoculum for blossom colonization.

The importance of groundcovers and weeds within and outside the orchard represent another potential source of inoculum reservoir of *P. syringae*. In particular, when no leaf surface is available on trees (autumn and winter) the pathogen can shift to the groundcovers where it multiplies thereby ensuring a constant source of inoculum. Work reported from California (Davis and English, 1969) was the first to implicate weeds as hosts for *P. syringae*. Successively, the association of *P. syringae* with stone fruit orchard weeds or grasses have been reported in the USA (Michigan (Latorre and Jones, 1979b), Oregon (Baca and Moore, 1987)), Poland (Lyskanowska, 1976), and South Africa (Roos and Hattingh, 1986b). Large populations of phytopathogenic *P. syringae* have been consistently isolated from perennial rye, red fescue, annual rye and broom grasses growing among ornamental trees in the maple nursery and on perennial rye grass in the pear orchard (Malvick and Moore, 1988).

In some cases, pollen can be an important inoculum source of the pathogen. On kiwifruit, *P. syringae* has been found in pollen samples (Vanneste et al., 2011a) and it is believed that pollen has been a source of *P. syringae* introduction in New Zealand. In addition, *P. syringae* is able to survive in detached kiwifruit organs, such as leaf litter and twigs, until 45 days post-leaf fall (<http://www.kvh.org.nz>). Leaf litter across the alpine environment has been reported as an important reservoir of *P. syringae* populations (Monteil et al., 2012). Finally, it is thought that *P. syringae* survives poorly in soil or host debris, mostly throughout the regions with warmer summer (McCarter et al., 1983) although it is possible that the pathogen can survive for a long period in regions with cooler summer temperature, mostly under a constant soil moisture. Indeed, the ability of *P. syringae* to survive in the soil for a longer period has been demonstrated especially when the source of the inoculum was associated with plant debris and in the presence of constant soil moisture (Kritzman and Zutra, 1983). It is also worth noting that *P. syringae* has been isolated from the rhizosphere of crops and weeds (Knoche et al., 1987; Valleu et al., 1944). The fact that *P. syringae* can't be

found in agricultural soil all year round (mostly during the summer) might be because such lands are irrigated generally until the beginning of the summer and no water supply occurs afterward once the crops are harvested. Hence, warmer summer temperatures associated with a drastic reduction in soil moisture result in fatal conditions for the survival of *P. syringae*.

Snow is another important source of *P. syringae* inoculums, which may play an important role in a disease occurrence. An example is bacterial canker of blueberry (Canfield et al., 1986). This species grows naturally or in cultivated conditions across mountain areas where snowfall events are very common. At higher altitudes, spring frosts frequently occur where freezing and thawing are accentuated through the fluctuations in day/night temperatures. Such events cause lesions on plant parts exposing them to a high risk of infection. Snow per se can harbor populations of *P. syringae* as recently demonstrated (Morris et al., 2010). Besides snow, other environmental reservoirs of *P. syringae* including headwaters and epilithic biofilm have been described (Morris et al., 2007, 2010), and these eventually can come into contact with crops as irrigation water.

4.2 Ports of Entry for Infection of Plant Tissues

Unlike fungal pathogens, phytopathogenic bacteria are not able to make their own ports of entry (Agrios, 2005). Woody plants present a wide range of entry ports for bacteria including natural openings and wounds caused by natural phenomena and man-made practices. Natural openings (lenticels, hydathodes, stomata, trichomes) that serve as water and gas pores, and the wounds made by biotic (humans, insects, animals) and abiotic factors (hailstones, frost), are the main ports of entry (Agrios, 2005). For *P. syringae* pathogens of woody plants, the literature reports a large diversity of ports of entry as summarized in Figure 4.1. To gain access into plant tissues, the pathogen can use more than one port of entry. In general, foliar pathogens that cause localized symptoms enter mainly through the stomata, although some of them also enter via hydathodes and broken trichomes (Agrios, 2005; Hirano and Upper, 1990). Pathogens that cause woody parenchymatic diseases enter through wounds occurring on woody tissues (Garcia de los Rios, 1999; Kamiunten et al., 2000; Ogimi et al., 1990; Young, 2004). On the other hand, vascular pathogens use a vast number of ports including natural openings and lesions (Crosse, 1966; Kennelly et al., 2007; Hattingh et al., 1989). Lesions on woody tissues that allow a direct access to the vascular system are the most accessible port for vascular pathogens while natural openings are not always exploited by the different *P. syringae* pathogens of woody plants. There seems to be a

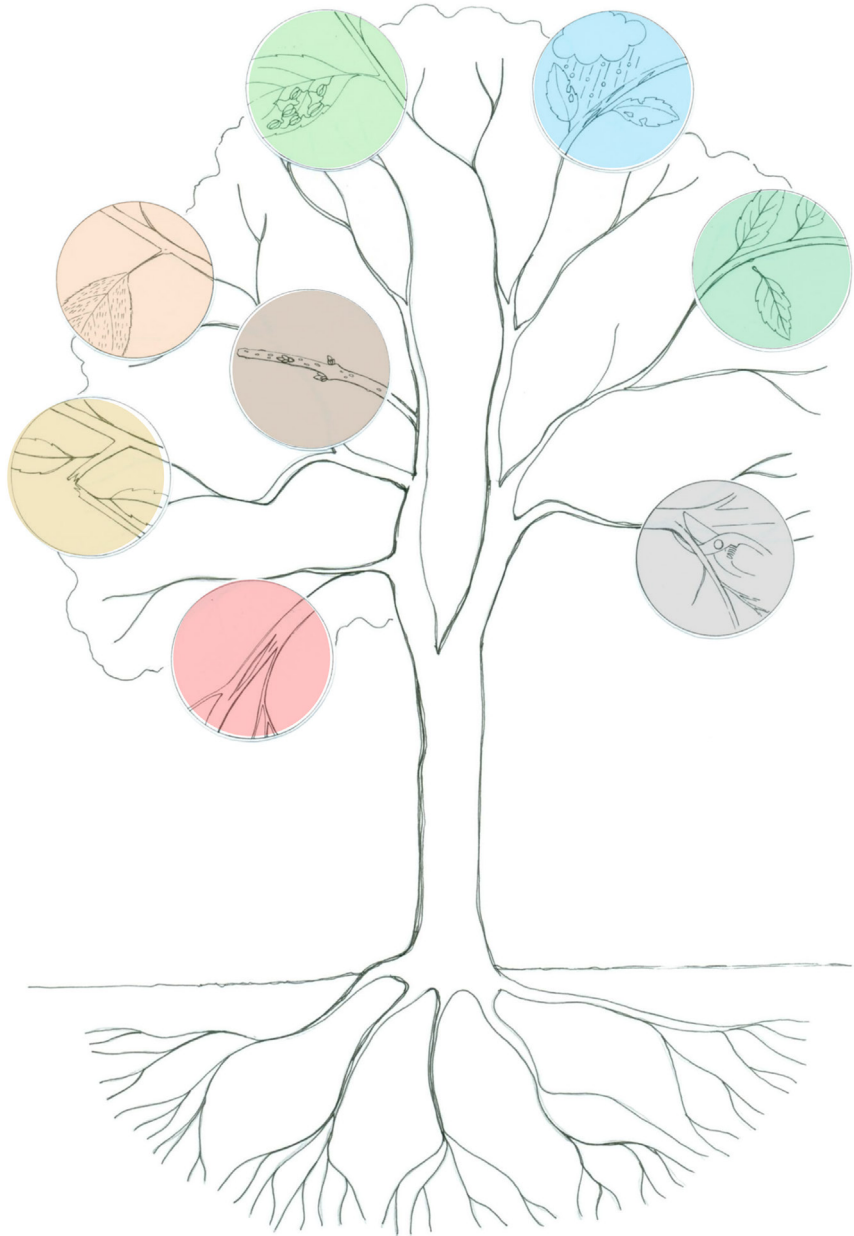


Figure 4.1 Schematic representation of infection ports of phytopathogenic *Pseudomonas syringae*. Clockwise from lower left: tissue damage caused by frost, branch breaking due to wind or mechanical damage, lenticels, broken trichomes, stomata, wounds caused by hailstones, leaf scars and wounds caused by pruning.

relationship between the port of entry and the symptoms caused by vascular *P. syringae* pathogens. Interestingly, leaf symptoms do not occur on infected hazelnut (Psallidas, 1993; Psallidas and Panagopoulos, 1979) and horse chestnut (Green et al., 2009) while they occur on infected kiwifruit (Scortichini et al., 2012; Young, 2012) and *Prunus* spp. (Bultreys and Kaluzna, 2010; Crosse, 1966; Freigoun and Crosse, 1975; Kennelly et al., 2007). On hazelnut, the only ports of entry used by *P. syringae* are leaf scars and lesions on woody tissues (Psallidas, 1993; Scortichini, 2002) giving the pathogen direct access to the vascular system. For horse chestnut, in addition to lesions, the role of lenticels as ports of entry has been demonstrated (Green et al., 2009). Indeed, lesions in proximity to lenticels appeared when stems of horse chestnut were spray-inoculated (Green et al., 2009). By contrast, *Prunus* spp. and in particular apricot and cherry, contain an impressive number of lenticels (Guirguis et al., 1995) although no report is available about ingress of *P. syringae* through the lenticels on these hosts. It is worth exploring why an enormous availability of this port does not seem to be exploited by the pathogen. In *Prunus* spp. the role of infection seems to be quite different. For example, on cherry most canker symptoms are located on the branches since the pathogen enters through leaf scars while the main stem is affected on plum where the pathogen seems to gain access through small wounds, although of unknown origin (Crosse and Garrett, 1970). Although leaf scar is one of the main ports of entry for *P. syringae* that cause vascular disease, on cherry it is not always utilized as an avenue of infection at warmer temperatures in particular. In South Africa, it seems that *P. syringae* reaches buds through the systemic movement before the leaf fall (Hattingh et al., 1989). Because *P. syringae* is a psychrophilic bacterium, it is possible that epiphytic populations of the pathogen do not survive in warmer temperatures, thereby favoring the organisms that colonize systemically. In Oregon, where mass destruction of dormant buds is the most conspicuous feature of the disease, attempts to infect cherry leaf scars with *P. syringae* failed (Cameron, 1962). Here, the author concluded that the infection was a result of direct bud infection, through the outer scales after the leaf-fall period. A recent study, based on the artificial inoculation experiments, showed that cherry is more susceptible to *P. syringae* infection through leaf scars than peach and “French” prune (Cao et al., 2013).

4.3 Means of Dissemination

Several natural and man-made phenomena favor the long- and short-distance dissemination of *P. syringae*. This pathogen can be carried in aerosols and thereby transported by wind-driven rain (Crosse, 1966). In addition,

the discovery that the life history of *P. syringae* is linked to the water cycle (Morris et al., 2008) explains how easily the pathogen can be disseminated over a wide range of distances. *P. syringae* can also be transmitted through mechanical equipment and pruning tools although their role in pathogen dissemination is often overlooked. Furthermore, insects such as aphids have been demonstrated to be potential vectors of *P. syringae* (Stavrinides et al., 2009). On stone fruits, the role of insects as a potential carrier of *P. syringae* inoculum has been demonstrated (Wormland, 1931). However, the most important dissemination source of *P. syringae* remains the transportation of infested nursery stock (Dowler and Petersen, 1967; Lyskanowska, 1976; Mansvelt and Hattingh, 1986).

4.4 Variability in Host Genotype Susceptibility

The underlying genetic variability and intensity of production is also important in the epidemiology of diseases of woody plants caused by *P. syringae*. A recent example of kiwifruit bacterial canker epidemics reveals how the cultivation of a very narrow range of plant diversity threatens durability of plant resistance. The genus *Actinidia* consists of over 50 species native to China where all wild germplasm is naturally distributed (Liang, 1983). However, the breeding of kiwifruit in New Zealand has been founded on imported planting materials where only two commercial varieties (cv. Hayward and Hort 16A, belonging to *Actinidia deliciosa* and *Actinidia chinensis*, respectively) have been developed and commercialized. For decades, the commercial kiwifruit industry was dominated by the sole cv. Hayward, grown in more than 80% of the world's kiwifruit production areas. It was not until 1999 that commercial marketing of cv. Hort16A was initiated (Ferguson, 1999). Suddenly, the kiwifruit industry has become vulnerable to *P. syringae* infection where the pathogen has jeopardized the entire kiwifruit industry (Butler et al., 2013; Scortichini et al., 2012). Intensive kiwifruit cultivation with very low genetic diversity in areas that are far from its center of origin has been detrimental for the long-term durability of the crop. Bacterial canker of European hazelnut (*Corylus avellana* L.) illustrates a marked contrast to the case of kiwifruit canker (Scortichini, 2002). Unlike kiwifruit, European hazelnut has a wide natural geographical distribution ranging from the Mediterranean coast of North Africa northward to the British Islands and the Scandinavian Peninsula, and eastward to the Ural Mountains of Russia, the Caucasus Mountains, Iran, and Lebanon (Rushforth, 1999). Moreover, there are other wild *Corylus* species native to North American (*Corylus americana*, *Corylus cornuta*), European and western Asian countries (*Corylus*

maxima, *C. colurna*), China (*Corylus chinensis*, *Corylus fargesii*, *Corylus yunnanensis*, *Corylus wangii*, *Corylus tibetica*), Japan (*Corylus sieboldiana*), and Siberia (*Corylus heterophylla*) (Mehlenbacher, 1991). A large number of European hazelnut varieties are grown around the globe. In Turkey, the world's most important hazelnut producer, an assorted number of varieties are grown together often in the same field. Bacterial canker has not been reported under these conditions. Indeed, the most extensive cultivated collection of hazelnut genetic resources resides in Turkey, which preserves 739 selections with over 700 genotypes of *C. avellana* (Hummer, 1995; Thompson et al., 1996). In contrast, in Greece where a hazelnut cultivar imported from Turkey (cv. Palaz) was intensively grown in monoculture, bacterial canker caused devastating losses making the cultivation impossible in some areas (Psallidas and Panagopoulos, 1979). Similarly, bacterial canker of hazelnut is a serious problem in some areas of central Italy (Scortichini, 2002) where only one cultivar (cv. Tonda Gentile Romana) is grown in more than 85% of the areas. By contrast, the disease is not reported from other Italian hazelnut growing areas such as Campania, Piedmont, Sardinia, and Sicily where several local varieties are grown (Siscaro et al., 2006; Viridis, 2008).

Among other economically important woody crop species, grapevine (*Vitis vinifera*), Mango (*Mangifera indica*), and citrus (*Citrus* spp.) are the hosts of *P. syringae*, although attacks and economic losses on these species have been reported sporadically. A very large genetic diversity has been described in the cultivated grapevine Arroyo-García et al., 2006). The genus *Vitis* is native to Transcaucasia (McGovern, 2003), which comprises about 60 infertile wild *Vitis* species. The natural distribution of such species ranges from Asia to Europe and North America (Terral et al., 2010). Species native to North America, such as *Vitis rupestris*, *Vitis riparia* or *Vitis berlandieri*, are widely used in breeding programs against different fungal pathogens that cause economically important diseases on grapevine. Several wild species of *Vitis* were found to grow along the river banks, and in alluvial and colluvial deciduous and semideciduous forests (Arnold et al., 1998). The distribution in the wild of these species ranges from Western Europe to the Trans-Caucasian zone and around the Mediterranean Basin except the most southern infra-Mediterranean and non-Mediterranean zones (Arnold et al., 1998). In Mango, in addition to commercial varieties, a large number of local and wild germplasm is reported to form a vast genetic resource to the mango breeder (Bally et al., 2008). In-depth lists of mango accessions in collections are also available (<http://www.ipgri.cgiar.org/germplasm/dbintro.htm>). Concerning *Citrus* spp., they originated in Southeast Asian countries. For

example, Key lime (*Corylus aurantifolia*) and citron (*Corylus medica*) are native to India while pomelo (*C. maxima*) is native to Malay Archipelago. Similarly, Mandarin orange (*Corylus reticulata*) is native to China while trifoliolate orange (*Corylus trifoliata*) is native to Korea and adjacent China. Finger lime (*Corylus australasica*), Australian round lime (*Corylus australis*), and desert lime (*Citrus glauca*) are native to Australia (Bally et al., 2008). In *Citrus* spp., lower genetic diversity is reported among the cultivars of orange, grapefruit and lemon since they have originated from nucellar seedlings or budsports. Conversely, mandarins, pummelos, and citrons are reported to have a high level of genetic diversity since many of the cultivars have arisen through sexual hybridization (The Citrus and Date Crop Germplasm Committee, 2004). Only few reports of *P. syringae* disease on *Citrus* spp. seem to be linked with the high genetic diversity of this crop, throughout the range of cultivations, thereby enhancing its durability of resistance to the pathogen.



5. THE DIVERSITY OF *P. SYRINGAE* CAUSING DISEASE TO WOODY PLANT SPECIES

Pseudomonas syringae is a species complex that encompasses a wide variety of strains that are grouped into numerous phylogroups (Parkinson et al., 2011) based on phylogeny of housekeeping genes using the Multi Locus Sequence Typing method. Strains known to attack woody species are found in all phylogroups except phylogroup 6 that contains strains causing disease on papaya and on sunflower (Parkinson et al., 2011). An exhaustive list of existing *P. syringae* pathogens of woody plants is presented in Table 4.2. The names of these pathogens were attributed after instauration of the pathovar nomenclature (Dye et al., 1980; Young et al., 1978) and they were translated to pathovars according to this system for pathogens identified before 1978. Most of the taxonomic descriptions were performed at a time when it was impossible to classify bacteria precisely on the basis of phylogenetic analysis (Cai et al., 2011). Furthermore, in only very few cases the attribution of a pathovar name was accomplished via host range tests (Table 4.3). It is a matter of debate whether the use of the so-called pathovar without thorough host-range description is justified. Among the *P. syringae* pathogens of woody plants, there are 14 existing pathovars, which were originally proposed as *species novel* on the basis of a few phenotypic tests (Table 4.3) and are still poorly circumscribed. Often, simply a few differences in biochemical traits in comparison to the lilac pathogen *P. syringae* pv. *syringae* were the basis of the proposal that the pathogen be considered as *species novel*. Such

Table 4.3 Tests and Number of Strains Used to Describe Novel *Pseudomonas syringae* Pathovars

Pathovar	No. of Strains Used	Tests Used for Characterization	Host Range and Species Used	Original References	pv. Designation
<i>aceris</i> ^b	1	Biochemical and pathogenicity	No	Ark (1939)	Young et al. (1978)
<i>actinidiae</i>	a			Takikawa et al. (1989)	Takikawa et al. (1989)
<i>aesculi</i>	a			Durgapal and Singh (1980)	Durgapal and Singh (1980)
<i>avellanae</i>	18	Biochemmical, serological, bacteriocin, phage typing, antibiotic resistance, pathogenicity and lesion tests	Yes (12 different species)	Psallidas (1993)	Psallidas (1993)
<i>avii</i> ^c	9	Biochemical tests, DNA–DNA hybridization, rep-PCR, cluster analysis, pathogenicity tests on different <i>Prunus</i> spp.	No	Menard et al. (2003)	Menard et al. (2003)
<i>berberidis</i> ^b	1	Biochemical and pathogenicity	No	Thornberry and Anderson (1931b)	Young et al. (1978)
<i>castaneae</i>	a			Takanashi and Shimizu (1989)	Takanashi and Shimizu (1989)
<i>cerasicola</i>	4	Biochemical and pathogenicity tests	Yes (66 species)	Kamiunten et al. (2000)	Kamiunten et al. (2000)
<i>cicaroneri</i> ^b	7	Biochemical and pathogenicity tests	No	Ercolani and Caldarola (1972)	Young et al. (1978)
<i>coryli</i> ^d	38	Fatty acid analysis, rep-PCR and genomic fingerprinting, 16S rDNA, hrpL gene, pathogenicity test	Yes (7 different species)	Scortichini et al. (2005)	Scortichini et al. (2005)
<i>daphniphylli</i>	a			Ogimi et al. (1990)	Ogimi et al. (1990)
<i>dysoxyl</i> ^b	NA			Hutchinson (1949)	Young et al. (1978)
<i>dendropanacis</i>	a			Ogimi et al. (1988b)	Ogimi et al. (1988b)

<i>erobotryae</i> ^b	a				Takimoto (1931)	Young et al. (1978)
<i>garcae</i> ^b	a				Do Amaral et al. (1956)	Young et al. (1978)
<i>lachrymans</i> ^b	3	Biochemical, copper resistance, pathogenicity	No		Smith and Bryan (1915)	Young et al. (1978)
<i>mori</i> ^b	a				Boyer and Lambert (1993)	Young et al. (1978)
<i>morsprunorum</i> ^b	1	Biocheical and pathogenicity	No		Wormland (1931)	Young et al. (1978)
<i>myricae</i>	a				Ogimi and Higuchi (1981)	Ogimi and Higuchi (1981)
<i>papulans</i> ^c	9	Biochemical, serological and pathogenicity	Yes (2 species)		Rose (1917)	Dhanvantari (1977)
<i>persicae</i> ^b	57	Biochemical tests	No		Prunier et al. (1970)	Young et al. (1978)
<i>philadelphii</i>	20	Biochemical, phage typing and pathogenicity tests	Yes (plants of 10 different genera)		Roberts (1985a)	Roberts (1985a)
<i>photiniae</i>	a				Goto (1983a)	Goto (1983a)
<i>rhapthiolepidis</i>	a				Ogimi et al. (1992)	Ogimi et al. (1992)
<i>ribicola</i> ^b	3	Biochemical and pathogenicity	No		Bohn and Maloit (1946)	Young et al. (1978)
<i>syringae</i>	a				Van Hall (1902)	Young (1992)
<i>theae</i> ^b	a				Hori (1915)	Young et al. (1978)
<i>ulmi</i> ^b	a				Sutic and Tescic (1958)	Young et al. (1978)
<i>viburni</i> ^b	1	Biochemical and pathogenicity	No		Thornberry and Anderson (1931a)	Young et al. (1978)

^aPublished in different language than English and in local journal, NA: not available.

^bPathogen, originally described as a novel species, not included in the approved list, successively translated to pathovar without any description.

^cIn pathogenicity tests the strains caused symptoms also on sweet cherry.

^dIn host range test the strains caused mild symptoms also on some other hosts.

^eIn host range test the strains caused symptoms also on peach.

discriminate criteria for defining new pathovars are inconsistent with the common observation of high phenotypic and genetic diversity of *P. syringae* in a very restricted area and even in association with a single species of host plant (Table 4.4). Indeed, a high phenotypic and genetic variability is typical of *P. syringae*. For each disease, differences in phenotypes and genotypes among the strains incriminated in the disease have been reported in the literature (Table 4.4). In a very recent work, Cinelli et al. (2013c) demonstrated that even the disease symptoms caused by the strains isolated from the same woody plant markedly differ. Similarly, a high phenotypic variability has been reported among the *P. syringae* strains isolated from different plant organs of the same annual plant affected by the disease (Morris et al., 2000).

Although attempts to clarify the naming of pathovars were made after 1978, confusions still occur. According to the standards, in designating a novel pathovar, it is necessary to demonstrate, through a pathogenicity testing regime, that the pathogen has a distinct host range or causes a distinct disease when compared with previously described pathogens (Young et al., 1978). However, it seems that old habits persist. For example, *P. syringae* pv. *avii* is the name attributed to the causal agent of bacterial canker of wild cherry (Menard et al., 2003) without a host range test. Bacterial canker with identical symptoms is caused by *P. syringae* pv. *syringae* and *P. syringae* pv. *morsprunorum* races on wild cherry (Vicente et al., 2004). On *Prunus* spp., four distinct *P. syringae* pathovars (*avii*, *morsprunorum* race 1 and 2, *persicae* and *syringae*) have been described on the basis of some phenotypic differences. All of them cause bacterial canker on the same hosts and most of them are frequently associated with the same disease (Hattingh et al., 1989; Kennelly et al., 2007). Another important example concerns the pathogens of olive and oleander knots caused by *Pseudomonas savastanoi* pv. *savastanoi* and *P. savastanoi* pv. *nerii*, respectively. Previous studies demonstrated that there is an overlapping host range among these pathovars (Alvarez et al., 1998; Janse, 1982). Recently, Young (2008) questioned if they should be considered as separate pathovars (pv. *savastanoi* pathogenic to olive and pv. *nerii* pathogenic to oleander) or as a single pathovar. The debate about the naming of these pathovars can be set into the context of the studies of host range that have been conducted for single pathovars. In many cases, these pathovars infect hosts other than that of the original isolation. Dhanvantari (1977) reported that *P. syringae* pv. *papulans*, previously described as *species novel* from apple (Rose, 1917), also infects peach. Similarly, Scortichini et al. (2005) reported a so-called novel pathovar from European hazelnut, *P. syringae* pv. *coryli*, which also causes mild disease symptoms on pear, apricot, and peach shoots.

Table 4.4 Phenotypic and Genetic Diversity Observed among Strains of *Pseudomonas syringae* Pathovars Pathogenic on Woody Plants

Pathogen(s)	Isolated Host	No. of Strains Used	Analysis	Haplotypes	References
Genetic diversity					
Pss	Stone fruits	91	ERIC PCR	11	Little et al. (1998)
Psa	Kiwifruit	44	MLST	4	Chapman et al. (2012)
Pss	Stone fruit and almond	78	ERIC, REP, BOXA1R, IS50	9	Abbasi et al. (2012)
Pss, Psm	Stone fruit and hazelnut	33	MLST	5,3	Kaluzna et al. (2010)
Pss	Pome and stone fruits	280	BOX PCR	4	Gilbert et al. (2009)
Pss	Cherry and plum	87	rep-PCR	10	Vicente and Roberts (2007)
Pss	Pome and stone fruits	101	rep-PCR	17	Scortichini et al. (2003)
Pss	Pear	90	BOX PCR	4	Natalini et al. (2006)
Psm1	Cherry and plum	19	Phage typing	6	Crosse and Garrett (1970)
Phenotypic diversity			Phenotypic patterns		
Pss	Apple	60	F, LOPAT, GATTa, INA, syringomycin	16	Mansvelt and Hattingh (1986)
Pss	Mixed hosts		LOPAT, syringomycin, other biochemical tests		Young (1991)
Psa	Kiwifruit	46	F, LOPAT, INA, syringomycin production, resistance to streptomycin and copper	3	Vanneste et al. (2013)
Psav	Olive	26	F, LOPAT	2	Marchi et al. (2005)
Psav	Myrtle	34	Pathogenicity	4	Cinelli et al. (2013b)
Pss	Pear	90	F, INA, LOPAT, GATTa, virulence tests on lemon fruits, pear and lilac leaves	4	Natalini et al. (2006)
Pss	Pome and stone fruits	70	F, LOPAT, GATTa, virulence tests	3	Gilbert et al. (2010)
Pss	Cherry and plum	54	Pathogenicity	4	Vicente et al. (2004)

Note: Pss, *Pseudomonas syringae* pv. *syringae*; Psav, *P. savastanoi*; Pssav, *P. savastanoi* pv. *savastanoi*; Psm1, *P. syringae* pv. *morsprunorum* race 1; Psa, *P. syringae* pv. *actinidiae*; Pav, *Pseudomonas avellanae*; F, fluorescence on KB, LOPAT, levan, oxidase, potato rot, arginine dihydrolase and tobacco hypersensitivity, respectively; GATTa, Gelatin hydrolysis, aesculin hydrolysis, tyrosinase activity and tartaric acid utilization, respectively; INA, ice nucleation activity.

Without comparative host range testing, it is difficult to know if apple is also a host of strains from peach or if hazelnut is a host of strains from pear and apricot cankers or if these are reports of truly novel pathotypes.

It is difficult to assess if the abundance of reports of different pathovars of *P. syringae* of woody species reflects a real diversification in host specialization or if it is a reflection of the wide range and inconsistency of tests used to characterize these pathogens. The literature reveals a surprising heterogeneity in tests used for the characterization of *P. syringae* from woody plants. Firstly, *in planta* pathogenicity tests on the original host of isolation, for the completion of Koch's postulate, is lacking in some cases (Gilbert et al., 2009; Ivanovic et al., 2012; Kaluzna et al., 2010). Secondly, host range tests have been performed only in a limited number of studies and on a very low number of host species (1–5) (Cirvilleri et al., 2007; Eltlbany et al., 2012; Golzar and Cother, 2008; Hall et al., 2004; Psallidas, 1993; Samavatian, 2006; Scortichini, 2006; Scortichini et al., 2005; Taghavi and Hasani, 2012; Vicente et al., 2004) making it difficult to know if the described pathovar is really different from previously described pathovars. On *Prunus* spp., where different pathovars cause the disease, cross-infection tests within the genus are lacking. There is also inconsistency in tests of ice nucleation activity (INA) of strains. INA has often been reported as a virulence factor of plant pathogenic *P. syringae* (Kennelly et al., 2007; Klement et al., 1984; Sule and Seemuller, 1987; Weaver, 1978) and in particular those attacking woody plants because flowering, leaf bud formation and surges of succulent growth can occur during periods with risk of frost. However, tests of ice nucleation activity are missing in many of the descriptions of *P. syringae* that are pathogenic to woody plants (Abbasi et al., 2012; Balestra et al., 2009c; Gilbert et al., 2009; Ivanovic et al., 2012; Kaluzna et al., 2010; Kamiunten et al., 2000; Mirik et al., 2005; Vicente et al., 2004). Biochemical tests, such as fluorescence on King's medium B, LOPAT (levan production, oxidase, potato rot, presence of arginine dihydrolase and induction of hypersensitivity on tobacco), GATTa (gelatin hydrolysis, aesculin hydrolysis, tyrosinase activity, and tartaric acid production), use of different carbohydrates as sole carbon sources, induction of lesions on detached plant organs, phytohormone production, resistance to copper compounds and antibiotics were among the most utilized for the characterization of strains (Table 4.4). While the identification of specific pathovars is the most common means for reporting new diseases, in some cases authors were reticent. Of the 55 outbreaks reported since 2000 (Table 4.1), 46 associated the causal agents to specific *P. syringae* pathovars, while only few reports described *P. syringae* “*in sensu lato*”

(Bardoux and Rousseau, 2007; González and Ávila, 2005; Hall et al., 2003; Ivanova, 2009; Mahdavian and Hasanzadeh, 2012; Ozakatan et al., 2008).



6. CONTROL OF DISEASES OF WOODY PLANTS CAUSED BY *P. SYRINGAE*

Strange and Scott (2005) described three categories of methods for minimizing plant disease: (1) exclusion, elimination or reduction of pathogen inoculum, (2) promotion of genetic diversity in the crop and (3) inhibition of pathogen virulence mechanisms. These measures are pertinent to limiting diseases of woody plants caused by *P. syringae*. In practice, these methods should not be used in exclusion but rather they are combined together through an integrated management approach.

6.1 Exclusion, Elimination, or Reduction of Pathogen Inoculum

In theory, hygiene and quarantine are effective control methods and they are currently being put to test for bacterial canker of kiwifruit. In 2012, *P. syringae* pv. *actinidiae* was declared a quarantine pathogen in the southern part of the EPPO region (http://www.eppo.int/QUARANTINE/recent_additions.htm). Similarly, *P. syringae* pv. *persicae*, the causal agent of bacterial dieback of peach, is another EPPO quarantine pathogen (OEPP/EPPO, 2005). Whether the quarantine regulation applied to a specific pathovar can be effective in controlling the introduction of the pathogen into new areas is a matter of debate. In some cases, the pathogen can be latently present in plant tissues for long periods of time without causing diseases as those reported from *Prunus* spp. (Dowler and Petersen, 1967; Lyskanowska, 1976; Mansvelt and Hattingh, 1986). The development of early detection methods should be the first step to avoid the introduction of latently infected nursery materials to a given area. Several detection methods have been developed with the aim of early detection of *P. syringae* from asymptomatic plant parts (Bertolini et al., 2003; Biondi et al., 2013; Gallelli et al., 2011). However, the limit of such methods is based on the fact that they can detect only a narrow range of the diversity of the *P. syringae* population, usually targeting the so-called pathovar level. Only detection methods that are able to identify a broader *P. syringae* diversity can be effective in order to promptly detect the emerging pathogens from asymptomatic propagation materials, given the high phenotypic and genetic diversity of this pathogen.

Freedom from pathogens in planting material is not a static event and requires constant monitoring and maintenance during all stages of production, storage, and distribution (Janse and Wenneker, 2002). Hence, a clear understanding of the causal agent of a given disease might be a good starting point to develop sensitive and effective detection methods from asymptomatic propagation materials. Besides propagation materials, the pathogen can spread for long distance also through migrating birds, insects (honey bees), wind-driven slime and undetected infections on wild hosts as those reported for the quarantine pathogen *Erwinia amylovora*, which led to a complete failure of the eradication campaign of fire blight disease (Calzolari et al., 2000; Vanneste, 2000). There are several examples in the literature on the reintroduction of an eradicated bacterial disease of woody plants that clearly indicate the difficulty of effective application of quarantine measures. Citrus canker, caused by *Xanthomonas axonopodis* pv. *citri* on citrus, in Florida (Graham and Gottwald, 1991; Schubert and Miller, 1997; Schubert et al., 2001) and fire blight of pome fruits, caused by *E. amylovora*, in many countries (Calzolari et al., 2000; Vanneste, 2000) are examples. Overall, a complete eradication of plants is rarely accomplished and often the common practice in the field is to eliminate only heavily damaged plants that are no longer productive. Current epidemics of kiwifruit bacterial canker fully reflects this scenario in which no reports on plant eradication exist, except those reported from some areas of Spain (Abelleira et al., 2011). Furthermore, an accurate definition of the pathovar responsible for the disease is essential for quarantine. As mentioned earlier, it is possible that these definitions are too narrow at present, thereby limiting the scope of quarantine actions to a range of strains that is narrower than the full diversity truly responsible for disease.

The only way to reduce *P. syringae* pathogen inoculum is effective cultural practices (Scortichini, 2002; Young, 2004, 2012). Treatments of propagative materials in nurseries with bactericides might be an effective solution but no efficient product is commercially available (see below). In fields, infected plants or plant parts may be either completely uprooted or pruned and burned. The nature of *P. syringae*, in that it lives, multiplies and overwinters on plant surfaces, makes its management extremely difficult compared to soil pathogens, for example. The reduction of inoculum of the latter is often successful through crop rotation and plowing (Summerell and Burgess, 1989), soil solarization (Katan, 1981), the addition of amendments (Lazarovits, 2001), and in some instances, by flooding (Thurston, 1990).

Overall, chemical control has been exclusively used for decades in the plant disease management. However, only a few effective and economical

bactericides have been developed to control bacterial pathogens. Plant pathogenic bacteria have been more recalcitrant to chemical treatments than their fungal counterparts (Jones et al., 2013). Unlike several products available for the control of phytopathogenic fungi (Oerke, 2005) (many of them systemic), only a limited number of products is commercially available for the control of phytopathogenic *P. syringae* (Agrios, 2005). The use of antibiotics is strictly forbidden in many countries including those in the European Union (Casewell et al., 2003), because of their implication for human health and the risk of resistance that the pathogen develops under selective pressure (Khachatourians, 1998; Lipsitch et al., 2002). Growers have to settle for only few commercially available chemicals. Among them, copper compounds are the standard bactericides, almost exclusively used, for the control of bacterial diseases (Agrios, 2005; Kennelly et al., 2007). Although these compounds often give satisfactory results on herbaceous plants, where *P. syringae* does not cause systemic disease, the success is limited on woody plants because they do not penetrate inside plant tissues to where the pathogen has invaded the vascular tissues (Alvarez, 2004; Kennelly et al., 2007). The only way to have success in controlling vascular pathogens is to intervene at the time of infection, by coinciding with periods when the host is susceptible, when the pathogen is accessible, and when conditions are favorable for disease (Kennelly et al., 2007). Previously, a predictive system for timing of chemical applications has been reported to improve chemical spray control of *P. syringae* (Jardine and Stephens, 1987). The authors used stagewise multiple linear regression techniques to identify meteorological and biological variables useful in predicting *P. syringae* disease development. However, it is worth noting that different hosts react differently to the same treatment. Stone fruits are examples of this differential reaction where preventive treatments, with copper-based compounds following leaf shedding, are effective to control *P. syringae* infection of peach and cherry but not of apricot. Knowledge of infection ports is useful for this reason. However, the phytotoxic effect of copper compounds on some species can be incompatible with such timings. For example, treatment during flower bloom is not possible for some species because flowers are highly sensitive to copper compounds (Lalancette and McFarland, 2007). Copper is one of the most used bactericides in agriculture, leading to the development of copper-resistant lines of *P. syringae* (Masami et al., 2004; Scheck et al., 1996; Sundin and Bender, 1993). Whatever the utility of copper, the environmental concerns provoked by its heavy use are leading to increasing restrictions in the European Union (Pietrzak and McPhail, 2004).

New directions in chemical control emerged recently to overcome the limitations of the common bactericides. Examples are elicitors such as harpins that activate plant defense and induce resistance, and polysaccharides such as chitosan (Dong et al., 1999; Reglinski and Elmer, 2011). Chitosan has attracted concern because of its strong antimicrobial activity toward a broad spectrum of pathogens, including common plant pathogenic bacteria and fungi. The major advantage of chitosan over conventional chemicals is its biocompatibility and biodegradability (Badawy and Rabea, 2011). In addition to chitosan, other compounds that have shown *in vitro* inhibitory effects on *P. syringae* include terpenes (Ferrante and Scortichini, 2010) and antimicrobial peptides (Cameron and Sarojini, 2014). The latter are reported also to inhibit biofilms (De Zoysa et al., 2013), commonly formed by *P. syringae*. However, the use of these compounds has been limited to controlled environments and no information is available for open conditions. Other chemicals used in fields are Acibenzolar-S-methyl (ASM, BTH, Bion or Actigard), an inducer of systemic acquired resistance (SAR) (Scortichini and Ligouri, 2003) and prohexadione calcium (Costa et al., 2001; Norelli and Miller, 2004), a growth regulator that has been tested on several species. While inducers of SAR can be effective under controlled conditions, the host response can be highly variable in the field, raising questions about their potential for disease management. Although SAR inducers may reduce disease to a certain extent in some species such as apple and hazelnut (Maxson-Stein et al., 2002; Scortichini and Ligouri, 2003), in fields they may also have deleterious effects on certain other plant species and/or affect yield (Gent and Schwartz, 2005; Romero et al., 2001). Furthermore, it has been reported that plant inducers did not result in any effective disease control in some pathosystems such as citrus canker (Graham and Leite, 2004). Studies carried out in Italy and New Zealand showed that in glasshouse conditions SAR can reduce the disease incidence on young kiwifruit seedlings (Vanneste et al., 2012) although no information is available from the field. Since a large number of similarities have been reported among *P. syringae* diseases of woody plants (such as bacterial cankers of stone fruit and kiwifruit) and citrus canker (<http://www.kvh.org.nz/vdb/document/91507>), the effect of SAR on *P. syringae* disease control might not be effective in natural field conditions. However, in-depth future investigations are needed before making a conclusion.

During the last decades, there is a growing interest in adopting biological control measures. At present, only inundative methods of biological control have been developed for diseases of woody species whereby

nonpathogenic microorganisms are applied to foliar or root tissues resulting in disease suppression. Such strategies include the use of nonpathogenic or pathogenically attenuated strains of the pathogen species (Frey et al., 1994; Liu, 1998; Hert, 2007), saprophytic bacteria (Ji et al., 2006), nonpathogenic bacteriocin-producing *Agrobacterium radiobacter* strains that inhibit closely related pathogenic strains (Kerr, 1974; Kerr and Htay, 1974), and plant growth-promoting rhizobacteria (Ji et al., 2006). These strategies aim to suppress pathogen populations or induce SAR or a similar response in the plant that reduces the ability of the pathogen to colonize the plant and cause disease. Biological control approaches have been used to control bacterial pathogens of several woody plants such as fire blight diseases of pome fruits (Boulé et al., 2011; Vanneste et al., 1992), caused by *E. amylovora* and bacterial spot of peach (Biondi et al., 2009) caused by *Xanthomonas arboricola* pv. *pruni*. However, throughout the literature, there is only an example on the biocontrol of *P. syringae*, which involved *in vitro* efficacy of aqueous plants extracts (Bhardwaj, 2011).

The use of bacteriophages is another form of biological control and has been successful for managing several annual plant diseases (Jackson, 1989). Phages have been under evaluation for controlling several woody plant-pathogenic bacteria. Examples are fire blight on apple and pear (Schnabel and Jones, 2001) and bacterial canker and bacterial spot of citrus (Balogh, 2006; Balogh et al., 2008). To date, all the successful application of phages concerns foliar pathogens and there are virtually no reports for woody tissues. Only one study has shown a preventative and beneficial effect with phage treatment, on vascular disease system on citrus, caused by *X. axonopodis* pv. *citri* (Balogh et al., 2008). The disease symptoms and location of infection within or on the plant can pose challenges for phage biocontrol. For example, most of the economically important diseases on trees are caused by vascular *P. syringae* pathogens (Kennelly et al., 2007; Scortichini, 2002; Scortichini et al., 2012). The latter spend some of the disease cycle inside the host plant following infection through plant openings or wounds (Kennelly et al., 2007; Scortichini, 2002; Scortichini et al., 2012). High numbers of bacteria can accumulate within cankers in the plant and are protected from any control agent applied to the outside of the plant that cannot penetrate to deeper tissues. However, the ability of phage to act as a curative agent of cankers was not directly assessed. In a recent report, use of bacteriophages has been indicated among the biocontrol agents with potential to control or suppress bacterial canker of kiwifruit, caused by *P. syringae* pv. *actinidiae* (Stewart et al., 2011). In addition, there are some ongoing studies on the

bacteriophage of this pathogen (Qing, 2007). Despite several attempts to use of bacteriophage to control different phytopathogenic bacteria, little is known on the possibility of control of *P. syringae* pathogens of woody plants.

6.2 Enhancing Crop Genetic Diversity

As mentioned above, the diversity of the woody crop can have a marked impact on epidemics as illustrated by the contrasting cases of the cankers of kiwifruit and hazelnut. In the case of bacterial canker of kiwifruit, there has been a call to try to increase the diversity of the crop in an attempt to reduce disease pressure (McCann et al., 2013). This needs to be done with foresight, in order to not enhance the abundance of disease sensitive plants as in the case of yellow-fleshed kiwifruit, *A. chinensis*. A thorough knowledge of crop genetic resources and their diversity is a prerequisite for their preservation and further use in breeding programs. The centers of origin and diversification of the most important woody hosts of *P. syringae* are listed in Table 4.5. Wild genetic resources of most of the woody crops are present in more than one country and they have been domesticated for centuries or even millennia. However, their origins and the natural distribution of their progenitor species are usually matters of debate (Frankel and Bennett, 1970) mostly for *Citrus* spp., *Prunus* spp. and *Vitis* spp. By contrast, the domestication of kiwifruit has occurred only a century ago and almost all the diversity of the genus *Actinidia* is present in China (Ferguson and Huang, 2007). Aside from *Prunus* spp., almost all woody fruit crop species have Asia as the center of origin and domestication and this occurred several centuries ago. Domestication is reported as the main cause of reduction of genetic diversity in crops relative to their wild progenitors, due to human selection and genetic drift through bottleneck effects (Tanksley and McCouch, 1997).

For woody plant species characterized by a high genetic diversity, spontaneous variation in disease resistance can be selected and used in breeding programs. In *Prunus* spp., some successful control of *P. syringae* has been reported using plant germplasm resistant to this pathogen. Example is the rootstock F12-1 used in Oregon, which is found to be quite resistant to the pathogen (Moore, 1988). Similarly, some cultivars of sour cherry in Germany were resistant to bacterial canker caused by *P. syringae* (Schmidle, 1981).

Plantation of mixtures of varieties or cultivars versus only one variety within the same field might be useful to improve the efficacy of control methods. Because different plant genotypes present different resistance to pathogen, the overall yield loss in this way may be significantly reduced. An example is rice blast control in China (Zhu et al., 2000) where a significant

Table 4.5 Centers of Origin and Diversication of the Most Economically Important Woody Hosts of *Pseudomonas syringae*

Species	Origin	Area of Domestication	References
Apple	Central Asia	Central and East Asia	Janick (2005), Watkins (1995)
Pear	Central Asia	Central and East Asia	Janick (2005), Watkins (1995)
Citrus	Southeast Asia	Southeast Asia	Gmitter et al. (2009)
European hazelnut	Western Asia	Mediterranean areas, Turkey, Iran	Kasapliligil (1964)
Grapevine	Transcaucasia	Transcaucasiaand-Mediterranean areas	McGovern (2003)
Kiwifruit	China	New Zealand	Ferguson and Bollard (1990)
Mango	South Asia	Tropical areas of Asia, Oceania and America	Bally et al. (2008)
Olive	Asia minor	Asia minor, Mediterranean basin	Zohary and Spiegel-Roy (1975)
<i>Prunus</i> spp.			
Almond	Southwest Asia	Central and East Asia	Janick (2005), Watkins (1995)
Apricot	Central and eastern Asia	Central and East Asia	Janick (2005), Watkins (1995)
Peach	China	Central and East Asia	Faust et al. (1998), Janick (2005), Watkins (1995)
Plum (Asian, European, American)	China, Europe and America	Central and East Asia, Europe, America	Janick (2005), Watkins (1995)
Sweet and tart cherry	Central Europe, western Asia	Central and East Asia, Europe	Janick (2005), Watkins (1995)

reduction of the disease has been observed through the interspaced cultivation of two rice cultivars, one resistant and the another susceptible to rice blast disease. Even more effective results might be obtained through intercropping whereby a mixture of different plant species is grown in close proximity. However, prior to intercropping, it is necessary to know whether two or more crop species that constitute the mixture are susceptible to the same pathogen. To date, the lack of comparative host range tests

limit our understanding of the full host range of *P. syringae* pathovars and make it difficult to predict the efficiency of intercropping as a means of disease control.

6.3 Inhibition of *P. syringae* Virulence Mechanisms

Exploitation of a pathogen's dependence on certain virulence mechanisms might be useful for their control. Table 4.6 presents a list of *P. syringae* virulence factors. It is well known that most of the virulence factors are induced by plant signal molecules (Ausubel, 2005; Tör et al., 2009). For example, the Type-Three Secretion System (TTSS) is the system in which bacteria can inject effector (virulence) proteins into the host cells Alfano and Collmer, 2004. These proteins, as well as the apparatus for the syringae, are coded by genes located in the exchangeable effector loci (EEL), *hrp/hrc* and conserved effector loci (CEL) (Block and Alfano, 2011). Type-III effectors are believed to contribute to pathogenesis in two ways: by eliciting the release of water and/or nutrients from the host cell in the apoplastic space; and by suppressing and/or evading plant host defense responses (Block and Alfano, 2011; Tampakaki et al., 2010). Recent studies have firmly established the concept that the suppression of various plant defenses, including basal defense, gene-for-gene resistance, and nonhost resistance (NHR), is a major virulence function of intracellular TTSS effectors (Nomura et al., 2005; Tampakaki et al., 2010). In particular, NHR is the most important form of resistance since it provides immunity to all members of plant species against all pathogens that cause disease to other plant species. Different plant genes have been reported to show NHR against plant pathogens. In Arabidopsis, *NONHOST1* was the first gene to confer NHR against *P. syringae* pv. *phaseolicola* (Kang et al., 2003). In tomato, host resistance to *P. syringae* disease is conferred by the Pto protein kinase, which acts in concert with the Prf nucleotide-binding lucine-rich repeat protein to recognize the pathogen expressing the TTSS effector genes *AvrPto* or *AvrPtoB* (Pedley and Martin, 2003). In tobacco and tomato, the successful use of a pattern recognition receptor gene, *EFR*, from Arabidopsis reduced the growth of *P. syringae* pv. *tabaci* and pv. *tomato*, respectively (Lacombe et al., 2010). In tomato, the R gene from pepper, *Bs2*, has been shown to impart resistance to bacterial pathogen *Xanthomonas campestris* pv. *vesicatoria* (Tai et al., 1999). The same pepper gene *Bs2* confers resistance to lemon against the bacterial pathogen *X. axonopodis* pv. *citri*. In barley, penetration deficient genes (*PEN*) 1, 2 and 3 provide NHR against the pathogen *Blumeria graminis* f. sp. *hordei* at the prehaustorial level (Lipka et al., 2005). In addition, NHR Arabidopsis gene *PSS1* confers immunity

Table 4.6 Virulence Factor of *Pseudomonas syringae* Pathogen of Woody Plants

Virulence Factor	Pathogen	References
Functional T3SS	All	Cunnac et al. (2009), Jin et al. (2003)
Ice nucleation activity	Pss	Klement et al. (1984), Sule and Seemuller (1987), Weaver (1978)
Exopolysaccharides	All	Corsaro et al. (2001), Denny (1995), Yu et al. (1999)
Coronatins	Psa; Psm	Bender et al. (1999), Gross (1991), Han et al. (2003), Liang and Jones (1995)
Mangotoxin	Pss, Pav	Arrebola et al. (2003), Carrión et al. (2013)
Persicomycin	Psp	Barzic and Guittet (1996)
Phaseolotoxin	Psa	Bender et al. (1999), Gross (1991)
Tabtoxin	Psg	Bender et al. (1999), Gross (1991), Mitchell (1984)
Tagetotoxin	Pst	Mitchell and Hart (1983)
Syringomycin	Pss	Bender et al. (1999), Gross (1991)
Yersiniabactin	Psm	Bender et al. (1999), Kaluzna et al. (2010)
Phytohormones	Pss, Psc, Psac, Psm, Psp, Psav, Pa, Psr, Psac	Bultreys et al. (2008), Glickmann et al. (1998), MacDonald et al. (1986), Young (2004)

Note: T3SS, Effectors and type-three secretion system; Pss, *Pseudomonas syringae* pv. *syringae*; Psc, *P. syringae* pv. *cicaronae*; Psa, *P. syringae* pv. *actiidae*; Psm, *P. syringae* pv. *morsprunorum*; Psp, *P. syringae* pv. *persicae*; Pav, *P. syringae* pv. *avellanae*; Psav, *P. savastanoi* pathovars; Psg, *P. syringae* pv. *garcae*; Pst, *P. syringae* pv. *tagetis*; Psm, *P. syringae* pv. *myricae*; Psp, *P. syringae* pv. *photinae*; Psr, *P. syringae* pv. *ribicola*; Psac, *P. syringae* pv. *aceris*; Pa, *P. amygdali*.

against *Phytophthora sojae* and *Fusarium virguliformae* (Sumit et al., 2012). Recognition of pathogen-associated molecular patterns (PAMPs) of nonadapted pathogens by PAMP recognition receptors (PRRs) triggers the PAMP-triggered immunity (PTI) in nonhost species (Dangl and Jones, 2001). PTI has been demonstrated to play a major role in NHR (Schwessinger and Zipfel, 2008). Both physical (callose deposition at the infection sites, waxy coating on leaves) and chemical (deposition of various reactive oxygen species such as H₂O₂ and phenolic compounds at the infection sites) barriers induced by PTI restrict nonadapted pathogens from invading nonhost species (Bittel and Robatzek, 2007; Mittler et al., 1999). Hence, identification, characterization, and the use of different NHR genes from various plants may be a good strategy to develop *P. syringae* disease resistant woody crops, through breeding.

The virulence of numerous phytopathogenic bacteria has been correlated with their ability to produce exopolysaccharide polymers *in planta* (Denny, 1995; Kao et al., 1992; Katzen et al., 1998). Studies on the exopolysaccharide molecules produced by *P. syringae* *in planta* indicated that alginate was the major exopolysaccharide produced in water-soaked lesions (Fett et al., 1989; Rudolph et al., 1989). Alginate production by *P. syringae* has been associated with increased epiphytic fitness, resistance to desiccation and toxic molecules, and the induction of water-soaked lesions on infected leaves (Fett et al., 1989; Yu et al., 1999). Furthermore, a positive correlation between the virulence of *P. syringae* and the quantity of alginate produced *in planta* has been demonstrated (Osman et al., 1986; Gross and Rudolph, 1987; Yu et al., 1999). A recent study demonstrated the presence of phase variation in *P. syringae* where the same clonal line can give rise to two phenotypes, a mucoid and a transparent (Bartoli et al., 2014). Only the mucoid phenotype, where the production of exopolysaccharide occurs, is reported to have pectolytic activity and to induce tobacco hypersensitivity. In addition, the two phases of the pathogen can be fixed *in vitro* and are not revertible. In addition, the disease is caused only by the mucoid phase *in planta*. Hence, targeting the molecular switch between these different phases could be a means to manipulate the pathogen.

Phytotoxins are products of plant pathogens or of the host–pathogen interaction that directly injure plant cells and influence the course of disease development or symptoms (Bender et al., 1999). Although phytotoxins are not required for pathogenicity in *P. syringae*, they generally function as factors that enhance aggressiveness of the pathogen leading to increased disease severity. For example, *P. syringae* phytotoxins can contribute to systemic movement of bacteria *in planta* (Patil et al., 1974), to lesion size (Bender et al., 1987; Xu and Gross, 1988), and to multiplication of the pathogen in the host (Bender et al., 1987; Feys et al., 1994; Mittal and Davis, 1995). In nature, other microorganisms resistant to the toxins produced by *P. syringae* may exist thereby allowing their use as biocontrol agents, to detoxify the effect of *P. syringae* produced toxins in plant. An example is the use of a strain of *Pantoea dispersa* as a biocontrol agent (Zhang and Birch, 1997) which is resistant to the toxin albicidin produced by *Xanthomonas albilineans*, the causal agent of sugarcane leaf scald.



7. THE CASE OF FROST DAMAGE DUE TO ICE NUCLEATION-ACTIVE *P. SYRINGAE*

In addition to its pathogenicity *sensu stricto*, *P. syringae* causes significant crop losses through frost damage. The frost sensitivity of plants is augmented

when they harbor large population of INA bacteria (Hirano and Upper, 2000). The amount of frost damage at a given temperature increases directly with increasing numbers of INA bacteria on that plant (Hirano and Upper, 1990; Lindow, 1980). In the presence of INA populations of *P. syringae*, the freezing point of plant tissue is raised compared to when INA bacteria are absent. Overall, plants can resist temperatures below freezing by supercooling. At temperatures below 0°C, a process known as ice nucleation can occur whereby a solid particle (dust, bacteria etc.) serves as a catalyst for ice formation. As discussed previously, *P. syringae* can survive and multiply both as an endophyte and epiphyte, even in association to symptomless plants thereby increasing the risk of frost injury.

Frost injury in association to *P. syringae* has been reported as a predisposing factor for blossom blight, bud and twig diebacks in numerous woody plants. Blossom blights are reported on kiwifruit (Balestra et al., 2009c; Young, 1987, 1988b), pear (Panagopoulos and Crosse, 1964), magnolia (Goto et al., 1988), pistachio (Rostami, 2012), and rhododendron (Baca et al., 1987). Similarly, twig dieback has been reported in tea (Goto et al., 1988) and coffee (Ramos and Kamidi, 1981). *P. syringae* is reported to affect ice nucleation of grapevine buds (Luisetti et al., 1991). In addition, the predisposition of plants to *P. syringae* leaf infection was increased in the presence of readily available inoculum, within 20 min of thawing. However, after 30 min, no effect of thawing has been observed in the formation of leaf lesions (Sule and Seemuller, 1987).

In contrast to its effect on tender and succulent plant parts, the contribution of *P. syringae* INA population to frost injury of lignified tissues is limited as demonstrated previously (Gross et al., 1983). Indeed, the woody stem tissue of these plants has a source of INA material that by itself can promote ice formation at -2 to -4°C (Andrews et al., 1983; Ashworth et al., 1985; Proebsting et al., 1982). Freezing and thawing events, irrespective of INA bacteria, have been reported to predispose woody plants to infection by phytopathogenic bacteria in orchards (Ferrante and Scortichini, 2014; Lamichhane et al., 2013). In nurseries, frost damage is reported to predispose a large number of woody plants to *P. syringae* infection (Baca et al., 1987). Moreover, in short-rotation forestry, twig dieback of poplar (Ramstedt et al., 1994) willow (Nejad et al., 2004; Ramstedt et al., 1994) and black alder (Scortichini, 1997) has been attributed to *P. syringae* in combination with freezing stress.

Preventive measures can be applied to reduce the propensity of ice nucleation. Prediction of critical conditions that favor frost damage is the basis to avoid crop losses. More specifically, prediction of INA *P. syringae* population sizes maybe compared to weather forecasting. Classical

methods of preventing frost damage include sprinkler irrigation and heating of orchards (Lindow, 1983a). In addition, bacterial ice nucleation can be inhibited by agents that kill whole cells such as bactericides (Kawahara et al., 2000; Menkissoglu-Spiroudi et al., 2001), antibiotics (Hirano et al., 1985; Lindow, 1983a, 1983b), various heavy metal ions in a soluble state (Hirano et al., 1985; Lindow, 1983a, 1983b; Menkissoglu and Lindow, 1991), surfactants (Himmelrick et al., 1991), organic solvents (Turner et al., 1990), and phospholipases (Govindarajan and Lindow, 1988; Turner et al., 1991). These compounds inactivate the nucleus produced by the INA bacteria. Copper compounds were used successfully to reduce frost injury induced by INA *P. syringae* (Lindow, 1983b). A combination of copper-streptomycin sprays was also used to control pear blossom blast in California (Bethell et al., 1977).

Efforts at biological control have been directed almost entirely at frost control using bacterial antagonists to prevent buildup of *P. syringae* INA populations (Lindemann and Suslow, 1987; Lindow, 1983b). Lindow and Staskawicz (1981), by using recombinant DNA technology, used an INA positive *P. syringae* strain from which the gene responsible for ice nucleation had been removed. Other tests for biocontrol of frost damage concerned the use of chemically mutated *P. syringae* INA⁻ strains and of naturally occurring INA⁻ bacterial antagonists, which reduced significantly the population sizes of naturally occurring INA⁺ *P. syringae* (Lindow, 1990, 1995). Application of these antagonists prior to budbreak (woody plants) or at seedling (annual plants) allowed the antagonist to obtain a dominant competitive position in the phylloplane. Examples are reduction of frost injury to strawberry (Lindemann and Suslow, 1987), almond (Lindow and Connell, 1984), and potato (Lindow and Panagopoulous, 1988). The use of bacterial ice nucleation inhibitors appears to offer a “day-before” type of immediate prevention of INA-bacteria-induced frost, which is not provided by bactericides or antagonistic bacteria (Lindow, 1980) and hence is reliant on accurate prediction of frost events. However, frost control was not achieved by using such antagonists or chemical bactericides in field trials on apple and pear in Washington (Gross et al., 1984). It is believed that, in these hosts, there are intrinsic INA molecules within plant tissue independent from the *P. syringae* INA populations.



8. CONCLUSIONS AND PERSPECTIVES

Within *P. syringae*, the designation of the so-called pathovars has complicated the understanding of disease epidemiology and the establishment of management practices. Such pathovar definitions are too narrow at present

thereby strongly limiting the objective of quarantine actions to a range of strains that is narrower than the full diversity involved in disease development. Do the pathovar names truly suggest that the strains within a pathovar are specialized to a host exclusive from other pathovars? If so how can we then explain the variability that can be observed among the strains of the same pathovar? Without comparative host range testing, it is difficult to know whether peach is also a host of strains from kiwifruit or if hazelnut is a host of strains from apricot canker or if these are reports of truly novel pathotypes. Such aspects are critical and should be addressed for the management of inoculum reservoirs, breeding for resistance and control targets.

Other criteria for grouping hosts, beyond that of shared sensitivity to *P. syringae*, might be informative. Groupings based on the availability of ports of entry may provide a clear picture on the gradient of sensitivity to *P. syringae* infection. To this aim, two major groups of woody plants (deciduous and evergreen) can be classified in different groups. For example, plants with a very high, moderate and low stomatal and lenticellular density on leaves and lignified tissues, respectively. Likewise, on the basis of the time required for suberization of leaf scar followed by leaf fall, a further sub-grouping in plants with a high, moderate, and low rate of suberization is needed. Such groupings of woody plants might allow us to investigate whether there is a correlation between the ports of entry and the rate of infection thereby allowing breeders to find further solutions.

Genetic diversity can be deployed at spatial scales down to the level of orchards. In the field, large-scale intensive cultivation of vegetatively propagated clonal plants leads to an increased vulnerability of plants to pathogen attacks. Only the promotion of genetic mixtures within a field can ensure a greater stability of plant resistance in the long term. With this mind, the introduction of either different plant cultivars of the same species or different species within the same field (intercropping) may significantly reduce the risk of severe infection. The cultivation of different landraces of the same species might present some disadvantages such as unsynchronized phenological phases among the genotypes with different flowering, fruiting, and ripening time. However, this technique may be economically advantageous in the long term if it reduces the severity of infections that could otherwise lead to drastic yield losses.

ACKNOWLEDGMENTS

The authors wish to thank Dr Enrico Scarici of the University of Tuscia, Viterbo for providing us a hand drawing of *P. syringae* entry ports of an imaginary tree. Many thanks to Drs Claudia Bartoli and Odile Berge for their constructive suggestions during the preparation of the manuscript.

REFERENCES

- Abbasi, V., Rahimian, H., Tajick-Ghanbari, M.A., 2012. Genetic variability of Iranian strains of *Pseudomonas syringae* pv. *syringae* causing bacterial canker disease of stone fruits. *Eur. J. Plant Pathol.* 135, 225–235.
- Abelleira, A., Lopez, M.M., Penalver, J., Aguin, O., Mansilla, J.P., Picoaga, A., Garcia, M.J., 2011. First report of bacterial canker of kiwifruit caused by *Pseudomonas syringae* pv. *actinidiae* in Spain. *Plant Dis.* 95, 1583–1583.
- Aerts, R., 1995. The advantages of being evergreen. *Trends Ecol. Evol.* 10, 402–407.
- Agrios, G.N., 2005. *Plant Pathology*. Elsevier-Academic Press, Amsterdam.
- Akbari, H., 2002. Shade trees reduce building energy use and CO₂ emissions from power plants. *Environ. Pollut.* 116, S119–S126.
- Alabdalla, N., Valentini, F., Moretti, C., Essa, S., Buonauro, R., Abu-Ghorra, M., 2009. First report of *Pseudomonas savastanoi* pv. *savastanoi* causing olive knot in Syria. *Plant Pathol.* 58, 1170.
- Alfano, J.R., Collmer, A., 2004. Type III secretion system effector proteins: double agents in bacterial disease and plant defense. *Annu. Rev. Phytopathol.* 42, 385–414.
- Alvarez, A.M., 2004. Integrated approaches for detection of plant pathogenic bacteria and diagnosis of bacterial diseases. *Annu. Rev. Phytopathol.* 42, 339–366.
- Alvarez, F., Garcia de los Rios, J.E., Jimenez, P., Rojas, A., Reche, P., Troya, M.T., 1998. Phenotypic variability in different strains of *Pseudomonas syringae* subsp. *savastanoi* isolated from different hosts. *Eur. J. Plant Pathol.* 104, 603–609.
- Andrews, P.K., Proebsting, E.L., Gross, D.C., 1983. Differential thermal analysis and freezing injury of deacclimating peach and sweet cherry reproductive organs. *J. Am. Soc. Hortic. Sci.* 108, 755–759.
- Ark, A.P., 1939. Bacterial leaf spot of maple. *Phytopathology* 29, 968–970.
- Arnold, C., Gillet, F., Gobat, G.M., 1998. Situation de la vigne sauvage *Vitis vinifera* subsp. *silvestris* en Europe. *Vitis* 37, 159–170.
- Arora, R., Wisniewski, M.E., Scorza, R., 1992. Cold acclimation in genetically related (sibling) deciduous and evergreen peach (*Prunus persica* [L.] Batsch): I. Seasonal changes in cold hardiness and polypeptides of bark and xylem tissues. *Plant Physiol.* 99, 1562–1568.
- Arora, R., Rowland, L.J., Tanino, K., 2003. Induction and release of bud dormancy in woody perennials: a science comes of age. *HortScience* 38, 911–921.
- Arrebola, E., Cazorla, F.M., Duran, V.E., Rivera, E., Olea, F., Codina, J.C., Pérez-García, A., de Vicente, A., 2003. Mangotoxin: a novel antimetabolite toxin produced by *Pseudomonas syringae*. *Physiol. Mol. Plant Pathol.* 63, 117–127.
- Arroyo-García, R., Ruiz-García, L., Bolling, L., Ocete, R., López, M.A., Arnold, C., Ergul, A., Söylemezoglu, G., Uzun, H.I., Cabello, F., Ibáñez, J., Aradhya, M.K., Atanassov, A., Atanassov, I., Balint, S., Cenis, J.L., Costantini, L., Goris-Lavets, S., Grando, M.S., Klein, B.Y., McGovern, P.E., Merdinoglu, D., Pejic, I., Pelsy, F., Primikiriros, N., Risovannaya, V., Roubelakis-Angelakis, K.A., Snoussi, H., Sotiri, P., Tamhankar, S., This, P., Troshin, L., Malpica, J.M., Lefort, F., Martínez-Zapater, J.M., 2006. Multiple origins of cultivated grapevine (*Vitis vinifera* L. ssp. *sativa*) based on chloroplast DNA polymorphisms. *Mol. Ecol.* 15, 3707–3714.
- Ashorpour, M., Kazempour, M.N., Ramezani, M., 2008. Occurrence of *Pseudomonas syringae* pv. *syringae* the causal agent of bacterial canker on olives (*Olea europaea*) in Iran. *ScienceAsia* 34, 323–326.
- Ashworth, E.N., Anderson, J.A., Davis, G.A., 1985. Properties of ice nuclei associated with peach trees. *J. Am. Soc. Hortic. Sci.* 110, 287–291.
- Ausubel, F.M., 2005. Are innate immune signaling pathways in plants and animals conserved? *Nat. Immunol.* 6, 973–979.
- Baca, S., Moore, L.W., 1987. *Pseudomonas syringae* colonization of grass species and cross infectivity to woody nursery plants. *Plant Dis.* 71, 724–726.

- Baca, S., Canfield, M.L., Moore, L.W., 1987. Variability in ice nucleation strains of *Pseudomonas syringae* isolated from diseased woody plants in Pacific Northwest nurseries. *Plant Dis.* 71, 412–415.
- Badawy, M.E.I., Rabea, E.I., 2011. A biopolymer chitosan and its derivatives as promising antimicrobial agents against plant pathogens and their applications in crop protection. *Int. J. Carbohydr. Chem.* <http://dx.doi.org/10.1155/2011/460381>.
- Balestra, G.M., Mazzaglia, A., Rossetti, A., 2008. Outbreak of bacterial blossom blight caused by *Pseudomonas viridiflava* on *Actinidia chinensis* kiwifruit plants in Italy. *Plant Dis.* 92, 707.
- Balestra, G.M., Lamichhane, J.R., Kshetri, M.B., Mazzaglia, A., Varvaro, L., 2009a. First report of olive knot caused by *Pseudomonas savastanoi* pv. *savastanoi* in Nepal. *Plant Pathol.* 58, 393.
- Balestra, G.M., Mazzaglia, A., Quattrucci, A., Renzi, M., Rossetti, A., 2009b. Current status of bacterial canker spread on kiwifruit in Italy. *Australas. Plant Dis. Notes* 4, 34–36.
- Balestra, G.M., Perestrelo, L., Mazzaglia, A., Rossetti, A., 2009c. First report of blossom blight caused by *Pseudomonas syringae* on kiwifruit plants in Portugal. *J. Plant Pathol.* 91, 231.
- Balestra, G.M., Renzi, M., Mazzaglia, A., 2010. First report on bacterial canker of *Actinidia deliciosa* caused by *Pseudomonas syringae* pv. *actinidiae* in Portugal. *New Dis. Rep.* 22, 10.
- Bally, I.S.E., Lu, P., Johnson, P.R., 2008. Mango breeding. In: Jain, S.M., Priyadarshan, P.M. (Eds.), *Breeding Plantation Tree Crops: Tropical Species*. Springer, The Netherlands, pp. 51–82.
- Balogh, B., 2006. Characterization and Use of Bacteriophages Associated with Citrus Bacterial Pathogens for Disease Control (Ph.D. dissertation). University of Florida, Gainesville.
- Balogh, B., Canteros, B.I., Stall, R.E., Jones, J.B., 2008. Control of citrus canker and citrus bacterial spot with bacteriophages. *Plant Dis.* 92, 1048–1052.
- Bardoux, S., Rousseau, P., 2007. Le deperissement bacterien du marronnier. *Phytoma* 605, 22–23.
- Bartoli, C., Berge, O., Monteil, C., Guilbaud, C., Balestra, G.M., Varvaro, L., Jones, C., Dangel, J.L., Baltrus, D.A., Sands, D.C., Morris, C.E., 2014. The *Pseudomonas viridiflava* phylogroups in the *P. syringae* species complex are characterized by genetic variability and phenotypic plasticity of pathogenicity-related traits. *Environmen. Microbiol.* <http://dx.doi.org/10.1111/1462-2920.12433>.
- Barzic, M.R., Guittet, E., 1996. Structure and activity of persicomycins, toxins produced by a *Pseudomonas syringae* pv. *persicae*/ *Prunus persica* isolate. *FEBS J.* 239, 702–709.
- Bastas, K.K., Karakaya, A., 2012. First report of bacterial canker of kiwifruit caused by *Pseudomonas syringae* pv. *actinidiae* in Turkey. *Plant Dis.* 96, 452.
- Bedford, K.E., MacNeill, B.H., Bonn, W.G., Dirks, V.A., 1988. Population dynamics of *Pseudomonas syringae* pv. *papulans* on Mutsu apple. *Can. J. Plant Pathol.* 10, 23–29.
- Bender, C.L., Stone, H.E., Sims, J.J., Cooksey, D.A., 1987. Reduced pathogen fitness of *Pseudomonas syringae* pv. *tomato* Tn mutants defective in coronatine production. *Physiol. Mol. Plant Pathol.* 30, 273–283.
- Bender, C.L., Alarcón-Chaidez, F., Gross, D.C., 1999. *Pseudomonas syringae* phytotoxins: mode of action, regulation, and biosynthesis by peptide and polyketide synthetases. *Microbiol. Mol. Biol. Rev.* 63, 266–292.
- Bertolini, E., Penyalver, R., García, A., Olmos, A., Quesada, J.M., Cambra, M., López, M.M., 2003. Highly sensitive detection of *Pseudomonas savastanoi* pv. *savastanoi* in asymptomatic olive plants by nested-PCR in a single closed tube. *J. Microbiol. Methods* 52, 261–266.
- Bethell, R.S., Ogawa, J.M., English, W.H., Hansen, R.R., Manji, B.T., Schick, F.J., 1977. Copper-streptomycin sprays control pear blossom blast. *Calif. Agric.* 31, 7–9.
- Bhardwaj, S.K., 2011. Potential use of some plant extracts against *Pseudomonas syringae* pv. *syringae*. *J. Med. Aromat. Plant Sci.* 33, 41–45.
- Biondi, E., Dallai, D., Brunelli, A., Bazzi, C., Stefani, E., 2009. Use of a bacterial antagonist for the biological control of bacterial leaf/fruit spot of stone fruits. *IOBC Bull.* 43, 277–281.

- Biondi, E., Galeone, A., Kuzmanovic, N., Ardizzi, S., Lucchese, C., Bertaccini, A., 2013. *Pseudomonas syringae* pv. *actinidiae* detection in kiwifruit plant tissue and bleeding sap. *Ann. Appl. Biol.* 162, 60–70.
- Bittel, P., Robatzek, S., 2007. Microbe-associated molecular patterns (MAMPs) probe plant immunity. *Curr. Opin. Plant Biol.* 10, 335–341.
- Block, A., Alfano, J.R., 2011. Plant targets for *Pseudomonas syringae* type III effectors: virulence targets or guarded decoys? *Curr. Opin. Microbiol.* 14, 39–46.
- Bobev, S.G., Baeyen, S., Vaerenbergh, J., Maes, M., 2008. First record of bacterial blight caused by *Pseudomonas syringae* pv. *syringae* on *Pyracantha coccinea* and an *Amelanchier* sp. in Bulgaria. *Plant Dis.* 92, 1251.
- Bohn, G.W., Maloit, J.C., 1946. Bacterial spot of native golden currant. *J. Agric. Res.* 73, 281–290.
- Boulé, J., Sholberg, P.L., Lehman, S.M., O’gorman, D.T., Svircev, A.M., 2011. Isolation and characterization of eight bacteriophages infecting *Erwinia amylovora* and their potential as biological control agents in British Columbia, Canada. *Can. J. Plant Pathol.* 33, 308–317.
- Boyer, G., Lambert, F., 1993. Sur deux nouvelles maladies du mûrier. *C. R. Hebd. Séances Acad. Sci.* 117, 342–343.
- Bull, C.T., De Boer, S.H., Denny, T.P., Firrao, G., Fischer-Le, S., Saddler, G.S., Scortichini, M., Stead, D.E., Takikawa, Y., 2010. Comprehensive list of names of plant pathogenic bacteria, 1980–2007. *J. Plant Pathol.* 92, 551–592.
- Bultreys, A., Kaluzna, M., 2010. Bacterial cankers caused by *Pseudomonas syringae* on stone fruit species with special emphasis on the pathovars *syringae* and *morsprunorum* race 1 and race 2. *J. Plant Pathol.* 92S, 21–33.
- Bultreys, A., Gheysen, I., Planchon, V., 2008. Characterization of *Pseudomonas syringae* strains isolated from diseased horse chestnut trees in Belgium. In: Fatmi, M.B., Collmer, A., Iacobellis, N.S. (Eds.), *Pseudomonas syringae* Pathovars and Related Pathogens – Identification, Epidemiology and Genomics. Springer, The Netherlands, pp. 283–293.
- Burr, T.J., Hurwitz, B., 1981. Seasonal susceptibility of “Mutsu” apples to *Pseudomonas syringae* pv. *papulans*. *Plant Dis.* 65, 334–336.
- Burr, T.J., Katz, B.H., 1984. Overwintering and distribution pattern of *Pseudomonas syringae* pv. *papulans* and pv. *syringae* in apple buds. *Plant Dis.* 68, 383–385.
- Butler, M.I., Stockwell, P.A., Black, M.A., Day, R.C., Lamont, I.L., Poulter, R.T.M., 2013. *Pseudomonas syringae* pv. *actinidiae* from recent outbreaks of kiwifruit bacterial canker belong to different clones that originated in China. *PLoS One* 8, e57464. <http://dx.doi.org/10.1371/journal.pone.0057464>.
- CABI/EPP0, 2008. *Pseudomonas syringae* pv. *actinidiae*. (Distribution Map). Distribution Maps of Plant Diseases. CABI, Wallingford.
- Cai, R., Lewis, J., Yan, S., Liu, H., Clarke, C.R., Campanile, F., Almeida, N.F., Studholme, D.J., Lindeberg, M., Schneider, D., Zaccardelli, M., Setubal, J.H., Morales-Lizcano, N.P., Bernal, A., Coaker, G., Baker, C., Bender, C.L., Leman, S., Vinatzer, B.A., 2011. The plant pathogen *Pseudomonas syringae* pv. *tomato* is genetically monomorphic and under strong selection to evade tomato immunity. *PLoS Pathog.* 7, e1002130.
- Calzolari, A., Finelli, F., Bazzi, C., Mazzucchi, U., 2000. Fire blight: prevention and control in the Emilia–Romagna region. *Riv. Frutticol. Ortofloricol.* 62, 23–28 (in Italian).
- Cameron, H.R., 1962. Mode of infection of sweet cherry by *Pseudomonas syringae*. *Phytopathology* 52, 917–921.
- Cameron, H.R., 1970. *Pseudomonas* content of cherry trees. *Phytopathology* 60, 1343–1346.
- Cameron, A., Sarojini, V., 2014. *Pseudomonas syringae* pv. *actinidiae*: chemical control, resistance mechanisms and possible alternatives. *Plant Pathol.* 63, 1–11. <http://dx.doi.org/10.1111/ppa.12066>.

- Canfield, M.L., Baca, S., Moore, L.W., 1986. Isolation of *Pseudomonas syringae* from 40 cultivars of diseased woody plants with tip dieback in Pacific Northwest nurseries. *Plant Dis.* 70, 647–650.
- Cao, T., Kirkpatrick, B.C., Shackle, K.A., DeJong, T.M., 2013. Effect of leaf scar age, chilling and freezing-thawing on infection of *Pseudomonas syringae* pv. *syringae* through leaf scars and lenticels in stone fruits. *Fruits* 68, 159–169.
- Carrión, V.J., Gutiérrez-Barranquero, J.A., Arrebola, E., Bardaji, L., Codina, J.C., de Vicente, A., Cazorla, F.M., Murillo, J., 2013. The mangotoxin biosynthetic operon (mbo) is specifically distributed within *Pseudomonas syringae* genomospecies 1 and was acquired only once during evolution. *Appl. Environ. Microbiol.* 79, 756–767.
- Casewell, M., Friis, C., Marco, E., McMullin, P., Phillips, I., 2003. The European ban on growth-promoting antibiotics and emerging consequences for human and animal health. *J. Antimicrob. Chemother.* 52, 159–161.
- Cazorla, F.M., Torés, J.A., Olalla, L., Pérez-García, A., Farré, J.M., De Vicente, A., 1998. Bacterial apical necrosis of mango in southern Spain: a disease caused by *Pseudomonas syringae* pv. *syringae*. *Phytopathology* 88, 614–620.
- Chapman, J.R., Taylor, R.K., Weir, B.S., Romberg, M.K., Vanneste, J.L., Luck, J., Alexander, B.J.R., 2012. Phylogenetic relationships among global populations of *Pseudomonas syringae* pv. *actinidiae*. *Phytopathology* 102, 1034–1044.
- Chase, M.W., 2004. Monocot relationships: an overview. *Am. J. Bot.* 91, 1645–1655.
- Cinelli, T., Rizzo, D., Marchi, G., Surico, G., 2013a. First report of knot disease caused by *Pseudomonas savastanoi* on sweet olive in central Italy. *Plant Dis.* 97, 419.
- Cinelli, T., Marchi, G., Cimmino, A., Marongiu, R., Evidente, A., Fiori, M., 2013b. Heterogeneity of *Pseudomonas savastanoi* populations infecting *Myrtus communis* in Sardinia (Italy). *Plant Pathol.* <http://dx.doi.org/10.1111/ppa.12096>.
- Cinelli, T., Rizzo, D., Marchi, G., Surico, G., 2013c. First report of knot disease caused by *Pseudomonas savastanoi* on sweet olive in central Italy. *Plant Dis.* 97, 419.
- Cirvilleri, G., Scuderi, G., Bonaccorsi, A., Scortichini, M., 2007. Occurrence of *Pseudomonas syringae* pv. *coryli* on hazelnut orchards in sicily, Italy and characterization by fluorescent amplified fragment length polymorphism. *J. Phytopathol.* 155, 397–402.
- Conn, K.E., Gubler, W.D., Hasey, J.K., 1993. Bacterial blight of kiwifruit in California. *Plant Dis.* 77, 228–230.
- Corsaro, M.M., Evidente, A., Lanzetta, R., Lavermicocca, P., Molinaro, A., 2001. Structural determination of the phytotoxic mannan exopolysaccharide from *Pseudomonas syringae* pv. *cicaronei*. *Carbohydr. Res.* 330, 271–277.
- Costa, G., Andreotti, C., Bucchi, F., Sabatini, E., Bazzi, C., Malaguti, S., Rademacher, W., 2001. Prohexadione-Ca (Apogee): growth regulation and reduced fire blight incidence in pear. *HortScience* 36, 931–933.
- Craker, L.E., Gusta, L.V., Weiser, C.J., 1969. Soluble proteins and cold hardiness of two woody species. *Can. J. Plant Sci.* 49, 279–286.
- Crosse, J.E., 1956. Bacterial canker of stone fruits. II. Leaf scar infection of cherry. *J. Hortic. Sci.* 31, 212–224.
- Crosse, J.E., 1966. Epidemiological relations of the pseudomonad pathogens of deciduous fruit trees. *Annu. Rev. Phytopathol.* 14, 291–310.
- Crosse, J.E., Garrett, C.M.E., 1970. Pathogenicity of *Pseudomonas morsprunorum* in relation to host specificity. *J. Gen. Microbiol.* 62, 315–327.
- Cunnac, S., Lindberg, M., Collmer, A., 2009. *Pseudomonas syringae* type III secretion system effectors: repertoires in search of functions. *Curr. Opin. Microbiol.* 12, 53–60.
- Dangl, J.L., Jones, J.D., 2001. Plant pathogens and integrated defence responses to infection. *Nature* 411, 826–833.
- Davis, J.R., English, H., 1969. Factors related to the development of bacterial canker in peach. *Phytopathology* 59, 588–595.

- De Zoysa, G.H., Washington, V., Lewis, G., Sarojini, V., 2013. The undiscovered potential of dehydroproline as a fire blight control option. *Plant Pathol.* 62, 767–776.
- Denny, T.P., 1995. Involvement of bacterial polysaccharide in plant pathogenesis. *Annu. Rev. Phytopathol.* 33, 173–197.
- Destéfano, S.A.L., Rodrigues, L.M.R., Beriam, L.O.S., Patrício, F.R.A., Thomaziello, R.A., Rodrigues-Neto, J., 2010. Bacterial leaf spot of coffee caused by *Pseudomonas syringae* pv. *tabaci* in Brazil. *Plant Pathol.* 59, 1162–1163.
- Dhanvantari, B.N., 1977. A taxonomic study of *Pseudomonas papulans* Rose 1917. *N.Z. J. Agric. Res.* 20, 557–561.
- Dijkshoorn-Dekker, M.W.C., 2005. Eindrapport onderzoeksprogramma Red de kastanje voor Nederland. Applied Plant Research, Boskoop, Wageningen University, The Netherlands.
- Do Amaral, J.F., Teixeira, C., Pinheiro, E.D., 1956. O bacterio causador da mancha aureolada do cafeeiro, vol. 23, Arquivos do Instituto Biológico, São Paulo. pp. 151–155.
- Dong, H., Delaney, T.P., Bauer, D.W., Beer, S.V., 1999. Harpin induces disease resistance in *Arabidopsis* through the systemic acquired resistance pathway mediated by salicylic acid and the NIM1 gene. *Plant J.* 20, 207–215.
- Dowler, W.M., Petersen, D.H., 1967. Transmission of *Pseudomonas syringae* in peach trees by bud propagation. *Plant Dis. Rep.* 51, 666–668.
- Dunquesne, J., Gall, H., 1975. L'influence des porte-greffes sur la sensibilité de l'abricotier aux bactérioses. *Phytoma* 1, 22–26.
- Durgapal, J.C., Singh, B., 1980. Taxonomy of pseudomonads pathogenic to horse-chestnut, wild fig and wild cherry in India. *Indian Phytopathol.* 33, 533–535.
- Dye, D.W., Bradbury, J.F., Goto, M., Hayward, A.C., Lelliott, R.A., Schroth, M.N., 1980. International standards for naming pathovars of phytopathogenic bacteria and a list of pathovar names and pathotypes. *Rev. Plant Pathol.* 59, 153–168.
- Eltbany, N., Prokscha, Z.-Z., Castañeda-Ojeda, M.P., Krögerrecklenfort, E., Heuer, H., Wohanka, W., Ramos, C., Smalla, K., 2012. A new bacterial disease on *Mandevilla sanderi*, caused by *Pseudomonas savastanoi*: lessons learned for bacterial diversity studies. *Appl. Environ. Microbiol.* 78, 8492–8497.
- English, H., DeVay, J.E., Lilleland, O., Davis, J.R., 1961. Effect of certain soil treatments on the development of bacterial canker in peach trees (Abstract). *Phytopathology* 51, 65.
- English, H., Davis, J.R., DeVay, J.E., 1980. Bacterial canker, an important decline disease of apricots and other stone fruits in California. *Acta Hortic.* 83, 235–242.
- EPPO, 2005. *Pseudomonas syringae* pv. *persicae*. Bull. OEPP/EPPO, no. 145. http://www.eppo.int/QUARANTINE/bacteria/Pseudomonas_persicae/PSDMPE_ds.pdf.
- EPPO, 2011a. First Report of *Pseudomonas syringae* pv. *actinidiae* in Australia. Number 6, 2011/130. <http://archives.eppo.org/EPPOReporting/2011/Rse-1106.pdf>.
- EPPO, 2011b. First Report of *Pseudomonas syringae* pv. *actinidiae* in Chile. Number 3, 2011/055. <http://archives.eppo.org/EPPOReporting/2011/Rse-1103.pdf>.
- EPPO, 2011c. Bleeding Canker of Horse Chestnut in Ireland. Number 6, 2011/077. <http://archives.eppo.org/EPPOReporting/2011/Rse-1108.pdf>.
- EPPO, 2011d. First Report of *Pseudomonas syringae* pv. *actinidiae* in Switzerland. Number 8, 2011/168. <http://archives.eppo.org/EPPOReporting/2011/Rse-1108.pdf>.
- Ercolani, G.L., Caldarella, M., 1972. *Pseudomonas ciccaraonei* sp. n., agente di una maculatura fogliare del carrubo in Puglia. *Phytopathol. Mediterr.* 11, 71–73.
- Everett, K.R., Taylor, R.K., Romberg, M.K., Rees-George, J., Fullerton, R.A., Vanneste, J.L., Manning, M.A., 2011. First report of *Pseudomonas syringae* pv. *actinidiae* causing kiwifruit bacterial canker in New Zealand. *Australas. Plant Dis. Notes* 6, 67–71.
- Fahy, P.C., Lloyd, A.B., 1983. *Pseudomonas*: the fluorescent pseudomonads. In: Fahy, G.J., Pearsley, P.C. (Eds.), *Plant Bacterial Diseases – A Diagnostic Guide*. Academic Press, Sydney, Australia, pp. 141–188.

- Faust, M., Surányi, D., Nyujtő, F., 1998. Origin and dissemination of apricot. *Hortic. Rev.* 22, 225–266.
- Ferguson, A.R., 1999. Kiwifruit cultivars: breeding and selection. *Acta Hort.* 498, 43–52.
- Ferguson, A.R., Bollard, E.G., 1990. Domestication of the kiwifruit. In: Warrington, I.J., Weston, G.C. (Eds.), *Kiwifruit: Science and Management*. Ray Richards Publisher, Auckland, New Zealand, pp. 165–246.
- Ferguson, A.R., Huang, H.W., 2007. Genetic resources of kiwifruit: domestication and breeding. *Hortic. Rev.* 33, 1–121.
- Ferrante, P., Scortichini, M., 2010. Molecular and phenotypic features of *Pseudomonas syringae* pv. *actinidiae* isolated during recent epidemics of bacterial canker on yellow kiwifruit (*Actinidia chinensis*) in central Italy. *Plant Pathol.* 59, 954–962.
- Ferrante, P., Scortichini, M., 2014. Frost promotes the pathogenicity of *Pseudomonas syringae* pv. *actinidiae* in *Actinidia chinensis* and *A. deliciosa* plants. *Plant Pathol.* 63, 12–19. <http://dx.doi.org/10.1111/ppa.12070>.
- Fett, W., Dunn, F., Michael, F., 1989. Exopolysaccharides produced by phytopathogenic *Pseudomonas syringae* pathovars in infected leaves of susceptible hosts. *Plant Physiol.* 89, 5–9.
- Feys, B., Benedetti, C.E., Penfold, C.N., Turner, J.G., 1994. Arabidopsis mutants selected for resistance to the phytotoxin coronatine are male sterile, insensitive to methyl jasmonate, and resistant to a bacterial pathogen. *Plant Cell* 6, 751–759.
- Frankel, O.H., Bennett, E., 1970. *Genetic Resources in Plants, Their Exploration and Conservation*. Blackwell Scientific Publications, Oxford, The UK.
- Fratantuono, M., Broquaire, J.-M., Esteve, L., 1998. Bactériose et choix du porte-greffe en Roussillon. *Fruits Légumes* 164, 52–53.
- Freigoun, S.O., Crosse, J.E., 1975. Host relations and distribution of a physiological and pathological variant of *Pseudomonas morsprunorum*. *Ann. Appl. Biol.* 81, 317–330.
- Frey, P., Prior, P., Marie, C., Kotoujansky, A., Trigalet-Demery, D., Trigalet, A., 1994. Hrp-mutants of *Pseudomonas solanacearum* as potential biocontrol agents of tomato bacterial wilt. *Appl. Environ. Microbiol.* 60, 3175–3181.
- Gallelli, A., Talocci, S., L'Aurora, A., Loreti, S., 2011. Detection of *Pseudomonas syringae* pv. *actinidiae*, causal agent of bacterial canker of kiwifruit, from symptomless fruits, and twigs, and from pollen. *Phytopathol. Mediterr.* 50, 473–483.
- García de los Ríos, J.E., 1999. *Retama sphaerocarpa* (L.) Boiss., a new host of *Pseudomonas savastanoi*. *Phytopathol. Mediterr.* 38, 54–60.
- Garibaldi, A., Bertetti, D., Scortichini, M., Gullino, M.L., 2005. First report of bacterial leaf spot caused by *Pseudomonas syringae* pv. *viburnii* on *Viburnum sargentii* in Italy. *Plant Dis.* 89, 777.
- Gent, D.H., Schwartz, H.F., 2005. Management of *Xanthomonas* leaf blight of onion with a plant activator, biological control agents, and copper bactericides. *Plant Dis.* 89, 631–639.
- Gilbert, V., Legros, F., Maraite, H., Bultreys, A., 2009. Genetic analyses of *Pseudomonas syringae* strains from Belgian fruit orchards reveal genetic variability and host preferences within pathovar syringae, and help identify both races of pathovar morsprunorum. *Eur. J. Plant Pathol.* 124, 199–218.
- Gilbert, V., Planchon, V., Legros, F., Maraite, H., Bultreys, A., 2010. Pathogenicity and aggressiveness in populations of *Pseudomonas syringae* from Belgian fruit orchards. *Eur. J. Plant Pathol.* 126, 263–277.
- Glickmann, E., Gardan, L., Jacquet, S., Hussain, S., Elasri, M., Petit, A., Dessaux, Y., 1998. Auxin production is a common feature of most pathovars of *Pseudomonas syringae*. *Mol. Plant Microbe Interact.* 11, 156–162.
- Gmitter, F.G., Soneji, J.R., Rao, M.N., 2009. Citrus breeding. In: Jain, S.M., Priyadarshan, P.M. (Eds.), *Breeding Plantation Tree Crops: Temperate Species*. Springer, The Netherlands, pp. 105–113.
- Golzar, H., Cother, E.J., 2008. First report of bacterial necrosis of mango caused by *Pseudomonas syringae* pv. *syringae* in Australia. *Australas. Plant Dis. Notes* 3, 107–109.

- González, J., Ávila, M., 2005. Disease of floral buds of kiwifruit in Spain caused by *Pseudomonas syringae*. *Plant Dis.* 85, 1287.
- Goto, M., 1983a. *Pseudomonas syringae* pv. *photiniae* pv. nov., the causal agent of bacterial leaf spot of *Photinia glabra* Maxim. *Ann. Phytopathol. Soc. Jpn.* 49, 457–462.
- Goto, M., 1983b. *Pseudomonas ficuserectae* sp. nov., the causal agent of bacterial leaf spot of *Ficus erecta* Thunb. *Int. J. Syst. Bacteriol.* 33, 546–550.
- Goto, M., Huang, B.L., Makino, T., Goto, T., Inaba, T., 1988. A taxonomic study on ice nucleation-active bacteria isolated from gemmisphere of tea (*Thea sinensis* L.), phyllosphere of vegetables, and flowers of *Magnolia denudata*. *Ann. Phytopathol. Soc. Jpn.* 54, 189–197.
- Govindarajan, A.G., Lindow, S.E., 1988. Phospholipid requirement for expression of ice nuclei in *Pseudomonas syringae* and in vitro. *J. Biol. Chem.* 263, 9333–9338.
- Graham, J.H., Gottwald, T.R., 1991. Research perspectives on eradication of citrus bacterial diseases in Florida. *Plant Dis.* 75, 1193–1200.
- Graham, J.H., Leite, J.R.P., 2004. Lack of control of citrus canker by induced systemic resistance compounds. *Plant Dis.* 88, 745–750.
- Green, S., A'Hara, S.W., Cottrell, J.E., Laue, B., Fossdal, C.G., 2009. Infection of horse chestnut (*Aesculus hippocastanum*) by *Pseudomonas syringae* pv. *aesculi* and its detection by quantitative real-time PCR. *Plant Pathol.* 58, 731–744.
- Green, Sarah, Studholme, D.J., Laue, B.E., Dorati, F., Lovell, H., Arnold, D.L., Cottrell, J.E., Bridgett, S., Blaxter, M., Huitema, E., Thwaites, R., Sharp, P.M., Jackson, R. W., Kamoun, S., 2010. Comparative genome analysis provides insights into the evolution and adaptation of *Pseudomonas syringae* pv. *aesculi* on *Aesculus hippocastanum*. *PLoS One* 5, e10224.
- Greer, G., Saunders, C., 2012. The Costs of Psa-V to the New Zealand Kiwifruit Industry and the Wider Community. <http://www.kvh.org.nz/vdb/document/91146>.
- Gross, D.C., 1991. Molecular and genetic analysis of toxin production by pathogens of *Pseudomonas syringae*. *Annu. Rev. Phytopathol.* 29, 247–278.
- Gross, M., Rudolph, K., 1987. Demonstration of levan and alginate in bean plants (*Phaseolus vulgaris*) infected by *Pseudomonas syringae* pv. *phaseolicola*. *J. Phytopathol.* 120, 9–19.
- Gross, D.C., Cody, S.Y., Proebsting, E.L., Rademaker, G.K., Spotts, R.A., 1983. Distribution, population dynamics, and characteristics of ice nucleation active bacteria in deciduous fruit tree orchards. *Appl. Environ. Microbiol.* 46, 1370–1379.
- Gross, D.C., Cody, Y.S., Pebsting, E.L., Rademaker, G.K., Spotts, R.A., 1984. Ecotypes and pathogenicity of ice nucleation-active *Pseudomonas syringae* isolated from deciduous fruit tree orchards. *Phytopathology* 74, 241–248.
- Guirguis, N.S., Soubhy, I., Khalil, M.A., Stino, G.R., 1995. Leaf stomata and stem lenticels as a means of identification of some stone fruits stocks. *Acta Hort.* 409, 229–240.
- Hall, B.H., Cother, E.J., Noble, D., McMahon, R., Wicks, T.J., 2003. First report of *Pseudomonas syringae* on olives (*Olea europaea*) in South Australia. *Australas. Plant Dis. Notes* 32, 119–120.
- Hall, B.H., Cother, E.J., Whattam, M., Noble, D., Lucj, J., Cartwright, D., 2004. First report of olive knot caused by *Pseudomonas savastanoi* pv. *savastanoi* on olives (*Olea europea*) in Australia. *Australas. Plant Dis. Notes* 33, 433–436.
- Hall, B.H., McMahon, R.L., Noble, D., Cother, E.J., McLintock, D., 2002. First report of *Pseudomonas syringae* on grapevines (*Vitis vinifera*) in South Australia. *Australas. Plant Pathol.* 31, 421–422.
- Han, H.S., Oak, E.J., Koh, Y.J., Hur, J.S., Jung, J.S., 2003. Characterization of *Pseudomonas syringae* pv. *actinidiae* isolated in Korea and genetic relationship among coronatine-producing pathogens based on *cmaU* sequences. *Acta Hort.* 610, 403–408.
- Hattingh, M.J., Roos, I.M.M., Mansvelt, E.L., 1989. Infection and systemic invasion of deciduous fruit trees by *Pseudomonas syringae* in South Africa. *Plant Dis.* 73, 784–789.
- Heaton, C.R., Ogawa, J.M., Nyland, G., 1981. Evaluating economic losses caused by pathogens of fruit and nut crops. *Plant Dis.* 65, 886–888.

- Hert, A.P., 2007. Evaluation of Bacteriocins in *Xanthomonas perforans* for Use in Biological Control of *Xanthomonas euvesicatoria*. University of Florida, Gainesville. http://ufdcimages.uflib.ufl.edu/UF/E0/01/99/80/00001/hert_a.pdf.
- Hickey, M., King, C., 2001. The Cambridge Illustrated Glossary of Botanical Terms. <http://www.cambridge.org/us/academic/subjects/life-sciences/botanical-reference/cambridge-illustrated-glossary-botanical-terms>.
- Himelrick, D.G., Pool, R.M., McInnis, P.J., 1991. Cryoprotectants influence freezing resistance of grapevine bud and leaf tissue. *HortScience* 26, 406–407.
- Hinrichs-Berger, J., 2004. Epidemiology of *Pseudomonas syringae* pathovars associated with decline of plum trees in the southwest of Germany. *J. Phytopathol.* 152, 153–160.
- Hirano, S.S., Upper, C.D., 1990. Population biology and epidemiology of *P. syringae*. *Annu. Rev. Phytopathol.* 28, 155–177.
- Hirano, S.S., Upper, C.D., 2000. Bacteria in the leaf ecosystem with emphasis on *Pseudomonas syringae*-a pathogen, ice nucleus, and epiphyte. *Microbiol. Mol. Biol. Rev.* 64, 624–653.
- Hirano, S.S., Baker, L.S., Upper, C.D., 1985. Ice nucleation temperature of individual leaves in relation to population sizes of ice nucleation active bacteria and frost injury. *Plant Physiol.* 77, 259–265.
- Hori, S., 1915. An important disease of tea caused by a bacterium. *J. Plant Prot.* 2, 1–7.
- Hummel, R.L., Teets, T.M., Guy, C.L., 1990. Protein comparisons of non- and cold-acclimated *Hibiscus syriacus* and *H. rosa-sinensis* bark. *HortScience* 25, 365.
- Hummer, K., 1995. The mystical powers and culinary delights of the hazelnut: a globally important Mediterranean crop. *Diversity* 11, 130.
- Hutchinson, P.B., 1949. A bacterial disease of *Dysoxylum* spectabile caused by the pathogen *Pseudomonas dysoxylis* n. sp. *N.Z. J. Sci. Technol.* B30, 274–286.
- Ivanova, L., 2009. First occurrence of apricot blast disease caused by *Pseudomonas syringae* in the north-eastern part of Bulgaria. *Acta Hort.* 825, 149–152.
- Ivanovic, Z., Stanković, S., Živković, S., Gavrilović, V., Kojić, M., Fira, D., 2012. Molecular characterization of *Pseudomonas syringae* isolates from fruit trees and raspberry in Serbia. *Eur. J. Plant Pathol.* 134, 191–203.
- Jackson, L.E., 1989. Bacteriophage prevention and control of harmful plant bacteria. Patent no. US4828999 A.
- James, W.C., 1974. Assessment of plant diseases and losses. *Annu. Rev. Phytopathol.* 12, 27–48.
- Janick, J., 2005. The origins of fruits, fruit growing, and fruit breeding. *Plant Breed.* 25, 255–320.
- Janse, J.D., 1982. *Oleaceae* and *Neriurn oleander* L. *Int. J. Syst. Bacteriol.* 32, 166–169.
- Janse, J.D., 2010. Diagnostic methods for phytopathogenic bacteria of stone fruits and nuts in COST 873. *EPPO/OEPP Bull.* 40, 68–85.
- Janse, J.D., Wenneker, M., 2002. Possibilities of avoidance and control of bacterial plant diseases when using pathogen-tested (certified) or -treated planting material. *Plant Pathol.* 51, 523–536.
- Jardine, D.J., Stephens, C.T., 1987. A predictive system for timing chemical applications to control *Pseudomonas syringae* pv. *tomato*, causal agent of bacterial speck. *Phytopathology* 77, 823–827.
- Ji, P., Campbell, H.L., Klopper, J.W., Jones, J.B., Suslow, T.V., Wilson, M., 2006. Integrated biological control of bacterial speck and spot of tomato under field conditions using foliar biological control agents and plant growth-promoting rhizobacteria. *Biol. Control* 36, 358–367.
- Jin, Q., Thilmony, R., Zwiesler-Vollick, J., He, S.Y., 2003. Type III protein secretion in *Pseudomonas syringae*. *Microbes Infect.* 5, 301–310.
- Jones, A.L., 1971. Bacterial canker of sweet cherry in Michigan. *Plant Dis.* 55, 961–965.

- Jones, J.B., Vallad, G.E., Iriarte, F.B., Obradović, A., Wernsing, M.H., Jackson, L.E., Balogh, B., Hong, J.C., Momol, M.T., 2013. Considerations for using bacteriophages for plant disease control. *Bacteriophage* 2, 208–214.
- Kaluzna, M., Ferrante, P., Sobiczewski, P., Scortichini, M., 2010. Characterization and genetic diversity of *Pseudomonas syringae* from stone fruits and hazelnut using repetitive-PCR and MLST. *J. Plant Pathol.* 92, 781–787.
- Kamiunten, H., Nakao, T., Oshida, S., 2000. *Pseudomonas syringae* pv. *cerasicola* pv. nov., the causal agent of bacterial gall of cherry tree. *J. Gen. Plant Pathol.* 66, 219–224.
- Kang, S.M., Titus, J.S., 1987. Specific proteins may determine maximum cold resistance in apple shoots. *J. Hortic. Sci.* 62, 281–285.
- Kang, L., Li, J., Zhao, T., Xiao, F., Tang, X., Thilmony, R., ShengYang, H., Zhou, J.-M., 2003. Interplay of the *Arabidopsis* nonhost resistance gene NHO1 with bacterial virulence. *Proc. Natl. Acad. Sci. U.S.A.* 100, 3519–3524.
- Kao, C.C., Barlow, E., Sequeira, L., 1992. Extracellular polysaccharide is required for wild-type virulence of *Pseudomonas solanacearum*. *J. Bacteriol.* 174, 1068–1071.
- Karimi-Kurdistani, G., Harighi, B., 2008. Phenotypic and molecular properties of *Pseudomonas syringae* pv. *syringae* the causal agent of bacterial canker of stone fruit trees in Kurdistan province. *J. Plant Pathol.* 90, 81–86.
- Kasaplilgil, B., 1964. A contribution to the histotaxonomy of *Corylus* (*Betulaceae*). *Adansonia* 4, 43–90.
- Katan, J., 1981. Solar heating (solarization) of soil for control of soilborne pests. *Annu. Rev. Phytopathol.* 19, 211–236.
- Katzen, F., Ferreira, D.U., Oddo, C.G., Ielmini, M.V., Becker, A., Puhler, A., Ielpi, L., 1998. *Xanthomonas campestris* pv. *campestris* gum mutants: effects on xanthan biosynthesis and plant virulence. *J. Bacteriol.* 180, 1607–1617.
- Kawahara, H., Masuda, K., Obata, H., 2000. Identification of a compound in *Chamaecyparis taiwanensis* inhibiting the ice-nucleating activity of *Pseudomonas fluorescens* KUIN-1. *Biosci. Biotechnol. Biochem.* 64, 2651–2656.
- Kennelly, M.M., Cazorla, E.M., De Vicente, A., Ramos, C., Sundin, G.W., 2007. *Pseudomonas syringae* diseases of fruit trees: progress toward understanding and control. *Plant Dis.* 91, 4–17.
- Kerr, A., 1974. Soil microbiological studies on *Agrobacterium radiobacter* and biological control of crown gall. *Soil Sci.* 118, 168–172.
- Kerr, A., Htay, K., 1974. Biological control of crown gall through bacteriocin production. *Physiol. Plant Pathol.* 4, 37–40.
- Khachatourians, G.G., 1998. Agricultural use of antibiotics and the evolution and transfer of antibiotic-resistant bacteria. *Can. Med. Assoc. J.* 159, 1129–1136.
- Klement, Z., Rozsnyay, D.S., Arsenijevic, M., 1974. Apoplexy of apricots. III. Relationship of winter frost and the bacterial canker dieback of apricots. *Acta Phytopathol. Entomol. Hung.* 9, 35–45.
- Klement, Z., Rozsnyay, D.S., Báló, E., Pánczél, M., Prileszky, G., 1984. The effect of cold on development of bacterial canker in apricot trees infected with *Pseudomonas syringae* pv. *syringae*. *Physiol. Plant Pathol.* 24, 237–246.
- Knoche, K.K., Parke, J.L., Durbin, R.D., 1987. Root colonization by *Pseudomonas syringae* pv. *tabaci*. In: Abstracts. 3rd International Working Group on *Pseudomonas syringae* pathovars. Lisbon, Portugal.
- Koh, Y.J., Kim, G.H., Koh, H.S., Lee, Y.S., Kim, S.C., Jung, J.S., 2012. Occurrence of a new type of *Pseudomonas syringae* pv. *actinidiae* strain of bacterial canker on kiwifruit in Korea. *Plant Pathol. J.* 28, 423–427.
- Kotan, R., Sahin, F., 2002. First record of bacterial canker caused by *Pseudomonas syringae* pv. *syringae*, on apricot trees in Turkey. *Plant Pathol.* 51, 798.

- Kritzman, G., Zutra, D., 1983. Survival of *Pseudomonas syringae* pv. *lachrymans* in soil, plant debris, and the rhizosphere of no-host plants. *Phytoparasitica* 11, 99–108.
- Kuroda, H., Sagisaka, S., Chiba, K., 1990. Frost induces cold acclimation and peroxidase-scavenging systems coupled with pentose phosphate cycle in apple twigs under natural conditions. *J. Jpn. Soc. Hortic. Sci.* 59, 409–416.
- Lacombe, S., Rougon-Cardoso, A., Sherwood, E., Peeters, N., Dahlbeck, D., Van Esse, H.P., Smoker, M., Rallapalli, G., Thomma, B.P., Staskawick, B., Jones, J.D., Zipfel, C., 2010. Interfamily transfer of a plant pattern-recognition receptor confers broad-spectrum bacterial resistance. *Nat. Biotechnol.* 28, 365–369.
- Lalancette, N., McFarland, K.A., 2007. Phytotoxicity of copper-based bactericides to peach and nectarine. *Plant Dis.* 91, 122–130.
- Lamichhane, J.R., Fabi, A., Ridolfi, R., Varvaro, L., 2013. Epidemiological study of hazelnut bacterial blight in central Italy by using laboratory analysis and geostatistics. *PLoS One* 8, e56298.
- Lang, G.A., Tao, J., 1990. Analysis of fruit bud proteins associated with plant dormancy. *Hort-Science* 29S, 1068.
- Latorre, B.A., Jones, A.L., 1979a. *Pseudomonas morsprunorum*, the cause of bacterial canker of sour cherry in Michigan, and its epiphytic association with *P. syringae*. *Phytopathology* 69, 335–339.
- Latorre, B.A., Jones, A.L., 1979b. Evaluation of weeds and plant refuse as potential sources of inoculum of *Pseudomonas syringae* in bacterial canker of cherry. *Phytopathology* 69, 1122–1125.
- Lazarovits, G., 2001. Management of soilborne plant pathogens with organic soil amendments: a disease control strategy salvaged from the past. *Can. J. Plant Pathol.* 23, 1–7.
- Liang, C.F., 1983. On the distribution of *Actinidia*. *Guihaia* 3, 229–248.
- Liang, L.Z., Jones, A.L., 1995. Organization of the *hrp* gene cluster and nucleotide sequence of the *hrpL* gene from *Pseudomonas syringae* pv. *morsprunorum*. *Phytopathology* 85, 118–123.
- Lindemann, J., Suslow, T.V., 1987. Competition between ice nucleation-active wild type and ice nucleation-deficient deletion mutant strains of *Pseudomonas syringae* and *P. fluorescens* biovar I and biological control of frost injury on strawberry blossoms. *Phytopathology* 77, 882–886.
- Lindow, S.E., 1980. New method of frost control through control of epiphytic ice nucleation-active bacteria. *Calif. Plant Pathol.* 41, 1–5.
- Lindow, S.E., 1983a. Methods of preventing frost injury caused by epiphytic ice-nucleation-active bacteria. *Plant Dis.* 67, 327–333.
- Lindow, S.E., 1983b. The role of bacterial ice nucleation in frost injury to plants. *Annu. Rev. Phytopathol.* 21, 363–384.
- Lindow, S.E., 1988. Field tests of recombinant Ice-*Pseudomonas syringae* for biological frost control in potato. In: Sussman, M., et al. (Ed.), *Release of Genetically-Engineered Micro-organisms*. Academic Press, New York, pp. 121–138.
- Lindow, S.E., 1990. Design and results of field tests of recombinant Ice-*Pseudomonas syringae* strains. In: Marois, J.J., Bruening, G. (Eds.), *Risk Assessment in Agricultural Biotechnology*. University of California, Davis, pp. 61–69.
- Lindow, S.E., 1995. Control of epiphytic ice nucleation-active bacteria for management of plant frost injury. In: Lee, R.E., et al. (Ed.), *Biological Ice Nucleation and its Applications*. American Phytopathological Society, St. Paul, Minn, pp. 239–256.
- Lindow, S.E., Connell, J.H., 1984. Reduction of frost injury to almond by control of ice nucleation active bacteria. *J. Am. Soc. Hortic. Sci.* 109, 48–53.
- Lindow, S.E., Panopoulos, N.J., 1988. Field tests of recombinant Ice negative *Pseudomonas syringae* for biological frost control in potato. In: Sussman, M., Collins, C.H., Skinner, F.A. (Eds.), *Release of Genetically Engineered Microorganisms*. Academic Press, London, pp. 121–138. *Proc. First Int'l Conf.*

- Lindow, S.F., Staskawicz, B.J., 1981. Isolation of ice nucleation deficient mutants of *Pseudomonas syringae* and *Erwinia herbicola* and their transformation with plasmid DNA. *Phytopathology* 71, 237.
- Lipka, V., Dittgen, J., Bednarek, P., Bhat, R., Wiermer, M., Stein, M., Landtag, J., Brandt, W., Rosahl, S., Scheel, D., Llorente, F., Molina, A., Parker, J., Somerville, S., Schulze-Lefert, P., 2005. Pre- and postinvasion defenses both contribute to nonhost resistance in Arabidopsis. *Science* 310, 1180–1183.
- Lipsitch, M., Singer, R.S., Levin, B.R., 2002. Antibiotics in agriculture: when is it time to close the barn door. *Proc. Natl. Acad. Sci.* 99, S572–S574.
- Little, E.L., Bostock, R.M., Kirkpatrick, B.C., 1998. Genetic characterization of *Pseudomonas syringae* pv. *syringae* strains from stone fruits in California. *Appl. Environ. Microbiol.* 64, 3818–3823.
- Liu, T., 1998. Biological Control with Tomato Bacterial Spot with hrp-Mutants of *Xanthomonas campestris* pv. *vesicatoria* (M. Sc. thesis). University of Florida, Gainesville.
- Lownsbery, B.F., English, H., Noel, G.R., Schick, F.J., 1977. Influence of Nemaguard and Lovell rootstocks and *Macrostothionia xenoplax* on bacterial canker of peach. *J. Nematol.* 9, 221–224.
- Luisetti, J., Gagnard, J.L., Devaux, M., 1991. *Pseudomonas syringae* pv. *syringae* as one of the factors affecting the ice nucleation of grapevine buds in controlled conditions. *J. Phytopathol.* 133, 334–344.
- Lyskanowska, M.K., 1976. Bacterial canker of sweet cherry (*Prunus avium*) in Poland. I. Symptoms, disease development and economic importance. *Plant Dis. Rep.* 60, 465–469.
- MacDonald, E.M.S., Powell, G.K., Regier, D.A., Glass, N.L., Roberto, F., Kosuge, T., Morris, R., 1986. Secretion of zeatin, ribosylzeatin, and ribosyl-1" -methylzeatin by *Pseudomonas savastanoi*. *Plant Physiol.* 82, 742–747.
- Mahdavian, S.E., Hasanzadeh, N., 2012. Isolation of *Pseudomonas syringae* from hazelnut trees in west part of Mazandaran province. *Int. J. Innov. Res. Sci. Eng. Tech.* 1, 226–229.
- Malvick, D.K., Moore, L.W., 1988. Population dynamics and diversity of *Pseudomonas syringae* on maple and pear trees and associated grasses. *Phytopathology* 78, 1366–1370.
- Manceau, C., Lalande, J., Lachaud, G., Chartier, R., Paulin, J., 1990. Bacterial colonization of flowers and leaf surface of pear trees. *Acta Hort.* 273, 73–81.
- Mansvelt, E.L., Hattingh, M.J., 1986. Bacterial blister bark and blight of fruit spurs of apple in south Africa caused by *Pseudomonas syringae* pv. *syringae*. *Plant Dis.* 70, 403–405.
- Marchi, G., Viti, C., Giovannetti, L., Surico, G., 2005. Spread of levan-positive populations of *Pseudomonas savastanoi* pv. *savastanoi*, the causal agent of olive knot, in central Italy. *Eur. J. Plant Pathol.* 112, 101–112. <http://dx.doi.org/10.1007/s10658-005-0804-0>.
- Masami, N., Masao, G., Katsumi, A., Tadaaki, H., 2004. Nucleotide sequence and organization of copper resistance genes from *Pseudomonas syringae* pv. *actinidiae*. *Eur. J. Plant Pathol.* 110, 223–226.
- Mattheis, J.P., Ketchie, D.O., 1990. Changes in parameters of the plasmalemma ATPase during cold acclimation of apple (*Malus domestica*) bark tissues. *Physiol. Plant.* 78, 616–622.
- Maxson-Stein, K., He, S.Y., Hammerschmidt, R., Jones, A.L., 2002. Effect of treating apple trees with acibenzolar-S-methyl on fire blight and expression of pathogenesis-related protein genes. *Plant Dis.* 86, 785–790.
- McCann, H.C., Rikkerink, E.H.A., Bertels, F., Fiers, M., Lu, A., Rees-George, J., Andersen, M.T., Gleave, A.P., Haubold, B., Wohlers, M.W., Guttman, D.S., Wang, P.W., Straub, C., Vanneste, J.L., Rainey, P.B., Templeton, M.W., 2013. Genomic analysis of the kiwifruit pathogen *Pseudomonas syringae* pv. *actinidiae* provides insight into the origins of an emergent plant disease. *PLoS Pathog.* 9, e100.

- McCarter, S.M., Jones, J.B., Gitaitis, R.D., Smitley, D.R., 1983. Survival of *Pseudomonas syringae* pathovar *tomato* in association with tomato lycopersicon esculentum seed, soil, host tissue and epiphytic hosts in Georgia. *Phytopathology* 73, 1393–1398.
- McGovern, P.E., 2003. *Ancient Wine: The Search for the Origins of Viticulture*. Princeton University Press, Princeton.
- McKeen, W.E., 1955. Pear blast in Vancouver Island. *Phytopathology* 45, 629–632.
- McRae, E.M., Hale, C.N., 1986. New plant disease record in New Zealand: loquat canker. *N.Z. J. Plant Prot.* 29, 547–550.
- Mehlenbacher, S.A., 1991. Hazelnut genetic resources in temperate fruit and nut crops. *Acta Hort.* 290, 789–836.
- Menard, M., Sutra, L., Luisetti, J., Prunier, J.P., Gardan, L., 2003. *Pseudomonas syringae* pv. *avii* (pv. nov.), the causal agent of bacterial canker of wild cherries (*Prunus avium*) in France. *Eur. J. Plant Pathol.* 109, 565–576.
- Menkissoglu, O., Lindow, S.E., 1991. Chemical form of copper on leaves in relation to the bactericidal activity of cupric hydroxide deposits on leaves. *Phytopathology* 81, 1263–1270.
- Menkissoglu-Spirooudi, U., Karamanoli, K., Spyroudis, S., Constantinidou, H.I., 2001. Hypervalent iodine compounds as potent antibacterial agents against ice nucleation active (INA) *Pseudomonas syringae*. *J. Agric. Food Chem.* 49, 3746–3752.
- Mertelik, J., Kloudova, K., Pankova, I., Krejzar, V., Kudela, V., 2013. Occurrence of horse chestnut bleeding canker caused by *Pseudomonas syringae* pv. *aesculi* in the Czech Republic. *For. Pathol.* <http://dx.doi.org/10.1111/efp.12021>.
- Mirik, M., Baloglu, S., Aysan, Y., Cetinkaya-Yildiz, R., Kusek, M., Sahin, F., 2005. First outbreak and occurrence of citrus blast disease, caused by *Pseudomonas syringae* pv. *syringae*, on orange and mandarin trees in Turkey. *Plant Pathol.* 54, 238.
- Mitchell, R.E., 1984. The relevance of non-host-specific toxins in the expression of virulence by pathogens. *Annu. Rev. Phytopathol.* 22, 215–245.
- Mitchell, R.E., Hart, P.A., 1983. The structure of tagetitoxin, a phytotoxin of *Pseudomonas syringae* pv. *tagetis*. *Phytochemistry* 22, 1425–1428.
- Mittal, S., Davis, K.R., 1995. Role of the phytotoxin coronatine in the infection of *Arabidopsis thaliana* by *Pseudomonas syringae* pv. *tomato*. *Mol. Plant Microbe Interact.* 8, 165–171.
- Mittler, R., Herr, E.H., Orvar, B.L., Van Camp, W., Willekens, H., Inzé, D., Ellis, B.E., 1999. Transgenic tobacco plants with reduced capability to detoxify reactive oxygen intermediates are hyperresponsive to pathogen infection. *Proc. Natl. Acad. Sci. U.S.A.* 96, 14165–14170.
- Mmbaga, M.T., Nnodu, E.C., 2006. Biology and control of bacterial leaf blight of *Cornus mas*. *HortScience* 41, 721–724.
- Monk, C.D., 1966. An ecological significance of evergreenness. *Ecology* 47, 504–505.
- Monteil, C.L., Guilbaud, C., Glaux, C., Lafolie, F., Soubeyrand, S., Morris, C.E., 2012. Emigration of the plant pathogen *Pseudomonas syringae* from leaf litter contributes to its population dynamics in alpine snowpack. *Environ. Microbiol.* 14, 2099–2112.
- Montesinos, E., Vilardell, P., 1991. Relationships among population-levels of *Pseudomonas syringae*, amount of ice nuclei, and incidence of blast of dormant flower buds in commercial pear orchards in Catalunya, Spain. *Phytopathology* 81, 113–119.
- Moore, L.W., 1988. *Pseudomonas syringae* disease and ice nucleation activity. *Ornam. Northwest Arch.* 12, 3–16.
- Moore, L.W., Malvick, D.K., 1987. Survival and dissemination of *Pseudomonas syringae* on maple trees and grasses. In: Abstracts. 3rd International Conference on Biological Ice Nucleation. Newport, Oregon.

- Moragrega, C., Llorente, I., Manceau, C., Montrinos, E., 2003. Susceptibility of European pear cultivar sto *Pseudomonas syringae* pv. *syringae* using immature fruit and detached leaf assays. *Eur. J. Plant Pathol.* 109, 319–326.
- Morris, C.E., Glaux, C., Latour, X., Gardan, L., Samson, R., Pitrat, M., 2000. The relationship of host range, physiology, and genotype to virulence on cantaloupe in *Pseudomonas syringae* from cantaloupe blight epidemics in France. *Phytopathology* 90, 636–646.
- Morris, C.E., Kinkel, L.L., Xiao, K., Prior, P., Sands, D.C., 2007. Surprising niche for the plant pathogen *Pseudomonas syringae*. *Infect. Genet. Evol.* 7, 84–92.
- Morris, C.E., Sands, D.C., Vinatzer, B.A., Glaux, C., Guilbaud, C., Buffière, A., Yan, S., Dominguez, H., Thompson, B.M., 2008. The life history of the plant pathogen *Pseudomonas syringae* is linked to the water cycle. *ISME J.* 2, 321–334.
- Morris, C.E., Sands, D.C., Vanneste, J.L., Montarry, J., Oakley, B., Guilbaud, C., Glaux, C., 2010. Inferring the evolutionary history of the plant pathogen *Pseudomonas syringae* from its biogeography in headwaters of rivers in North America, Europe, and New Zealand. *MBio* 1, e00107–e00110.
- Natalini, E., Rossi, M.P., Barionovi, D., Scortichini, M., 2006. Genetic and pathogenic diversity of *Pseudomonas syringae* pv. *syringae* isolates associated with bud necrosis and leaf spot of pear in a single orchard. *J. Plant Pathol.* 88, 219–223.
- Nejad, P., Ramstedt, M., Granhall, U., 2004. Pathogenic ice–nucleation active bacteria in willows for short rotation forestry. *For. Pathol.* 34, 369–381.
- Nomura, K., Melotto, M., He, S.Y., 2005. Suppression of host defense in compatible plant–*Pseudomonas syringae* interactions. *Curr. Opin. Plant Biol.* 8, 361–368.
- Norelli, J.L., Miller, S.S., 2004. Effect of prohexadione–calcium dose level on shoot growth and fire blight in young apple trees. *Plant Dis.* 88, 1099–1106.
- Novaes, E., Kirst, M., Chiang, V., Winter–Sederoff, H., Sederoff, R., 2010. Lignin and biomass: a negative correlation for wood formation and lignin content in trees. *Plant Physiol.* 154, 555–561.
- Nowak, D.J., Crane, D.E., 2002. Carbon storage and sequestration by urban trees in the USA. *Environ. Pollut.* 116, 381–389.
- Nowak, D.J., Crane, D.E., Stevens, J.C., 2006. Air pollution removal by urban trees and shrubs in the United States. *Urban For. Urban Gree.* 4, 115–123.
- Oerke, E.C., 2005. Crop losses to pests. *J. Agric. Sci.* 144, 31–43.
- Oerke, E.C., Dehne, H.W., Schonbeck, F., Weber, A., 1994. *Crop Production and Crop Protection Estimated Losses in Major Food and Cash Crops*. Elsevier Science, Amsterdam.
- Ogimi, C., 1977. Studies on bacterial gall of chinaberry (*Melia azedarach* Lin.), caused by *Pseudomonas meliae* n. sp. *Bull. Coll. Agric. Univ. Ryukyus* 24, 497–556.
- Ogimi, C., Higuchi, H., 1981. Bacterial gall of yamamomo (*Myrica rubra* S. et Z.) caused by *Pseudomonas syringae* pv. *myricae* pv. nov. *Ann. Phytopathol. Soc. Jpn.* 47, 443–448.
- Ogimi, C., Higuchi, H., Takikawa, Y., 1988a. Bacterial gall disease of urajiroenoki (*Trema orientalis* Blume) caused by *Pseudomonas syringae* pv. *tremae* pv. nov. *J. Jpn. For. Soc.* 70, 441–446.
- Ogimi, C., Higuchi, H., Takikawa, Y., 1988b. Bacterial gall disease of kakuremino (*Dendropanax trifidus* Mak.) caused by *Pseudomonas syringae* pv. *dendropanacis* pv. nov. *Ann. Phytopathol. Soc. Jpn.* 54, 296–302.
- Ogimi, C., Kubo, Y., Higuchi, H., Takikawa, Y., 1990. Bacterial gall diseases of himeyuzuriha (*Daphniphyllum teijsmanni* Z.) caused by *Pseudomonas syringae* pv. *daphniphylli* pv. nov. *J. Jpn. For. Soc.* 72, 17–22.
- Ogimi, C., Kawano, C., Higuchi, H., Takikawa, Y., 1992. Bacterial gall disease of sharinbai (*Rhaphiolepis umbellata* Makino) caused by *Pseudomonas syringae* pv. *rhaphiolepidis* pv. nov. *J. Jpn. For. Soc.* 74, 308–313.
- Osman, S.F., Fett, W.F., Fishman, M.L., 1986. Exopolysaccharides of the phytopathogen *Pseudomonas syringae* pv. *glycinea*. *J. Bacteriol.* 166, 66–71.

- Ozakatan, H., Akkorpu, A., Bozkurt, A., Erdal, M., 2008. Information on peach bacterial canker in Aegean region of Turkey. In: Abstracts. COST Meeting. Skierniewice, Poland.
- O'Brien, H.E., Thakur, S., Gong, Y., Fung, P., Zhang, J., Yuan, L., Wang, P.W., Yong, C., Scortichini, M., Guttman, D.S., 2012. Extensive remodeling of the *Pseudomonas syringae* pv. *avellanae* type III secretome associated with two independent host shifts onto hazelnut. *BMC Microbiol.* 12, 141. <http://dx.doi.org/10.1186/1471-2180-12-141>.
- Panagopoulos, C.G., Crosse, J.E., 1964. Frost injury as a predisposing factor in blossom blight of pear caused by *Pseudomonas syringae* van Hall. *Nature* 202, 1352.
- Parkinson, N., Bryant, R., Bew, J., Elphinstone, J., 2011. Rapid phylogenetic identification of members of the *Pseudomonas syringae* species complex using the rpoD locus. *Plant Pathol.* 60, 338–344.
- Patil, S.S., Hayward, A.C., Emmons, R., 1974. An ultraviolet-induced nontoxigenic mutant of *Pseudomonas phaseolicola* of altered pathogenicity. *Phytopathology* 64, 590–595.
- Pearl, I.W., 1967. *The Chemistry of Lignin*. Marcel Dekker, Inc., New York.
- Pedley, K.F., Martin, G.B., 2003. Molecular basis of Pto-mediated resistance to bacterial speck disease in tomato. *Annu. Rev. Phytopathol.* 41, 215–243.
- Pietrzak, U., McPhail, D.C., 2004. Copper accumulation, distribution and fractionation in vineyard soils of Victoria, Australia. *Geoderma* 122, 151–166.
- Plomion, C., Leprovost, G., Stokes, A., 2001. Wood formation in trees. *Plant Physiol.* 127, 1513–1523.
- Polizzi, G., Castello, I., Parlavecchio, G., Cirvilleri, G., 2005. First report of bacterial blight of *Strelitzia augusta* caused by *Pseudomonas syringae* pv. *lachrymans*. *Plant Dis.* 89, 1010.
- Poschenrieder, G., Czech, I., Friedrich-Zorn, M., Huber, B., Theil, S., et al., 2006. Ester nachweis von *Pseudomonas syringae* pv. *coryli* (pv. nov.) und *Xanthomonas arboricola* pv. *corylina* an *Corylus avellana* (Haselnuss) in Deutschland. In: Abstracts Bayerische Landesanstalt für Landwirtschaft–Institut für Pflanzenschutz, pp. 32–33.
- Proebsting, E.L., Andrews, P.K., Gross, D.C., 1982. Supercooling young developing fruit and floral buds in deciduous orchards. *HortScience* 17, 67–68.
- Prunier, J.-P., Luisetti, J., Gardan, L., 1970. Études sur les bactérioses des arbres fruitiers. II. Caractérisation d'un *Pseudomonas* non-fluorescent agent d'une bactériose nouvelle du pêcher. *Ann. Phytopathol.* 2, 181–197.
- Prunier, J.P., Jullian, J.-P., Audergon, J.-M., 1999. Influence of rootstocks and height of grafting on the susceptibility of apricot cultivars to bacterial canker. *Acta Hort.* 488, 643–648.
- Psallidas, P.G., 1993. *Pseudomonas syringae* pv. *avellanae* pathovar nov., the bacterium causing canker disease on *Corylus avellana*. *Plant Pathol.* 42, 358–363.
- Psallidas, P.G., Panagopoulos, C.G., 1975. A new bacteriosis of almond caused by *Pseudomonas amygdali* sp. nov. *Ann. Inst. Phytopathol. Benaki* 11, 94–108.
- Psallidas, P.G., Panagopoulos, C.G., 1979. A bacterial canker of hazelnut in Greece. *J. Phytopathol.* 94, 103–111.
- Qing, L., 2007. Primary study of bacteriophage of *Pseudomonas syringae* pv. *actinidiae*. *J. Anhui Agric. Sci.* 19, S436.634 (in Chinese).
- Ramos, A.H., Kamidi, R.E., 1981. Seasonal periodicity and distribution of bacterial blight of coffee in Kenya. *Plant Dis.* 65, 581–584.
- Ramstedt, M., ÅRström, B., von Fircks, H.A., 1994. Dieback of poplar and willow caused by *Pseudomonas syringae* in combination with freezing stress. *Eur. J. For. Pathol.* 24, 305–315.
- Reglinski, T.W.K., Elmer, P., 2011. Short Report on Commercially Available Elicitors, Natural Products and Microbes for Evaluation against *Pseudomonas syringae* pv. *actinidiae*. Retrieved April 14, 2013, from: <http://www.kvh.org.nz/vdb/>.
- Renick, L.J., Cogal, A.G., Sundin, G.W., 2008. Phenotypic and genetic analysis of epiphytic *Pseudomonas syringae* populations from sweet cherry in Michigan. *Plant Dis.* 92, 372–378.

- Roberts, S.J., 1985a. Variation within *Pseudomonas syringae* pv. *philadelphia*, the cause of a leaf spot of *Philadelphus* spp. J. Appl. Bacteriol. 59, 283–290.
- Roberts, S.J., 1985b. A note on *Pseudomonas syringae* pv. *berberidis* infections of *Berberis*: comparative infection studies in attached and detached leaves. J. Appl. Microbiol. 59, 369–374.
- Robinson, J.M., 1990. Lignin, land plants, and fungi: biological evolution affecting Phanerozoic oxygen balance. Geology 18, 607–610.
- Romero, A.M., Kousik, C.S., Ritchie, D.F., 2001. Resistance to bacterial spot in bell pepper induced by acibenzolar-S-methyl. Plant Dis. 85, 189–194.
- Roos, I.M.M., Hattingh, M.J., 1986. Resident populations of *Pseudomonas syringae* on stone fruit tree leaves in South Africa. Phytophylactica 18, 55–58.
- Roos, I.M.M., Hattingh, M.J., 1986a. Pathogenic *Pseudomonas* spp. in stone fruit buds. Phytophylactica 18, 7–9.
- Roos, I.M.M., Hattingh, M.J., 1986b. Weeds in orchards as potential source of inoculum for bacterial canker on stone fruit. Phytophylactica 18, 5–6.
- Rose, D.H., 1917. Blister spot of apples and its relation to a disease of apple bark. Phytopathology 7, 198–208.
- Rostami, M., 2012. Isolation and identification of ice-nucleating – active bacteria and their antagonistic bacteria from pistachio trees in Rafsanjan region. Adv. Environ. Biol. 6, 1460–1467.
- Rudolph, K.W.E., Gross, M., Neugebauer, M., Hokawat, S., Zachowski, A., Wydra, K., et al., 1989. Extracellular polysaccharides as determinants of leaf spot diseases caused by pseudomonads and xanthomonads. In: Graniti, A., et al. (Ed.), Phytotoxins and Plant Pathogenesis. Springer, Berlin, pp. 177–218.
- Rushforth, K., 1999. Trees of Britain and Europe. Collins. ISBN: 0-00-220013-9.
- Sakamoto, Y., 1999. Anatomy of bacterial canker on *Maackia amurensis* var. *burgeri*. J. For. Res. 4, 281–285.
- Samavatian, H., 2006. Identification and distribution of bacterial disease agent of almond. Tree canker in Isfahan province. Acta Hort. 726, 667–672.
- Sarkanen, K.V., Ludwig, C.H., 1971. Lignins: Occurrence, Formation, Structure and Reactions. John Wiley and Sons, New York.
- Scheck, H.J., Pscheidt, J.W., Moore, L.W., 1996. Copper and streptomycin resistance in strains of *Pseudomonas syringae* from Pacific Northwest nurseries. Plant Dis. 80, 1034–1039.
- Schmidle, A., 1981. Zur resistaenz von sauerkirschosorten gegen den bakteenbrand *Pseudomonas syringae* van Hall. Erwerbsobstbau 23, 110–113.
- Schmidt, O., Dujesiefken, D., Stobbe, H., Moreth, U., Kehr, R., Schroder, T., 2008. *Pseudomonas syringae* pv. *aesculi* associated with horse chestnut bleeding canker in Germany. For. Pathol. 38, 124–128.
- Schnabel, E.L., Jones, A.L., 2001. Isolation and characterization of five *Erwinia amylovora* bacteriophages and assessment of phage resistance in strains of *Erwinia amylovora*. Appl. Environ. Microbiol. 67, 59–64.
- Schubert, T.S., Miller, J.W., 1997. Bacterial citrus canker. Plant Pathol. Cir. 377, 1–6.
- Schubert, T.S., Rizvi, S.A., Sun, X.A., Gottwald, T.R., Graham, J.H., Dixon, W.N., 2001. Meeting the challenge of eradicating citrus canker in Florida again. Plant Dis. 85, 340–356.
- Schwessinger, B., Zipfel, C., 2008. News from the frontline: recent insights into PAMP-triggered immunity in plants. Curr. Opin. Plant Biol. 11, 389–395.
- Scortichini, M., 1997. Leaf necrosis and sucker and twig dieback of *Alnus glutinosa* incited by *Pseudomonas syringae* pv. *syringae*. Eur. J. For. Pathol. 27, 331–336.
- Scortichini, M., 2002. Bacterial canker and decline of European hazelnut. Plant Dis. 86, 704–709.
- Scortichini, M., 2006. Severe outbreak of *Pseudomonas syringae* pv. *syringae* on new apricot cultivars in central Italy. J. Plant Pathol. 88, S65–S70.

- Scortichini, M., 2010. Epidemiology and predisposing factors of some major bacterial diseases of stone and nut fruit trees species. *J. Plant Pathol.* 92S, S173–S178.
- Scortichini, M., Janse, J.D., 2008. Nectarine fruit scab caused by *Pseudomonas syringae* pv. *syringae*. *J. Plant Pathol.* 90, 397.
- Scortichini, M., Ligouri, R., 2003. Integrated management of bacterial decline of hazelnut, by using Bion as an activator of systemic acquired resistance (SAR). In: Iacobellis, N.S., et al. (Ed.), *Pseudomonas syringae* and Related Pathogens. Kluwer Academic Publishers, Dordrecht, The Netherlands, pp. 483–487.
- Scortichini, M., Morone, C., 1997. Apoplexy of peach trees caused by *Pseudomonas viridiflava*. *J. Phytopathol.* 145, 397–399.
- Scortichini, M., Marchesi, U., Rossi, M.P., Di Prospero, P., 2002. Bacteria associated with hazelnut (*Corylus avellana* L.) decline are of two groups: *Pseudomonas avellanae* and strains resembling *P. syringae* pv. *syringae*. *Appl. Environ. Microbiol.* 68, 476–484.
- Scortichini, M., Marchesi, U., Dettori, M.T., Rossi, M.P., 2003. Genetic diversity, presence of the *syrB* gene, host preference and virulence of *Pseudomonas syringae* pv. *syringae* strains from woody and herbaceous host plants. *Plant Pathol.* 52, 277–286.
- Scortichini, M., Rossi, M.P., Loreti, S., Bosco, A., Fiori, M., Jackson, R.W., Stead, D.E., Aspin, A., Marchesi, U., Zini, M., Janse, J.D., 2005. *Pseudomonas syringae* pv. *coryli*, the causal agent of bacterial twig dieback of *Corylus avellana*. *Phytopathology* 95, 1316–1324.
- Scortichini, M., Marcelletti, S., Ferrante, P., Petriccione, M., Firrao, G., 2012. *Pseudomonas syringae* pv. *actinidiae*: a re-emerging, multi-faceted, pandemic pathogen. *Mol. Plant Pathol.* 13, 631–640.
- Scortichini, M., Tropiano, F.G., 1994. Severe outbreak of *Pseudomonas syringae* pv. *avellanae* on hazelnut in Italy. *J. Phytopathol.* 140, 65–70.
- Siscaro, G., Longo, S., Catara, V., Cirvilleri, G., 2006. Le principali avversità del nocciolo in Sicilia. *Petria* 16, 59–70.
- Smith, E.F., Bryan, M.K., 1915. Angular leaf-spot of cucumbers. *J. Agric. Res.* 5, 465–476.
- Sobiczewski, P., Jones, A.L., 1992. Effect of exposure to freezing temperature on necrosis in sweet cherry shoots inoculated with *Pseudomonas syringae* pv. *syringae* or *P. s. morsprunorum*. *Plant Dis.* 76, 447–451.
- Spotts, R.A., Facteau, T.J., Cervantes, L.A., Chestnut, N.E., 1990. Incidence and control of cytospora canker and bacterial canker in a young sweet cherry orchard on Oregon. *Plant Dis.* 74, 577–580.
- Stavriniades, J., McCloskey, J.K., Ochman, H., 2009. Pea aphid as both host and vector for the phytopathogenic bacterium *Pseudomonas syringae*. *Appl. Environ. Microbiol.* 75, 2230–2235.
- Stead, D.E., Stanford, H., Aspin, A., Weller, S.A., 2006. First record of *Pseudomonas syringae* pv. *viburni* in the UK. *Plant Pathol.* 55, 571.
- Stewart, A., Hill, R., Stark, C., 2011. Desktop Evaluation on Commercially Available Microbial-Based Products for Control or Suppression of *Pseudomonas syringae* pv. *actinidiae*. <http://www.kvh.org.nz/vdb/document/481>.
- Strange, R.N., Scott, P.R., 2005. Plant disease: a threat to global food security. *Annu. Rev. Phytopathol.* 43, 83–116.
- Sule, S., Seemuller, E., 1987. The role of ice formation in the infection of sour cherry leaves by *Pseudomonas syringae* pv. *syringae*. *Phytopathology* 77, 173–177.
- Sullivan, J.T., 1955. Cellulose and lignin in forage grasses and their digestion coefficients. *J. Anim. Sci.* 14, 710–717.
- Sumit, R., Sahu, B.B., Xu, M., Sandhu, D., Bhattacharyya, M.K., 2012. Arabidopsis nonhost resistance gene PSS1 confers immunity against an oomycete and a fungal pathogen but not a bacterial pathogen that cause diseases in soybean. *BMC Plant Biol.* 12, 87.

- Summerell, B.A., Burgess, L.W., 1989. Factors influencing survival of *Pyrenophora tritici repentis*-stubble management. *Mycol. Res.* 93, 38–40.
- Sundin, G.W., Bender, C.L., 1993. Ecological and genetic analysis of copper and streptomycin resistance in *Pseudomonas syringae* pv. *syringae*. *Appl. Environ. Microbiol.* 59, 1018–1024.
- Sundin, G.W., Olson, B.D., Jones, A.L., 1988. Overwintering and population dynamics of *Pseudomonas syringae* pv. *syringae* and *P. s.* pv. *morsprunorum* on sweet and sour cherry trees. *Can. J. Plant Pathol.* 10, 281–288.
- Sutic, D., Tesic, Z., 1958. A new elm bacteriosis caused by *Pseudomonas ulmi*, sp. nov. *Zast Bilja* 45, 13–25.
- Taghavi, S.M., Hasani, Y., 2010. Etiology of chinaberry gall disease in Iran. *Iran Agric. Res.* 29, 13–20.
- Taghavi, M., Hasani, S., 2012. Occurrence of *Pseudomonas savastanoi* the causal agent of winter jasmine gall in Iran. *Iran Agric. Res.* 31, 39–48.
- Tai, T.H., Dahlbeck, D., Clark, E.T., Gajiwala, P., Pasion, R., Whalen, M.C., Stall, R.E., Staskawicz, B.J., 1999. Expression of the Bs2 pepper gene confers resistance to bacterial spot disease in tomato. *Proc. Natl. Acad. Sci. USA.* 96, 14153–14158.
- Takahashi, K., 1980. The causal pathogen of bacterial blight of mulberry and its control. *Jpn. Agric. Res. Q.* 14, 41–45.
- Takanashi, K., Shimizu, K., 1989. *Pseudomonas syringae* pv. *castaneae* pv. nov., causal agent of bacterial canker of chestnut (*Castanea crenata* Sieb. et Zucc.). *Ann. Phytopathol. Soc. Jpn.* 55, 397–403.
- Takikawa, Y., Serizawa, S., Ichikawa, T., Tsuyumu, S., Goto, M., 1989. *Pseudomonas syringae* pv. *actinidiae* pv. nov.: the causal bacterium of canker of kiwifruit in Japan. *Ann. Phytopathol. Soc. Jpn.* 55, 437–444.
- Takimoto, S., 1931. Bacterial bud rot of loquat. *J. Plant Prot.* 18, 349–355.
- Talgø, V., Perminow, J.I.S., Sletten, A., Brurberg, M.B., Herrero, M.L., Strømeng, G.M., Stensvand, A., 2012. Fungal and bacterial diseases on horse chestnut in Norway. *J. Agric. Ext. Rural. Dev.* 4, 256–258.
- Tampakaki, A.P., Skandalis, N., Gazi, A.D., Bastaki, M.N., Sarris, P.F., Charova, S.N., Kokkinidis, M., Panopoulos, N.J., 2010. Playing the “Harp”: evolution of our understanding of hrp/hrc genes. *Annu. Rev. Phytopathol.* 48, 347–370.
- Tanksley, S.D., McCouch, S.R., 1997. Seed banks and molecular maps: unlooked genetic potential from the wild. *Science* 277, 1063–1066.
- Temsah, M., Hanna, L., Saad, A.T., 2007a. Histology of pathogenesis of *Pseudomonas savastanoi* on *Myrtus communis*. *J. Plant Pathol.* 89, 241–249.
- Temsah, M., Hanna, L., Saad, A.T., 2007b. Anatomical observations of *Pseudomonas savastanoi* on *Rhamnus alaternus*. *For. Pathol.* 37, 64–72.
- Terral, J.-F., Tabard, E., Bouby, L., Ivorra, S., et al., 2010. Evolution and history of grapevine (*Vitis vinifera*) under domestication: new morphometric perspectives to understand seed domestication syndrome and reveal origins of ancient European cultivars. *Ann. Bot.* 105, 443–455.
- The Citrus and Date Crop Germplasm Committee, (CDCGC) Report, 2004. Citrus and date germplasm: crop vulnerability, germplasm activities. *Germplasm Needs*, 1–30.
- Thompson, M.M., Lagerstedt, H.B., Mehlenbacher, S.A., 1996. Hazelnuts. In: Janick, J., Moore, J. (Eds.), *Fruit Breeding*. John Wiley and Sons, Inc, UK, pp. 125–184.
- Thornberry, H.H., Anderson, H.W., 1931a. Bacterial leaf spot of viburnum. *Phytopathology* 21, 907–912.
- Thornberry, H.H., Anderson, H.W., 1931b. A bacterial disease of barberry caused by *Phytomonas berberidis*, n. sp. *J. Agric. Res.* 43, 29–36.

- Thurston, H.D., 1990. Plant-disease management- practices of traditional farmers. *Plant Dis.* 74, 96–102.
- Tomihama, T., Nonaka, T., Nishi, Y., Arai, K., 2009. Environmental control in tea fields to reduce infection by *Pseudomonas syringae* pv. *theae*. *Phytopathology* 99, 209–216.
- Tör, M., Lotze, M.T., Holton, N., 2009. Receptor mediated signalling in plants: molecular patterns and programmes. *J. Exp. Bot.* 60, 3645–3654.
- Turner, M.A., Arellano, F., Kozloff, L.M., 1990. Three separate classes of bacterial ice nucleation structures. *J. Bacteriol.* 172, 2521–2526.
- Turner, M.A., Arellano, F., Kozloff, L.M., 1991. Components of ice nucleation structures of bacteria. *J. Bacteriol.* 173, 6515–6527.
- Valleu, W.D., Johnson, E.M., Diachun, S., 1944. Root infection of crop plants and weeds by tobacco leaf spot bacteria. *Phytopathology* 34, 163–174.
- Van Hall, C.J.J., 1902. Bijdragen tot de kennis der Bakterieele Plantenziekten. Coöperatieve Drukkerij-vereeninging “Plantijn” (Inaugural dissertation).
- Vanneste, J.L., 2000. The Disease and its Causative Agent, *Erwinia amylovora*. CAB International, Wallingford, UK.
- Vanneste, J.L., 2012. *Pseudomonas syringae* pv. *actinidiae* (Psa): a threat to the New Zealand and global kiwifruit industry. *N.Z. J. Crop Hortic. Sci.* 40, 265–267.
- Vanneste, J.L., Yu, J., Beer, S.V., 1992. Role of antibiotic production by *Erwinia herbicola* Eh252 in biological control of *Erwinia amylovora*. *J. Bacteriol.* 174, 2785–2796.
- Vanneste, J.L., Giovanardi, D., Yu, J., Cornish, D.A., Kay, C., Spinelli, F., Stefani, E., 2011a. Detection of *Pseudomonas syringae* pv. *actinidiae* in pollen samples. *N.Z. J. Plant Prot.* 64, 246–251.
- Vanneste, J., Poliakov, F., Audusseau, C., Cornish, D., Paillard, S., Rivoal, C., Yu, J., 2011b. First report of *Pseudomonas syringae* pv. *actinidiae* the causal agent of bacterial canker of kiwifruit on *Actinidia deliciosa* in France. *Plant Dis.* 95, 1311.
- Vanneste, J.L., Spinelli, F., Fiorentini, L., Yu, J., Cellini, A., Cornish, D.A., Donati, I., Costa, G., Moffat, B., Felman, C., 2012. Reducing susceptibility of kiwifruit plant to *Pseudomonas syringae* pv. *actinidiae* by manipulating the plant metabolism using elicitors and hormones. In: A Snapshot of Psa (*Pseudomonas syringae* pv. *actinidiae*). New Zealand Plant Protection Society Symposium, 13 August 2012, Nelson, New Zealand. http://www.nzpps.org/symposia/2012_Psa.pdf (accessed 17.09.13.).
- Vanneste, J.L., Yu, J., Cornish, D.A., Tanner, D.J., Windner, R., Chapman, J.R., Taylor, R.K., Mackay, J.F., Dowlut, S., 2013. Identification, virulence and distribution of two biovars of *Pseudomonas syringae* pv. *actinidiae* in New Zealand. *Plant Dis.* 97, 708–719.
- Vasinauskienė, M., Baranauskaitė, L., Burokienė, D., 2008. Search for *Pseudomonas syringae* on Stone Fruits in Lithuania. COST meeting. Skierniewice, Poland.
- Vicente, J.G., Roberts, S.J., 2007. Discrimination of *Pseudomonas syringae* isolates from sweet and wild cherry using rep-PCR. *Eur. J. Plant Pathol.* 117, 383–392.
- Vicente, J.G., Alves, J.P., Russell, K., Roberts, S.J., 2004. Identification and discrimination of *Pseudomonas syringae* isolates from wild cherry in England. *Eur. J. Plant Pathol.* 110, 337–351.
- Vigoroux, A., 1989. Ingress and spread of *Pseudomonas* in stems of peach and apricot promoted by frost-related water soaking tissue. *Plant Dis.* 73, 854–855.
- Vigoroux, A., 1999. Bacterial Canker of Peach: Effect of Tree Winter Water Content on the Spread of Infection Through Frost-related Water Soaking in Stems. *J. Phytopathol.* 147, 442–448.
- Vigoroux, A., Berger, J.-F., Bussi, C., 1987. La sensibilité de pecher au dépérissement bactérien en France: incidence de certaines caractéristiques du sol et de l'irrigation. Relations avec la nutrition. *Agronomie* 7, 483–495.

- Vigouroux, A., Bussi, C., 1994. Une action possible des sols sur la prédisposition des pêchers au dépérissement bactérien par modification de la teneur en eau hivernale des tiges. *Agronomie* 14, 319–326 (in French).
- Vigouroux, A., Bussi, C., Chalvon, V., Girard, T., 1997. Bactériose du pecher et de l'abricotier. Influence combinée du froid et du sol. *Arboric. Frut.* 511, 35–40.
- Viridis, S., 2008. Studio delle principali malattie del nocciolo in Sardegna (Ph.D. thesis). University of Sassari, Sardegna, Italy.
- Watkins, R., 1995. Cherry, plum, peach, apricot and almond: *Prunus* spp. (*Rosaceae*). In: Smartt, J., Simmonds, N.W. (Eds.), *Evolution of Crop Plants*, second ed. Longman Scientific and Technical, Essex, England, pp. 423–429.
- Weaver, D.J., 1978. Interaction of *Pseudomonas syringae* and freezing in bacterial canker on excised peach twigs. *Phytopathology* 68, 1460–1463.
- Webber, J.F., Parkinson, N.M., Rose, J., Stanford, H., Cook, R.T.A., Elphinstone, J.G., 2008. Isolation and identification of *Pseudomonas syringae* pv. *aesculi* causing bleeding canker of horse chestnut in the UK. *Plant Pathol.* 57, 368.
- Welsh, S.L., 1981. New taxa of western plants in tribute. *Brittonia* 33, 294–303.
- Weneker, M., Janse, J.D., de Bruine, A., Vink, P., Pham, K., 2012. Bacterial canker of plum caused by *Pseudomonas syringae* pathovars, as a serious threat for plum production in the Netherlands. *J. Plant Pathol.* 94, S11–S13.
- Whitebread, R., 1967. Bacterial canker of poplars in Britain: the cause of the disease and the role of leaf-scars in infection. *Ann. Appl. Biol.* 59, 123–131.
- Whitelaw-Weckert, M.A., Whitelaw, E.S., Rogiers, S.Y., Quirk, L., Clark, A.C., Huang, C.X., 2011. Bacterial inflorescence rot of grapevine caused by *Pseudomonas syringae* pv. *syringae*. *Plant Pathol.* 60, 325–337.
- Whitesides, S.K., Spotts, R.A., 1991. Frequency, distribution, and characteristics of endophytic *Pseudomonas syringae* in pear trees. *Phytopathology* 81, 453–457.
- Wilkinson, A.G., 1999. Poplars and willows for soil erosion control in New Zealand. *Biomass Bioenergy* 16, 263–274.
- Wormland, H., 1931. Bacterial diseases of stone fruit trees in Britain. III. The symptoms of bacterial canker in plum trees. *J. Pomol. Hortic. Sci.* 9, 239–256.
- Xu, G.W., Gross, D.C., 1988. Evaluation of the role of syringomycin in plant pathogenesis by using Tn5 mutants of *Pseudomonas syringae* pv. *syringae* defective in syringomycin production. *Appl. Environ. Microbiol.* 54, 1345–1353.
- Xu, L.H., Xie, G.L., Zhu, B., Xu, F.S., Qian, J., 2008. First report of pear blossom blast caused by *Pseudomonas syringae* pv. *syringae* in China. *Plant Dis.* 92, 832.
- Young, J.M., 1987. Ice-nucleation on kiwifruit. *Ann. Appl. Biol.* 111, 697–704.
- Young, J.M., 1988a. *Pseudomonas syringae* pv. *persicae* from nectarine, peach and Japanese plum in New Zealand. *EPPPO Bull.* 18, 141–151.
- Young, J.M., 1988b. Bacterial blight of kiwifruit. *J. Appl. Biol.* 112, 91–105.
- Young, J.M., 1991. Pathogenicity and identification of the lilac pathogen, *Pseudomonas syringae* pv. *syringae* van Hall 1902. *Ann. Appl. Biol.* 118, 283–298.
- Young, J.M., 1992. *Pseudomonas syringae* pv. *japonica* (Mukoo 1955) Dye et al. 1980 is a junior synonym of *P. syringae* pv. *syringae* van Hall 1902. *Lett. Appl. Microbiol.* 15, 129–130.
- Young, J.M., 2004. Olive knot and its pathogens. *Australas. Plant Pathol.* 33, 33–39.
- Young, J.M., 2008. An overview of bacterial nomenclature with special reference to plant pathogens. *Syst. Appl. Microbiol.* 31, 405–424.
- Young, J.M., 2012. *Pseudomonas syringae* pv. *actinidiae* in New Zealand. *J. Plant Pathol.* 94S, 5–10.
- Young, J.M., Dye, D.W., Bradbury, J.F., Panagopoulos, C.G., Robbs, C.F., 1978. A proposed nomenclature and classification for plant pathogenic bacteria. *N.Z. J. Agric. Res.* 21, 153–177.

- Yu, J., Peñaloza-Vázquez, A., Chakrabarty, A.M., Bender, C.L., 1999. Involvement of the exopolysaccharide alginate in the virulence and epiphytic fitness of *Pseudomonas syringae* pv. *syringae*. *Mol. Microbiol.* 33, 712–720.
- Zhang, L.H., Birch, R.G., 1997. The gene for albicidin detoxification from *Pantoea dispersa* encodes an esterase and attenuates pathogenicity of *Xanthomonas albilineans* to sugarcane. *Proc. Natl. Acad. Sci.* 94, 9984–9989.
- Zhu, Y., Chen, H., Fan, J., Wang, Y., Li, Y., Chen, J., Fan, J., Yang, S., Hu, L., Leung, H., Mew, T.W., Teng, P.S., Wang, Z., Mundt, C.C., 2000. Genetic diversity and disease control in rice. *Nature* 406, 718–722.
- Zohary, D., Spiegel-Roy, P., 1975. Beginning of fruit growing in the old world. *Science* 187, 319–327.

This page intentionally left blank

INDEX

Note: Page numbers with “f” denote figures; “t” tables.

A

- Abscisic acid (ABA), 209–210
- Allophane/imogolite
 - characteristics, 26
 - computer-aided subtraction, 27–28
 - DRIFTS, 26–27, 27f
 - IR spectroscopy, 26
- Antimicrobial organic compounds, 64, 65t–66t
- p*-Arsanilic acid, 71
- Attenuated total reflectance Fourier transform infrared spectroscopy (ATR–FTIR), 9f
 - angle of incidence, 11, 12f
 - critical angle, 10–11
 - crystal materials, 10–11
 - internal reflection element, 10
 - penetration, 11
- Auxin (IAA), 209–210

B

- Bacterial cankers, 240–241
- Benzoic acid (BA), 69
- Biochar
 - vs.* charcoal, 49–50
 - chemical characteristics, 50–51
 - Dispersive Raman, 50
 - FTIR spectroscopy, 51–52
 - functional group assignments, 50–51, 51t
 - structural order, 52–53
 - Terra Preta de Indio soils, 49–50
- Biosolids, 53–54
- Biotic stress, 221–222

C

- Calcium-bound humic acid (CaHA), 97–98
- Carbohydrates synthesis, 205–206
- CF systems. *See* Conventional uncovered/flat-plot (CF) systems
- Chinese agriculture. *See* Water-saving innovations
- Ciprofloxacin, 70–71

- Cold stress, 219–220
- Compost, 53
- Conventional uncovered/flat-plot (CF) systems, 173–174, 175t
- Crop water requirement (CWR), 157–158

D

- Diffuse reflectance infrared Fourier transform spectroscopy (DRIFTS), 9, 9f
- Diketetonitrile (DKN), 69
- 4,6-Dinitro-*o*-cresol, 64–69
- Dinitrophenol herbicides, 64–69
- Dispersive Raman spectroscopy
 - fluorescence interferences, 16–17
 - instrument setup, 15–16, 16f
 - sample preparation, 16–17
 - solid samples, 15–16
- Drought stress, 218–219

E

- Evapotranspiration (ET), 156–157

F

- Fluoroquinolones, 70–71
- Fourier transformed Raman spectroscopy (FT-Raman)
 - instrument setup, 16f
 - interferometers, 17–18
 - MARS Rover, 17–18
- Fourier transform infrared (FTIR) spectroscopy
 - polychromatic radiation, 4–5
 - sampling techniques, 8, 9f
 - ATR–FTIR, 10–12
 - DRIFTS, 9–10
 - IRMS, 12–13
 - SR–FTIR spectromicroscopy, 13–15, 14f
 - transmission, 8–9, 9f
 - soil amendments. *See* Vibrational spectroscopy techniques

- Fourier transform infrared (FTIR) spectroscopy (*Continued*)
 SOM analysis, 91
 fractions and extracts, 92–103
 soil carbon and nitrogen, 109–110
 spectral analysis, 107–108, 109f
 subtraction spectra, 104–107
 in whole soils, 91–92
- Fringing, 13
- G**
- Gibberellin (GA), 209–210
- Gibbsite
 FTIR spectra, 29–31, 30f
 OH stretching, 31
 structure, 28–29
- Glyphosate, 69–70
- Gravel-sand mulching system, 179, 180f
- H**
- Herbicides, 64–69
- Hydrous Mn oxide (HMO), 77–78
- I**
- Infrared microspectroscopy (IRMS)
 cryomicrotoming, 12–13
 factors, 13
 fringing, 13
 with IR spectrometer, 4
 measurement modes, 12–13
- K**
- Kiwifruit bacterial canker, 255–256
- L**
- Low molecular weight organic acids, 59–64, 60t–62t
- M**
- Methylphosphonic acid (MPA), 69–70
- Michelson interferometer, 3–4
- Molecular-scale analysis, 54
 ATR-FTIR, 54
 bacteria and biomolecule adhesion, 79t
 ATR-FTIR spectra, 83–85, 84f
 carboxyl groups, 82
Cryptosporidium parvum oocyst, 82–83
 Mn-oxides, 81
 phosphate groups, 83–85
Pseudomonas aeruginosa, 83
 PZNPC, 80–81
Shewanella putrefaciens, 85
 siderophores, 83
 silica, 80–81
 surface molecules, 78–80
- inorganic molecule interactions, mineral surfaces, 72
 ATR-FTIR, 72, 77–78
 ferrihydrite, 76–77
 HMO, 77–78
 inorganic ions, 72, 73t–75t
 phosphate sorption, 72–76
 Raman microspectroscopy, 76
- organic molecule interactions, mineral surfaces
 adsorbate surrogates, 55
 adsorption complexes, 57–59, 58f
 aqueous ofloxacin spectra, 56–57, 57f
 carboxyl band separations, 57–59, 58t
 FTIR and DRIFTS analyses, 55–56
 herbicides and pharmaceuticals, 64–71, 65t–68t
 inner-and outer-sphere complex, 57–59
 low molecular weight organic acids, 59–64, 60t–62t
- Mulching systems
 gravel-sand mulching, 179, 180f
 RF plastic mulching, 174f
 factors, 176
 plastic-covered RF *vs.* CF system, 173–174, 175t
 rain-simulation study, 173–174
- straw mulching
 allelopathic effects, 177
 mean root weight densities, winter wheat, 177, 179f
 soil moisture conservation, 176–177
 tillage system effects, 177, 178t
 types, 173
- N**
- Nonhost resistance (NHR), 270–271
- O**
- Organoarsenicals, 71
- Osmotic adjustment, 207–208

P

- PAMP-triggered immunity (PTI), 270–271
 Partial Least Squares (PLS), 102
 Partial root zone drying (PRD), 181–182, 182f
 Penman–Monteith equation, 156
 Pesticide compounds, 64, 67t–68t
 Photophosphorylation, 213
 Phyllosilicates/layer silicates
 composition, 21
 differentiation and characterization, 21
 FTIR spectroscopy, 25
 kaolin group minerals, 24
 kaolinite and dickite, 22–23
 OH bending vibrations, 23
 Raman spectroscopy, 25–26
 Si–O stretching, 23
 transmission infrared spectra, 21, 22f
 Point of zero net proton charge (PZNPC), 80–81
 Potassium (K) nutrition
 biotic stress, 221–222
 channels, 217–218
 characteristics, 204–205
 cold stress, 219–220
 drought stress, 218–219
 enzyme and organic compound synthesis, 205–206
 leaf movements, 208
 meristematic and plant growth regulation, 209–211
 nitrate transport–potassium interactions, 215–216
 optimal plant growth, 204
 photosynthesis, 212–214
 respiration, 214
 salt stress, 220–221
 stomatal regulation, 211–212
 and stress signaling, 222
 transpiration, 214–215
 water relations, 206–208
 PRD. *See* Partial root zone drying (PRD)
 Precipitation use efficiency (PUE), 155–156
Pseudomonas syringae. *See also* Woody plants disease
 biochemical tests, 262–263
 host range tests, 262–263

- multi locus sequence typing method, 257–260
 novel pathovar, 260–262
 pathovars, host range test, 257–260, 258t–259t
 phenotypic and genetic diversity, 257–260, 261t
 in planta pathogenicity tests, 262–263
 Pyrophosphate-extractable organic matter (PEOM), 93
 Pyruvate kinase, 205–206

R

- Raman microspectroscopy, 18
 Raman spectroscopy
 energy level transitions, 6–7, 6f
 inelastic scattering, 6–7
 vs. infrared spectroscopic analysis, 7, 8t
 molecular bond measurement, 7
 near-infrared excitation laser source, 5–6
 positions, 7, 7f
 sample photodecomposition, 5
 sampling techniques
 dispersive Raman spectroscopy, 15–17, 16f
 FT-Raman, 16f, 17–18
 Raman microspectroscopy/
 micro-Raman, 18
 SERS, 18–20, 19f
 Regulated deficit irrigation (RDI)
 PRD, 181–182, 182f
 RDIC, 181
 supplement irrigation, 183
 Ridge-furrow plastic mulching system, 174f
 factors, 176
 plastic-covered RF *vs.* CF system, 173–174, 175t
 rain-simulation study, 173–174

S

- Salt stress, 220–221
 “She-shi agriculture,” 190–192, 191f
 Soil-crop system, 156
 Soil mineral analysis
 allophane/imogolite
 characteristics, 26
 computer-aided subtraction, 27–28
 DRIFTS, 26–27, 27f

- Soil mineral analysis (*Continued*)
- IR spectroscopy, 26
 - metal oxides
 - Fe oxides, 31–32
 - FTIR spectra, 30f
 - gibbsite, 28–29
 - goethite and hematite, 31–32
 - midinfrared spectra, 28, 29f
 - Mn oxides, 33
 - SERS, 33
 - micro-Raman and FT-Raman, 20–21
 - phyllosilicates/layer silicates
 - composition, 21
 - differentiation and characterization, 21
 - FTIR spectroscopy, 25
 - kaolin group minerals, 24
 - kaolinite and dickite, 22–23
 - OH bending vibrations, 23
 - Raman spectroscopy, 25–26
 - Si–O stretching, 23
 - transmission infrared spectra, 21, 22f
 - weathering and pedogenesis
 - DRIFTS analyses, 34
 - gypsum, 34
 - limestone, 35
 - in situ measurements, 35
 - X-ray diffraction, 20
- Soil organic matter (SOM) analysis
- chemical extracts and fractionation, 93
 - FTIR analyses of HS
 - agricultural management effects, 96
 - binding mechanisms, 95
 - calcium-bound humic acid, 97–98
 - carboxyl groups, 95–96
 - components, 93–94
 - humification processes, 96–97
 - mobile humic acid, 97–98
 - NMR spectroscopy, 94
 - molecular resolution, 92
 - physical fractionation, 98
 - aggregate fractions, 101–102
 - clay fraction, 101
 - DRIFTS spectra, 100–101, 100f
 - Haplic Chernozem, 102
 - PLS, 102
 - POM, 99–100
 - pyrosequencing, 102–103
 - soil physical fractions, 99–100
 - soil carbon and nitrogen, 109–110
 - spectral analysis, 107–108, 109f
 - subtraction spectra, 104
 - ashing subtraction method, 105
 - chemical fractions, 106–107, 106f
 - fractionation method, 104–105
 - hydrogen peroxide, 106–107
 - in whole soils, 91–92
- SR-FTIR. *See* Synchrotron radiation-based Fourier transform infrared
- (SR-FTIR) spectromicroscopy
- Straw mulching system
- allelopathic effects, 177
 - mean root weight densities, winter wheat, 177, 179f
 - soil moisture conservation, 176–177
 - tillage system effects, 177, 178t
- Surface Energy Balance Algorithm for Land (SEBAL) model, 157
- Surface-enhanced Raman scattering spectroscopy (SERS), 19f
- applications, 19–20
 - metals, 19
 - plasmons, 18–19
- Synchrotron radiation-based Fourier transform infrared (SR-FTIR) spectromicroscopy
- applications, 15
 - components, 13–14, 14f
 - light source, 13–14
- Systemic acquired resistance (SAR), 266
- T**
- Type-Three Secretion System (TTSS), 270–271
- V**
- Vibrational spectroscopy techniques
- bacteria and biomolecules, 44
 - components, 47
 - FTIR spectroscopy, 44–46, 46f, 48f
 - microbial identification, 44–46
 - pertinent infrared assignments, 44–46, 45t
 - Raman techniques, 47, 48f
 - SERS, 48–49
- FTIR. *See* Fourier transform infrared (FTIR) spectroscopy

- mineral and organic spectral absorbance
 - ashing subtraction, 89
 - carbonate, 87–88
 - DRIFTS spectra, 87–89, 88f
 - NMR spectroscopy, 88
 - soil C, 87
 - SOM, 90–91
 - wet chemistry extraction, 89–90
 - molecular-scale analysis. *See* Molecular-scale analysis
 - Raman spectroscopy. *See* Raman spectroscopy
 - soil amendments
 - biochar, 49–53, 51t
 - biosolids, 53–54
 - compost, 53
 - FTIR spectroscopy, 49
 - soil heterogeneity and mineral analysis, 85–87
 - soil mineral analysis
 - allophane and imogolite, 26–28, 27f
 - metal oxides, 28–33, 29f–30f
 - mineral weathering and pedogenesis, 34–36
 - phyllosilicates, 21–26, 22f
 - SOM spectral components
 - fingerprint soils/OM samples, 40–41
 - FTIR vibrational assignments, 36, 37t–39t
 - IRMS technique, 41
 - limitation, 40
 - mapping, 41–42
 - molecular bonds, 36
 - Raman peak assignments, 42, 43t
 - SERS, 42, 44
 - SR-FTIR spectroscopy, 41
- W**
- Water-extractable organic matter (WEOM), 93
 - Water-saving innovations
 - chemical regulation, 183–184
 - components, 161
 - crop responses, water deficits
 - carbohydrate sources, 171
 - drought resistance, types, 169–170
 - irrigation scheduling, 170
 - plant growth, 170
 - transpiration and photosynthesis, 170
 - crop water use
 - CWR, 157–158
 - ET, 156–157
 - footprint, 160–161
 - soil water balance, 158–159
 - WUE, 159–160
 - engineering systems
 - contoured terraces, 184, 185f
 - drip and subsurface drip irrigation, 189
 - fertigation, 189–190
 - irrigation canals, 187, 188f
 - land leveling, 184, 185f
 - rainwater catchments, 184–187, 186f
 - “She-shi agriculture,” 190–192, 191f
 - spray irrigation, 188–189
 - fertilized and unfertilized plots, 171
 - freshwater resources, 151
 - global food demands, 193
 - global warming, arid and semiarid regions, 192
 - groundwater overexploitation, 192
 - irrigation network, 161
 - Loess Plateau soils, 171–172
 - mulching systems
 - gravel-sand mulching, 179, 180f
 - RF plastic mulching. *See* Ridge-furrow (RF) plastic mulching system
 - straw mulching. *See* Straw mulching system
 - types, 173
 - natural rainfall and irrigation resources, 155–156
 - no-till and subsoiling, 172–173
 - PUE, 155–156
 - Qilian Mountain snowmelt, 162
 - RDI
 - PRD, 181–182, 182f
 - RDIC, 181
 - supplement irrigation, 183
 - sand dunes, 152–155, 154f
 - scarcity and management, 193–194
 - socioeconomic and political consequences, 194
 - water-based food production systems, 151

- Water-saving innovations (*Continued*)
- water-resource management, 162
 - coordination needs, 168
 - economic factors, 168
 - farmers' educational backgrounds, 168
 - governmental policies, 168
 - groundwater pollution, 163
 - groundwater use, 163
 - guidelines for, 163
 - natural environmental factors, 168
 - off-farm employment, 169
 - prices and fees, 166–168
 - social environmental factors, 168
 - villagers' committee, 164–165
 - water-use rights, 165–166, 167f
 - Water Users' Association, 164
 - withdrawal permission license, 163
 - water-saving agriculture, definition, 155–156
 - water shortage, northern China, 152, 153f
 - WUE, 151
- Water-use efficiency (WUE), 151, 159–160
- Woody plants disease
- bacterial cankers, 240–241
 - crop genetic diversity
 - breeding programs, 268
 - host range tests, 268–270
 - origin and diversification, 268, 269t
 - disease control
 - chemical control, 264–265
 - chitosan, 266
 - citrus canker, 264
 - copper compounds, 264–265
 - disease cycle, 267–268
 - early detection methods, 263
 - inoculum reduction, 264
 - nonpathogenic microorganisms, 266–267
 - pathovar level, 263
 - quarantine pathogen, 263
 - SAR, 266
 - vascular pathogens, 264–265
 - disease outbreaks, 236–240, 237t–239t
 - economic losses, 240
 - epidemiology
 - abiotic and biotic factors, 249
 - dormant buds, 250–251
 - environmental reservoirs, 252
 - epiphytic populations, 249–250
 - genetic diversity, 256–257
 - genetic variability and intensity, 255–256
 - hazelnut, large-scale dissemination, 250
 - inoculum reservoir, 249–250
 - kiwifruit bacterial canker, 255–256
 - long- and short-distance dissemination, 254–255
 - plant tissues infections, 252–254, 253f
 - soil moisture, 251–252
 - warmer summer temperatures, 251–252
 - frost damage, ice nucleation
 - copper-streptomycin sprays, 273–274
 - freezing and thawing events, 273
 - frost sensitivity, 272–273
 - INA bacteria, 272–273
 - genetic diversity, 275
 - perennial plants, 236–240
 - risk analysis, 240–241
 - secondary products, 236–240
 - types
 - parenchymatic/localized diseases, 242
 - pathogens, 241–242, 243t–247t
 - vascular/systemic diseases, 242–249
 - virulence mechanisms
 - exopolysaccharide molecules, 272
 - factors, 270–271, 271t
 - NHR, 270–271
 - phytotoxins, 272
 - PTI, 270–271
 - TTSS, 270–271
 - type-III effectors, 270–271